Studies of Concentrated Electrolyte Solutions using the Electrodynamic Balance

Thesis by
Mark D. Cohen

In Partial Fulfillment of the Requirements
for the Degree of
Doctor of Philosophy

California Institute of Technology
Pasadena, California

1987
(submitted October 9, 1986)

Acknowledgments

I would like to thank my research advisors, Profs. John Seinfeld and Rick Flagan, for their help and guidance throughout the course of my research.

I'd also like to thank Profs. Jim Morgan and Fred Shair for their participation in my final examination committee.

Thanks also are due to many other people who have contributed to my work with helpful discussions and assistance, including Prof. Steve Arnold of Brooklyn Polytechnic University, Prof. Glen Cass, Fred Gelbard, Carol Jones, Brian Newport, Gidi Sageev, Craig Steele, and Dale Warren.

Several people helped with the design and construction of the apparatus used in this work, including Elton Daly, Rich Eastvedt, Concetto Geremia, George Griffith, Joe Fontana, Louis Johnson, Floyd Litreal, Leonard Montenegro, "Chic" Nakawatase, William Schuelke, and Tony Stark. I greatly appreciated their skill, advice and patience as they helped to build the various parts of the experimental apparatus.

My family has been very supportive during my time at Caltech (and before!). Each person has helped me in special ways, and I'd like to express my deepest appreciation and affection to them all. Howard, Mom, Dad, Barb, Joel, Bubba, Zady, Grandma, Grandpa and everyone else – thanks for your inexhaustible moral support and love.

Finally, I'd like to thank Serena for her understanding when my graduate

work borrowed from our time together. Her encouragement and love kept me going during the difficult periods. I treasure her companionship and hope to be the full-time friend that she deserves.

Abstract

An electrodynamic balance has been used to measure the water activity as a function of solute concentration at 20 °C for eleven single-electrolyte aqueous solutions — NaCl, NaBr, KCl, KBr, NH_4Cl, Na_2SO_4, $(NH_4)_2SO_4$, $CaCl_2$, $MnCl_2$, $MnSO_4$, and $FeCl_3$ — and three mixed-electrolyte aqueous solutions — NaCl–KCl, NaCl–KBr, and NaCl–$(NH_4)_2SO_4$. The measurements were performed by levitating single, charged, 20-micron diameter droplets of these solutions within the balance and measuring the mass of the particles as a function of the surrounding relative humidity. The deliquescence behavior of the particles was also observed.

Heterogeneous nucleation was inhibited due to the absence of container walls and because the small droplets were less likely than a bulk sample to contain foreign particles. Thus, this technique allowed the thermodynamics of highly concentrated solutions to be studied. For most of the solutions, water activity measurements were made to higher solute concentrations than have previously been reported. At low concentrations, the results were consistent with previously published data. Nucleation theory was used to estimate the surface excess free energy and critical nucleus size from the measured supersaturation at which nucleation occurred.

For the single-electrolyte solutions, the dependence of the solute activity coefficient on concentration was calculated, and the features of this dependence are discussed in relationship to ionic hydration and association. Several semi-

empirical electrolyte solution models were tested against the data, and it was found that salt-specific model parameters estimated from low concentration data could not be reliably used to predict the solution behavior at high concentrations. However, with estimated parameters based on the full range of the data, the models were able to represent the experimental data for single-electrolyte solutions to within the uncertainty in the measurements.

Three models of mixed-electrolyte solutions — the Zdanovskii-Stokes-Robinson, Reilly-Wood-Robinson and Pitzer methods — agreed well with the experimental data for the NaCl–KCl and NaCl–KBr systems over the range of concentration that the models could be applied. The mixing rules' predictions were consistent with the experimental observations for the NaCl–$(NH_4)_2SO_4$ particles assuming a small amount of water was retained in the dry state.

Contents

List of Tables in Chapter 1

List of Tables in Chapter 2

List of Tables in Chapter 3

List of Figures in Chapter 1

List of Figures in Chapter 2

List of Figures in Chapter 3

List of Appendices

Introduction

Aqueous electrolyte solutions occur in many biological, environmental, and industrial situations, and so, a characterization of the properties and an understanding of the underlying physics and chemistry of such solutions continue to be important areas of research. Two aspects of electrolyte solutions, their thermodynamics and nucleation, are the subject of this thesis.

Previous experimental investigations have generally involved a bulk sample of the solution of interest. Using conventional measurement methods, solution properties typically can be obtained only up to the saturation limit for a given salt or mixture. Further, it has been very difficult to study the homogeneous nucleation of electrolytes from aqueous solution, because it has not been generally possible to avoid the influences of container walls and foreign dust particles that can provide sites for heterogeneous, catalyzed nucleation.

Recently, the usefulness of the electrodynamic balance for the study of aqueous electrolyte solutions has been recognized. The apparatus allows a single, micron-sized, charged particle to be levitated in a controlled environment and continuously weighed. By measuring the relative mass of the particle as a function of the relative humidity of the surrounding vapor, information about the water activity's dependence on solute concentration can be obtained.

There are no container walls in contact with a levitated solution droplet. Further the likelihood that the tiny droplet will contain contaminating dust particles is much less than for a large, bulk sample of the solution. For these reasons,

the heterogeneous nucleation of crystals from solution is inhibited. Without this catalysis, very high supersaturations are observed within suspended droplets before crystallization occurs. Thus, the use of the electrodynamic balance allows the properties of highly supersaturated electrolyte solutions to be investigated. In addition, because of the supression of heterogeneous nucleation, the technique may possibly allow the homogeneous nucleation of electrolytes from aqueous solution to be investigated.

In Chapter 1, the experimental system is described and measurements of the water activity of several single-electrolyte solutions are presented. Calculations of solute activity coefficients are also given. For most of the salts, data were obtained at higher solute concentrations than have previously been reported. These data allow existing models of electrolyte solutions to be tested at higher concentrations than normally used for their evaluation.

Results for mixed-electrolyte solutions are given in Chapter 2. Three different mixtures were studied. The water activity dependence on solute concentration for one of the mixtures, $NaCl–(NH_4)_2SO_4$, had not been studied previously. These two salts are known to be important constituents of the atmospheric aerosol and so the properties of their mixed aqueous solution is of considerable interest. The measurements for all the mixtures extend to very high ionic strengths. These data thus allow the testing of existing mixed-electrolyte solution models at concentrations higher than typically employed in their assessment.

In Chapter 3, measurements of the solute concentration at which crys-

tallization occurred in the levitated droplets are presented. For the single-electrolyte solutions, the measured critical supersaturations are used with an existing theory to estimate the surface excess free energy and size of the critical embryo for homogeneous nucleation from aqueous solution. Two features of the present work are improvements over some of the earlier single-particle nucleation investigations. First, the particle size has been measured and explicitly accounted for in the theoretical interpretation of the results. Second, the supersaturation has been accurately estimated at the critical solute concentration by using the water activity measurements obtained in this work. The supersaturations found were much higher than those observed with conventional techniques, and it is thought that true homogeneous nucleation from solution was occurring.

Chapters 1-3 will be submitted for publication as a three-part series. Therefore, within the text, Chapters 1, 2, and 3 are referred to as Parts I, II, and III.

Chapter 1: Water Activities for Single-Electrolyte Solutions

Studies of Concentrated Electrolyte Solutions using the Electrodynamic Balance. I. Water Activities for Single-Electrolyte Solutions

Mark D. Cohen, Richard C. Flagan*,
and John H. Seinfeld†

Chemical Engineering
California Institute of Technology
Pasadena, CA 91125

*Environmental Engineering Science
†To whom correspondence should be sent

Abstract

An electrodynamic balance apparatus has been used to suspend single, twenty-micron diameter, charged droplets of aqueous salt solutions in a humid environment. From measurements of the humidity surrounding the droplet and the relative mass of the particle in its wet and dry states, the dependence of water activity on solute concentration was determined for aqueous solutions of the following salts at 20 ℃ : NaCl, NaBr, KCl, KBr, NH_4Cl, Na_2SO_4, $(NH_4)_2SO_4$, $CaCl_2$, $MnCl_2$, and $FeCl_3$. This technique allowed the thermodynamics of highly supersaturated solutions to be studied, and for most of the salts, the measurements were made to higher concentrations than have previously been reported at comparable temperatures. The dependence of the solute activity coefficient on concentration was calculated for each of the salts, and the features of this dependence are discussed in relationship to ionic hydration and association. Several semi-empirical electrolyte solution models were tested against the data, and it was found that salt-specific model parameters estimated from low concentration data could not be reliably used to predict the solution behavior at high concentrations. However, with estimated parameters based on the full range of the data, the models were able to represent the experimental data to within the uncertainty in the measurements.

Introduction

The thermodynamics of aqueous electrolyte solutions continues to be an area of experimental and theoretical interest. Knowledge of solution properties is required for the understanding of many important phenomena in industrial, biological, and environmental settings. While the theoretical details of the behavior at very low concentrations are reasonably well established, that at high concentrations remains less well understood. At high concentrations, many of the simplifying assumptions made for dilute solutions are no longer valid. A deeper understanding of the processes occurring in highly concentrated solutions may lead to a more complete understanding of electrolyte solutions in general. For many electrolytes, however, there are little or no data available at high solute concentrations. With conventional methods of measurement, crystallization generally occurs at relatively low supersaturations and so data can normally be obtained only up to the saturation limit of the salt.

Recently, the electrodynamic balance has been used to investigate the thermodynamics of aqueous solutions at high concentrations [1,2,3,4,5]. In this technique, a single, charged solution droplet is trapped by the fields created by the electrodes of the apparatus and can be continuously weighed. Because of the lack of foreign surfaces, heterogeneous nucleation is suppressed, allowing the solute concentration in a suspended droplet to reach very high degrees of supersaturation before crystallization occurs. Thus, the use of the electrodynamic balance allows the properties of highly concentrated solutions to be investigated.

We have used the electrodynamic balance to study the thermodynamics of concentrated aqueous electrolyte solutions. In this paper, Part I, the thermodynamics of concentrated aqueous solutions of single electrolytes are studied. In Part II [6], results for aqueous solutions of salt mixtures are presented. In Part III [7], results for the nucleation of the solute from aqueous electrolyte solutions are given.

Experimental Method

In recent years, the bihyperboloidal electrodynamic balance has proven to be a useful experimental tool for the investigation of a wide variety of problems involving micron-sized particles, including gas-phase mass transfer [8], vapor-liquid equilibrium for multicomponent oils [9], chemical reaction kinetics [10], light scattering [11], and solute nucleation in electrolyte solutions [3,4,5,12]. The design of the bihyperboloidal electrodynamic balance and the theory underlying its ability to levitate charged particles have been treated fully by others [13,14,15,16] and will not be repeated here.

Rubel [1] has measured the water activity as a function of solute concentration for aqueous solutions of phosphoric acid using the electrodynamic balance. As humid air was directed past a suspended droplet at atmospheric pressure, its relative mass was measured as a function of relative humidity. The results were consistent with other literature data for phosphoric acid solutions.

Richardson and coworkers [2,3,4,5] have also studied the thermodynamics of aqueous solutions by suspending droplets in an electrodynamic balance. In

their experiments, the chamber was first evacuated to dry the particle. Small amounts of water vapor were then admitted into the chamber to establish a controlled humidity atmosphere. The experiments were performed at low pressure. With this technique, the properties of LiBr, LiI, $(NH_4)_2SO_4$, and mixed $(NH_4)_2SO_4$–NH_4HSO_4 solutions were studied.

Particle Containment System

A schematic diagram of the apparatus used for this study is shown in Figure 1. In the electrodynamic balance technique, a single, charged particle is suspended in a gaseous atmosphere by means of an electric field. The electric field is created by imposing voltages on the electrodes shown in Figure 2. The surfaces of the top and bottom electrodes are given by

$$z^2 = \frac{r^2}{2} + z_0^2 \tag{1}$$

where z is the vertical displacement from the geometric center of the chamber, r is the radial distance from the axis of symmetry, and z_0 is the characteristic length of the electrode assembly, equal to one–half the distance between the top and bottom electrodes at their closest point of approach. For our electrodes, z_0 was 0.5 cm. The surface of the ring electrode satifies

$$z^2 = \frac{r^2}{2} - z_0^2 \tag{2}$$

A dc voltage difference between the top and bottom electrodes creates a dc field that balances the particle against gravity. On this field is superimposed a

field created by an ac voltage applied to the ring electrode. This ac field creates an unsteady force on an off-center charged particle that, on a time-averaged basis, pushes it toward the center of the chamber.

In the absence of any gas flows, a particle will remain at rest at the center of the chamber as long as the force due to the dc field exactly balances the gravitational force on the particle. If the vertical electrical force due to the dc field is greater or less than the gravitational force on the particle, the particle will oscillate vertically above or below the center of the chamber, respectively. Thus, in the absence of any gas flows within the chamber, the balancing voltage is determined by finding the voltage such that the particle remains at rest in the center of the chamber. The ac field is exactly zero at the center. However, if a balanced particle is moved from the center by the action of any small, transient force, it oscillates in the ac field and is quickly forced back to the center.

In the presence of a horizontal gas flow, the particle oscillates at the frequency of the ac voltage in a stable limit cycle. The time-averaged horizontal electrical force on the particle during this oscillation exactly equals the aerodynamic drag force on the particle due to the flowing gas. The trajectory of a particle cannot be completely horizontal because the vertical field strength is dependent on position while the force due to gravity is constant. For a small-amplitude oscillation, however, the particle's oscillation will be approximately horizontal if the average dc field encountered by the particle over its trajectory balances the gravitational force on the particle. If, however, the average dc field does not exactly balance gravity, the particle's oscillation will have a noticeable

vertical component. Thus, even in the presence of an added, horizontal force, the dc voltage required to balance a charged, suspended particle against gravity can be determined.

A particle is balanced when the dc field force exactly counteracts the gravity force, *i.e.*,

$$mg = ne\frac{CV_{dc}^{bal}}{z_0} \tag{3}$$

where m is the mass of the particle, g is the gravitational constant, n is the number of elementary charges on the particle, e is the charge on an electron, V_{dc}^{bal} is the dc balancing voltage, and C is a geometrical constant. This condition is valid whether or not a horizontal flow is present.

We performed a numerical calculation of the dc field within the electrodes, neglecting the holes in the ring and endcap electrodes, and found that the geometrical constant C was equal to 0.401 ($\pm$0.001) at the center of the chamber, in good agreement with a previous calculation [16]. Calculations were also performed for a modified electrode geometry with a slot in the ring electrode, as if holes were drilled continuously all around the ring. No effect on the geometrical factor C was found for a slot with vertical dimension of 0.636 z_0 (*i.e.*, 0.318 cm), the diameter of the holes in our ring electrode. It should be noted that the value of C is not required for relative mass measurements and is only needed when the absolute mass of a particle is to be determined.

The electrodes were gold plated to inhibit corrosion and to ensure a smooth distribution of surface charge. Spacers made of the machinable ceramic MACOR [18] maintained the electrode orientation. A teflon spacer insulated

the electrodes from the base of the overall chamber. Electrical connections to the ring and endcap electrodes were made by insulated screws. The electrode assembly was secured to the base of the environmental chamber by two plastic screws.

One set of holes on opposite sides of the ring electrode allowed the introduction and removal of gases. The unfocused beam from a 3 milliwatt He-Ne laser was directed through another set of oppositely placed holes in order to illuminate the particle at the center of the chamber. A suspended particle was observed by viewing the scattered laser light through an additional hole in the ring electrode with a microscope. The microscope contained a 1.5x objective and a 10x eyepiece with a movable hairline reticle. The laser and visual observation holes in the ring were covered with windows, and the hole in the top electrode was covered with a stainless steel sphere.

The particles to be studied were inserted using a piezoelectric droplet generator [17]. The tip of the injector was immersed in a beaker of the solution of interest, and a small quantity of that solution was drawn into the tip of the injector by applying a small relative vacuum to the fluid in the injector. An electrical pulse applied to the piezoelectric element of the injector caused the expulsion of a small jet of solution from a glass capillary nozzle. The jet eventually broke up into one or more droplets. Just beyond the the end of the glass nozzle was a small metal ring held at a dc voltage different from that of the electrically grounded fluid in the generator. In this way, the surface of an emerging jet of solution was charged inductively. When the jet broke away,

the charge remained on the resulting droplet(s). To insert a particle into the electrodynamic balance, the top of the chamber and the ball covering the 0.15 cm hole in the top electrode were removed and the tip of the injector was positioned directly above the hole in the top electrode. The ac field was activated, and the generator was pulsed until a suitable particle was captured.

Measurement of Water Activity and Solute Concentration

In order to measure water activities for electrolyte solutions, this experimental method exploits the fact that at equilibrium the chemical potential of water in the droplet's solution and the surrounding vapor will be equal. The droplets studied were typically about 20 microns in diameter. It was, therefore, unnecessary to include the Kelvin effect in describing the droplet-vapor equilibrium. Assuming an ideal gas, the condition of phase equilibrium for water requires that

$$\mu^0_{w,liq} + RT \ln a_w = \mu^0_{w,vap} + RT \ln \frac{p_w}{p^{sat}_w} \tag{4}$$

in which $\mu^0_{w,liq}$ and $\mu^0_{w,vap}$ are the standard state chemical potentials of water in the liquid and vapor phases at the temperature and pressure of interest, R is the gas constant, T is the absolute temperature, a_w is the activity of the water in the liquid phase, p_w is the partial pressure of water present, and p^{sat}_w is the saturation vapor pressure of water at temperature T. Since the standard state chemical potentials are equal in this instance, eq 4 reduces to

$$a_w = \frac{p_w}{p^{sat}_w} = rh \tag{5}$$

where rh is the relative humidity of the vapor phase. Thus, if the relative humidity of the gas flowing past the particle is known, then the activity of water in the suspended droplet is also known.

The humid air flowing past the particle was produced in the following way. First, the air was purified and dried by passing it through beds of activated charcoal, molecular sieve, and Drierite. The air was then filtered to remove any particles. Part of the gas stream was then split off to be humidified. The humidification was carried out by passing the air through two bubblers filled with pure water, the second of which was immersed in a constant temperature bath. The humidified air was filtered to remove any particles that may have been formed as a result of the humidification process. This humidified air was then recombined with the remaining dry flow to produce air at a particular relative humidity. At this point, a small fraction, 7 cm^3/minute, of this mixed stream was split off and pulled through the electrode assembly and a capillary flow meter by a vacuum pump. The remaining humid air passed through a dewpoint hygrometer to measure the absolute humidity of this air stream. In this way, a constant flow of known absolute humidity could be directed past a suspended particle.

If the charge on a particle remains constant, then the relative mass of the particle at any two states can be obtained from the ratio of the balancing voltages for the two states. For these experiments, the amount of solute in a particle remained essentially constant unless, as noted below, the solute was volatile. For a nonvolatile solute, any change in the particle's mass must be due

to a change in the water content of the particle. Therefore, if the composition of the particle at any particular balancing voltage was known, the composition at any other state could be easily determined from the relative masses of the two states. For example, if a particle was anhydrous in its dry state, then the weight fraction solute at any other state is given simply by $V_{dc}^{dry}/V_{dc}^{wet}$. If the weight fraction solute is known, then the molality can be calculated from

$$m = \left(\frac{1}{wfs} - 1\right)^{-1} \frac{1}{w_s} \tag{6}$$

in which wfs is the weight fraction solute and w_s is the molecular weight of the solute. As discussed below, the overall uncertainty in the weight fraction solute measured in the present experiments was at most 0.01.

The electrode assembly was housed in an insulated chamber for safety and for temperature control. Water from a constant temperature bath was circulated through an O-ring-sealed sleeve on the outer wall of the chamber. The temperature inside the chamber was measured with a thermistor. The tip of the thermistor was outside the the electrode assembly, approximately 8 cm away from the center of the electrodes. In order to estimate the relative humidity to which the particle is exposed, the temperature of the gas surrounding the particle must be known accurately. Unfortunately, it was not possible to directly measure the temperature in the vicinity of a suspended particle because the probe would have altered the electric fields in the electrode region. If the dependence of water activity on molality is known for a particular salt solution and the dry composition of the particle is known, however, then the temperature of the particle and the gas immediately surrounding it can be calculated from the

relative balancing voltage of the particle in the wet and dry states and the absolute humidity of the gas. In this way, a suspended particle was used as a temperature probe.

It was found that the temperature of the particle and the immediately surrounding gas was slightly higher than that measured by the thermistor. This slight temperature increase was due to heat dissipation related to the ac voltage. Evidence for this heating and its source came from a variety of observations. First, by changing the position of the thermistor, a temperature gradient radially and vertically away from the ring electrode was found. Also, when the ac voltage was increased, the temperature measured by the thermistor at any given location increased. Finally, when the ac voltage was increased, the temperature of a suspended particle increased. The temperature difference between the thermistor and the particle increased approximately as the square of the ac voltage.

In order to calculate the relative humidity to which a suspended particle was exposed, it was necessary to relate the temperature of the particle to that indicated by the thermistor. The difference between these two temperatures, $\triangle T$, depends on the flow rate through the electrodes, the ac voltage, and the position of the thermistor. An ac potential of 400 volts and an electrode flow of 7 cm^3/minute were found to be optimal and were used for all measurements. The thermistor position was also fixed for all the measurements reported in this paper. Using particles of sodium chloride, potassium chloride, potassium bromide, sodium sulfate, ammonium sulfate, and calcium chloride at humidities

where the water activity as a function of concentration is known, it was found that $\triangle T$ for the chosen flow rate and ac voltage was equal to 0.3 ± 0.1 °C.

The relative humidity of the air flowing past the particle was calculated from the measured absolute humidity and the measured chamber temperature with a $\triangle T$ of 0.3 °C. The uncertainty in our estimate of the relative humidity is approximately 0.01–0.02 considering uncertainties in the thermistor calibration, the value of $\triangle T$, and the absolute humidity indicated by the hygrometer. Since the relative humidity is exactly equivalent to the water activity in our experiments, the uncertainty in our reported water activities is also approximately 0.01–0.02.

After the particle was inserted, dry air was passed through the electrodes, causing the particle to lose water until it crystallized. The balancing voltage corresponding to the dry mass of the particle was thus determined. The relative humidity was then changed in steps, allowing adequate time for the equilibration of the chamber humidity at each step. The variation of the the balancing voltage with time for a part of a typical experiment is shown in Figure 3. Each of the steady states in Figure 3 represents a particular particle concentration in equilibrium with a particular relative humidity. The particle responds rapidly to the slowly changing conditions. The gas stream equilibrates more slowly with the tubing and the walls of the apparatus, resulting in the slow approach of the particle mass to steady state. At high humidities this equilibration time became prohibitively long. Therefore, measurements were not generally attempted at relative humidities above 0.90.

There are several advantages in making water activity measurements for electrolyte solutions using micron-sized, levitated droplets. First, because the sample of solution is so small, it reaches phase equilibrium with its surroundings extremely quickly. In practice, measurements of the water activity as a function of concentration are limited only by the time it takes to establish and measure the relative humidity in the chamber. An entire experiment, with measurements over a wide range of humidites, can be performed in a single day. This can be compared to the long equilibration times typically required for conventional isopiestic measurements, in which it is not uncommon to wait 2–28 days for each water activity measurement [22,23]. Thus, the electrodynamic balance offers a relatively quick way to obtain water activity data.

In addition, heterogeneous nucleation is supressed because there is no containing vessel and because the tiny droplet is less likely than a larger sample to be contaminated with particles. Thus, very high supersaturations can be reached before crystallization occurs. It is unlikely that water activity data for such highly supersaturated solutions could be obtained by conventional measurement methods.

Particle Size and Charge Measurement

A measurement of the particle size and net charge was required for several reasons. First, an estimate of the particle size was needed in order to determine whether the Kelvin effect is significant. An estimate of the net particle charge was needed to assess the possible influence of the surface charge. Furthermore,

the cystallization process, discussed in Part III of this work [7], depends on the particle size. The following procedure was used to estimate the particle size and charge.

In the absence of flow through the electrodes and with no ac voltage, a particle will simply rise or fall vertically if the dc field does not exactly balance gravity. A force balance on a spherical particle of diameter d_p moving at its terminal velocity, u, under the influence of gravity and the constant electric field near the center of the chamber, yields

$$u = \frac{-neCA(d_p)[V_{dc} - V_{dc}^{bal}]}{3z_0\pi\mu d_p} \tag{7}$$

in which μ is the viscosity of air, V_{dc} is the dc voltage during the measurement, and V_{dc}^{bal} is the balancing voltage of the particle. The slip correction factor [20,21], $A(d_p)$, is is given by

$$A(d_p) = 1 + \frac{2\ell}{d_p}\left[A_1 + A_2 \exp\left(\frac{-A_3 d_p}{\ell}\right)\right] \tag{8}$$

in which ℓ is the mean free path of the air molecules, $A_1 = 1.257$, $A_2 = 0.400$, and $A_3 = 0.55$.

From eq 7, it is seen that a plot of the measured particle velocity versus the dc voltage should yield a straight line. After substitution from eq 3, it can be shown that the slope, S, of this straight line is given by

$$S = \frac{\rho_p g A(d_p) d_p^2}{18\mu V_{dc}^{bal}} \tag{9}$$

where ρ_p is the density of the particle.

With no flow through the chamber and no ac voltage, the particle's terminal velocity was measured as a function of the dc voltage between the endcap

electrodes. Particle velocity was determined by measuring the time required for the particle to travel a known distance. The measurments were made by first changing the dc voltage from the balance condition, setting the movable crosshair to a specific distance away from the particle, and then turning off the ac voltage and timing the particle's sedimentation. Several velocity measurements were made at each voltage setting, and dc voltage settings both greater and less than the balancing voltage were used.

The velocities were measured over distances on the order of 0.5 mm and times on the order of 1–5 seconds. Over this distance the vertical dc field changed by only about 1 %, and so the field was assumed constant at its value at the center of the chamber. A twenty-micron particle subjected to the above sudden imposition of unbalanced force would achieve its terminal settling velocity in approximately 0.01 seconds. It was assumed, for the purposes of calculating the particle velocity, that the terminal velocity was reached instantaneously.

A straight line was fit to the measurements using a least-squares procedure to estimate the slope in eq 9. A typical set of measurements and best-fit straight line are shown in Figure 4. Using the estimated slope and measured balancing voltage, eq 9 was then solved for the particle diameter by iteration. Once the diameter of the particle was known, the particle's charge could then be obtained from eq 3. As an example, the measurements presented in Figure 4 for an ammonium sulfate particle resulted in a particle diameter of 19 microns and a charge of 8.9×10^4 elementary charges.

As stated above, the velocity measurements were made in the absence

of flow through the electrodes. Since the humidity in the chamber was not stable in the absence of flow, a solution droplet would have changed size during the series of velocity measurements. Therefore, the velocity measurements were made on dried particles. The shape of the dry particles was unknown, so the measurements provide an equivalent aerodynamic spherical diameter for the dry particle.

Additional Factors in Data Analysis

The estimation of the solute concentration in the droplet was ocassionally complicated by one or more factors. First, there is no general, *a priori* way to predict what the composition of a suspended particle will be after it has crystallized and/or dried. One cannot simply assume the dry particle will be the most thermodynamically stable crystalline phase at the temperature of the experiment. In fact, there are several additional possibilities. Even if a crystalline phase is obtained, it may not be the most stable phase. This phenomenon is often found in crystallization experiments and is known as Ostwald's Law of Stages [19] which states that a less stable crystalline phase can be formed from a supersaturated solution because the free energy change required for its formation is less than that for a more stable crystalline phase. There could also be more than one crystalline phase present. Water could be retained in the particle, possibly trapped between different crystalline phases. Finally, the particle may not crystallize at all but instead pass into a glassy state.

The following algorithm was used to determine the particle's dry com-

position. First, an experiment was performed in which the particle's balancing voltage was measured at various relative humidities. A measurement of the deliquescence humidity at which the crystalline phase and a liquid solution phase have equal thermodynamic stability was also attempted. At humidities above the deliquescence point, a crystalline particle quickly absorbs water from the vapor phase. The crystal then dissolves, forming a solution droplet in which the activity of the water equals the relative humidity.

From the measurements of relative particle mass as a function of relative humidity, the solute concentration as a function of water activity was initially estimated by assuming the dry-particle stoichiometry was that of the most stable crystalline phase. If the resulting dependence of water activity on solute concentration was consistent with literature data, then the dry-particle stoichiometry was taken to be this equilibrium value. This was the case for sodium chloride, potassium chloride, potassium bromide, ammonium chloride, ammonium sulfate, and ferric chloride. For all of these salts except for ferric chloride, this assumption was confirmed by the fact that deliquescence occurred at the relative humidity expected for crystalline particles of this equilibrium composition.

If the salt particle deliquesced at a lower relative humidity than expected and if the $a_w(m)$ results were consistent with the another less stable, but known, crystalline phase, then it was assumed that the dry particle was comprised of this phase. This was true for sodium bromide, sodium sulfate, and calcium chloride.

In some cases, the $a_w(m)$ results were not consistent with the assumption

that the dry particle consisted of a single, known crystalline phase, suggesting that the dry particle either contained several different crystalline phases, contained some trapped water, or had a glassy structure. The stoichiometry of the dry particle was estimated from literature values of the thermodynamic properties [*i.e.*, $a_w(m)$] at high humidity. This procedure was necessary for manganese chloride and manganese sulfate.

Thus, while there is no general way to predict the composition of a suspended particle after drying, there was no difficulty in inferring the dry-particle stoichiometry in the present experiments. In almost all cases, the dry-particle stoichiometry corresponded to a known crystalline form. Although not attempted in the present work, it would be possible to circumvent this problem completely by inserting a *dry* particle of *known* stoichiometry into the chamber.

A second factor slightly complicating the interpretation of the experimental data was that the particle's charge did not always remain constant. The dry state for a given particle generally corresponded to a constant, particular amount of water and solute. If the charge on the particle remained constant, the same dry balancing voltage would be obtained throughout the experiment. It was sometimes found, however, that the dry balancing voltage would increase with each successive measurement, probably resulting from a loss of net charge on the particle. With less charge, the particle required a higher balancing voltage for its mass to be supported against gravity. The decharging was more pronounced at high humidity and when the ac voltage applied to the ring electrode was increased. The precise source of the decharging was not determined.

However, it is believed that the generation of the ions was related to the high ac voltage on the ring, that the ion generation process was aided by water vapor and impurities on the surfaces of the apparatus, and that suitably charged ions were captured by the particle. As a result, the net charge on the particle could decrease over the course of an experiment.

The rate of charge loss was typically less than about 0.1 % per hour. When decharging occurred, the change in particle charge was assumed to occur linearly with time between two successive dry balancing voltage determinations. In most cases, this procedure amounted to only a very small correction to the calculated solute concentration for a given steady state. The decharging process, while noticeable, did not introduce a significant uncertainty in the calculation of the solute concentration from the ratio of dry and wet balancing voltages.

The particle's motion in the electric field introduced a small systematic error in the calculation of the solute concentration from the measured balancing voltages. The dc field within the electrodynamic balance decreases with increasing radial distance away from the center. As mentioned earlier, the air flow within the electrodes caused the suspended particle to oscillate horizontally away from the center. The amplitude of this oscillation depends on the particle charge, particle shape, particle mass, flow rate, and ac voltage. For a constant flow rate and ac voltage, the oscillation amplitude and the particle's average displacement from the center increase with increasing particle size. In this way, a large particle encounters, on the average, a weaker vertical dc field than a small particle. Because of this, the ratio of the mass of a particle when it is

large to that when it is small is actually less than that calculated from the ratio of the balancing voltages for the two particle states, introducing a systematic underestimation of the solute concentration in the droplet that increases as the particle mass increases.

By changing the ac field while observing a dry particle in the presence of a horizontal gas flow, we determined the balancing voltage for a particle of constant mass as a function of the average displacement of the particle from the center of the chamber. The trajectory of the particle could be easily measured using a calibrated, movable hairline reticle. The magnitude of the decrease in vertical dc field strength with increasing radial distance away from the center was estimated from our numerical calculations of the dc field within the electrodynamic balance. The increase in balancing voltage required as the particle oscillated at greater and greater distances from the center of the chamber corresponded exactly to our numerical estimation of the decrease in the dc field. In the measurements of particle mass as a function of chamber relative humidity, the systematic underestimation of the weight fraction solute for the largest amplitude oscillations encountered was less than 0.01 at the highest humidities measured. At lower humidities, the systematic error was even smaller.

Considering the above factors and the uncertainty in determing the particle balancing voltage, the overall uncertainty in the estimation of the weight fraction of solute in the droplet is, at most, 0.01 in the present experiments. The corresponding uncertainty in droplet molality depends on the solute concentration and molecular weight. For example, in a sodium chloride droplet with a

nominal concentration of 10.00 molal, the uncertainty in molality corresponding to a 0.01 uncertainty in the weight fraction solute is approximately 0.22 molal or about 2 %.

A additional question that needs to be addressed is whether the charge will affect the thermodynamics of the suspended particle. First, we note that in the 60 Hz ac field, a suspended aqueous electrolyte droplet will behave as a conductor. Therfore, the excess charge will reside on the droplet surface, and there will be no electric fields within the particle. The presence of a surface charge can alter the phase equilibrium between a droplet and the surrounding vapor. According to a result obtained by Fletcher, cited by Rubel [1], the correction to the vapor pressure over a solution droplet due to the surface charge is given by

$$\ln \frac{p}{p_0} = \frac{-2q^2 w_w(\epsilon - 1)}{\pi \rho \epsilon R T d_p^4} \tag{10}$$

where p and p_0 are the vapor pressures over the droplet in the presence and absence of surface charge, respectively, q is the surface charge, w_w is the molecular weight of water, ϵ is the dielectric constant of the solution, and ρ is the solution density. The smallest particles that we studied had a diameter of about ten microns, and the maximum charge was less than 10^6 elementary charges. For a ten-micron diameter water droplet with 10^6 elementary charges, eq 10 predicts that the surface charge will have a negligible effect on the vapor pressure above the droplet.

The laser used to illuminate the particle might possibly affect its behavior, but the effect was found to be negligible. Even if it is assumed that the particle

absorbed all the light incident upon it and that heat dissipation was limited to conduction alone, heating of the particle due to the laser beam was found to be insignificant. Estimates of the magnitude of the radiation pressure and photophoretic force due to the laser beam's interaction with the particle showed that these phenomena are also unimportant. Furthermore, no evidence that the laser beam influenced the suspended particles was observed in the experiments.

Results and Discussion

Water Activity Measurements and Deliquescence

Measurements of particle mass as a function of relative humidity were performed for eleven different salts at 20 °C. In most cases, measurements for a given salt were made on two or more particles. For a given salt, the results from particle to particle and for different measurements on the same particle generally agreed to within the experimental uncertainties described above. An attempt was made to measure the deliquescence humidity for each salt. Crystallization measurements were also made, and these are presented and discussed in Part III of this work [7].

In Table 1, the stoichiometries of the dry particles, the deliquescence observations, and the range of molalities over which water activity measurements were made are presented. The compositions, deliquescence humidity, and solubility of the most stable crystalline phase at 20 °C are also listed. For practical reasons, it was not possible to determine the deliquescence humidity exactly, but

upper and lower bounds were measured. The meaning of the bounds given in Table 1 for the deliquescence humidity is that deliquescence did not occur at the lower humidity but did occur at the upper humidity. Thus, the deliquescence humidity lies somewhere in this range.

Using the dry-particle compositions listed in Table 1, the weight fraction solute was calculated for each steady state from the measured dry and wet balancing voltages. In Figures 5–15, the measurements of the weight fraction solute are shown as a function of relative humidity for each of the salts studied. Each point represents a different steady state. Also shown are data from the literature. Where the present results can be compared with literature data, the agreement is generally within our experimental uncertainty. In most cases, data were not available in the literature for water activity as a function of concentration at 20 °C, so literature data at 25 °C were used for comparison. For a given solute concentration, the change in water activity for a temperature change from 20 °C to 25 °C is generally much less than 0.001 [31], well within our experimental uncertainty.

Richardson and Spann have also made water activity measurements on ammonium sulfate particles suspended in an electrodynamic balance [4]. Their data are shown along with ours and those from conventional measurements [27] in Figure 11. The difference in the water activities in the two single-particle data sets at high concentration is as high as 0.04–0.05, larger than the estimated uncertainty of our measurements. The source of this discrepancy is not known. The only other system for which data are available at low humidities is calcium

chloride for which good agreement is obtained, even at very low humidities.

For each salt, the literature data and experimental data represented in Figures 5–15 were combined, molalities were calculated from the weight fraction solute, and the resulting data for water activity dependence on molality were fitted by a least-squares procedure to a polynomial of the form

$$a_w = a_0 + a_1 m + a_2 m^2 + a_3 m^3 + \ldots \tag{11}$$

The coefficients of the best-fit polynomial, the standard deviation between the polynomial's predictions and the data, and the highest molality for which the fit is valid are given in Table 2. While the accuracy of these fits is less than that for data obtained by the isopiestic method, these polynomials represent our data to within the experimental uncertainty and extend well beyond the range of most previous determinations. Two polynomial fits are presented for ammonium sulfate. One fit includes our results and those given by Robinson and Stokes [27]. The second fit also includes the results reported by Richardson and Spann [4].

In the experiments with ammonium chloride particles, it was found that the dry balancing voltage decreased slightly as the experiment progressed. Over the 72 hours that one particle was suspended in the electrodynamic balance, the dry balancing voltage decreased by a total of about 10 %. The only reasonable explanation for this was that the ammonium chloride in the particle was evaporating during the experiment. The volatilization rate appeared to be greatest for an aqueous droplet at low humidity (*i.e.*, high solute concentration). Since the vapor pressure of a volatile solute over an aqueous droplet increases with increas-

ing solute concentration, this observation was not surprising. The volatilization rate was relatively low when the particle was dry. Between any two successive dry states, the particle lost at most a few percent of its solute mass. In general, longer times were spent reaching steady state at higher humidities than those for lower humidities, and so, the solute mass lost by volatilization was roughly the same during each of the various steady states. In order to calculate the droplet concentrations in the experiments, it was therefore assumed that the decrease in solute mass between any two successive dry balancing voltage determinations decreased the same amount during each wet steady state. As with the treatment of the decharging phenomenon, the uncertainty in solute molality introduced by this assumption is relatively small.

The most thermodynamically stable crystalline form was obtained for sodium chloride, potassium chloride, potassium bromide, ammonium chloride, and ammonium sulfate. For these salts, it is seen in Table 1 that the measured deliquescence humidities were consistent with the available literature data. With sodium bromide, sodium sulfate, and calcium chloride, manganese chloride and manganese sulfate, the dry particles obtained were not the equilibrium crystalline forms. As expected, each of these exhibited a lower deliquescence humidity than that of the most stable phase at 20 ℃. The sodium bromide and sodium sulfate particles both crystallized to their known, anhydrous crystalline form.

The water activity results for $CaCl_2$ were consistent with a dry–particle stoichiometry of $CaCl_2 \cdot 4(H_2O)$. Although there is a stable crystalline form with

this stoichiometry, the calcium chloride particles did not appear to crystallize. Instead, when dried at a humidity of 0.10 at 20 ℃, the particles consistently attained the same $CaCl_2 \cdot 4(H_2O)$ stoichiometry. The particles did not exhibit a deliquescence above a certain humidity but simply absorbed water as relative humidity was increased above 0.10. From the solubility of $\alpha CaCl_2 \cdot 4(H_2O)$ and $\beta CaCl_2 \cdot 4(H_2O)$ crystalline forms at 20 ℃, we estimated from our water activity results that deliquescence would be expected at relative humidities of 0.24 or 0.19, respectively. Thus, our deliquescence observations suggest that the dry particles of $CaCl_2 \cdot 4(H_2O)$ were not crystalline. Instead, the particles may have been gelatinous or glassy.

The $CaCl_2$ particles were dried further from the $CaCl_2 \cdot 4(H_2O)$ state by increasing the temperature from 20 ℃ to 50 ℃ while keeping the absolute humidity constant. In this process, the particle lost almost half of its water. A further temperature increase at constant absolute humidity, to 90 ℃, dried the particle slightly more and the resulting particle had a stoichiometry of $CaCl_2 \cdot 2(H_2O)$. Measurements of the balancing voltage at high temperatures were difficult because of buoyancy-driven flows within the chamber. A variability of 5 % in balancing voltage was found in repeated measurements at elevated temperatures, at least ten times higher than the variability found at 20 ℃. The behavior of our calcium chloride particles upon heating are reasonably consistent with the recent results of Meisingset and Gronvold [32], who found that a bulk sample of $CaCl_2 \cdot 4(H_2O)$ dehydrated to $CaCl_2 \cdot 2(H_2O)$ at 45 ℃.

With manganese chloride and manganese sulfate, the stoichiometry of

the dry particles did not correspond to a particular, known crystalline phase. Manganese chloride droplets appeared to crystallize, however, while manganese sulfate droplets, like the calcium chloride droplets, did not. For manganese sulfate, the dry particle's stoichiometry was not changed when dried at 50 ℃ or 85 ℃. Drying at temperatures higher than 20 ℃ was not attempted for manganese chloride. As discussed earlier, the composition of the dry particles for these two salts had to be estimated by matching our measurements to the known $a_w(m)$ properties reported in the literature for low molalities. From the estimated dry composition, the solute concentration at any other balancing voltage could be estimated.

Manganese sulfate is unusual in that there are three different crystalline hydrates that have very similar thermodynamic stabilities 20 ℃. From solubility data for the various $MnSO_4$ crystalline hydrates [26] and the dependence of water activity on concentration for manganese sulfate solutions, we have estimated the deliquescence humidities for $MnSO_4 \cdot 5(H_2O)$, $MnSO_4 \cdot 4(H_2O)$, and $MnSO_4 \cdot 1(H_2O)$ to be 0.847, 0.839, and 0.822, respectively, at 20 ℃. The manganese sulfate particles deliquesced in the relative humidity range 0.51-0.55, much lower than the deliquescence points for the above crystalline phases. Because the particle's mass at humidities slightly greater than the observed deliquescence humidity was the same whether the particle had come from a dry state or from a state at a high humidity, we can conclude that the manganese sulfate was completely dissolved after deliquescence occurred. Thus, the dry particles of manganese sulfate, with an overall stoichiometry of $MnSO_4 \cdot 2.8(H_2O)$, may have been glassy or contained only very small regions of crystalline order.

Other investigators have experienced difficulties in working with manganese sulfate and manganese chloride aqueous solutions. In an attempt to measure the solubility of manganese sulfate in water, Rard [23] explained the observed variability in solubility by suggesting that the solid phases obtained were a mixture of metastable hydrates of unknown composition, and that the solid phase underwent continuous changes with time. In the same investigation, Rard also found that the solid phase obtained upon crystallization of manganese chloride from solution did not correspond to a known crystalline form.

Ferric chloride solutions in suspended droplets at constant humidity gradually lost mass. Slow polymer or colloid formation is known to occur in aqueous solutions of inorganic ferric salts [33]. In the highly concentrated ferric chloride solutions within our suspended droplets, it is possible that polymeric or colloidal iron-hydroxide species were being formed, removing ferric ions from the solution and lowering the pH. As the pH is lowered, the evaporation of HCl from the droplet would be enhanced. A loss of HCl and the loss of water due to a decrease in dissolved ferric and chloride ions could have accounted for the observed decrease in the droplet mass with time.

The deliquescence of ferric chloride particles was unusual. The particles absorbed a small but measurable amount of water below a relative humidity of 0.77, and the amount of water absorbed increased as the humidity increased. The particle mass asymptotically approached a steady state at these low humidities. At relative humidities above 0.77, however, the particle appeared to truly deliquesce, and a relatively large amount of water was absorbed. The known

crystalline forms of the various ferric chloride hydrates all deliquesce at relative humidities far below 0.77. Thus, our deliquescence observations suggest that at least part of the iron in the particle was present in a form (*e.g.*, a polymeric ferric hydroxide species) more thermodynamically stable than any of the known, crystalline ferric chloride hydrates.

Solute Activity Coefficients

The chemical potential of the solute in an electrolyte solution, μ, may be expressed as

$$\mu = \mu^0 + \nu RT \ln(\gamma_{\pm} m_{\pm}) \tag{12}$$

where μ^0 is the chemical potential of the solute in a hypothetical, one molal solution which behaves ideally, ν is the number of ions formed when one molecule of the electrolyte dissolves, $\gamma_{\pm}$ is the mean molal solute activity coefficient, and $m_{\pm}$ is the mean solute molality. The mean solute molality is defined by

$$m_{\pm} = [m_+^{\nu_+} m_-^{\nu_-}]^{\frac{1}{\nu}} \tag{13}$$

where m_+ and m_- are the cation and anion molalities, and ν_+ and ν_- are the stoichiometric coefficients of the cation and anion.

Changes in the chemical potential of the solute are related to changes in the chemical potential of the solvent through the Gibbs-Duhem equation, integration of which leads to

$$\int_{m_1}^{m_2} \frac{\phi - 1}{m} dm + \phi(m_2) - \phi(m_1) = \ln \gamma_{\pm}(m_2) - \ln \gamma_{\pm}(m_1) \tag{14}$$

where ϕ, the osmotic coefficient, is given by

$$\phi = \frac{-1000.0 \ln a_w}{m w_w} \tag{15}$$

Using the polynomial expressions for the water activity as a function of molality given in Table 2, the integral in eq 14 was evaluated numerically. The lower limit of the integral was taken to be 1 molal for all salts, and the value of the mean molal solute activity coefficient at this reference concentration was taken from the literature. In this way, the solute activity coefficient for each salt was calculated as a function of molality, and the results of this calculation are shown in Figures 16–18.

The relative magnitudes and the concentration dependence of the solute activity coefficient for the different salts can be understood by considering the physical processes occurring in solution [27,34,35]. The solute activity coefficient is unity at infinite dilution and decreases as the concentration increases due to the electrostatic interaction between the ions in solution. For electrolytes whose ions associate in solution, the solute activity coefficient remains relatively low as the concentration increases. The effective ion concentration is lowered because the ions are associated. In contrast, some ions do not associate strongly in solution but are more completely surrounded by water; *i.e.*, they are extensively hydrated. As the solute increases in concentration, an increasing amount of solvent is bound by the ions, and the amount of free solvent decreases. Thus, the effective concentration of the solute – the number of ions for a given amount of free solvent – is increased. The solute activity coefficient for electrolytes whose ions are extensively solvated in solution thus goes through a minimum and then

increases with increasing concentration.

Ion association generally increases with increasing ionic charge, size, and polarizability. The sulfate ion, with its high charge and polarizability, is highly associative with most cations in aqueous solution. Thus, it is understandable that the three sulfate-containing electrolytes studied exhibited relatively low solute activity coefficients.

Ion hydration typically increases with increasing ionic charge and decreasing ionic size. Also, cations are believed to be hydrated more extensively than anions [35,36]. In comparing the relative magnitudes of the solute activity coefficients for the uni-univalent salts with a common anion shown in Figure 16, it is apparent that cation hydration increases in the order $NH_4^+ < K^+ < Na^+$. As expected, this ordering is the inverse of the relative ordering of the sizes of these cations. In light of their higher activity coefficients, the multiply-charged cations appear to be more extensively hydrated than the singly-charged cations. Of all the salts studied in this work, calcium chloride appears to be the most extensively hydrated. The relative ordering of cation hydration suggested by the solute activity coefficient results is consistent with other estimates of the hydration of ions in solution [37,38].

For the salts where hydration was important (*i.e.*, those that did not contain sulfate), the rate of increase of the solute activity coefficient with concentration diminishes at high concentration. This is demonstrated most strikingly by calcium chloride for which the solute activity coefficient actually begins to decrease at very high concentration. This behavior can be understood by

recognizing that, at high concentration, the water in the solution becomes increasingly scarce. In fact, at very high concentrations, there may not even be enough water in the solution to hydrate the ions to their normal level. Thus, it is understandable that the most extensively hydrated salt, calcium chloride, is affected most strongly by this phenomenon. It is possible that ion association begins to play a role in these highly concentrated solutions. In the limit of very high concentrations, ion association must eventually occur, for there is not enough water to keep the ions apart.

The behavior of the solute activity coefficients for sodium sulfate and manganese sulfate is interesting. The maximum in the $\gamma_{\pm}(m)$ curve for sodium sulfate occurs at a concentration for which there are seven water molecules per solute molecule. For manganese sulfate, the $\gamma_{\pm}(m)$ curve goes through a plateau at a concentration of 4–5 waters per solute molecule. It is intriguing that these stoichiometries correspond to stable crystalline phases for the two salts. Concentrated electrolyte solutions are very highly ordered, but it might be expected that the structure of the solution would be particularly ordered at special concentrations, equivalent to stoichiometries that are particularly favored. Thus, it appears that the thermodynamics of concentrated electrolyte solutions can be influenced by special configurational effects.

The above descriptions and rationalizations of the dependence of the solute activity coefficient on concentration are certainly not new, but our results demonstrate that these ideas remain valid as the concentration is increased to very high supersaturations. Also, the logical consequences of these ideas at

high concentrations, such as the effects due to the scarcity of water, have been demonstrated experimentally.

Because the solute activity coefficients calculated from experimental data were compared with the predictions of several electrolyte solution models (see below), it was desired to estimate the uncertainty in our calculated $\gamma_{\pm}(m)$ due to uncertainties in the measured water activities and balancing voltages. This was accomplished in the usual way from

$$d[\gamma_{\pm}(m)] = \left\{ \left[\frac{\partial \gamma_{\pm}(m)}{\partial a_w} d[a_w] \right]^2 + \left[\frac{\partial \gamma_{\pm}(m)}{\partial m} d[m] \right]^2 \right\}^{1/2} \qquad (16)$$

The partial derivatives in eq 16 were obtained by differentiating eq 14, and the resulting expression for the uncertainty contained an additional integral. The 0.01 uncertainty in water activity and weight fraction solute estimated above were used for the calculations. Detailed results for the uncertainty in the solute activity coefficient as a function of molality will not be presented here, but for all salts, the uncertainty in $\ln \gamma_{\pm}$ was in the range 0.10 to 0.35. Examples of these uncertainty calculations are shown in Figures 19–21, discussed below, in which the calculated solute activity coefficients are compared against the predictions of electrolyte solution models.

Electrolyte Solution Models

We have tested the applicability of three previously published electrolyte solution models to our results. Each of the models is based, in different ways, on the underlying physics of electrolyte solutions, but the models are semi-empirical

in that salt-specific model parameters are obtained by fitting the model to the experimental data.

Pitzer's Method

Pitzer and coworkers have developed an effective and widely used model for electrolyte solutions [39,40]. In this model, it is assumed that the behavior of electrolyte solutions can be described by a combination of terms characterizing the long-range and short-range forces between ions and molecules in solution. An improved Debye-Huckel-type electrostatic term is derived for the long-range interactions. For the short-range forces, a virial expansion in concentration is employed in which the virial coefficients are a function of ionic strength. The virial coefficients characterizing a particular single-electrolyte solution depend on three parameters, $\beta_{mx}^{(0)}$, $\beta_{mx}^{(1)}$, and C_{mx}^{ϕ}. With these parameters, the water activity and solute activity coefficient can be predicted. Equations giving the water activity and solute activity coefficient as a function of concentration are presented elsewhere [39,40] and will not be repeated here.

Pitzer and Mayorga [40] have applied this method to 227 pure aqueous electrolytes with one or both ions univalent and have shown that the available literature data can be correlated very well with their model. Pitzer and coworkers have also treated 2-2 electrolytes [41], electrolyte mixtures [42], and have estimated the effect of higher order electrostatic terms than are included in the basic version of their model [43].

Model predictions, obtained using the parameter values derived by Pitzer and Mayorga [40] from low concentration data, have been compared with our data. Pitzer's equations employ two additional parameters, α and b, for which values of $\alpha = 2.0$ and $b = 1.2$ have been recommended. These values were used in the calculations. As examples, the solute activity coefficients predicted by Pitzer's method and those calculated from our experimental results are given as a function of concentration for calcium chloride in Figure 19 and potassium bromide in Figure 20. The uncertainties in our calculated solute activity coefficients are also shown. With potassium bromide, the agreement is quite good, but with calcium chloride, there is a large discrepancy at high concentrations. These salts were chosen as representative of the range of success found when Pitzer's method was used to predict solution properties at higher concentrations than were used in the original fit of the parameters. The results of these calculations for all the salts studied are summarized in Table 3.

If a semi-empirical model of electrolyte solutions is globally valid, parameters obtained over one concentration range could be used to predict the solution's properties at concentrations outside this range. While satisfactory results were found with some of salts, it is clear from Table 3 and Figure 19 that for any particular salt, Pitzer's equation cannot be used with confidence at concentrations much greater than those for which its parameters were estimated. This should not be taken as a criticism of Pitzer's method, for there is no known method of accurately predicting the behavior of concentrated electrolyte solutions from their behavior at low concentrations.

Using a least-squares fit to water and solute activities over the full range of our data together with data from the literature, we have estimated new parameters to be used with Pitzer's equations for the salts studied in this work. The water activities for this fit were calculated from the $a_w(m)$ polynomial fits given in Table 2. Solute activity coefficients for the fit were calculated from the $a_w(m)$ polynomials at high concentrations and taken from the literature at low concentrations. The parameters estimated from this procedure and the success of Pitzer's method in representing the experimental data are presented in Table 4. Figures 19 and 20 also show examples of the agreement obtained with these re-estimated parameters for the concentration dependence of the solute activity coefficient.

The agreement obtained is within the experimental uncertainty for both the water activity and the solute activity coefficient for all salts over the entire concentration range except for ferric chloride and manganese sulfate at very high concentrations. Pitzer and coworkers have pointed out that a more sophisticated approach needs to be taken to obtain good fits for 2-2 electrolytes [41] and for electrolytes containing highly charged ions [43]. Thus, the relatively poor results for manganese sulfate and ferric chloride are not surprising. Pitzer has also stated that their basic approach is less likely to be successful for electrolytes that are extensively associated in solution. This may be the reason for the comparitively poor representation of the sodium sulfate data.

Local Composition Model for Electrolytes

Chen et al. [44] have developed a local composition model for electrolyte solutions. Like the Pitzer model, short-range and long-range interactions are treated separately and then combined for a complete description of the electrolyte solution. This model uses the modified Debye-Huckel-type electrostatic expression obtained by Pitzer [39] to characterize the effects of long-range forces. The short-range forces are treated using a variation of the local composition model of Renon and Prausnitz [45]. This model, developed for non-electrolyte liquid mixtures, postulates that the local composition around a molecule in solution is determined by the energetics of the interactions between the molecule and the other entities in solution. It is further assumed [46] that the distribution of species around a central molecule is governed by a Boltzmann-type expression. Chen and coworkers made two important modifications to the usual local composition formulation in order to account for the physics of electrolyte solutions. First, it was stipulated that ions of like charge cannot be immediate neighbors in the solution. Second, it was assumed that the immediate environment surrounding each solvent molecule is electrically neutral. Recently, these investigators have extended their local composition model to allow mixed-electrolyte solutions [47] and mixed-solvent electrolyte solutions [48] to be treated.

Chen et al. [44] derived expressions for the solute activity coefficient and solvent activity for a solution containing anions, cations, and a molecular solvent [49]. Their model requires the specification of two salt-specific parameters, τ_{m-ca} and τ_{ca-m}, that characterize the short-range interactions in the electrolyte

solution. The molecule-salt parameter, τ_{m-ca}, is the difference in the dimensionless interaction energies between the molecule-ion pair and the cation-anion pair. The salt-molecule parameter, τ_{ca-m}, is the difference in the dimensionless interaction energies between the ion-molecule pair and the molecule-molecule pair. With these two adjustable parameters, this model was very successful in its description of the thermodynamics of aqueous electrolytes over the range of available literature data [44].

As with Pitzer's method, we first compared our data with the predictions of this model using the parameters estimated in the original work. These parameters were obtained from data at relatively low concentrations. It was found that the given parameters worked satisfactorily for some of the salts but not for others. As an example of one case in which it did not, the results for sodium bromide are presented in Figure 21. In most cases, the deviation at high concentrations was greater than the experimental uncertainty. The results of this comparison are summarized in Table 5. In general, the agreement found with Chen's low-concentration parameters was slightly better than that obtained from Pitzer's equations and the corresponding low-concentration parameters.

We have estimated a new set of parameters for this local composition model by a least-squares fit to the solute activity coefficient data calculated in this work. The new parameters and relative success of the model in fitting the experimental data are summarized in Table 6. For all of the salts studied except ferric chloride, the predictions based on the new parameters agree with the our data to within the experimental uncertainty. As an example, the results with

the re-estimated parameters for sodium bromide are also shown in Figure 21.

Thus, as with Pitzer's method, it is not advisable to use this local composition model to predict thermodynamic properties at concentrations much higher than those used to determine the salt-specific parameters for the model. With re-estimated parameters, however, the model can successfully correlate the thermodynamic properties of many aqueous salt solutions over the entire range of the experimental data.

BET Model of Robinson and Stokes

Robinson and Stokes [36] postulated that ion-solvent forces are more important than ion-ion forces in determining the thermodynamic properties of highly concentrated electrolyte solutions. By treating the solvent as an adsorbate and the electrolyte as a substrate, they constructed a model of electrolyte solutions based on adsorption theory. Using the BET adsorption isotherm, Robinson and Stokes hypothesized that the dependence of the water activity on concentration should be consistent with

$$\frac{ma_w}{55.51(1-a_w)} = \frac{1}{cr} + \frac{c-1}{cr}a_w \tag{17}$$

in which r is the total number of water molecules in completed monomolecular hydration layers around both the anion and cation. For an enthalpy of adsorption E_{ads} and an enthalpy of liquefaction E_{liq}, the energy parameter c in eq 17 is given by

$$c = \exp\left(\frac{E_{ads} - E_{liq}}{RT}\right) \tag{18}$$

The suitability of this model for describing electrolyte solution behavior can be assessed by plotting the left-hand-side of eq 17 as a function of water activity. If a straight line results, then the model is applicable and the values of the parameters r and c can be calculated from the slope and intercept of the line.

This procedure was carried out for all the salts studied in this work in order to test the validity of the BET model of Robinson and Stokes. As an example, Figure 22 shows the $a_w(m)$ data for calcium chloride plotted in the form of eq 17. Calcium chloride was similar to the other salts in that a reasonably linear relationship was found only at high concentrations. In Table 7, the range of molality over which the fit was valid, the parameters r and c, and the standard deviation in the model's predictions from the experimental data are given for each salt. In most cases, the model was able to represent the experimental $a_w(m)$ data within the uncertainty in those data. However, unlike the models discussed earlier, only a limited range of concentrations could be fit for a given set of parameters.

Conclusions

By suspending single, charged droplets in an electrodynamic balance, the water activity as a function of concentration has been measured for aqueous solutions of eleven inorganic salts. The water activity and weight fraction of solute in the solutions were measured to within approximately 0.01.

One difficulty with the present experiments is that the composition of a

particle after drying cannot be predicted *a priori*. The dry-particle composition is needed to calculate the solute concentration at high humidities when the particle is a solution droplet. However, if some auxiliary water activity data are available from other measurements, the composition of the dry particle can be determined. For most of the salts studied, the dry particle was crystalline and its stoichiometry corresponded to a known crystalline form for the salt. Alternatively, this difficulty could be overcome by direct introduction of dry particles of known composition into the electrodynamic balance.

Water activity measurements can be made in a much shorter time with this technique than with the isopiestic method. The principal advantage of this experimental method, however, is that measurements can be made on solutions that have solute concentrations much higher than can be studied with conventional methods. For many of the salts, data were obtained at much higher concentrations than have previously been reported.

Solute activity coefficients were calculated as function of molality using our experimental water activity results and data taken from the literature. The concentration dependence and relative magnitudes of the solute activity coefficients for the different salts were consistent with commonly held views of ion hydration and ion association phenomena in solution. At very high concentrations, the effects of the scarcity of water in the solution on the solute activity coefficient were seen. Also, a special configurational effect seemed to be present for some of the salts when the solution stoichiometry was equivalent to a stable crystalline phase.

Three different semi-empirical electrolyte solution models were evaluated by comparison with our results. With each model, it was found that parameters estimated from low concentration data could not be reliably used to predict thermodynamic properties of the solution at high concentrations. However, with parameters estimated from the full range of the data, Pitzer's virial coefficient model and Chen's local composition model were able to represent the experimental observations over the full range of the data within the experimental uncertainty. With the BET-based model of Robinson and Stokes, only a limited range of data at high concentration could be represented.

Acknowledgements

This work was supported by the U.S. Environmental Protection Agency under grant number R-810857. The authors would like to thank Prof. Steven Arnold of the Polytechnic Institute of New York, for many useful discussions and for the particle injector used in this work.

References

[1] G. O. Rubel. *J. Aerosol Science*, 12:551, 1981.

[2] C.B. Richardson and C.A. Kurtz. *J. Amer. Chem. Soc.*, 106:6615, 1984.

[3] C.A. Kurtz and C.B. Richardson. *Chem. Phys. Letters*, 109:190, 1984.

[4] C.B. Richardson and J.F. Spann. *J. Aerosol Sci.*, 15:563, 1984.

[5] J.F. Spann and C.B. Richardson. *Atmospheric Environment*, 19:819, 1985.

[6] M.D. Cohen, R.C. Flagan, and J.H. Seinfeld. To be submitted to *J. Phys. Chem.*, 1986.

[7] M.D. Cohen, R.C. Flagan, and J.H. Seinfeld. To be submitted to *J. Phys. Chem.*, 1986.

[8] E.J. Davis. *Aerosol Science and Technology*, 2:121, 1983.

[9] G.O. Rubel. *J. Colloid and Interface Sci.*, 81:188, 1981.

[10] G.O. Rubel and J.W. Gentry. *J. Aerosol Science*, 15:661, 1984.

[11] E.J. Davis and R. Periasamy. *Langmuir*, 1:373, 1985.

[12] I.N. Tang and H.R. Munkelwitz. *J. Colloid and Interface Sci.*, 98:430, 1984.

[13] R.F. Wuerker, H. Shelton, and R.V. Langmuir. *J. Appl. Phys.*, 30:342, 1959.

[14] R.H. Frickel, R.E. Schaffer, and J.B. Stamatoff. Technical Report ARCSL-TR-77041, U.S. Army Armament Research and Development Command, Chemical Systems Laboratory, Aberdeen Proving Ground, Maryland, 1978.

[15] E.J. Davis. *Langmuir*, 1:379, 1985.

[16] M.A. Philip, F. Gelbard, and S. Arnold. *J. Colloid and Interface Sci.*, 91:507, 1983.

[17] Uni-Photon Systems, New York, N.Y.

[18] Corning Glass Works, Corning, N.Y.

[19] A. Van Hook. *Crystallization: Theory and Practice.* Reinhold, New York, 1961.

[20] C.N. Davies. *Proc. Phys. Soc.*, 57:259, 1945.

[21] M.D. Allen and O.G. Raabe. *Aerosol Sci. and Tech.*, 4:269, 1985.

[22] R.F. Platford. Experimental Methods: Isopiestic. In R.M. Pytkowicz, editor, *Activity Coefficients in Electrolyte Solutions*, Volume 1, pages 65–79, CRC Press, 1979.

[23] J.A. Rard. *J. Chem. Engr. Data*, 29:443, 1984.

[24] I.N. Tang, H.R. Munkelwitz, and J.G. Davis. *J. Aerosol Sci.*, 8:149, 1977.

[25] R.C. Weast, editor. *Handbook of Chemsitry and Physics.* CRC Press, 1975.

[26] E.W. Washburn, editor. *International Critical Tables.* McGraw Hill, New York, 1926.

[27] R.A. Robinson and R.H. Stokes. *Electrolyte Solutions.* Butterworths, London, 2nd edition, 1959.

[28] J.A. Rard and D.G. Miller. *J. Chem. Engr. Data*, 26:33, 1981.

[29] J.A. Rard, A. Habenschuss, and F. Spedding. *J. Chem. Engr. Data*, 22:180, 1977.

[30] W. Kangro and A. Groeneveld. *Z. Physik. Chem.*, 32:110, 1962.

[31] F.J. Millero. Effects of Pressure and Temperature on Activity Coefficients. In R.M. Pytkowicz, editor, *Activity Coefficients in Electrolyte Solutions*, Volume 2, pages 63–151, CRC Press, 1979.

[32] K.K. Mesingset and F. Gronvold. *J. Chem. Thermodynamics*, 18:159, 1986.

[33] C.M. Flynn. *Chem. Rev.*, 84:31, 1984.

[34] J. O'M. Bockris and A.K.N. Reddy. *Modern Electrochemistry.* Plenum Press, New York, 1970.

[35] B.E. Conway. *Ionic Hydration in Chemistry and Biophysics.* Elsevier Scientific Publishing Company, New York, 1981.

[36] R.H. Stokes and R.A. Robinson. *J. Amer. Chem. Soc.*, 70:1870, 1948.

[37] J. Burgess. *Metal Ions in Solution.* John Wiley and Sons, 1978.

[38] Y. Marcus. *Ion Solvation.* Wiley Interscience, New York, 1985.

[39] K.S. Pitzer. *J. Phys. Chem.*, 77:268, 1973.

[40] K.S. Pitzer and G. Mayorga. *J. Phys. Chem.*, 77:2300, 1973.

[41] K.S. Pitzer and G. Mayorga. *J. Solution Chem.*, 3:539, 1974.

[42] K.S. Pitzer and J.J. Kim. *J. Amer. Chem. Soc.*, 96:5701, 1974.

[43] K.S. Pitzer. *J. Solution Chem.*, 4:249, 1975.

[44] C.-C. Chen, H.I. Britt, J.F. Boston, and L.B. Evans. *A.I.Ch.E. Journal*, 28:588, 1982.

[45] H. Renon and J.M. Prausnitz. *A.I.Ch.E. Journal*, 14:135, 1968.

[46] G.M. Wilson. *J. Amer. Chem. Soc.*, 86:127, 1964.

[47] C.-C. Chen and L.B. Evans. *A.I.Ch.E. Journal*, 32:444, 1986.

[48] B. Mock, L.B. Evans, and C.-C. Chen. *A.I.Ch.E. Journal*, 32:1655, 1986.

[49] There appear to be typographical errors in eqs 23-25 of Ref [44]. In these equations, the following substitutions should be made: τ_{mc} should be changed to $\tau_{m,ca}$; τ_{ma} should be changed to $\tau_{m,ca}$; G_{mc} should be changed to $G_{mc,ac}$; and G_{ma} should be changed to $G_{ma,ca}$.

salt	number of water molecules per salt molecule in most stable crystal form at 20 ℃	number of water molecules per salt molecule measured for dry particle	deliq. relative humidity for most stable crystal form	deliq. relative humidity observed	solubility of most stable crystal phase at 20 ℃ (molal) (Ref [26])	range of molalities over which a_w was measured
NaCl	0	0	0.753 (a) 0.748 (c)	0.74–0.76	6.13	4.1–13.6
NaBr	2	0	0.58 (b)	0.445–0.455	8.77	5.5–20.1
KCl	0	0	0.843 (a) 0.851 (c)	0.830–0.860	4.61	4.4–12.7
KBr	0	0	0.817 (c) 0.84 (b)	0.799–0.820	5.42	4.9–14.6
NH_4Cl	0	0	0.795 (b) 0.777 (c)	0.765–0.773	6.97	3.7–23.2
Na_2SO_4	10	0	0.93 (b)	0.854–0.865	1.33	3.5–12.8
$(NH_4)_2SO_4$	0	0	0.810 (b)	0.806–0.813	5.73	3.8–17.9
$CaCl_2$	6	4	0.323 (b)	(d)	6.70	2.2–14.1
$MnCl_2$	4	2.3 ± 0.1	0.574 (c)	0.395–0.409	5.93	4.5–12.0
$MnSO_4$	5	2.8 ± 0.1	0.841 (c)	0.513–0.554	4.16	3.5–17.0
$FeCl_3$	6	6 ± 1	0.45 (c)	0.77 (e)	5.68	1.2–5.1

Table 1: Stoichiometric amount of water in crystal, deliquescence, and molality range of data; (a) Ref [24] at 25 ℃; (b) Ref [25] at 20 ℃; (c) deliquescence relative humidity estimated from International Critical Tables solubility data at 20 ℃ (Ref [26]) and $a_w(m)$ polynomial fit given in Table 2; (d) deliquescence not observed; (e) partial deliquescence at relative humidities lower than 0.77, see text.

salt	a_0	a_1	a_2	a_3	a_4	a_5	a_6
NaCl	1.0084	-4.939(-2)	8.888(-3)	-2.157(-3)	1.617(-4)	-1.990(-6)	-1.142(-7)
NaBr	0.9996	-3.116(-2)	-2.112(-3)	-9.347(-5)	2.000(-5)	-5.472(-7)	0
KCl	0.9975	-2.173(-2)	-1.053(-2)	4.253(-3)	-7.780(-4)	6.203(-5)	-1.764(-6)
KBr	1.0008	-3.531(-2)	2.490(-3)	-6.729(-4)	5.318(-5)	-8.040(-7)	-2.866(-8)
NH_4Cl	0.9968	-2.611(-2)	-1.599(-3)	1.355(-4)	-2.317(-6)	-1.113(-8)	0
Na_2SO_4	1.0052	-6.484(-2)	3.519(-2)	-1.319(-2)	1.925(-3)	-1.224(-4)	2.870(-6)
$(NH_4)_2SO_4$ (a)	0.9968	-2.969(-2)	1.753(-5)	-3.253(-4)	3.571(-5)	-9.787(-7)	0
$(NH_4)_2SO_4$ (b)	1.0151	-4.478(-2)	1.041(-3)	-8.258(-6)	0	0	0
$CaCl_2$	0.9947	-6.062(-3)	-4.122(-2)	6.091(-3)	-3.433(-4)	7.009(-6)	0
$MnCl_2$	0.9989	-3.639(-2)	-2.049(-2)	4.286(-3)	-4.137(-4)	1.960(-5)	-3.417(-7)
$MnSO_4$	0.9817	3.294(-2)	-2.773(-2)	3.483(-3)	-1.773(-4)	3.229(-6)	0
$FeCl_3$	1.0930	-1.782(-1)	3.041(-2)	-6.872(-3)	8.728(-4)	-5.089(-5)	1.096(-6)

Table 2: Coefficients of $a_w(m)$ polynomial fit, $a_w = a_0 + a_1 m + a_2 m^2 + \ldots$; see Table 3 for range of validity, standard error in fit's representation of data, and sources of literature data; (a) fit of data from this work and from Ref [27]; (b) fit of data in "a" and data from Ref [4].

salt	maximum molality for which fit is valid	σ_{a_w}	range of literature data used in fit	source of literature data used in fit [Ref #]
NaCl	13.6	.0053	0.5–6.0	[27]
NaBr	20.1	.0055	0.1–8.75	[26,27]
KCl	12.7	.0041	0.1–4.8	[27]
KBr	14.6	.0025	0.1–5.5	[27]
NH_4Cl	23.2	.0043	0.1–6.0	[27]
Na_2SO_4	12.8	.0026	0.1–4.0	[27,28]
$(NH_4)_2SO_4$ (a)	17.9	.0027	0.1–5.5	[27]
$(NH_4)_2SO_4$ (b)	36.2	.0145	0.1–36.2	[4,27]
$CaCl_2$	14.1	.0066	0.005–9.0	[29]
$MnCl_2$	12.0	.0032	0.1–7.699	[23,27]
$MnSO_4$	17.0	.0115	0.1–4.966	[23,27]
$FeCl_3$	15.0	.0085	1.0-15.0	[30]

Table 3: Molality range for which coefficients given in Table 2 are valid, standard error in fit of $a_w(m)$ data over this range, and sources of literature data used in polynomial fits; (a) fit of data from this work and from Ref [27]; (b) fit of data in "a" and data from Ref [4].

salt	$\beta_{mx}^{(0)}$ (a)	$\beta_{mx}^{(1)}$ (a)	C_{mx}^{ϕ} (a)	maximum molality used in original estimation of parameters (a)	molality range for model evaluation	σ_{a_w} over this molality range
NaCl	0.0765	0.2664	0.00127	6.0	0.1–13.6	0.025
NaBr	0.0973	0.2791	0.00116	4.0	0.1–20.1	0.063
KCl	0.04835	0.2122	-0.00084	4.8	0.1–12.7	0.013
KBr	0.0569	0.2212	-0.00180	5.5	0.1–14.6	0.010
NH_4Cl	0.0522	0.1918	-0.00301	6.0	0.1–23.2	0.097
Na_2SO_4	0.01958	1.1130	0.00497	4.0	0.1–12.8	0.143
$(NH_4)_2SO_4$	0.04888	0.6585	-0.00116	5.5	0.1–17.9	0.022
$CaCl_2$	0.31590	1.6140	-0.00339	2.5	0.1–14.1	0.065
$MnCl_2$	0.32723	1.5503	-0.02050	2.5	0.1–12.0	0.212

Table 4: Evaluation of Pitzer's model using parameters estimated from low-concentration data; (a) from Ref [40].

salt	$\beta_{mx}^{(0)}$	$\beta_{mx}^{(1)}$	C_{mx}^{ϕ}	molality range used for parameter estimation	σ_{a_w}	$\sigma_{\ln \gamma_{\pm}}$
NaCl	0.10820	0.03127	-0.002469	0.1–13.6	0.010	0.052
NaBr	0.13523	0.02917	-0.003478	0.1–20.1	0.006	0.034
KCl	0.06577	0.09351	-0.002160	0.1–12.7	0.009	0.040
KBr	0.06292	0.16046	-0.001981	0.1–14.6	0.005	0.021
NH_4Cl	0.04568	0.20431	-0.001731	0.1–23.2	0.006	0.019
Na_2SO_4	0.08610	0.13037	-0.003104	0.1–12.8	0.021	0.091
$(NH_4)_2SO_4$	0.04763	0.44459	-0.001311	0.1–17.9	0.006	0.020
$CaCl_2$	0.41328	0.53043	-0.014250	0.1–14.1	0.008	0.083
$MnCl_2$	0.25811	2.31108	-0.010540	0.1–12.0	0.014	0.070
$MnSO_4$	0.33089	3.14630	-0.014731	0.1–17.0	0.029	0.129
$FeCl_3$	0.31583	10.4224	-0.010078	0.1–15.0	0.048	0.214

Table 5: Re-estimated parameters and evaluation of Pitzer's method.

salt	τ_{m-ca} (a)	τ_{ca-m} (a)	maximum molality used in original estimation of parameters (a)	molality range"1" for model evaluation	$\sigma_{\ln\gamma_\pm}$ over molality range "1"	molality range"2" for model evaluation	$\sigma_{\ln\gamma_\pm}$ over molality range "2"
NaCl	8.885	-4.549	6.0	1.0–13.6	0.29	7.0–13.6	0.43
NaBr	8.793	-4.562	4.0	1.0–20.1	0.68	5.0–20.1	0.79
KCl	8.064	-4.107	4.5	1.0–12.7	0.17	5.0–12.7	0.24
KBr	8.093	-4.143	5.5	1.0–14.6	0.15	6.0–14.6	0.19
NH_4Cl	7.842	-4.005	6.0	1.0–23.2	0.04	7.0–23.2	0.05
Na_2SO_4	8.389	-4.539	4.0	1.0–12.8	0.46	5.0–12.8	0.56
$(NH_4)_2SO_4$	8.623	-4.602	4.0	1.0–17.9	0.22	5.0–17.9	0.25
$CaCl_2$	11.396	-6.218	6.0	1.0–14.1	0.78	6.5–14.1	1.11
$MnCl_2$	9.554	-5.508	6.0	1.0–12.0	0.24	7.0–12.0	0.39
$MnSO_4$	11.294	-6.805	4.0	1.0–17.0	0.22	5.0–17.0	0.24

Table 6: Comparison of experimental results with predictions of local composition model of Chen et al. (Ref [44]) using parameters estimated from low-concentration data; (a) from Ref [44].

salt	τ_{m-ca}	τ_{ca-m}	molality range for fit	$\sigma_{\ln \gamma_\pm}$
NaCl	9.935	-4.929	0.1–13.6	0.07
NaBr	10.432	-5.152	0.1–20.1	0.11
KCl	8.803	-4.413	0.1–12.7	0.04
KBr	8.730	-4.393	0.1–14.6	0.03
NH_4Cl	7.962	-4.053	0.2–23.2	0.03
Na_2SO_4	9.480	-5.021	0.1–12.8	0.09
$(NH_4)_2SO_4$	9.147	-4.826	0.1–17.9	0.03
$CaCl_2$	12.500	-6.551	0.1–14.1	0.30
$MnCl_2$	10.282	-5.741	0.1–12.0	0.10
$MnSO_4$	11.188	-6.794	0.2–17.0	0.12
$FeCl_3$	11.596	-6.378	0.5–16.0	0.33

Table 7: Comparison of experimental results with predictions of local composition model of Chen et al. (Ref [44]) using re-estimated parameters.

salt	molality range for which model is approx. valid	r	c	σ_{a_w}
NaCl	8.0–13.6	2.72	7.51 (0)	0.005
NaBr	6.5–20.1	2.65	1.92 (1)	0.017
KCl	10.0–12.7	4.76	4.14 (-1)	0.001
KBr	8.5–14.6	2.23	3.86 (0)	0.002
NH_4Cl	13.5–23.2	3.17	7.15 (-1)	0.001
Na_2SO_4	7.5–12.8	312.	5.43 (-3)	0.004
$(NH_4)_2SO_4$	10.5–17.9	3.08	1.23 (0)	0.003
$CaCl_2$	3.0–14.1	5.32	3.08 (1)	0.034
$MnCl_2$	2.5–12.0	4.02	1.69 (1)	0.013
$MnSO_4$	5.2–17.0	2.92	2.69 (0)	0.011
$FeCl_3$	2.5–15.0	5.73	1.24 (1)	0.012

Table 8: Parameters and range of validity of BET model at high concentrations.

Figure Captions

Figure 1: Schematic of apparatus.

Figure 2: Electrodynamic balance electrical circuitry and cross-sectional schematic of electrode assembly; R = 181 kΩ , C = 0.47 μF, z_0 = 0.5 cm.

Figure 3: dc balancing voltage vs. time during a typical experiment; measurements for an ammonium chloride particle; (a), dry state; (b), deliquescence; (c), crystallization; each steady state in this figure corresponds to a datum point in Figure 9.

Figure 4: Velocity (meters/sec) vs. V_{dc} for a dry ammonium sulfate particle.

Figure 5: Weight fraction solute vs. water activity for sodium chloride; ○, particle 1, expt 1; □, particle 1, expt 2; △, particle 2; solid line, data from Robinson and Stokes (Ref [27]) at 25 ℃; filled points indicate measurements beginning with a dry particle.

Figure 6: Weight fraction solute vs. water activity for sodium bromide; □, expt 1; △, expt 2; solid line, fit to data from Int'l Crit. Tables (Ref [26]) at 20 ℃ and data from Robinson and Stokes (Ref [27]) at 25 ℃; filled points indicate measurements beginning with a dry particle.

Figure 7: Weight fraction solute vs. water activity for potassium chloride; □, expt 1; △, expt 2; solid line, data from Robinson and Stokes (Ref [27]) at 25 ℃; filled points indicate measurements beginning with a dry particle.

Figure 8: Weight fraction solute vs. water activity for potassium bromide; △, expt 1; □, expt 2; solid line, data from Robinson and Stokes (Ref [27]) at 25 ℃; filled points indicate measurements beginning with a dry particle.

Figure 9: Weight fraction solute vs. water activity for ammonium chloride; □, expt 1; △, expt 2; ○, expt 3; solid line, data from Robinson and Stokes (Ref [27]) at 25 ℃; filled points indicate measurements beginning with a dry particle.

Figure 10: Weight fraction solute vs. water activity for sodium sulfate; □, particle 1; △, particle 2; solid line, fit to data from Rard et al. (Ref [28]) at 25 ℃ and data from Robinson and Stokes (Ref [27]) at 25 ℃; filled points indicate measurements beginning with a dry particle.

Figure 11: Weight fraction solute vs. water activity for ammonium sulfate; □, particle 1; △, particle 2; ○, data from Richardson and Spann (Ref [4]) at 24 ℃; solid line, data from Robinson and Stokes (Ref [27]) at 25 ℃; filled points indicate measurements beginning with a dry particle.

Figure 12: Weight fraction solute vs. water activity for calcium chloride; ○, particle 1; △, particle 2, expt 1; □, particle 2, expt 2; solid line, data from Rard et al. (Ref [29]) at 25 ℃ ; horizontal line corresponds to the stoichiometry of $CaCl_2 \cdot 4(H_2O)$; filled points indicate measurements beginning with a dry particle.

Figure 13: Weight fraction solute vs. water activity for manganese chloride; □, expt 1; △, expt 2; ○, expt 3; solid line, fit to data from Rard (Ref [23]) at 25 ℃ and data from Robinson and Stokes (Ref [27]) at 25 ℃; horizontal line corresponds to the stoichiometry of $MnCl_2 \cdot 2(H_2O)$; filled points indicate measurements beginning with a dry particle.

Figure 14: Weight fraction solute vs. water activity for manganese sulfate; □, particle 1, expt 1; △, particle 1, expt 2; ○, particle 2, expt 1; ◇, particle 2, expt 2; solid line, data from Rard (Ref [23]) at 25 ℃; filled points indicate measurements beginning with a dry particle.

Figure 15: Weight fraction solute vs. water activity for ferric chloride; □, expt 1; △, expt 2; ◇, expt 2, partial deliquesence ; ⊕, expts 1 and 2, after droplets had aged for several hours; ○, data from Kangro et al (Ref [30]) at 25 ℃; horizontal line corresponds to the stoichiometry of $FeCl_3 \cdot 6(H_2O)$; filled points indicate measurements beginning with a dry particle.

Figure 16: Solute activity coefficient vs. solute molality for 1:1 electrolytes. The curves are calculated from integration of Gibbs-Duhem equation using $a_w(m)$ polynomials in Table 2: (a), NaBr; (b), NaCl; (c), KBr; (d), KCl; (e), NH_4Cl. The data points are from Ref [27] at 25 ℃: ◇, NaBr; □, NaCl; +, KBr; ○, KCl; △, NH_4Cl.

Figure 17: Solute activity coefficient vs. solute molality. The curves are calculated from integration of Gibbs-Duhem equation using $a_w(m)$ polynomials in Table 2: (a), $CaCl_2$; (b), $FeCl_3$; (c), $MnCl_2$. The data points are from the following sources: □, $CaCl_2$ data from Ref [29] at 25 ℃; ○, $FeCl_3$ data from Ref [30] at 25 ℃; △, $MnCl_2$ data from Ref [23] at 25 ℃.

Figure 18: Solute activity coefficient vs. solute molality for electrolytes containing sulfate ion. The curves are calculated from integration of Gibbs-Duhem equation using $a_w(m)$ polynomials in Table 2: (a), Na_2SO_4; (b), $(NH_4)_2SO_4$, calculated from combined $a_w(m)$ fit to data from this work and Refs [27,4]; (c), $(NH_4)_2SO_4$, calculated from combined $a_w(m)$ fit to data from this work and Ref [27]; (d), $MnSO_4$. The data points are from the following sources: □, Na_2SO_4 data from Ref [28] at 25 ℃; ○, $(NH_4)_2SO_4$ data from Ref [27] at 25 ℃; △, $MnSO_4$ data from Ref [23] at 25 ℃.

Figure 19: Solute activity coefficient vs. solute molality for potassium bromide; solid line, calc. of $\gamma_\pm$(m) from a_w(m) polynomial in Table 2; dotted lines, upper and lower bounds for $\gamma_\pm$(m) based on calculated uncertainty; △, data from Robinson and Stokes at 25 ℃ (Ref [27]); □, calculated using Pitzer's method with parameters given in Ref [40] (Table 3); ○, calculated using Pitzer's method with re-estimated parameters (Table 4).

Figure 20: Solute activity coefficient vs. solute molality for calcium chloride; solid line, calc. of $\gamma_\pm$(m) from a_w(m) polynomial in Table 2; dotted lines, upper and lower bounds for $\gamma_\pm$(m) based on calculated uncertainty; △, data from Rard et al (Ref [29]) at 25 ℃; □, calculated using Pitzer's method with parameters given in Ref [40] (Table 3); ○, calculated using Pitzer's method with re-estimated parameters (Table 4).

Figure 21: Solute activity coefficient vs. solute molality for sodium bromide; solid line, calc. of $\gamma_\pm$(m) from a_w(m) polynomial in Table 2; dotted lines, upper and lower bounds for $\gamma_\pm$(m) based on calculated uncertainty; △, data from Robinson and Stokes (Ref [27]) at 25 ℃; □, calculated using Chen's model with parameters given in Ref [44] (Table 5); ○, calculated using Chen's model with re-estimated parameters (Table 6).

Figure 22: Evaluation of BET model for calcium chloride; left-hand-side of eq 17 vs. a_w; □, calculated from a_w(m) polynomial in Table 2; solid line, best-fit line for $3.0 \leq$ molality ≤ 14.0.

Figure 1

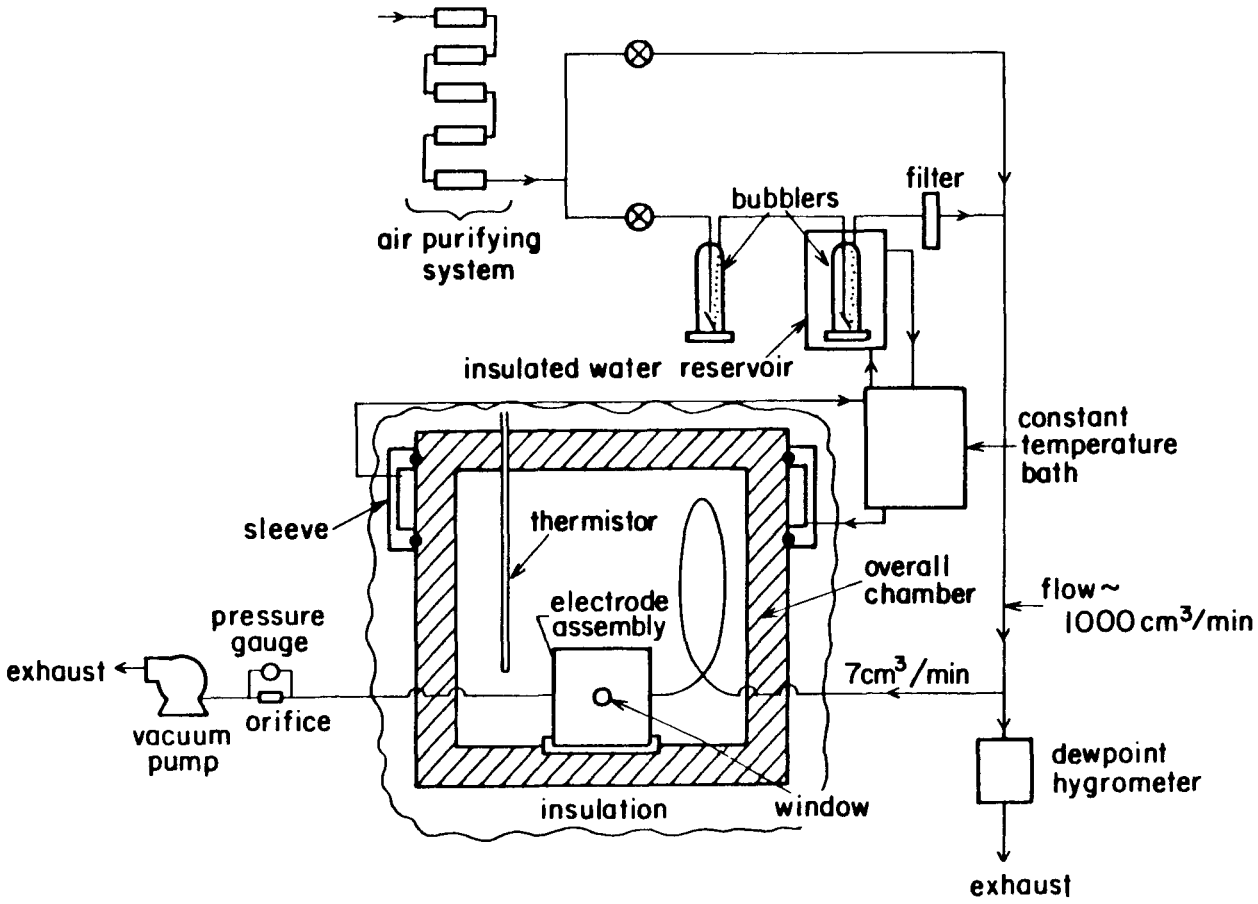
air purifying system
bubblers
filter
insulated water reservoir
constant temperature bath
sleeve
thermistor
overall chamber
flow ~ 1000 cm³/min
electrode assembly
pressure gauge
exhaust
vacuum pump
orifice
7cm³/min
dewpoint hygrometer
insulation
window
exhaust

Figure 2

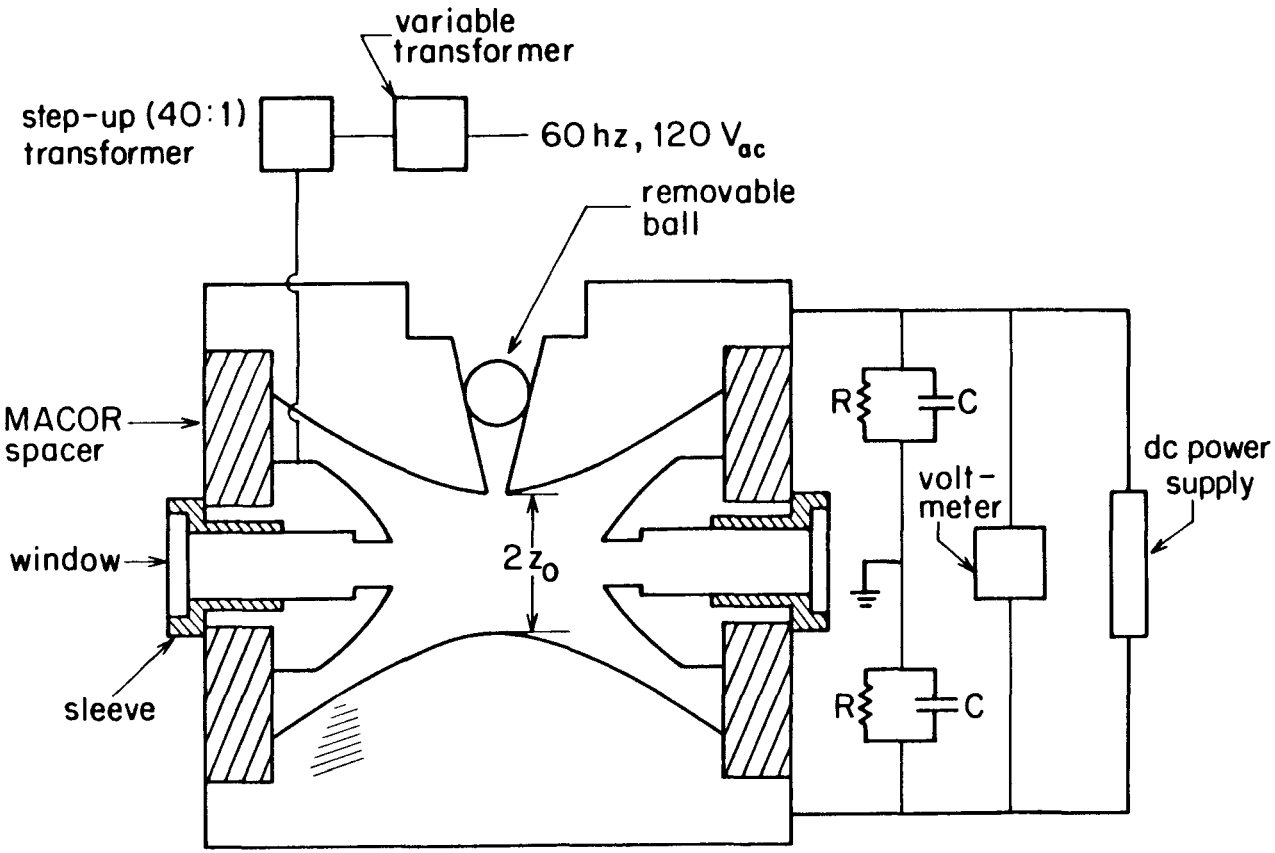
variable
transformer
step-up (40:1)
transformer
60 hz, 120 V_{ac}
removable
ball
MACOR
spacer
window
sleeve
$2z_o$
R
C
R
C
volt-
meter
dc power
supply

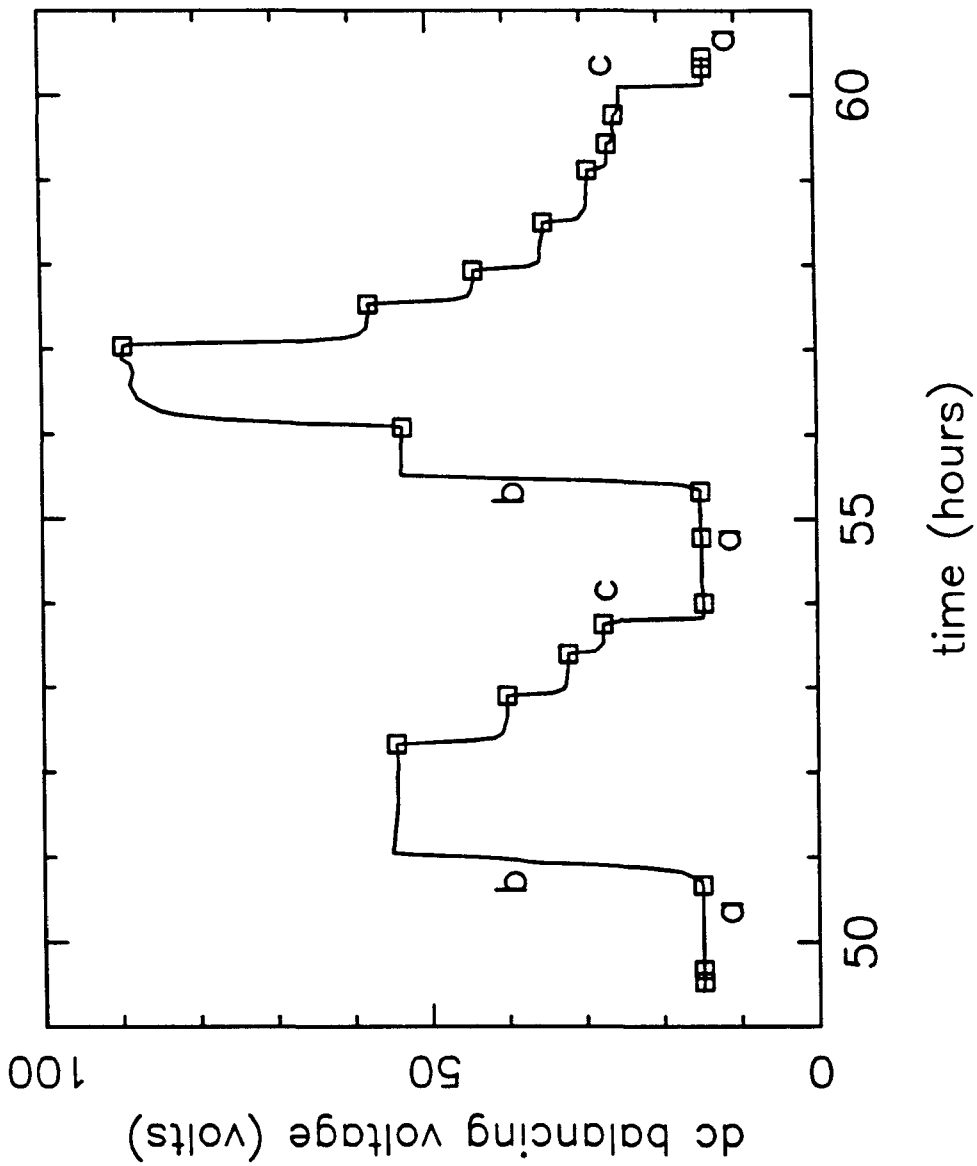
dc balancing voltage (volts)
0
50
100
time (hours)
50
55
60
a
b
c
d
a
b
c
d

Figure 3

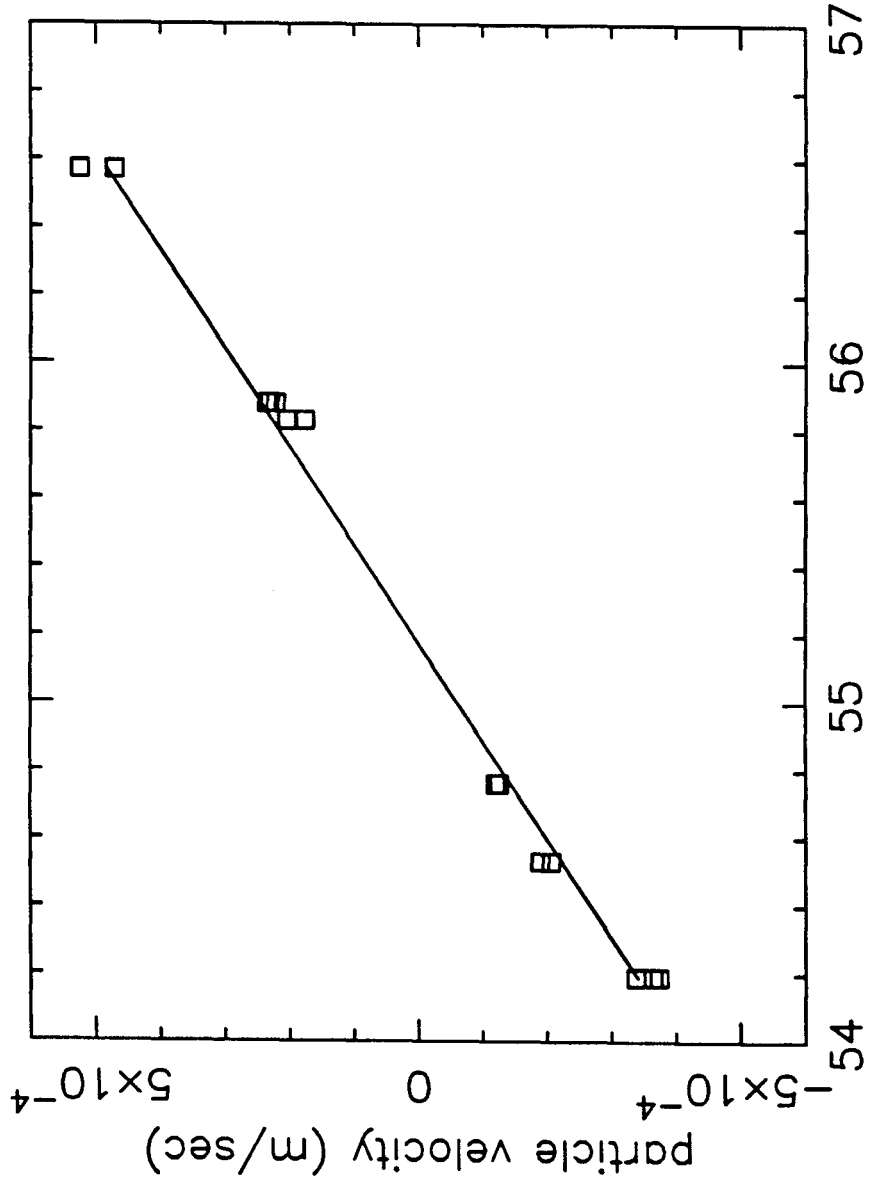
particle velocity (m/sec)
−5×10⁻⁴
0
5×10⁻⁴
54
55
56
57
dc voltage (volts)

Figure 4

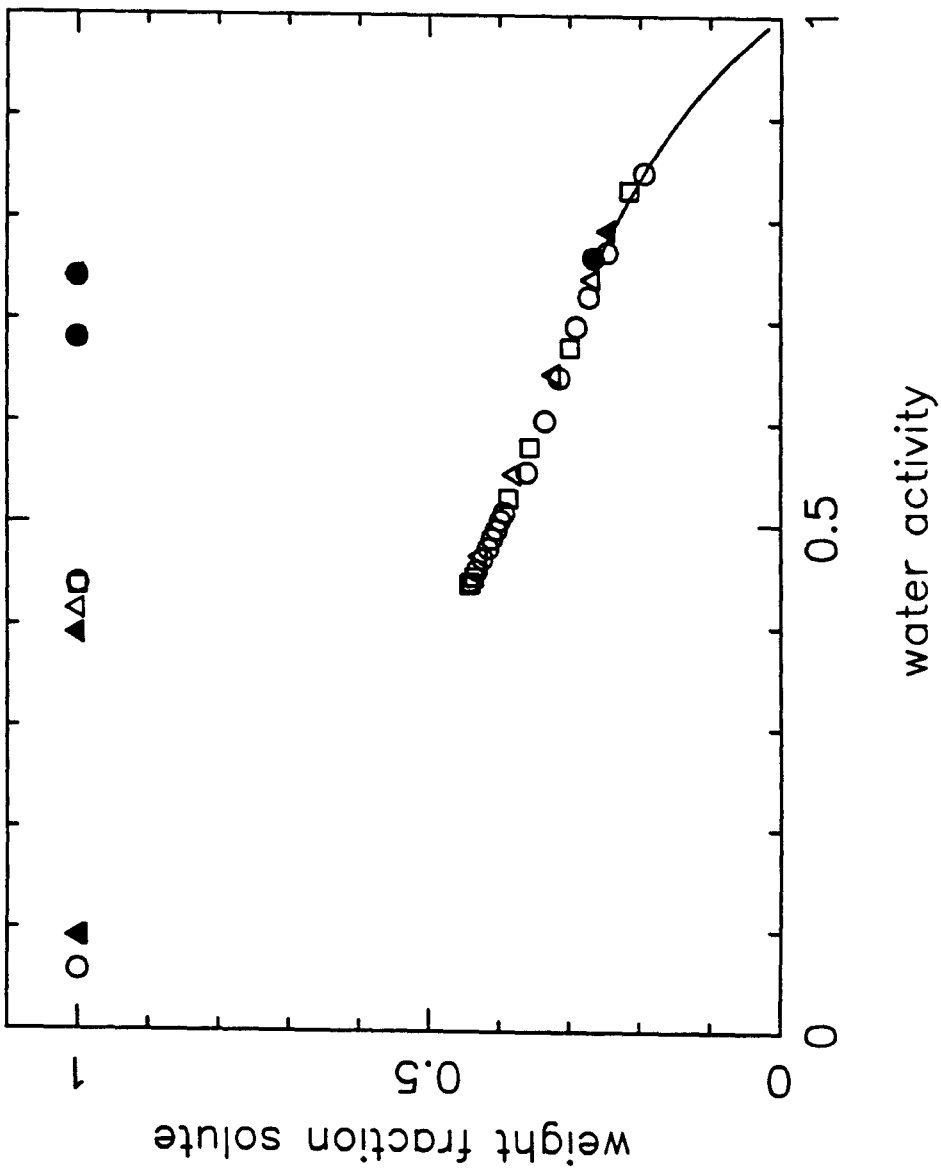

Figure 5

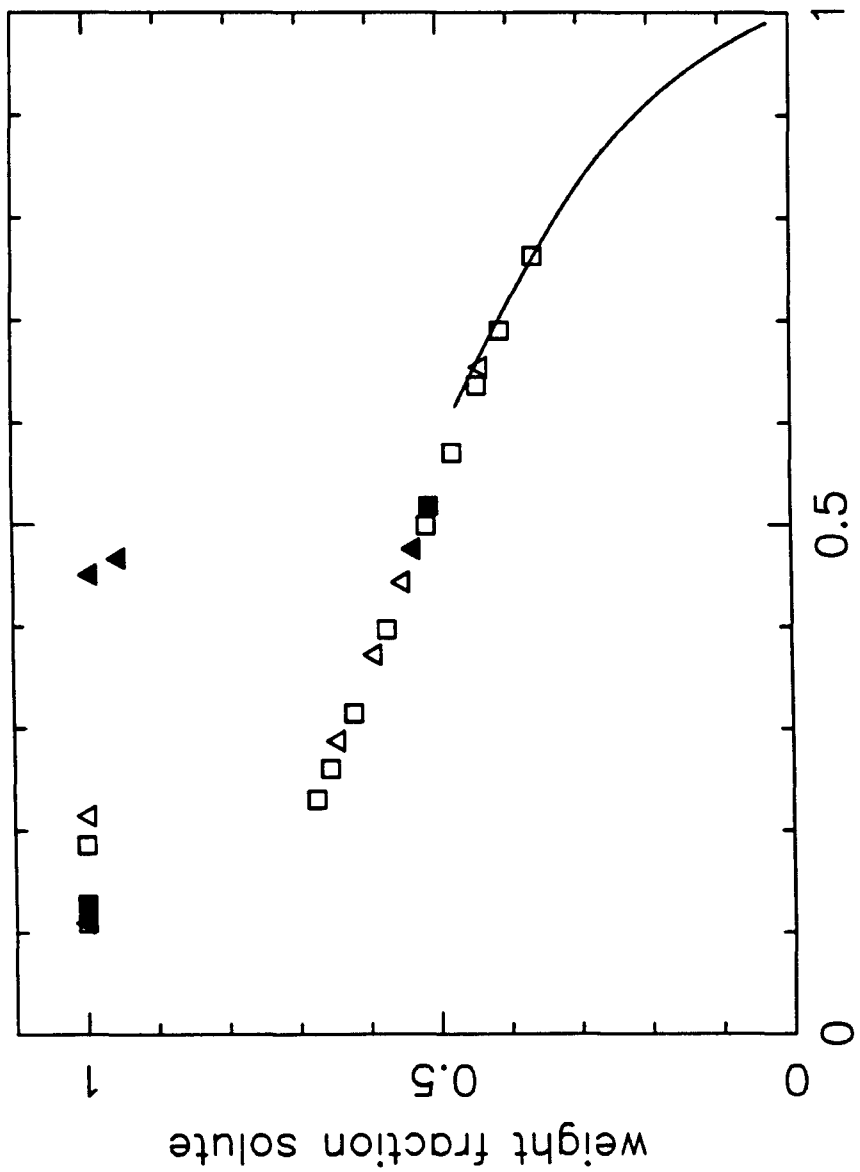

Figure 6

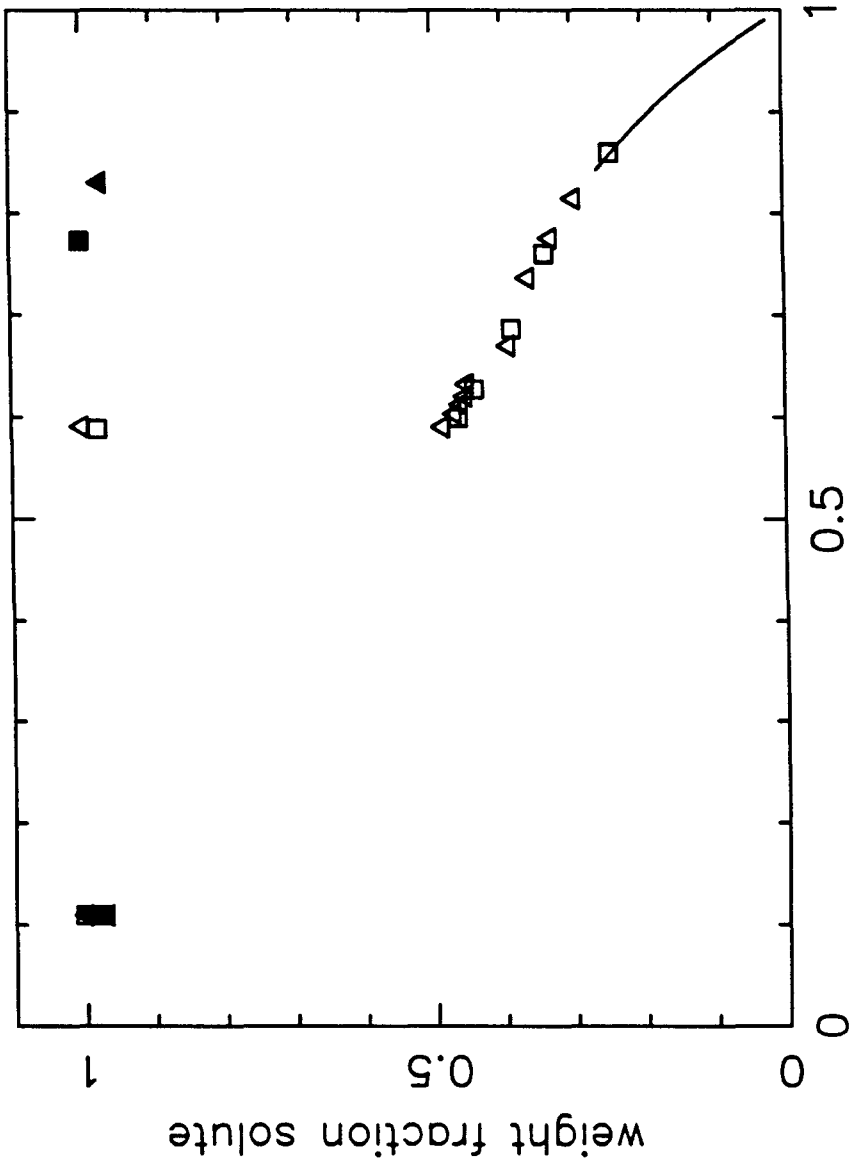

Figure 7

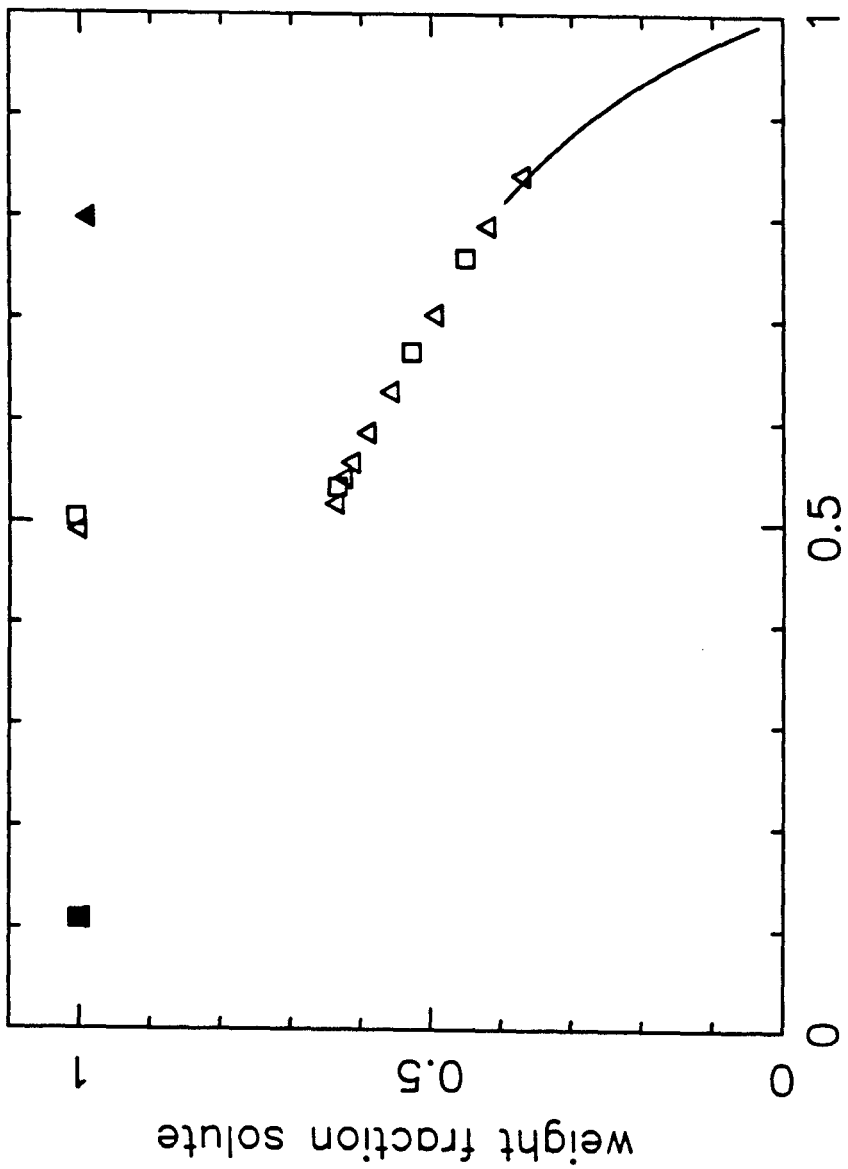

Figure 8

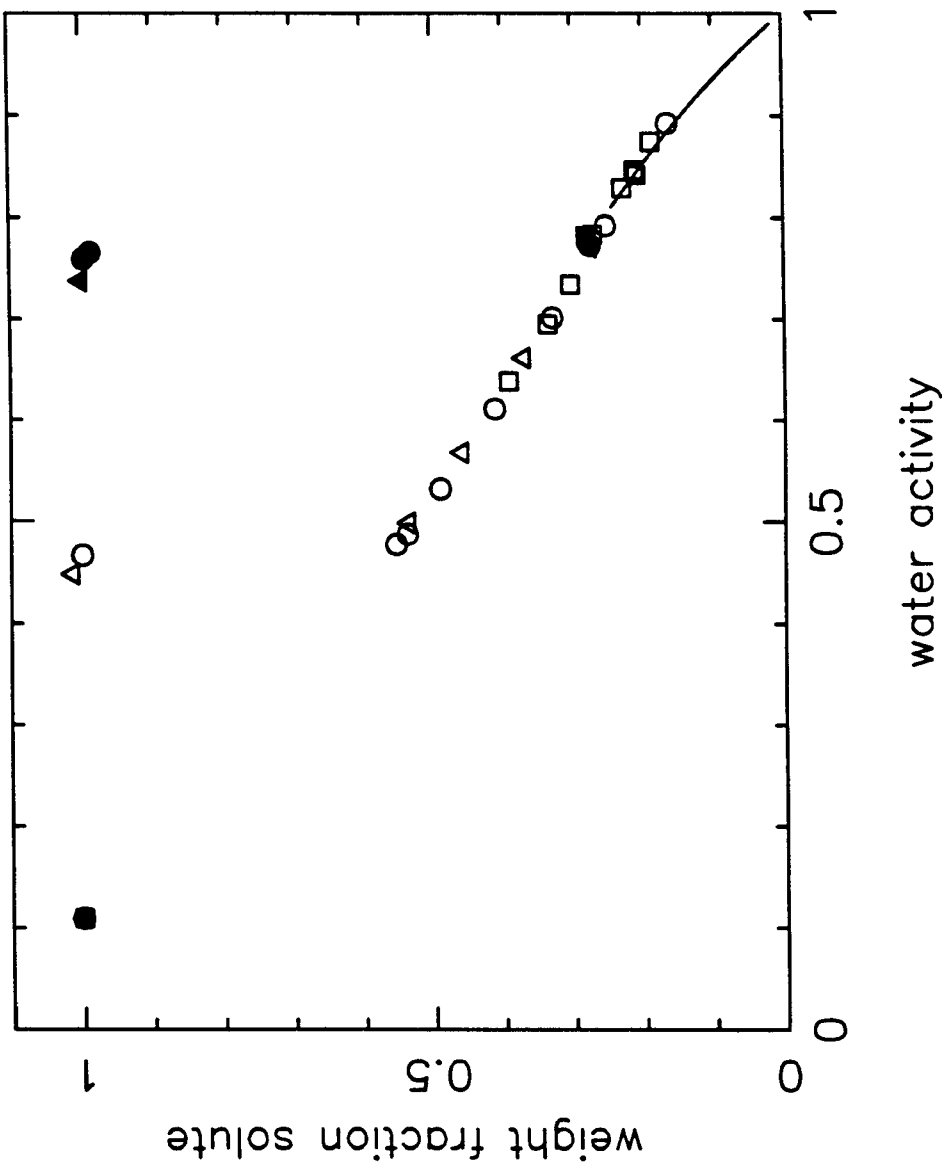

Figure 9

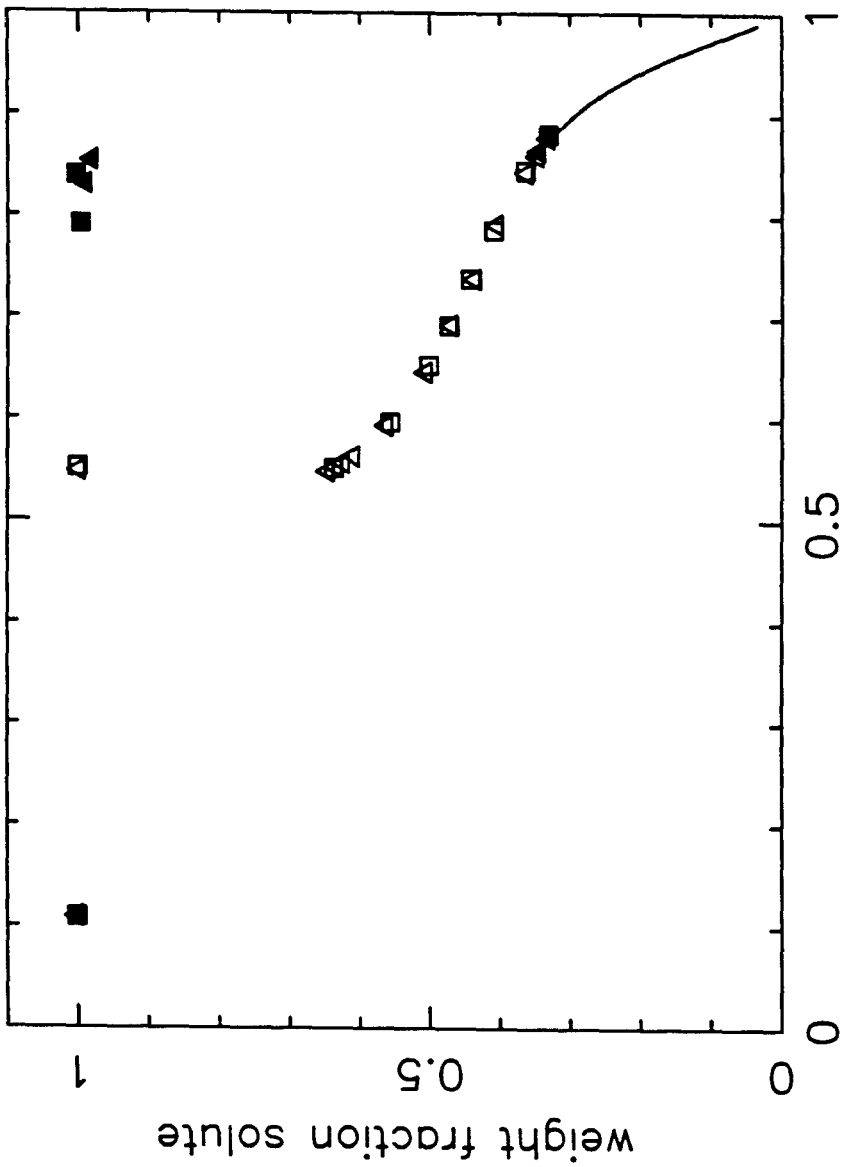

Figure 10

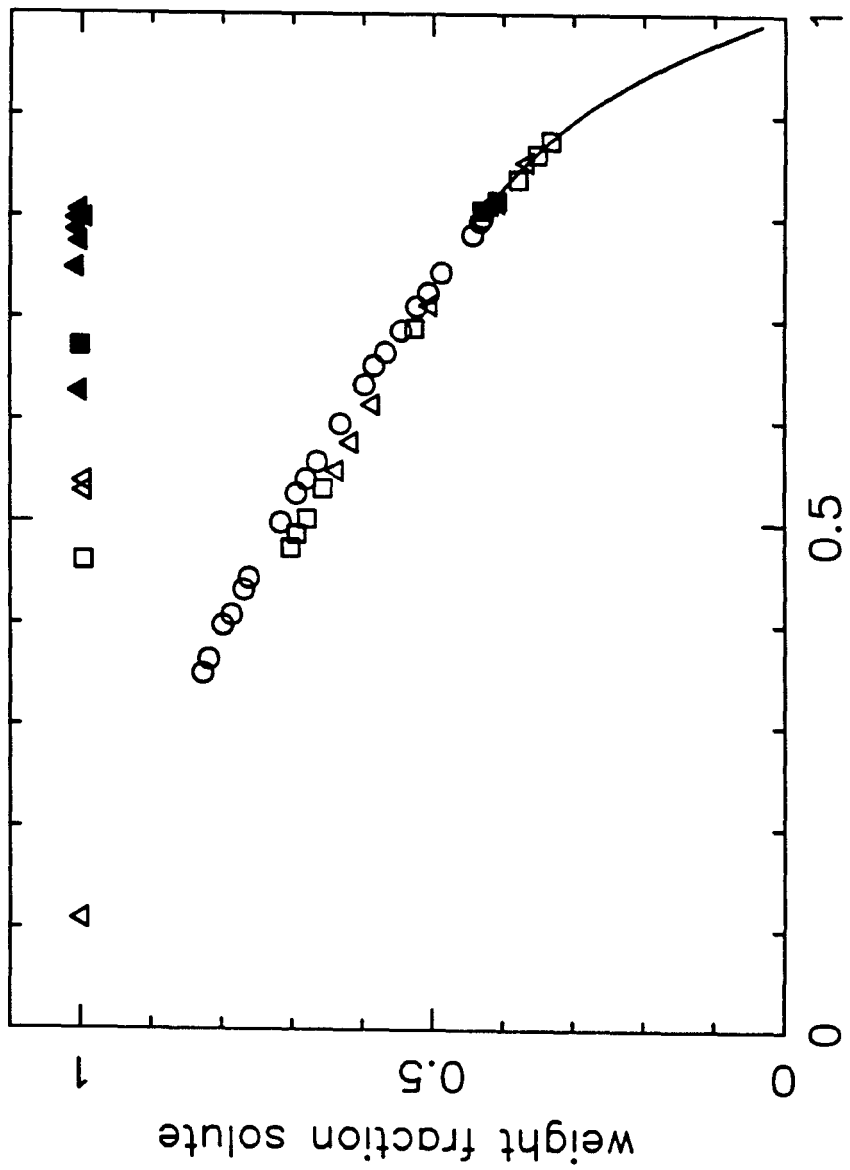

Figure 11

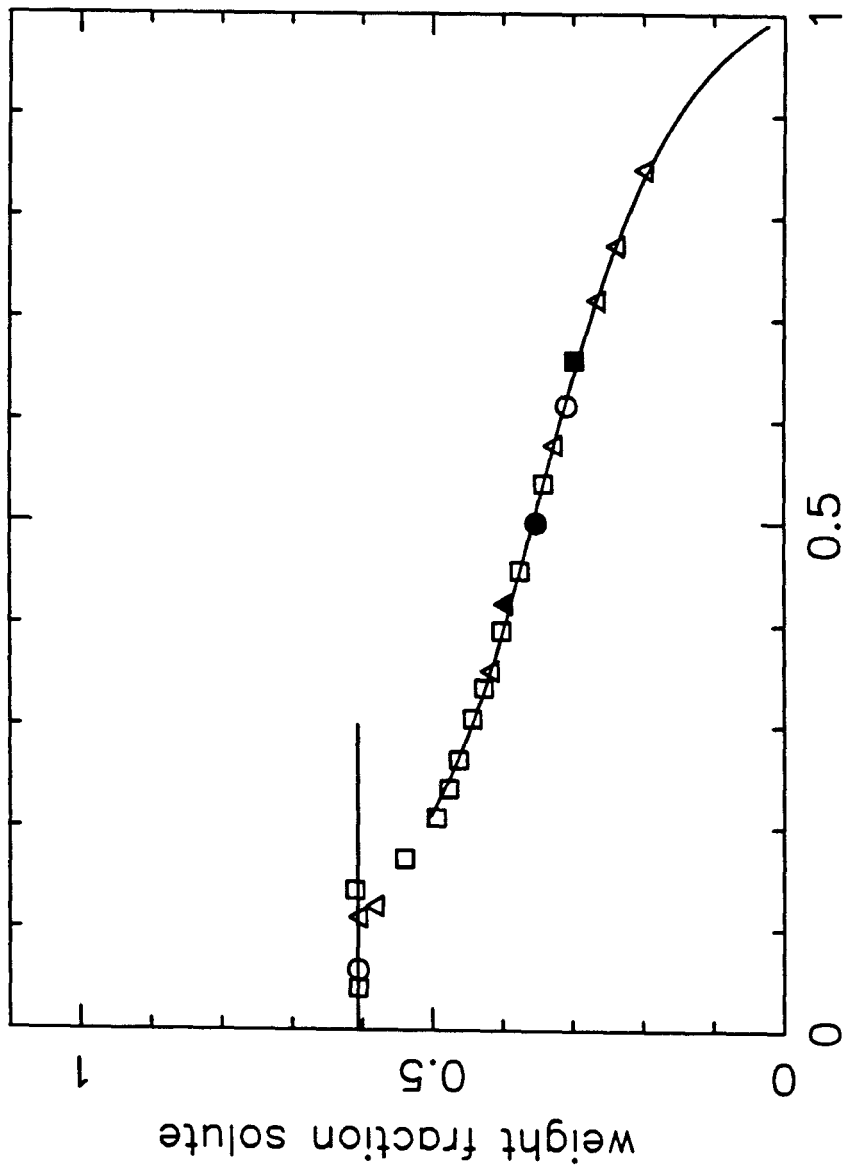

Figure 12

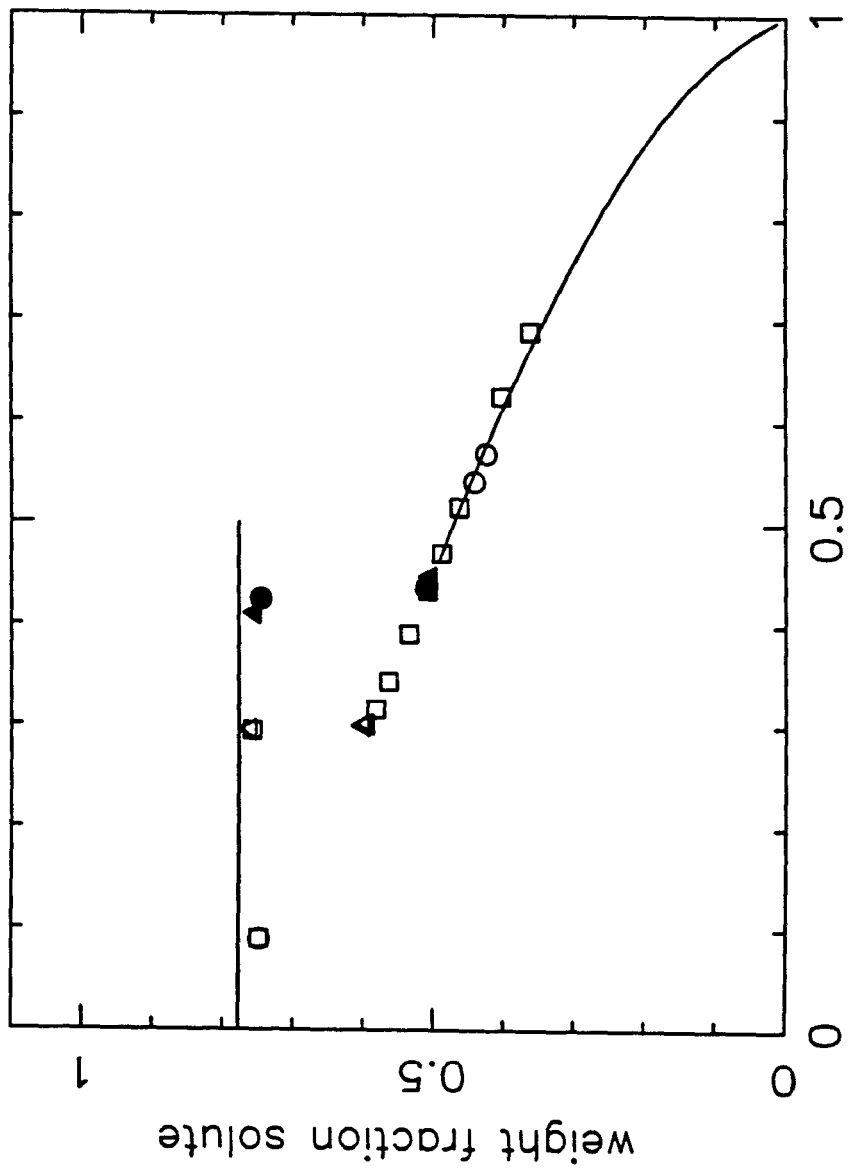

Figure 13

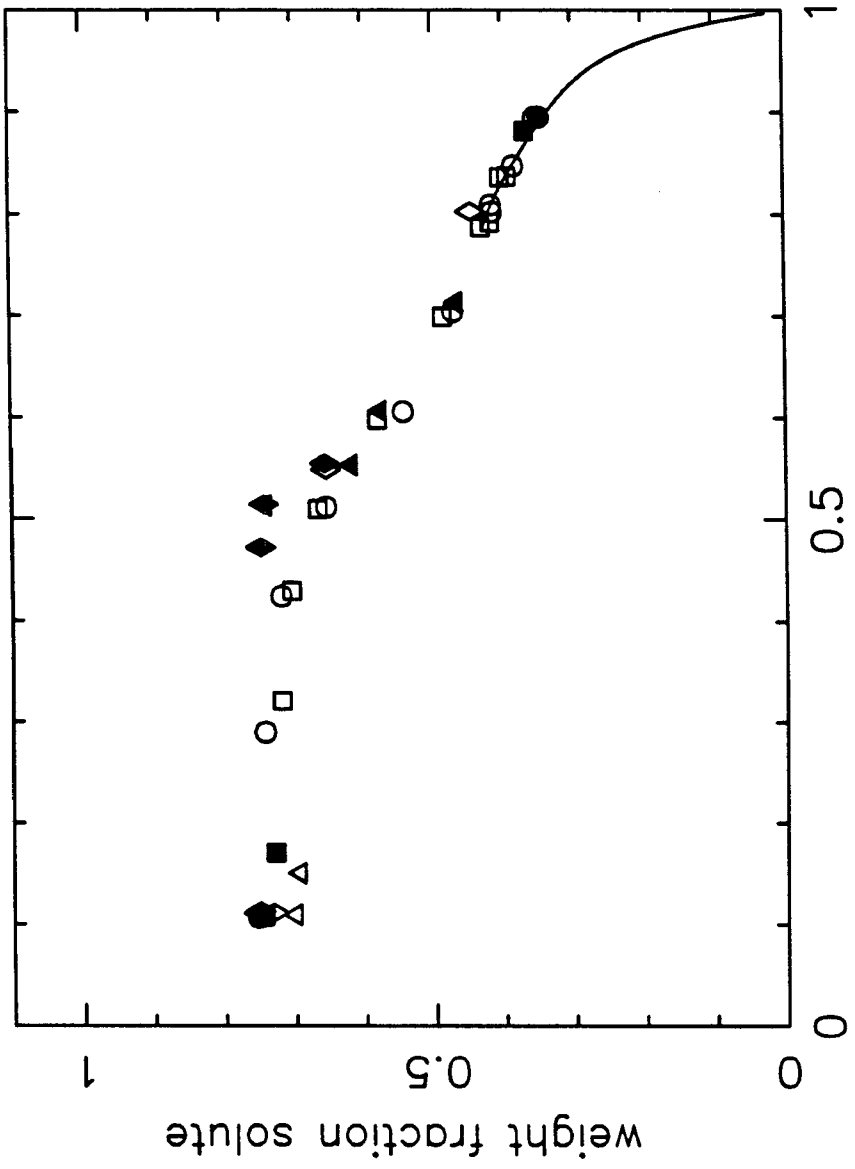

Figure 14

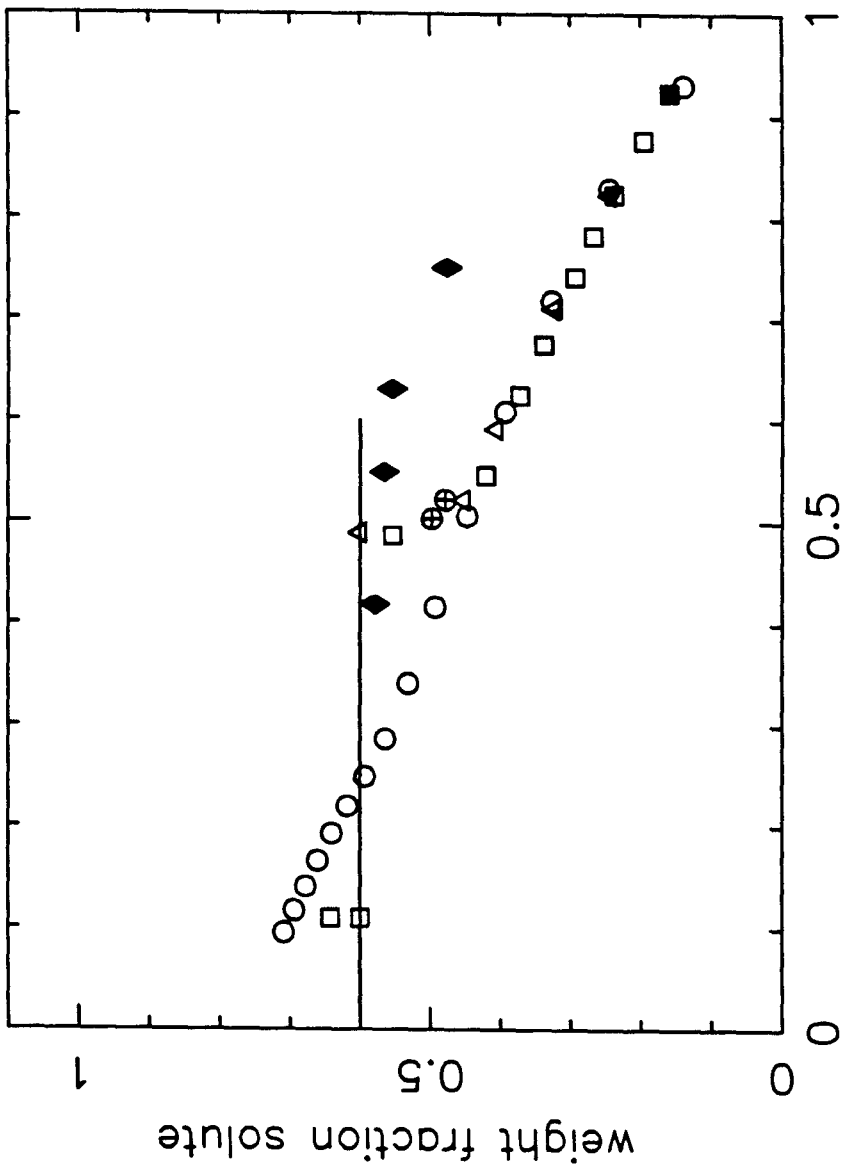

Figure 15

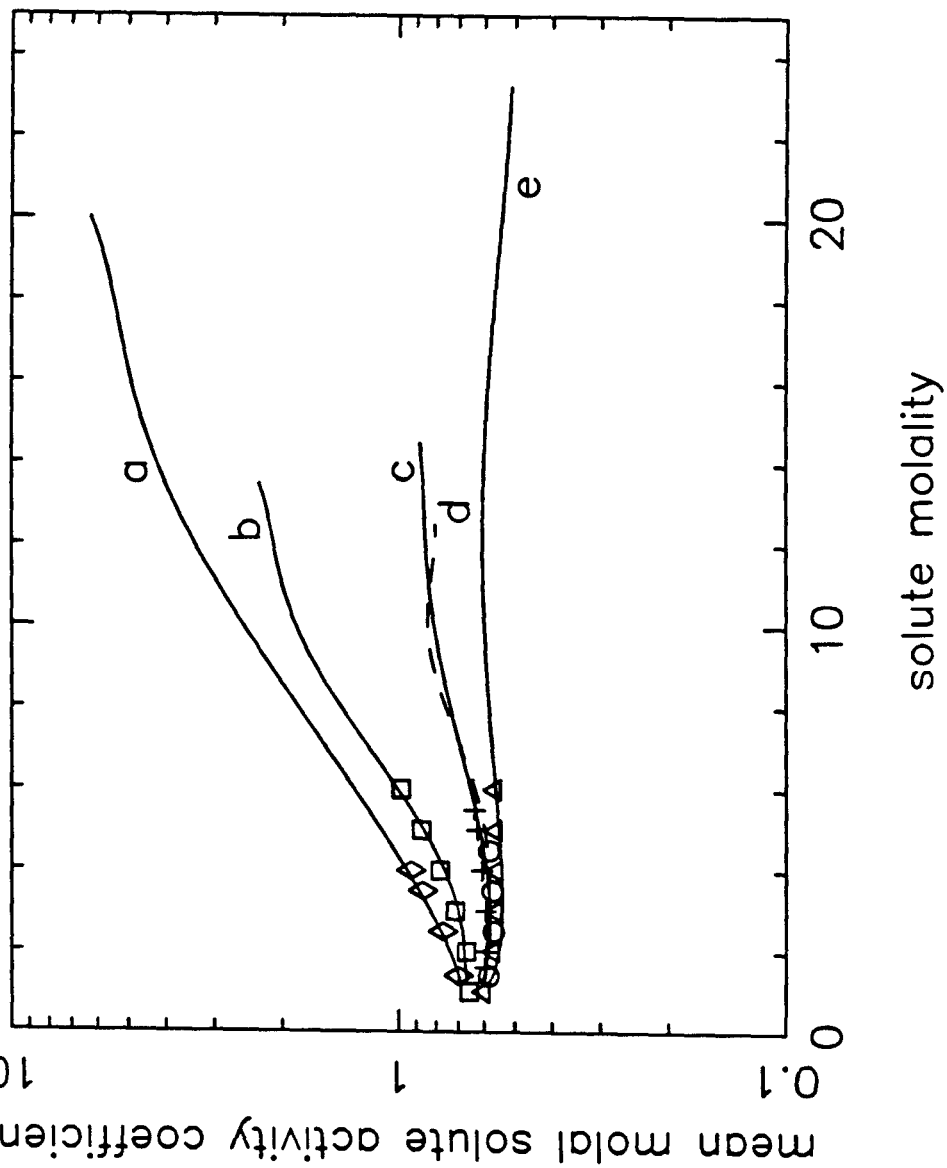
mean molal solute activity coefficient
10
1
0.1
0
10
20
solute molality
a
b
c
d
e

Figure 16

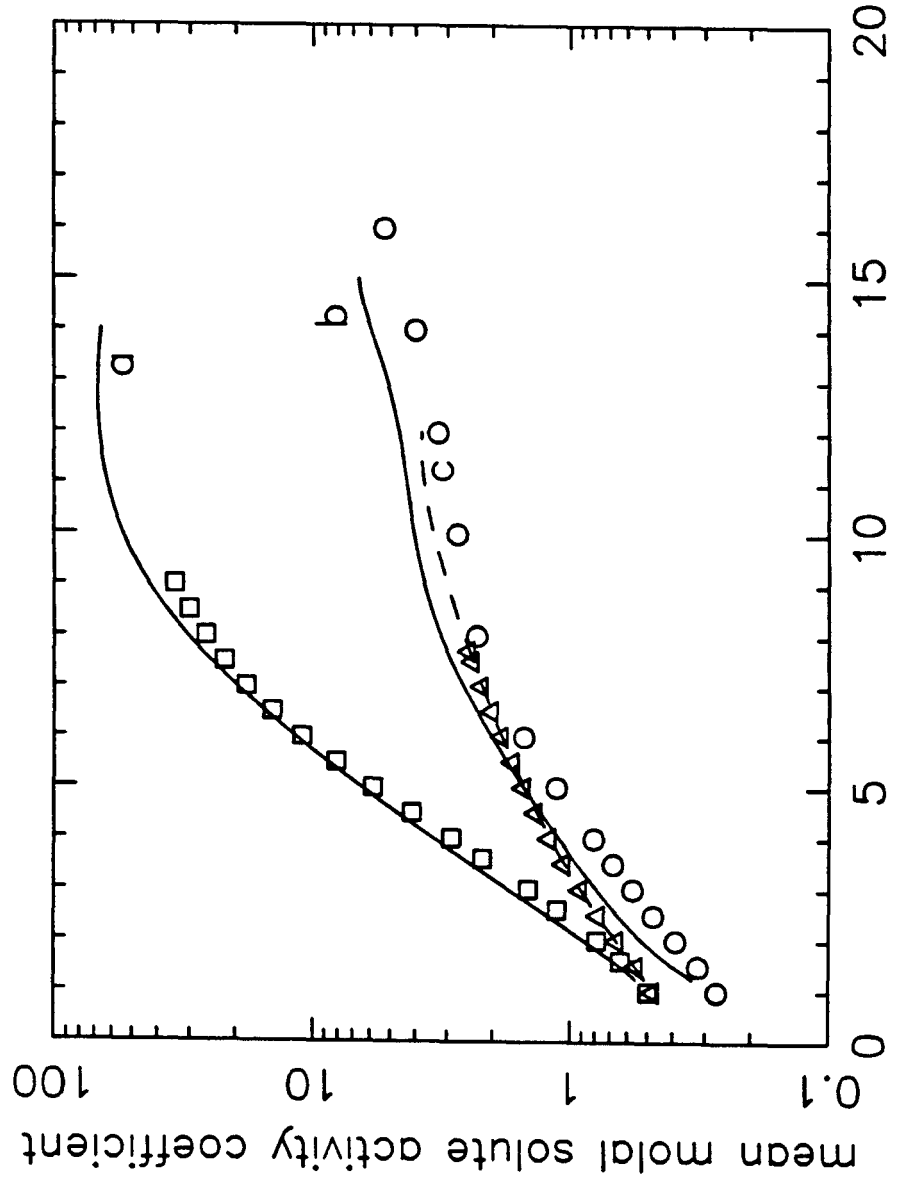
mean molal solute activity coefficient
100
10
1
0.1
0
5
10
15
20
solute molality
a
b

Figure 17

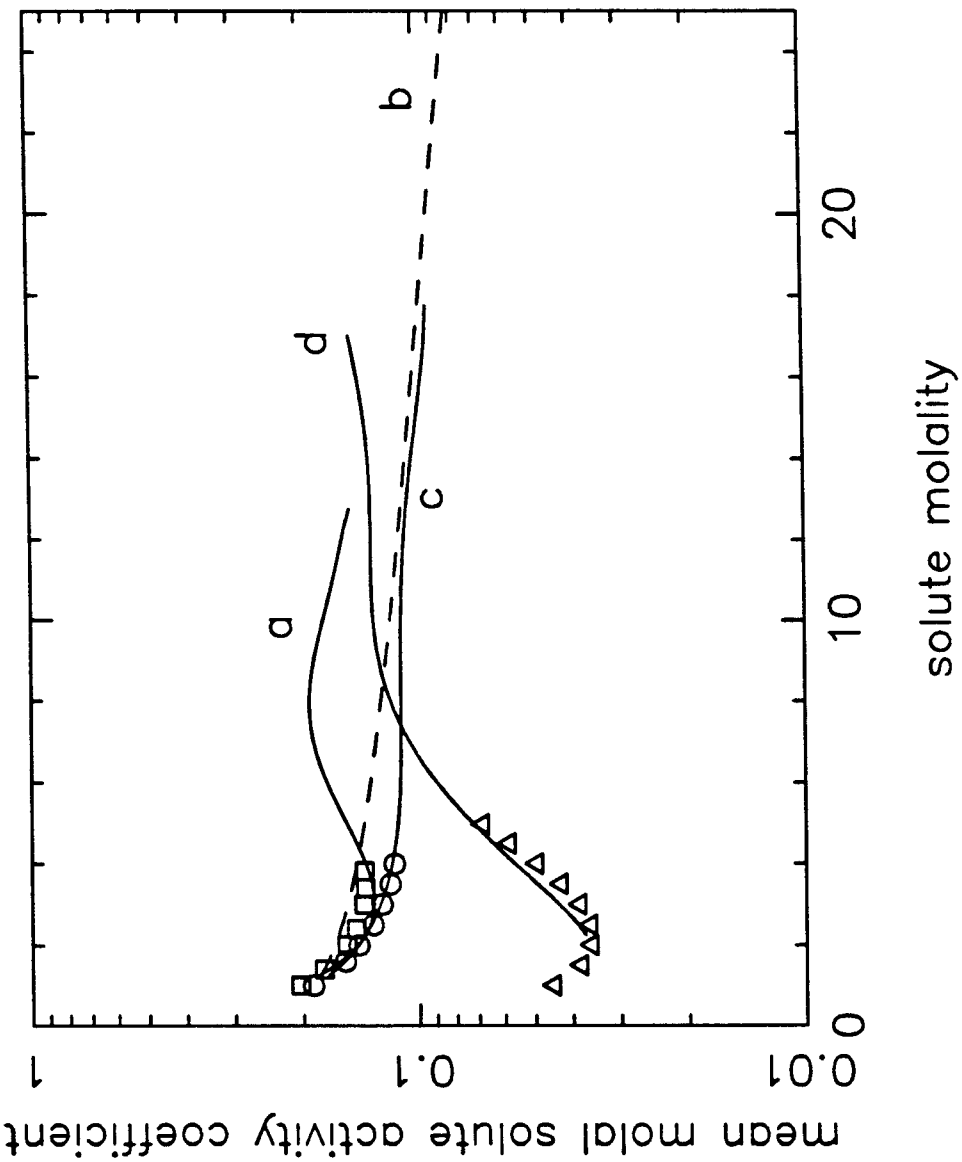
mean molal solute activity coefficient
1
0.1
0.01
0
10
20
solute molality
a
b
c
d

Figure 18

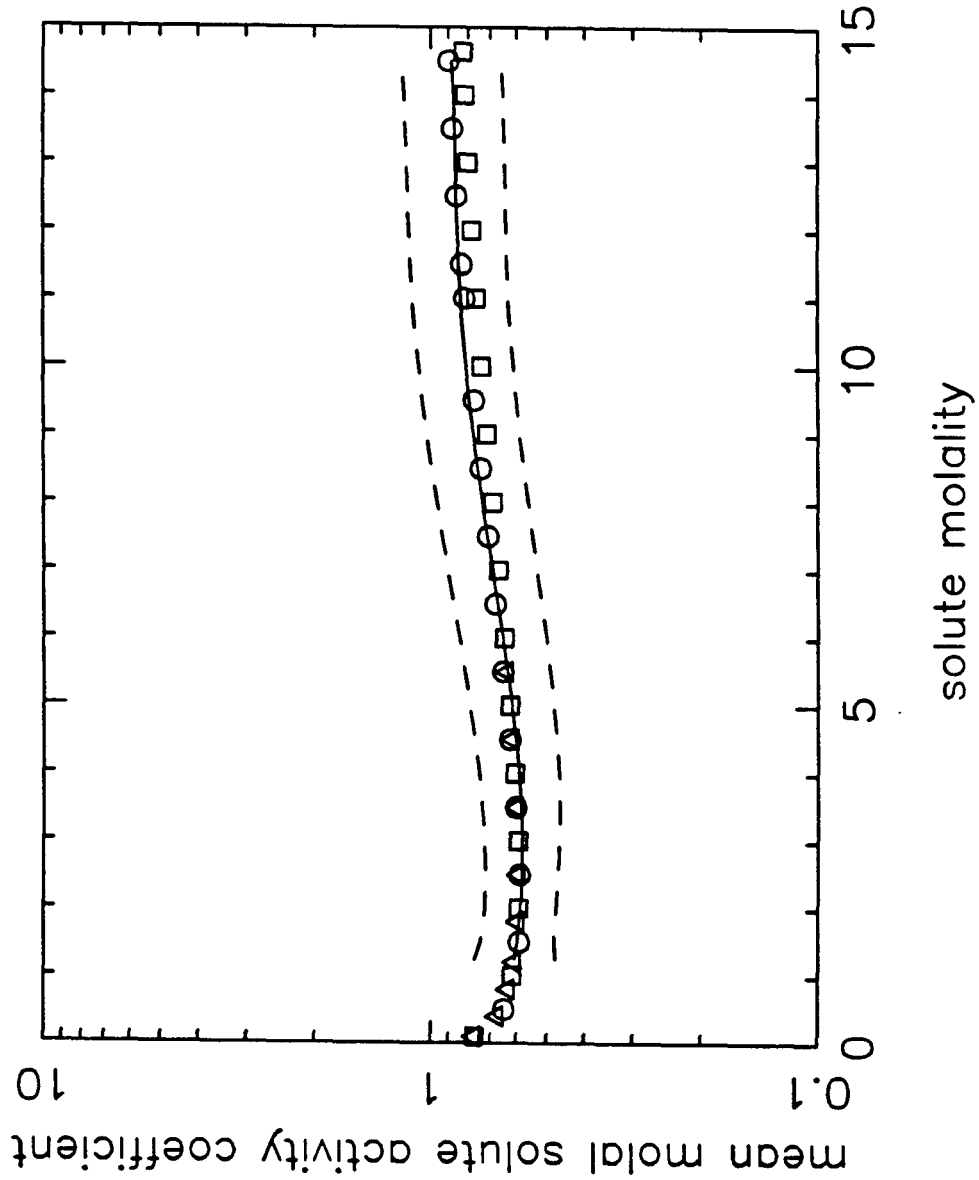
mean molal solute activity coefficient
10
1
0.1
0
5
10
15
solute molality

Figure 19

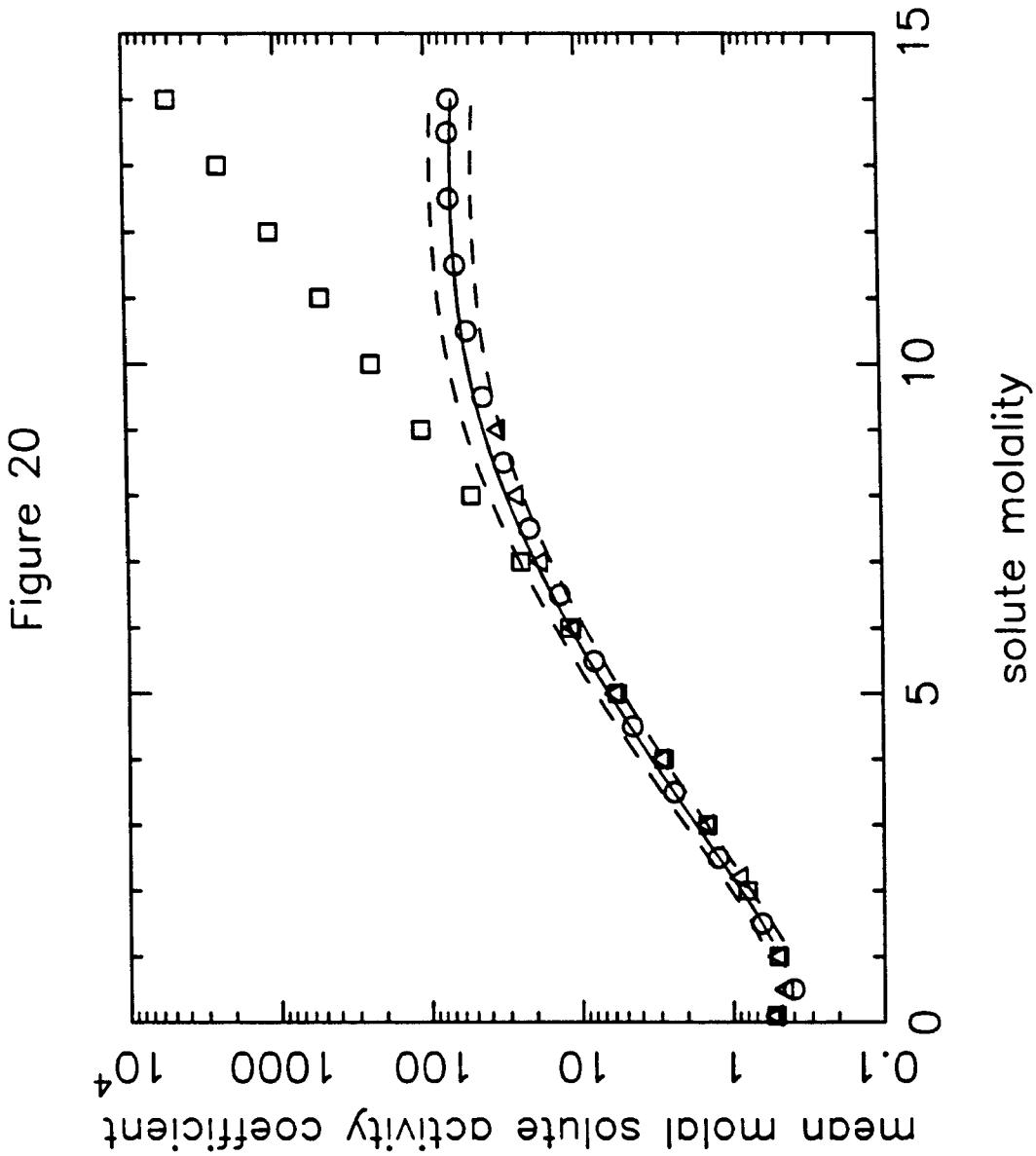
mean molal solute activity coefficient
0.1
1
10
100
1000
10⁴
0
5
10
15
solute molality

Figure 20

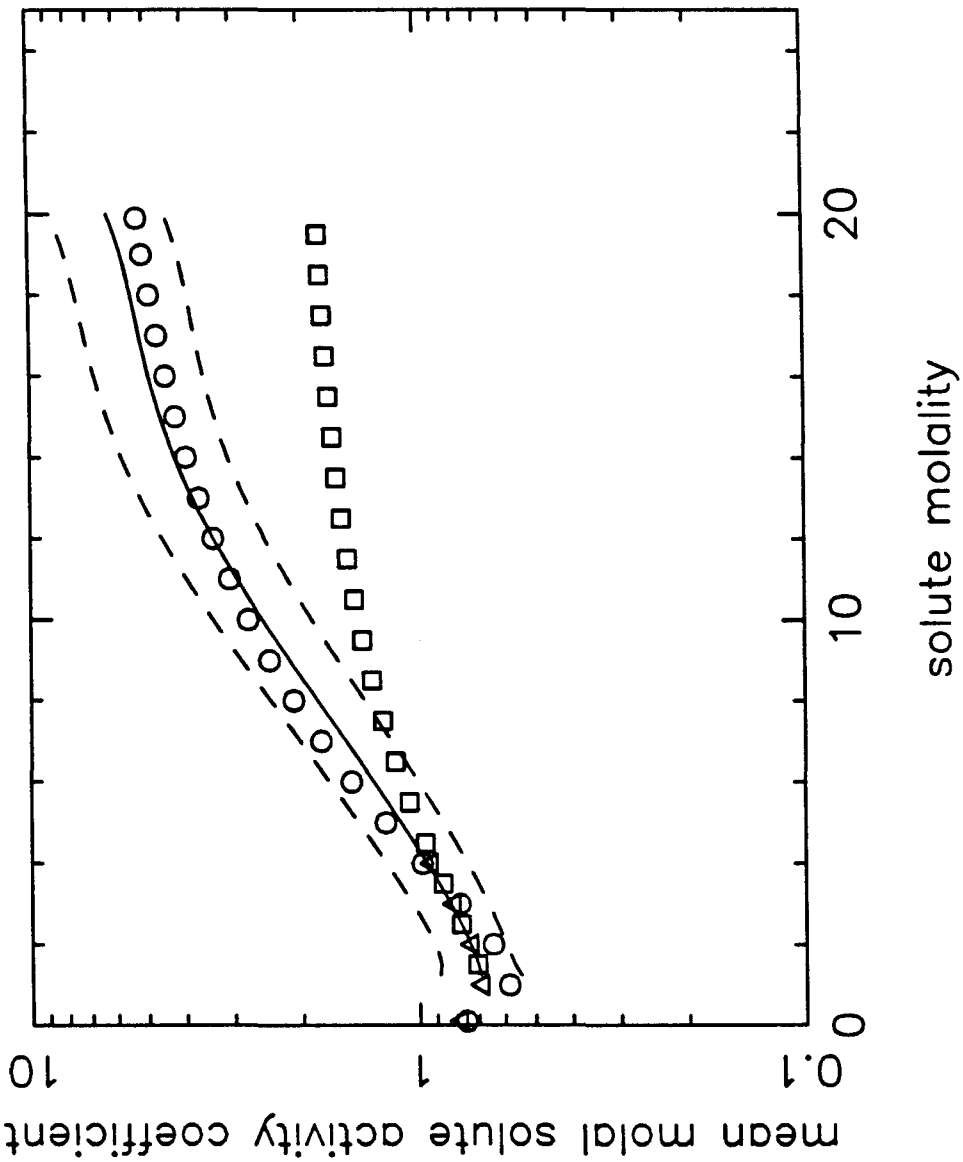
mean molal solute activity coefficient
10
1
0.1
0
10
20
solute molality

Figure 21

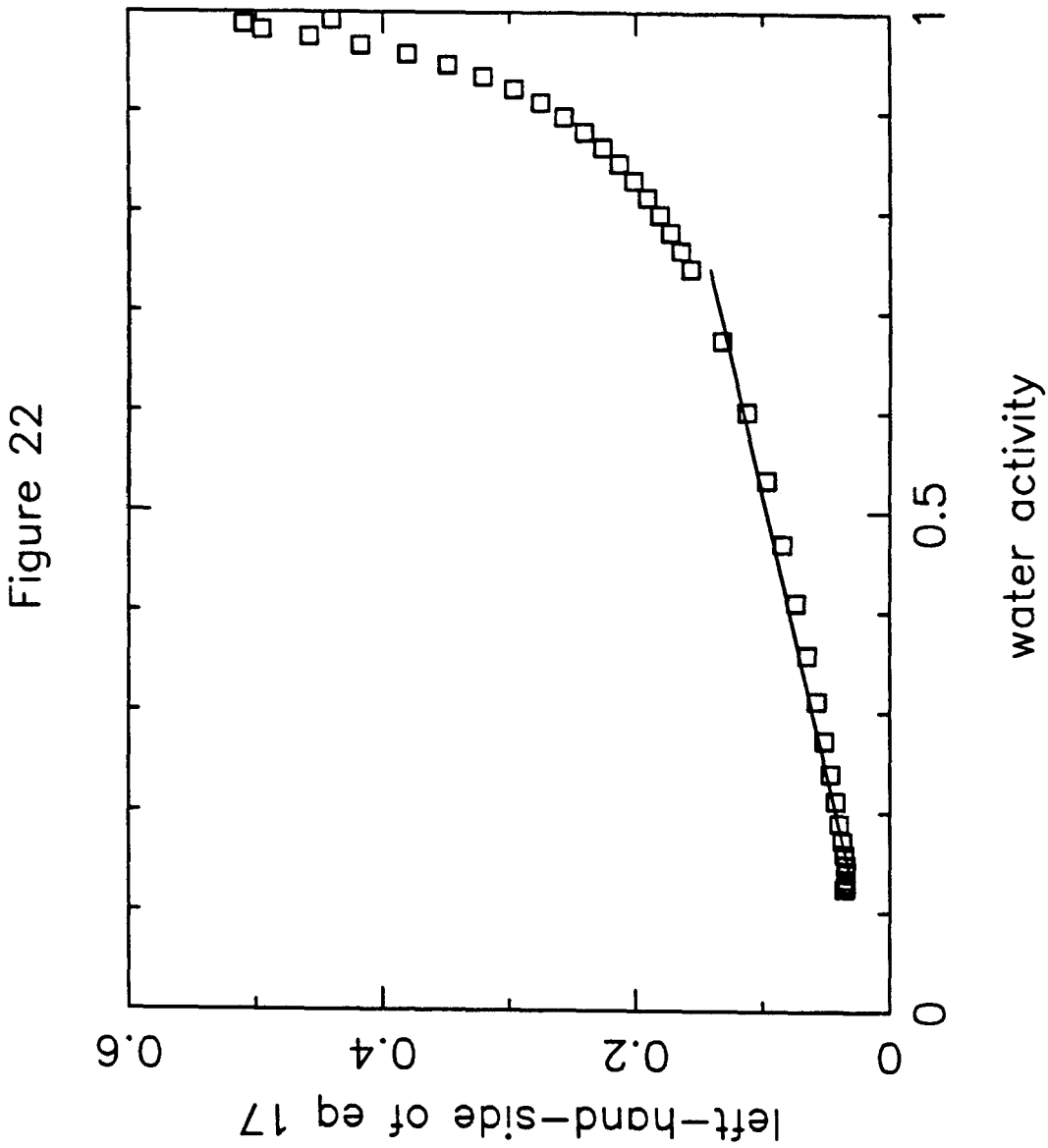

Figure 22

Chapter 2: Water Activities for Mixed-Electrolyte Solutions

Studies of Concentrated Electrolyte Solutions using the Electrodynamic Balance. II. Water Activities for Mixed-Electrolyte Solutions

Mark D. Cohen, Richard C. Flagan*,
and John H. Seinfeld†

Chemical Engineering
California Institute of Technology
Pasadena, CA 91125

*Environmental Engineering Science
†To whom correspondence should be sent

Abstract

An electrodynamic balance has been used to measure the water activity as a function of solute concentration at 20 ℃ for three aqueous electrolyte mixtures: NaCl–KCl, NaCl–KBr, and NaCl–$(NH_4)_2SO_4$. The measurements were performed by levitating single, charged particles of these electrolyte mixtures within the balance and measuring the mass of the particles as a function of the surrounding relative humidity. The deliquescence behavior of the mixed-electrolyte particles was also observed. For the alkali halide mixtures, the low concentration data were consistent with earlier investigations. Data were obtained at higher concentrations than previously reported. The amount of water in the NaCl–$(NH_4)_2SO_4$ particles after drying was unknown. This, together with the lack of previously reported water activity data for this mixture complicated the analysis of these experiments. Three models of mixed-electrolyte solutions — the Zdanovskii-Stokes-Robinson, Reilly-Wood-Robinson and Pitzer methods — agreed well with the experimental data for the NaCl–KCl and NaCl–KBr systems over the range of concentration that the models could be applied. The mixing rules' predictions were consistent with the experimental observations for the NaCl–$(NH_4)_2SO_4$ system assuming a small amount of water was retained in the particles after drying.

Introduction

An understanding of the thermodynamics of mixed-electrolyte solutions is important in such diverse problems as geochemistry, oceanography, biology, atmospheric chemistry, desalinization, waste treatment, and many manufacturing processes. As an example, the atmospheric aerosol consists, in part, of a complex, aqueous mixture of inorganic salts [1,2]. As a prerequisite to the understanding and modeling of the light scattering, growth, and health effects of this aerosol, the composition of an aerosol particle in equilibrium with a given ambient temperature and humidity must be known. This requires knowledge of the water activity as a function of solute concentrations for mixed-electrolyte solutions [3]. As atmospheric relative humidities are often low, the thermodynamics of highly concentrated solutions needs to be understood.

With the electrodynamic balance, water activity measurements can generally be made to much higher solute concentrations than with conventional techniques. The data are obtained by measuring the relative mass of a micron-sized levitated droplet as a function of the relative humidity. Measurements of the water activity as a function of solution concentration were made for aqueous electrolyte mixtures NaCl–KCl, NaCl–KBr, and NaCl–$(NH_4)_2SO_4$ at 20 °C. For the NaCl–KCl and NaCl–KBr mixtures, the measurements were made to much higher ionic strengths than have previously been reported. The NaCl–$(NH_4)_2SO_4$ mixture was studied because of its importance to the understanding of the atmospheric aerosol and because no water activity data could be found in the literature for this mixture.

It has long been recognized that some form of mixing rule is necessary in order to relate the thermodynamic properties of electrolyte mixtures to the concentrations of the individual components in the solution. Many different mixing rules have been proposed [4,5,6,7,8,9,10,11,12,13] and these have been reviewed [14,15,16]. The simplest and most convenient mixing rules are those that allow the properties of mixed-electrolyte solutions to be predicted from those of the aqueous solutions of the individual component salts. Most modern theories of electrolyte mixtures, however, attempt to take into account more complicated interactions in solution than those that occur in single-electrolyte solutions, such as the interactions between different ions of like sign, by employing data from common-ion electrolyte mixtures. Often, however, such data are not available, and so the simple mixing rules, based only on the properties of single-electrolyte solutions, must be used. The measurements obtained in this investigation provide an opportunity to test the validity of these simple mixing rules for very concentrated mixed-electrolyte solutions. The results of this evaluation are presented.

Experimental Method

The electrodynamic balance apparatus employed in this investigation is described in Part I of this work [17], and so only a brief summary of the experimental method need be given here. The methods used in the study of mixed-electrolyte solutions with the electrodynamic balance are essentially the same as those for the investigation of single-electrolyte solutions. The gravita-

tional force on a charged, suspended particle is balanced by the electrical force created by the imposition of a dc voltage difference between the top and bottom electrodes of the electrodyamic balance. By measuring the electric field required to balance the gravitational force, the relative mass of a trapped particle can be determined at any time. Particles of known solute composition were suspended and their relative mass measured as a function of the surrounding relative humidity. Using knowledge of the composition of the particle at some reference state, *e.g.,* dry, the composition of the suspended particle at any other relative mass can be easily determined by the relative balancing voltages for the two states.

The charge and aerodynamic diameter of the particles in their dry state were estimated from measurements of the particle's terminal velocity as a function of the dc field within the chamber [17]. The aerodynamic diameters of the dry particles studied here were 11.0–21.2 microns. For such large particles, the effect of curvature on the vapor pressure of water over the droplet, *i.e.,* the Kelvin effect, is negligible. The charge levels on the various particles varied from 1.3×10^5 to 3.1×10^5 elementary charges. It has previously been shown [17] that the surface charge does not significantly influence the vapor pressure of volatile components within the suspended droplet under these conditions. Thus, at equilibrium, the activity of water in a suspended droplet exactly equals the relative humidity of the surrounding vapor. In the present experiments, the water activity of the mixed-electrolyte solution as a function of the solute concentration within the droplet was determined by measuring the relative particle mass as a function of the chamber relative humidity. The relative humidities

were determined with an uncertainty of about 0.01–0.02. The weight fraction solute was determined to within 0.01, excluding uncertainties in the dry-particle stoichiometry.

As discussed in Part I of this work, one of the drawbacks of this technique is that the composition of a particle after drying cannot be predicted *a priori*. With single-electrolyte solutions, it was shown that the composition of the dry particle could be inferred from other measurements made on the particle. With mixed-electrolyte solutions, the uncertainty in the dry-particle composition is potentially more serious than for single-electrolyte solutions for the following reasons. First, after a mixed-electrolyte solution droplet has crystallized, the possibility that the dry particle will contain trapped water is enhanced. For example, Hanel and Zankl [5] found that a considerable amount of water apparently remained in the crystals obtained from some electrolyte mixtures and that the water could not be removed using physical methods.

In addition, there are generally several possibilities for the compositions of the various crystalline phases that are present in dry particle. As an example, for the (NH_4^+,Na^+,SO_4^{2-},Cl^-,H_2O) system studied here, one previous investigator found that depending on the composition of the system, six different crystalline phases in nineteen different combinations could be obtained after crystallization [18]. The wide range of possibilities for the crystalline phase(s) coupled with the fact that non-equilibrium crystal forms are often found after nucleation within suspended particles [17] suggest that difficulties in determining the dry particle composition may arise.

Three different aqueous electrolyte mixtures were studied in this work. The first mixture, NaCl–KCl, has previously been well characterized at low concentrations, making it relatively easy to infer the dry particle's compostion for the particular mixing ratio we studied. The second mixture, NaCl–KBr, has not been characterized so extensively. Experiments were performed for one of the few mixing ratios that had been previously studied, allowing us to infer the composition of the dry particles at this solute mixing ratio for this system. For the final mixture studied, NaCl–$(NH_4)_2SO_4$, there were no water activity data available in the literature, and this complicated data analysis.

Results and Discussion

1. Sodium Chloride – Potassium Chloride

The thermodynamics of the NaCl–KCl–H_2O system have been extensively characterized at low concentrations [19,20,21,22,23,24,25]. An aqueous solution was prepared with a mole ratio of KCl to NaCl of 1.0026 and a droplet of this solution was injected into the electrodynamic balance and trapped as described in Part I. The particle, when dry, had an aerodynamic diameter of 13.1 microns and had 1.74×10^5 elementary charges. A series of measurements was made of the relative particle mass as a function of relative humidity at 20 ℃.

The mass fraction solute for each of the steady states is shown in Figure 1 as a function of the relative humidity in the chamber. It was assumed in calculating the mass fraction solute from the relative balancing voltages that af-

ter crystallization the dry particle was anhydrous, the most thermodynamically stable state under these conditions [26]. In Figure 1, and in later figures, the predictions of models of electrolyte solutions are compared with the experimental data. These predictions will be discussed later. Also shown in Figure 1 are data calculated from the equations presented in Robinson's [19] investigation of this system at 25 °C. As mentioned in Part I of this work, the comparison of data at 25 °C with data at 20 °C does not introduce significant errors. Good agreement was found with Robinson's results over the range that the data can be directly compared. We have extended the data for this particular Na^+ / K^+ mixing ratio down to a water activity of 0.46 from the lower limit of 0.76 of Robinson's data.

For any particle composed of a single, crystalline inorganic salt, there is a particular humidity, the deliquescence humidity, above which the particle will transform into a solution droplet. However, as Tang and coworkers have pointed out [26,27], the deliquescence of a multicomponent particle will, in general, be more complicated. These investigators studied the deliquescence behavior of crystalline NaCl–KCl particles at 25 °C theoretically [26], by reference to the phase diagram for the system, and experimentally [27], by measuring the size changes of a monodisperse aerosol as a function of relative humidity. In their study, they assumed that the dry particles were anhydrous and that there were no mixed-crystalline phases present. They found that at 25 °C, a dry particle of a special composition, the eutonic compostion, will deliquesce at a humidity of 0.738 ($\pm$0.003). The eutonic composition corresponds to a mass ratio of NaCl to KCl of 1.78 at 25 °C.

For all NaCl / KCl mixing ratios different than the eutonic ratio, however, Tang et al. found that the particle would deliquesce over a range of humidities. At the eutonic relative humidity of 0.738 the component in least abundance relative to the eutonic compostion will dissolve completely, while the other component will dissolve partially. As the humidity is increased, the remaining crystalline phase dissolves continuously until at a certain humidity, it is completely dissolved. Tang and coworkers [27] measured the eutonic humidity and observed a deliquescence range for non-eutonic mixing ratios, but they did not measure the concentration of solute within the droplet during the deliquescence.

The deliquescence behavior of the particle we studied was completely consistent with the above theoretical and experimental results. When the dry particle was exposed to a humidity higher than the eutonic humidity, the deliquescence occured in two stages. The particle first absorbed a certain amount of water very quickly, and this was followed by a slower water gain. The ratio of total mass to solute mass is shown in Figure 2 as a function of time during two of the humidity transients in which a partial deliquescence occurred. The initial, rapid water gain up to point (a) in Figure 2 corresponds to the dissolution of a portion of the crystalline material in the particle when the relative humidity in the chamber reached the eutonic value. The ratio of total mass to solute mass in the particle at the end of this initial deliquescence was 2.48. From the phase diagram and explanation given by Tang and coworkers [26], one can estimate for the NaCl / KCl mixing ratio of our particle that the ratio of total mass to solute mass after the first stage of deliquescence should be 2.46, in close agreement with the present measurements.

The relative humidity at which the initial deliquescence began is estimated to be approximately 0.74 (±0.01). This is consistent with the previously reported eutonic humidity of 0.738.

We observed two other deliquescence events with the suspended NaCl–KCl mixed-electrolyte particle. One of these is shown, in addition to the aforementioned first stage of the deliquescence, in Figure 2. In both of these cases the final relative humidity that the chamber reached was greater than 0.86, and for both, when the deliquescence was completed (*i.e.*, point (b) in Figure 2) the ratio of total to solute mass in the particle was equal to 3.65 (±0.07). From the phase diagram mentioned earlier [26], one can estimate for the NaCl / KCl mixing ratio of our particle that, when the solute is completely dissolved, the ratio of total to solute mass in the particle will be 3.41. Our observations are reasonably consistent with this prediction. One can calculate from the results of Robinson [19] that for our mixing ratio and a ratio of total mass to solute mass of 3.65 that the water activity would be 0.798.

The agreement of our water activity results and deliquescence measurements with previous results suggest that the dry particle of NaCl–KCl was, indeed, anhydrous and contained only two different, pure crystalline phases — NaCl and KCl.

2. Sodium Chloride – Potassium Bromide

The aqueous electrolyte mixture of NaCl and KBr has been studied previously at ionic strengths less than 5 molal [21]. To aid in the interpretation of our data, we chose a particular mixing ratio, moles NaCl / moles KBr = 1.6142, that corresponded closely to one that was studied in the earlier investigation.

Assuming that the particles were anhydrous after crystallization and drying at low humidity, the weight fraction solute was calculated for each of the steady states measured. The results are shown in Figure 3 along with the two data points at this mixing ratio from the earlier investigation [21]. The data for this salt mixture showed more scatter than usually observed in our investigations. Nevertheless, our results were consistent with the earlier measurements, indicating that the dry particles were anhydrous. Our measurements extend down to a relative humidity of 0.37, considerably lower than the lowest relative humidity, 0.848, measured for this mixing ratio in the earlier investigation.

The deliquescence observations with particles of this electrolyte mixture were particularly interesting. When one of the particles was exposed to a relative humidity of about 0.70 after being in a dry state, it continued to gain water very slowly over a period of 6 hours. Since the length of this transient was considerably longer than the time it normally took for the chamber humidity to reach steady state at a relative humidity of 0.70 (c.f. Figure 2), the slow particle response was definitely a consequence of a particle-related phenomenon. When the particles of this system were exposed to higher humidities (*e.g.*, around 0.85),

the deliquescence was quite fast but appeared to be seemed extremely violent. In these deliquescences, the particle seemed to be shaking, as if the structure of the particle was being rapidly altered. The weight gain during the humidity transients when the violent deliquescences occurred slowed significantly when the weight fraction solute was approximately equal to 0.38 ($\pm$0.02), suggesting that a deliquescence event had been completed. It is not clear, however, whether the particle was completely dissolved at the end of this deliquescence or if this was only the end of the first stage of dissolution of the solid material in the particle.

Another unusual phenomenon observed with some of the particles of the NaCl–KBr mixture was that after crystallization, the particle would slowly lose a small amount of mass until it reached its apparently anhydrous dry state. Thus, the particle apparently contained a small amount of water immediately after crystallization. Crystallization and drying of the particle at 50 ℃ yielded the same dry mass was found as when the particle was dried at 20 ℃.

The deliquescence and slow-drying observations with particles of this system suggest that the particles were spatially inhomogeneous in the dry state. In other words, the particles may have dried to a state in which there was a complex juxtaposition of different crystalline regions. The slow-drying phenomenon could have arisen because water had been trapped between the crystalline regions within the particle. Since the dry particles were assumed to be anhydrous, physical trapping of variable amounts of water could have accounted for the scatter in the measurements. The slow rate of water gain at a relative humidity

of 0.70 might also have been due to the complexity of the particle structure. Water may have been unable to diffuse easily within the particle to dissolve crystalline regions in the particle's interior.

3. Sodium Chloride – Ammonium Sulfate

Although Hanel and Zankl [5] have studied multicomponent electrolyte aqueous solutions that contain NaCl and $(NH_4)_2SO_4$, there has to our knowledge been no experimental investigation of the water activity as a function of solute concentrations for the system NaCl–$(NH_4)_2SO_4$–H_2O. This system is important from an atmospheric perspective in that the components are often present in significant concentrations in the atmospheric aerosol [1,2]. An important source of sodium and chloride ions in the aerosol is sea spray. Ammonium ions and sulfate ions are often incorporated into the atmospheric aerosol as a result of gas-to-particle conversion. Gaseous ammonia and sulfuric acid can be absorbed and directly influence the concentration of ammonium and sulfate ions within an aerosol particle, and sulfur dioxide can be absorbed and oxidized to sulfate within an aqueous droplet [28,29,1].

The mass was measured as a function of relative humidity for NaCl–$(NH_4)_2SO_4$ particles with three different solute mixing ratios: moles $(NH_4)_2SO_4$ / moles NaCl = 0.5, 1, and 2. With all the mixing ratios, a small amount of solute was lost from the particles during the course of the experiments. As with the volatilization observed with aqueous solutions of ammonium chloride in Part I of this work [17], the evidence for this solute volatilization was

that over the course of an experiment for a particular particle, the dry-particle balancing voltage would decrease with each successive determination. The most likely species to volatilize from the NaCl–$(NH_4)_2SO_4$ particles are NH_3 and HCl.

The volatilization of solute from a mixed-electrolyte solution is potentially a more serious problem than for a single-electrolyte solution. At the beginning of an experiment, the particle was composed of a particular stoichiometric mixture of NaCl and $(NH_4)_2SO_4$, but, because of the volatilization of NH_3 and HCl, the relative proportions of the ions in the solution changed continuously throughout the experiment.

Volatilization from this electrolyte mixture was generally less than 2 % of the solute mass over the course of the measurements for a particular particle. In the calculation of the weight fraction solute for a steady state at a particular relative humidity from our measurements of the wet and dry balancing voltages, we have, as in our previous study [17], simply assumed that the solute mass decreased the same amount during each of the steady states between any two successive dry balancing voltage determinations. We have further assumed that the relative amounts of the various ions within the particle remained constant at the initial mixing ratio. An experimental test of these two assumptions is discussed below.

The data obtained for the three different mixing ratios are presented in Figures 4–6. Individually, aqueous solutions of both sodium chloride and ammonium sulfate crystallized to an anhydrous dry state [17]. It was therefore assumed that the dry mixed-salt particles were anhydrous in calculating the

weight fraction solute from the dry and wet balancing voltages for the different steady states represented in Figures 4–6. As far as we are aware, there are no water activity data for this system in the literature with which to compare our results and to verify this assumed dry-particle stoichiometry.

The sensitivity of the results to the above assumptions regarding the treatment of the volatilization phenomenon was investigated using the 1:1 NaCl–$(NH_4)_2SO_4$ particles. First, two particles were extensively studied, with the particles' relative mass being measured at many relative humidities. For these particles, steady states at low humidities were consistently measured at the end of a given experiment, after most of the volatilization had taken place.

A fresh 1:1 NaCl–$(NH_4)_2SO_4$ solution was then prepared and a droplet of this solution was immediately inserted into the chamber. With this particle, only three steady states were measured: a dry state at low humidity after the initial crystallization of the particle, a steady state for a solution droplet at a relative humidity of 0.359, and a final dry state at low humidity after the particle had re-crystallized. To transform the particle into a solution droplet for the steady state at a relative humidity of 0.359, the dry particle was first exposed to a relatively high humidity (*i.e.*, about 0.90) for a few minutes in order to dissolve the particle. The humidity was then quickly lowered. The entire experiment was completed in less than 30 minutes, and the particle's balancing voltage was the same for the initial and final dry states. Thus, as was expected for such a short experiment, the amount of solute volatilization that occurred with this particle was negligible.

As can be seen in Figure 5, the weight fraction solute at a relative humidity of 0.359 for this particle, for which no significant volatilization took place, agrees well with the data at low humidites for the other particles, for which a small amount of volatilization was observed. Thus, within the uncertainty of our measurements, the change in relative ion concentrations and uncertainty in total solute mass caused by the volatilization phenomenon can be satisfactorily accounted for with the above assumptions.

As with the other systems studied, the particles of this mixed-electrolyte system deliquesced at a lower humidity than did any of the component salts by themselves. For the 1:1 mixing ratio, no water was absorbed at a humidity of 0.644, but a small amount of water was absorbed beginning at a relative humidity of 0.660. At a relative humidity of 0.682, the particle absorbed a large amount of water quickly (*i.e.*, it deliquesced), but the amount of water eventually gained by the particle was not quite as much as would be expected if the crystalline material in the particle had completely dissolved. This partial deliquescence corresponds to point A in Figure 5.

The deliquescence was similar for the other mixing ratios studied. For an NaCl / $(NH_4)_2SO_4$ mixing ratio of 2:1, no water was absorbed at a relative humidity of 0.607, but a partial deliquescence occurred during a humidity transient in which the chamber eventually reached a relative humidity of 0.706. With the 1:2 mixing ratio, water was not absorbed at a relative humidity of 0.651, but during a transient in which the chamber relative humidity reached 0.704, a partial deliquescence was found. The points labelled A in Figures 4 and 6

have the same meaning as that in Figure 5 – *i.e.*, the particle had only partially deliquesced and had not completely dissolved. Measurements of the water gain as a function of time for the partial deliquescence observations with this mixed-electrolyte system are presented in Figure 7. As can be seen, the particles of all mixing ratios exhibited a clearly defined deliquescence that occurred at a relative humidity in the range 0.65 - 0.70. This behavior is similar to that of the NaCl–KCl system in which particles of different mixing ratios all experience an initial deliquescence at the eutonic relative humidity. It thus appears that the NaCl–$(NH_4)_2SO_4$ system may have a eutonic relative humidity between 0.65 and 0.68 at 20 ℃.

Models of Multicomponent Electrolyte Solutions

The water activity predictions of three different models of mixed-electrolyte solutions have been compared to the above data. All of the methods combine only the properties of single-electrolyte solutions, each of which is a subset of the mixture, in order to predict the mixed-electrolyte solution's properties. For all the mixtures studied, the relevant single component solutions were investigated in Part I of this work [17]. Because the data in this and the previous work extend to very high concentrations, the validity of the various mixing rules can be tested at higher concentrations than typically used in their evaluation.

1. The Zdanovskii-Stokes-Robinson Method

One of the simplest mixing rules is that developed independently by Zdanovskii and by Stokes and Robinson [6,7]. This approach, called the ZSR method, is defined by the following relation:

$$\sum_i \frac{m_i}{m_{0,i}(a_w)} = 1 \tag{1}$$

In eq 1, m_i is the molality of component i in the multicomponent solution, and $m_{0,i}$ is the molality of a single-electrolyte solution of component i for which the water activity, a_w, equals that of the multicomponent solution. The summation in eq 1 is over a set of individual salts that, if mixed together, would be equivalent to the solute in the electrolyte mixture. The choice of this set is not necessarily unique. For example, for an equimolar solution of Na^+, K^+, Cl^-, and Br^-, one could consider the solution to be composed of NaCl and KBr or NaBr and KCl.

In order to test the predictions of the ZSR model against the mixture data, measurements of the molality as a function of water activity for each of the relevant single-salt solutions were fit to polynomial of the form

$$m = a_0 + a_1 a_w + a_2 a_w^2 + a_3 a_w^3 + \ldots \tag{2}$$

using a least-squares procedure. The data sets used for these fits, combining data from the literature and from our experiments, were the same as that used for the $a_w(m)$ polynomial fits presented in Part I of this work [17]. For a given weight-fraction-solute of the mixed solution, the molalities of the various components were calculated, and the particular water activity for which eq 1 was satisfied was determined by iteration.

The predictions of the ZSR method for the mixtures studied in this work are presented along with the experimental data in Figures 1 and 3–6 above. This method requires single-electrolyte data at the water activity of the mixture, and for each of the systems studied, data for the mixed solutions were obtained at lower water activities than were available for one or more of the component salts. Thus, the model could not be used to predict the properties of the mixtures at the highest concentrations at which data were obtained. Over the range of data for which the model could be applied, however, the agreement with the NaCl–KCl and NaCl–KBr systems was very satisfactory. For these systems, the predicted water activity agrees with the experimentally observed value to within about 0.01–0.02.

For the NaCl–$(NH_4)_2SO_4$ system, however, the agreement is poor. As mentioned earlier, the data for this system were interpreted with the assumption that the dry particles were anhydrous. The discrepancy between the ZSR model's prediction and the experimental observations shown in Figures 4–6 suggest that this assumption may have been in error. Water could have been incorporated into various crystalline phases within the particle (*e.g.*, $Na_2SO_4 \cdot 10(H_2O)$) or could have been trapped between crystalline regions. While the structure and composition of the dry particles is not known, it is very likely that widely different crystalline morphologies were present. In contrast with the similarity in the crystalline forms of NaCl and KCl, the crystalline forms of ammonium and sodium sulfate salts are very different from those of the chloride salts of the same cations. Because of this, it possible that non-crystalline water could have been trapped within the interstitial regions between differing

crystalline morphologies.

In Figures 8–10 the results for the NaCl–$(NH_4)_2SO_4$ system are replotted with the assumption that the dry particles were not anhydrous, and that the amount of water in the dry particles for each of the different mixing ratios was that which brought the ZSR model's predictions in agreement with the experimental observations. The number of moles of water per mole of solute determined in this way for the dry particles of the 1:2, 1:1, and 2:1 ammonium sulfate : sodium chloride mixing ratios was 0.51, 0.59, and 0.66, respectively. With these assumed dry-particle stoichiometries, the predictions of the ZSR model agree well with the experimental data over the entire concentration range that the comparison could be made, even at very high ionic strengths. In Figure 7, the measurements of the particle concentration during deliquescence are also shown using the above dry-particle stoichiometries.

2. The Reilly-Wood-Robinson Method

Another model of mixed electrolyte solutions is that developed by Reilly, Wood, and Robinson [12]. As pointed out by Sangster and Lenzi [15], the methods of Kusik and Meissner [9] and Robinson and Bower [11] are special cases of this model. For a solution containing m_i^M moles of cation M_i with charge Z_i^M, m_j^X moles of anion X_j with charge Z_j^X, etc., in each kilogram of solvent, the RWR method's prediction of the osmotic coefficient of the mixed-

electrolyte solution is given by

$$RTm(1-\phi) = -\frac{RT}{E}\sum_{\ell=1}^{\ell=i}\sum_{m=1}^{m=j}\frac{E_\ell^M E_m^X Z_{\ell m}}{Z_\ell^M Z_m^X}(1-\phi^0_{M_\ell X_m}) + \cdots \tag{3}$$

in which

$$E_\ell^M = Z_\ell^M m_\ell^M \tag{4}$$

$$E_\ell^X = -Z_\ell^X m_\ell^X \tag{5}$$

$$E = \sum_{k=1}^{k=i} E_k^M = \sum_{\ell=1}^{\ell=j} E_\ell^X \tag{6}$$

$$Z_{km} = Z_k^M - Z_m^X \tag{7}$$

In eq 3, $\phi^0_{M_\ell X_m}$ is the osmotic coefficient of a solution of electrolyte $M_\ell X_m$ at the ionic strength of the mixture. The omitted terms involve parameters obtained from common ion mixtures for interactions between different ions of like charge.

The complete RWR treatment requires data from common-ion solutions to estimate terms describing the binary interactions between different, like-charged ions in solution and ternary interactions between three different ions not all of the same sign. For example, data from solutions of sodium chloride and potassium cloride can be used to characterize the binary (Na^+,K^+) and ternary (Na^+,K^+,Cl^-) interactions in any mixed-electrolyte solution containing these three ions. However, as shown by Reilly et al. [12], to a first approximation, the model can be used with only the single-electrolyte terms (i.e. eq 3, above). To estimate the water activity of a mixed-electrolyte solution with eq 3, one needs single-electrolyte solution data for all possible cation-anion combinations in the multicomponent solution. As an example, for the NaCl–KBr system, data for NaCl, KCl, NaBr and KBr solutions are required.

Calculations were made with eq 3 to predict the water activity as a function of solute concentration for the mixtures studied in this work. The $a_w(m)$ polynomials presented in Part I of this work were used to calculate the osmotic coefficients for the appropriate single-electrolyte solutions as needed in eq 3. In Figures 1, 3–6, and 8–10, the predictions of the simplified RWR method are compared with the experimental observations. The predictions are very similar to those of the ZSR model – in these figures, the predictions of the two models are indistinguishable over most of the concentration range where they can be compared. With the RWR model, the water activity cannot be estimated up to the highest concentrations measured, because the single-component data for one or more of the salts do not extend to sufficiently high ionic strengths.

The predictions of the RWR method, with only single-electrolyte terms, agree quite well with the experimental data for the NaCl–KCl and NaCl–KBr systems. However, as with the ZSR method, it is seen in Figures 4–6 that the RWR method poorly describes the NaCl–$(NH_4)_2SO_4$ mixture with the assumption that the dry particles for this system were anhydrous. However, Figures 8–10 demonstrate that if the dry-particle stoichiometry estimated above by comparing the ZSR method's predictions with the experimental data is used, the RWR method's predictions are consistent with the experimental observations.

3. Pitzer's Method

Pitzer and Kim [30,10] have extended the Pitzer model for single-electrolyte solutions [30,31] to allow the prediction of the properties of mixed-electrolyte

solutions. This model has been used by many investigators, *e.g.*, Rosenblatt [32] and Harvie et al. [33,34], to describe the thermodynamics of mixed-electrolyte solutions. Like the RWR model, the full version of their method requires parameters estimated from common-ion solutions in order to characterize binary interactions among different ions of the same sign and ternary interactions between different ions not all of the same sign in a mixed-electrolyte solution. As with the RWR method, however, these terms can be omitted, to first approximation, and information from only single-electrolyte solutions can be used.

The following equations were developed by Pitzer and Kim for the description of mixed-electrolyte solutions:

$$(\phi - 1)\sum_i m_i = 2If^\phi + 2\sum_c\sum_a m_c m_a \left[B^\phi_{ca} + \frac{(\Sigma mz)}{(z_c z_a)^{1/2}} C^\phi_{ca}\right] + \cdots \qquad (8)$$

where

$$B^\phi_{ca} = \beta^{(0)}_{ca} + \beta^{(1)}_{ca} e^{-\alpha I^{1/2}} \qquad (9)$$

$$(\Sigma mz) = \sum_c m_c z_c = \sum_a m_a \,|\, z_c \,| \qquad (10)$$

$$f^\phi = -A_\phi \left[\frac{I^{1/2}}{1.0 + 1.2\, I^{1/2}}\right] \qquad (11)$$

In the above equations, $A_\phi = 0.392$ for water at 25 °C, $\alpha = 0.2$, the parameters $\beta^{(0)}_{ca}$, $\beta^{(1)}_{ca}$ and C^ϕ_{ca} are for the single-electrolyte solution of anion a of charge z_a and cation c of charge z_c, and the sums in eq 8 cover all possible cation-anion combinations. The omitted terms involve parameters obtained from common ion mixtures for interactions between different ions of like charge.

Pitzer's model of electrolyte solutions allows for model parameters determined for single-electrolyte solutions to be applied to multicomponent elec-

trolyte solutions. For example, the modified Debye-Huckel expression developed by Pitzer for the long range electrostatic interactions between ions in solution (*i.e.*, the first term on the right-hand-side of eq 8) depends only on ionic strength and not on the properties of specific ions. In Part I of this work, parameters were found for the Pitzer model that characterized the solutions of the individual salts that are components of the mixtures studied here. The new parameters — $\beta^{(0)}_{mx}$, $\beta^{(1)}_{mx}$, and C^{ϕ}_{mx} for each salt — were able to correlate the experimental measurements within their uncertainty over the full range of the data. These parameters were used in the above equations to estimate the properties of the mixtures studied in this work and the results are presented in Figures 11–15. For the NaCl–$(NH_4)_2SO_4$ system, it was assumed at the outset that the dry particles contained the same amount of water as that suggested by the ZSR model's predictions.

Pitzer's method requires single-electrolyte parameters for all possible cation-anion pairings in the solution which are valid at the ionic strength of the solution. As with the other methods, this restriction meant that only a portion of the concentration range could be treated. However, with this method, one can attempt to use the parameters beyond the maximum ionic strengths for which they were estimated. It was found in Part I of this work that this procedure was occasionally successful with single-electrolyte solutions. In Figures 11–15, the predictions of Pitzer's method at higher ionic strengths than are supported by the single-salt parameters are also compared to the experimental observations.

It is seen from Figures 11–15 that Pitzer's method works very well over the range of ionic strengths for which the single-salt parameters are valid. In addition, the model can be successfully used to somewhat higher ionic strengths. At very high ionic strengths, however, the model can no longer satisfactorily predict the properties of the mixtures. The degree to which the model can be extrapolated to high ionic strengths varied among the systems studied here. For the NaCl–$(NH_4)_2SO_4$ mixing ratio of 2:1, for example, Pitzer's method was able to predict the experimental water activity to within 0.04 up to an ionic strength of 32 molal even though the NaCl parameters used in the prediction were only valid up to an ionic strength of 13.6 molal. In contrast, with the 1:2 NaCl to $(NH_4)_2SO_4$ mixing ratio, the model could not be used past an ionic strength of 19 molal before the discrepancy between predicted and experimental water activity exceeded 0.04.

4. Discussion of Mixing Rules Results

The results of the comparison of the above mixing rules with the experimental data are summarized in Table 1. All of the mixing rules used above were generally able to predict the water activity of the mixture within the uncertainty in in the measurements over the range of concentrations for which the model could be considered to be strictly valid.

For the ZSR method, the valid concentration range was different than that for the RWR or Pitzer models because this method used single-electrolyte data at the water activity — instead of the ionic strength — of the mixed-electrolyte

solution. This difference was most pronounced for the NaCl–$(NH_4)_2SO_4$ mixture, in which very high ionic strengths were encountered. Because of the extensive association in these solutions, the decrease in water activity at very high concentrations was less than it would have been if the ions had been more extensively hydrated. As is seen in Table 1, the ZSR method could be used to much higher ionic strengths than either of the other two methods for the NaCl–$(NH_4)_2SO_4$ aqueous solutions.

The ZSR method generally requires less data to predict the properties of mixed-electrolyte solutions than does the RWR or Pitzer methods. For example, to predict the properties of an aqueous solution of ammonium sulfate and sodium chloride, only data from the single-electrolyte solutions of these two salts are needed with the ZSR method. However, with even the simplified version of the other two methods used here, data for sodium sulfate and ammonium chloride solutions are also needed to estimate the mixture's properties.

The simplified versions of the RWR and Pitzer method, using only information from single-electrolyte solutions, were found to be quite satisfactory in predicting the water activities in mixed-electrolyte solutions. That is, the terms characterizing the interactions of different ions of the same charge polarity were not needed to predict the properties of the mixture.

Conclusions

The water activity as a function of solute concentration has been determined for several aqueous electrolyte mixtures to high ionic strengths with the

use of an electrodynamic balance apparatus. For two of the systems, NaCl–KCl and NaCl–KBr, the results were consistent with previous investigations and data were obtained to higher concentrations than have been previously reported. The deliquescence behavior of the NaCl–KCl particle studied was consistent with the findings of Tang et al. [26,27], and the measured solute concentration at the eutonic point verified their theoretical predictions. For the NaCl–$(NH_4)_2SO_4$ mixture, there were no data available in the literature, and so it was not possible to determine unambiguously the composition of the particles in their dry state and therefore the absolute solute concentration.

Three different mixing rules were evaluated in their ability to predict the water activity as a function of solute concentration for the mixed-electrolyte solutions studied. The ZSR method and the simplified versions of the RWR and Pitzer methods, using only information from single-electrolyte solutions, were generally able to predict the mixture's water activity to within the uncertainty of the experimental data for the NaCl–KCl and NaCl–KBr systems. For the NaCl–$(NH_4)_2SO_4$ mixture, the different models' predictions were consistent with each other but were inconsistent with the experimental observations if it was assumed that the dry particles were anhydrous. The possibility that water could be contained within the dry particles for this system was considered. If a small amount of water, slightly different for each of the three mixing ratios studied, was assumed to be present in the dry particles for this system, then the mixing rules' predictions agreed closely with the experimental findings even at high ionic strengths.

Acknowledgements

This work was supported by the U.S. Environmental Protection Agency under grant number R-810857.

References

[1] J.H. Seinfeld. *Atmospheric Chemistry and Physics of Air Pollution.* John Wiley and Sons, New York, 1986.

[2] J.M. Prospero, R.J. Charlson, V. Mohnen, R. Jaenicke, A.C. Delany, J. Moyers, W. Zoller, and K. Rahn. *Rev. Geophys. and Space Phys.*, 21:1607, 1983.

[3] P. Saxena, A.B. Hudischewsky, C. Seigneur, and J.H. Seinfeld. *Atmospheric Environment*, 20:1471, 1986.

[4] L.A. Bromley. *A.I.Ch.E. Journal*, 19:313, 1973.

[5] G. Hanel and B. Zankl. *Tellus*, 31:478, 1979.

[6] J. Sangster, T.T. Tang, and F. Lenzi. *Can. J. Chem. Engr.*, 51:234, 1973.

[7] R.H. Stokes and R.A. Robinson. *J. Phys. Chem.*, 70:2126, 1966.

[8] M.H. Lietzke and R.W. Stoughton. *J. Solution Chem.*, 1:299, 1972.

[9] C.L. Kusik and H.P. Meissner. *Ind. Engr. Chem. Proc. Des. Develop.*, 12:112, 1973.

[10] K.S. Pitzer and J.J. Kim. *J. Amer. Chem. Soc.*, 96:5701, 1974.

[11] R.A. Robinson and V.E. Bower. *J. Res. Nat. Bur. Stand.*, 69A:365, 1965.

[12] P.J. Reilly, R.H. Wood, and R.A. Robinson. *J. Phys. Chem.*, 75:1305, 1971.

[13] G. Scatchard, R.M. Rush, and J.S. Johnson. *J. Phys. Chem.*, 74:3786, 1970.

[14] K.H. Khoo. *J. Chem. Soc., Faraday Trans. 1*, 82:1, 1986.

[15] J. Sangster and F. Lenzi. *Can. J. Chem. Engr.*, 52:392, 1974.

[16] P. Saxena and T.W. Peterson. *J. Colloid and Interface Sci.*, 79:496, 1981.

[17] M.D. Cohen, R.C. Flagan, and J.H. Seinfeld. To be submitted to *J. Phys. Chem.*, 1986.

[18] A.C.D. Rivett. *J. Chem. Soc.*, 121:379, 1922.

[19] R.A. Robinson. *J. Phys. Chem.*, 65:662, 1961.

[20] A.N. Kirgintsev and A.V. Luk'yanov. *Russ. J. Phys. Chem.*, 37:1501, 1963.

[21] A.K. Covington, T.H. Lilley, and R.A. Robinson. *J. Phys. Chem.*, 72:2759, 1968.

[22] R. Huston and J.N. Butler. *Analytical Chem.*, 41:1695, 1969.

[23] J.H. Stern and C.W. Anderson. *J. Phys. Chem.*, 68:2528, 1968.

[24] M.C.P. de Lima and K.S. Pitzer. *J. Solution Chem.*, 12:171, 1983.

[25] M.A. Clynne, R.W. Potter, II, and J.L. Hass, Jr. *J. Chem. Engr. Data*, 26:396, 1981.

[26] I.N. Tang. *J. Aerosol Sci.*, 7:361, 1976.

[27] I.N. Tang, H.R. Munkelwitz, and J.G. Davis. *J. Aerosol Sci.*, 9:505, 1978.

[28] L.R. Martin. Kinetic studies of sulfite oxidation in aqueous solutions. In J.G. Calvert, editor, *Acid Precipitation: SO_2, NO, NO_2 Oxidation Mechanisms - Atmospheric Considerations*, Ann Arbor Science Publishers, 1982.

[29] T.E. Graedel and C.J. Weschler. *Rev. Geophys. and Space Phys.*, 19:505, 1981.

[30] K.S. Pitzer. *J. Phys. Chem.*, 77:268, 1973.

[31] K.S. Pitzer and G. Mayorga. *J. Phys. Chem.*, 77:2300, 1973.

[32] G.M. Rosenblatt. *A.I.Ch.E. Journal*, 27:619, 1981.

[33] C.E. Harvie and J.H. Weare. *Geochim. et Cosmochim. Acta*, 44:981, 1980.

[34] C.E. Harvie, N. Moller, and J.H. Weare. *Geochim. et Cosmochim. Acta*, 48:723, 1984.

electrolyte mixture		moles of comp. 2 per mole of comp. 1	range of ionic strengths for which a_w measured	range of a_w measured	I_{max} for ZSR	σ_{a_w} for ZSR (n_{pts})	I_{max} for RWR and Pitzer	σ_{a_w} for RWR (n_{pts})	σ_{a_w} for Pitzer (n_{pts})
comp. 1	comp. 2				(e)	(f)	(g)	(f)	(f)
NaCl	KCl	1.0027	4.8–16.0	0.46–0.84	11.0	0.012 (6)	12.7	0.016 (6)	0.015 (6)
NaCl	KBr	0.6195	2.0–16.9	0.37–0.92	11.8	0.022 (19)	12.7	0.018 (20)	0.019 (20)
NaCl	$(NH_4)_2SO_4$	0.5003	8.8–33.3 (b)	0.38–0.81	23.8	0.011 (4)	13.6	0.024 (3)	0.027 (3)
NaCl	$(NH_4)_2SO_4$	1.0002	9.4–74.5 (c)	0.29–0.84	32.8	0.015 (10)	13.6	0.009 (4)	0.010 (4)
NaCl	$(NH_4)_2SO_4$	1.9981	12.9–76.8 (d)	0.28–0.80	36.9	0.009 (5)	13.6	0.002 (1) (h)	0.003 (1) (h)
NaCl	$(NH_4)_2SO_4$	(a)	8.8–76.8	0.28–0.84		0.012 (19)	13.6	0.014 (8)	0.016 (8)

Table 1: Summary of experimental measurements, range of applicability, and success of electrolyte solution models in prediction of water activities; (a) summary for all NaCl–$(NH_4)_2SO_4$ mixing ratios; (b) assuming dry-particle stoichiometry of 0.512 moles of water per mole of solute; (c) assuming dry-particle stoichiometry of 0.588 moles of water per mole of solute; (d) assuming dry-particle stoichiometry of 0.663 moles of water per mole of solute; (e) limited by range of water activity data for relevant single-salt solutions; (f) there were n_{pts} data points at ionic strengths less than I_{max} ; standard deviation calculated from comparison of these data points with model predictions; (g) limited by maximum ionic strength for which relevant single-salt solution data are available; (h) absolute value of deviation between measured and predicted a_w .

Figure Captions

Figure 1: Weight fraction solute vs. water activity for NaCl–KCl mixture; particle assumed anhydrous when dry; moles KCl / moles NaCl = 1.0; ○, calculated from 25 ℃ data of Ref [19]; □, experiment 1; △, experiment 2; filled points indicate measurements beginning with a dry particle; datum point (A) is a partially dissolved state; solid line, predictions of ZSR model; dotted line, prediction of RWR model (note: the two models' predictions are indistinguishable over most of the concentration range).

Figure 2: Ratio of total particle mass to solute mass vs. time for NaCl–KCl particle during humidity transients in which deliquescence occurred; moles KCl / moles NaCl = 1.0; (a),(b), end of deliquescence events; (c), chamber relative humidity increased from 0.70, eventually reached 0.76; (d), chamber relative humidity increased from 0.76, eventually reached 0.86.

Figure 3: Weight fraction solute vs. water activity for NaCl–KBr mixture; particles assumed anhydrous when dry; moles KBr / moles NaCl = 0.6195; △, 25 ℃ data from Ref [21]; ○, particle 1, expts 1–5; □, particle 2, expts 1 and 2; filled points indicate measurements beginning with a dry particle; solid line, predictions of ZSR model; dotted line, prediction of RWR model (note: the two models' prediction are indistinguishable over most of the concentration range).

Figure 4: Weight fraction solute vs. water activity for NaCl–$(NH_4)_2SO_4$ mixture # 1; particle assumed anhydrous when dry; moles $(NH_4)_2SO_4$ / moles NaCl = 0.5; □, experimental measurements; filled points indicate measurements beginning with a dry particle; datum point (A) is a partially dissolved state; solid line, predictions of ZSR model; dotted line, prediction of RWR model (note: the two models' prediction are indistinguishable over most of the concentration range).

Figure 5: Weight fraction solute vs. water activity for NaCl–$(NH_4)_2SO_4$ mixture # 2; particles assumed anhydrous when dry; moles $(NH_4)_2SO_4$ / moles NaCl = 1.0; □, particle 1; △, particle 2; ○, particle 3; filled points indicate measurements beginning with a dry particle; datum point (A) is a partially dissolved state; solid line, predictions of ZSR model; dotted line, prediction of RWR model (note: the two models' prediction are indistinguishable over most of the concentration range).

Figure 6: Weight fraction solute vs. water activity for NaCl–$(NH_4)_2SO_4$ mixture # 3; particle assumed anhydrous when dry; moles $(NH_4)_2SO_4$ / moles NaCl = 2.0; □, experimental measurements; filled points indicate measurements beginning with a dry particle; datum point (A) is a partially dissolved state; solid line, predictions of ZSR model; dotted line, prediction of RWR model (note: the two models' prediction are indistinguishable over most of the concentration range).

Figure 7: Ratio of total particle mass to solute mass vs. time for NaCl–$(NH_4)_2SO_4$ particles during humidity transients in which deliquescence occurred; solid lines, particles assumed anhydrous in dry state; dotted lines, particles assumed to have dry-particle stoichiometry as given in Table 1; □, moles $(NH_4)_2SO_4$ / moles NaCl = 0.5; △, moles $(NH_4)_2SO_4$ / moles NaCl = 1.0; ◇, moles $(NH_4)_2SO_4$ / moles NaCl = 2.0; (note: the starting point for each curve plotted corresponds to the beginning of a humidity transient, but the times plotted are not the actual, absolute times during the measurements; *e.g.*, for a 1:1 $(NH_4)_2SO_4$: NaCl particle assumed anhydrous in dry state, the humidity transient begins at "t = 5 minutes" in this figure).

Figure 8: Weight fraction solute vs. water activity for NaCl–$(NH_4)_2SO_4$ mixture # 1; assuming dry-particle stoichiometry of 0.512 moles of water per mole of solute; moles $(NH_4)_2SO_4$ / moles NaCl = 0.5; □, experimental measurements; filled points indicate measurements beginning with a dry particle; datum point (A) is a partially dissolved state; solid line, predictions of ZSR model; dotted line, prediction of RWR model (note: the two models' prediction are indistinguishable over most of the concentration range).

Figure 9: Weight fraction solute vs. water activity for NaCl–$(NH_4)_2SO_4$ mixture # 2; assuming dry-particle stoichiometry of 0.588 moles of water per mole of solute; moles $(NH_4)_2SO_4$ / moles NaCl = 1.0; □, particle 1; △, particle 2; ○, particle 3; filled points indicate measurements beginning with a dry particle; datum point (A) is a partially dissolved state; solid line, predictions of ZSR model; dotted line, prediction of RWR model (note: the two models' prediction are indistinguishable over most of the concentration range).

Figure 10: Weight fraction solute vs. water activity for NaCl–$(NH_4)_2SO_4$ mixture # 3; assuming dry-particle stoichiometry of 0.663 moles of water per mole of solute; moles $(NH_4)_2SO_4$ / moles NaCl = 2.0; □, experimental measurements; filled points indicate measurements beginning with a dry particle; datum point (A) is a partially dissolved state; solid line, predictions of ZSR model; dotted line, prediction of RWR model (note: the two models' prediction are indistinguishable over most of the concentration range).

Figure 11: Water activity vs. molal ionic strength, I, for NaCl–KCl mixture; particle assumed anhydrous when dry; moles KCl / moles NaCl = 1.0; □, experiment measurements; only data corresponding to fully-dissolved solute are plotted; solid line, predictions of Pitzer model for $I < I_{max}$; dotted line, predictions of Pitzer model for $I > I_{max}$.

Figure 12: Water activity vs. molal ionic strength, I, for NaCl–KBr mixture; particle assumed anhydrous when dry; moles KBr / moles NaCl = 0.6195; ○, particle 1; □, particle 2; only data corresponding to fully-dissolved solute are plotted; solid line, predictions of Pitzer model for $I < I_{max}$; dotted line, predictions of Pitzer model for $I > I_{max}$.

Figure 13: Water activity vs. molal ionic strength, I, for NaCl–$(NH_4)_2SO_4$ mixture # 1; assuming dry-particle stoichiometry of 0.512 moles of water per mole of solute; moles $(NH_4)_2SO_4$ / moles NaCl = 0.5; □, experimental measurements; only data corresponding to fully-dissolved solute are plotted; solid line, predictions of Pitzer model for $I < I_{max}$; dotted line, predictions of Pitzer model for $I > I_{max}$.

Figure 14: Water activity vs. molal ionic strength, I, for NaCl–$(NH_4)_2SO_4$ mixture # 2; assuming dry-particle stoichiometry of 0.588 moles of water per mole of solute; moles $(NH_4)_2SO_4$ / moles NaCl = 1.0; □, particle 1; △, particle 2; ○, particle 3; only data corresponding to fully-dissolved solute are plotted; solid line, predictions of Pitzer model for $I < I_{max}$; dotted line, predictions of Pitzer model for $I > I_{max}$.

Figure 15: Water activity vs. molal ionic strength, I, for NaCl–$(NH_4)_2SO_4$ mixture # 3; assuming dry-particle stoichiometry of 0.663 moles of water per mole of solute; moles $(NH_4)_2SO_4$ / moles NaCl = 2.0; □, experimental measurements; only data corresponding to fully-dissolved solute are plotted; solid line, predictions of Pitzer model for $I < I_{max}$; dotted line, predictions of Pitzer model for $I > I_{max}$.

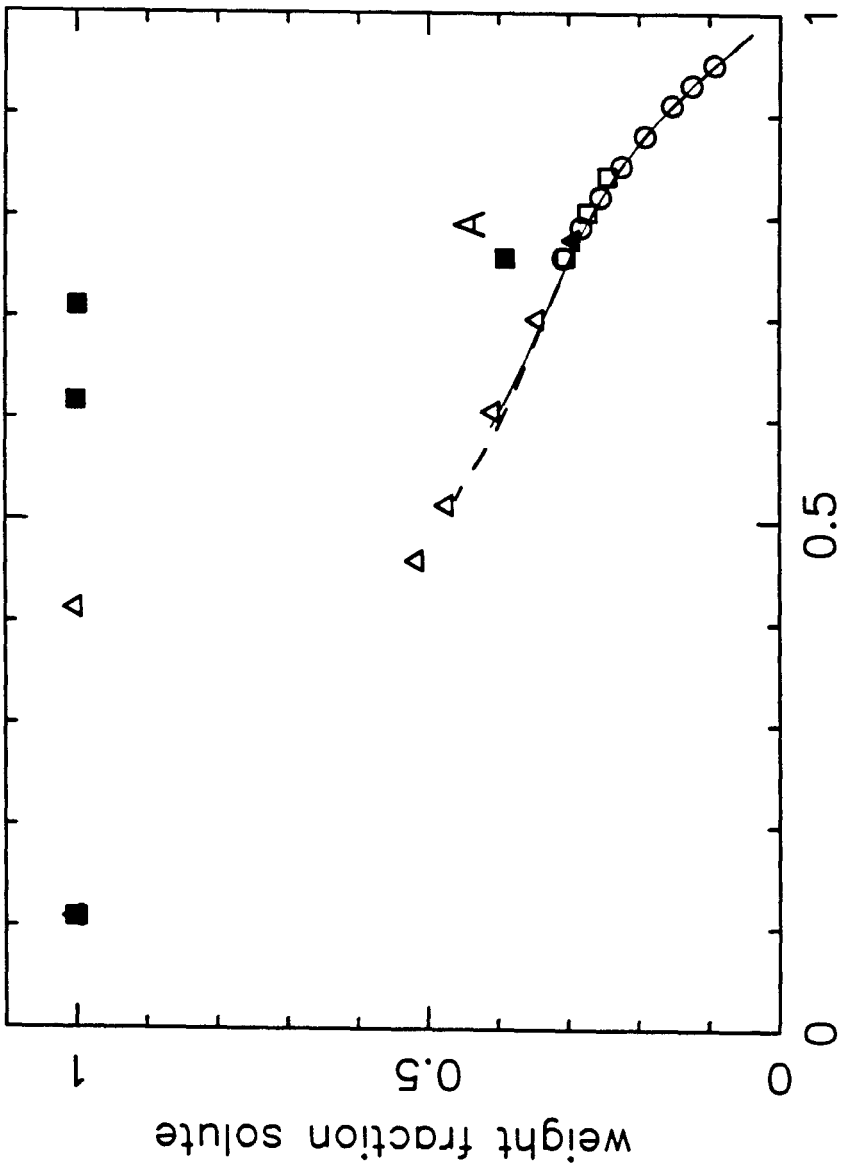

Figure 1

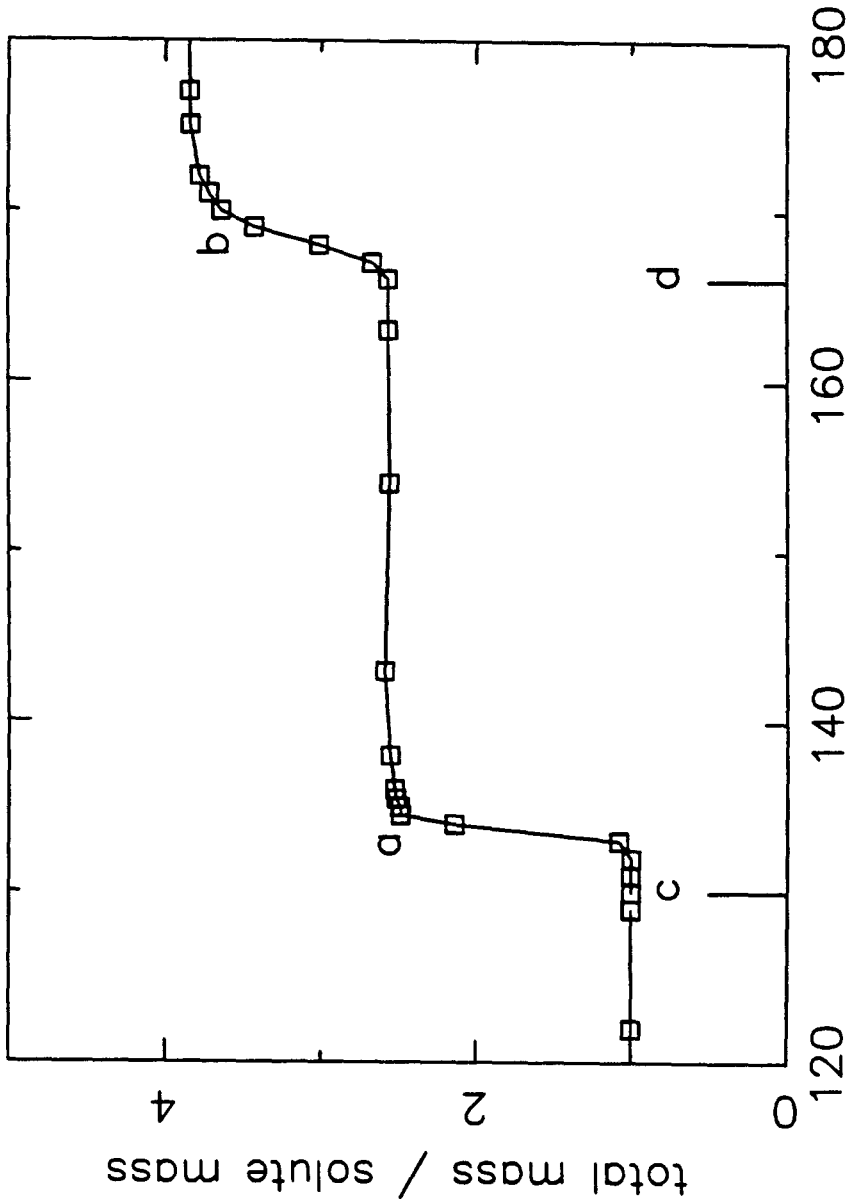

Figure 2

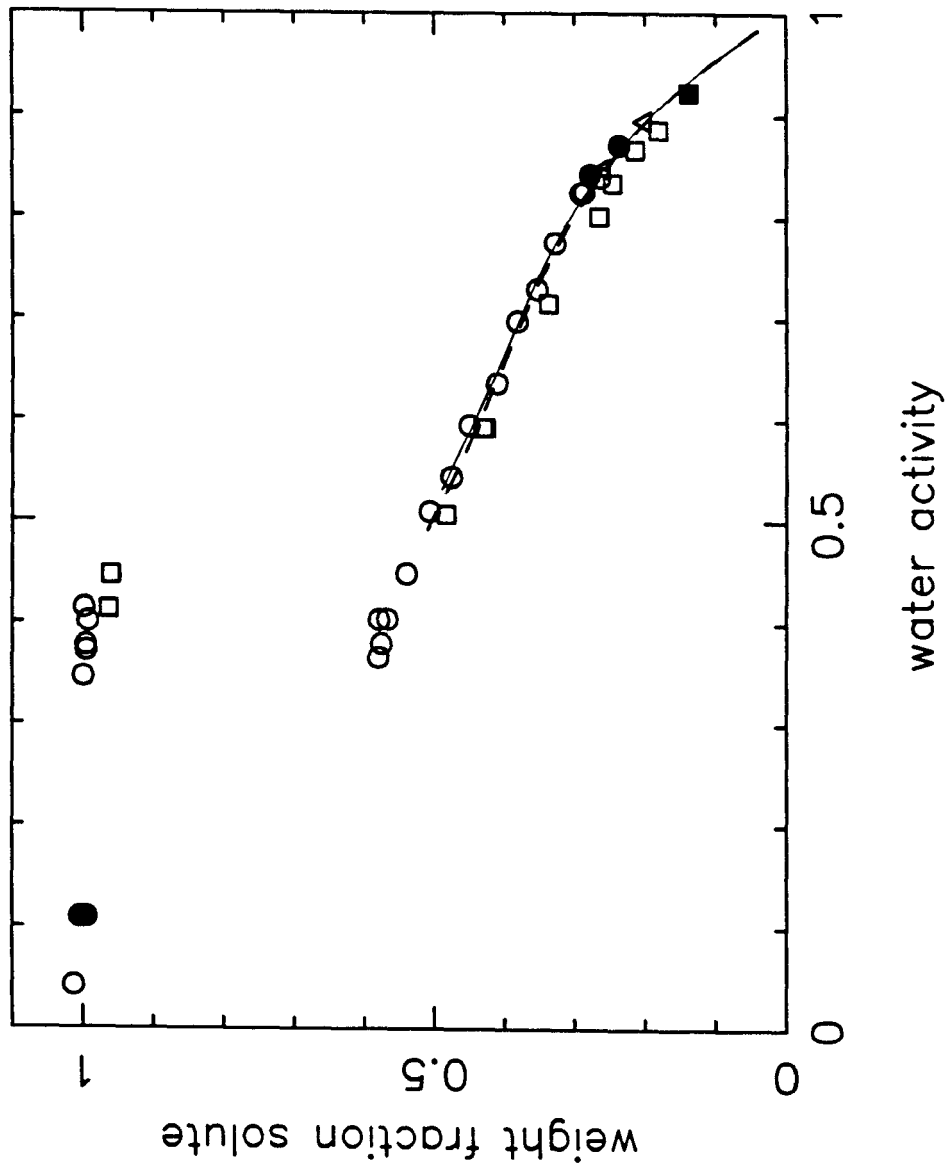

Figure 3

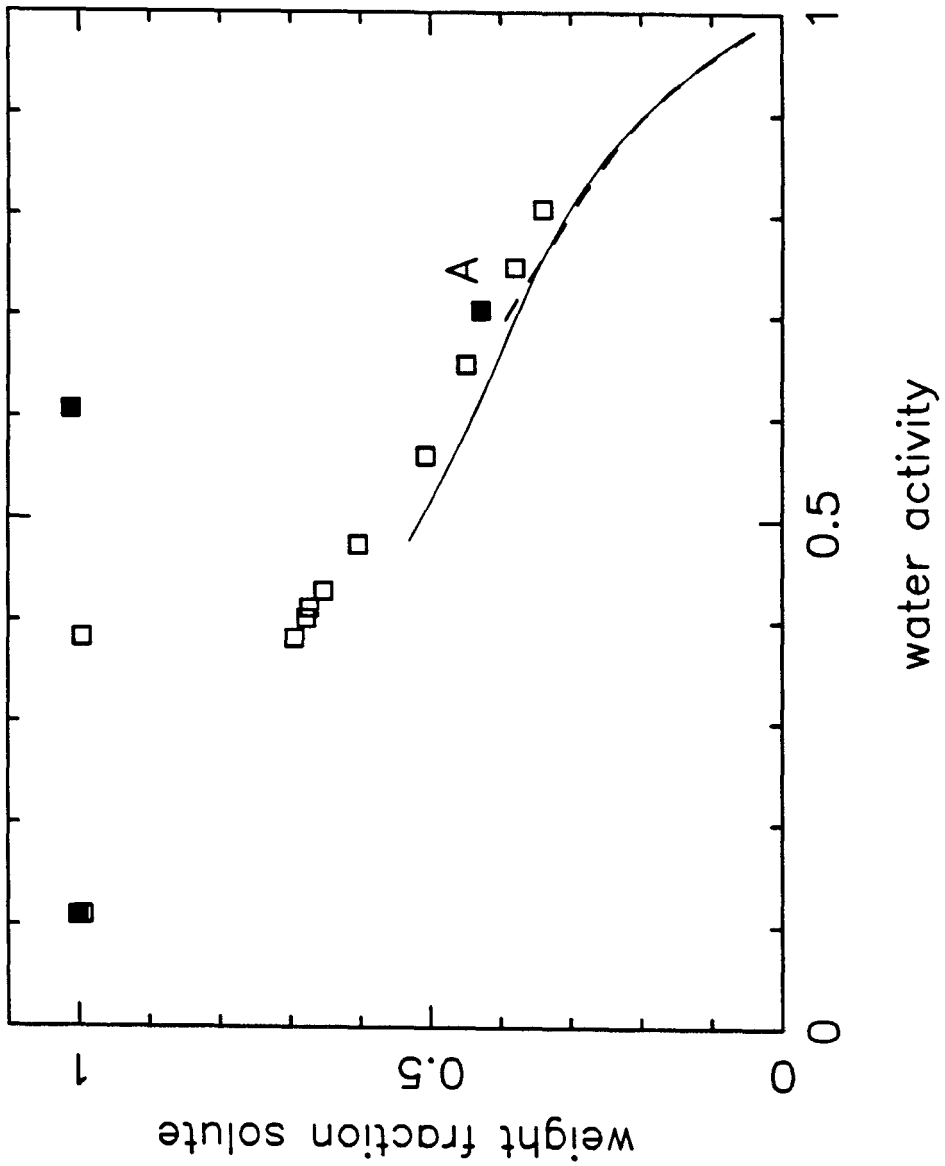

Figure 4

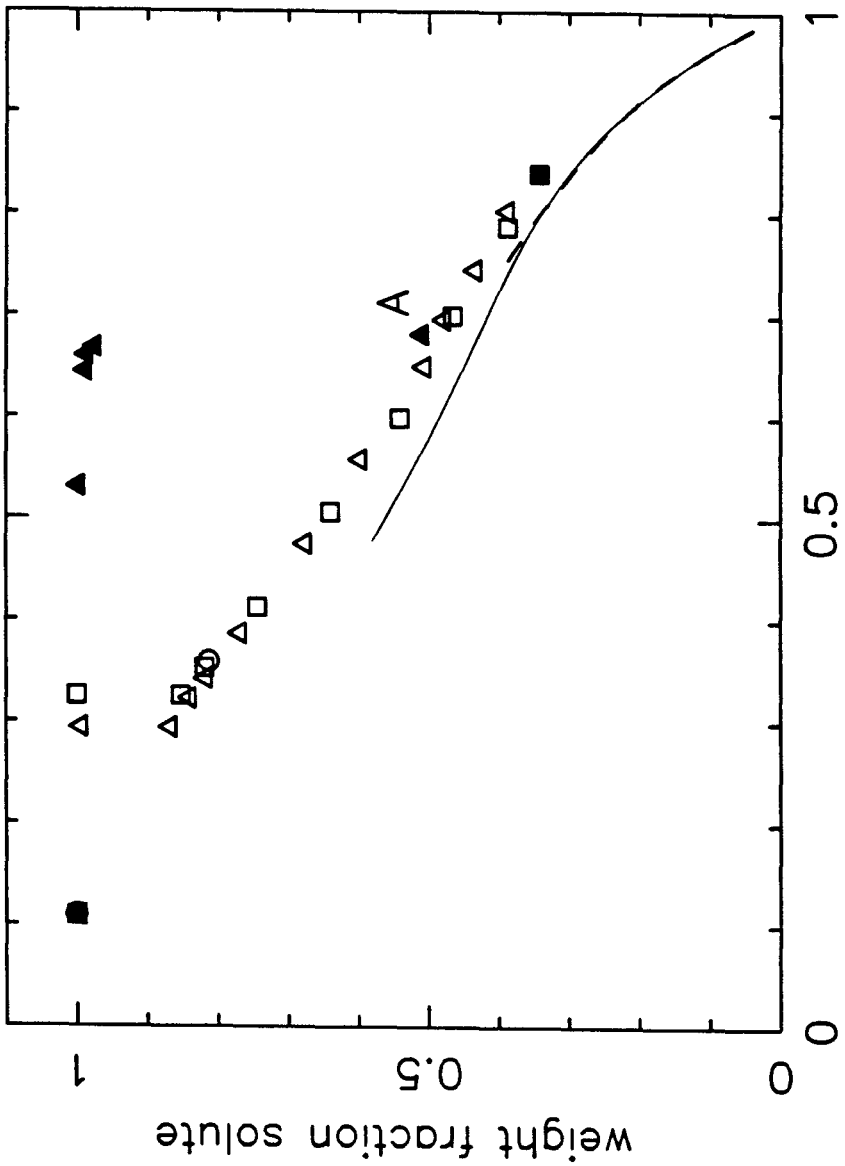

Figure 5

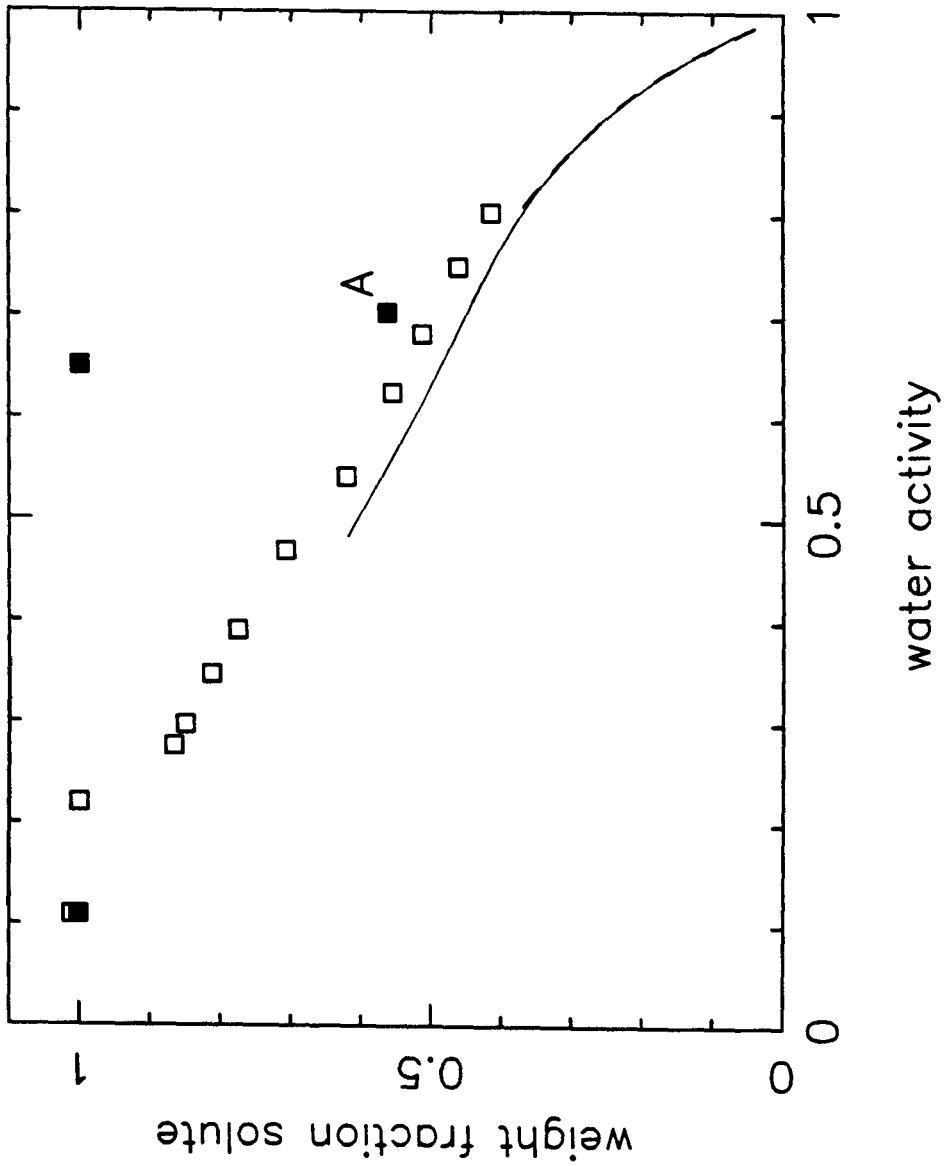

Figure 6

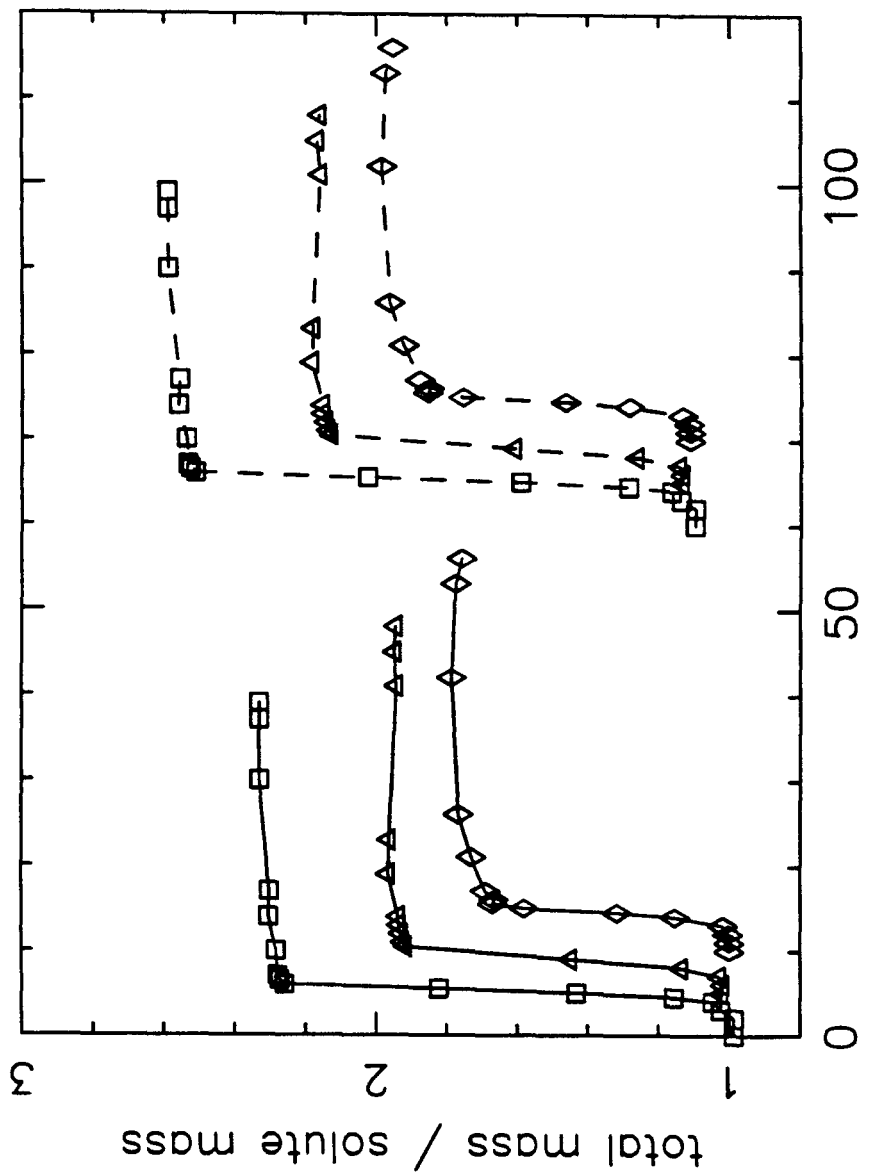

Figure 7

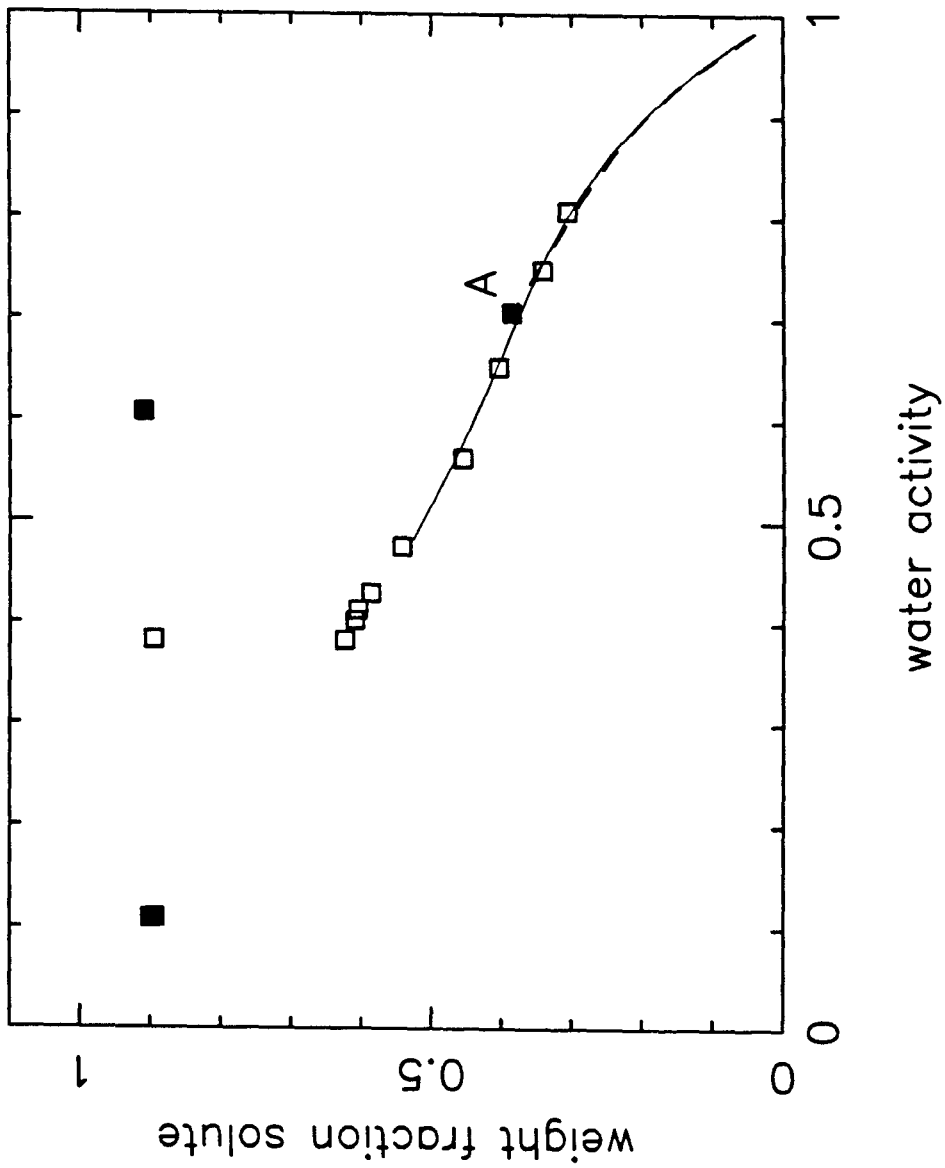

Figure 8

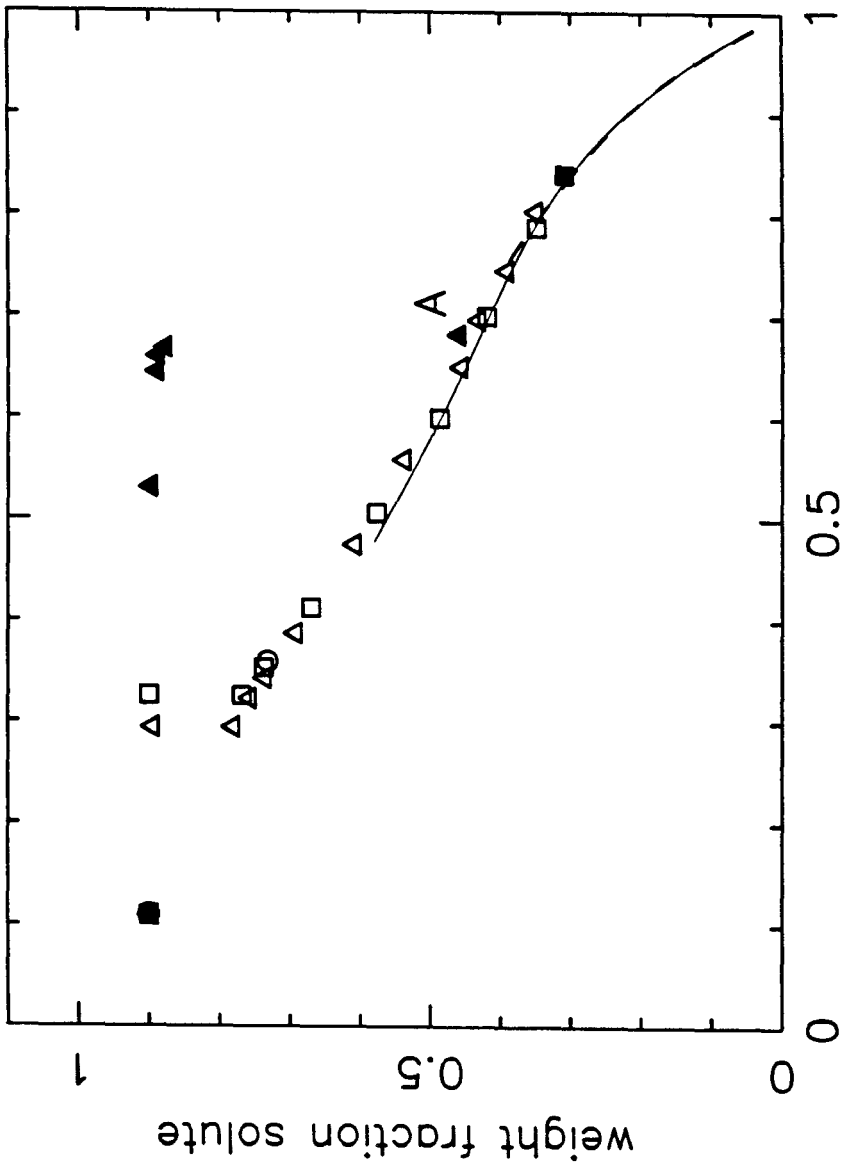

Figure 9

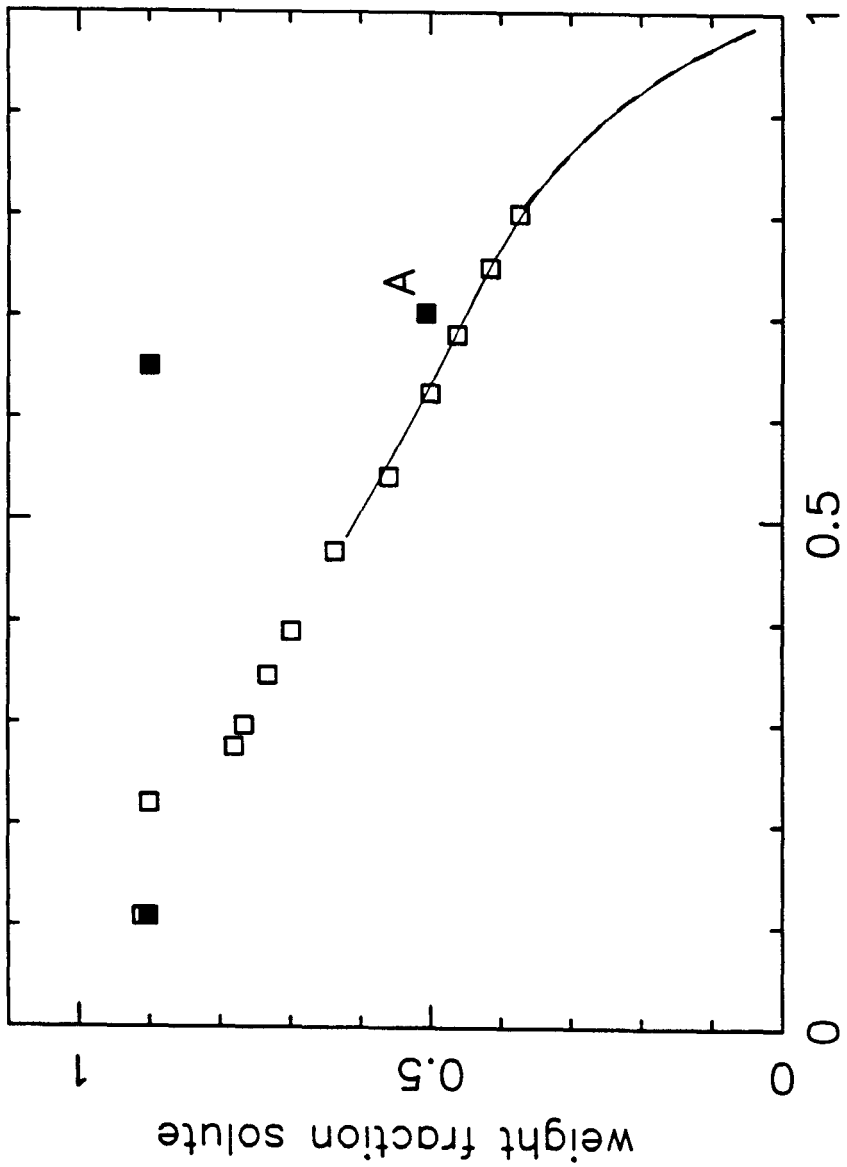

Figure 10

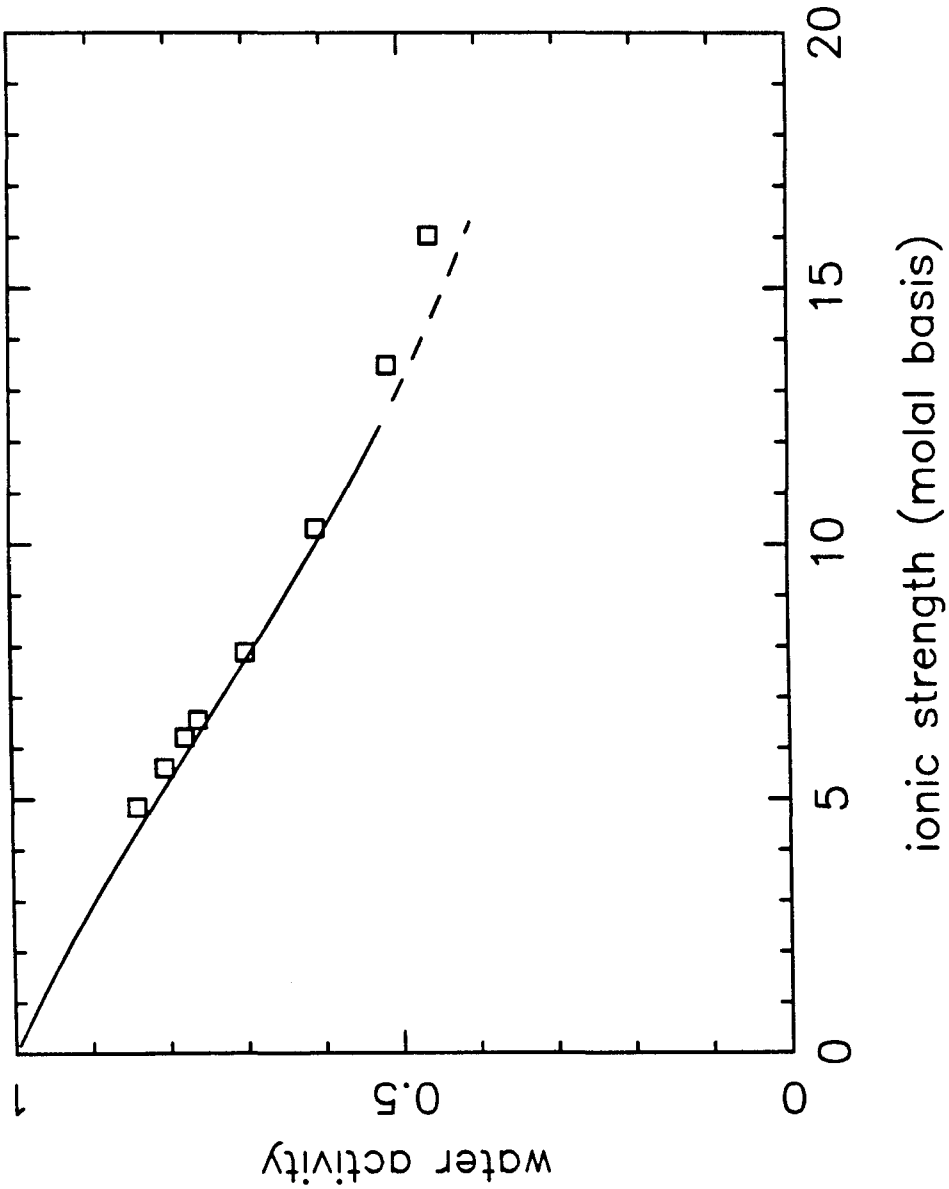

Figure 11

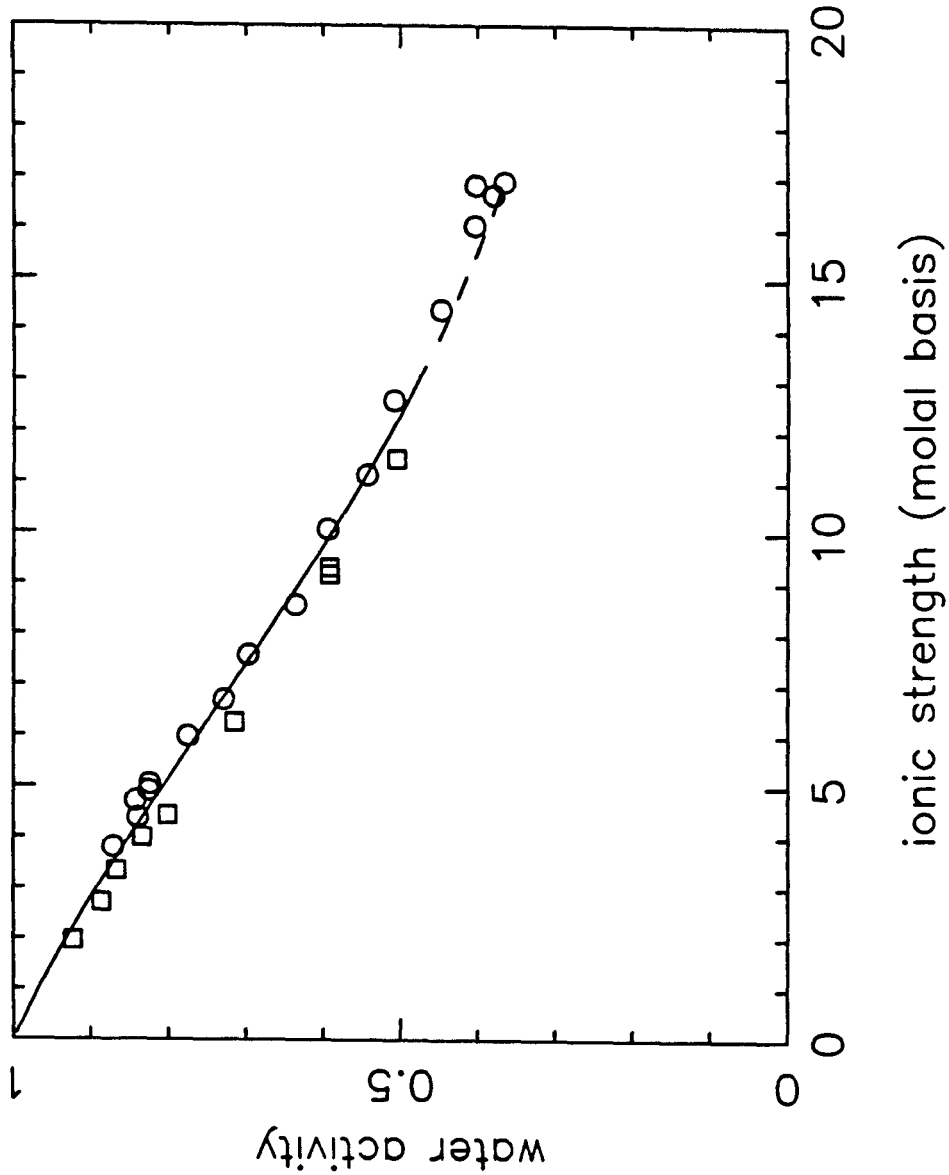

Figure 12

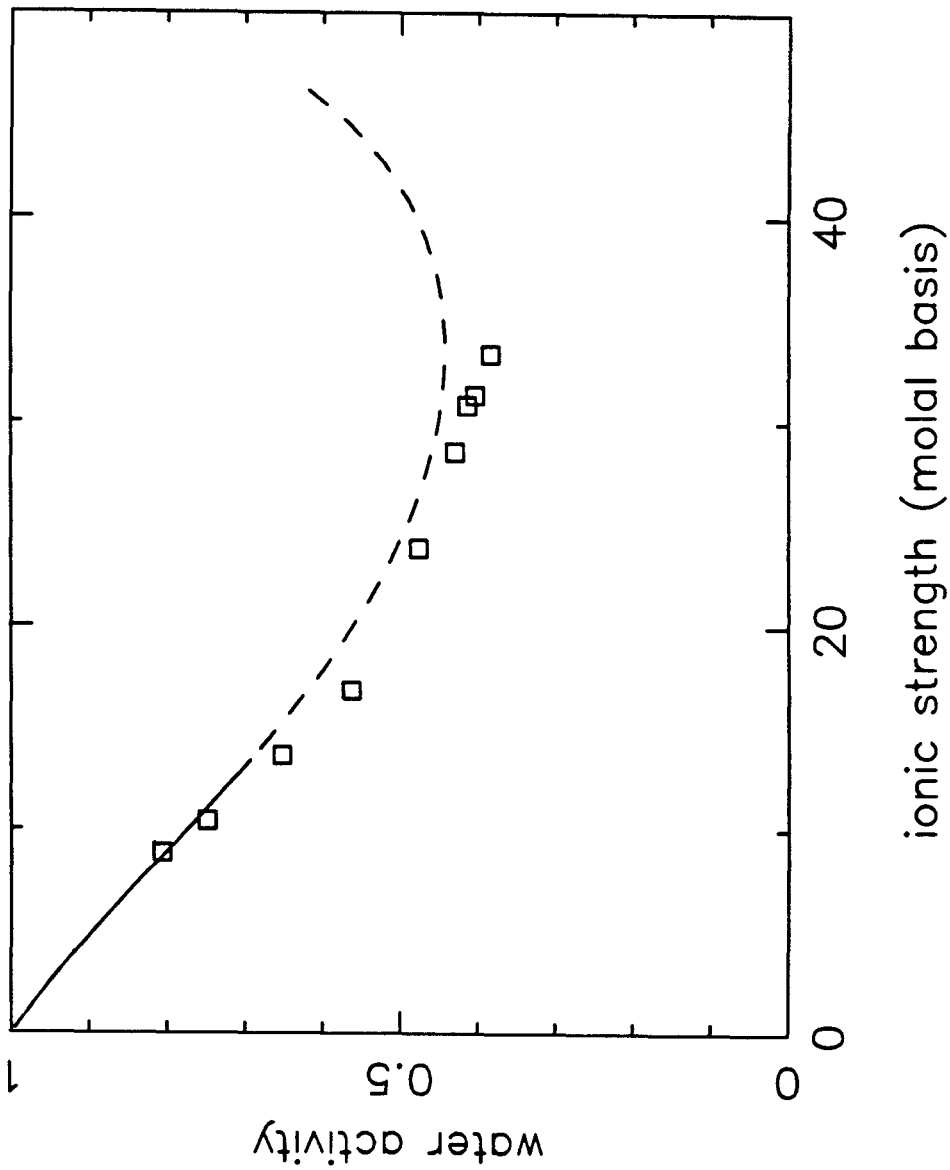

Figure 13

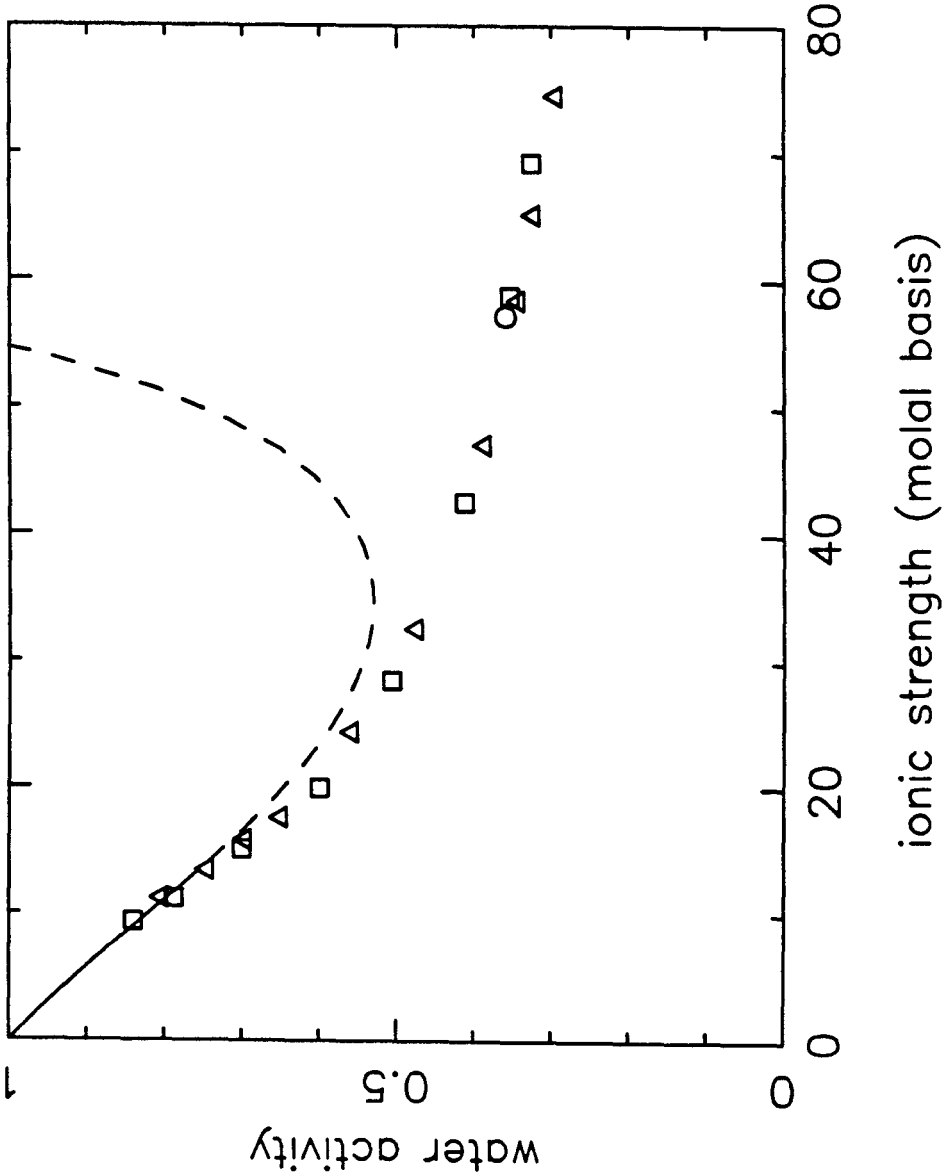

Figure 14

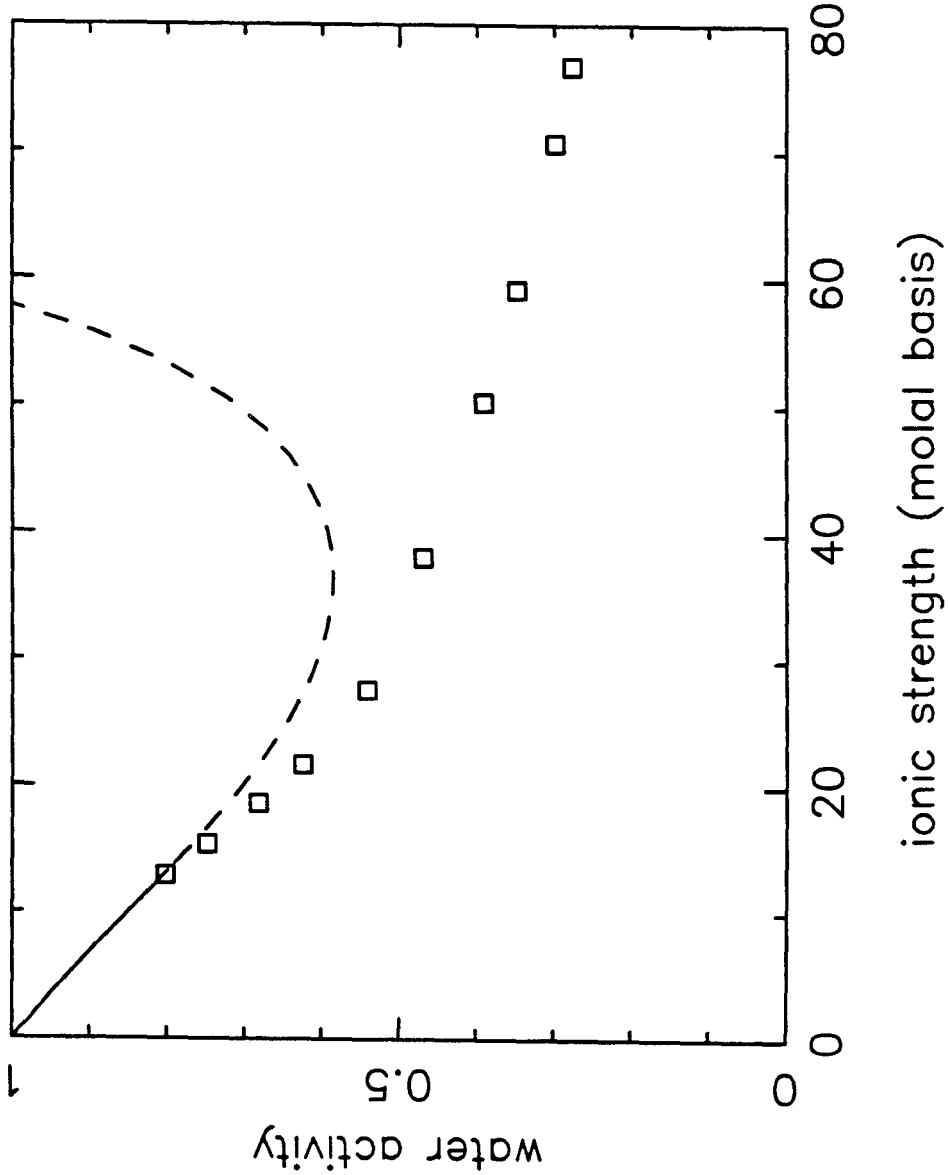

Figure 15

Chapter 3: Solute Nucleation

Studies of Concentrated Electrolyte Solutions using the Electrodynamic Balance. III. Solute Nucleation

Mark D. Cohen, Richard C. Flagan*,
and John H. Seinfeld†

Chemical Engineering
California Institute of Technology
Pasadena, CA 91125

*Environmental Engineering Science
†To whom correspondence should be sent

Abstract

The nucleation of crystals from aqueous solution has been investigated for several common inorganic salts alone and in mixtures. Single, charged solution droplets approximately 20 microns in diameter were suspended in an electrodynamic balance and continuously weighed. The solute concentration in the droplet was changed by adjusting the relative humidity of the air surrounding the particle. Nucleation theory was used to estimate the surface excess free energy and critical nucleus size from the measured supersaturation at which nucleation occurred.

Introduction

The nucleation of crystals from solution is a phenomenon of widespread importance, with occurrences in many biological, environmental, and industrial situations. The nucleation may be heterogeneous or homogeneous. In heterogeneous nucleation, the formation of the new phase is catalyzed by foreign surfaces or foreign ions. For example, dust particles or the walls of the containing vessel can act as nucleation catalysts. Homogeneous nucleation requires higher supersaturations than heterogeneous nucleation and refers to initiation of the new phase by itself, directly from solution. Homogeneous nucleation has traditionally been difficult to study, because with conventional techniques, it is hard to eliminate the effects of foreign surfaces in even the most careful of experiments [1,2,3]. Thus, there are few published data on homogeneous nucleation from solution. On the other hand, there is considerably more information available about heterogeneous nucleation [4,5,6].

It has long been known that small droplets can often be supercooled to a much higher degree than bulk samples before crystallization occurs [7], presumably because some of the droplets do not contain foreign particles [8]. This has been exploited in attempts to study homogeneous nucleation. In one technique, the aqueous solution of interest was dispersed as droplets in oil [9,10,11], and nucleation in the droplets was measured as a function of supercooling. As will be shown later, the nucleation observed in at least some of these experiments was probably heterogeneous.

Aqueous salt solutions have also been prepared as a monodisperse aerosol population [12,13,14,15] in order to study homogeneous nucleation. In these experiments, supersaturation of the salt was achieved by lowering the humidity of the air surrounding the droplets. With this technique, the size of the particles before and after crystallization is measured. However, since accurate density data do not exist for highly supersaturated solutions, the salt concentration at which nucleation occurs can only be roughly estimated from the relative particle sizes. For very small droplets, the calculation is further complicated by the necessity of including the effect of curvature on vapor pressure, the Kelvin effect, since surface tension data for supersaturated solutions are not generally available.

Recently, homogeneous nucleation in aqueous solutions has been studied by suspending single, charged particles in an electrodynamic balance [16,17,18,19]. In these investigations, solute concentration in a levitated droplet was increased by lowering the surrounding humidity until the solute crystallized. The solute concentration at which nucleation occurred was determined from the relative mass of particle before and after crystallization. In the present work, this single-particle technique has been used to study the homogeneous nucleation of several common inorganic salts from their supersaturated aqueous solutions. Both single-electrolyte and mixed-electrolyte solutions were studied. A simple nucleation theory was used in conjunction with the results for the single-electrolyte solutions to estimate the surface excess free energy and critical size of the crystalline embryo.

Experimental Method

The experimental system has previously been described in detail [20]. Briefly, a single, charged particle of known composition is suspended in an electrodynamic balance. The humidity of the air surrounding the particle could be varied. Because of the small size of the droplet, the droplet solution rapidly equilibrates with the vapor-phase water. By changing the relative humidity of the vapor, the droplet can be made to absorb or evaporate water and thereby change the concentration of solute. The relative mass of the particle at any humidity is obtained from the balancing voltage required to levitate the particle. The solute concentration in a droplet can be calculated from the ratio of the dry particle's balancing voltage to the wet particle's balancing voltage.

During the course of the water activity measurements described in Parts I and II [20,21], it was found with most substances that a suspended droplet suddenly and violently crystallized when the solute concentration reached a certain critical value. Figures 1,2, and 3 show some typical crystallization measurements for NaCl. The crystallization usually occurred while the humidity was being lowered and the particle was losing water in response to this changing humidity. The crystallization was very fast, and was normally completed in less than 1 second. With a few salts, the particle did not transform immediately to its final dry weight. In these cases, most of the water loss occurred quickly, but the droplet then continued to lose water slowly until the final dry weight was reached.

There are two small systematic errors in our measurements. The first lies in the measurement of the critical balancing voltage (point A in Figures 1–3). It is difficult to follow the particle's balancing voltage exactly during a humidity transient. Thus, it is difficult to precisely determine the voltage at point A, and generally, this voltage will be overestimated because the observer will usually be slightly behind in tracking the particle's balancing voltage. In contrast, the dry voltage (*e.g.*, point B in Figures 1–3) is easy to measure precisely because it is unchanging. Because of this systematic error, the solute concentration at the critical state will generally be slightly underestimated. With the incorporation of an automatic balancing voltage-tracking system [22,23], this problem could be avoided although such a system was not used here. A second systematic error, discussed in Part I, is related to the fact that the particle's displacement from the center of the chamber due to the gas flow increases with particle size. Since the electric field supporting the particle decreases with distance away from the center, this also leads to a slight underestimation of the critical solute concentration. The critical weight fraction of solute in the droplet has been underestimated by at most 0.01 due to these systematic biases.

Theory of Homogeneous Nucleation from Solution

Following Tang et al. [16], we shall use an elementary version of classical nucleation theory [3] to interpret our results. According to this theory, the free energy barrier to nucleation of a given sized crystalline embryo is

$$\triangle G = A\sigma + V\triangle G_v \tag{1}$$

where A is the total interfacial area of the embryo, V is the total volume of the embryo, σ is the average interfacial energy based on A, and $\triangle G_v$ is the excess free energy of the solute per unit volume in the crystalline phase over that in solution. $\triangle G_v$ is given by

$$\triangle G_v = \frac{\rho_{cryst}}{w_s}(\mu^{sat} - \mu^{supersat}) \tag{2}$$

where ρ_{cryst} is the density of the crystalline phase, w_s is the molecular weight of the solute, μ^{sat} is the chemical potential of the solute in a solution saturated with respect to the crystalline phase of interest, and $\mu^{supersat}$ is the chemical potential of the solute in the supersaturated solution. A characteristic dimension, y, is defined such that the local surface area for each type of surface and the total volume of the crystalline embryo are given by

$$A_i = k_i y^2 \tag{3}$$

$$V = \ell y^3 \tag{4}$$

where the k_i and ℓ are geometrical constants dependent on the morphology of the particular crystal of interest. By definition,

$$A = \sum_i A_i = \sum_i k_i y^2 \tag{5}$$

and so the average surface energy is given by

$$\sigma = \frac{\sum_i A_i \sigma_i}{A} = \frac{\sum_i k_i \sigma_i}{\sum_i k_i} \tag{6}$$

Substitution into eq 1 leads to

$$\triangle G = (\textstyle\sum_i k_i)\sigma y^2 + \ell \triangle G_v y^3 \tag{7}$$

According to this simple theory, the critical size of the nucleus is that for which $\triangle G$ is maximized with respect to y. Once the embryo has reached this size, nucleation has occurred and the crystal grows spontaneously from solution. This critical size, y_c, is given by

$$y_c = -\frac{2\alpha\sigma}{3\triangle G_v} \tag{8}$$

where $\alpha = \sum_i k_i/\ell$. Substitution of this critical size into eq 7 yields the critical free energy change for nucleation,

$$\triangle G_c = \frac{4(\sum_i k_i)\alpha^2\sigma^3}{27\triangle {G_v}^2} \tag{9}$$

The rate of nucleation is then written as

$$J = K \exp\left(\frac{-\triangle G_c}{k_b T}\right) \tag{10}$$

where $\triangle G_c$ is given by eq 9, k_b is Boltzman's constant, and T is the absolute temperature. The correct value of the pre-exponential factor, K, is not known at the present time. Theoretical estimates of its value range from 10^{24} to 10^{36} $cm^{-3}sec^{-1}$. An intermediate value that has been commonly used [9,24,25] is 10^{30} $cm^{-3}sec^{-1}$. The sensitivity of the calculated results to variations in the parameter K is examined below. The formation of a single critical-sized nucleus is assumed to be sufficient to initiate the rapid and complete crystallization of the entire droplet. Then, for a given rate of critical nucleus formation per unit volume per unit time, J, the expected induction time, t_i, before a nucleation event happens in a droplet of volume V_{drop} would be

$$t_i = \frac{1}{V_{drop} J} \tag{11}$$

Thus, if one knows the time required for crystallization to occur, the droplet volume, the concentration at crystallization, the chemical potential of the solute in the saturated and supersaturated solution, and the shape factors for the crystalline phase, one can calculate the average interfacial free energy from the above equations to be

$$\sigma = \left[\frac{4(\sum_i k_i)\alpha^2}{27\triangle G_v{}^2 k_b T} \ln(V_{drop} K t_i)\right]^{1/3} \tag{12}$$

The droplet volume at the crystallization concentration must be estimated in order to calculate σ from eq 12. To accomplish this, the absolute mass of the dry particle was measured as described in Part I. The mass of the droplet at the critical concentration was then known from the ratio of its balancing voltage to that of the dry particle. The densities of aqueous salt solutions are, however, generally known only up to the saturation concentration. Because the value of σ calculated from eq 12 is relatively insensitive to the droplet volume, we used the following procedure to estimate the density of the supersaturated solutions.

We assumed that the density of the solution could be written as

$$\rho_s = \frac{n_w w_w + n_s w_s}{n_w v_w + n_s v_s} \tag{13}$$

where n_w and n_s are the number of moles, w_w and w_s are the molecular weights, and v_w and v_s are the molar volumes of the water and the solute in the solution, respectively. Eq 13 can be rearranged into the following form:

$$\frac{w_w + 0.018\, m w_s}{\rho_s} = v_w + 0.018\, m v_s \tag{14}$$

where m is the molality of the solute. If v_w and v_s are constants, independent of concentration, then a plot of the left-hand-side of eq 14 against molality would yield a straight line. Using available density data, we found that the relationship was reasonably linear at high concentrations for all the single-electrolyte solutions studied in this work. From the slope and intercept of the lines, we obtained values of v_w and v_s for each salt, and these are presented in Table 1. Assuming that these parameters remained constant at supersaturated concentrations, the density of the droplet could then be estimated at the critical concentration.

Water activity measurements and calculations of solute activity coefficients have previously been presented [20] for all the salts studied in this work. The same data base and procedure was used to calculate the solute activity coefficients at the saturation and critical concentration, parameters that are necessary for the calculation of $\triangle G_v$ from eq 2. In many crystallization studies, activity data are not available, and so, it is commonly assumed that the supersaturation ratio is given by the ratio of the concentrations of the supersaturated and saturated solutions. One of the advantages of this single-particle technique is that activity data for supersaturated solutions can be obtained along with the crystallization data.

The dependence of the nucleation time delay, t_i, on the concentration of the droplet is extremely strong. The data in Table 2 demonstrate this dependence for NaCl, assuming an interfacial energy of 81.6 ergs cm^{-2} and a dry particle diameter of 13.4 microns. Between a molality of 12.91 and 14.00, the predicted t_i drops from more than 54 minutes to less than 0.04 seconds. Thus,

for a time scale of seconds or minutes, the crystallization of a droplet of NaCl occurs at a critical concentration of roughly 13.5 molal.

In our experiments, it was not possible to make a precise determination of t_i, because most of the crystallizations occurred during a humidity transient and not from a steady state condition. In these transients the particle mass was generally changing at a rate of several percent per minute. The interfacial free energies calculated depend only weakly on the value of t_i, and so the uncertainty introduced by the need to assume a value of t_i is not large. In the calculations presented here, we will assume that $t_i = 1$ sec; a variation of t_i from 0.01 to 100 seconds changes the calculated σ by a maximum of 4 %. Experimentally, we did not see an influence of the concentrating rate on the observed crystallization concentrations. Figures 1–3 give an example of this for some of our sodium chloride measurements. Within the experimental uncertainty, the crystallization concentrations measured during each of these differing transients were equivalent.

For a cubic crystal morphology, the characteristic length, y, was chosen to be the length of a side of the cube. With this assumption, $\sum_i k_i = 6$ and $\alpha = 6$. For crystals of the orthorhombic class, y was defined to be the length of the longest diagonal of the crystal. For an orthorhombic crystal with dimensions a,b, and c, it can be shown [16] that $\sum_i k_i$ and α are given by

$$\sum_i k_i = \frac{2(ab + bc + ca)}{a^2 + b^2 + c^2} \tag{15}$$

$$\alpha = \frac{2(ab + bc + ca)}{abc} (a^2 + b^2 + c^2)^{1/2} \tag{16}$$

For crystals of monoclinic morphology, y was again defined as the length of the longest diagonal of the crystal. For a monoclinic crystal of dimensions a,b, and c, with an angle β between sides a and c, it can be shown that $\sum_i k_i$ and α are given by

$$\sum_i k_i = \frac{2[ab + bc + ac\ \cos(\beta - \pi/2)]}{a^2 + b^2 + c^2 - 2ac\ \cos(\beta)} \tag{17}$$

$$\alpha = \frac{2[ab + bc + ac\ \cos(\beta - \pi/2)]\,[a^2 + b^2 + c^2 - 2ac\ \cos(\beta)]^{1/2}}{abc\ \cos(\beta - \pi/2)} \tag{18}$$

In Table 3, the calculated values of $\sum_i k_i$ and α and the characteristic length of the unit cell are presented for the salts of this investigation.

When calculating $\triangle G_v$ from eq 2, one needs to know the chemical potential of the solute in a solution that is saturated with respect to the actual crystalline phase that is nucleating. If this phase is not the most stable phase at the temperature of the experiment, then solubility information may not be available. As discussed in Part I, non-equilibrium crystal forms were found with sodium bromide, manganese chloride, and sodium sulfate.

For sodium sulfate, the most stable phase at 20 ℃ is $Na_2SO_4 \cdot 10(H_2O)$. However, the crystalline phase that formed upon droplet evaporation was the anhydrous form. The solubility of the anhydrous form is reported to be 3.72 molal [29].

For sodium bromide, the most stable phase at 20 ℃ is $NaBr \cdot 2(H_2O)$. However, the observed crystalline phase was, once again, the anhydrous form. The solubility of anhydrous NaBr at 20 ℃ could not be found in the literature. So, the activity of aqueous NaBr in a solution saturated with respect to the

anhydrous NaBr crystalline phase was calculated by noting that at equilibrium,

$$\mu_{cryst} = \mu^0_{aq} + \nu RT \ln(a^{sat}_{aq}) \tag{19}$$

Thus,

$$a^{sat}_{aq} = \exp\left(\frac{\triangle G^\circ_{f,cryst} - \triangle G^\circ_{f,aq}}{\nu RT}\right) \tag{20}$$

where $\triangle G^\circ_{f,cryst}$ is the standard free energy of formation of the crystalline phase and $\triangle G^\circ_{f,aq}$ is the standard free energy of formation of the aqueous, ionized salt. Using eq 20 and values for $\triangle G^\circ_{f,cryst}$ and $\triangle G^\circ_{f,aq}$ obtained from standard references [30,31], a^{sat}_{aq} for anhydrous NaBr was estimated to be 23.92 molal. This value of a^{sat}_{aq} was then used in the calculation of $\triangle G_v$ for the driving force in the nucleation equations. The activity of the aqueous solute at the concentration saturated with respect to the more stable $NaBr \cdot 2(H_2O)$ crystalline phase is only 18.14 molal.

With manganese chloride, the most stable phase at 20 ℃ is $MnCl_2 \cdot 4(H_2O)$. As discussed in Part I, the quantity of water retained in the crystal was stoichiometrically equivalent to $MnCl_2 \cdot 2.3(H_2O)$. Thus, the nature of the crystalline phase with $MnCl_2$ was not known. The crystalline phase controlling nucleation was assumed to be $MnCl_2 \cdot 2(H_2O)$. Unfortunately, there is no solubility data for $MnCl_2 \cdot 2(H_2O)$ at 20 ℃. A solubility of 6.09 molal, obtained by Rard [32] for an unidentified, mixed, hydrated crystalline phase of $MnCl_2$, has been used for the present calculations.

There are many approximations involved in the calculation of the interfacial free energy and critical nucleus size from the above theory. For example, the

formulation of the free energy change upon embryo formation, eq 2, ignores any mixing effects or the free energy change of water, the other component in the solution. Also, it has been assumed that the free energy density of the embryo is the same as that of a bulk crystal. Finally, it has been assumed that the concept of surface energy can be applied to a small cluster of atoms and that this surface energy is independent of cluster size, an assumption that has frequently been questioned [33,34,35,36]. In spite of these uncertainties, we have attempted to interpret our experimental results using the above description of nucleation.

Results

In Tables 4 and 5, the experimental observations and calculations performed using the above theory are summarized for single-electrolyte solutions. The calculated values of σ and y_c are, of course, dependent on the assumptions made about the parameters K and t_i, and are influenced by uncertainties in the experimentally measured weight-fraction-solute at crystallization, wfs_{crit}, the calculated solute activity coefficient at this critical concentration, $\gamma_{\pm,crit}$, and d_p. In Table 6, the sensitivity of the calculated results for NaCl to the estimated uncertainties is presented. As described in Part I, the uncertainty in $\gamma_{\pm,crit}$ was obtained assuming an uncertainty of 0.01 in the water activity data used in its calculation. The most significant uncertainties are associated with the values of K and the solute activity coefficient and are on the order of 10–15 % in the calculated values of σ.

The experimental observations on nucleation in mixed-electrolyte solu-

tions are presented in Table 7. A theoretical interpretation of the results for these mixed systems was not attempted.

Discussion

In our experiments, we did not see a dependence of nucleation phenomena on particle size, as is predicted by eq 11. However, with the narrow range of particle sizes used, our experimental resolution was not sufficient to allow us to make any conclusions about the validity of eq 11.

The particles studied generally had about 2×10^5 charges on their surface. While these charges did not affect the vapor-liquid equilibrium of water [20], it is possible that they influenced the nucleation process. Such an influence could have resulted, for example, if the charges induced a slightly enhanced ordering of the solution near the surface. The polarity or magnitude of the particle's charge did not, however, appear to influence the nucleation phenomenon in the present experiments. Since concentrated electrolyte solutions are highly ordered anyway, and since the individual particles contained on the order of 10^{14} dissolved, charged ions, it is not surprising that particle charge would not influence nucleation. However, as is suggested by the results presented in Table 5, nucleation involves a very small number of atoms, and so the influence of any inhomogeneity in the solution cannot be ruled out. For experimental reasons, it was not possible to vary the particle charge levels over a wide range in order to investigate this issue.

The supersaturations reported here are much higher than those found in

bulk-sample experiments with the same salts. For example, Nyvlt and coworkers [37] measured the maximum supercooling before crystallization for 25 different inorganic salt solutions in the presence and absence of added seed crytals. In Table 8, the maximum supercoolings they measured for crystallization at 30 ℃ and the corresponding supersaturation ratio (based on concentration) are listed. Also listed are the same concentration ratios obtained in the present experiments for crystallization at 20 ℃. Although the two data sets are not exactly comparable due to differences in method and temperature, it is likely that the crystallization that they observed even in the absence of added seed crystals was heterogeneous.

Glasner and Kenat [38] investigated the crystallization of potassium chloride with and without added lead ions and found that the nucleation was catalyzed by the added lead. Without lead ions the nucleation commenced at a solute concentration of 5.43 molal at temperatures ranging from 33.41 to 35.6 ℃. At 20 ℃, crystallization did not occur in our suspended droplets of potassium chloride until the concentration reached about 12.33 molal. Again, while the results are not directly comparable, it is likely that, even without the added lead ions, the nucleation that they observed was heterogeneously catalyzed.

The above differences are not surprising. It is generally accepted that the nucleation from aqueous solution that occurs in bulk samples is almost always heterogeneously catalyzed [3,4]. A more stringent test of the present results involves a comparison with results obtained by other investigators who utilized small droplets.

Melia and Moffit [10] studied the nucleation of ammonium chloride by dispersing solution droplets in oil and following the crystallization visually. They found a marked dependence of nucleation on the volume of the sample, as is suggested by eq 11. For an aqueous ammonium chloride droplet of diameter 2.36 mm, crystallization occured at a solute concentration of 11.2 molal at 20.8 ℃. Using the interfacial energy calculated from our results and the simple theory presented above, we estimate that a droplet of this size would be able to reach a concentration of approximately 23 molal before homogeneous nucleation from solution occurred. It thus appears that the nucleation that they observed was heterogeneously catalyzed.

In the same investigation, Melia and Moffit also employed Turnbull's microscopic method [9] and investigated a thirty-micron-diameter droplet with an ammonium chloride concentration of 11.2 molal. They found that this particle did not crystallize even when held at 0 ℃ for 3 days. Using our estimated interfacial free energy and the above simple theory, a droplet of this size with as high a concentration of 18 molal would not crystallize for over 10 days if held at 0 ℃. Thus, their observation is consistent with the results obtained using the electrodynamic balance.

Orr et al. [12] observed the nucleation of sodium chloride in very small aqueous droplets. Working with particles of dry diameter 0.056 microns, Orr and coworkers found that droplets of aqueous sodium chloride crystallized at a relative humidity of about 0.42. Water activity data for sodium chloride solutions do not extend down to 0.42, but the data obtained using single particles

at water activities as low as 0.44 [20] can be extrapolated with reasonable confidence to yield a concentration estimate of 14.23 molal at this humidity. We have neglected the Kelvin effect and thus have underestimated the concentration within their droplets at crystallization. The inclusion of the Kelvin effect requires surface tension data that are not available for such highly supersaturated solutions of sodium chloride. Using the above estimated concentration and their measured dry particle size, we calculate a surface excess free energy, σ, of 75.4 ergs cm^{-2}, in reasonable agreement with our results. The direction of the deviation is consistent with having neglected the Kelvin effect.

In the same investigation, Orr and coworkers also studied other aqueous salt solutions, including potassium chloride, ammonium sulfate, and calcium chloride. With calcium chloride, crystallization was not observed even at a relative humidity as low as 0.20, consistent with our observations. We have estimated σ for potassium chloride and ammonium sulfate from their reported results following the procedure outlined above for sodium chloride. For potassium chloride, σ was calculated to be 58.8 ergs cm^{-2}. A large extrapolation of the $a_w(m)$ data from Part I of this work was required for this calculation and so this result is fairly uncertain. For ammonium sulfate, a combined fit of the water activity data of Robinson and Stokes [39], Richardson and Spann [18], and our measurements [20] was used to estimate the solute concentration and the solute activity coefficient at the critical concentration. The surface excess free energy for ammonium sulfate corresponding to Orr's results was then calculated to be 33.6 ergs cm^{-2}. For the purposes of comparison, the same combined fit yields an estimate of $\sigma = 33.1$ ergs cm^{-2} from our crystallization data.

Tang and coworkers [16] studied the nucleation of sodium chloride and ammonium sulfate within very small aqueous droplets. Their experiments were on single, charged droplets suspended in an electrodynamic balance similar to that used in the present study. They did not report droplet size measurements but state that the diameters of their particles when dry were generally about 2–3 microns. Nucleation of sodium chloride was found to occur at a concentration of 11.2($\pm$0.7) molal at 25 °C. Ammonium sulfate nucleation occurred at 29.9($\pm$3) molal. They performed nucleation calculations with their data using the above theory but did not explicitly take into account the particle size. Instead, the critical state was defined as that which would produce a nucleation rate of one critical-sized embryo per cm^3 per second, an assumption commonly employed in nucleation studies. Also, these workers did not have solute activity data available to them and so the activity of the salts at very high supersaturations had to be estimated by extrapolation from dilute solution data.

Based on their estimated particle size and measured crystallization concentrations, we have recalculated values of σ for the data of Tang et al. [16]. For sodium chloride, σ was found to be 67.7 ergs cm^{-2}, a value lower than that calculated from our results. Using the aforementioned combined fit for aqueous-phase thermodynamics, σ for ammonium sulfate was calculated to be 37.4 ergs cm^{-2}, higher than that calculated for our data on the same basis. The differences between the two studies remain unresolved.

Richardson and Spann [18] have also measured the nucleation of ammonium sulfate within single aqueous droplets suspended in an electrodynamic

balance. They did not measure the size of their particles but state that the particles used were micron sized. Nucleation did not occur within their ammonium sulfate droplets until the concentration reached 35.9($\pm$0.5) molal at 24 °C. They used a slightly different version of nucleation theory to analyze their results than that employed here, and so, for the purposes of comparison, we have calculated σ from their data using the formulation used in the present work. According to this theory, their data indicate an average interfacial energy of 37.5 ergs cm^{-2}, higher than the value we obtained from our results but consistent with the results of Tang et al. [16]. In this calculation, a dry particle diameter of one micron was assumed.

The differences in nucleation in the various single-particle experiments might be caused by catalysis of nucleation by soluble or insoluble impurities in the solution from which the droplet was created. It is also possible that catalyzing impurities were introduced after the particle was inserted into the electrodynamic balance. This could occur if, for example, submicron dust particles were scavenged by the suspended particle. In any event, the differences in the estimated surface excess interfacial energy are small; *e.g.*, for ammonium sulfate, the estimate of σ from the present data is only 12 % less than that calculated from the results of previous studies [16,18] of nucleation of this salt in small suspended droplets.

The value of the surface excess free energy for ferric chloride hexahydrate calculated from our results is extremely low. It is possible that formation of colloidal particles during the observed aging of these droplets [20] provided sites

to catalyze the nucleation, thereby reducing the apparent surface energy. That is, the nucleation of this salt in our experiments may have been heterogeneous. On the other hand, the large amount of water in the crystal may mean that the energy penalty for surface formation is greatly lessened relative to anhydrous crystals. It is possible, therefore, that the low surface energy estimate is reasonable.

With two of the substances studied, manganese sulfate and calcium chloride, crystallization did not occur even when the humidity was lowered below 0.10. The solute concentration in the dry particles was, however, reasonably consistent for multiple determinations with several particles. As discussed in Part I, the dry state of calcium chloride at 20 ℃ corresponded to $CaCl_2 \cdot 4(H_2O)$, but it is not known whether this state was crystalline or amorphous, with no long range order. Since the calcium chloride particles studied did not exhibit a definite deliquescence humidity but instead absorbed water continuously as the humidity was increased over 0.10, it is possible that the particle was amorphous. With manganese sulfate, the situation was even more complicated, because the dry state did not correspond to any single hydrate stoichiometry. The particles we studied consistently dried to a stoichiometry of $MnSO_4 \cdot 2.8(H_2O)$. As discussed in Part I, the deliquescence and drying observations with $MnSO_4$ suggest that the dry particle was either amorphous or was composed of very small regions of crystalline phases in juxtaposition.

The formation of an amorphous or glassy material can be understood in the following way [40]. As the supersaturation increases, the driving force

for nucleation is increased. The viscosity of the solution also increases as the solute concentration is increased. Eventually, the solution is so viscous that the molecules can no longer rearrange themselves into an ordered crystalline lattice. The nucleation process can be effectively quenched for some substances by this phenomenon, and the solution is left in a frozen liquid state.

The solublilities of the α and β forms of $CaCl_2 \cdot 4(H_2O)$ at 20 ℃ are 8.17 and 9.41 molal, respectively. The maximum molality reached within our suspended particles even at the lowest humidities was only about 14 molal. The supersaturation achieved was considerably lower than for the other salts studied. Thus, it is perhaps understandable that calcium chloride did not crystallize homogeneously.

For manganese sulfate, the high charge on both the cation and the anion make the viscosity of a concentrated solution very high [31]. Moreover, there is extensive association of the manganese and sulfate ions in these solutions. The local structure of the hydrated complex in solution may well be different than that for any of the stable crystalline hydrates that exist for this salt. Because of the very high viscosity, rearrangement would occur slowly in a very concentrated manganese sulfate solution. It is not surprising, therefore, that a homogeneous crystalline phase was not found in our experiments.

The manganese sulfate and calcium chloride results suggest that the simple treatment of nucleation theory that we have employed is insufficient to deal with very concentrated solutions in which diffusional limitations to embryo formation may become important.

The calculated critical sizes of embryos required for nucleation presented in Table 4 are remarkably consistent for the four alkali halide electrolytes studied. For each of these salts, the ratio of the characteristic length of the critical nucleus to that of the unit cell is approximately $2.0(\pm 0.1)$. As mentioned earlier, these crystals are of cubic morphology and the characteristic length is defined to be the length of the cube's side. Thus, our results suggest that the critical embryo for the nucleation of each of these salts is a cube whose side-length is approximately two unit-cell-lengths long. It is interesting that while each of these salts nucleated at a different supersaturation and has a different surface excess free energy, all appear to have nucleated in a very similar way.

There are no independent measurements or estimates of the surface excess free energy of these inorganic salts in supersaturated aqueous solution with which to compare our results. For the alkali halides, however, there are theoretical calculations of the surface energy of crystals at 0 °K in a vacuum [41]. Also, surface energies of the crystals have been estimated from measurements of molten salt nucleation [42]. Finally, the surface excess free energy arises, at least in part, because the crystal structure is abruptly terminated at the surface, and so, the normal crystal bonding requirements for surface ions are not satisfied. Thus, it might be expected that the surface energy would be related to the lattice energy of the crystalline phase [2].

In Table 9, the lattice energy and various surface energies noted above are listed along with our calculated results for the four alkali halide salts studied. All of the various energies exhibit the same relative ordering as our calculations.

The energy of the crystal surface in the molten salt are of the same order as our calculated surface energies. However, the estimates of the surface energies of the crystal in vacuum are much higher. This can be partly understood by realizing that, in the electrolyte solution or molten salt, there will be liquid-phase ions near the crystal surface. These ions will interact with the exposed surface ions and the energy penalty imposed by the existence of the surface will be lessened. In this way, the surface excess free energy of a crystal next to an ionic liquid or solution is lowered relative to the same crystal in relation to a vacuum.

For sodium bromide, our calculated surface excess free energy seems slightly high with respect to the relative magnitudes of the various energy terms contained in Table 9. One possible explanation for this is that, since solubility information was not available for this salt, the saturation activity estimate may have been in error. On the other hand, sodium bromide is qualitatively different than the other salts at 20 °C in that the crystalline dihydrate, $NaBr \cdot 2(H_2O)$, is more thermodynamically stable than the anhydrous crystal. This may be the reason for what appears to be an anomolously high NaBr surface energy.

In all cases with the mixed-salt solutions, the droplet reached a lower relative humidity before crystallization occurred than with any of the component salts individually. For the NaCl–KCl and NaCl–KBr mixtures, crystallization occurred at lower individual component concentrations than was required when the same components were alone in solution. However, the ionic strength of the solution was greater than that for either of the individual critical solutions. For these systems, no water was retained in the particle after crystallization

occurred. By inference from deliquescence observations, it was demonstrated in Part II [21] that the NaCl–KCl system probably did not form mixed crystals. Instead, the crystalline particle of NaCl–KCl most likely contained separate phases of pure NaCl and pure KCl. With the NaCl–KBr mixture, however, the nature of the crystalline particle is unclear. That is, it is not known if the dry particle contained mixed-crystalline phases or pure crystalline phases.

For the NaCl–$(NH_4)_2SO_4$ mixtures, NaCl reached a higher concentration in the mixture before crystallization occurred than in the absence of $(NH_4)_2SO_4$. Except for the mixture with an $(NH_4)_2SO_4$ to NaCl mole ratio of 0.5, $(NH_4)_2SO_4$ also reached higher concentrations before crystallization occurred than when in solution by itself. As discussed in Part II, it is probable that there was some water retained in the particles for all of the NaCl–$(NH_4)_2SO_4$ mixtures after crystallization had occurred. As with NaCl–KBr, the composition and spatial arrangement of the phases within the dry particles could not be inferred. The dry particles may have been composed of tiny pockets of crystalline $(NH_4)_2SO_4$ and NaCl interspersed throughout, although the existence of regions of crystalline Na_2SO_4 and NH_4Cl cannot be ruled out. The water in the crystal may have been trapped or could have been incorporated into a crystalline region (*e.g.*, $Na_2SO_4 \cdot 7(H_2O)$, $Na_2SO_4 \cdot 10(H_2O)$, or a more complicated double salt [44]).

With these mixed solutions, the nature and composition of the nucleating embryo is not known. In the mixture with a mole ratio of $(NH_4)_2SO_4$ to NaCl of 0.5, it seems plausible that NaCl initiated nucleation since its individual concentration was higher than its critical nucleation concentration when alone.

With the other mixtures, it is not as easy to speculate about which component may have initiated the nucleation. Once a single crystal phase started growing, however, the concentration of the components remaining in solution would be increased and their nucleation would follow shortly after. For the crystalline phases to nucleate and grow, however, the ions must untangle themselves from their configurations in solution in order to be incorporated within whatever lattices are being formed. It seems reasonable that nucleation and growth within mixtures of simple, similar salts would occur more easily than within mixtures containing dissimilar salts. Thus, the extraordinarily high concentrations required for NaCl–$(NH_4)_2SO_4$ mixtures to crystallize relative to mixtures of alkali halides is understandable.

Conclusions

The electrodynamic balance is an effective tool for investigating the nucleation of crystals from aqueous solutions. The small, suspended droplets are much less influenced by nucleation catalysts than are solutions studied in bulk samples, and much higher supersaturations can be achieved. Furthermore, solute activity coefficients and droplet volume can be measured and incorporated into nucleation theory calculations.

The surface excess free energies obtained from the present experiments agree reasonably well with those calculated from the results of other investigations in which small droplets were used.

The relative magnitudes of the surface energies for the four alkali halides

we studied appear reasonable in light of other experimental and theoretical evidence. Despite differences in surface energy and supersaturation, the ratio of the characteristic length of the critical nucleus to that of the unit cell for each of the alkali halides studied was equal to $2.0(\pm 0.1)$. Since it might be expected that these salts would nucleate in a very similar fashion, this consistency gives support to the experimental results and their theoretical interpretation.

Nucleation of crystals from mixtures of dissimilar electrolytes appears to be slower than from mixtures of similar electrolytes. Moreover, some of the salts studied did not nucleate but appeared to form glasses. These results suggest that diffusional resistances need to be included for a more accurate description of nucleation phenomena from aqueous solution.

Despite the ubiquity of the salts studied, for some of the salts, this is the first time that nucleation measurements have been made under conditions in which homogeneous nucleation might be observed. The measured supersaturations required before nucleation occurred were generally very high. Further improvements in the experimental technique and studies of much larger numbers of particles will be required before unambiguous measurements of homogeneous nucleation in aqueous solutions can be made.

Acknowledgements

This work was supported by the U.S. Environmental Protection Agency under grant number R-810857.

References

[1] A.G. Walton. *Science*, 148:601, 1965.

[2] A.G. Walton. *The Formation and Properties of Precipitates.* Interscience Publishers, John Wiley and Sons, New York, 1967.

[3] A.G. Walton. Nucleation in Liquids and Solutions. In A.C. Zettlemoyer, editor, *Nucleation*, Marcel Dekker, Inc., New York, 1969.

[4] G.R. Youngquist, editor. Advances in Crystallization From Solutions. *A.I.Ch.E. Symposium Series # 240, Volume 80*, 1984.

[5] B.R. Pamplin, editor. *Crystal Growth.* Pergamon Press, 1980.

[6] M. Ohara and R.C. Reid. *Modeling Crystal Growth Rates from Solution.* Prentice Hall, Englewood Cliffs, New Jersey, 1973.

[7] L.R. Ingersoll and C.E. Mendenhall. *Phil. Mag.*, 15:205, 1908.

[8] J.H. Holloman and D. Turnbull. *Prog. Metal Phys.*, 4:333, 1953.

[9] J.B. Newkirk and D. Turnbull. *J. Appl. Phys.*, 26:579, 1955.

[10] T.P. Melia and W.P Moffit. *J. Colloid Sci.*, 19:433, 1964.

[11] M.L. White and A.A. Frost. *J. Colloid Sci.*, 14:247, 1957.

[12] C. Orr, F. Hurd, and W.J. Corbett. *J. Colloid Sci.*, 13:472, 1958.

[13] C. Orr, F. Hurd, W.P. Hendrix, and C. Junge. *J. Meteorology*, 15:240, 1958.

[14] I.N. Tang, H.R. Munkelwitz, and J.G. Davis. *J. Aerosol Sci.*, 8:149, 1977.

[15] I.N. Tang, H.R. Munkelwitz, and J.G. Davis. *J. Aerosol Sci.*, 9:505, 1978.

[16] I.N. Tang and H.R. Munkelwitz. *J. Colloid and Interface Sci.*, 98:430, 1984.

[17] C.A. Kurtz and C.B. Richardson. *Chem. Phys. Letters*, 109:190, 1984.

[18] C.B. Richardson and J.F. Spann. *J. Aerosol Sci.*, 15:563, 1984.

[19] J.F. Spann and C.B. Richardson. *Atmospheric Environment*, 19:819, 1985.

[20] M.D. Cohen, R.C. Flagan, and J.H. Seinfeld. To be submitted to *J. Phys. Chem.*, 1986.

[21] M.D. Cohen, R.C. Flagan, and J.H. Seinfeld. To be submitted to *J. Phys. Chem.*, 1986.

[22] S. Arnold. *J. Aerosol Sci.*, 10:49, 1979.

[23] S. Arnold, Y. Amani, and A. Orenstein. *Rev. Sci. Instr.*, 51:1202, 1980.

[24] A.E. Nielson. *Kinetics of Precipitation.* Pergamon Press, MacMillan Co., New York, 1964.

[25] W. Stumm and J.J. Morgan. *Aquatic Chemistry.* Wiley Interscience, New York, 1981.

[26] J.D.H. Donnay and H. Ondik, editors. *Crystal Data Determinative Tables, Inorganic Compounds.* Volume 2, U.S. Dept. of Commerce, Natl. Bur. Stds., and the Joint Comm. on Powder Diffraction Stds., 3 edition, 1973.

[27] M.D. Lind. *J. Chem. Phys.*, 47:990, 1967.

[28] B. Morosin and E. Graeber. *J. Chem. Phys.*, 42:898, 1965.

[29] E.W. Washburn, editor. *International Critical Tables.* McGraw Hill, New York, 1926.

[30] D.D. Wagman, W.H. Evans, V.B. Parker, R.H. Schumm, I. Halow, S.M. Bailey, K.L. Churney, and R.L. Nuttal. The N.B.S. Tables of Chemical Thermodynamic Properties. *J. Phys. Chem. Ref. Data*, 11, Supplement 2, 1982.

[31] R.C. Weast, editor. *Handbook of Chemsitry and Physics.* CRC Press, 1975.

[32] J.A. Rard. *J. Chem. Engr. Data*, 29:443, 1984.

[33] G.C. Benson and R. Shuttleworth. *J. Chem. Phys.*, 19:130, 1951.

[34] A.G. Walton. *J. Chem. Phys.*, 39:3162, 1963.

[35] F.F. Abraham. *Homogeneous Nucleation Theory.* Academic Press, New York, 1974.

[36] B. Lewis. Nucleation and Growth Theory. In B.R. Pamplin, editor, *Crystal Growth*, Pergamon Press, New York, 1980.

[37] J. Nyvlt, R. Rychly, J. Gottfried, and J. Wurzelova. *J. Cryst. Growth*, 6:151, 1970.

[38] A. Glasner and J. Kenatt. *J. Cryst. Growth*, 2:119, 1968.

[39] R.A. Robinson and R.H. Stokes. *Electrolyte Solutions.* Butterworths, London, 2nd edition, 1959.

[40] R.F. Strickland-Constable. *Kinetics and Mechanism of Crystallization.* Academic Press, London, 1968.

[41] F. van Zeggeren and G.C. Benson. *J. Chem. Phys.*, 26:1077, 1957.

[42] E.R. Buckle and A.R. Ubbelohde. *Proc. Royal Soc., A*, 261:197, 1961.

[43] M.P. Tosi. Cohesion of Ionic Solids in the Born Model. In F. Seitz and D. Turnbull, editors, *Solid State Physics, Vol. 16*, pages 1–120, Academic Press, New York, 1964.

[44] A.C.D. Rivett. *J. Chem. Soc.*, 121:379, 1922.

salt	molar volume of water, v_w (cm^3)	molar volume of solute, v_s (cm^3)	range of wt. frac. solute over which v_w and v_s estimated
NaCl	17.88	22.59	0.15–0.26
NaBr	17.92	28.32	0.20–0.40
KCl	17.94	32.10	0.15–0.24
KBr	17.94	38.58	0.20–0.40
NH_4Cl	17.93	40.17	0.15–0.24
Na_2SO_4	17.68	38.96	0.18–0.22
$(NH_4)_2SO_4$	17.59	72.21	0.20–0.40
$MnCl_2$	17.88	31.56	0.20–0.30
$FeCl_3$	17.64	47.71	0.32–0.40

Table 1: Parameters for density estimation of supersaturated droplets.

weight fraction NaCl	molality of NaCl	supersaturation ratio, $S = a_{crit}/a_{sat}$	calculated time until a nucleation event occurs in a droplet with a dry diameter of 13.4 μm (seconds)
.40	11.41	3.719	3.314×10^{11}
.41	11.89	3.969	2.776×10^{8}
.42	12.39	4.229	7.407×10^{5}
.43	12.91	4.518	3.284×10^{3}
.44	13.44	4.880	1.385×10^{1}
.45	14.00	5.395	3.344×10^{-2}
.46	14.58	6.228	3.128×10^{-5}

Table 2: Time until nucleation event occurs in an aqueous droplet of NaCl; diameter of particle when dry is 13.4 μm.

salt	cystal type	reference for unit cell dimensions	characteristic length for unit cell, y_c^0 (Å)	α	$\sum_i k_i$
NaCl	cubic	[26]	5.64	6	6
NaBr	cubic	[26]	5.97	6	6
KCl	cubic	[26]	6.29	6	6
KBr	cubic	[26]	6.60	6	6
NH_4Cl	cubic	[26]	6.52	6	6
Na_2SO_4	orthorhombic	[26]	16.76	11.878	1.7752
$(NH_4)_2SO_4$	orthorhombic	[26]	14.50	11.276	1.8429
$MnCl_2 \cdot 2(H_2O)$	monoclinic	[27]	12.42	13.019	1.6176
$FeCl_3 \cdot 6(H_2O)$	monoclinic	[28]	15.90	12.633	1.5506

Table 3: Geometric factors for salt crystals.

salt	N_{part} (N_{meas}) (a)	d_p^{dry} (μm) (b)	$q \div 10^5$ (c)	average rh at cryst'n, rh_{crit}	average weight frac. of solute at cryst'n, wfs_{crit} (d)	std. dev. in measurements of wfs_{crit}
NaCl	2 (5)	11.7 13.4	1.48 2.25	0.44	0.446	0.004
NaCl (Ref [16]) (e)	3 (19)	2 (f)		0.51 (g)	0.395	0.015
NaBr	1 (4)	12.9	1.29	0.22	0.685	0.003
KCl	2 (4)	18.8 16.4	2.53 1.55	0.59	0.479	0.007
KBr	3 (5)	13.3 12.5 10.1	1.60 1.10 0.84	0.52	0.629	0.020
NH_4Cl	1 (3)	18.6	2.55	0.45	0.585	0.024
Na_2SO_4	2 (3)	12.5 15.5	1.81 1.82	0.55	0.652	0.018
$(NH_4)_2SO_4$	6 (14)	12.0–24.2	0.67–3.63	0.48	0.699	0.034
$(NH_4)_2SO_4$ (Ref [16]) (e)	2 (11)	2 (f)		0.39 (h)	0.798	0.012
$(NH_4)_2SO_4$ (Ref [18]) (i)	4	1 (f)		0.35	0.826	0.002
$MnCl_2 \cdot 2(H_2O)$	1 (3)	10.8	2.30	0.30	0.611	0.019
$FeCl_3 \cdot 6(H_2O)$	1 (3)	14.8	2.18	0.48	0.491	0.034

Table 4: Characteristics of particles studied and conditions at which crystallization occurred in single-electrolyte aqueous droplets; (a) a total of N_{meas} crystallization measurements were made with N_{part} different particles; (b) aerodynamic diameter; (c) q is number of elementary charges on particle; (d) based on anhydrous solute; (e) at 25 °C; (f) assumed value; (g) calculated from $a_w(m)$ polynomial given in Ref [20]; (h) calculated from $a_w(m)$ polynomial obtained from fit to data of Refs [18,20,39] (*i.e.*, fit "b" in Table 2 of Ref [20]); (i) at 24 °C.

salt	average molality of anhydrous solute at crystallization, m_{crit}	super-saturation ratio, $S = a_{crit}/a_{sat}$	surface excess free energy, σ (erg/cm^2)	characteristic length of critical nucleus, y_c (Å)	ratio of characteristic length of critical nucleus to that of unit cell, y_c/y_c^0
NaCl	13.8	5.16	81.6	11.0	2.0
NaCl (Ref [16])	11.2	3.58	67.7	11.6	2.1
NaBr	21.1	6.42	79.0	11.2	1.9
KCl	12.3	3.64	56.2	13.4	2.1
KBr	14.3	3.64	51.0	13.9	2.1
NH_4Cl	26.4	3.44	57.2	13.3	2.0
Na_2SO_4	13.2	3.71	56.7	24.3	1.5
$(NH_4)_2SO_4$	17.5	2.57 (a)	36.8	29.9	2.1
$(NH_4)_2SO_4$	17.5	2.23 (b)	33.1	31.5	2.2
$(NH_4)_2SO_4$ (Ref [16])	29.9	2.77 (b)	37.4	27.7	1.9
$(NH_4)_2SO_4$ (Ref [18])	35.9	2.86 (b)	37.5	27.0	1.9
$MnCl_2 \cdot 2(H_2O)$	12.5	3.78	46.5	27.8	2.2
$FeCl_3 \cdot 6(H_2O)$	6.0	1.13	7.1	73.4	4.6

Table 5: Calculation of surface excess free energy and characteristic length of critical nucleus from measured critical solute concentration; $K = 10^{30}$, $t_i = 1$ second; (a) calculated from $a_w(m)$ polynomial obtained from fit to data of Refs [20,39] (*i.e.*, fit "a" in Table 2 of Ref [20]); (b) calculated from $a_w(m)$ polynomial obtained from fit to data of Refs [18,20,39] (*i.e.*, fit "b" in Table 2 of Ref [20]).

parameter which has been varied	t_i (sec)	$\log_{10} K$ $K[=]cm^{-3}sec^{-1}$	aero-dynamic diameter of particle when dry (μm)	weight fraction solute at crystalli-zation, wfs_{crit}	$\gamma_{\pm}$ at critical solute concen-tration	surface excess free energy, σ (erg/cm^2)	characteristic length of critical nucleus, y_c (Å)
base case	1	30	12.5	0.446	2.36	81.6	11.0
t_i	0.01 100	30 30	13.4 13.4	0.446 0.446	2.36 2.36	79.3 84.3	10.7 11.4
$\log_{10} K$	1 1	24 36	13.4 13.4	0.446 0.446	2.36 2.36	73.7 88.8	12.0 9.9
d_p^{dry} (a)	1 1	30 30	11.7 13.4	0.446 0.446	2.36 2.36	81.6 81.6	11.0 11.0
wfs_{crit} (b)	1 1	30 30	12.5 12.5	0.442 0.450	2.36 2.36	80.4 83.0	11.1 10.9
$\gamma_{\pm}^{crit}$ (c)	1 1	30 30	12.5 12.5	0.446 0.446	1.74 3.20	71.2 91.4	11.8 10.4

Table 6: Sensitivity of calculated surface excess free energy and critical nucleus size for NaCl to variations in t_i , K , d_p^{dry} , wfs_{crit} , and $\gamma_{\pm}^{crit}$; (a) values correspond to measurements of the two different particles of NaCl studied; (b) variation corresponds to standard deviation in measurements; (c) variation corresponds to uncertainty in $\gamma_{\pm}$ estimated from experimental uncertainties in measured water activity and weight fraction solute as described in Part I.

A	B	moles of B per mole of A	N_{part} (N_{meas}) (a)	d_p^{dry} (μm) (b)	$q \div 10^5$ (c)	average rh at cryst'n, rh_{crit}	average weight frac. of solute at cryst'n, wfs_{crit} (d)	std. dev. measure-ments of wfs_{crit}	m^A_{crit} (e)	m^B_{crit} (e)
NaCl	KCl	1.0026	1 (3)	13.1	1.74	0.43	0.539	0.007	8.79	8.81
NaCl	KBr	1.6142	4 (14)	18.3 13.7 13.2 (f)	1.72 2.06 2.51 (f)	0.41	0.558	0.029	9.55	5.92
NaCl	$(NH_4)_2SO_4$	0.5002	1 (2)	11.0	1.70	0.38	0.699 (g)	0.004	18.61	9.31
NaCl	$(NH_4)_2SO_4$	1.0029	3 (6)	15.1 14.4 11.4	1.30 1.81 1.12	0.30	0.869 (h)	0.011	34.92	34.93
NaCl	$(NH_4)_2SO_4$	1.9980	1 (2)	21.2	3.05	0.21	0.886 (i)	0.014	24.15	48.25

Table 7: Characteristics of particles studied and conditions at which crystallization occurred in mixed-electrolyte aqueous droplets; (a) a total of N_{meas} crystallization measurements were made with N_{part} different particles; (b) aerodynamic diameter; (c) q is number of elementary charges on particle; (d) based on anhydrous solute; (e) corresponding to average value of wfs_{crit} ; (f) 4th particle was lost before size measurement was made; (g) assuming dry-particle stoichiometry of 0.512 moles of water per mole of solute; (h) assuming dry-particle stoichiometry of 0.588 moles of water per mole of solute; (i) assuming dry-particle stoichiometry of 0.663 moles of water per mole of solute.

salt	maximum under-cooling without added crystals, ΔT (℃) (a)	solubility at 30 ℃ (molal)	solubility at 30 ℃ - ΔT (molal)	supersaturation, $S_m = m_{crit}/m_{sat}$ for measurements of Ref [37]	supersaturation, $S_m = m_{crit}/m_{sat}$ for measurements of this work
KCl	2.35	5.01	4.92	1.018	2.67
KBr	4.00	5.88	5.70	1.032	2.63
NH_4Cl	1.80	7.78	7.64	1.018	3.78
$(NH_4)_2SO_4$	4.6	5.91	5.83	1.014	3.06

Table 8: Comparison of measured critical supersaturations found in a typical bulk-solution crystallization investigation with those measured in the present work for levitated droplets; (a) data from Nyvlt et al. (Ref [37]) for solutions saturated at 30 ℃ .

salt	surface excess free energy found in this work (erg/cm^2)	theoretical surface energy of crystal at 0 °K (Ref [41]) (erg/cm^2)	surface energy estimated from molten salt nucleation (Ref [42]) (erg/cm^2)	cohesive energy density of crystal (Ref [43]) (kcal/mole)
NaCl	81.6	188	84.1	-182.6
NaBr	79.0	177	71.5	-173.6
KCl	56.2	163	65.6	-165.8
KBr	51.0	151	57.1	-158.5

Table 9: Surface and lattice energies for alkali halide salts studied in this investigation.

Figure Captions

Figure 1: Balancing voltage vs. time for a sodium chloride particle during a humidity transient in which crystallization occurred; point A: balancing voltage immediately before crystallization; point B: balancing voltage in dry state; particle aerodynamic diameter when dry is 11.7 microns; at $t = 0$, chamber relative humidity lowered from a steady state value of 0.455 to an eventual value of 0.440; from balancing voltages at points A and B, weight fraction solute at crystallization calculated to be 0.443.

Figure 2: Balancing voltage vs. time for a sodium chloride particle during a humidity transient in which crystallization occurred; point A: balancing voltage immediately before crystallization; point B: balancing voltage in dry state; particle aerodynamic diameter when dry is 13.4 microns; at $t = 0$, chamber relative humidity lowered from a value greater than 0.90 to an eventual value of 0.391; from balancing voltages at points A and B, weight fraction solute at crystallization calculated to be 0.442.

Figure 3: Balancing voltage vs. time for a sodium chloride particle during a humidity transient in which crystallization occurred; point A: balancing voltage immediately before crystallization; point B: balancing voltage in dry state; particle aerodynamic diameter when dry is 13.4 microns; at $t = 0$, air with relative humidity 0.11 began to flow through chamber; from balancing voltages at points A and B, weight fraction solute at crystallization calculated to be 0.450.

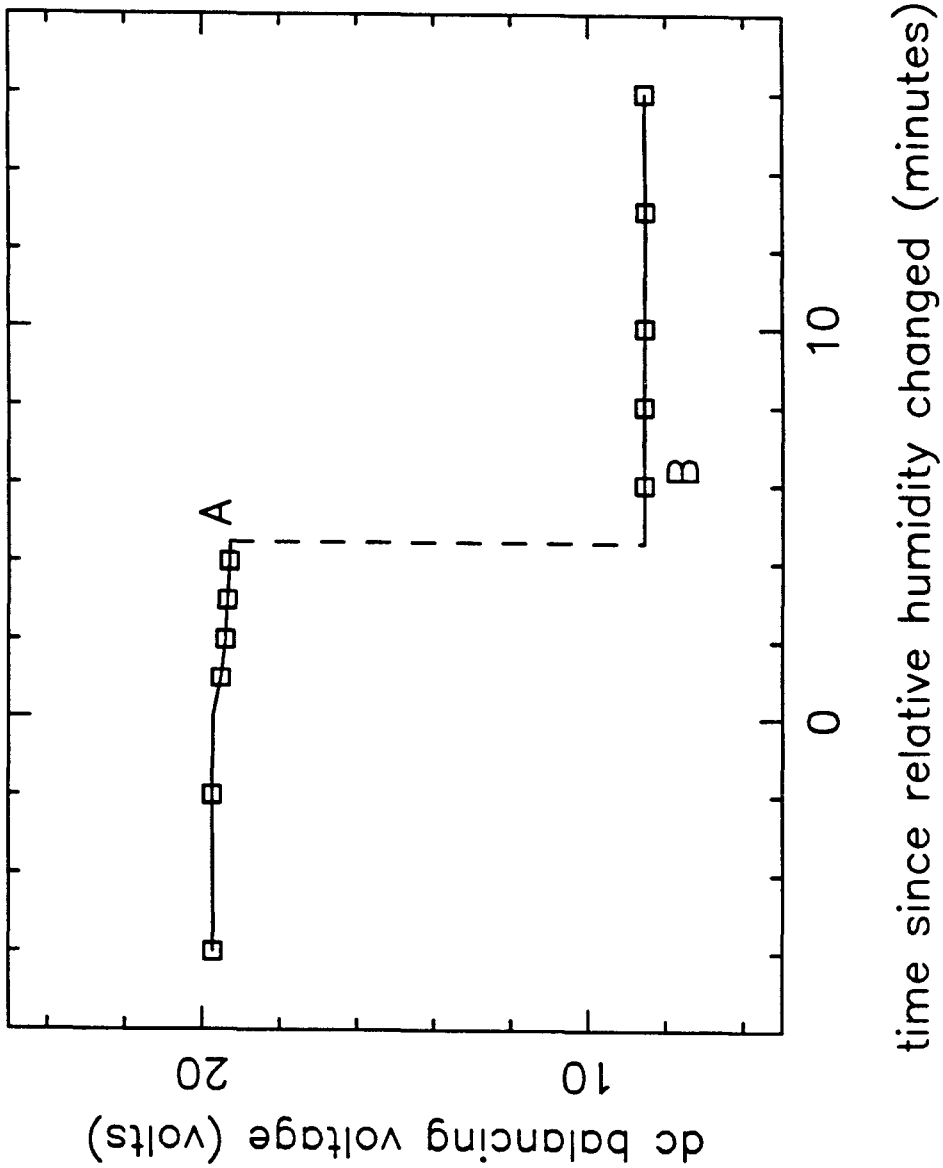
dc balancing voltage (volts)
20
10
0
10
time since relative humidity changed (minutes)
A
B

Figure 1

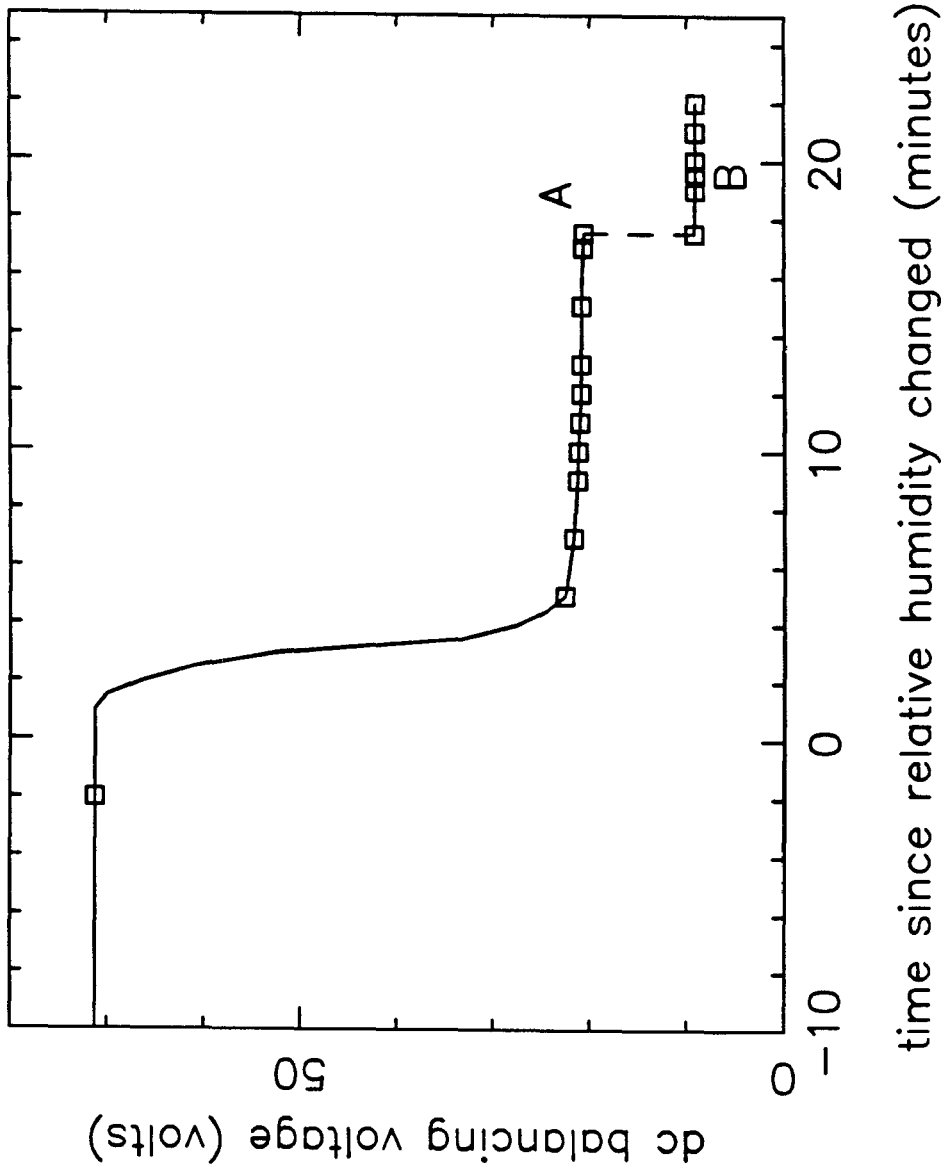
dc balancing voltage (volts)
50
0
−10
0
10
20
time since relative humidity changed (minutes)
A
B

Figure 2

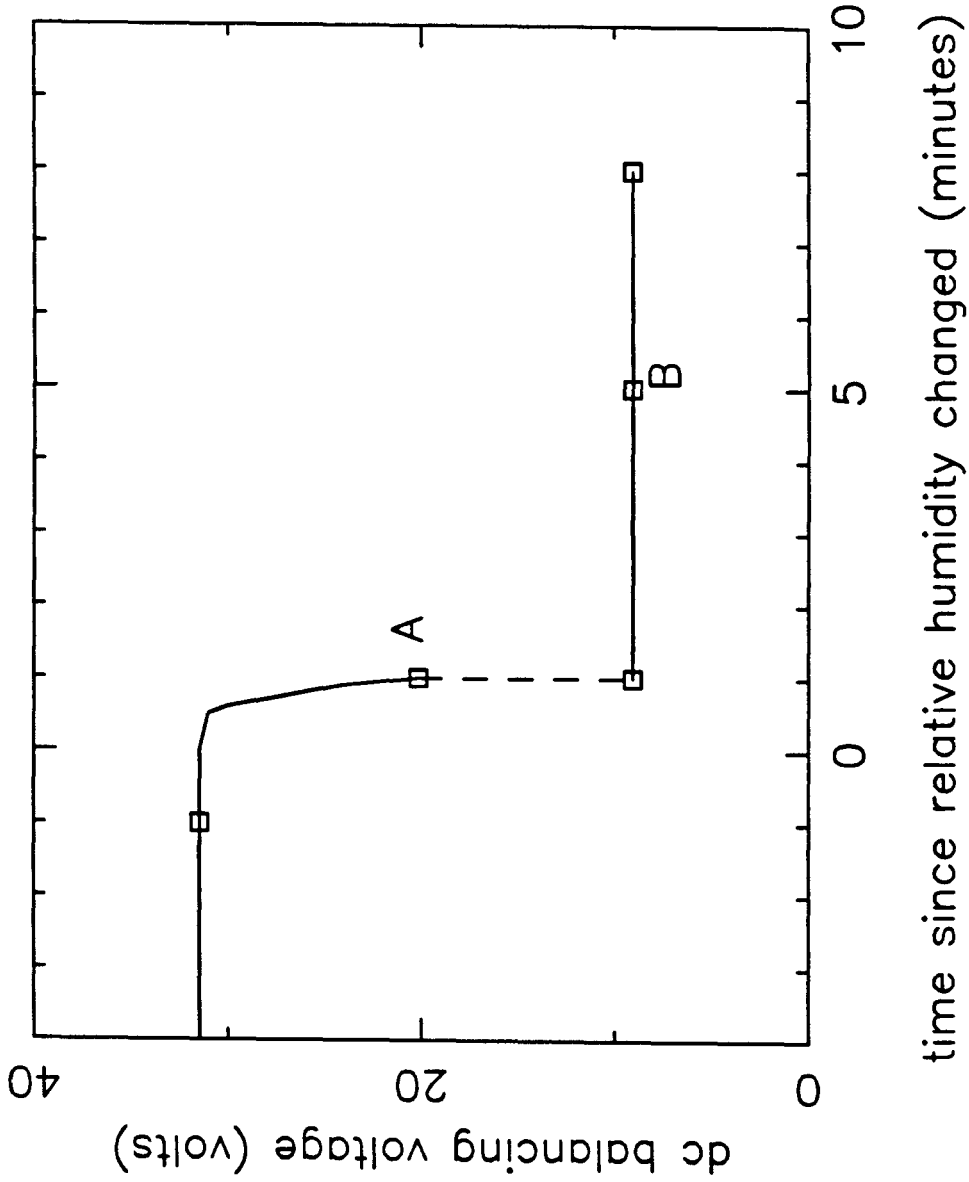
dc balancing voltage (volts)
0
20
40
time since relative humidity changed (minutes)
0
5
10
A
B

Figure 3

Conclusions

By suspending single, charged droplets in an electrodynamic balance, the water activity as a function of concentration has been measured for aqueous solutions of eleven inorganic salts and three inorganic salt mixtures at 20 ℃. The water activity and weight fraction of solute in the solutions were measured to within approximately 0.01.

One difficulty with this technique is that the composition of a particle of a particular salt or salt mixture after drying cannot be predicted *a priori*. The dry-particle composition is needed to calculate the solute concentration at high humidities when the particle is a solution droplet. However, if some auxiliary water activity data are available from other measurements, the composition of the dry particle can be determined. For most of the solutions studied, the dry particle was crystalline and its stoichiometry corresponded to a known crystalline form.

As compensation for the relatively high uncertainty, water activity measurements can be made in a much shorter time with this technique than with the isopiestic method. The principal advantage of this experimental method, however, is that measurements can be made on solutions that have solute concentrations much higher than can be studied with conventional methods. For most of the solutions, data were obtained at much higher concentrations than have previously been reported.

Solute activity coefficients in the single-electrolyte solutions were calculated as function of molality using our experimental water activity results and data taken from the literature. The concentration dependence and relative magnitudes of the solute activity coefficients for the different salts were consistent with commonly held views of ion hydration and ion association phenomena in solution. At very high concentrations, the effects of the scarcity of water in the solution on the solute activity coefficient were seen. Also, a special configurational effect seemed to be present for some of the salts when the solution stoichiometry was equivalent to a stable crystalline phase.

The validities of three different semi-empirical electrolyte solution models were evaluated by comparison with our single-salt results. With each model, it was found that parameters estimated from low concentration data could not be reliably used to predict thermodynamic properties of the solution at high concentrations. However, with parameters estimated from the full range of the data, Pitzer's virial coefficient model and Chen's local composition model were able to represent the experimental observations over the full range of the data within the experimental uncertainty. With the BET-based model of Robinson and Stokes, only a limited range of data at high concentration could be represented.

For two of the mixtures studied, NaCl–KCl and NaCl–KBr , the water activities as a function of solute concentration were consistent with previous investigations, and data were obtained to higher concentrations than have been previously reported. The deliquescence behavior of the NaCl–KCl particle stud-

ied was consistent with the theoretical predictions and experimental results of Tang and coworkers. For the NaCl–$(NH_4)_2SO_4$ system, there were no data available in the literature, and so it was not possible to determine unambiguously the composition of the particles in their dry state and therefore the absolute solute concentration.

Three different mixing rules were evaluated in their ability to predict the water activity as a function of solute concentration for the mixed-electrolyte solutions studied. The ZSR method and the simplified versions of the RWR and Pitzer methods, using only information from single-electrolyte solutions, were generally able to predict the mixture's water activity to within the uncertainty of the experimental data for the NaCl–KCl and NaCl–KBr systems. For the NaCl–$(NH_4)_2SO_4$ system, the different models' predictions were consistent with each other but were inconsistent with the experimental observations if it was assumed that the dry particles were anhydrous. The possibility that water could be contained within the dry particles for this system was considered. If a small amount of water, slightly different for each of the three mixing ratios studied, was assumed to be present in the dry particles for this system, then the predictions of the mixing rules agreed closely with the experimental findings even at high ionic strengths.

The electrodynamic balance is an effective tool for investigating the nucleation of crystals from aqueous solutions. The small, suspended droplets are much less influenced by nucleation catalysts than are solutions studied in bulk samples, and so, much higher supersaturations can be achieved. Furthermore,

solute activity coefficients and droplet volume can be measured and incorporated into nucleation theory calculations.

The surface excess free energies obtained from the present experiments agree reasonably well with those calculated from the results of other investigations in which small droplets were used.

The relative magnitudes of the surface energies for the four alkali halides studied appear reasonable in light of other experimental and theoretical evidence. Despite differences in surface energy and supersaturation, the ratio of the characteristic length of the critical nucleus to that of the unit cell for each of the alkali halides studied was equal to $2.0(\pm\ 0.1)$. Since it might be expected that these salts would nucleate in a very similar fashion, this consistency gives support to the experimental results and their theoretical interpretation.

Nucleation of crystals from mixtures of dissimilar electrolytes appears to be slower than from mixtures of similar electrolytes. Moreover, some of the salts studied did not nucleate but appeared to form glasses. These results suggest that diffusional resistances need to be included for a more accurate description of nucleation phenomena from aqueous solution.

Despite the ubiquity of the salts studied, for some of the salts, this is the first time that nucleation measurements have been made under conditions in which homogeneous nucleation might be observed. The measured supersaturations required before nucleation occurred were generally very high, but it cannot be stated definitively that true homogeneous nucleation has been ob-

served. Further improvements in the experimental technique and studies of much larger numbers of particles will be required before unambiguous measurements of homogeneous nucleation in aqueous solutions can be made with the electrodynamic balance.

Appendices

In the appendices that follow, many of the tabulated quantities are presented using more significant figures than justified. The extra significant figures are retained because many of the quantities are intermediate and are used in further calculations. In this way, round-off error is kept to a minimum.

Appendix A: Tables of experimental data for particle relative mass as a function of chamber relative humidity for single-electrolyte particles

This appendix documents the experimental data taken for single-electrolyte solutions. There are two kinds of tables included in this appendix.

In the first type of table, there are seven columns of data. Each line represents a datum point in which the particle mass and relative humidity had reached a steady state. This first type of table contains essentially the "raw" experimental data. The columns of data in this first type of table have the following meanings.

- Column 1 contains the point label. When a particular portion of an experiment was obviously not a steady state (*e.g.*, if a high-humidity was imposed for a short time in order to deliquesce the particle) the datum point was not included in these tables. Thus, in some cases there are missing numbers. Also, for measurements on a particular particle, the numbers of the steady states increase consecutively (with the exceptions just noted). When measurements on a *different* particle of the *same* salt or salt mixture are being reported, the point numbers start again at 1. Thus, for example, in the data for NaCl, the Oct 24, 1985 table (starting with point number 1) and the Oct 25, 1985 table (starting with point number 22) refer to measurements on the *same* particle. However, the Dec 24, 1985 tables, starting again with point number 1, refer to measurements on a

different NaCl particle.

- Column 2 contains the voltage output (volts) from the thermistor used to measure the chamber temperature. The thermistor was calibrated against a mercury thermometer, and 33 calibration datum points were obtained in the temperature range from 11.58 ℃ to 41.35 ℃. The uncertainty in reading the the mercury thermometer was about approximately 0.02–0.05 ℃. The calibration data of thermistor voltage output as a function of temperature were fit to a polynomial. The relation between temperature and thermistor output was found to be

$$T(℃) = a_0 + a_1(\#1) + a_2(\#1)^2 + \ldots,$$

where

(# 1) = voltage output (volts) from thermistor # 1

$$a_0 = 0.929943771 \times 10^2$$

$$a_1 = -0.785485458 \times 10^2$$

$$a_2 = 0.470811577 \times 10^2$$

$$a_3 = -0.187670517 \times 10^2$$

$$a_4 = 0.451940346 \times 10^1$$

$$a_5 = -0.592991590 \times 10^0$$

$$a_6 = 0.324333906 \times 10^{-1}.$$

The standard error in the polynomial fit's representation of the calibration data was 0.02 ℃.

- Column 3 contains the voltage output (millivolts) from the dewpoint hygrometer used to measure the absolute humidity of the air that was drawn through the electrode assembly. From this measurement, the absolute humidity of the gas stream was determined as described below.

  Measurements of the same humid air stream were made simultaneously with each hygrometer. The dewpoint indicated digitally by the EG&G 911 and the corresponding voltage output of the EG&G 880 were noted. The nominal uncertainty, given in the instrument specifications, for the EG&G 880 hygrometer is 1.11 ℃ in the measured dewpoint. For the EG&G 911 hygrometer, the corresponding uncertainty is 0.3 ℃ in the measured dewpoint. The vapor pressure of water corresponding to the EG&G 911 dewpoint was determined. Finally, the resulting calibration data of absolute humidity as a function of EG&G 880 voltage output was fit to a polynomial:

$$p_{H_2O}(\text{mmHg}) = a_0 + a_1(880mv) + a_2(880mv)^2 + \ldots,$$

  where

  (880mv) = voltage output (millivolts) from EG&G 880

$$a_0 = 0.146884 \times 10^1$$

$$a_1 = -0.508924 \times 10^0$$

$$a_2 = 0.666104 \times 10^{-1}$$

$$a_3 = -0.224123 \times 10^{-2}$$

$$a_4 = 0.240279 \times 10^{-4}$$

$$a_5 = 0.208391 \times 10^{-6}$$

The standard error in the polynomial fit's representation of the calibration data was 0.15 mmHg in absolute humidity. The calibration was over an absolute humidity range of 1.0–17.0 mmHg.

- Column 4 contains the balancing voltage (volts) for the particle for the steady state.

- Column 5 contains the dry-particle balancing voltage (volts) from which the solute concentration in the "wet" particle is to be calculated. The dry balancing voltage listed has been corrected for dry-particle water, decharging, and solute volatilization. Thus, the weight fraction solute in the particle is given by the ratio of the dry balancing voltage in Column 4 and the wet balancing voltage in Column 5.

- Column 6 describes whether the particle was dry, denoted by a "d" entry, or wet, denoted by a "w" entry. In general, points that were wet were used in the $a_w(m)$ polynomial fits. Points that were dry were not used to construct these fits.

- Finally, in Column 7, comments are listed.

In the second type of table, there are eleven columns of data. Again, each line represents a datum point in which the particle mass and relative humidity had reached a steady state. This type of table contains useful quantities which

have been calculated from the "raw" data of the previous type of table. For each table of the first type there is corresponding table of this second type. The columns of data in this second type of table have the following meanings.

- Column 1 contains the point label for the steady state corresponding to the earlier table for this particular experiment.
- Column 2 lists the relative humidity calculated from the dewpoint hygrometer output, the thermistor output, and the temperature difference between the particle and the thermistor, determined to be 0.3 ℃. As discussed in the text of the thesis, because the water in the particle is in equilibrium with the surrounding vapor, the relative humidity is equivalent to the water activity in the droplet solution. The uncertainty in this calculated relative humidity is approximately 0.01–0.02
- Columns 3 and 4 contain the wet and dry balancing voltages given in the earlier table of "raw" data for this experiment.
- Column 5 describes whether the particle was dry, denoted by a "d" entry, or wet, denoted by a "w" entry.
- Column 6 contains the weight fraction solute, calculated from the ratio of the dry to the wet balancing voltage.
- Column 7 contains the solute molality.
- Column 8 gives the ionic strength of the solution, calculated on molal basis.

- Column 9 lists the mole fraction of solute in the solution.
- Column 10 contains the "hydration number", *i.e.*, the number of moles of water per mole of salt in the particle.
- Finally, Column 11 gives the osmotic coefficient calculated from the water activity and solute molality.

SPECIES ..... SODIUM CHLORIDE
DATE(S) OF EXPERIMENT .. OCT 24, 1985

pt #	#1	880mv	Vdc(w)	Vdc(d)	comments
1	2.971	10.	8.53	8.53	d
2	2.969	32.17	8.53	8.53	d
3	2.971	33.075	8.53	8.53	d
4	2.970	33.38	32.10	8.53	w
6	2.967	34.47	44.0	8.53	w
7	2.965	33.48	34.66	8.53	w
8	2.966	32.85	31.29	8.53	w
9	2.966	32.40	29.37	8.53	w
10	2.967	31.58	27.07	8.53	w
11	2.967	30.81	25.48	8.53	w
12	2.966	29.81	23.62	8.53	w
13	2.966	28.92	21.68	8.53	w
14	2.966	28.74	21.38	8.53	w
15	2.966	28.52	21.10	8.53	w
16	2.965	28.31	20.77	8.53	w
17	2.965	28.065	20.48	8.53	w
18	2.963	27.81	20.11	8.53	w
19	2.963	27.50	19.73	8.53	w
20b	2.963	27.10	8.53	8.53	d

DATE(S) OF EXPERIMENT .. OCT 25, 1985

pt #	#1	880mv	Vdc(w)	Vdc(d)	comments
22	2.961	34.29	39.72	8.53	w
23	2.959	32.11	28.52	8.53	w
24	2.959	30.35	23.92	8.54	w
25	2.959	29.28	22.07	8.54	w
26	2.958	27.34	19.6	8.55	w
27	2.958	27.195	19.38	8.55	w
28	2.958	27.145	19.30	8.56	w
29	2.957	27.075	8.56	8.56	d

DATE(S) OF EXPERIMENT .. DEC 24, 1985

pt #	#1	880mv	Vdc(w)	Vdc(d)	comments
1	3.005	12.0	9.08	9.04	d
2	3.005	32.91	9.04	9.04	d
3	3.005	33.57	37.01	9.04	w
4	3.004	32.91	33.93	9.04	w
5	3.005	31.44	28.04	9.04	w
6	3.006	29.54	23.88	9.04	w
7	3.006	27.63	21.14	9.04	w
8	3.005	26.10	9.04	9.04	d
9	3.005	12.0	9.04	9.04	d
11	3.002	25.37	9.09	9.09	d
12	3.005	12.0	9.09	9.09	d

SPECIES ..... SODIUM BROMIDE
DATE(S) OF EXPERIMENT .. DEC 26, 1985

pt #	#1	880mv	Vdc(w)	Vdc(d)		comments
1	3.0	13.	21.08	21.08	d	
2	3.008	28.83	41.16	21.08	w	
3	3.006	33.20	58.06	21.08	w	
4	3.005	32.13	51.46	21.08	w	
5	3.005	31.24	47.58	21.08	w	
6	3.004	29.99	44.0	21.08	w	
7	3.004	28.40	40.82	21.08	w	
8	3.004	25.54	36.78	21.08	w	
9	3.004	22.58	33.93	21.08	w	
10	3.004	20.3	32.15	21.08	w	Vdc,880: +/- 0.1
11	3.003	18.96	31.25	21.08	w	
12	3.003	16.87	21.08	21.08	d	
13	3.003	13.96	21.08	21.08	d	

DATE(S) OF EXPERIMENT .. DEC 27, 1985

pt #	#1	880mv	Vdc(w)	Vdc(d)		comments
14	3.0	13.	21.21	21.21	d	
17	3.011	27.11	21.39	21.21	d	
18	3.011	27.54	22.3	21.21	d	
19	3.010	27.79	39.68	21.21	w	
20	3.009	31.53	48.6	21.21	w	
21	3.0075	26.92	38.55	21.21	w	
22	3.008	24.69	35.96	21.21	w	
23	3.0075	21.45	32.96	21.21	w	Vdc +/- 0.1 at least
24	3.0075	18.21	21.29	21.21	d	
25	3.0	13.	21.23	21.21	d	

SPECIES ..... POTASSIUM CHLORIDE
DATE(S) OF EXPERIMENT .. DEC 4,1985

pt #	#1	880mv	Vdc(w)	Vdc(d)		comments
1	3.	13.	22.57	22.61	d	
2	3.055	33.10	22.61	22.61	d	
4	3.045	34.26	93.77	23.0	w	
7	3.0495	32.95	68.67	23.28	w	
8	3.049	31.85	60.02	23.28	w	
9	3.048	30.85	52.72	23.28	w	
10	3.049	30.32	50.03	23.28	w	
11	3.049	30.11	23.80	23.28	d	
12	3.	13.	23.8	23.28	d	

DATE(S) OF EXPERIMENT .. DEC 5, 1985

pt #	#1	880mv	Vdc(w)	Vdc(d)		comments
13	3.	13.	24.22	23.50	d	
14	3.057	33.84	24.20	23.50	d	
16	3.056	33.65	79.24	23.50	w	
17	3.054	33.14	71.20	23.50	w	
18	3.052	32.60	64.61	23.50	w	
19	3.050	31.58	59.94	23.50	w	
20	3.050	30.93	52.03	23.50	w	
21	3.049	30.72	51.74	23.50	w	
22	3.049	30.57	51.02	23.50	w	
23	3.049	30.40	50.00	23.50	w	
24	3.049	30.15	48.28	23.50	w	just before crystn
25	3.049	30.15	23.5	23.50	d	
26	3.	13.	23.5	23.50	d	

SPECIES ..... POTASSIUM BROMIDE
DATE(S) OF EXPERIMENT .. DEC 25, 1985

pt #	#1	880mv	Vdc(w)	Vdc(d)		comments
1	3.	13.	13.40	13.33	d	
2	3.005	33.685	13.48	13.33	d	
4	3.004	34.23	36.2	13.33	w	
5	3.004	33.60	31.91	13.33	w	
6	3.003	32.37	27.00	13.33	w	
7	3.003	31.12	23.95	13.33	w	
8	3.003	30.37	22.60	13.33	w	
9	3.002	29.78	21.79	13.33	w	
10	3.002	29.45	21.37	13.33	w	
11	3.002	28.89	20.98	13.33	w	
12	3.001	28.25	13.31	13.33	d	
13	3.	13.	13.35	13.33	d	

DATE(S) OF EXPERIMENT .. DEC 26, 1985

pt #	#1	880mv	Vdc(w)	Vdc(d)		comments
15	3.002	33.18	29.54	13.33	w	
16	3.003	31.79	25.196	13.33	w	
17	3.002	29.26	21.00	13.33	w	
18	3.002	28.55	13.25	13.33	d	
19	3.	13.	13.3	13.33	d	Vdc +/- 0.1 at least

SPECIES ..... AMMONIUM CHLORIDE
DATE(S) OF EXPERIMENT .. OCT 11, 1985

pt #	#1	880mv	Vdc(w)	Vdc(d)		comments
1	3.	13.	15.33	15.33	d	
3	2.954	33.72	54.65	15.29	w	
4	2.961	33.70	56.58	15.28	w	
5	2.956	34.31	66.89	15.26	w	
6	2.953	34.87	81.4	15.24	w	Vdc increasing...
7	2.951	34.55	72.4	15.22	w	
8	2.944	34.53	73.36	15.20	w	
9	2.945	33.10	50.13	15.18	w	
10	2.942	32.53	45.16	15.17	w	
11	2.937	31.63	38.63	15.15	w	Vdc decreasing...
12	3.	13.	15.13	15.13	d	

DATE(S) OF EXPERIMENT .. OCT 12A, 1985

pt #	#1	880mv	Vdc(w)	Vdc(d)		comments
13	3.	13.	14.92	14.92	d	
14	2.950	33.12	14.92	14.92	d	
15	2.945	33.62	54.35	14.90	w	
16	2.941	32.00	40.15	14.88	w	
17	2.939	30.29	32.30	14.86	w	
18	2.940	28.75	27.66	14.83	w	
19	2.939	27.46	14.60	14.8	d	

DATE(S) OF EXPERIMENT .. OCT 12B, 1985

pt #	#1	880mv	Vdc(w)	Vdc(d)		comments
20	2.939	33.48	14.85	14.8	d	
21	2.938	33.57	15.00	14.8	d	
22	2.939	33.67	53.65	14.73	w	
23	2.939	35.14	89.7	14.66	w	
24	2.938	33.93	57.8	14.59	w	
25	2.938	32.65	44.11	14.52	w	
26	2.939	31.13	35.0	14.45	w	
27	2.940	29.53	29.28	14.38	w	
28	2.941	28.48	26.57	14.30	w	
29	2.941	28.23	25.68	14.23	w	
30	2.940	27.95	14.15	14.15	d	
31	3.	13.	14.137	14.15	d	

SPECIES ..... SODIUM SULFATE
DATE(S) OF EXPERIMENT .. OCT 21, 1985

pt #	#1	880mv	Vdc(w)	Vdc(d)		comments
1	3.	13.	11.66	11.66	d	
2	2.973	33.75	11.72	11.68	d	
3	2.971	34.37	11.7	11.73	d	Vdc +/- 0.2
5	2.968	34.87	35.85	11.84	w	
6	2.967	34.46	32.65	11.86	w	
7	2.970	33.695	29.19	11.94	w	
8	2.968	33.04	27.06	11.98	w	
9	2.968	32.345	25.37	12.00	w	
10	2.968	31.705	23.93	12.01	w	
11	2.967	30.70	21.62	12.03	w	
12	2.967	29.79	18.90	12.04	w	may not have reached ss
13	2.969	29.79	12.06	12.06	d	
14	3.	13.	12.06	12.07	d	

DATE(S) OF EXPERIMENT .. OCT 22, 1985

pt #	#1	880mv	Vdc(w)	Vdc(d)		comments
1	3.	13.	22.08	22.07	d	
2	2.979	34.22	22.29	22.07	d	
3	2.977	34.79	66.72	22.07	w	
4	2.976	34.59	63.61	22.07	w	
5	2.973	34.405	60.93	22.07	w	
6	2.973	33.755	54.50	22.07	w	
7	2.973	33.01	50.5	22.07	w	
8	2.973	32.33	46.9	22.07	w	
9	2.972	31.57	43.55	22.07	w	
10	2.973	30.61	39.25	22.07	w	
11	2.971	30.02	36.2	22.07	w	
12	2.971	29.88	35.38	22.07	w	
13	2.972	29.80	34.77	22.07	w	
14	2.971	29.71	34.17	22.07	w	just before crystn
15	2.971	29.71	22.09	22.07	d	
16	2.971	34.54	22.49	22.07	d	
17	2.971	34.67	64.07	22.07	w	
18	3.	13.	22.04	22.07	d	

SPECIES ..... AMMONIUM SULFATE
DATE(S) OF EXPERIMENT .. AUG 25-27,1985

pt #	#1	880mv	Vdc(w)	Vdc(d)	comments
2	3.006	33.91	50.31	20.54	w
3	2.997	34.51	58.50	20.54	w
4	2.996	34.22	54.3	20.54	w
5	2.995	34.68	61.93	20.54	w
6	2.996	32.18	39.07	20.54	w
7	2.994	29.25	31.3	20.54	w
8	2.993	28.57	30.24	20.54	w
9	2.994	28.20	29.59	20.54	w
10	2.995	27.85	29.23	20.54	w
11	2.993	27.52	20.63	20.54	d
13	2.991	31.91	20.71	20.71	d
15	2.983	33.90	48.5	20.86	w

DATE(S) OF EXPERIMENT .. SEPT 20-24, 1985

pt #	#1	880mv	Vdc(w)	Vdc(d)	comments
1	2.955	31.34	5.42	5.424	d
2	2.953	33.27	5.39	5.424	d
3	2.953	33.78	5.40	5.424	d
4	2.955	34.16	13.22	5.424	w
5a	3.	13.	5.43	5.424	d
5b	2.956	33.61	5.42	5.424	d
6	2.956	33.91	5.40	5.424	d
7	2.953	33.93	5.46	5.424	d
8	2.950	34.05	5.42	5.424	d
10	2.951	34.13	13.02	5.424	w
12	2.949	34.65	14.86	5.424	w
13	2.949	34.17	13.33	5.424	w
14	2.949	32.77	10.78	5.424	w
15	2.950	31.15	9.27	5.424	w
16	2.950	29.43	5.45	5.424	d
17	2.951	30.44	8.81	5.424	w
18	2.950	29.88	8.52	5.424	w
19	2.950	29.64	5.45	5.424	d

SPECIES ..... CALCIUM CHLORIDE
DATE(S) OF EXPERIMENT .. JAN 10, 1986

pt #	#1	880mv	Vdc(w)	Vdc(d)		comments
1	3.023	9.92	76.38	46.26	d	
2	3.019	28.33	131.27	46.26	w	
3	3.020	30.77	149.64	46.26	w	

DATE(S) OF EXPERIMENT .. JAN 11, 1986

pt #	#1	880mv	Vdc(w)	Vdc(d)		comments
1	3.022	13.	9.37	5.64	w	
2	3.023	26.14	14.29	5.64	w	
3	3.018	34.23	28.91	5.64	w	
4	3.018	33.27	23.96	5.64	w	
5	3.018	30.03	17.4	5.64	w	#1,880mv not stable
6	3.018	32.50	21.49	5.64	w	
7	3.018	23.99	13.64	5.64	w	
8	3.019	13.6	9.75	5.64	w	

DATE(S) OF EXPERIMENT .. JAN 12, 1986

pt #	#1	880mv	Vdc(w)	Vdc(d)		comments
11	3.022	8.55	9.32	5.64	d	
12	3.020	31.55	18.93	5.64	w	880mv increasing
13	3.019	29.22	16.50	5.64	w	
14	3.019	27.10	15.02	5.64	w	
15	3.019	25.34	14.07	5.64	w	
16	3.019	23.35	13.23	5.64	w	
17	3.019	22.16	12.75	5.64	w	
18	3.016	20.48	12.21	5.64	w	
19	3.016	19.23	11.85	5.64	w	
20	3.016	17.91	11.42	5.64	w	
21	3.014	16.0	10.46	5.64	w	
22	3.016	14.42	9.25	5.64	w	

SPECIES MNCL2
DATE(S) OF EXPERIMENT .. SEPT 27a, 1985

pt #	#1	880mv	Vdc(w)	Vdc(d)		comments
1	2.963	12.00	4.90	3.67	d	
3	2.962	31.26	9.10	3.67	w	
4	2.960	32.34	10.14	3.67	w	
5	2.960	29.06	7.92	3.67	w	
6	2.960	27.95	7.51	3.67	w	#1 and 880mv changing
7	2.956	26.97	7.22	3.67	w	
8	2.956	25.65	6.86	3.67	w	
9	2.956	23.99	6.51	3.67	w	
10	2.956	22.92	6.30	3.67	w	
11	2.956	22.04	4.84	3.67	d	

DATE(S) OF EXPERIMENT .. SEPT 27b, 1985

pt #	#1	880mv	Vdc(w)	Vdc(d)		comments
12	2.956	26.27	4.86	3.67	d	
13	2.956	27.35	7.27	3.67	w	
14	2.956	22.33	6.17	3.67	w	
15	2.956	22.27	6.11	3.67	w	880mv changing
16	2.954	22.08	4.82	3.67	d	

DATE(S) OF EXPERIMENT .. SEPT 27c, 1985

pt #	#1	880mv	Vdc(w)	Vdc(d)		comments
17	2.954	26.72	4.92	3.67	d	
18	2.952	27.08	7.18	3.67	w	
22	2.953	30.24	8.63	3.67	w	
23	2.953	29.66	8.3	3.67	w	
24	2.953	12.00	4.90	3.67	d	

SPECIES ..... MANGANESE SULFATE
DATE(S) OF EXPERIMENT .. SEPT 1, 1985

pt #	#1	880mv	Vdc(w)	Vdc(d)		comments
0a	2.955	13.	9.40	7.03	d	
0b	2.969	13.	9.44	7.03	d	
2	2.960	34.38	17.5	7.03	w	
3	2.957	33.77	16.36	7.03	w	
4	2.957	32.51	14.46	7.03	w	
5	2.9545	30.80	12.12	7.03	w	
6	2.953	28.94	10.55	7.03	w	not sure if steady state
7	2.952	26.85	9.98	7.03	w	
8	2.946	23.16	9.78	7.03	d	
9	2.937	16.39	9.65	7.03	d	
10	2.934	35.04	19.19	7.03	w	not sure if steady state
11	2.935	34.51	17.94	7.03	w	
12	2.933	33.95	16.87	7.03	w	

DATE(S) OF EXPERIMENT .. SEPT 3, 1985

pt #	#1	880mv	Vdc(w)	Vdc(d)		comments
13h	2.987	13.	9.45	7.03	d	
14	2.983	28.86	9.48	7.03	d	
15	2.976	32.63	15.07	7.03	w	
16	3.0	13.	10.03	7.03	d	
17	3.0155	30.635	12.20	7.03	w	
18	3.010	15.1	10.12	7.03	d	
19	3.009	29.605	11.36	7.03	w	very close to deliq boundary

DATE(S) OF EXPERIMENT .. SEPT 4, 1985

pt #	#1	880mv	Vdc(w)	Vdc(d)		comments
1	3.021	34.78	30.93	10.7	w	
2	3.021	34.22	27.93	10.7	w	
3	3.020	33.66	25.845	10.7	w	
4	3.021	32.27	22.7	10.7	w	
5	3.022	30.59	19.68	10.7	w	
6	3.022	28.60	16.34	10.7	w	
7	3.022	26.28	14.87	10.7	w	
8	3.021	21.46	14.40	10.7	d	
9	3.020	33.75	25.76	10.7	w	
10a	3.020	34.78	30.36	10.7	w	
10b	2.95	13.	14.2	10.7	d	

DATE(S) OF EXPERIMENT .. SEPT 7, 1985

pt #	#1	880mv	Vdc(w)	Vdc(d)		comments
12	3.026	13.	14.2	10.7	d	
13	3.040	27.51	14.3	10.7	d	
14	3.042	28.55	14.4	10.7	d	
15	3.041	29.46	16.31	10.7	w	
16	3.040	33.57	24.07	10.7	w	
17	3.040	29.33	16.35	10.7	w	
18	3.041	13.	14.61	10.7	d	
19	3.067	13.	14.25	10.7	d	

SPECIES ..... FERRIC CHLORIDE
DATE(S) OF EXPERIMENT .. OCT 3, 1985

pt #	#1	880mv	Vdc(w)	Vdc(d)		comments
0	3.	13.	10.8	6.943	d	
1	3.043	34.99	43.62	6.943	w	
2	3.044	34.46	35.49	6.943	w	
3	3.044	33.82	29.22	6.943	w	
4	3.046	33.28	26.05	6.943	w	
5	3.046	32.71	23.70	6.943	w	
6	3.045	31.68	20.56	6.943	w	
7	3.049	30.80	18.66	6.943	w	
8	3.049	29.23	16.50	6.943	w	
9	3.050	27.83	12.54	6.943	w	aged, not used in aw(m) fit
10	3.	13.	11.57	6.943	d	

DATE(S) OF EXPERIMENT .. OCT 4, 1985

pt #	#1	880mv	Vdc(w)	Vdc(d)		comments
11	3.050	25.95	12.00	6.943	w	partial deliq from "dry"
12	3.051	29.29	12.27	6.943	w	further partial deliq
13	3.051	30.89	12.53	6.943	w	further partial deliq
14	3.051	32.82	14.57	6.943	w	further partial deliq
15	3.053	33.77	28.45	6.943	w	after full deliq completed
16	3.054	32.21	21.56	6.943	w	
17	3.057	32.18	21.36	6.943	w	
18	3.055	30.14	17.10	6.943	w	
19	3.052	28.67	15.35	6.943	w	
20	3.044	28.72	14.51	6.943	w	aged, not used in aw(m) fit
21	3.042	28.29	13.94	6.943	w	aged, not used in aw(m) fit
22	3.042	27.94	11.57	6.943	w	aged, not used in aw(m) fit
23	3.	13.	10.72	6.943	d	

CHEMICAL SPECIES: SODIUM CHLORIDE
DATE(S) OF EXPT: OCT 24, 1985

pt	rh	Vdc(w)	Vdc(d)		wt. frac. sol.	sol. molal.	ionic strgth	sol. mole frac.	hydr. #	osm. coeff.
1	.0586	8.530	8.530	d	1.0000					
2	.6810	8.530	8.530	d	1.0000					
3	.7416	8.530	8.530	d	1.0000					
4	.7630	32.100	8.530	w	.2657	6.197	6.197	.1004	8.96	1.211
6	.8465	44.000	8.530	w	.1939	4.118	4.118	.0691	13.48	1.123
7	.7685	34.660	8.530	w	.2461	5.590	5.590	.0915	9.93	1.307
8	.7244	31.290	8.530	w	.2726	6.417	6.417	.1036	8.65	1.395
9	.6946	29.370	8.530	w	.2904	7.009	7.009	.1121	7.92	1.443
10	.6447	27.070	8.530	w	.3151	7.878	7.878	.1243	7.05	1.546
11	.6018	25.480	8.530	w	.3348	8.617	8.617	.1344	6.44	1.635
12	.5515	23.620	8.530	w	.3611	9.679	9.679	.1485	5.73	1.707
13	.5115	21.680	8.530	w	.3935	11.107	11.107	.1667	5.00	1.675
14	.5039	21.380	8.530	w	.3990	11.367	11.367	.1700	4.88	1.674
15	.4948	21.100	8.530	w	.4043	11.620	11.620	.1731	4.78	1.681
16	.4861	20.770	8.530	w	.4107	11.933	11.933	.1769	4.65	1.678
17	.4764	20.480	8.530	w	.4165	12.223	12.223	.1805	4.54	1.683
18	.4662	20.110	8.530	w	.4242	12.613	12.613	.1852	4.40	1.679
19	.4547	19.730	8.530	w	.4323	13.041	13.041	.1902	4.26	1.677
20b	.4404	8.530	8.530	d	1.0000					

DATE(S) OF EXPT: OCT 25, 1985

pt	rh	Vdc(w)	Vdc(d)		wt. frac. sol.	sol. molal.	ionic strgth	sol. mole frac.	hydr. #	osm. coeff.
22	.8294	39.720	8.530	w	.2148	4.683	4.683	.0778	11.85	1.109
23	.6740	28.520	8.530	w	.2991	7.307	7.307	.1163	7.60	1.498
24	.5759	23.920	8.540	w	.3570	9.508	9.508	.1462	5.84	1.611
25	.5254	22.070	8.540	w	.3870	10.808	10.808	.1630	5.14	1.652
26	.4478	19.600	8.550	w	.4362	13.249	13.249	.1927	4.19	1.683
27	.4427	19.380	8.550	w	.4412	13.518	13.518	.1958	4.11	1.673
28	.4409	19.300	8.560	w	.4435	13.648	13.648	.1973	4.07	1.665
29	.4382	8.560	8.560	d	1.0000					

DATE(S) OF EXPT: DEC 24, 1985

pt	rh	Vdc(w)	Vdc(d)		wt. frac. sol.	sol. molal.	ionic strgth	sol. mole frac.	hydr. #	osm. coeff.
1	.0916	9.080	9.040	d	.9956					
2	.7419	9.040	9.040	d	1.0000					
3	.7898	37.010	9.040	w	.2443	5.534	5.534	.0907	10.03	1.183
4	.7415	33.930	9.040	w	.2664	6.219	6.219	.1008	8.93	1.334
5	.6481	28.040	9.040	w	.3224	8.147	8.147	.1280	6.81	1.478
6	.5491	23.880	9.040	w	.3786	10.431	10.431	.1582	5.32	1.595
7	.4689	21.140	9.040	w	.4276	12.793	12.793	.1873	4.34	1.643
8	.4149	9.040	9.040	d	1.0000					
9	.0916	9.040	9.040	d	1.0000					
11	.3914	9.090	9.090	d	1.0000					
12	.0916	9.090	9.090	d	1.0000					

CHEMICAL SPECIES: SODIUM BROMIDE
DATE(S) OF EXPT: DEC 26, 1985

pt	rh	Vdc(w)	Vdc(d)		wt. frac. sol.	sol. molal.	ionic strgth	sol. mole frac.	hydr. #	osm. coeff.
1	.1093	21.080	21.080	d	1.0000					
2	.5178	41.160	21.080	w	.5121	10.203	10.203	.1553	5.44	1.790
3	.7628	58.060	21.080	w	.3631	5.540	5.540	.0908	10.02	1.356
4	.6900	51.460	21.080	w	.4096	6.744	6.744	.1083	8.23	1.527
5	.6365	47.580	21.080	w	.4430	7.731	7.731	.1223	7.18	1.622
6	.5701	44.000	21.080	w	.4791	8.939	8.939	.1387	6.21	1.745
7	.4987	40.820	21.080	w	.5164	10.379	10.379	.1575	5.35	1.860
8	.3970	36.780	21.080	w	.5731	13.049	13.049	.1903	4.25	1.965
9	.3147	33.930	21.080	w	.6213	15.944	15.944	.2231	3.48	2.012
10	.2603	32.150	21.080	w	.6557	18.507	18.507	.2500	3.00	2.018
11	.2303	31.250	21.080	w	.6746	20.145	20.145	.2663	2.76	2.023
12	.1858	21.080	21.080	d	1.0000					
13	.1274	21.080	21.080	d	1.0000					

DATE(S) OF EXPT: DEC 27, 1985

pt	rh	Vdc(w)	Vdc(d)		wt. frac. sol.	sol. molal.	ionic strgth	sol. mole frac.	hydr. #	osm. coeff.
14	.1093	21.210	21.210	d	1.0000					
17	.4507	21.390	21.210	d	.9916					
18	.4665	22.300	21.210	d	.9511					
19	.4758	39.680	21.210	w	.5345	11.161	11.161	.1674	4.97	1.847
20	.6545	48.600	21.210	w	.4364	7.526	7.526	.1194	7.38	1.563
21	.4432	38.550	21.210	w	.5502	11.888	11.888	.1764	4.67	1.900
22	.3722	35.960	21.210	w	.5898	13.976	13.976	.2011	3.97	1.963
23	.2876	32.960	21.210	w	.6435	17.544	17.544	.2402	3.16	1.972
24	.2146	21.290	21.210	d	.9962					
25	.1093	21.230	21.210	d	.9991					

CHEMICAL SPECIES: POTASSIUM CHLORIDE
DATE(S) OF EXPT: DEC 4,1985

pt	rh	Vdc(w)	Vdc(d)		wt. frac. sol.	sol. molal.	ionic strgth	sol. mole frac.	hydr. #	osm. coeff.
1	.1093	22.570	22.610	d	1.0018					
2	.7729	22.610	22.610	d	1.0000					
4	.8600	93.770	23.000	w	.2453	4.359	4.359	.0728	12.73	.960
7	.7602	68.670	23.280	w	.3390	6.879	6.879	.1103	8.07	1.106
8	.6864	60.020	23.280	w	.3879	8.498	8.498	.1328	6.53	1.229
9	.6272	52.720	23.280	w	.4416	10.606	10.606	.1604	5.23	1.221
10	.5990	50.030	23.280	w	.4653	11.672	11.672	.1737	4.76	1.219
11	.5882	23.800	23.280	d	.9782					
12	.1093	23.800	23.280	d	.9782					

DATE(S) OF EXPT: DEC 5, 1985

pt	rh	Vdc(w)	Vdc(d)		wt. frac. sol.	sol. molal.	ionic strgth	sol. mole frac.	hydr. #	osm. coeff.
13	.1093	24.220	23.500	d	.9703					
14	.8302	24.200	23.500	d	.9711					
16	.8148	79.240	23.500	w	.2966	5.655	5.655	.0925	9.82	1.005
17	.7755	71.200	23.500	w	.3301	6.608	6.608	.1064	8.40	1.068
18	.7365	64.610	23.500	w	.3637	7.667	7.667	.1214	7.24	1.107
19	.6701	59.940	23.500	w	.3921	8.649	8.649	.1348	6.42	1.285
20	.6322	52.030	23.500	w	.4517	11.047	11.047	.1660	5.02	1.152
21	.6203	51.740	23.500	w	.4542	11.161	11.161	.1674	4.97	1.188
22	.6122	51.020	23.500	w	.4606	11.453	11.453	.1710	4.85	1.189
23	.6032	50.000	23.500	w	.4700	11.894	11.894	.1765	4.67	1.180
24	.5902	48.280	23.500	w	.4867	12.719	12.719	.1864	4.36	1.151
25	.5902	23.500	23.500	d	1.0000					
26	.1093	23.500	23.500	d	1.0000					

CHEMICAL SPECIES: POTASSIUM BROMIDE
DATE(S) OF EXPT: DEC 25, 1985

pt	rh	Vdc(w)	Vdc(d)		wt. frac. sol.	sol. molal.	ionic strgth	sol. mole frac.	hydr. #	osm. coeff.
1	.1093	13.400	13.330	d	.9948					
2	.7986	13.480	13.330	d	.9889					
4	.8414	36.200	13.330	w	.3682	4.898	4.898	.0811	11.33	.979
5	.7917	31.910	13.330	w	.4177	6.029	6.029	.0980	9.21	1.075
6	.7048	27.000	13.330	w	.4937	8.195	8.195	.1286	6.77	1.185
7	.6292	23.950	13.330	w	.5566	10.548	10.548	.1597	5.26	1.219
8	.5889	22.600	13.330	w	.5898	12.084	12.084	.1788	4.59	1.216
9	.5594	21.790	13.330	w	.6117	13.241	13.241	.1926	4.19	1.217
10	.5439	21.370	13.330	w	.6238	13.933	13.933	.2006	3.98	1.213
11	.5189	20.980	13.330	w	.6354	14.643	14.643	.2087	3.79	1.243
12	.4919	13.310	13.330	d	1.0015					
13	.1093	13.350	13.330	d	.9985					

DATE(S) OF EXPT: DEC 26, 1985

pt	rh	Vdc(w)	Vdc(d)		wt. frac. sol.	sol. molal.	ionic strgth	sol. mole frac.	hydr. #	osm. coeff.
15	.7600	29.540	13.330	w	.4513	6.911	6.911	.1107	8.03	1.102
16	.6683	25.196	13.330	w	.5291	9.441	9.441	.1454	5.88	1.185
17	.5353	21.000	13.330	w	.6348	14.605	14.605	.2083	3.80	1.188
18	.5045	13.250	13.330	d	1.0060					
19	.1093	13.300	13.330	d	1.0023					

CHEMICAL SPECIES: AMMONIUM CHLORIDE
DATE(S) OF EXPT: OCT 11, 1985

pt	rh	Vdc(w)	Vdc(d)		wt. frac. sol.	sol. molal.	ionic strgth	sol. mole frac.	hydr. #	osm. coeff.
1	.1093	15.330	15.330	d	1.0000					
3	.7823	54.650	15.290	w	.2798	7.262	7.262	.1157	7.64	.938
4	.7834	56.580	15.280	w	.2701	6.916	6.916	.1108	8.03	.980
5	.8290	66.890	15.260	w	.2281	5.525	5.525	.0905	10.05	.942
6	.8746	81.400	15.240	w	.1872	4.306	4.306	.0720	12.89	.863
7	.8467	72.400	15.220	w	.2102	4.976	4.976	.0823	11.16	.928
8	.8422	73.360	15.200	w	.2072	4.886	4.886	.0809	11.36	.975
9	.7343	50.130	15.180	w	.3028	8.120	8.120	.1276	6.84	1.056
10	.6951	45.160	15.170	w	.3359	9.456	9.456	.1456	5.87	1.068
11	.6385	38.630	15.150	w	.3922	12.062	12.062	.1785	4.60	1.032
12	.1093	15.130	15.130	d	1.0000					

DATE(S) OF EXPT: OCT 12A, 1985

pt	rh	Vdc(w)	Vdc(d)		wt. frac. sol.	sol. molal.	ionic strgth	sol. mole frac.	hydr. #	osm. coeff.
13	.1093	14.920	14.920	d	1.0000					
14	.7374	14.920	14.920	d	1.0000					
15	.7715	54.350	14.900	w	.2741	7.061	7.061	.1128	7.86	1.020
16	.6616	40.150	14.880	w	.3706	11.008	11.008	.1655	5.04	1.042
17	.5675	32.300	14.860	w	.4601	15.929	15.929	.2230	3.48	.987
18	.4981	27.660	14.830	w	.5362	21.609	21.609	.2802	2.57	.895
19	.4481	14.600	14.800	d	1.0137					

DATE(S) OF EXPT: OCT 12B, 1985

pt	rh	Vdc(w)	Vdc(d)		wt. frac. sol.	sol. molal.	ionic strgth	sol. mole frac.	hydr. #	osm. coeff.
20	.7591	14.850	14.800	d	.9966					
21	.7653	15.000	14.800	d	.9867					
22	.7730	53.650	14.730	w	.2746	7.075	7.075	.1131	7.85	1.010
23	.8924	89.700	14.660	w	.1634	3.652	3.652	.0617	15.20	.865
24	.7922	57.800	14.590	w	.2524	6.312	6.312	.1021	8.79	1.024
25	.7015	44.110	14.520	w	.3292	9.173	9.173	.1418	6.05	1.072
26	.6110	35.000	14.450	w	.4129	13.145	13.145	.1915	4.22	1.040
27	.5319	29.280	14.380	w	.4911	18.042	18.042	.2453	3.08	.971
28	.4874	26.570	14.300	w	.5382	21.787	21.787	.2819	2.55	.916
29	.4775	25.680	14.230	w	.5541	23.233	23.233	.2951	2.39	.883
30	.4664	14.150	14.150	d	1.0000					
31	.1093	14.137	14.150	d	1.0009					

CHEMICAL SPECIES: SODIUM SULFATE
DATE(S) OF EXPT: OCT 21, 1985

pt	rh	Vdc(w)	Vdc(d)		wt. frac. sol.	sol. molal.	ionic strgth	sol. mole frac.	hydr. #	osm. coeff.
1	.1093	11.660	11.660	d	1.0000					
2	.7916	11.720	11.680	d	.9966					
3	.8398	11.700	11.730	d	1.0026					
5	.8809	35.850	11.840	w	.3303	3.473	10.418	.0589	15.98	.676
6	.8457	32.650	11.860	w	.3632	4.017	12.052	.0675	13.82	.772
7	.7863	29.190	11.940	w	.4090	4.874	14.623	.0807	11.39	.912
8	.7381	27.060	11.980	w	.4427	5.595	16.784	.0916	9.92	1.004
9	.6917	25.370	12.000	w	.4730	6.321	18.962	.1022	8.78	1.079
10	.6523	23.930	12.010	w	.5019	7.095	21.286	.1133	7.82	1.114
11	.5960	21.620	12.030	w	.5564	8.834	26.502	.1373	6.28	1.084
12	.5508	18.900	12.040	w	.6370	12.360	37.080	.1821	4.49	.893
13	.5513	12.060	12.060	d	1.0000					
14	.1093	12.060	12.070	d	1.0008					

DATE(S) OF EXPT: OCT 22, 1985

pt	rh	Vdc(w)	Vdc(d)		wt. frac. sol.	sol. molal.	ionic strgth	sol. mole frac.	hydr. #	osm. coeff.
1	.1093	22.080	22.070	d	.9995					
2	.8308	22.290	22.070	d	.9901					
3	.8776	66.720	22.070	w	.3308	3.481	10.443	.0590	15.95	.694
4	.8601	63.610	22.070	w	.3470	3.742	11.225	.0631	14.84	.745
5	.8435	60.930	22.070	w	.3622	4.000	11.999	.0672	13.88	.787
6	.7920	54.500	22.070	w	.4050	4.793	14.378	.0795	11.58	.900
7	.7378	50.500	22.070	w	.4370	5.467	16.401	.0897	10.15	1.029
8	.6924	46.900	22.070	w	.4706	6.259	18.778	.1013	8.87	1.087
9	.6456	43.550	22.070	w	.5068	7.236	21.707	.1153	7.67	1.119
10	.5930	39.250	22.070	w	.5623	9.047	27.140	.1401	6.14	1.069
11	.5628	36.200	22.070	w	.6097	10.999	32.998	.1654	5.05	.967
12	.5561	35.380	22.070	w	.6238	11.677	35.031	.1738	4.75	.930
13	.5526	34.770	22.070	w	.6347	12.238	36.714	.1806	4.54	.897
14	.5481	34.170	22.070	w	.6459	12.845	38.535	.1879	4.32	.866
15	.5481	22.090	22.070	d	.9991					
16	.8539	22.490	22.070	d	.9813					
17	.8649	64.070	22.070	w	.3445	3.701	11.102	.0625	15.00	.726
18	.1093	22.040	22.070	d	1.0014					

CHEMICAL SPECIES: AMMONIUM SULFATE
DATE(S) OF EXPT: AUG 25-27,1985

pt	rh	Vdc(w)	Vdc(d)	wt. frac. sol.	sol. molal.	ionic strgth	sol. mole frac.	hydr. #	osm. coeff.
2	.8164	50.310	20.540 w	.4083	5.221	15.664	.0860	10.63	.719
3	.8619	58.500	20.540 w	.3511	4.095	12.285	.0687	13.56	.672
4	.8374	54.300	20.540 w	.3783	4.604	13.813	.0766	12.06	.713
5	.8755	61.930	20.540 w	.3317	3.756	11.267	.0634	14.78	.655
6	.6903	39.070	20.540 w	.5257	8.389	25.166	.1313	6.62	.818
7	.5328	31.300	20.540 w	.6562	14.446	43.339	.2065	3.84	.806
8	.5032	30.240	20.540 w	.6792	16.025	48.075	.2240	3.46	.793
9	.4883	29.590	20.540 w	.6942	17.176	51.527	.2363	3.23	.772
10	.4748	29.230	20.540 w	.7027	17.887	53.662	.2437	3.10	.770
11	.4619	20.630	20.540 d	.9956					
13	.6719	20.710	20.710 d	1.0000					
15	.8069	48.500	20.860 w	.4301	5.711	17.134	.0933	9.72	.695

DATE(S) OF EXPT: SEPT 20-24, 1985

pt	rh	Vdc(w)	Vdc(d)	wt. frac. sol.	sol. molal.	ionic strgth	sol. mole frac.	hydr. #	osm. coeff.
1	.6273	5.420	5.424 d	1.0007					
2	.7490	5.390	5.424 d	1.0063					
3	.7864	5.400	5.424 d	1.0044					
4	.8166	13.220	5.424 w	.4103	5.265	15.796	.0866	10.54	.712
5a	.1093	5.430	5.424 d	.9989					
5b	.7748	5.420	5.424 d	1.0007					
6	.7975	5.400	5.424 d	1.0044					
7	.7979	5.460	5.424 d	.9934					
8	.8060	5.420	5.424 d	1.0007					
10	.8127	13.020	5.424 w	.4166	5.404	16.211	.0887	10.27	.710
12	.8543	14.860	5.424 w	.3650	4.350	13.050	.0727	12.76	.670
13	.8151	13.330	5.424 w	.4069	5.192	15.576	.0855	10.69	.729
14	.7132	10.780	5.424 w	.5032	7.664	22.991	.1213	7.24	.816
15	.6153	9.270	5.424 w	.5851	10.673	32.018	.1613	5.20	.842
16	.5299	5.450	5.424 d	.9952					
17	.5782	8.810	5.424 w	.6157	12.123	36.368	.1792	4.58	.836
18	.5506	8.520	5.424 w	.6366	13.258	39.775	.1928	4.19	.833
19	.5394	5.450	5.424 d	.9952					

CHEMICAL SPECIES: CALCIUM CHLORIDE
DATE(S) OF EXPT: JAN 10, 1986

pt	rh	Vdc(w)	Vdc(d)	wt. frac. sol.	sol. molal.	ionic strgth	sol. mole frac.	hydr. #	osm. coeff.
1	.0589	76.380	46.260 d	.6057			.1995	4.01	
2	.4994	131.270	46.260 w	.3524	4.903	14.709	.0812	11.32	2.621
3	.6148	149.640	46.260 w	.3091	4.032	12.095	.0677	13.77	2.233

DATE(S) OF EXPT: JAN 11, 1986

pt	rh	Vdc(w)	Vdc(d)	wt. frac. sol.	sol. molal.	ionic strgth	sol. mole frac.	hydr. #	osm. coeff.
1	.1104	9.370	5.640 w	.6019	13.623	40.870	.1971	4.07	2.993
2	.4197	14.290	5.640 w	.3947	5.875	17.624	.0957	9.45	2.734
3	.8469	28.910	5.640 w	.1951	2.184	6.551	.0379	25.42	1.408
4	.7722	23.960	5.640 w	.2354	2.774	8.321	.0476	20.01	1.724
5	.5758	17.400	5.640 w	.3241	4.321	12.963	.0722	12.85	2.363
6	.7183	21.490	5.640 w	.2624	3.206	9.618	.0546	17.31	1.909
7	.3541	13.640	5.640 w	.4135	6.352	19.056	.1027	8.74	3.024
8	.1215	9.750	5.640 w	.5785	12.364	37.092	.1822	4.49	3.155

DATE(S) OF EXPT: JAN 12, 1986

pt	rh	Vdc(w)	Vdc(d)	wt. frac. sol.	sol. molal.	ionic strgth	sol. mole frac.	hydr. #	osm. coeff.
11	.0410	9.320	5.640 d	.6052			.1992	4.02	
12	.6591	18.930	5.640 w	.2979	3.824	11.471	.0644	14.52	2.017
13	.5377	16.500	5.640 w	.3418	4.679	14.037	.0777	11.86	2.454
14	.4520	15.020	5.640 w	.3755	5.417	16.252	.0889	10.25	2.712
15	.3935	14.070	5.640 w	.4009	6.028	18.084	.0980	9.21	2.863
16	.3369	13.230	5.640 w	.4263	6.695	20.085	.1076	8.29	3.007
17	.3064	12.750	5.640 w	.4424	7.147	21.441	.1141	7.77	3.062
18	.2659	12.210	5.640 w	.4619	7.734	23.203	.1223	7.18	3.169
19	.2377	11.850	5.640 w	.4759	8.183	24.548	.1285	6.78	3.249
20	.2089	11.420	5.640 w	.4939	8.792	26.375	.1367	6.31	3.295
21	.1687	10.460	5.640 w	.5392	10.543	31.628	.1596	5.27	3.123
22	.1372	9.250	5.640 w	.6097	14.076	42.229	.2023	3.94	2.611

CHEMICAL SPECIES: MNCL2
DATE(S) OF EXPT: SEPT 27a, 1985

pt	rh	Vdc(w)	Vdc(d)	wt. frac. sol.	sol. molal.	ionic strgth	sol. mole frac.	hydr. #	osm. coeff.
1	.0898	4.900	3.670 d	.7490					
3	.6249	9.100	3.670 w	.4033	5.371	16.112	.0882	10.34	1.620
4	.6888	10.140	3.670 w	.3619	4.507	13.522	.0751	12.31	1.530
5	.5161	7.920	3.670 w	.4634	6.862	20.586	.1100	8.09	1.784
6	.4709	7.510	3.670 w	.4887	7.595	22.784	.1204	7.31	1.835
7	.4344	7.220	3.670 w	.5083	8.215	24.645	.1289	6.76	1.878
8	.3915	6.860	3.670 w	.5350	9.142	27.426	.1414	6.07	1.898
9	.3439	6.510	3.670 w	.5637	10.269	30.806	.1561	5.41	1.923
10	.3162	6.300	3.670 w	.5825	11.089	33.266	.1665	5.01	1.921
11	.2946	4.840	3.670 d	.7583					

DATE(S) OF EXPT: SEPT 27b, 1985

pt	rh	Vdc(w)	Vdc(d)	wt. frac. sol.	sol. molal.	ionic strgth	sol. mole frac.	hydr. #	osm. coeff.
12	.4110	4.860	3.670 d	.7551					
13	.4478	7.270	3.670 w	.5048	8.101	24.303	.1274	6.85	1.835
14	.3016	6.170	3.670 w	.5948	11.665	34.996	.1737	4.76	1.901
15	.3002	6.110	3.670 w	.6007	11.952	35.856	.1772	4.64	1.863
16	.2953	4.820	3.670 d	.7614					

DATE(S) OF EXPT: SEPT 27c, 1985

pt	rh	Vdc(w)	Vdc(d)	wt. frac. sol.	sol. molal.	ionic strgth	sol. mole frac.	hydr. #	osm. coeff.
17	.4254	4.920	3.670 d	.7459					
18	.4374	7.180	3.670 w	.5111	8.309	24.926	.1302	6.68	1.842
22	.5688	8.630	3.670 w	.4253	5.880	17.639	.0958	9.44	1.776
23	.5411	8.300	3.670 w	.4422	6.299	18.896	.1019	8.81	1.804
24	.0894	4.900	3.670 d	.7490					

CHEMICAL SPECIES: MANGANESE SULFATE
DATE(S) OF EXPT: SEPT 1, 1985

pt	rh	Vdc(w)	Vdc(d)	wt. frac. sol.	sol. molal.	ionic strgth	sol. mole frac.	hydr. #	osm. coeff.
0a	.1070	9.400	7.030 d	.7479			.2614	2.83	
0b	.1077	9.440	7.030 d	.7447			.2582	2.87	
2	.8363	17.500	7.030 w	.4017	4.447	17.787	.0742	12.48	1.116
3	.7872	16.360	7.030 w	.4297	4.990	19.960	.0825	11.12	1.331
4	.6987	14.460	7.030 w	.4862	6.266	25.065	.1014	8.86	1.588
5	.5978	12.120	7.030 w	.5800	9.147	36.587	.1415	6.07	1.561
6	.5092	10.550	7.030 w	.6664	13.227	52.906	.1924	4.20	1.416
7	.4294	9.980	7.030 w	.7044	15.782	63.129	.2214	3.52	1.487
8	.3207	9.780	7.030 d	.7188			.2337	3.28	
9	.1705	9.650	7.030 d	.7285			.2425	3.12	
10	.8815	19.190	7.030 w	.3663	3.829	15.315	.0645	14.50	.915
11	.8370	17.940	7.030 w	.3919	4.267	17.070	.0714	13.01	1.157
12	.7919	16.870	7.030 w	.4167	4.731	18.926	.0785	11.73	1.369

DATE(S) OF EXPT: SEPT 3, 1985

pt	rh	Vdc(w)	Vdc(d)	wt. frac. sol.	sol. molal.	ionic strgth	sol. mole frac.	hydr. #	osm. coeff.
13h	.1086	9.450	7.030 d	.7439			.2574	2.89	
14	.5130	9.480	7.030 d	.7416			.2550	2.92	
15	.7130	15.070	7.030 w	.4665	5.791	23.163	.0945	9.59	1.622
16	.1093	10.030	7.030 d	.7009			.2185	3.58	
17	.6062	12.200	7.030 w	.5762	9.005	36.021	.1396	6.16	1.542
18	.1502	10.120	7.030 d	.6947			.2135	3.68	
19	.5529	11.360	7.030 w	.6188	10.752	43.009	.1623	5.16	1.529

DATE(S) OF EXPT: SEPT 4, 1985

pt	rh	Vdc(w)	Vdc(d)	wt. frac. sol.	sol. molal.	ionic strgth	sol. mole frac.	hydr. #	osm. coeff.
1	.8950	30.930	10.700 w	.3459	3.503	14.011	.0594	15.85	.879
2	.8472	27.930	10.700 w	.3831	4.113	16.451	.0690	13.50	1.119
3	.8022	25.845	10.700 w	.4140	4.679	18.716	.0777	11.86	1.307
4	.7042	22.700	10.700 w	.4714	5.905	23.621	.0962	9.40	1.648
5	.6057	19.680	10.700 w	.5437	7.891	31.565	.1245	7.03	1.763
6	.5113	16.340	10.700 w	.6548	12.564	50.257	.1846	4.42	1.482
7	.4242	14.870	10.700 w	.7196	16.993	67.974	.2344	3.27	1.401
8	.2896	14.400	10.700 w	.7431	19.152	76.608	.2565	2.90	1.796
9	.8092	25.760	10.700 w	.4154	4.705	18.821	.0781	11.80	1.249
10a	.8946	30.360	10.700 w	.3524	3.604	14.418	.0610	15.40	.858
10b	.1067	14.200	10.700 d	.7535			.2673	2.74	

DATE(S) OF EXPT: SEPT 7, 1985

pt	rh	Vdc(w)	Vdc(d)	wt. frac. sol.	sol. molal.	ionic strgth	sol. mole frac.	hydr. #	osm. coeff.
12	.1106	14.200	10.700 d	.7535			.2673	2.74	
13	.4717	14.300	10.700 d	.7483			.2618	2.82	
14	.5139	14.400	10.700 d	.7431			.2565	2.90	
15	.5543	16.310	10.700 w	.6560	12.632	50.526	.1854	4.39	1.296
16	.8027	24.070	10.700 w	.4445	5.300	21.201	.0872	10.47	1.151
17	.5480	16.350	10.700 w	.6544	12.542	50.168	.1843	4.43	1.331
18	.1113	14.610	10.700 d	.7324			.2461	3.06	
19	.1127	14.250	10.700 d	.7509			.2645	2.78	

CHEMICAL SPECIES: FERRIC CHLORIDE
DATE(S) OF EXPT: OCT 3, 1985

pt	rh	Vdc(w)	Vdc(d)	wt. frac. sol.	sol. molal.	ionic strgth	sol. mole frac.	hydr. #	osm. coeff.
0	.1093	10.800	6.943 d	.6429			.1666	5.00	
1	.9231	43.620	6.943 w	.1592	1.167	7.002	.0206	47.56	.952
2	.8765	35.490	6.943 w	.1956	1.499	8.996	.0263	37.02	1.220
3	.8237	29.220	6.943 w	.2376	1.921	11.529	.0335	28.89	1.401
4	.7830	26.050	6.943 w	.2665	2.240	13.441	.0388	24.78	1.515
5	.7421	23.700	6.943 w	.2930	2.554	15.326	.0440	21.73	1.621
6	.6746	20.560	6.943 w	.3377	3.143	18.860	.0536	17.66	1.738
7	.6247	18.660	6.943 w	.3721	3.653	21.919	.0617	15.19	1.787
8	.5456	16.500	6.943 w	.4208	4.479	26.873	.0747	12.39	1.877
9	.4863	12.540	6.943 w	.5537			.1211	7.26	
10	.1093	11.570	6.943 d	.6001			.1428	6.00	

DATE(S) OF EXPT: OCT 4, 1985

pt	rh	Vdc(w)	Vdc(d)	wt. frac. sol.	sol. molal.	ionic strgth	sol. mole frac.	hydr. #	osm. coeff.
11	.4187	12.000	6.943 w	.5786			.1323	6.56	
12	.5489	12.270	6.943 w	.5659			.1265	6.91	
13	.6303	12.530	6.943 w	.5541			.1213	7.25	
14	.7515	14.570	6.943 w	.4765			.0918	9.89	
15	.8232	28.450	6.943 w	.2440	1.990	11.941	.0346	27.89	1.357
16	.7110	21.560	6.943 w	.3220	2.928	17.570	.0501	18.96	1.616
17	.7100	21.360	6.943 w	.3250	2.969	17.814	.0508	18.70	1.601
18	.5913	17.100	6.943 w	.4060	4.214	25.285	.0706	13.17	1.730
19	.5214	15.350	6.943 w	.4523	5.091	30.549	.0840	10.90	1.775
20	.5217	14.510	6.943 w	.4785			.0925	9.81	
21	.5030	13.940	6.943 w	.4981			.0993	9.07	
22	.4889	11.570	6.943 w	.6001			.1428	6.00	
23	.1093	10.72	6.943 d	.6447			.1695	4.90	

Appendix B: Comparison of experimental water activity data with literature data for single-electrolyte solutions

Appendix B contains plots of water activity as a function of molality for each of the eleven single-electrolyte solutions studied in this work. Each plot contains experimental data and data from the literature. The experimental data is taken from the tables of Appendix A. The sources for the literature data are given in the figure captions. The following abbreviations are used:

- **Robinson and Stokes** or **R & S**:
  R.A. Robinson and R.H. Stokes. *Electrolyte Solutions.* Butterworths, London, 2nd edition, 1959.
- **Intl Crit Tables** or **ICT**:
  E.W. Washburn, editor. *International Critical Tables.* McGraw Hill, New York, 1926.
- **Rard et al. (1981)**:
  J.A. Rard and D.G. Miller. *J. Chem. Engr. Data*, 26:33, 1981.
- **Spann5** and **Spann6**:
  Tables 5 and 6 of J.F. Spann and C.B. Richardson. *Atmospheric Environment*, 19:819, 1985.
- **Richardson**:
  C.B. Richardson and J.F. Spann. *J. Aerosol Sci.*, 15:563, 1984.
- **Rard (1983)**:
  J.A. Rard, A. Habenschuss, and F. Spedding. *J. Chem. Engr. Data*, 22:180, 1977.
- **Rard (1984)**:
  J.A. Rard. *J. Chem. Engr. Data*, 29:443, 1984.
- **Kangro (1962)**:
  W. Kangro and A. Groeneveld. *Z. Physik. Chem.*, 32:110, 1962.

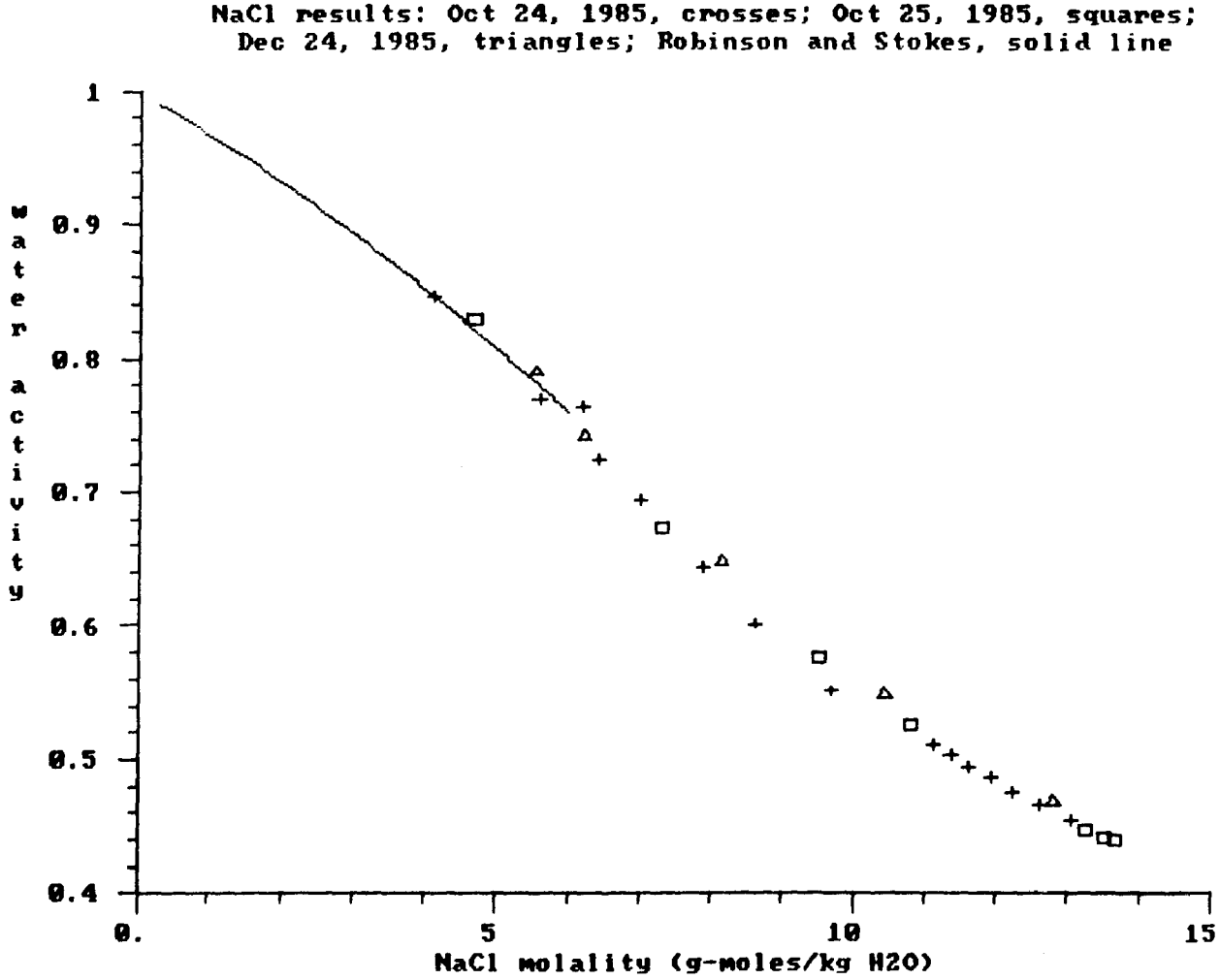
NaCl results: Oct 24, 1985, crosses; Oct 25, 1985, squares;
Dec 24, 1985, triangles; Robinson and Stokes, solid line
water activity
1
0.9
0.8
0.7
0.6
0.5
0.4
0.
5
10
15
NaCl molality (g-moles/kg H2O)

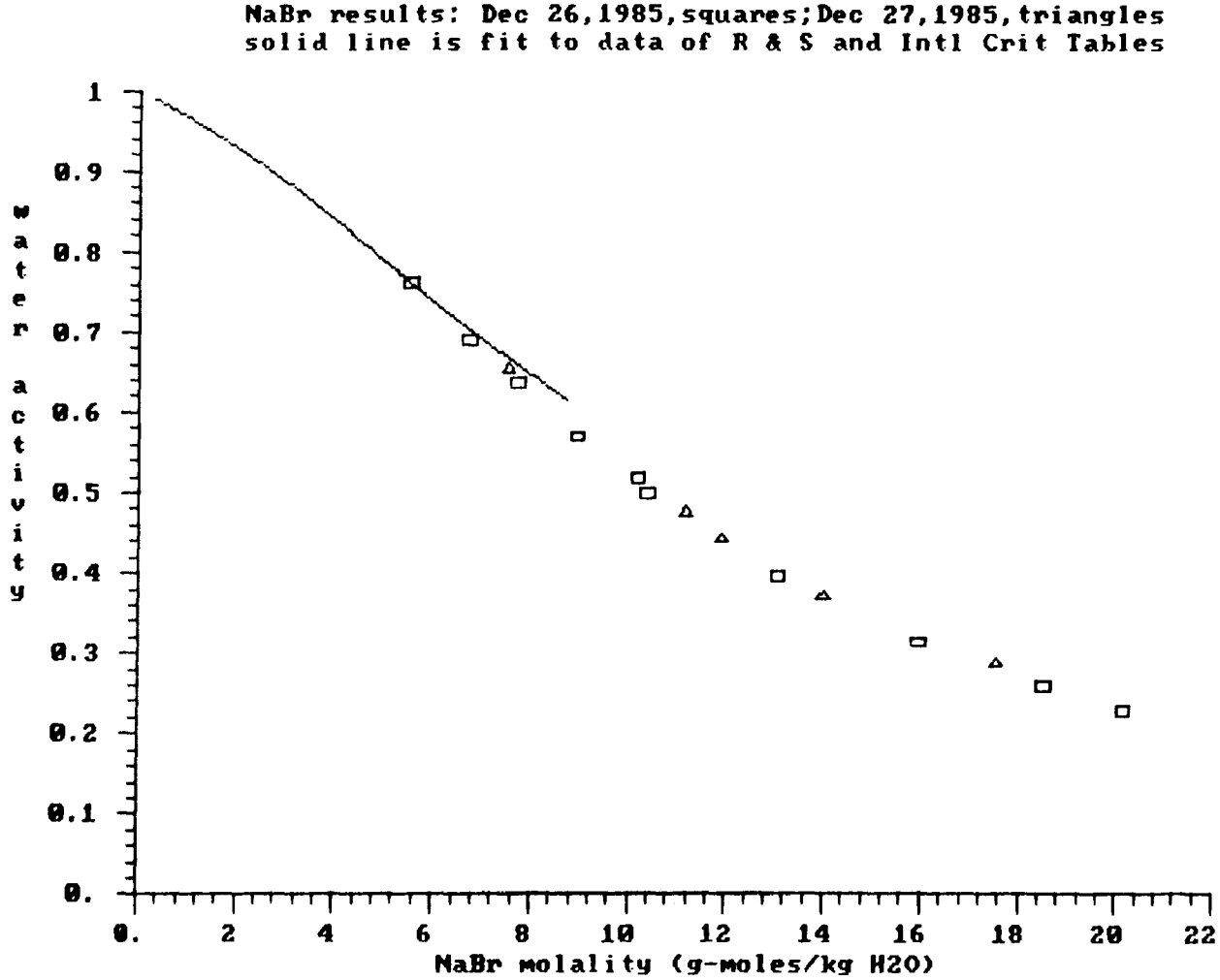
NaBr results: Dec 26,1985,squares;Dec 27,1985,triangles
solid line is fit to data of R & S and Intl Crit Tables
water activity
1
0.9
0.8
0.7
0.6
0.5
0.4
0.3
0.2
0.1
0.
0.
2
4
6
8
10
12
14
16
18
20
22
NaBr molality (g-moles/kg H2O)

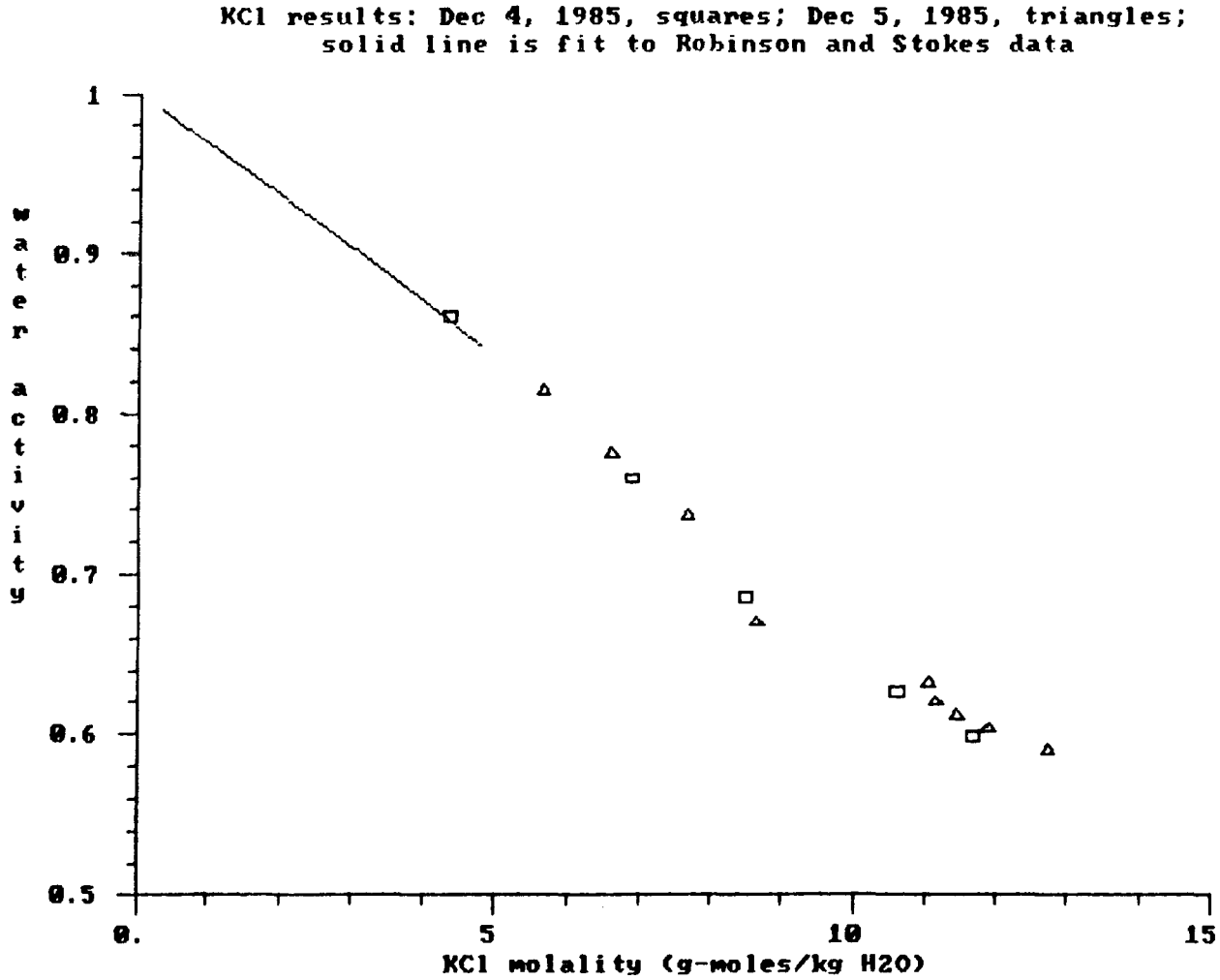
KCl results: Dec 4, 1985, squares; Dec 5, 1985, triangles;
solid line is fit to Robinson and Stokes data
water activity
1
0.9
0.8
0.7
0.6
0.5
0.
5
10
15
KCl molality (g-moles/kg H2O)

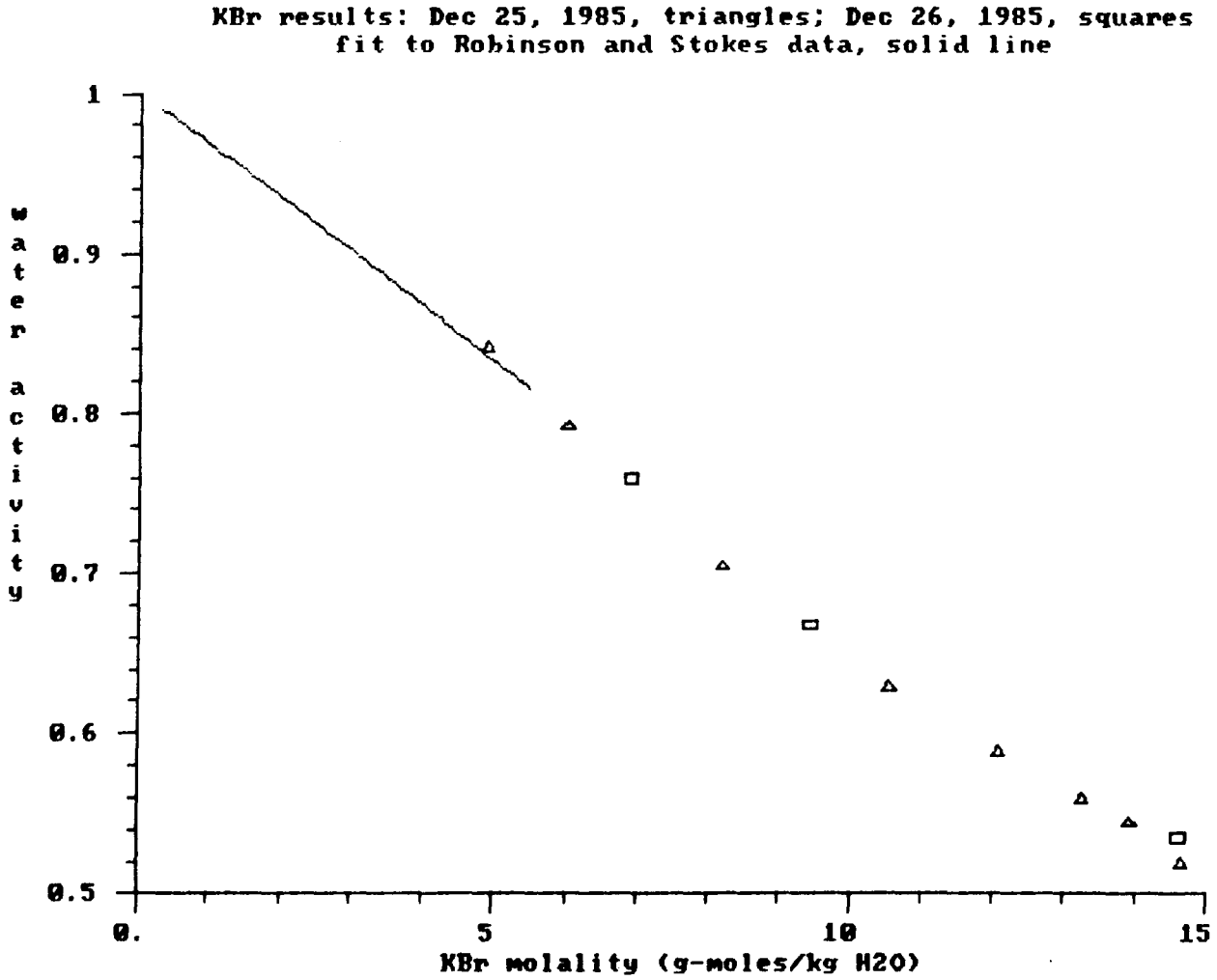
KBr results: Dec 25, 1985, triangles; Dec 26, 1985, squares
fit to Robinson and Stokes data, solid line
water activity
1
0.9
0.8
0.7
0.6
0.5
0.
5
10
15
KBr molality (g-moles/kg H2O)

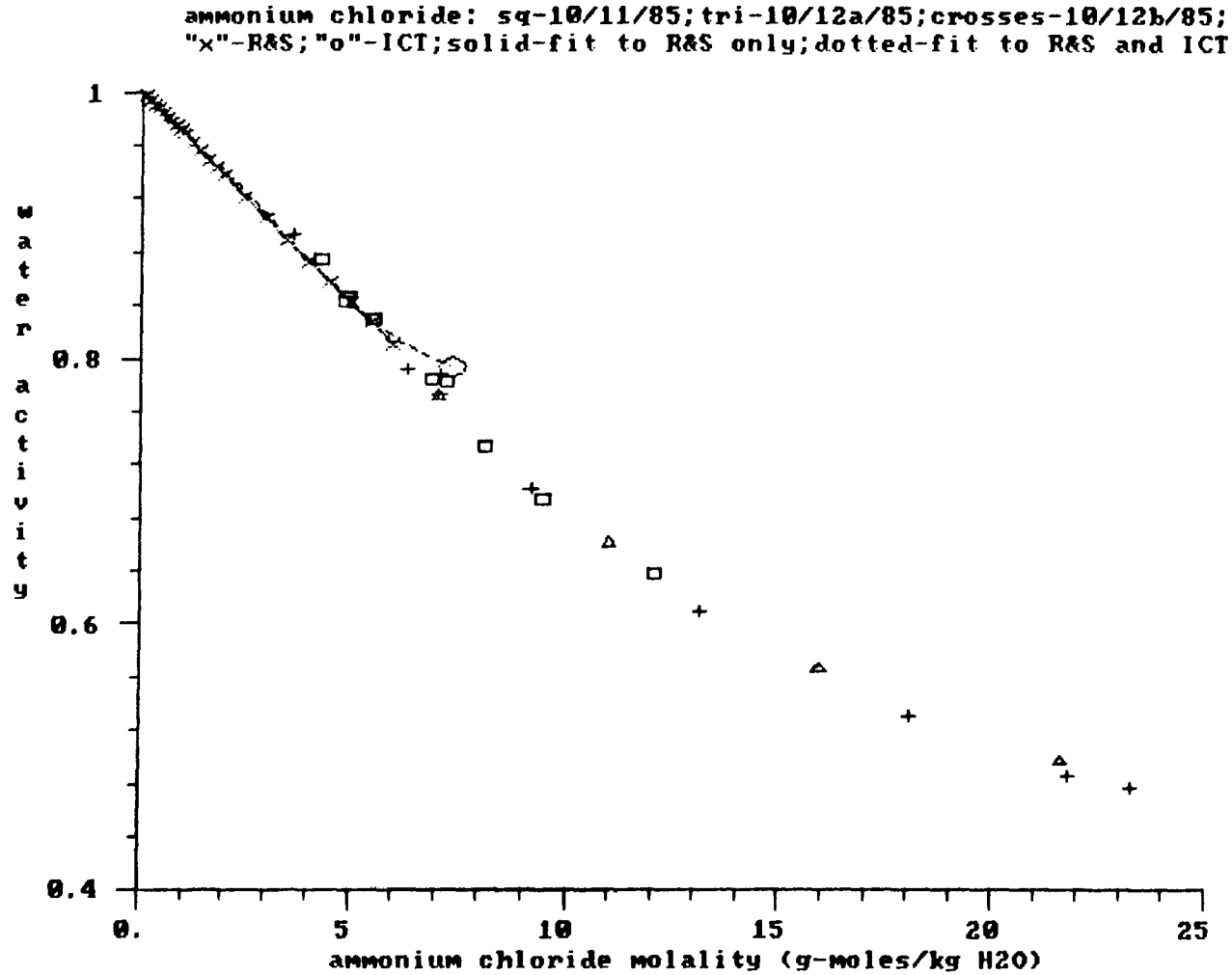
ammonium chloride: sq-10/11/85;tri-10/12a/85;crosses-10/12b/85;
"x"-R&S;"o"-ICT;solid-fit to R&S only;dotted-fit to R&S and ICT
water activity
1
0.8
0.6
0.4
0.
5
10
15
20
25
ammonium chloride molality (g-moles/kg H2O)

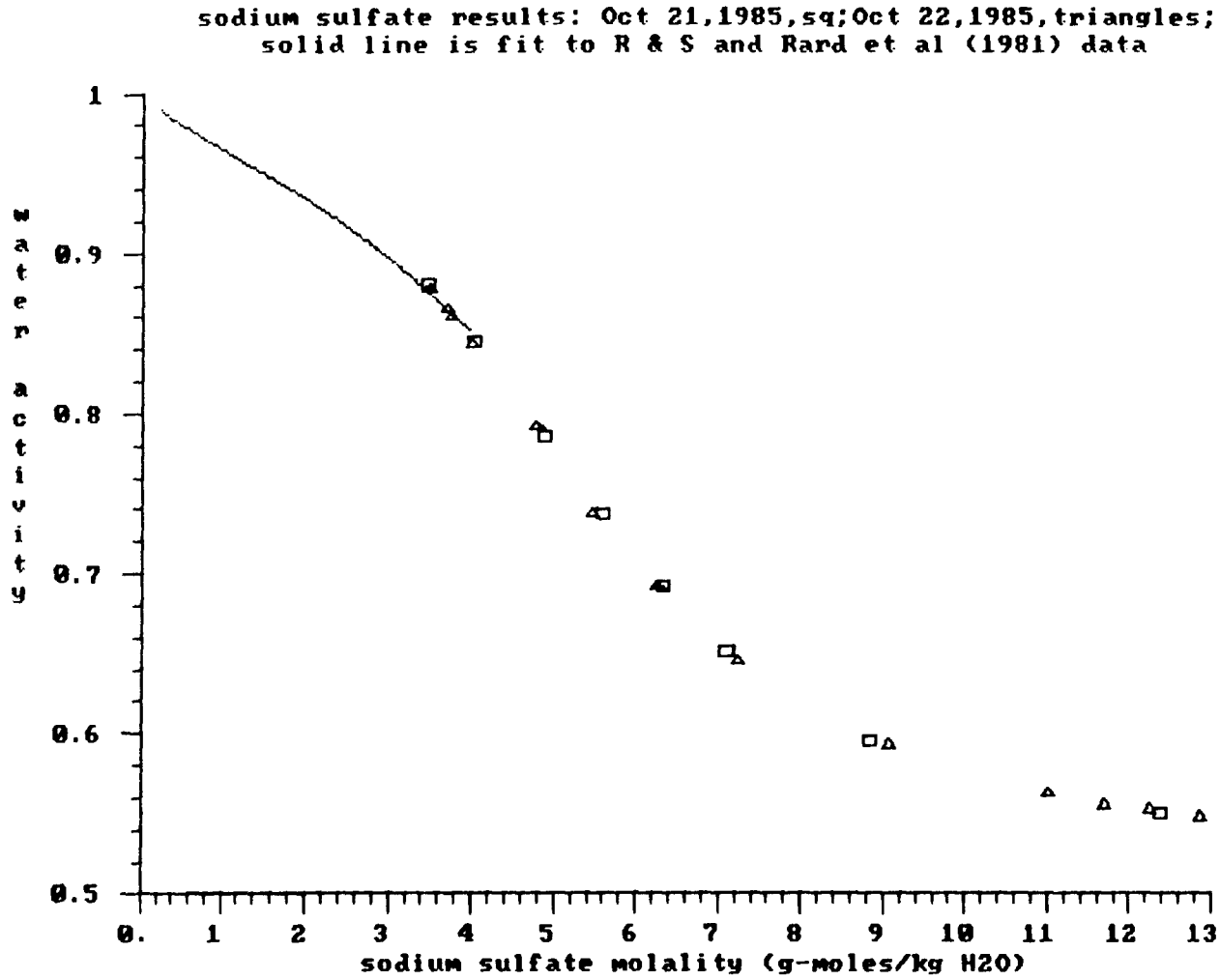
sodium sulfate results: Oct 21,1985,sq;Oct 22,1985,triangles;
solid line is fit to R & S and Rard et al (1981) data
water activity
1
0.9
0.8
0.7
0.6
0.5
0.
1
2
3
4
5
6
7
8
9
10
11
12
13
sodium sulfate molality (g-moles/kg H2O)

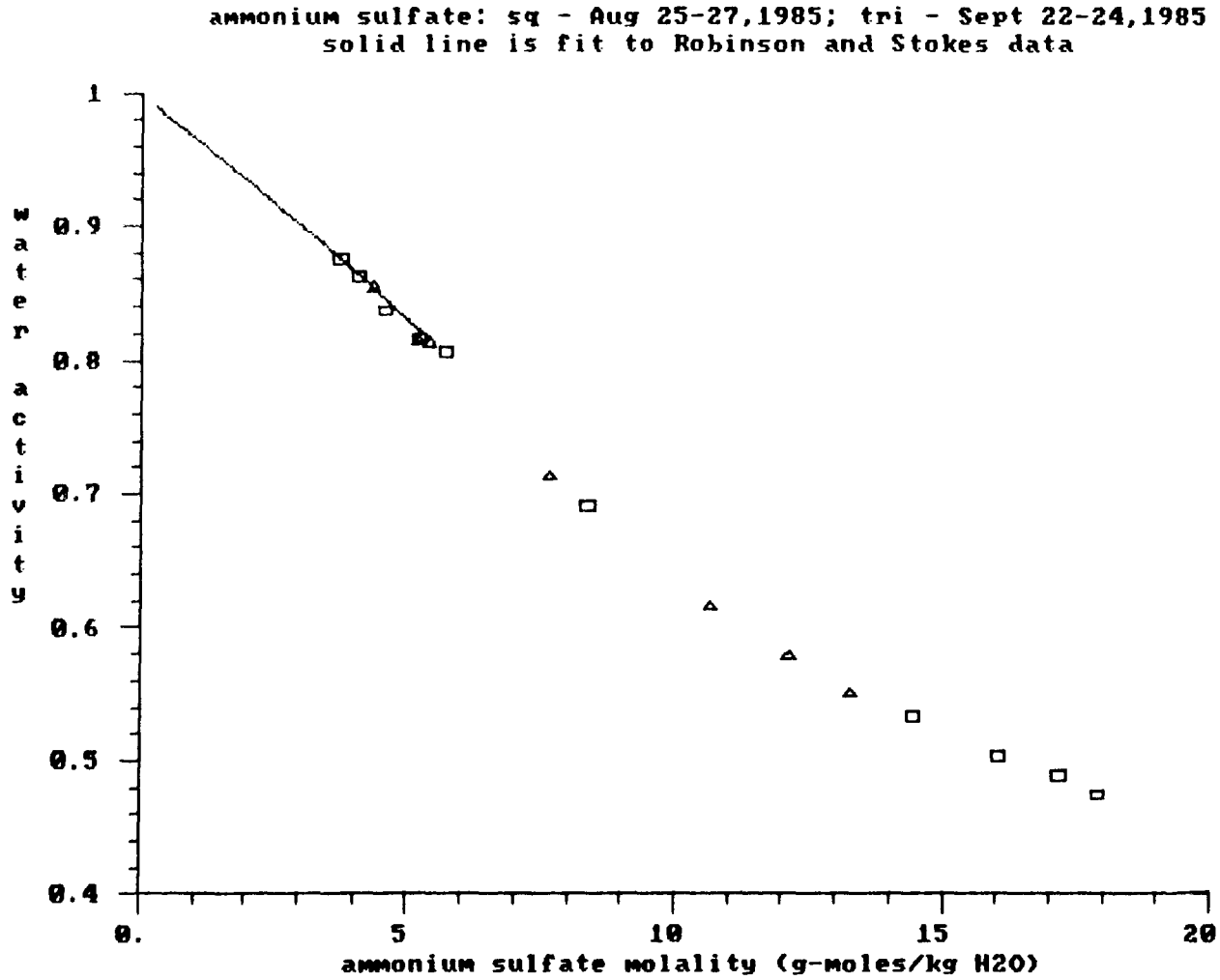
ammonium sulfate: sq - Aug 25-27,1985; tri - Sept 22-24,1985
solid line is fit to Robinson and Stokes data
water activity
1
0.9
0.8
0.7
0.6
0.5
0.4
0.
5
10
15
20
ammonium sulfate molality (g-moles/kg H2O)

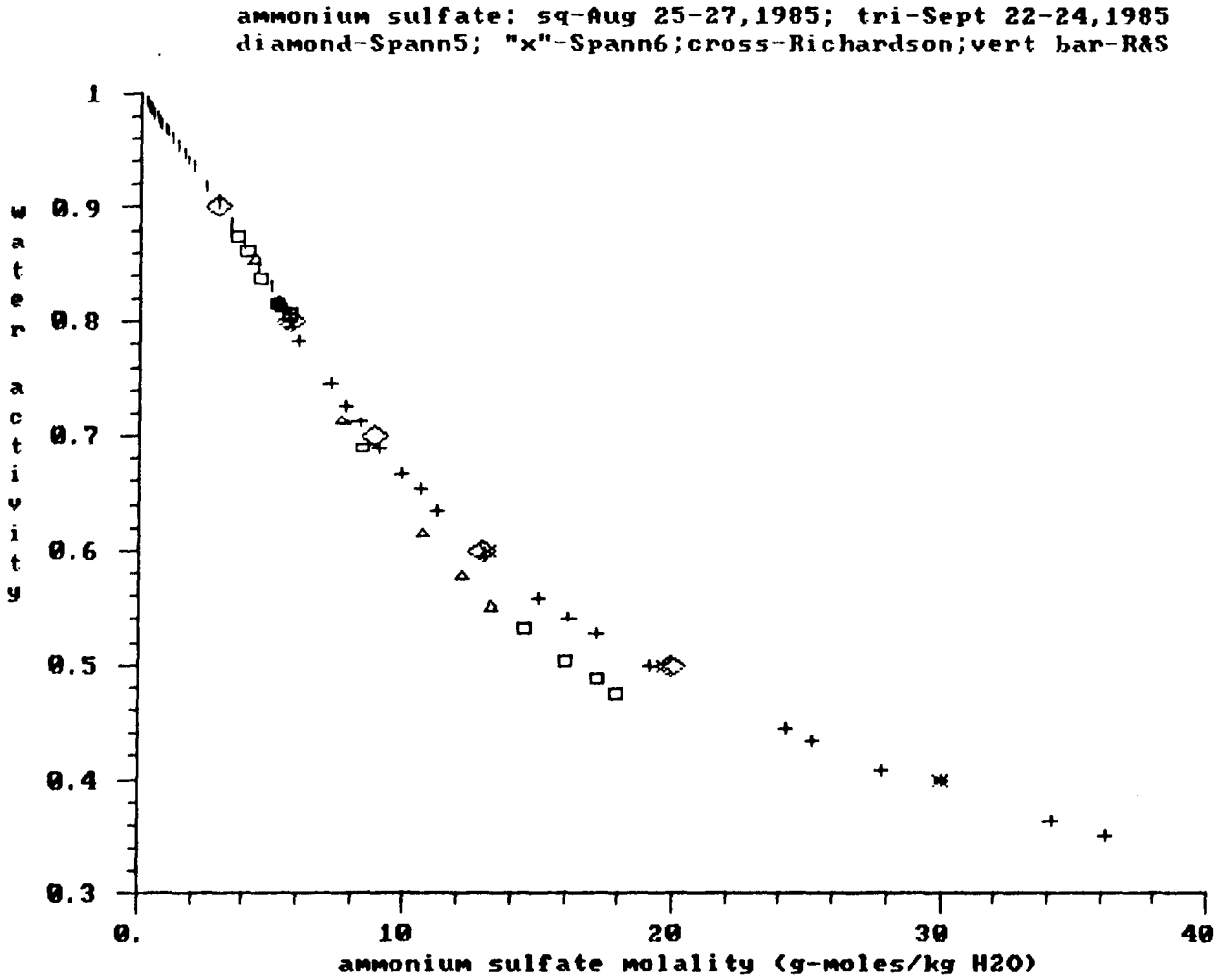
ammonium sulfate: sq-Aug 25-27,1985; tri-Sept 22-24,1985
diamond-Spann5; "x"-Spann6;cross-Richardson;vert bar-R&S
water activity
1
0.9
0.8
0.7
0.6
0.5
0.4
0.3
0.
10
20
30
40
ammonium sulfate molality (g-moles/kg H2O)

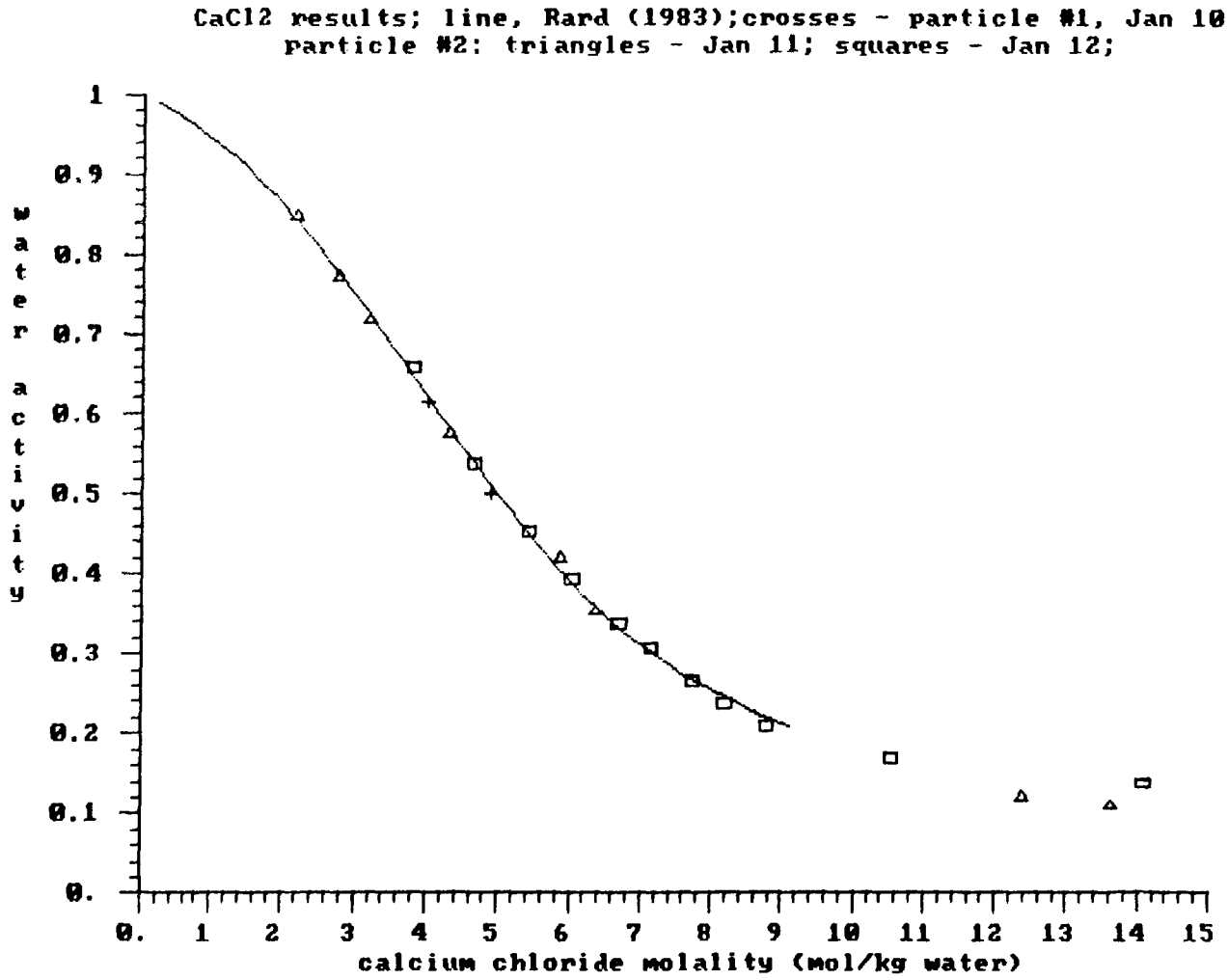
CaCl2 results; line, Rard (1983);crosses - particle #1, Jan 10
particle #2: triangles - Jan 11; squares - Jan 12;
water activity
1
0.9
0.8
0.7
0.6
0.5
0.4
0.3
0.2
0.1
0.
0. 1 2 3 4 5 6 7 8 9 10 11 12 13 14 15
calcium chloride molality (mol/kg water)

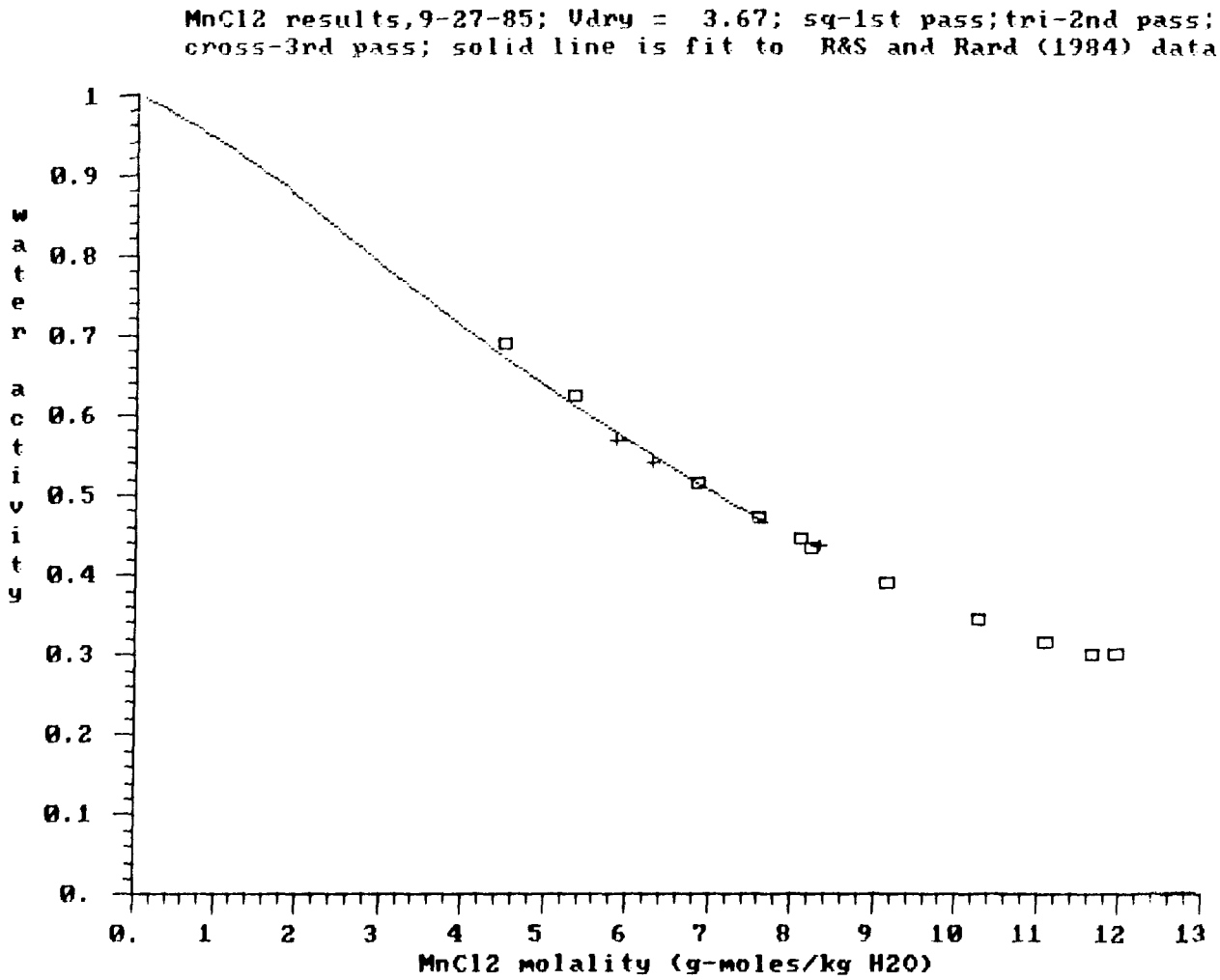
MnCl2 results,9-27-85; Vdry = 3.67; sq-1st pass;tri-2nd pass;
cross-3rd pass; solid line is fit to R&S and Rard (1984) data
water activity
1
0.9
0.8
0.7
0.6
0.5
0.4
0.3
0.2
0.1
0.
0.
1
2
3
4
5
6
7
8
9
10
11
12
13
MnCl2 molality (g-moles/kg H2O)

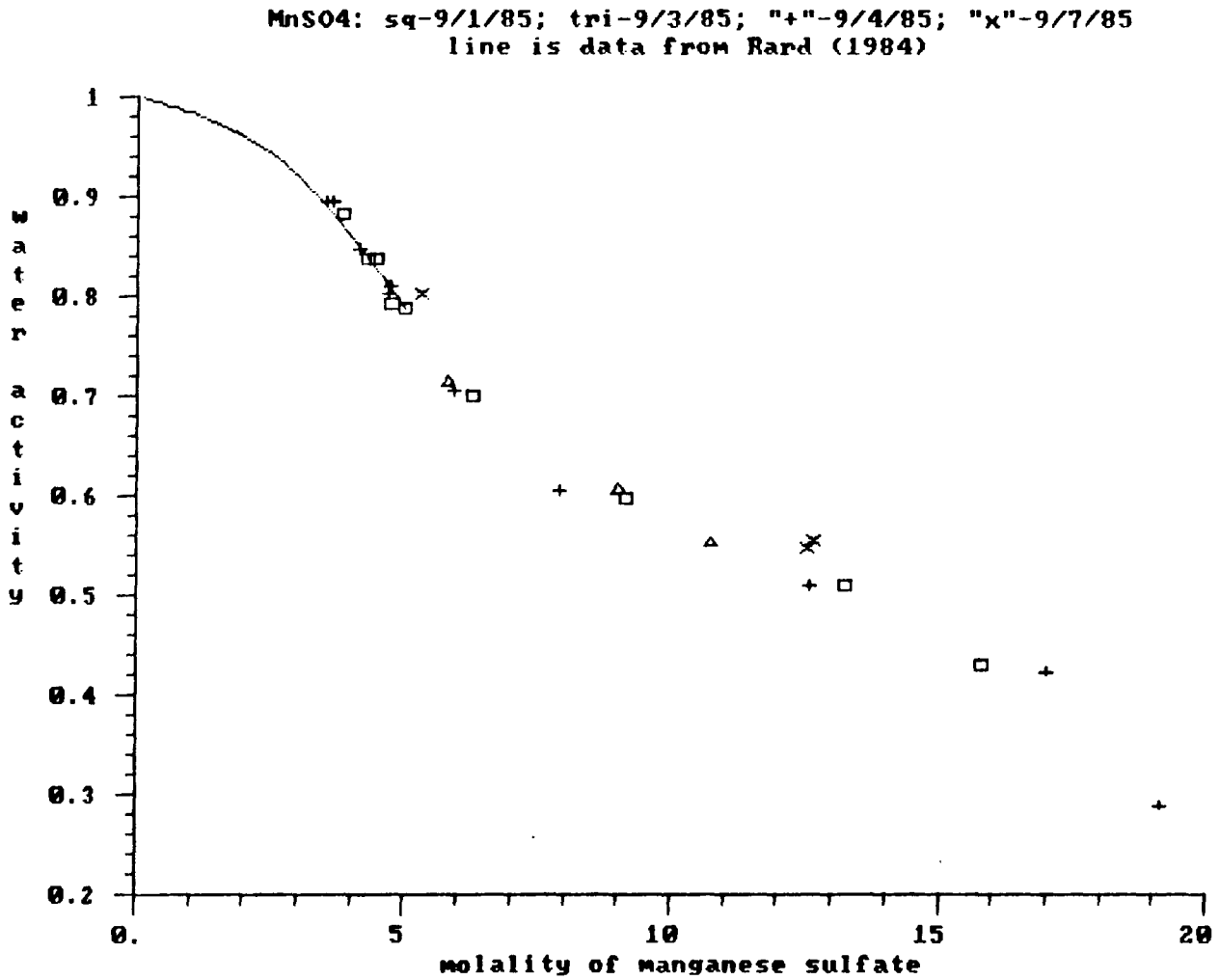
MnSO4: sq-9/1/85; tri-9/3/85; "+"-9/4/85; "x"-9/7/85
line is data from Rard (1984)
water activity
1
0.9
0.8
0.7
0.6
0.5
0.4
0.3
0.2
0.
5
10
15
20
molality of manganese sulfate

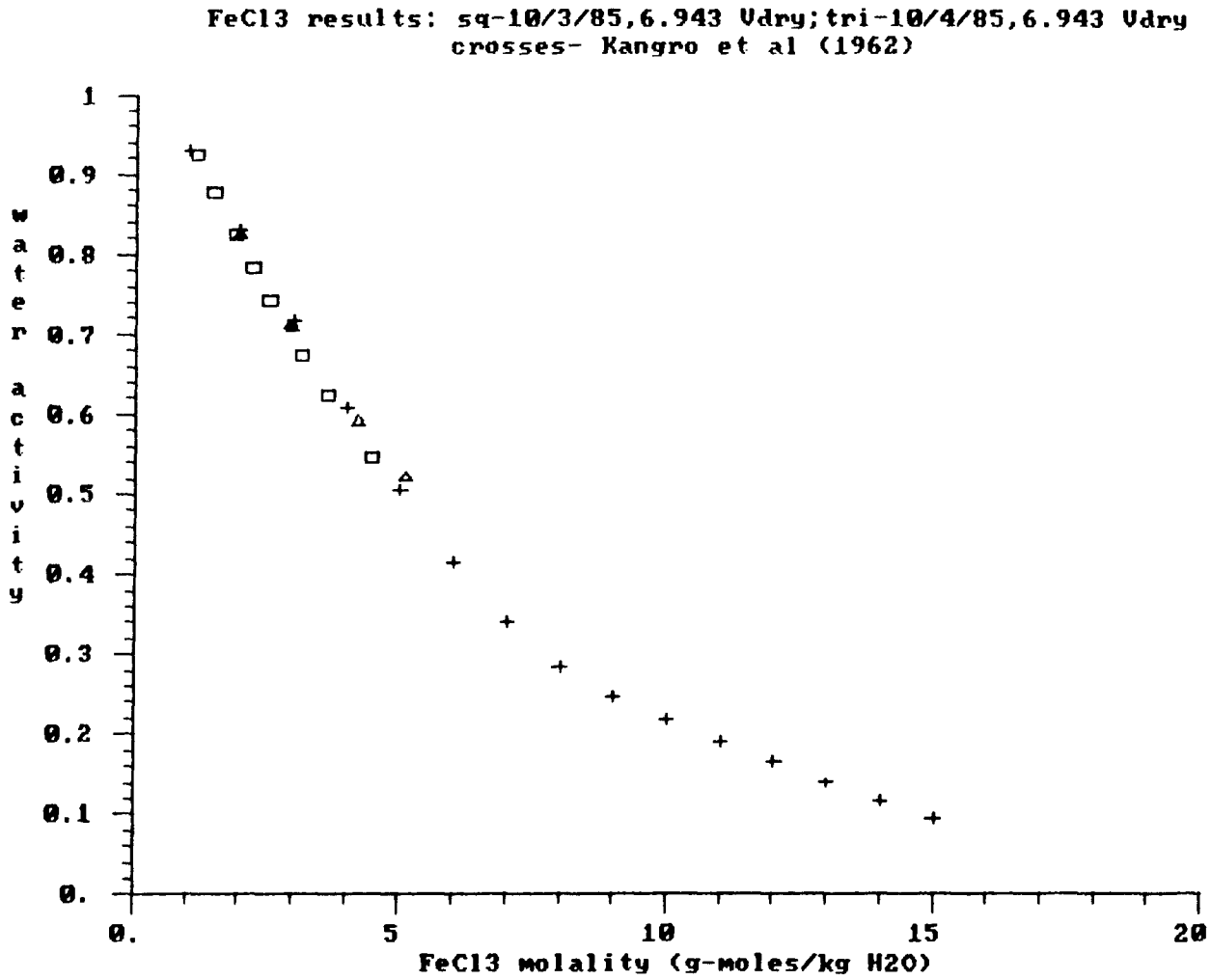
FeCl3 results: sq-10/3/85,6.943 Vdry;tri-10/4/85,6.943 Vdry
crosses- Kangro et al (1962)
water activity
1
0.9
0.8
0.7
0.6
0.5
0.4
0.3
0.2
0.1
0.
0.
5
10
15
20
FeCl3 molality (g-moles/kg H2O)

Appendix C: Detailed results for polynomial fits to water activity data for single-electrolyte solutions

This appendix contains tables detailing the fitting of the present $a_w(m)$ results and literature $a_w(m)$ data to polynomials.

Each table represents a particular salt, and for all of the salts except $(NH_4)_2SO_4$, there is only one table for each salt. In each table, there are $a_w(m)$ data from the present experiments and from the literature. The sources of the literature data for each salt are the same as those for the plots of Appendix B. The sources are also listed in Table 3 of Chapter 1. The fits are summarized in Tables 2 and 3 of Chapter 1.

Each table begins by listing the number of data points for the fit and the order of polynomial used. Then, the coefficients of the best fit polynomial for the $a_w(m)$ data are given. These are the same coefficients that are presented in Table 2 of Chapter 1. Then, a table of the data, the fit's predictions, and the fractional and actual error between the data and the fit's prediction are given. The numbering of the data points does not correspond to the numbering in the tables of Appendix A. In almost all cases, it is very easy to tell whether the data comes from the literature or from the present experiments, because the literature data used was already smoothed and had been reported at even molalities (*e.g.*, 0.1, 0.2, ..., 1.0, 1.2, ...).

After the tabulated data, the average value of the absolute value of the

error, the average fractional error, and the standard deviation in the fit's representation of the data are given.

The $a_w(m)$ polynomials presented in this appendix were used to calculate the mean molal solute activity coefficient. The fits were also used in estimating parameters for models of single-electrolyte solutions and in the estimation of the properties of mixed-electrolyte solutions from mixing rules.

SODIUM CHLORIDE

number of data points : 58
order of polynomial : 6

coefficients of best-fit polynomial:

a(0) = .100841E+01
a(1) = -.493917E-01
a(2) = .888798E-02
a(3) = -.215690E-02
a(4) = .161717E-03
a(5) = -.198961E-05
a(6) = -.114186E-06

i	x(i)	y(i)	f(x(i))	act err	frac err
1	.500000E+00	.983550E+00	.985673E+00	-.212262E-02	-.215812E-02
2	.600000E+00	.980250E+00	.981526E+00	-.127560E-02	-.130130E-02
3	.700000E+00	.976920E+00	.977486E+00	-.565615E-03	-.578977E-03
4	.800000E+00	.973590E+00	.973542E+00	.478020E-04	.490987E-04
5	.900000E+00	.970230E+00	.969685E+00	.544758E-03	.561473E-03
6	.100000E+01	.966900E+00	.965905E+00	.994989E-03	.102905E-02
7	.120000E+01	.960100E+00	.958538E+00	.156242E-02	.162735E-02
8	.140000E+01	.953200E+00	.951369E+00	.183078E-02	.192067E-02
9	.160000E+01	.946100E+00	.944335E+00	.176511E-02	.186567E-02
10	.180000E+01	.938900E+00	.937375E+00	.152490E-02	.162413E-02
11	.200000E+01	.931600E+00	.930436E+00	.116420E-02	.124968E-02
12	.220000E+01	.924200E+00	.923468E+00	.731780E-03	.791798E-03
13	.240000E+01	.916600E+00	.916429E+00	.171197E-03	.186774E-03
14	.260000E+01	.908900E+00	.909279E+00	-.379026E-03	-.417016E-03
15	.280000E+01	.901100E+00	.901985E+00	-.885283E-03	-.982446E-03
16	.300000E+01	.893200E+00	.894519E+00	-.131874E-02	-.147642E-02
17	.320000E+01	.885100E+00	.886855E+00	-.175518E-02	-.198303E-02
18	.340000E+01	.876900E+00	.878975E+00	-.207487E-02	-.236614E-02
19	.360000E+01	.868600E+00	.870862E+00	-.226237E-02	-.260462E-02
20	.380000E+01	.860000E+00	.862506E+00	-.250642E-02	-.291444E-02
21	.400000E+01	.851500E+00	.853900E+00	-.239972E-02	-.281822E-02
22	.420000E+01	.842800E+00	.845039E+00	-.223877E-02	-.265635E-02
23	.440000E+01	.833900E+00	.835924E+00	-.202372E-02	-.242682E-02
24	.460000E+01	.825000E+00	.826558E+00	-.155816E-02	-.188868E-02
25	.480000E+01	.816000E+00	.816949E+00	-.948916E-03	-.116289E-02
26	.500000E+01	.806800E+00	.807106E+00	-.305899E-03	-.379151E-03
27	.520000E+01	.797600E+00	.797042E+00	.558135E-03	.699769E-03
28	.540000E+01	.788300E+00	.786772E+00	.152777E-02	.193806E-02
29	.560000E+01	.778800E+00	.776315E+00	.248515E-02	.319100E-02
30	.580000E+01	.769300E+00	.765690E+00	.361018E-02	.469282E-02
31	.600000E+01	.759800E+00	.754919E+00	.488078E-02	.642377E-02
32	.619693E+01	.763001E+00	.744195E+00	.188061E-01	.246475E-01
33	.411789E+01	.846484E+00	.848707E+00	-.222347E-02	-.262671E-02
34	.558981E+01	.768491E+00	.776852E+00	-.836089E-02	-.108796E-01
35	.641747E+01	.724356E+00	.732075E+00	-.771885E-02	-.106562E-01

36	.700872E+01	.694601E+00	.699283E+00	-.468232E-02	-.674102E-02
37	.787819E+01	.644698E+00	.651557E+00	-.685896E-02	-.106390E-01
38	.861721E+01	.601844E+00	.613031E+00	-.111871E-01	-.185881E-01
39	.967937E+01	.551467E+00	.563607E+00	-.121404E-01	-.220147E-01
40	.111073E+02	.511504E+00	.511317E+00	.186827E-03	.365251E-03
41	.113667E+02	.503897E+00	.503475E+00	.422240E-03	.837949E-03
42	.116199E+02	.494804E+00	.496194E+00	-.139013E-02	-.280945E-02
43	.119331E+02	.486094E+00	.487578E+00	-.148441E-02	-.305375E-02
44	.122227E+02	.476446E+00	.479841E+00	-.339484E-02	-.712535E-02
45	.126133E+02	.466229E+00	.469413E+00	-.318398E-02	-.682923E-02
46	.130412E+02	.454699E+00	.457379E+00	-.268006E-02	-.589414E-02
47	.468296E+01	.829378E+00	.822601E+00	.677668E-02	.817080E-02
48	.730674E+01	.674037E+00	.682765E+00	-.872838E-02	-.129494E-01
49	.950799E+01	.575877E+00	.571008E+00	.486938E-02	.845558E-02
50	.108080E+02	.525441E+00	.520934E+00	.450665E-02	.857689E-02
51	.132492E+02	.447829E+00	.451039E+00	-.321045E-02	-.716892E-02
52	.135184E+02	.442658E+00	.442098E+00	.559743E-03	.126450E-02
53	.136476E+02	.440893E+00	.437433E+00	.345958E-02	.784677E-02
54	.553431E+01	.789811E+00	.779769E+00	.100419E-01	.127143E-01
55	.621914E+01	.741546E+00	.742979E+00	-.143309E-02	-.193257E-02
56	.814708E+01	.648054E+00	.637239E+00	.108149E-01	.166882E-01
57	.104309E+02	.549114E+00	.534025E+00	.150888E-01	.274785E-01
58	.127929E+02	.468851E+00	.464486E+00	.436549E-02	.931103E-02

average actual error (abs values) = .356201E-02
average fractional error = .538329E-02

SODIUM BROMIDE

number of data points : 44
order of polynomial : 5

coefficients of best-fit polynomial:

a(0) = .999608E+00
a(1) = -.311570E-01
a(2) = -.211238E-02
a(3) = -.934741E-04
a(4) = .200024E-04
a(5) = -.547248E-06

i	x(i)	y(i)	f(x(i))	act err	frac err
1	.100000E+00	.996640E+00	.996472E+00	.168454E-03	.169022E-03
2	.200000E+00	.993340E+00	.993292E+00	.481513E-04	.484742E-04
3	.300000E+00	.990020E+00	.990069E+00	-.488812E-04	-.493739E-04
4	.400000E+00	.986700E+00	.986802E+00	-.102200E-03	-.103578E-03
5	.500000E+00	.983330E+00	.983491E+00	-.161410E-03	-.164146E-03
6	.600000E+00	.979950E+00	.980136E+00	-.186157E-03	-.189966E-03
7	.700000E+00	.976520E+00	.976736E+00	-.216136E-03	-.221333E-03
8	.800000E+00	.973070E+00	.973291E+00	-.221084E-03	-.227202E-03
9	.900000E+00	.969570E+00	.969801E+00	-.230781E-03	-.238024E-03
10	.100000E+01	.966070E+00	.966265E+00	-.195051E-03	-.201901E-03
11	.120000E+01	.958970E+00	.959057E+00	-.868118E-04	-.905261E-04
12	.140000E+01	.951620E+00	.951666E+00	-.457848E-04	-.481125E-04
13	.160000E+01	.944140E+00	.944092E+00	.479711E-04	.508093E-04
14	.180000E+01	.936470E+00	.936336E+00	.133776E-03	.142851E-03
15	.200000E+01	.928600E+00	.928400E+00	.200349E-03	.215754E-03
16	.250000E+01	.908360E+00	.907781E+00	.579075E-03	.637495E-03
17	.300000E+01	.887220E+00	.886089E+00	.113058E-02	.127430E-02
18	.350000E+01	.865000E+00	.863389E+00	.161125E-02	.186272E-02
19	.400000E+01	.841300E+00	.839760E+00	.153978E-02	.183023E-02
20	.485900E+00	.983500E+00	.983961E+00	-.460916E-03	-.468649E-03
21	.971900E+00	.969300E+00	.967263E+00	.203681E-02	.210132E-02
22	.194380E+01	.929400E+00	.930648E+00	-.124799E-02	-.134279E-02
23	.291570E+01	.889400E+00	.889819E+00	-.419305E-03	-.471447E-03
24	.388760E+01	.843800E+00	.845148E+00	-.134799E-02	-.159753E-02
25	.485950E+01	.792500E+00	.797262E+00	-.476241E-02	-.600935E-02
26	.583140E+01	.746900E+00	.746991E+00	-.914581E-04	-.122450E-03
27	.680330E+01	.701300E+00	.695308E+00	.599238E-02	.854467E-02
28	.777520E+01	.655700E+00	.643270E+00	.124300E-01	.189568E-01
29	.874710E+01	.615800E+00	.591968E+00	.238324E-01	.387016E-01
30	.102030E+02	.517773E+00	.518787E+00	-.101373E-02	-.195786E-02
31	.554017E+01	.762827E+00	.762250E+00	.577201E-03	.756661E-03
32	.674377E+01	.690020E+00	.698495E+00	-.847452E-02	-.122816E-01
33	.773115E+01	.636528E+00	.645621E+00	-.909286E-02	-.142851E-01
34	.893873E+01	.570126E+00	.582032E+00	-.119058E-01	-.208828E-01
35	.103787E+02	.498744E+00	.510385E+00	-.116406E-01	-.233398E-01
36	.130494E+02	.396957E+00	.398547E+00	-.158986E-02	-.400512E-02

37	.159436E+02	.314741E+00	.315756E+00	-.101544E-02	-.322627E-02
38	.185073E+02	.260336E+00	.265353E+00	-.501679E-02	-.192705E-01
39	.201451E+02	.230345E+00	.229128E+00	.121657E-02	.528150E-02
40	.111608E+02	.475843E+00	.474386E+00	.145707E-02	.306208E-02
41	.752607E+01	.654549E+00	.656582E+00	-.203336E-02	-.310651E-02
42	.118881E+02	.443235E+00	.443201E+00	.344844E-04	.778015E-04
43	.139755E+02	.372202E+00	.367736E+00	.446574E-02	.119982E-01
44	.175438E+02	.287566E+00	.283461E+00	.410533E-02	.142761E-01

average actual error (abs values) = .280033E-02
average fractional error = .508841E-02

POTASSIUM CHLORIDE

number of data points : 43
order of polynomial : 6

coefficients of best-fit polynomial:

a(0) = .997541E+00
a(1) = -.217333E-01
a(2) = -.105276E-01
a(3) = .425263E-02
a(4) = -.778035E-03
a(5) = .620300E-04
a(6) = -.176359E-05

i	x(i)	y(i)	f(x(i))	act err	frac err
1	.100000E+00	.996668E+00	.995267E+00	.140109E-02	.140577E-02
2	.200000E+00	.993443E+00	.992806E+00	.636622E-03	.640824E-03
3	.300000E+00	.990250E+00	.990183E+00	.674554E-04	.681195E-04
4	.400000E+00	.987090E+00	.987416E+00	-.326497E-03	-.330767E-03
5	.500000E+00	.983940E+00	.984528E+00	-.587670E-03	-.597262E-03
6	.600000E+00	.980780E+00	.981534E+00	-.753921E-03	-.768695E-03
7	.700000E+00	.977630E+00	.978452E+00	-.821594E-03	-.840393E-03
8	.800000E+00	.974480E+00	.975296E+00	-.815590E-03	-.836949E-03
9	.900000E+00	.971330E+00	.972079E+00	-.749433E-03	-.771554E-03
10	.100000E+01	.968180E+00	.968815E+00	-.635334E-03	-.656215E-03
11	.120000E+01	.961900E+00	.962186E+00	-.285969E-03	-.297296E-03
12	.140000E+01	.955600E+00	.955481E+00	.118685E-03	.124199E-03
13	.160000E+01	.949200E+00	.948758E+00	.441867E-03	.465515E-03
14	.180000E+01	.942800E+00	.942058E+00	.742027E-03	.787046E-03
15	.200000E+01	.936400E+00	.935409E+00	.991046E-03	.105836E-02
16	.220000E+01	.929900E+00	.928827E+00	.107255E-02	.115341E-02
17	.240000E+01	.923400E+00	.922320E+00	.108031E-02	.116992E-02
18	.260000E+01	.916900E+00	.915883E+00	.101668E-02	.110882E-02
19	.280000E+01	.910300E+00	.909509E+00	.791182E-03	.869144E-03
20	.300000E+01	.903700E+00	.903181E+00	.519142E-03	.574462E-03
21	.320000E+01	.897100E+00	.896880E+00	.220377E-03	.245655E-03
22	.340000E+01	.890400E+00	.890582E+00	-.181985E-03	-.204386E-03
23	.360000E+01	.883700E+00	.884263E+00	-.562639E-03	-.636686E-03
24	.380000E+01	.877000E+00	.877895E+00	-.895138E-03	-.102068E-02
25	.400000E+01	.870200E+00	.871453E+00	-.125285E-02	-.143973E-02
26	.420000E+01	.863400E+00	.864910E+00	-.150986E-02	-.174874E-02
27	.440000E+01	.856600E+00	.858242E+00	-.164172E-02	-.191656E-02
28	.460000E+01	.849800E+00	.851426E+00	-.162622E-02	-.191365E-02
29	.480000E+01	.842900E+00	.844444E+00	-.154398E-02	-.183175E-02
30	.435886E+01	.859980E+00	.859625E+00	.355293E-03	.413142E-03
31	.687887E+01	.760164E+00	.760591E+00	-.427181E-03	-.561959E-03
32	.849842E+01	.686386E+00	.689672E+00	-.328619E-02	-.478767E-02
33	.106057E+02	.627178E+00	.625939E+00	.123944E-02	.197621E-02
34	.116722E+02	.598976E+00	.609945E+00	-.109694E-01	-.183136E-01
35	.565451E+01	.814850E+00	.812436E+00	.241440E-02	.296300E-02

36	.660760E+01	.775507E+00	.772553E+00	.295367E-02	.380869E-02
37	.766681E+01	.736506E+00	.725369E+00	.111374E-01	.151219E-01
38	.864935E+01	.670080E+00	.683611E+00	-.135309E-01	-.201930E-01
39	.110474E+02	.632213E+00	.618641E+00	.135720E-01	.214674E-01
40	.111609E+02	.620311E+00	.616990E+00	.332136E-02	.535435E-02
41	.114528E+02	.612192E+00	.612959E+00	-.766946E-03	-.125279E-02
42	.118937E+02	.603163E+00	.606682E+00	-.351901E-02	-.583425E-02
43	.127192E+02	.590208E+00	.587611E+00	.259748E-02	.440095E-02

average actual error (abs values) = .217163E-02
average fractional error = .306818E-02

POTASSIUM BROMIDE

number of data points : 33
order of polynomial : 6

coefficients of best-fit polynomial:

a(0) = .100083E+01
a(1) = -.353130E-01
a(2) = .248991E-02
a(3) = -.672925E-03
a(4) = .531836E-04
a(5) = -.803975E-06
a(6) = -.286628E-07

i	x(i)	y(i)	f(x(i))	act err	frac err
1	.100000E+00	.996662E+00	.997318E+00	-.656329E-03	-.658527E-03
2	.200000E+00	.993421E+00	.993857E+00	-.436097E-03	-.438985E-03
3	.300000E+00	.990212E+00	.990438E+00	-.225852E-03	-.228085E-03
4	.400000E+00	.987027E+00	.987057E+00	-.298734E-04	-.302660E-04
5	.500000E+00	.983846E+00	.983711E+00	.135437E-03	.137660E-03
6	.600000E+00	.980647E+00	.980395E+00	.251551E-03	.256515E-03
7	.700000E+00	.977458E+00	.977108E+00	.349820E-03	.357888E-03
8	.800000E+00	.974251E+00	.973846E+00	.405475E-03	.416191E-03
9	.900000E+00	.971048E+00	.970604E+00	.443622E-03	.456849E-03
10	.100000E+01	.967849E+00	.967382E+00	.467253E-03	.482775E-03
11	.120000E+01	.961419E+00	.960981E+00	.438335E-03	.455925E-03
12	.140000E+01	.954942E+00	.954621E+00	.321295E-03	.336455E-03
13	.160000E+01	.948509E+00	.948282E+00	.226878E-03	.239195E-03
14	.180000E+01	.941957E+00	.941947E+00	.100331E-04	.106514E-04
15	.200000E+01	.935382E+00	.935599E+00	-.217043E-03	-.232037E-03
16	.250000E+01	.918731E+00	.919582E+00	-.851393E-03	-.926706E-03
17	.300000E+01	.901922E+00	.903218E+00	-.129627E-02	-.143723E-02
18	.350000E+01	.884974E+00	.886386E+00	-.141160E-02	-.159508E-02
19	.400000E+01	.867781E+00	.869019E+00	-.123815E-02	-.142680E-02
20	.450000E+01	.850325E+00	.851104E+00	-.779392E-03	-.916582E-03
21	.500000E+01	.832889E+00	.832672E+00	.216917E-03	.260439E-03
22	.550000E+01	.815694E+00	.813793E+00	.190149E-02	.233113E-02
23	.489823E+01	.841359E+00	.836463E+00	.489614E-02	.581932E-02
24	.602920E+01	.791711E+00	.793439E+00	-.172783E-02	-.218240E-02
25	.819477E+01	.704801E+00	.709782E+00	-.498065E-02	-.706675E-02
26	.105483E+02	.629157E+00	.629535E+00	-.378077E-03	-.600926E-03
27	.120844E+02	.588926E+00	.587893E+00	.103322E-02	.175442E-02
28	.132414E+02	.559421E+00	.560697E+00	-.127614E-02	-.228118E-02
29	.139331E+02	.543922E+00	.544475E+00	-.552925E-03	-.101655E-02
30	.146435E+02	.518916E+00	.526123E+00	-.720722E-02	-.138890E-01
31	.691070E+01	.759966E+00	.759116E+00	.850309E-03	.111888E-02
32	.944063E+01	.668279E+00	.665037E+00	.324161E-02	.485069E-02
33	.146053E+02	.535260E+00	.527185E+00	.807545E-02	.150870E-01

average actual error (abs values) = .140999E-02
average fractional error = .209997E-02

AMMONIUM CHLORIDE

number of data points : 44
order of polynomial : 5

coefficients of best-fit polynomial:

a(0) = .996797E+00
a(1) = -.261139E-01
a(2) = -.159902E-02
a(3) = .135474E-03
a(4) = -.231700E-05
a(5) = -.111301E-07

i	x(i)	y(i)	f(x(i))	act err	frac err
1	.726212E+01	.782276E+00	.768041E+00	.142351E-01	.181971E-01
2	.691647E+01	.783366E+00	.779033E+00	.433326E-02	.553159E-02
3	.552540E+01	.829033E+00	.824325E+00	.470810E-02	.567903E-02
4	.430626E+01	.874635E+00	.864696E+00	.993872E-02	.113633E-01
5	.497601E+01	.846711E+00	.842498E+00	.421311E-02	.497586E-02
6	.488574E+01	.842245E+00	.845490E+00	-.324491E-02	-.385270E-02
7	.811962E+01	.734262E+00	.741398E+00	-.713619E-02	-.971886E-02
8	.945628E+01	.695077E+00	.702057E+00	-.697989E-02	-.100419E-01
9	.120622E+02	.638468E+00	.635020E+00	.344781E-02	.540013E-02
10	.706074E+01	.771502E+00	.774429E+00	-.292713E-02	-.379406E-02
11	.110080E+02	.661597E+00	.660460E+00	.113674E-02	.171817E-02
12	.159288E+02	.567463E+00	.562070E+00	.539291E-02	.950355E-02
13	.216086E+02	.498134E+00	.495174E+00	.296009E-02	.594236E-02
14	.707524E+01	.772998E+00	.773968E+00	-.969658E-03	-.125441E-02
15	.365218E+01	.892394E+00	.886276E+00	.611844E-02	.685621E-02
16	.631222E+01	.792211E+00	.798531E+00	-.631979E-02	-.797740E-02
17	.917345E+01	.701548E+00	.710131E+00	-.858314E-02	-.122346E-01
18	.131452E+02	.611007E+00	.611390E+00	-.382701E-03	-.626345E-03
19	.180420E+02	.531854E+00	.533989E+00	-.213461E-02	-.401353E-02
20	.217873E+02	.487362E+00	.493177E+00	-.581516E-02	-.119319E-01
21	.232333E+02	.477451E+00	.475488E+00	.196325E-02	.411195E-02
22	.100000E+00	.996666E+00	.994169E+00	.249665E-02	.250500E-02
23	.200000E+00	.993442E+00	.991511E+00	.193106E-02	.194381E-02
24	.300000E+00	.990255E+00	.988822E+00	.143285E-02	.144695E-02
25	.400000E+00	.987099E+00	.986104E+00	.995200E-03	.100821E-02
26	.500000E+00	.983935E+00	.983357E+00	.578325E-03	.587767E-03
27	.600000E+00	.980795E+00	.980582E+00	.213437E-03	.217616E-03
28	.700000E+00	.977655E+00	.977779E+00	-.124247E-03	-.127087E-03
29	.800000E+00	.974504E+00	.974951E+00	-.446503E-03	-.458185E-03
30	.900000E+00	.971363E+00	.972096E+00	-.733102E-03	-.754715E-03
31	.100000E+01	.968197E+00	.969217E+00	-.101981E-02	-.105331E-02
32	.120000E+01	.961918E+00	.963387E+00	-.146858E-02	-.152672E-02
33	.140000E+01	.955617E+00	.957466E+00	-.184882E-02	-.193469E-02
34	.160000E+01	.949275E+00	.951460E+00	-.218544E-02	-.230222E-02
35	.180000E+01	.942935E+00	.945376E+00	-.244128E-02	-.258902E-02
36	.200000E+01	.936596E+00	.939219E+00	-.262305E-02	-.280063E-02

37	.250000E+01	.920637E+00	.923543E+00	-.290613E-02	-.315665E-02
38	.300000E+01	.904754E+00	.907531E+00	-.277710E-02	-.306945E-02
39	.350000E+01	.888664E+00	.891265E+00	-.260082E-02	-.292666E-02
40	.400000E+01	.872672E+00	.874822E+00	-.215042E-02	-.246418E-02
41	.450000E+01	.856829E+00	.858278E+00	-.144926E-02	-.169143E-02
42	.500000E+01	.841486E+00	.841703E+00	-.216893E-03	-.257750E-03
43	.550000E+01	.826269E+00	.825163E+00	.110599E-02	.133853E-02
44	.600000E+01	.811005E+00	.808721E+00	.228357E-02	.281573E-02

average actual error (abs values) = .315839E-02
average fractional error = .417503E-02

SODIUM SULFATE

number of data points : 65
order of polynomial : 6

coefficients of best-fit polynomial:

a(0) = .100524E+01
a(1) = -.648418E-01
a(2) = .351882E-01
a(3) = -.131861E-01
a(4) = .192518E-02
a(5) = -.122350E-03
a(6) = .286982E-05

i	x(i)	y(i)	f(x(i))	act err	frac err
1	.347273E+01	.880861E+00	.875420E+00	.544098E-02	.617689E-02
2	.401737E+01	.845656E+00	.843202E+00	.245358E-02	.290140E-02
3	.487446E+01	.786327E+00	.786727E+00	-.399519E-03	-.508083E-03
4	.559457E+01	.738112E+00	.738301E+00	-.188566E-03	-.255470E-03
5	.632065E+01	.691726E+00	.692914E+00	-.118800E-02	-.171744E-02
6	.709542E+01	.652343E+00	.651820E+00	.522529E-03	.801004E-03
7	.883402E+01	.596038E+00	.594098E+00	.193989E-02	.325464E-02
8	.123599E+02	.550782E+00	.550352E+00	.430102E-03	.780894E-03
9	.348091E+01	.877647E+00	.874967E+00	.267966E-02	.305323E-02
10	.374151E+01	.860141E+00	.860020E+00	.120920E-03	.140581E-03
11	.399955E+01	.843503E+00	.844316E+00	-.812998E-03	-.963836E-03
12	.479255E+01	.791990E+00	.792276E+00	-.285567E-03	-.360569E-03
13	.546685E+01	.737766E+00	.746749E+00	-.898252E-02	-.121753E-01
14	.625947E+01	.692398E+00	.696519E+00	-.412092E-02	-.595167E-02
15	.723569E+01	.645636E+00	.645374E+00	.261943E-03	.405713E-03
16	.904671E+01	.593019E+00	.589961E+00	.305817E-02	.515695E-02
17	.109995E+02	.562832E+00	.565035E+00	-.220332E-02	-.391470E-02
18	.116771E+02	.556096E+00	.557315E+00	-.121923E-02	-.219248E-02
19	.122380E+02	.552556E+00	.551389E+00	.116708E-02	.211214E-02
20	.128448E+02	.548062E+00	.548211E+00	-.149101E-03	-.272051E-03
21	.370054E+01	.864890E+00	.862435E+00	.245523E-02	.283878E-02
22	.100000E+00	.995700E+00	.999093E+00	-.339268E-02	-.340734E-02
23	.200000E+00	.991900E+00	.993575E+00	-.167470E-02	-.168837E-02
24	.300000E+00	.988300E+00	.988612E+00	-.311649E-03	-.315339E-03
25	.400000E+00	.984900E+00	.984136E+00	.764495E-03	.776216E-03
26	.500000E+00	.981500E+00	.980082E+00	.141758E-02	.144430E-02
27	.600000E+00	.978300E+00	.976393E+00	.190741E-02	.194972E-02
28	.700000E+00	.975100E+00	.973010E+00	.208987E-02	.214323E-02
29	.800000E+00	.972000E+00	.969883E+00	.211705E-02	.217804E-02
30	.900000E+00	.968900E+00	.966963E+00	.193743E-02	.199962E-02
31	.100000E+01	.965900E+00	.964204E+00	.169596E-02	.175584E-02
32	.120000E+01	.959900E+00	.959010E+00	.890479E-03	.927679E-03
33	.140000E+01	.953800E+00	.954005E+00	-.205175E-03	-.215113E-03
34	.160000E+01	.947800E+00	.948945E+00	-.114491E-02	-.120797E-02
35	.180000E+01	.941500E+00	.943627E+00	-.212696E-02	-.225912E-02

36	.200000E+01	.935100E+00	.937890E+00	-.279011E-02	-.298376E-02
37	.250000E+01	.917800E+00	.920982E+00	-.318233E-02	-.346734E-02
38	.300000E+01	.898500E+00	.899683E+00	-.118334E-02	-.131702E-02
39	.350000E+01	.876700E+00	.873907E+00	.279316E-02	.318600E-02
40	.400000E+01	.852300E+00	.844288E+00	.801208E-02	.940054E-02
41	.100000E+00	.995748E+00	.999093E+00	-.334468E-02	-.335897E-02
42	.200000E+00	.991920E+00	.993575E+00	-.165470E-02	-.166818E-02
43	.300000E+00	.988290E+00	.988612E+00	-.321649E-03	-.325460E-03
44	.400000E+00	.984820E+00	.984136E+00	.684495E-03	.695046E-03
45	.500000E+00	.981460E+00	.980082E+00	.137758E-02	.140361E-02
46	.600000E+00	.978210E+00	.976393E+00	.181741E-02	.185790E-02
47	.700000E+00	.975040E+00	.973010E+00	.202987E-02	.208183E-02
48	.800000E+00	.971930E+00	.969883E+00	.204705E-02	.210617E-02
49	.900000E+00	.968860E+00	.966963E+00	.189743E-02	.195842E-02
50	.100000E+01	.965820E+00	.964204E+00	.161596E-02	.167315E-02
51	.120000E+01	.959780E+00	.959010E+00	.770479E-03	.802766E-03
52	.140000E+01	.953720E+00	.954005E+00	-.285175E-03	-.299013E-03
53	.160000E+01	.947550E+00	.948945E+00	-.139491E-02	-.147213E-02
54	.180000E+01	.941230E+00	.943627E+00	-.239696E-02	-.254662E-02
55	.200000E+01	.934690E+00	.937890E+00	-.320011E-02	-.342371E-02
56	.220000E+01	.927890E+00	.931610E+00	-.372021E-02	-.400932E-02
57	.240000E+01	.920800E+00	.924697E+00	-.389666E-02	-.423182E-02
58	.260000E+01	.913380E+00	.917089E+00	-.370915E-02	-.406090E-02
59	.280000E+01	.905600E+00	.908754E+00	-.315444E-02	-.348325E-02
60	.300000E+01	.897400E+00	.899683E+00	-.228334E-02	-.254439E-02
61	.320000E+01	.888800E+00	.889888E+00	-.108781E-02	-.122390E-02
62	.340000E+01	.879800E+00	.879398E+00	.401861E-03	.456764E-03
63	.360000E+01	.870200E+00	.868260E+00	.193966E-02	.222898E-02
64	.380000E+01	.860100E+00	.856534E+00	.356640E-02	.414649E-02
65	.381400E+01	.859400E+00	.855692E+00	.370757E-02	.431414E-02

average actual error (abs values) = .203112E-02
average fractional error = .238353E-02

AMMONIUM SULFATE (fit "a")

number of data points : 40
order of polynomial : 5

coefficients of best-fit polynomial:

a(0) = .996848E+00
a(1) = -.296887E-01
a(2) = .175281E-04
a(3) = -.325337E-03
a(4) = .357116E-04
a(5) = -.978654E-06

i	x(i)	y(i)	f(x(i))	act err	frac err
1	.522140E+01	.816425E+00	.818742E+00	-.231723E-02	-.283826E-02
2	.409487E+01	.861861E+00	.862146E+00	-.284812E-03	-.330462E-03
3	.460430E+01	.837410E+00	.842792E+00	-.538217E-02	-.642716E-02
4	.375553E+01	.875547E+00	.874738E+00	.808612E-03	.923551E-03
5	.838863E+01	.690294E+00	.693172E+00	-.287793E-02	-.416914E-02
6	.144462E+02	.532816E+00	.530381E+00	.243518E-02	.457040E-02
7	.160249E+02	.503195E+00	.507576E+00	-.438051E-02	-.870540E-02
8	.171758E+02	.488342E+00	.488685E+00	-.343275E-03	-.702939E-03
9	.178874E+02	.474831E+00	.473244E+00	.158697E-02	.334218E-02
10	.571139E+01	.806913E+00	.799295E+00	.761753E-02	.944033E-02
11	.526518E+01	.816631E+00	.817015E+00	-.384340E-03	-.470641E-03
12	.540381E+01	.812713E+00	.811532E+00	.118092E-02	.145305E-02
13	.435008E+01	.854252E+00	.852514E+00	.173834E-02	.203493E-02
14	.519193E+01	.815100E+00	.819903E+00	-.480330E-02	-.589290E-02
15	.766381E+01	.713181E+00	.721226E+00	-.804520E-02	-.112807E-01
16	.106727E+02	.615309E+00	.614305E+00	.100417E-02	.163198E-02
17	.121227E+02	.578217E+00	.574955E+00	.326158E-02	.564076E-02
18	.132582E+02	.550599E+00	.550627E+00	-.280191E-04	-.508885E-04
19	.100000E+00	.995863E+00	.993879E+00	.198425E-02	.199249E-02
20	.200000E+00	.992130E+00	.990908E+00	.122182E-02	.123151E-02
21	.300000E+00	.988602E+00	.987934E+00	.667766E-03	.675465E-03
22	.400000E+00	.985194E+00	.984955E+00	.238832E-03	.242421E-03
23	.500000E+00	.981872E+00	.981969E+00	-.973253E-04	-.991222E-04
24	.600000E+00	.978603E+00	.978975E+00	-.372126E-03	-.380263E-03
25	.700000E+00	.975414E+00	.975971E+00	-.557073E-03	-.571114E-03
26	.800000E+00	.972203E+00	.972956E+00	-.752744E-03	-.774267E-03
27	.900000E+00	.969066E+00	.969928E+00	-.861799E-03	-.889309E-03
28	.100000E+01	.966002E+00	.966886E+00	-.883972E-03	-.915083E-03
29	.120000E+01	.959840E+00	.960756E+00	-.915977E-03	-.954302E-03
30	.140000E+01	.953594E+00	.954557E+00	-.963115E-03	-.100998E-02
31	.160000E+01	.947471E+00	.948282E+00	-.810883E-03	-.855839E-03
32	.180000E+01	.941193E+00	.941924E+00	-.730889E-03	-.776555E-03
33	.200000E+01	.934877E+00	.935478E+00	-.600810E-03	-.642662E-03
34	.250000E+01	.918897E+00	.918952E+00	-.545360E-04	-.593494E-04
35	.300000E+01	.902166E+00	.901810E+00	.355917E-03	.394514E-03
36	.350000E+01	.884807E+00	.884048E+00	.758898E-03	.857699E-03

37	.400000E+01	.867031E+00	.865692E+00	.133921E-02	.154459E-02
38	.450000E+01	.849016E+00	.846795E+00	.222077E-02	.261570E-02
39	.500000E+01	.830792E+00	.827437E+00	.335530E-02	.403868E-02
40	.550000E+01	.812387E+00	.807715E+00	.467197E-02	.575092E-02

average actual error (abs values) = .182240E-02
average fractional error = .242944E-02

AMMONIUM SULFATE (fit "b")

number of data points : 61
order of polynomial : 3

coefficients of best-fit polynomial:

a(0) = .101507E+01
a(1) = -.447827E-01
a(2) = .104060E-02
a(3) = -.825825E-05

i	x(i)	y(i)	f(x(i))	act err	frac err
1	.100000E+00	.995863E+00	.101060E+01	-.147391E-01	-.148004E-01
2	.200000E+00	.992130E+00	.100616E+01	-.140250E-01	-.141363E-01
3	.300000E+00	.988602E+00	.100173E+01	-.131266E-01	-.132780E-01
4	.400000E+00	.985194E+00	.997323E+00	-.121289E-01	-.123112E-01
5	.500000E+00	.981872E+00	.992938E+00	-.110658E-01	-.112701E-01
6	.600000E+00	.978603E+00	.988573E+00	-.997025E-02	-.101882E-01
7	.700000E+00	.975414E+00	.984229E+00	-.881521E-02	-.903741E-02
8	.800000E+00	.972203E+00	.979906E+00	-.770264E-02	-.792287E-02
9	.900000E+00	.969066E+00	.975602E+00	-.653649E-02	-.674514E-02
10	.100000E+01	.966002E+00	.971320E+00	-.531770E-02	-.550485E-02
11	.120000E+01	.959840E+00	.962815E+00	-.297502E-02	-.309950E-02
12	.140000E+01	.953594E+00	.954391E+00	-.797215E-03	-.836011E-03
13	.160000E+01	.947471E+00	.946048E+00	.142312E-02	.150202E-02
14	.180000E+01	.941193E+00	.937785E+00	.340838E-02	.362133E-02
15	.200000E+01	.934877E+00	.929601E+00	.527595E-02	.564347E-02
16	.250000E+01	.918897E+00	.909488E+00	.940889E-02	.102393E-01
17	.300000E+01	.902166E+00	.889865E+00	.123015E-01	.136355E-01
18	.350000E+01	.884807E+00	.870724E+00	.140830E-01	.159164E-01
19	.400000E+01	.867031E+00	.852061E+00	.149705E-01	.172664E-01
20	.450000E+01	.849016E+00	.833868E+00	.151482E-01	.178421E-01
21	.500000E+01	.830792E+00	.816140E+00	.146525E-01	.176367E-01
22	.550000E+01	.812387E+00	.798870E+00	.135173E-01	.166390E-01
23	.361806E+02	.350805E+00	.365869E+00	-.150637E-01	-.429403E-01
24	.341249E+02	.364758E+00	.370485E+00	-.572740E-02	-.157019E-01
25	.300300E+02	.399001E+00	.385021E+00	.139796E-01	.350365E-01
26	.278056E+02	.408709E+00	.396870E+00	.118391E-01	.289672E-01
27	.252353E+02	.433522E+00	.414931E+00	.185914E-01	.428846E-01
28	.242178E+02	.444913E+00	.423550E+00	.213631E-01	.480163E-01
29	.191275E+02	.499727E+00	.481415E+00	.183121E-01	.366443E-01
30	.171601E+02	.528082E+00	.511291E+00	.167913E-01	.317968E-01
31	.161452E+02	.542054E+00	.528541E+00	.135126E-01	.249284E-01
32	.150151E+02	.559195E+00	.549305E+00	.988952E-02	.176853E-01
33	.130001E+02	.596426E+00	.590612E+00	.581411E-02	.974826E-02
34	.106114E+02	.653611E+00	.647170E+00	.644131E-02	.985496E-02
35	.112053E+02	.634808E+00	.632305E+00	.250295E-02	.394284E-02
36	.991096E+01	.666633E+00	.665407E+00	.122623E-02	.183943E-02
37	.904524E+01	.688295E+00	.689027E+00	-.732029E-03	-.106354E-02
38	.829564E+01	.712181E+00	.710467E+00	.171442E-02	.240728E-02

39	.775975E+01	.725370E+00	.726368E+00	-.997794E-03	-.137557E-02
40	.720149E+01	.745648E+00	.743451E+00	.219691E-02	.294631E-02
41	.601809E+01	.783342E+00	.781452E+00	.189004E-02	.241279E-02
42	.576396E+01	.796137E+00	.789935E+00	.620164E-02	.778966E-02
43	.566608E+01	.800497E+00	.793234E+00	.726331E-02	.907350E-02
44	.522140E+01	.816425E+00	.808436E+00	.798872E-02	.978500E-02
45	.409487E+01	.861861E+00	.848573E+00	.132884E-01	.154182E-01
46	.460430E+01	.837410E+00	.830132E+00	.727849E-02	.869167E-02
47	.375553E+01	.875547E+00	.861127E+00	.144203E-01	.164701E-01
48	.838863E+01	.690294E+00	.707756E+00	-.174624E-01	-.252970E-01
49	.144462E+02	.532816E+00	.560400E+00	-.275840E-01	-.517702E-01
50	.160249E+02	.503195E+00	.530673E+00	-.274777E-01	-.546065E-01
51	.171758E+02	.488342E+00	.511034E+00	-.226919E-01	-.464673E-01
52	.178874E+02	.474831E+00	.499711E+00	-.248803E-01	-.523982E-01
53	.571139E+01	.806913E+00	.791705E+00	.152083E-01	.188475E-01
54	.526518E+01	.816631E+00	.806924E+00	.970738E-02	.118871E-01
55	.540381E+01	.812713E+00	.802157E+00	.105562E-01	.129889E-01
56	.435008E+01	.854252E+00	.839274E+00	.149784E-01	.175339E-01
57	.519193E+01	.815100E+00	.809456E+00	.564353E-02	.692372E-02
58	.766381E+01	.713181E+00	.729266E+00	-.160848E-01	-.225536E-01
59	.106727E+02	.615309E+00	.645610E+00	-.303012E-01	-.492455E-01
60	.121227E+02	.578217E+00	.610398E+00	-.321807E-01	-.556551E-01
61	.132582E+02	.550599E+00	.585004E+00	-.344047E-01	-.624859E-01

average actual error (abs values) = .118947E-01
average fractional error = .187730E-01

CALCIUM CHLORIDE

number of data points : 66
order of polynomial : 5

coefficients of best-fit polynomial:

a(0) = .994696E+00
a(1) = -.606175E-02
a(2) = -.412174E-01
a(3) = .609061E-02
a(4) = -.343346E-03
a(5) = .700906E-05

i	x(i)	y(i)	f(x(i))	act err	frac err
1	.500000E-02	.999749E+00	.994665E+00	.508443E-02	.508571E-02
2	.100000E-01	.999510E+00	.994631E+00	.487883E-02	.488122E-02
3	.200000E-01	.999042E+00	.994558E+00	.448377E-02	.448807E-02
4	.300000E-01	.998583E+00	.994477E+00	.410588E-02	.411170E-02
5	.400000E-01	.998128E+00	.994388E+00	.374012E-02	.374714E-02
6	.500000E-01	.997674E+00	.994291E+00	.338347E-02	.339135E-02
7	.600000E-01	.997221E+00	.994185E+00	.303587E-02	.304433E-02
8	.700000E-01	.996768E+00	.994072E+00	.269630E-02	.270504E-02
9	.800000E-01	.996314E+00	.993950E+00	.236372E-02	.237247E-02
10	.900000E-01	.995859E+00	.993821E+00	.203810E-02	.204657E-02
11	.100000E+00	.995403E+00	.993684E+00	.171939E-02	.172733E-02
12	.200000E+00	.990753E+00	.991883E+00	-.113004E-02	-.114058E-02
13	.300000E+00	.985910E+00	.989329E+00	-.341949E-02	-.346836E-02
14	.400000E+00	.980850E+00	.986057E+00	-.520750E-02	-.530917E-02
15	.500000E+00	.975570E+00	.982101E+00	-.653076E-02	-.669430E-02
16	.600000E+00	.970040E+00	.977492E+00	-.745220E-02	-.768237E-02
17	.700000E+00	.964250E+00	.972264E+00	-.801396E-02	-.831108E-02
18	.800000E+00	.958190E+00	.966447E+00	-.825741E-02	-.861772E-02
19	.900000E+00	.951850E+00	.960073E+00	-.822314E-02	-.863912E-02
20	.100000E+01	.945210E+00	.953171E+00	-.796101E-02	-.842247E-02
21	.120000E+01	.931020E+00	.937899E+00	-.687877E-02	-.738842E-02
22	.140000E+01	.915580E+00	.920855E+00	-.527464E-02	-.576099E-02
23	.160000E+01	.898890E+00	.902251E+00	-.336099E-02	-.373905E-02
24	.180000E+01	.880960E+00	.882289E+00	-.132889E-02	-.150845E-02
25	.200000E+01	.861800E+00	.861158E+00	.641633E-03	.744527E-03
26	.220000E+01	.841600E+00	.839039E+00	.256129E-02	.304336E-02
27	.240000E+01	.820200E+00	.816099E+00	.410131E-02	.500038E-02
28	.260000E+01	.797900E+00	.792497E+00	.540313E-02	.677169E-02
29	.280000E+01	.774700E+00	.768382E+00	.631814E-02	.815560E-02
30	.300000E+01	.750800E+00	.743893E+00	.690743E-02	.920009E-02
31	.320000E+01	.726200E+00	.719159E+00	.704149E-02	.969636E-02
32	.340000E+01	.701100E+00	.694300E+00	.679998E-02	.969901E-02
33	.360000E+01	.675600E+00	.669429E+00	.617140E-02	.913469E-02
34	.380000E+01	.649900E+00	.644647E+00	.525290E-02	.808263E-02
35	.400000E+01	.624100E+00	.620050E+00	.404994E-02	.648925E-02
36	.450000E+01	.560100E+00	.559913E+00	.187332E-03	.334462E-03

37	.500000E+01	.498800E+00	.502590E+00	-.379023E-02	-.759869E-02
38	.550000E+01	.442100E+00	.448947E+00	-.684736E-02	-.154883E-01
39	.600000E+01	.391600E+00	.399597E+00	-.799652E-02	-.204201E-01
40	.650000E+01	.348200E+00	.354924E+00	-.672425E-02	-.193115E-01
41	.700000E+01	.311700E+00	.315117E+00	-.341750E-02	-.109641E-01
42	.750000E+01	.281200E+00	.280190E+00	.101013E-02	.359222E-02
43	.800000E+01	.255300E+00	.250008E+00	.529207E-02	.207288E-01
44	.850000E+01	.232700E+00	.224318E+00	.838250E-02	.360228E-01
45	.900000E+01	.213500E+00	.202770E+00	.107301E-01	.502580E-01
46	.490289E+01	.499352E+00	.513459E+00	-.141067E-01	-.282500E-01
47	.403167E+01	.614774E+00	.616178E+00	-.140385E-02	-.228351E-02
48	.136234E+02	.110376E+00	.124358E+00	-.139821E-01	-.126677E+00
49	.587461E+01	.419745E+00	.411545E+00	.820028E-02	.195363E-01
50	.218373E+01	.846853E+00	.840871E+00	.598200E-02	.706380E-02
51	.277377E+01	.772201E+00	.771569E+00	.632246E-03	.818758E-03
52	.432104E+01	.575831E+00	.581167E+00	-.533583E-02	-.926631E-02
53	.320602E+01	.718339E+00	.718412E+00	-.725018E-04	-.100930E-03
54	.635192E+01	.354074E+00	.367652E+00	-.135781E-01	-.383483E-01
55	.123638E+02	.121493E+00	.132125E+00	-.106321E-01	-.875121E-01
56	.382358E+01	.659088E+00	.641736E+00	.173522E-01	.263276E-01
57	.467913E+01	.537694E+00	.539002E+00	-.130805E-02	-.243271E-02
58	.541742E+01	.452047E+00	.457525E+00	-.547761E-02	-.121173E-01
59	.602792E+01	.393543E+00	.396976E+00	-.343310E-02	-.872358E-02
60	.669504E+01	.336903E+00	.338813E+00	-.191032E-02	-.567023E-02
61	.714703E+01	.306414E+00	.304344E+00	.207035E-02	.675671E-02
62	.773446E+01	.265928E+00	.265459E+00	.468982E-03	.176357E-02
63	.818283E+01	.237702E+00	.240110E+00	-.240770E-02	-.101291E-01
64	.879159E+01	.208948E+00	.211273E+00	-.232535E-02	-.111289E-01
65	.105426E+02	.168729E+00	.157744E+00	.109848E-01	.651030E-01
66	.140763E+02	.137162E+00	.123446E+00	.137165E-01	.100002E+00

average actual error (abs values) = .538751E-02
average fractional error = .143186E-01

MANGANESE CHLORIDE

number of data points : 65
order of polynomial : 6

coefficients of best-fit polynomial:

a(0) = .998933E+00
a(1) = -.363852E-01
a(2) = -.204943E-01
a(3) = .428627E-02
a(4) = -.413655E-03
a(5) = .196031E-04
a(6) = -.341674E-06

i	x(i)	y(i)	f(x(i))	act err	frac err
1	.537073E+01	.624930E+00	.611610E+00	.133204E-01	.213150E-01
2	.450743E+01	.688798E+00	.673931E+00	.148669E-01	.215838E-01
3	.686190E+01	.516060E+00	.514614E+00	.144633E-02	.280263E-02
4	.759455E+01	.470890E+00	.471688E+00	-.797582E-03	-.169377E-02
5	.821496E+01	.434370E+00	.437724E+00	-.335366E-02	-.772075E-02
6	.914203E+01	.391456E+00	.391355E+00	.101351E-03	.258909E-03
7	.102687E+02	.343933E+00	.343640E+00	.293211E-03	.852523E-03
8	.110886E+02	.316172E+00	.316888E+00	-.715918E-03	-.226433E-02
9	.810086E+01	.447765E+00	.443802E+00	.396278E-02	.885014E-02
10	.116652E+02	.301610E+00	.303355E+00	-.174451E-02	-.578398E-02
11	.119521E+02	.300155E+00	.298557E+00	.159774E-02	.532306E-02
12	.830857E+01	.437366E+00	.432795E+00	.457137E-02	.104520E-01
13	.587966E+01	.568779E+00	.577007E+00	-.822753E-02	-.144653E-01
14	.629872E+01	.541104E+00	.549693E+00	-.858885E-02	-.158728E-01
15	.100000E+00	.995414E+00	.995093E+00	.320637E-03	.322114E-03
16	.200000E+00	.990786E+00	.990869E+00	-.834030E-04	-.841787E-04
17	.300000E+00	.985990E+00	.986285E+00	-.294958E-03	-.299149E-03
18	.400000E+00	.980990E+00	.981363E+00	-.373339E-03	-.380574E-03
19	.500000E+00	.975770E+00	.976127E+00	-.356935E-03	-.365798E-03
20	.600000E+00	.970320E+00	.970597E+00	-.277232E-03	-.285712E-03
21	.700000E+00	.964640E+00	.964795E+00	-.154841E-03	-.160517E-03
22	.800000E+00	.958720E+00	.958740E+00	-.195145E-04	-.203547E-04
23	.900000E+00	.952570E+00	.952450E+00	.119829E-03	.125796E-03
24	.100000E+01	.946190E+00	.945945E+00	.245084E-03	.259022E-03
25	.120000E+01	.932810E+00	.932355E+00	.454834E-03	.487595E-03
26	.140000E+01	.918680E+00	.918100E+00	.580325E-03	.631694E-03
27	.150000E+01	.911370E+00	.910760E+00	.610488E-03	.669857E-03
28	.160000E+01	.903910E+00	.903296E+00	.613803E-03	.679053E-03
29	.180000E+01	.888600E+00	.888051E+00	.548515E-03	.617280E-03
30	.200000E+01	.872900E+00	.872462E+00	.438078E-03	.501865E-03
31	.250000E+01	.832300E+00	.832525E+00	-.225459E-03	-.270887E-03
32	.300000E+01	.791200E+00	.792066E+00	-.865610E-03	-.109405E-02
33	.350000E+01	.750400E+00	.751896E+00	-.149625E-02	-.199393E-02
34	.400000E+01	.711000E+00	.712582E+00	-.158200E-02	-.222504E-02
35	.450000E+01	.673200E+00	.674487E+00	-.128679E-02	-.191145E-02

36	.500000E+01	.637200E+00	.637818E+00	-.618490E-03	-.970637E-03
37	.550000E+01	.602700E+00	.602670E+00	.302106E-04	.501254E-04
38	.600000E+01	.569400E+00	.569055E+00	.344824E-03	.605593E-03
39	.650000E+01	.537000E+00	.536944E+00	.559120E-04	.104119E-03
40	.700000E+01	.505600E+00	.506290E+00	-.690226E-03	-.136516E-02
41	.750000E+01	.475900E+00	.477057E+00	-.115701E-02	-.243121E-02
42	.769900E+01	.465000E+00	.465815E+00	-.814778E-03	-.175221E-02
43	.100000E+00	.995401E+00	.995093E+00	.307637E-03	.309058E-03
44	.200000E+00	.990758E+00	.990869E+00	-.111403E-03	-.112442E-03
45	.300000E+00	.985961E+00	.986285E+00	-.323958E-03	-.328571E-03
46	.400000E+00	.981389E+00	.981363E+00	.256611E-04	.261477E-04
47	.500000E+00	.975762E+00	.976127E+00	-.364935E-03	-.374000E-03
48	.600000E+00	.970324E+00	.970597E+00	-.273232E-03	-.281589E-03
49	.700000E+00	.964698E+00	.964795E+00	-.968414E-04	-.100385E-03
50	.800000E+00	.958886E+00	.958740E+00	.146486E-03	.152766E-03
51	.900000E+00	.952755E+00	.952450E+00	.304829E-03	.319945E-03
52	.100000E+01	.946263E+00	.945945E+00	.318084E-03	.336148E-03
53	.120000E+01	.932837E+00	.932355E+00	.481834E-03	.516525E-03
54	.140000E+01	.918470E+00	.918100E+00	.370325E-03	.403198E-03
55	.160000E+01	.903542E+00	.903296E+00	.245803E-03	.272044E-03
56	.180000E+01	.888002E+00	.888051E+00	-.494850E-04	-.557262E-04
57	.200000E+01	.872295E+00	.872462E+00	-.166922E-03	-.191359E-03
58	.250000E+01	.831465E+00	.832525E+00	-.106046E-02	-.127541E-02
59	.300000E+01	.789981E+00	.792066E+00	-.208461E-02	-.263881E-02
60	.350000E+01	.748985E+00	.751896E+00	-.291125E-02	-.388692E-02
61	.400000E+01	.710041E+00	.712582E+00	-.254100E-02	-.357867E-02
62	.450000E+01	.672067E+00	.674487E+00	-.241979E-02	-.360052E-02
63	.500000E+01	.636640E+00	.637818E+00	-.117849E-02	-.185111E-02
64	.550000E+01	.602592E+00	.602670E+00	-.777894E-04	-.129091E-03
65	.600000E+01	.569717E+00	.569055E+00	.661824E-03	.116167E-02

average actual error (abs values) = .145800E-02
average fractional error = .248932E-02

MANGANESE SULFATE

note: points 1-13 are "artificial" points included so that fit would not be unreasonable

number of data points : 78
order of polynomial : 5

coefficients of best-fit polynomial:

a(0) = .981720E+00
a(1) = .329389E-01
a(2) = -.277295E-01
a(3) = .348275E-02
a(4) = -.177325E-03
a(5) = .322935E-05

i	x(i)	y(i)	f(x(i))	act err	frac err
1	.110000E+02	.547600E+00	.548195E+00	-.595063E-03	-.108667E-02
2	.115000E+02	.536700E+00	.538233E+00	-.153270E-02	-.285579E-02
3	.120000E+02	.525900E+00	.528688E+00	-.278760E-02	-.530063E-02
4	.125000E+02	.515000E+00	.519267E+00	-.426652E-02	-.828450E-02
5	.130000E+02	.504100E+00	.509701E+00	-.560087E-02	-.111106E-01
6	.135000E+02	.493200E+00	.499759E+00	-.655884E-02	-.132985E-01
7	.140000E+02	.482300E+00	.489257E+00	-.695748E-02	-.144256E-01
8	.145000E+02	.471400E+00	.478075E+00	-.667483E-02	-.141596E-01
9	.150000E+02	.460500E+00	.466162E+00	-.566201E-02	-.122954E-01
10	.155000E+02	.449700E+00	.453555E+00	-.385537E-02	-.857321E-02
11	.160000E+02	.438800E+00	.440389E+00	-.158856E-02	-.362024E-02
12	.165000E+02	.427900E+00	.426905E+00	.995356E-03	.232614E-02
13	.170000E+02	.417000E+00	.413468E+00	.353176E-02	.846946E-02
14	.100000E+00	.997901E+00	.984740E+00	.131614E-01	.131891E-01
15	.200000E+00	.996117E+00	.987226E+00	.889131E-02	.892597E-02
16	.300000E+00	.994460E+00	.989198E+00	.526187E-02	.529119E-02
17	.400000E+00	.992856E+00	.990677E+00	.217927E-02	.219495E-02
18	.500000E+00	.991260E+00	.991681E+00	-.420936E-03	-.424648E-03
19	.600000E+00	.989640E+00	.992230E+00	-.258976E-02	-.261687E-02
20	.700000E+00	.987990E+00	.992342E+00	-.435182E-02	-.440472E-02
21	.800000E+00	.986280E+00	.992035E+00	-.575533E-02	-.583539E-02
22	.900000E+00	.984510E+00	.991328E+00	-.681809E-02	-.692537E-02
23	.100000E+01	.982660E+00	.990238E+00	-.757754E-02	-.771125E-02
24	.120000E+01	.978730E+00	.986974E+00	-.824421E-02	-.842338E-02
25	.140000E+01	.974410E+00	.982377E+00	-.796694E-02	-.817617E-02
26	.150000E+01	.972080E+00	.979618E+00	-.753755E-02	-.775405E-02
27	.160000E+01	.969640E+00	.976571E+00	-.693129E-02	-.714831E-02
28	.180000E+01	.964350E+00	.969677E+00	-.532685E-02	-.552378E-02
29	.200000E+01	.958460E+00	.961807E+00	-.334742E-02	-.349250E-02
30	.250000E+01	.940680E+00	.938564E+00	.211606E-02	.224950E-02
31	.300000E+01	.917890E+00	.911426E+00	.646364E-02	.704185E-02
32	.350000E+01	.889900E+00	.881728E+00	.817151E-02	.918250E-02
33	.400000E+01	.857100E+00	.850611E+00	.648919E-02	.757110E-02

34	.450000E+01	.820900E+00	.819033E+00	.186741E-02	.227483E-02
35	.496640E+01	.785800E+00	.789860E+00	-.405998E-02	-.516668E-02
36	.100000E+00	.997900E+00	.984740E+00	.131604E-01	.131881E-01
37	.200000E+00	.996100E+00	.987226E+00	.887431E-02	.890906E-02
38	.300000E+00	.994400E+00	.989198E+00	.520187E-02	.523117E-02
39	.400000E+00	.992800E+00	.990677E+00	.212327E-02	.213867E-02
40	.500000E+00	.991200E+00	.991681E+00	-.480936E-03	-.485206E-03
41	.600000E+00	.989700E+00	.992230E+00	-.252976E-02	-.255609E-02
42	.700000E+00	.988100E+00	.992342E+00	-.424182E-02	-.429290E-02
43	.800000E+00	.986500E+00	.992035E+00	-.553533E-02	-.561107E-02
44	.900000E+00	.984800E+00	.991328E+00	-.652809E-02	-.662885E-02
45	.100000E+01	.983000E+00	.990238E+00	-.723754E-02	-.736271E-02
46	.120000E+01	.979700E+00	.986974E+00	-.727421E-02	-.742494E-02
47	.140000E+01	.974900E+00	.982377E+00	-.747694E-02	-.766945E-02
48	.160000E+01	.970100E+00	.976571E+00	-.647129E-02	-.667075E-02
49	.180000E+01	.964600E+00	.969677E+00	-.507685E-02	-.526317E-02
50	.200000E+01	.958500E+00	.961807E+00	-.330742E-02	-.345062E-02
51	.250000E+01	.940800E+00	.938564E+00	.223606E-02	.237676E-02
52	.300000E+01	.918900E+00	.911426E+00	.747364E-02	.813325E-02
53	.350000E+01	.891700E+00	.881728E+00	.997151E-02	.111826E-01
54	.400000E+01	.859800E+00	.850611E+00	.918919E-02	.106876E-01
55	.444676E+01	.836296E+00	.822392E+00	.139041E-01	.166258E-01
56	.499009E+01	.787164E+00	.788396E+00	-.123184E-02	-.156491E-02
57	.626615E+01	.698745E+00	.714034E+00	-.152888E-01	-.218804E-01
58	.914686E+01	.597770E+00	.593789E+00	.398149E-02	.666058E-02
59	.132266E+02	.509216E+00	.505254E+00	.396197E-02	.778052E-02
60	.157822E+02	.429429E+00	.446180E+00	-.167510E-01	-.390075E-01
61	.382874E+01	.881470E+00	.861366E+00	.201042E-01	.228076E-01
62	.426742E+01	.837000E+00	.833725E+00	.327528E-02	.391312E-02
63	.473146E+01	.791852E+00	.804484E+00	-.126321E-01	-.159526E-01
64	.579074E+01	.712957E+00	.740529E+00	-.275721E-01	-.386729E-01
65	.900533E+01	.606248E+00	.598101E+00	.814669E-02	.134379E-01
66	.107523E+02	.552929E+00	.553379E+00	-.450028E-03	-.813899E-03
67	.350286E+01	.894976E+00	.881554E+00	.134225E-01	.149976E-01
68	.411276E+01	.847207E+00	.843499E+00	.370827E-02	.437705E-02
69	.467896E+01	.802220E+00	.807774E+00	-.555406E-02	-.692336E-02
70	.590523E+01	.704185E+00	.733999E+00	-.298141E-01	-.423384E-01
71	.789118E+01	.605682E+00	.637510E+00	-.318282E-01	-.525494E-01
72	.125643E+02	.511299E+00	.518050E+00	-.675078E-02	-.132032E-01
73	.169935E+02	.424196E+00	.413641E+00	.105554E-01	.248832E-01
74	.470537E+01	.809183E+00	.806118E+00	.306479E-02	.378752E-02
75	.360442E+01	.894560E+00	.875313E+00	.192474E-01	.215160E-01
76	.126315E+02	.554304E+00	.516775E+00	.375290E-01	.677048E-01
77	.530014E+01	.802713E+00	.769454E+00	.332588E-01	.414330E-01
78	.125421E+02	.547992E+00	.518470E+00	.295218E-01	.538727E-01

average actual error (abs values) = .823182E-02
average fractional error = .114525E-01

FERRIC CHLORIDE

number of data points : 28
order of polynomial : 6

coefficients of best-fit polynomial:

a(0) = .109295E+01
a(1) = -.178216E+00
a(2) = .304142E-01
a(3) = -.687180E-02
a(4) = .872843E-03
a(5) = -.508931E-04
a(6) = .109601E-05

i	x(i)	y(i)	f(x(i))	act err	frac err
1	.116704E+01	.923067E+00	.916978E+00	.608864E-02	.659610E-02
2	.149941E+01	.876532E+00	.874984E+00	.154828E-02	.176638E-02
3	.192143E+01	.823723E+00	.824680E+00	-.956836E-03	-.116160E-02
4	.224021E+01	.782985E+00	.788338E+00	-.535288E-02	-.683650E-02
5	.255437E+01	.742056E+00	.753567E+00	-.115108E-01	-.155120E-01
6	.314339E+01	.674623E+00	.690489E+00	-.158661E-01	-.235185E-01
7	.365312E+01	.624701E+00	.637723E+00	-.130218E-01	-.208448E-01
8	.447877E+01	.545643E+00	.555823E+00	-.101797E-01	-.186563E-01
9	.199022E+01	.823161E+00	.816733E+00	.642793E-02	.780884E-02
10	.292834E+01	.711026E+00	.713238E+00	-.221230E-02	-.311143E-02
11	.296897E+01	.710041E+00	.708917E+00	.112400E-02	.158301E-02
12	.421420E+01	.591323E+00	.581542E+00	.978084E-02	.165406E-01
13	.509142E+01	.521428E+00	.498536E+00	.228920E-01	.439026E-01
14	.100000E+01	.930100E+00	.939100E+00	-.900035E-02	-.967675E-02
15	.200000E+01	.829200E+00	.815608E+00	.135918E-01	.163914E-01
16	.300000E+01	.718000E+00	.705624E+00	.123759E-01	.172366E-01
17	.400000E+01	.608500E+00	.602741E+00	.575882E-02	.946396E-02
18	.500000E+01	.505800E+00	.506862E+00	-.106186E-02	-.209937E-02
19	.600000E+01	.416300E+00	.420853E+00	-.455279E-02	-.109363E-01
20	.700000E+01	.341600E+00	.347989E+00	-.638857E-02	-.187019E-01
21	.800000E+01	.286300E+00	.290185E+00	-.388487E-02	-.135692E-01
22	.900000E+01	.248600E+00	.247021E+00	.157941E-02	.635321E-02
23	.100000E+02	.219600E+00	.215549E+00	.405089E-02	.184467E-01
24	.110000E+02	.192200E+00	.190899E+00	.130125E-02	.677027E-02
25	.120000E+02	.165400E+00	.167662E+00	-.226230E-02	-.136777E-01
26	.130000E+02	.140300E+00	.142076E+00	-.177566E-02	-.126562E-01
27	.140000E+02	.116900E+00	.114986E+00	.191427E-02	.163753E-01
28	.150000E+02	.952000E-01	.956072E-01	-.407229E-03	-.427762E-02

average actual error (abs values) = .631671E-02
average fractional error = .123025E-01

Appendix D: Plots of experimental and literature $a_w(m)$ data compared with predictions of polynomial fits for single-electrolyte solutions

Appendix D contains plots of water activity as a function of molality for each of the eleven single-electrolyte solutions studied in this work. Each plot contains experimental data and data from the literature. Also shown in each plot is the polynomial fit to the complete data set. The fit curves were calculated from the coefficients listed in Appendix C and in Table 2 of Chapter 1.

The abbreviations used in the figure captions to describe the literature data sources are the same as those used in Appendix B.

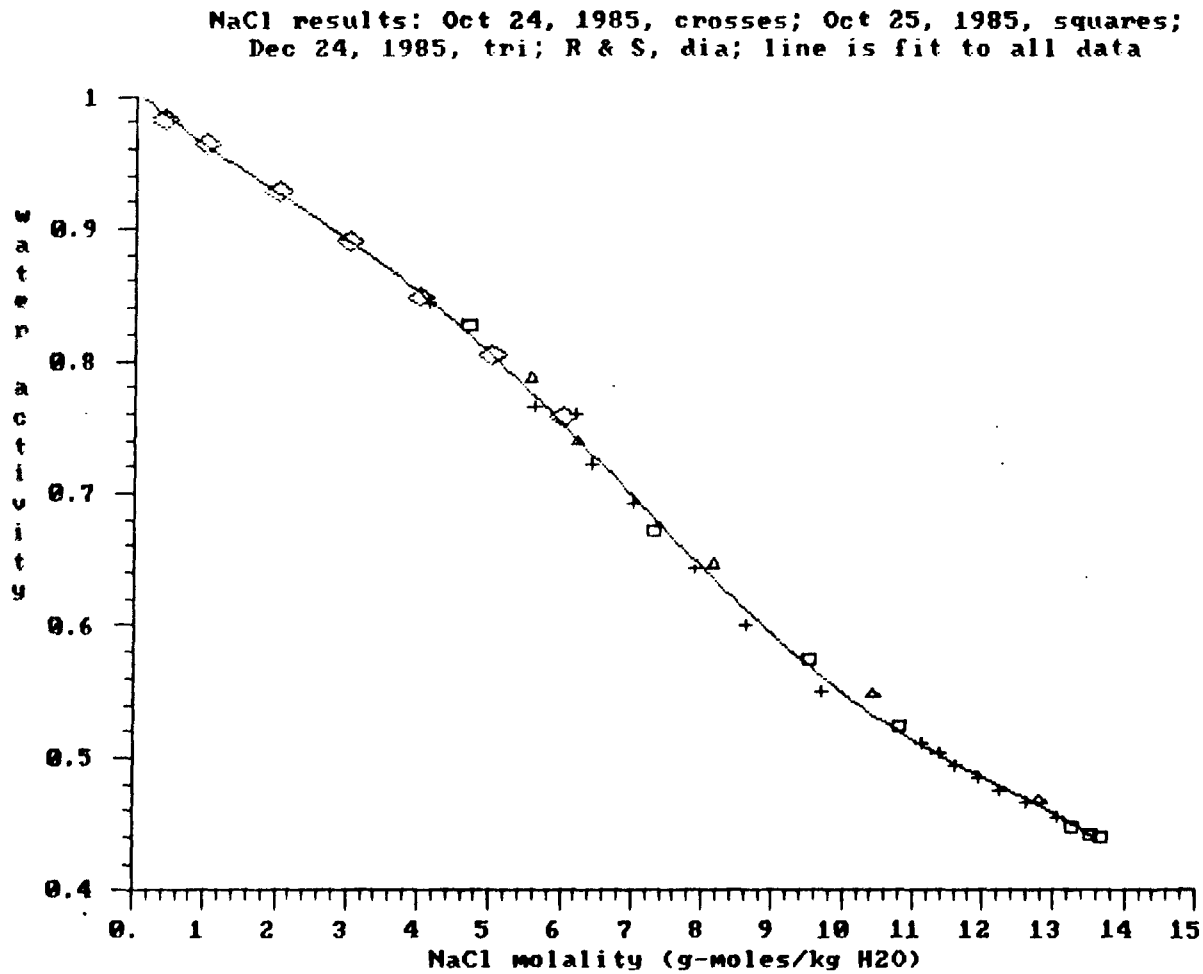
NaCl results: Oct 24, 1985, crosses; Oct 25, 1985, squares;
Dec 24, 1985, tri; R & S, dia; line is fit to all data
water activity
1
0.9
0.8
0.7
0.6
0.5
0.4
0.
1
2
3
4
5
6
7
8
9
10
11
12
13
14
15
NaCl molality (g-moles/kg H2O)

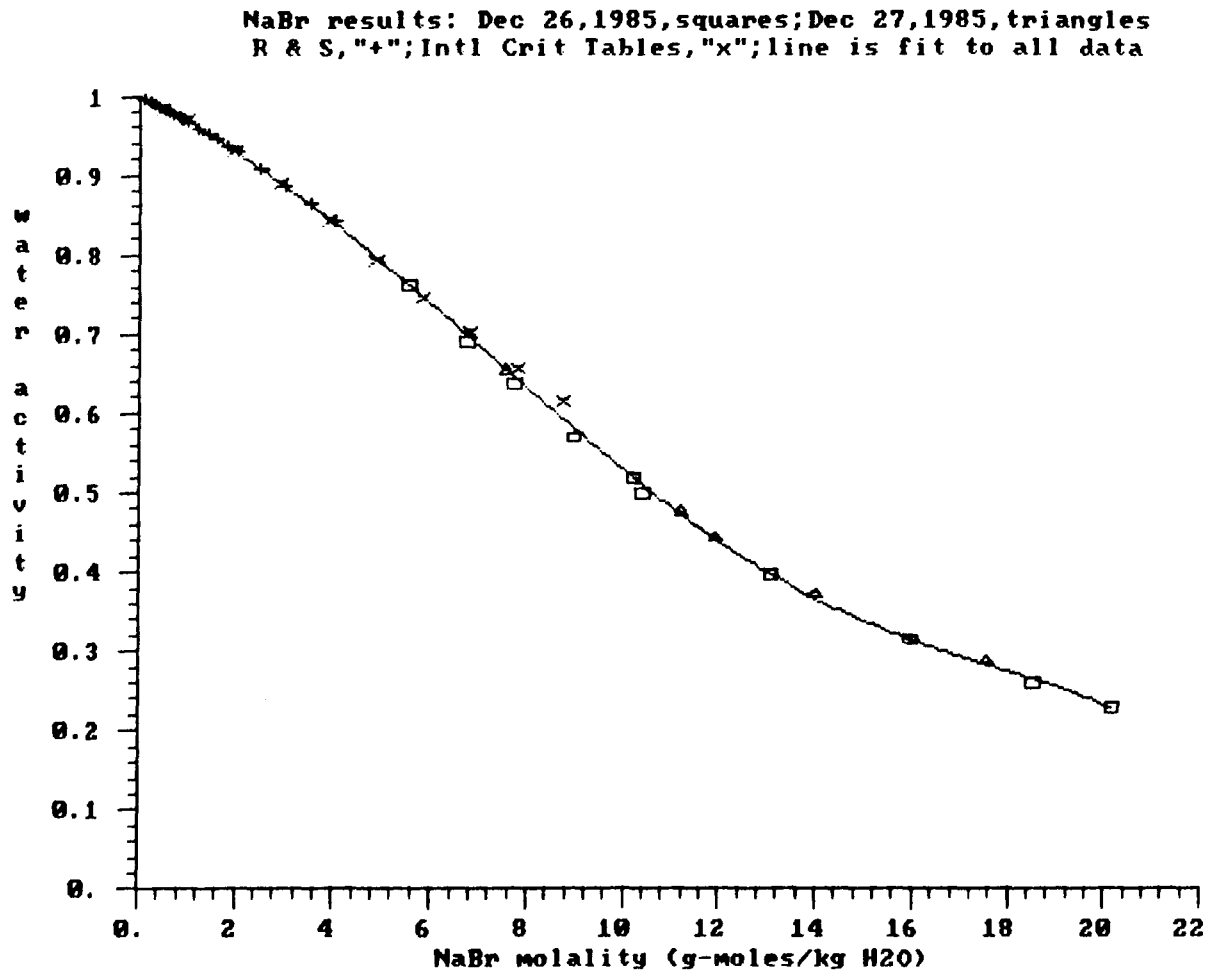
NaBr results: Dec 26,1985,squares;Dec 27,1985,triangles
R & S,"+";Intl Crit Tables,"x";line is fit to all data
water activity
1
0.9
0.8
0.7
0.6
0.5
0.4
0.3
0.2
0.1
0.
0.
2
4
6
8
10
12
14
16
18
20
22
NaBr molality (g-moles/kg H20)

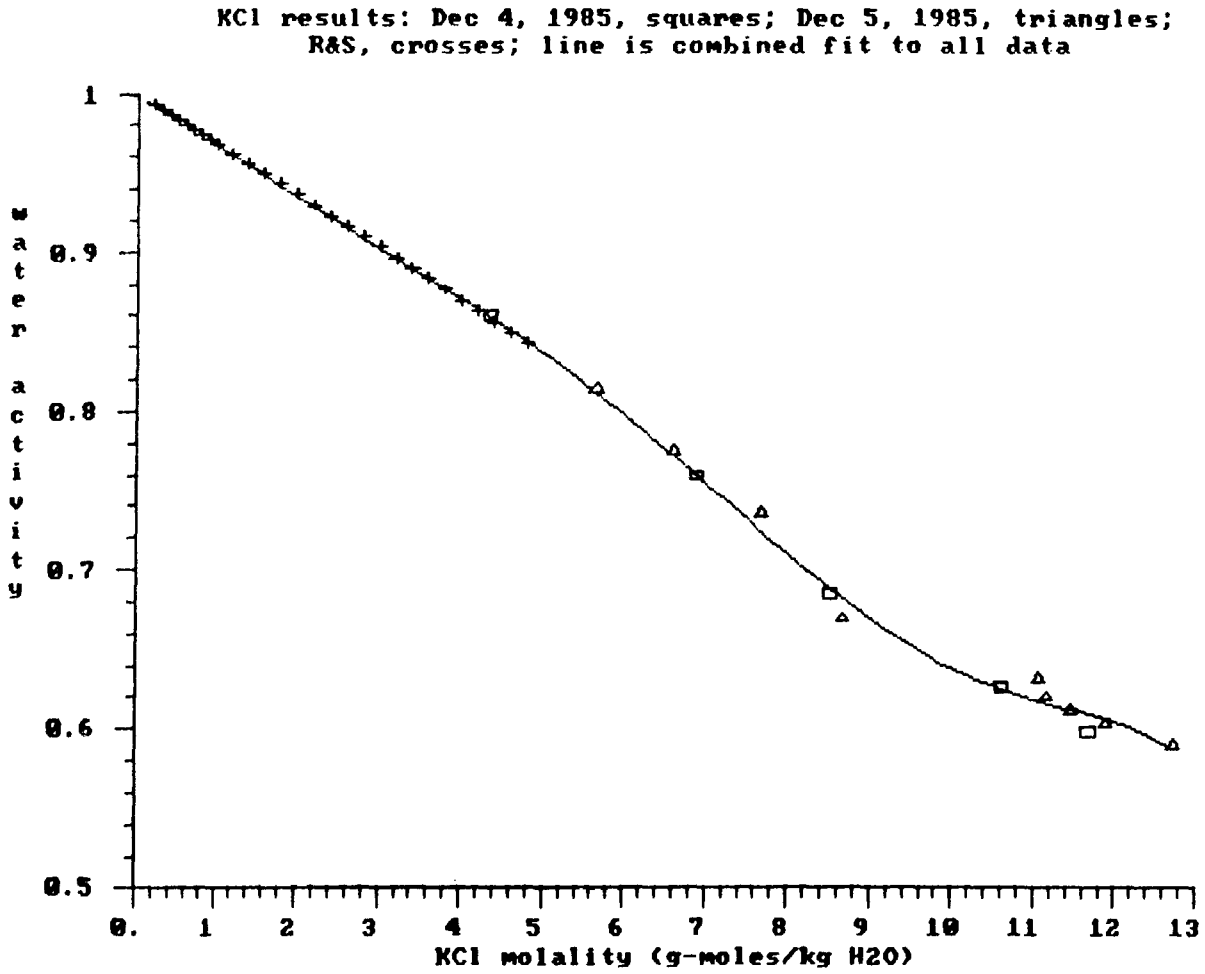
KCl results: Dec 4, 1985, squares; Dec 5, 1985, triangles;
R&S, crosses; line is combined fit to all data
water activity
1
0.9
0.8
0.7
0.6
0.5
0.
1
2
3
4
5
6
7
8
9
10
11
12
13
KCl molality (g-moles/kg H2O)

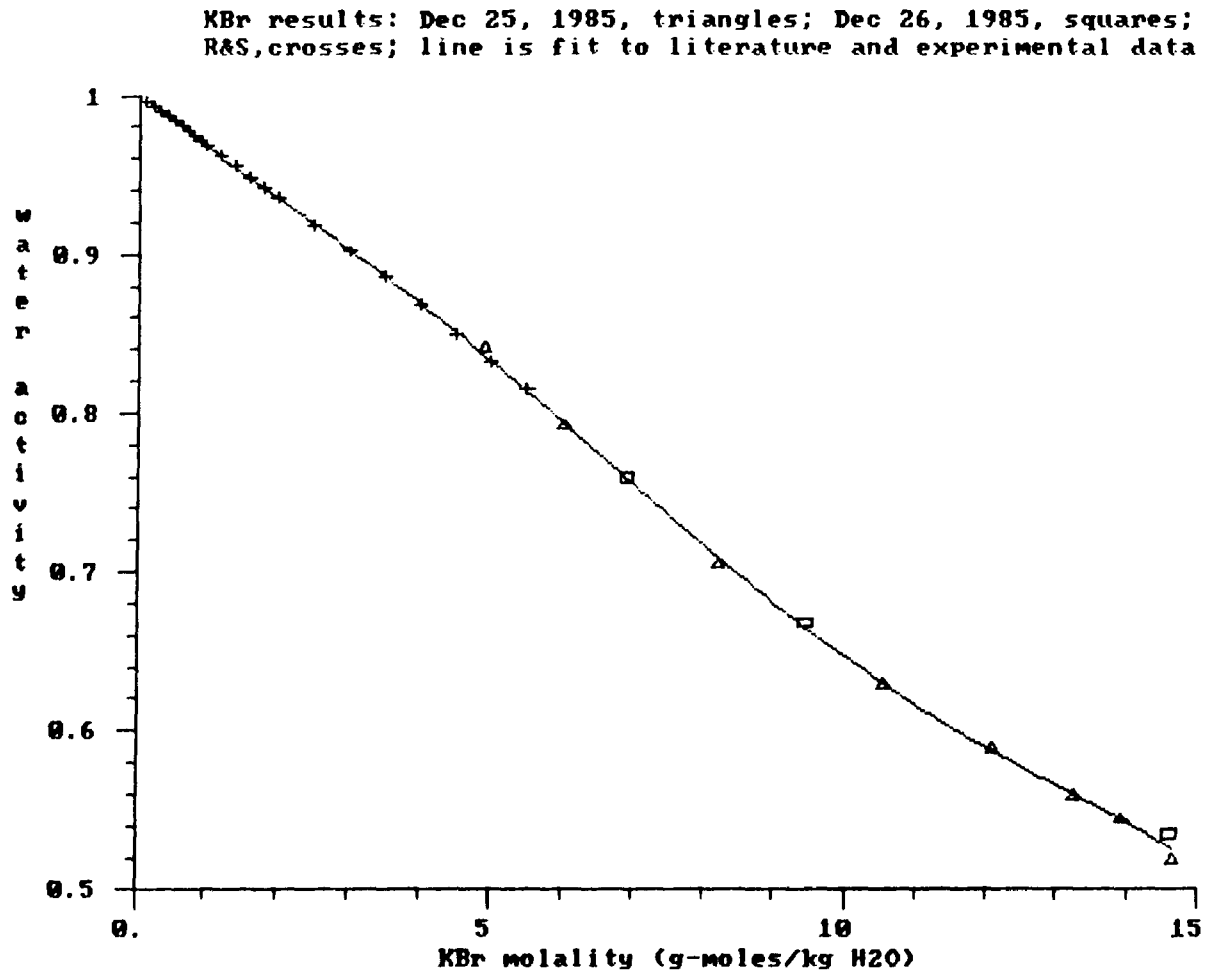
KBr results: Dec 25, 1985, triangles; Dec 26, 1985, squares;
R&S,crosses; line is fit to literature and experimental data
water activity
1
0.9
0.8
0.7
0.6
0.5
0.
5
10
15
KBr molality (g-moles/kg H2O)

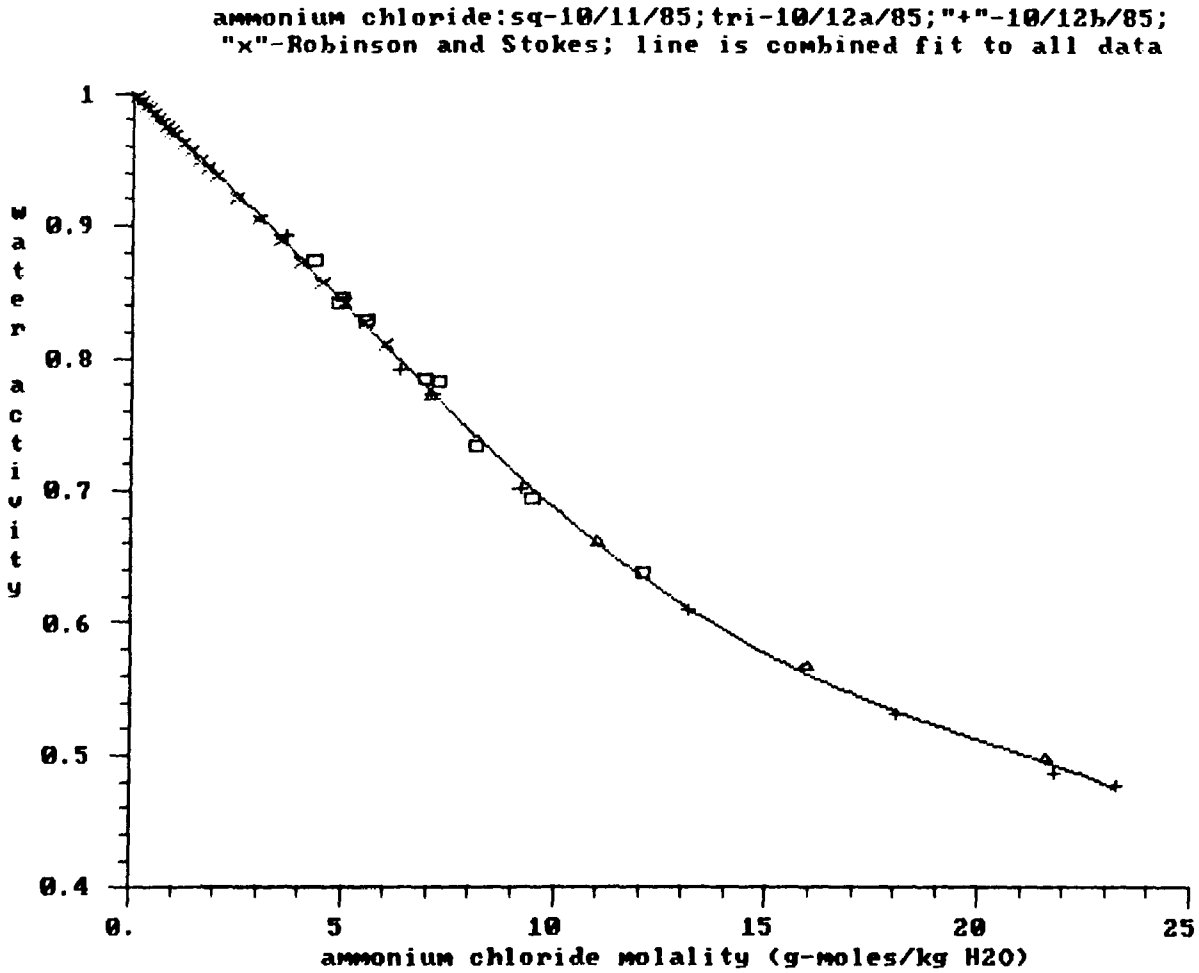
ammonium chloride:sq-10/11/85;tri-10/12a/85;"+"-10/12b/85;
"x"-Robinson and Stokes; line is combined fit to all data
water activity
1
0.9
0.8
0.7
0.6
0.5
0.4
0.
5
10
15
20
25
ammonium chloride molality (g-moles/kg H2O)

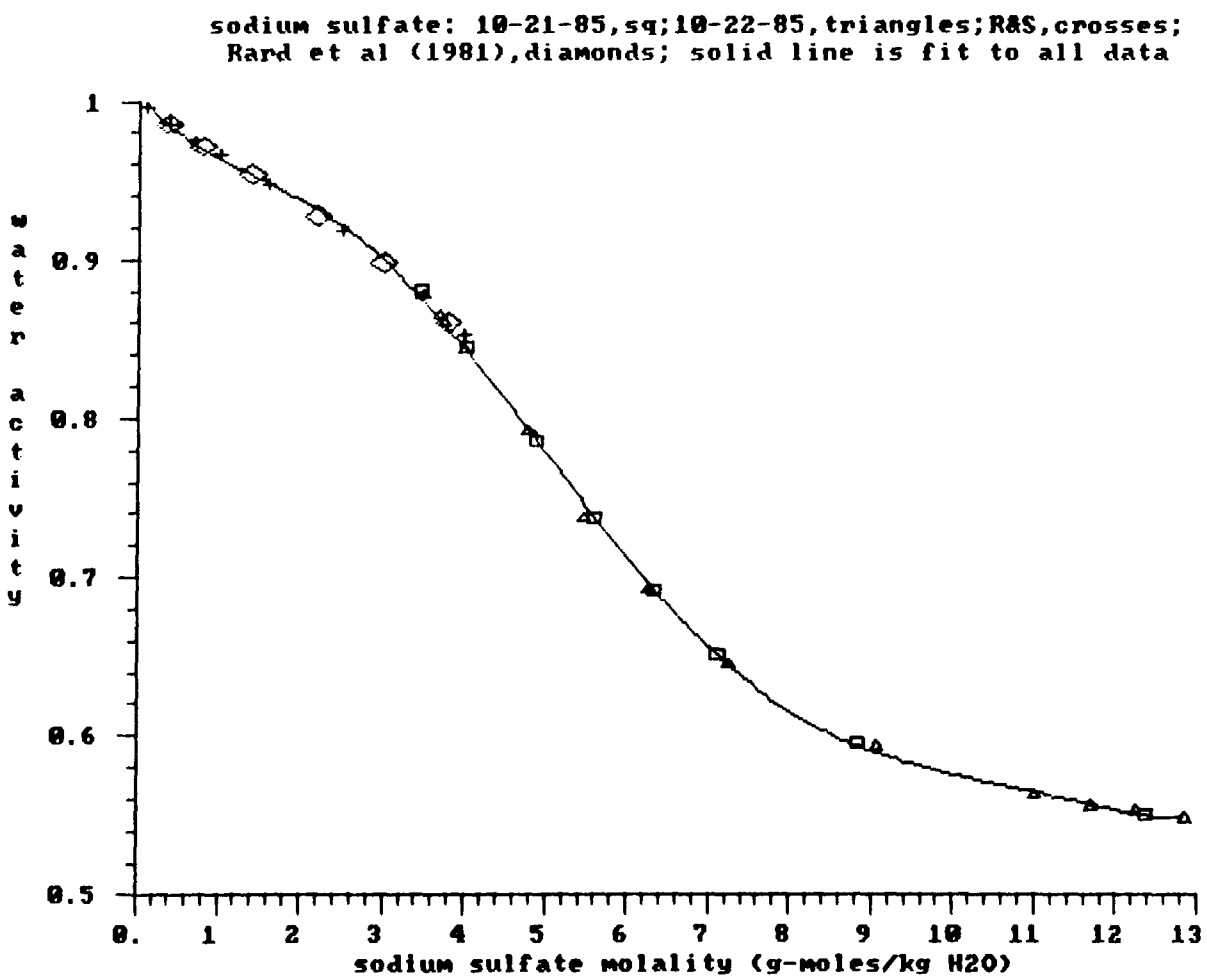
sodium sulfate: 10-21-85,sq;10-22-85,triangles;R&S,crosses;
Rard et al (1981),diamonds; solid line is fit to all data
water activity
1
0.9
0.8
0.7
0.6
0.5
0.
1
2
3
4
5
6
7
8
9
10
11
12
13
sodium sulfate molality (g-moles/kg H2O)

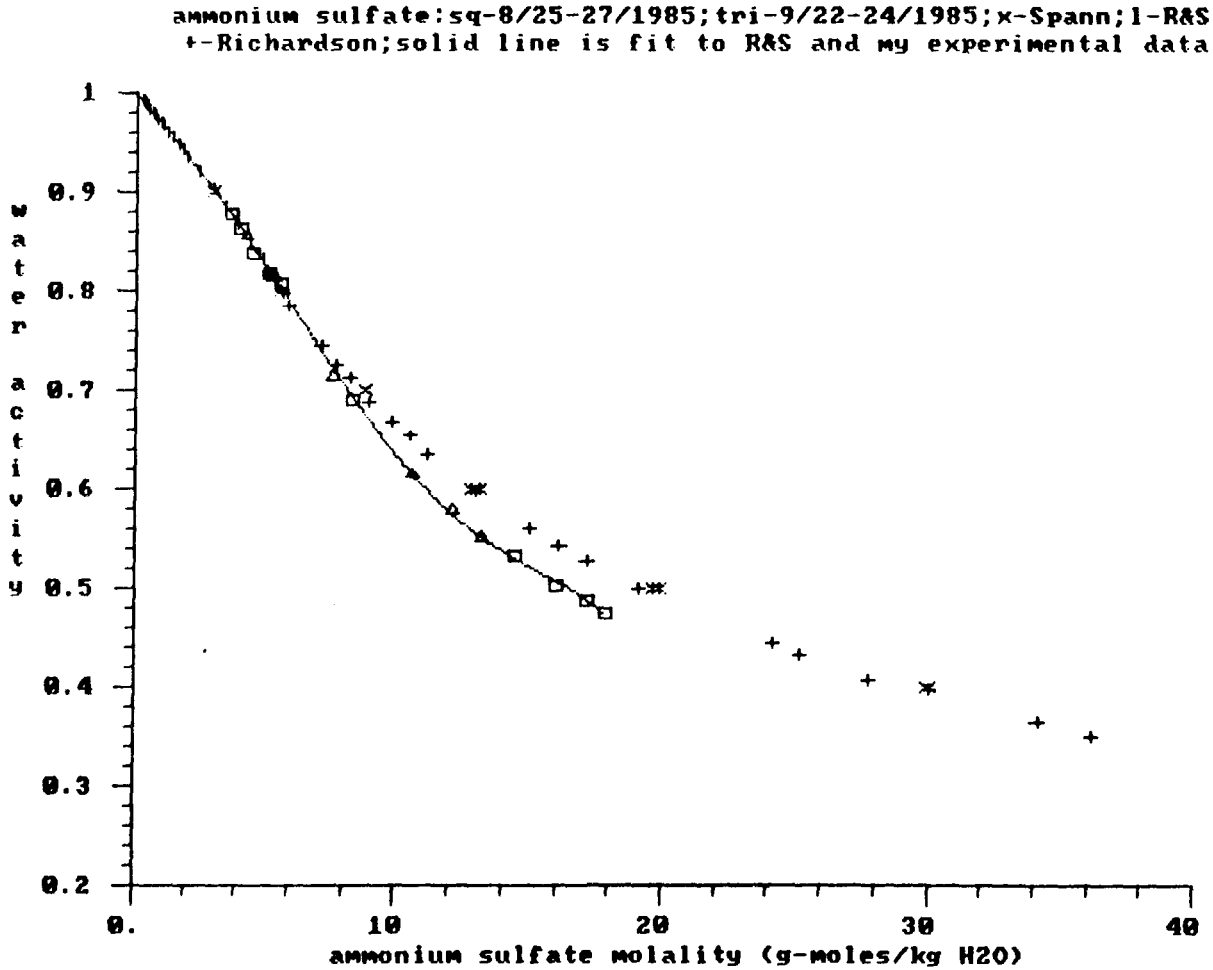
ammonium sulfate:sq-8/25-27/1985;tri-9/22-24/1985;x-Spann;1-R&S;
+-Richardson;solid line is fit to R&S and my experimental data
water activity
1
0.9
0.8
0.7
0.6
0.5
0.4
0.3
0.2
0.
10
20
30
40
ammonium sulfate molality (g-moles/kg H2O)

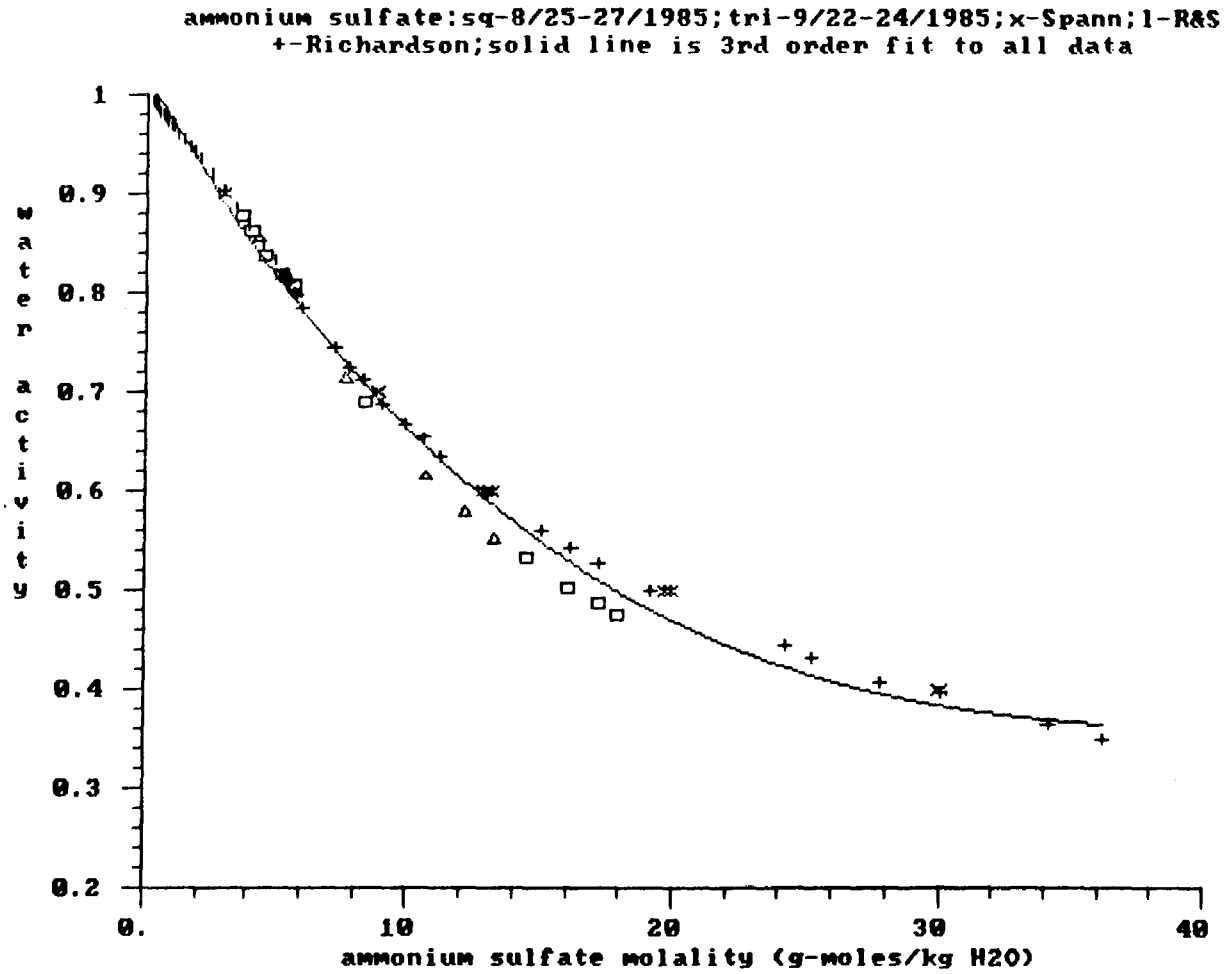
ammonium sulfate:sq-8/25-27/1985;tri-9/22-24/1985;x-Spann;l-R&S;
+-Richardson;solid line is 3rd order fit to all data
water activity
1
0.9
0.8
0.7
0.6
0.5
0.4
0.3
0.2
0.
10
20
30
40
ammonium sulfate molality (g-moles/kg H2O)

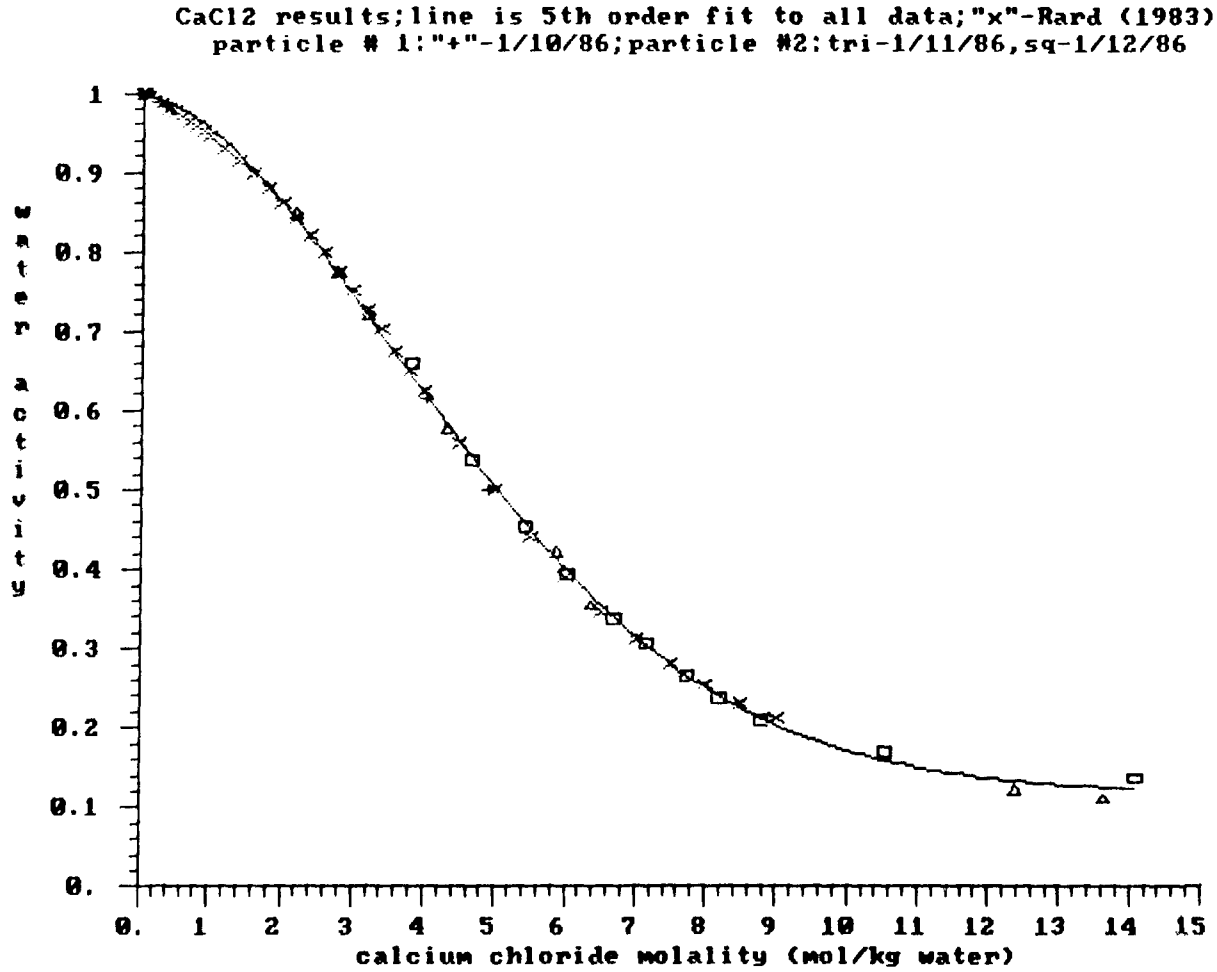
CaCl2 results;line is 5th order fit to all data;"x"-Rard (1983);
particle # 1:"+"-1/10/86;particle #2:tri-1/11/86,sq-1/12/86
water activity
1
0.9
0.8
0.7
0.6
0.5
0.4
0.3
0.2
0.1
0.
0. 1 2 3 4 5 6 7 8 9 10 11 12 13 14 15
calcium chloride molality (mol/kg water)

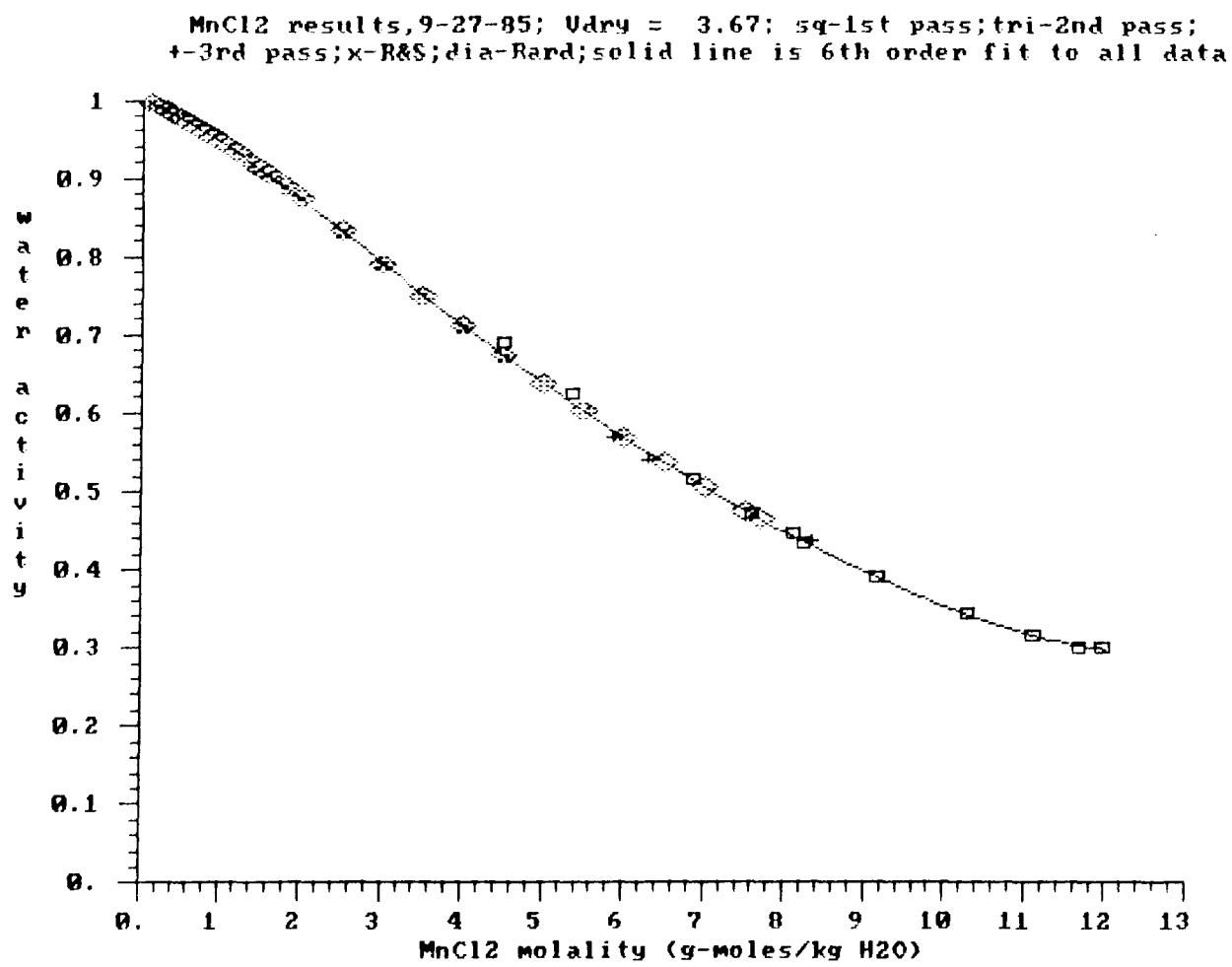
MnCl2 results,9-27-85; Vdry = 3.67; sq-1st pass;tri-2nd pass;
+-3rd pass;x-R&S;dia-Rard;solid line is 6th order fit to all data
water activity
1
0.9
0.8
0.7
0.6
0.5
0.4
0.3
0.2
0.1
0.
0. 1 2 3 4 5 6 7 8 9 10 11 12 13
MnCl2 molality (g-moles/kg H2O)

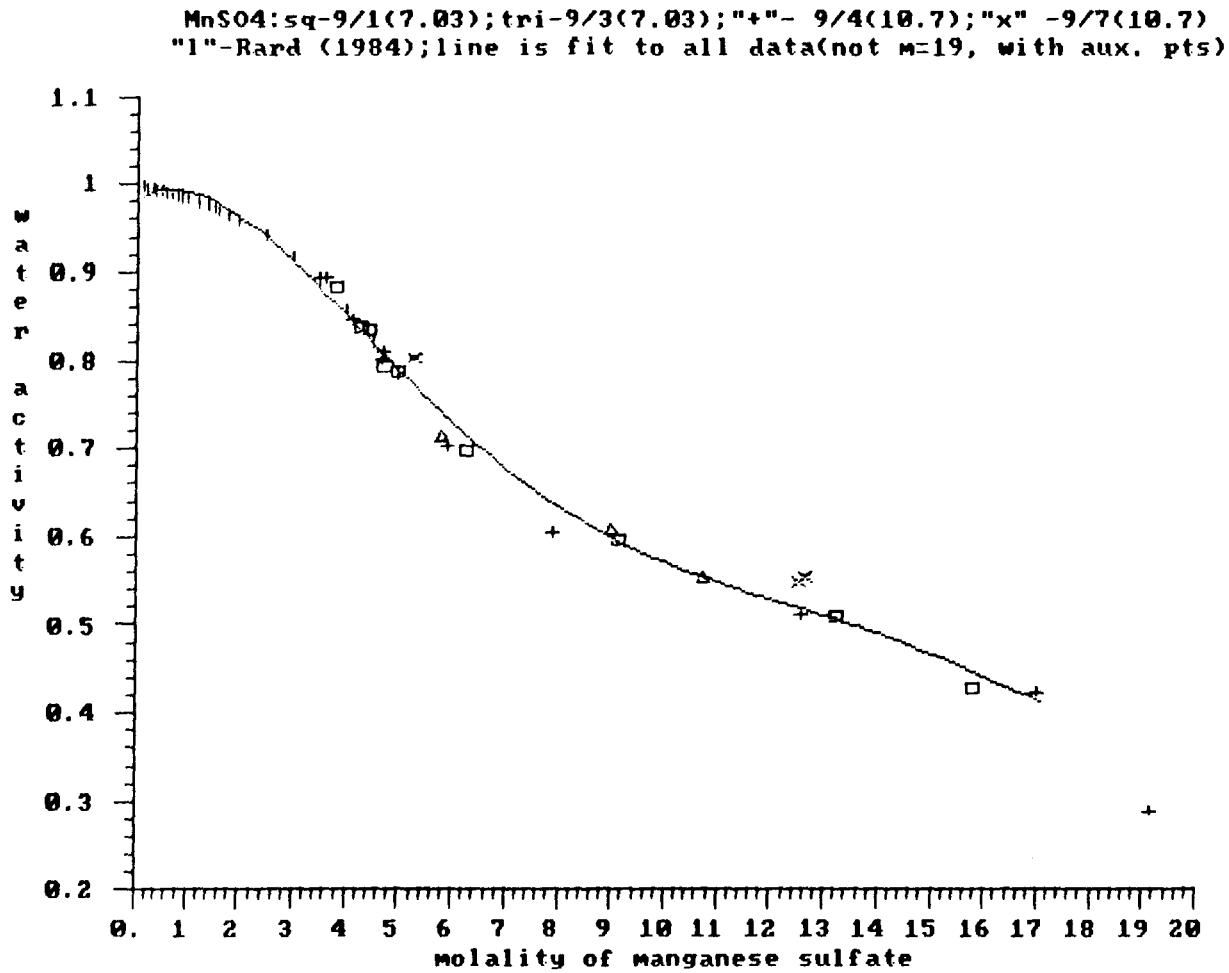
MnSO4:sq-9/1(7.03);tri-9/3(7.03);"+"- 9/4(10.7);"x" -9/7(10.7)
"1"-Rard (1984);line is fit to all data(not m=19, with aux. pts)
water activity
1.1
1
0.9
0.8
0.7
0.6
0.5
0.4
0.3
0.2
0. 1 2 3 4 5 6 7 8 9 10 11 12 13 14 15 16 17 18 19 20
molality of manganese sulfate

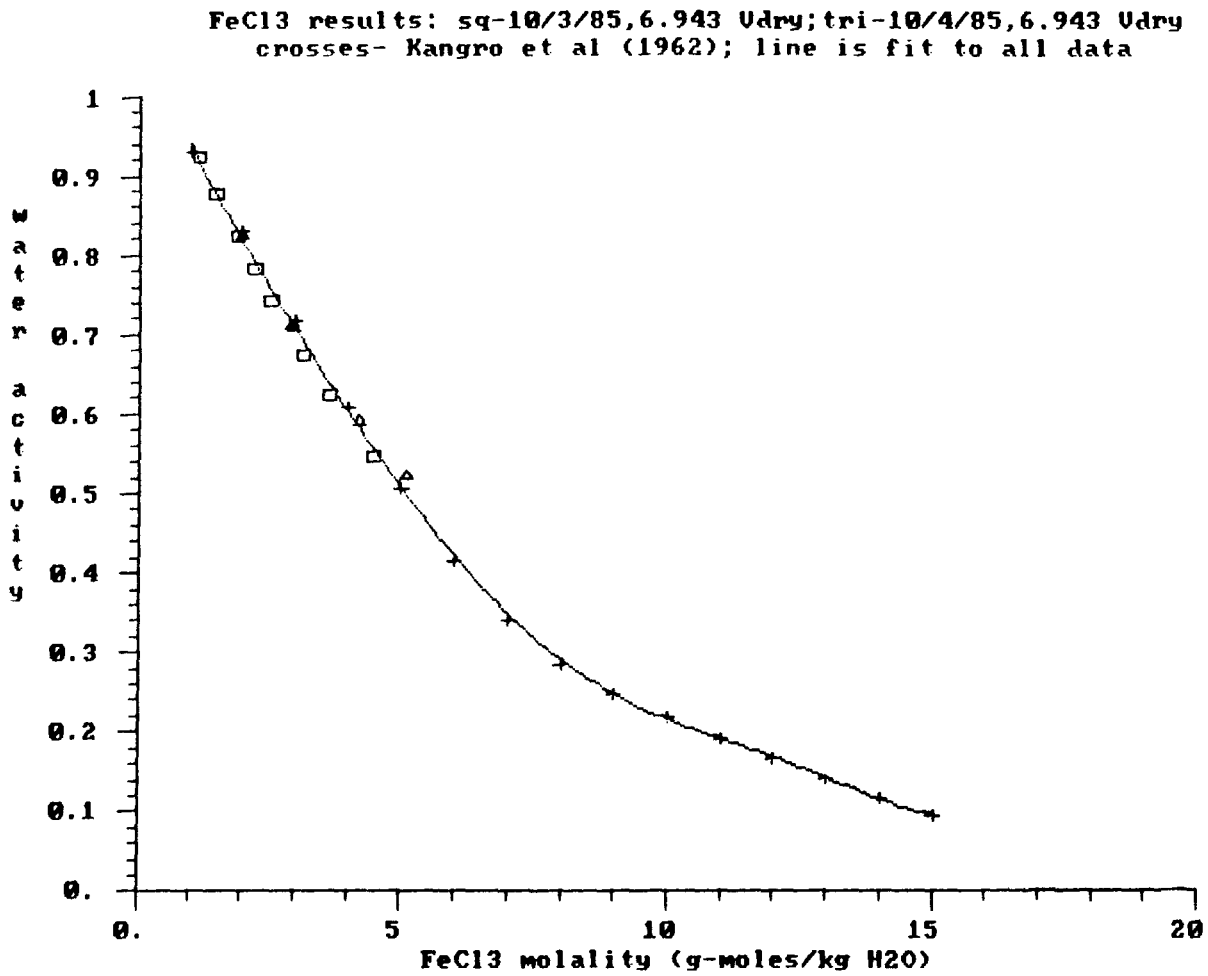
FeCl3 results: sq-10/3/85,6.943 Vdry;tri-10/4/85,6.943 Vdry
crosses- Kangro et al (1962); line is fit to all data
water activity
1
0.9
0.8
0.7
0.6
0.5
0.4
0.3
0.2
0.1
0.
0.
5
10
15
20
FeCl3 molality (g-moles/kg H2O)

Appendix E: Calculations of mean molal solute activity coefficient as a function of molality for single-electrolyte solutions

For each of the single-salt solutions studied, this appendix contains the calculated mean molal solute activity coefficient and estimated uncertainty as a function of molality. The calculations were performed using the Gibbs-Duhem equation, with the polynomial fits to the $a_w(m)$ data, as described in Chapter 1.

Each table begins with some of the data used for the calculation. This includes the lower, or "reference", molality and the mean molal solute activity coefficient at this molality. The value of the activity coefficient at the reference molality for each salt was taken from the same literature sources that were used in constructing the $a_w(m)$ fits. Also included is the "number of subintervals in each dm interval". This refers to the numerical integration used in the calculation — Simpson's rule was used, and the step size for the integration for each calculation was $0.25/50 = 0.005$ molal. Finally, in the introductory data, the uncertainty in the water activity and balancing voltages used in the estimation of the uncertainty in the solute activity coefficient are given. For each salt, values of 0.01 for each of these two experimental uncertainties were used. A discussion of the uncertainties is presented in Chapter 1.

In the tables, there are four columns: the molality, the mean molal solute activity coefficient, the natural logarithm of the mean molal solute activity coefficient, and the estimated uncertainty in the natural logarithm of the mean molal solute activity coefficient.

The uncertainty was estimated, as described in Chapter 1, from the following equation:

$$(\triangle \ln \gamma_{\pm}(m))^2 = \left[\frac{1000.0 \ln a_w(m)}{m^2 \nu w_w} \triangle m\right]^2 + \left[\frac{1000.0 \ln a_w(m_0)}{m_0^2 \nu w_w} \triangle m_0\right]^2$$

$$+2\alpha^2 \left[(\phi(m_0) - 1)^2 (1 + m_0 w_s)^2 + (\phi(m) - 1)^2 (1 + m w_s)^2\right]$$

$$+ \left[\frac{1000.0}{m \nu w_w a_w(m)} \triangle a_w\right]^2 + \left[\frac{1000.0}{m_0 \nu w_w a_w(m_0)} \triangle a_w\right]^2$$

$$+ \left[\frac{1000. \triangle a_w}{\nu w_w} \int_{m_0}^{m} \frac{1}{m^2 a_w(m)} dm\right]^2,$$

where

- m = solute molality at which uncertainty desired,
- m_0 = reference molality (equal to 1.0 for these calculations),
- ν = the number of moles of ions formed when one mole of salt completely dissociates,
- w_w = the molecular weight of water,
- w_s = the molecular weight of the solute,

- ϕ = the osmotic coefficient,
- $\triangle a_w$ = uncertainty in water activity, equal to 0.01 for these calculations,
- $\triangle m$ = uncertainty in molality calculated from an uncertainty in balancing voltage from the following equation:

$$\triangle m = \sqrt{2}\alpha m(1 + mw_s)$$

in which

- $\alpha = \triangle V_{dc}/V_{dc}$

It was assumed in the derivation of the above equation that the uncertainty in the mean molal solute activity coefficient taken from the literature was insignificant. Further, in the calculation, the uncertainty in the water activity at the reference molality (*i.e.*,m = 1.0) was assumed to be 0.001.

SODIUM CHLORIDE

lower limit of molal : .100000E+01
act coeff at lowest molality: .657000E+00
upper limit of molal : .136000E+02
number of subintervals in each dm interval: .5000E+02

uncertainty in water activity (absolute) = .100000E-01
uncertainty in bal voltages (fractional) = .100000E-01

molality	mean molal solute activity coeff, (GAMMA)	ln(GAMMA)	uncertainty in ln(GAMMA)
1.250	.6659E+00	-.4066E+00	.2418E+00
1.500	.6704E+00	-.3999E+00	.2207E+00
1.750	.6732E+00	-.3958E+00	.2129E+00
2.000	.6759E+00	-.3917E+00	.2116E+00
2.250	.6795E+00	-.3864E+00	.2135E+00
2.500	.6845E+00	-.3790E+00	.2169E+00
2.750	.6914E+00	-.3690E+00	.2208E+00
3.000	.7004E+00	-.3561E+00	.2249E+00
3.250	.7117E+00	-.3401E+00	.2289E+00
3.500	.7253E+00	-.3212E+00	.2328E+00
3.750	.7414E+00	-.2992E+00	.2365E+00
4.000	.7600E+00	-.2744E+00	.2400E+00
4.250	.7813E+00	-.2468E+00	.2433E+00
4.500	.8051E+00	-.2167E+00	.2464E+00
4.750	.8317E+00	-.1843E+00	.2493E+00
5.000	.8610E+00	-.1497E+00	.2521E+00
5.250	.8930E+00	-.1132E+00	.2547E+00
5.500	.9277E+00	-.7501E-01	.2572E+00
5.750	.9652E+00	-.3538E-01	.2596E+00
6.000	.1005E+01	.5439E-02	.2618E+00
6.250	.1048E+01	.4719E-01	.2640E+00
6.500	.1094E+01	.8961E-01	.2660E+00
6.750	.1142E+01	.1324E+00	.2680E+00
7.000	.1192E+01	.1754E+00	.2699E+00
7.250	.1244E+01	.2183E+00	.2718E+00
7.500	.1298E+01	.2608E+00	.2735E+00
7.750	.1353E+01	.3026E+00	.2752E+00
8.000	.1410E+01	.3436E+00	.2769E+00
8.250	.1467E+01	.3834E+00	.2785E+00
8.500	.1525E+01	.4219E+00	.2801E+00
8.750	.1582E+01	.4587E+00	.2816E+00
9.000	.1638E+01	.4938E+00	.2830E+00

9.250	.1694E+01	.5268E+00	.2844E+00
9.500	.1747E+01	.5578E+00	.2858E+00
9.750	.1798E+01	.5865E+00	.2871E+00
10.000	.1846E+01	.6129E+00	.2884E+00
10.250	.1891E+01	.6369E+00	.2896E+00
10.500	.1932E+01	.6586E+00	.2908E+00
10.750	.1970E+01	.6780E+00	.2919E+00
11.000	.2004E+01	.6953E+00	.2930E+00
11.250	.2035E+01	.7106E+00	.2941E+00
11.500	.2063E+01	.7243E+00	.2951E+00
11.750	.2089E+01	.7366E+00	.2961E+00
12.000	.2113E+01	.7480E+00	.2970E+00
12.250	.2136E+01	.7590E+00	.2980E+00
12.500	.2160E+01	.7702E+00	.2989E+00
12.750	.2186E+01	.7822E+00	.2998E+00
13.000	.2216E+01	.7958E+00	.3007E+00
13.250	.2252E+01	.8120E+00	.3016E+00
13.500	.2297E+01	.8317E+00	.3026E+00

SODIUM BROMIDE

lower limit of molal : .100000E+01
act coeff at lowest molality: .687000E+00
upper limit of molal : .201000E+02
number of subintervals in each dm interval: .5000E+02

uncertainty in water activity (absolute) = .100000E-01
uncertainty in bal voltages (fractional) = .100000E-01

molality	mean molal solute activity coeff, (GAMMA)	ln(GAMMA)	uncertainty in ln(GAMMA)
1.250	.6936E+00	-.3659E+00	.2417E+00
1.500	.7045E+00	-.3502E+00	.2207E+00
1.750	.7189E+00	-.3301E+00	.2131E+00
2.000	.7360E+00	-.3066E+00	.2120E+00
2.250	.7555E+00	-.2803E+00	.2141E+00
2.500	.7773E+00	-.2519E+00	.2176E+00
2.750	.8012E+00	-.2216E+00	.2217E+00
3.000	.8272E+00	-.1897E+00	.2259E+00
3.250	.8552E+00	-.1565E+00	.2301E+00
3.500	.8851E+00	-.1220E+00	.2341E+00
3.750	.9172E+00	-.8648E-01	.2379E+00
4.000	.9512E+00	-.5001E-01	.2416E+00
4.250	.9874E+00	-.1271E-01	.2450E+00
4.500	.1026E+01	.2535E-01	.2482E+00
4.750	.1066E+01	.6406E-01	.2512E+00
5.000	.1109E+01	.1034E+00	.2541E+00
5.250	.1154E+01	.1432E+00	.2568E+00
5.500	.1201E+01	.1835E+00	.2594E+00
5.750	.1251E+01	.2241E+00	.2619E+00
6.000	.1304E+01	.2651E+00	.2642E+00
6.250	.1359E+01	.3064E+00	.2664E+00
6.500	.1416E+01	.3480E+00	.2686E+00
6.750	.1476E+01	.3897E+00	.2707E+00
7.000	.1540E+01	.4315E+00	.2727E+00
7.250	.1605E+01	.4734E+00	.2746E+00
7.500	.1674E+01	.5153E+00	.2765E+00
7.750	.1746E+01	.5572E+00	.2783E+00
8.000	.1820E+01	.5990E+00	.2801E+00
8.250	.1898E+01	.6407E+00	.2819E+00
8.500	.1978E+01	.6822E+00	.2836E+00
8.750	.2062E+01	.7235E+00	.2852E+00
9.000	.2148E+01	.7645E+00	.2868E+00

9.250	.2237E+01	.8052E+00	.2884E+00
9.500	.2329E+01	.8454E+00	.2900E+00
9.750	.2424E+01	.8853E+00	.2916E+00
10.000	.2521E+01	.9246E+00	.2931E+00
10.250	.2620E+01	.9633E+00	.2946E+00
10.500	.2722E+01	.1001E+01	.2961E+00
10.750	.2826E+01	.1039E+01	.2975E+00
11.000	.2932E+01	.1076E+01	.2990E+00
11.250	.3040E+01	.1112E+01	.3004E+00
11.500	.3148E+01	.1147E+01	.3018E+00
11.750	.3258E+01	.1181E+01	.3032E+00
12.000	.3369E+01	.1214E+01	.3046E+00
12.250	.3479E+01	.1247E+01	.3060E+00
12.500	.3590E+01	.1278E+01	.3073E+00
12.750	.3700E+01	.1308E+01	.3086E+00
13.000	.3809E+01	.1337E+01	.3099E+00
13.250	.3918E+01	.1365E+01	.3112E+00
13.500	.4024E+01	.1392E+01	.3125E+00
13.750	.4128E+01	.1418E+01	.3137E+00
14.000	.4230E+01	.1442E+01	.3149E+00
14.250	.4329E+01	.1465E+01	.3161E+00
14.500	.4426E+01	.1487E+01	.3173E+00
14.750	.4518E+01	.1508E+01	.3185E+00
15.000	.4608E+01	.1528E+01	.3196E+00
15.250	.4694E+01	.1546E+01	.3207E+00
15.500	.4776E+01	.1564E+01	.3218E+00
15.750	.4854E+01	.1580E+01	.3229E+00
16.000	.4930E+01	.1595E+01	.3239E+00
16.250	.5001E+01	.1610E+01	.3249E+00
16.500	.5071E+01	.1623E+01	.3259E+00
16.750	.5137E+01	.1637E+01	.3269E+00
17.000	.5202E+01	.1649E+01	.3279E+00
17.250	.5266E+01	.1661E+01	.3289E+00
17.500	.5329E+01	.1673E+01	.3298E+00
17.750	.5393E+01	.1685E+01	.3308E+00
18.000	.5459E+01	.1697E+01	.3318E+00
18.250	.5528E+01	.1710E+01	.3327E+00
18.500	.5602E+01	.1723E+01	.3337E+00
18.750	.5681E+01	.1737E+01	.3347E+00
19.000	.5769E+01	.1753E+01	.3357E+00
19.250	.5868E+01	.1769E+01	.3368E+00
19.500	.5979E+01	.1788E+01	.3379E+00
19.750	.6107E+01	.1809E+01	.3391E+00
20.000	.6255E+01	.1833E+01	.3403E+00

POTASSIUM CHLORIDE

lower limit of molal : .100000E+01
act coeff at lowest molality: .604000E+00
upper limit of molal : .127000E+02
number of subintervals in each dm interval: .5000E+02

uncertainty in water activity (absolute) = .100000E-01
uncertainty in bal voltages (fractional) = .100000E-01

molality	mean molal solute activity coeff, (GAMMA)	ln(GAMMA)	uncertainty in ln(GAMMA)
1.250	.5979E+00	-.5143E+00	.2407E+00
1.500	.5952E+00	-.5189E+00	.2196E+00
1.750	.5936E+00	-.5216E+00	.2118E+00
2.000	.5922E+00	-.5239E+00	.2105E+00
2.250	.5908E+00	-.5263E+00	.2124E+00
2.500	.5892E+00	-.5290E+00	.2156E+00
2.750	.5875E+00	-.5319E+00	.2195E+00
3.000	.5859E+00	-.5346E+00	.2235E+00
3.250	.5846E+00	-.5368E+00	.2274E+00
3.500	.5838E+00	-.5382E+00	.2312E+00
3.750	.5837E+00	-.5384E+00	.2347E+00
4.000	.5844E+00	-.5372E+00	.2381E+00
4.250	.5861E+00	-.5342E+00	.2412E+00
4.500	.5890E+00	-.5293E+00	.2441E+00
4.750	.5931E+00	-.5223E+00	.2469E+00
5.000	.5985E+00	-.5133E+00	.2495E+00
5.250	.6053E+00	-.5020E+00	.2519E+00
5.500	.6135E+00	-.4886E+00	.2542E+00
5.750	.6230E+00	-.4732E+00	.2564E+00
6.000	.6339E+00	-.4559E+00	.2584E+00
6.250	.6460E+00	-.4369E+00	.2604E+00
6.500	.6594E+00	-.4164E+00	.2622E+00
6.750	.6738E+00	-.3948E+00	.2640E+00
7.000	.6892E+00	-.3722E+00	.2657E+00
7.250	.7053E+00	-.3492E+00	.2673E+00
7.500	.7218E+00	-.3260E+00	.2689E+00
7.750	.7386E+00	-.3031E+00	.2704E+00
8.000	.7552E+00	-.2808E+00	.2719E+00
8.250	.7713E+00	-.2597E+00	.2732E+00
8.500	.7866E+00	-.2400E+00	.2746E+00
8.750	.8007E+00	-.2223E+00	.2758E+00
9.000	.8132E+00	-.2068E+00	.2771E+00

9.250	.8237E+00	-.1939E+00	.2782E+00
9.500	.8321E+00	-.1838E+00	.2794E+00
9.750	.8380E+00	-.1768E+00	.2804E+00
10.000	.8413E+00	-.1728E+00	.2814E+00
10.250	.8421E+00	-.1718E+00	.2824E+00
10.500	.8405E+00	-.1737E+00	.2833E+00
10.750	.8368E+00	-.1781E+00	.2842E+00
11.000	.8314E+00	-.1846E+00	.2850E+00
11.250	.8249E+00	-.1925E+00	.2858E+00
11.500	.8180E+00	-.2009E+00	.2865E+00
11.750	.8116E+00	-.2088E+00	.2873E+00
12.000	.8066E+00	-.2149E+00	.2880E+00
12.250	.8043E+00	-.2178E+00	.2887E+00
12.500	.8060E+00	-.2157E+00	.2894E+00

POTASSIUM BROMIDE

lower limit of molal : .100000E+01
act coeff at lowest molality: .617000E+00
upper limit of molal : .146000E+02
number of subintervals in each dm interval: .5000E+02

uncertainty in water activity (absolute) = .100000E-01
uncertainty in bal voltages (fractional) = .100000E-01

molality	mean molal solute activity coeff, (GAMMA)	ln(GAMMA)	uncertainty in ln(GAMMA)
1.250	.6063E+00	-.5005E+00	.2411E+00
1.500	.5977E+00	-.5146E+00	.2199E+00
1.750	.5911E+00	-.5258E+00	.2121E+00
2.000	.5862E+00	-.5342E+00	.2107E+00
2.250	.5827E+00	-.5400E+00	.2126E+00
2.500	.5807E+00	-.5436E+00	.2159E+00
2.750	.5799E+00	-.5449E+00	.2198E+00
3.000	.5803E+00	-.5443E+00	.2238E+00
3.250	.5817E+00	-.5418E+00	.2277E+00
3.500	.5842E+00	-.5376E+00	.2316E+00
3.750	.5876E+00	-.5318E+00	.2352E+00
4.000	.5918E+00	-.5245E+00	.2386E+00
4.250	.5969E+00	-.5160E+00	.2417E+00
4.500	.6028E+00	-.5062E+00	.2447E+00
4.750	.6094E+00	-.4953E+00	.2475E+00
5.000	.6166E+00	-.4836E+00	.2501E+00
5.250	.6244E+00	-.4709E+00	.2526E+00
5.500	.6328E+00	-.4576E+00	.2549E+00
5.750	.6417E+00	-.4436E+00	.2571E+00
6.000	.6511E+00	-.4292E+00	.2592E+00
6.250	.6608E+00	-.4143E+00	.2612E+00
6.500	.6709E+00	-.3992E+00	.2631E+00
6.750	.6812E+00	-.3839E+00	.2648E+00
7.000	.6918E+00	-.3685E+00	.2665E+00
7.250	.7025E+00	-.3532E+00	.2682E+00
7.500	.7132E+00	-.3379E+00	.2697E+00
7.750	.7240E+00	-.3229E+00	.2712E+00
8.000	.7348E+00	-.3082E+00	.2726E+00
8.250	.7454E+00	-.2939E+00	.2740E+00
8.500	.7558E+00	-.2800E+00	.2753E+00
8.750	.7659E+00	-.2667E+00	.2766E+00
9.000	.7757E+00	-.2540E+00	.2779E+00

9.250	.7851E+00	-.2419E+00	.2790E+00
9.500	.7941E+00	-.2305E+00	.2802E+00
9.750	.8026E+00	-.2199E+00	.2813E+00
10.000	.8105E+00	-.2101E+00	.2824E+00
10.250	.8178E+00	-.2012E+00	.2834E+00
10.500	.8245E+00	-.1930E+00	.2844E+00
10.750	.8306E+00	-.1856E+00	.2854E+00
11.000	.8360E+00	-.1791E+00	.2863E+00
11.250	.8408E+00	-.1733E+00	.2872E+00
11.500	.8451E+00	-.1683E+00	.2881E+00
11.750	.8488E+00	-.1640E+00	.2889E+00
12.000	.8519E+00	-.1602E+00	.2897E+00
12.250	.8547E+00	-.1570E+00	.2905E+00
12.500	.8571E+00	-.1542E+00	.2913E+00
12.750	.8594E+00	-.1516E+00	.2921E+00
13.000	.8615E+00	-.1491E+00	.2928E+00
13.250	.8637E+00	-.1465E+00	.2935E+00
13.500	.8661E+00	-.1437E+00	.2943E+00
13.750	.8690E+00	-.1404E+00	.2950E+00
14.000	.8725E+00	-.1364E+00	.2956E+00
14.250	.8769E+00	-.1314E+00	.2963E+00
14.500	.8824E+00	-.1251E+00	.2970E+00

AMMONIUM CHLORIDE

lower limit of molal : .100000E+01
act coeff at lowest molality: .603000E+00
upper limit of molal : .232000E+02
number of subintervals in each dm interval: .5000E+02

uncertainty in water activity (absolute) = .100000E-01
uncertainty in bal voltages (fractional) = .100000E-01

molality	mean molal solute activity coeff, (GAMMA)	ln(GAMMA)	uncertainty in ln(GAMMA)
1.250	.5817E+00	-.5417E+00	.2403E+00
1.500	.5673E+00	-.5669E+00	.2190E+00
1.750	.5572E+00	-.5849E+00	.2111E+00
2.000	.5501E+00	-.5976E+00	.2098E+00
2.250	.5453E+00	-.6065E+00	.2116E+00
2.500	.5420E+00	-.6124E+00	.2148E+00
2.750	.5401E+00	-.6161E+00	.2187E+00
3.000	.5391E+00	-.6179E+00	.2227E+00
3.250	.5389E+00	-.6182E+00	.2266E+00
3.500	.5394E+00	-.6173E+00	.2304E+00
3.750	.5404E+00	-.6155E+00	.2339E+00
4.000	.5418E+00	-.6129E+00	.2372E+00
4.250	.5436E+00	-.6096E+00	.2404E+00
4.500	.5456E+00	-.6059E+00	.2433E+00
4.750	.5479E+00	-.6017E+00	.2460E+00
5.000	.5504E+00	-.5972E+00	.2485E+00
5.250	.5530E+00	-.5924E+00	.2509E+00
5.500	.5557E+00	-.5875E+00	.2532E+00
5.750	.5585E+00	-.5824E+00	.2553E+00
6.000	.5614E+00	-.5773E+00	.2572E+00
6.250	.5643E+00	-.5721E+00	.2591E+00
6.500	.5672E+00	-.5670E+00	.2609E+00
6.750	.5701E+00	-.5619E+00	.2625E+00
7.000	.5730E+00	-.5568E+00	.2641E+00
7.250	.5759E+00	-.5518E+00	.2656E+00
7.500	.5787E+00	-.5470E+00	.2670E+00
7.750	.5814E+00	-.5423E+00	.2684E+00
8.000	.5840E+00	-.5378E+00	.2697E+00
8.250	.5866E+00	-.5334E+00	.2709E+00
8.500	.5890E+00	-.5293E+00	.2721E+00
8.750	.5913E+00	-.5254E+00	.2733E+00
9.000	.5935E+00	-.5216E+00	.2744E+00
9.250	.5956E+00	-.5182E+00	.2754E+00
9.500	.5975E+00	-.5150E+00	.2764E+00

9.750	.5993E+00	-.5120E+00	.2774E+00
10.000	.6009E+00	-.5093E+00	.2783E+00
10.250	.6024E+00	-.5069E+00	.2792E+00
10.500	.6036E+00	-.5048E+00	.2801E+00
10.750	.6048E+00	-.5029E+00	.2810E+00
11.000	.6057E+00	-.5014E+00	.2818E+00
11.250	.6064E+00	-.5001E+00	.2826E+00
11.500	.6070E+00	-.4992E+00	.2833E+00
11.750	.6074E+00	-.4986E+00	.2841E+00
12.000	.6076E+00	-.4982E+00	.2848E+00
12.250	.6076E+00	-.4982E+00	.2855E+00
12.500	.6075E+00	-.4985E+00	.2861E+00
12.750	.6071E+00	-.4990E+00	.2868E+00
13.000	.6066E+00	-.4999E+00	.2874E+00
13.250	.6059E+00	-.5011E+00	.2880E+00
13.500	.6050E+00	-.5026E+00	.2886E+00
13.750	.6039E+00	-.5043E+00	.2892E+00
14.000	.6027E+00	-.5064E+00	.2898E+00
14.250	.6013E+00	-.5087E+00	.2903E+00
14.500	.5997E+00	-.5113E+00	.2909E+00
14.750	.5980E+00	-.5142E+00	.2914E+00
15.000	.5961E+00	-.5173E+00	.2919E+00
15.250	.5941E+00	-.5206E+00	.2924E+00
15.500	.5920E+00	-.5243E+00	.2929E+00
15.750	.5897E+00	-.5281E+00	.2934E+00
16.000	.5874E+00	-.5321E+00	.2938E+00
16.250	.5849E+00	-.5364E+00	.2943E+00
16.500	.5823E+00	-.5408E+00	.2947E+00
16.750	.5796E+00	-.5454E+00	.2951E+00
17.000	.5768E+00	-.5502E+00	.2955E+00
17.250	.5740E+00	-.5551E+00	.2960E+00
17.500	.5711E+00	-.5602E+00	.2964E+00
17.750	.5682E+00	-.5653E+00	.2967E+00
18.000	.5652E+00	-.5706E+00	.2971E+00
18.250	.5622E+00	-.5760E+00	.2975E+00
18.500	.5591E+00	-.5814E+00	.2979E+00
18.750	.5561E+00	-.5868E+00	.2982E+00
19.000	.5530E+00	-.5923E+00	.2986E+00
19.250	.5500E+00	-.5978E+00	.2989E+00
19.500	.5470E+00	-.6033E+00	.2992E+00
19.750	.5440E+00	-.6087E+00	.2996E+00
20.000	.5411E+00	-.6141E+00	.2999E+00
20.250	.5382E+00	-.6194E+00	.3002E+00
20.500	.5354E+00	-.6247E+00	.3005E+00
20.750	.5327E+00	-.6297E+00	.3008E+00
21.000	.5301E+00	-.6347E+00	.3011E+00
21.250	.5276E+00	-.6395E+00	.3014E+00
21.500	.5252E+00	-.6440E+00	.3017E+00
21.750	.5229E+00	-.6484E+00	.3020E+00
22.000	.5207E+00	-.6525E+00	.3023E+00
22.250	.5187E+00	-.6564E+00	.3026E+00
22.500	.5169E+00	-.6599E+00	.3029E+00
22.750	.5152E+00	-.6631E+00	.3032E+00
23.000	.5138E+00	-.6660E+00	.3034E+00

SODIUM SULFATE

lower limit of molal : .100000E+01
act coeff at lowest molality: .203600E+00
upper limit of molal : .128000E+02
number of subintervals in each dm interval: .5000E+02

uncertainty in water activity (absolute) = .100000E-01
uncertainty in bal voltages (fractional) = .100000E-01

molality	mean molal solute activity coeff, (GAMMA)	ln(GAMMA)	uncertainty in ln(GAMMA)
1.250	.1820E+00	-.1704E+01	.1613E+00
1.500	.1657E+00	-.1798E+01	.1470E+00
1.750	.1536E+00	-.1874E+01	.1417E+00
2.000	.1448E+00	-.1933E+01	.1408E+00
2.250	.1386E+00	-.1976E+01	.1420E+00
2.500	.1345E+00	-.2006E+01	.1443E+00
2.750	.1321E+00	-.2024E+01	.1470E+00
3.000	.1312E+00	-.2031E+01	.1498E+00
3.250	.1314E+00	-.2030E+01	.1526E+00
3.500	.1326E+00	-.2020E+01	.1553E+00
3.750	.1348E+00	-.2004E+01	.1579E+00
4.000	.1376E+00	-.1983E+01	.1604E+00
4.250	.1410E+00	-.1959E+01	.1628E+00
4.500	.1450E+00	-.1931E+01	.1651E+00
4.750	.1493E+00	-.1902E+01	.1673E+00
5.000	.1539E+00	-.1871E+01	.1693E+00
5.250	.1587E+00	-.1841E+01	.1713E+00
5.500	.1636E+00	-.1811E+01	.1732E+00
5.750	.1683E+00	-.1782E+01	.1750E+00
6.000	.1729E+00	-.1755E+01	.1767E+00
6.250	.1772E+00	-.1731E+01	.1784E+00
6.500	.1811E+00	-.1709E+01	.1799E+00
6.750	.1844E+00	-.1690E+01	.1814E+00
7.000	.1872E+00	-.1675E+01	.1828E+00
7.250	.1894E+00	-.1664E+01	.1842E+00
7.500	.1909E+00	-.1656E+01	.1854E+00
7.750	.1917E+00	-.1652E+01	.1866E+00
8.000	.1918E+00	-.1651E+01	.1877E+00
8.250	.1913E+00	-.1654E+01	.1887E+00
8.500	.1903E+00	-.1659E+01	.1896E+00
8.750	.1887E+00	-.1668E+01	.1905E+00
9.000	.1868E+00	-.1678E+01	.1914E+00

9.250	.1845E+00	-.1690E+01	.1922E+00
9.500	.1820E+00	-.1704E+01	.1929E+00
9.750	.1793E+00	-.1719E+01	.1936E+00
10.000	.1766E+00	-.1734E+01	.1943E+00
10.250	.1738E+00	-.1750E+01	.1949E+00
10.500	.1712E+00	-.1765E+01	.1956E+00
10.750	.1686E+00	-.1780E+01	.1962E+00
11.000	.1661E+00	-.1795E+01	.1968E+00
11.250	.1638E+00	-.1809E+01	.1973E+00
11.500	.1615E+00	-.1823E+01	.1979E+00
11.750	.1594E+00	-.1836E+01	.1984E+00
12.000	.1573E+00	-.1850E+01	.1989E+00
12.250	.1551E+00	-.1864E+01	.1994E+00
12.500	.1528E+00	-.1879E+01	.1999E+00
12.750	.1502E+00	-.1896E+01	.2003E+00

AMMONIUM SULFATE (fit "a")

lower limit of molal : .100000E+01
act coeff at lowest molality: .189000E+00
upper limit of molal : .179000E+02
number of subintervals in each dm interval: .5000E+02

uncertainty in water activity (absolute) = .100000E-01
uncertainty in bal voltages (fractional) = .100000E-01

molality	mean molal solute activity coeff, (GAMMA)	ln(GAMMA)	uncertainty in ln(GAMMA)
1.250	.1725E+00	-.1758E+01	.1610E+00
1.500	.1604E+00	-.1830E+01	.1469E+00
1.750	.1512E+00	-.1889E+01	.1417E+00
2.000	.1440E+00	-.1938E+01	.1409E+00
2.250	.1382E+00	-.1979E+01	.1421E+00
2.500	.1334E+00	-.2014E+01	.1443E+00
2.750	.1295E+00	-.2044E+01	.1469E+00
3.000	.1263E+00	-.2069E+01	.1496E+00
3.250	.1235E+00	-.2091E+01	.1523E+00
3.500	.1212E+00	-.2110E+01	.1548E+00
3.750	.1193E+00	-.2126E+01	.1573E+00
4.000	.1176E+00	-.2140E+01	.1596E+00
4.250	.1163E+00	-.2152E+01	.1617E+00
4.500	.1151E+00	-.2162E+01	.1637E+00
4.750	.1142E+00	-.2170E+01	.1656E+00
5.000	.1134E+00	-.2177E+01	.1674E+00
5.250	.1127E+00	-.2183E+01	.1690E+00
5.500	.1122E+00	-.2187E+01	.1706E+00
5.750	.1118E+00	-.2191E+01	.1721E+00
6.000	.1115E+00	-.2194E+01	.1735E+00
6.250	.1113E+00	-.2196E+01	.1748E+00
6.500	.1111E+00	-.2197E+01	.1761E+00
6.750	.1110E+00	-.2198E+01	.1773E+00
7.000	.1110E+00	-.2199E+01	.1784E+00
7.250	.1109E+00	-.2199E+01	.1795E+00
7.500	.1109E+00	-.2199E+01	.1806E+00
7.750	.1110E+00	-.2198E+01	.1816E+00
8.000	.1110E+00	-.2198E+01	.1826E+00
8.250	.1111E+00	-.2198E+01	.1835E+00
8.500	.1111E+00	-.2197E+01	.1844E+00
8.750	.1111E+00	-.2197E+01	.1853E+00
9.000	.1112E+00	-.2197E+01	.1861E+00

9.250	.1112E+00	-.2197E+01	.1869E+00
9.500	.1111E+00	-.2197E+01	.1877E+00
9.750	.1111E+00	-.2197E+01	.1885E+00
10.000	.1110E+00	-.2198E+01	.1892E+00
10.250	.1109E+00	-.2199E+01	.1899E+00
10.500	.1107E+00	-.2201E+01	.1906E+00
10.750	.1105E+00	-.2203E+01	.1913E+00
11.000	.1102E+00	-.2205E+01	.1919E+00
11.250	.1099E+00	-.2208E+01	.1925E+00
11.500	.1096E+00	-.2211E+01	.1931E+00
11.750	.1091E+00	-.2215E+01	.1937E+00
12.000	.1087E+00	-.2219E+01	.1943E+00
12.250	.1082E+00	-.2224E+01	.1949E+00
12.500	.1076E+00	-.2229E+01	.1954E+00
12.750	.1070E+00	-.2235E+01	.1959E+00
13.000	.1063E+00	-.2241E+01	.1964E+00
13.250	.1056E+00	-.2248E+01	.1969E+00
13.500	.1049E+00	-.2255E+01	.1974E+00
13.750	.1041E+00	-.2262E+01	.1978E+00
14.000	.1033E+00	-.2270E+01	.1983E+00
14.250	.1025E+00	-.2278E+01	.1987E+00
14.500	.1017E+00	-.2286E+01	.1991E+00
14.750	.1009E+00	-.2294E+01	.1995E+00
15.000	.1001E+00	-.2302E+01	.1999E+00
15.250	.9927E-01	-.2310E+01	.2003E+00
15.500	.9847E-01	-.2318E+01	.2007E+00
15.750	.9770E-01	-.2326E+01	.2011E+00
16.000	.9697E-01	-.2333E+01	.2015E+00
16.250	.9629E-01	-.2340E+01	.2018E+00
16.500	.9565E-01	-.2347E+01	.2022E+00
16.750	.9509E-01	-.2353E+01	.2026E+00
17.000	.9460E-01	-.2358E+01	.2029E+00
17.250	.9420E-01	-.2362E+01	.2033E+00
17.500	.9390E-01	-.2366E+01	.2036E+00
17.750	.9372E-01	-.2367E+01	.2040E+00

AMMONIUM SULFATE (fit "b")

lower limit of molal : .100000E+01
act coeff at lowest molality: .189000E+00
upper limit of molal : .362000E+02
number of subintervals in each dm interval: .5000E+02

uncertainty in water activity (absolute) = .100000E-01
uncertainty in bal voltages (fractional) = .100000E-01

molality	mean molal solute activity coeff, (GAMMA)	ln(GAMMA)	uncertainty in ln(GAMMA)
1.250	.1813E+00	-.1708E+01	.1607E+00
1.500	.1752E+00	-.1742E+01	.1470E+00
1.750	.1702E+00	-.1771E+01	.1420E+00
2.000	.1660E+00	-.1796E+01	.1413E+00
2.250	.1623E+00	-.1818E+01	.1426E+00
2.500	.1591E+00	-.1839E+01	.1449E+00
2.750	.1562E+00	-.1857E+01	.1476E+00
3.000	.1536E+00	-.1874E+01	.1504E+00
3.250	.1512E+00	-.1889E+01	.1531E+00
3.500	.1490E+00	-.1904E+01	.1557E+00
3.750	.1470E+00	-.1917E+01	.1581E+00
4.000	.1451E+00	-.1930E+01	.1604E+00
4.250	.1434E+00	-.1942E+01	.1626E+00
4.500	.1417E+00	-.1954E+01	.1646E+00
4.750	.1402E+00	-.1965E+01	.1665E+00
5.000	.1387E+00	-.1975E+01	.1683E+00
5.250	.1373E+00	-.1986E+01	.1699E+00
5.500	.1360E+00	-.1995E+01	.1715E+00
5.750	.1347E+00	-.2005E+01	.1730E+00
6.000	.1335E+00	-.2014E+01	.1743E+00
6.250	.1323E+00	-.2023E+01	.1756E+00
6.500	.1312E+00	-.2031E+01	.1769E+00
6.750	.1301E+00	-.2040E+01	.1781E+00
7.000	.1290E+00	-.2048E+01	.1792E+00
7.250	.1280E+00	-.2056E+01	.1802E+00
7.500	.1270E+00	-.2063E+01	.1812E+00
7.750	.1261E+00	-.2071E+01	.1822E+00
8.000	.1251E+00	-.2078E+01	.1831E+00
8.250	.1242E+00	-.2086E+01	.1840E+00
8.500	.1233E+00	-.2093E+01	.1849E+00
8.750	.1225E+00	-.2100E+01	.1857E+00
9.000	.1216E+00	-.2107E+01	.1865E+00

9.250	.1208E+00	-.2114E+01	.1872E+00
9.500	.1200E+00	-.2120E+01	.1879E+00
9.750	.1192E+00	-.2127E+01	.1886E+00
10.000	.1184E+00	-.2134E+01	.1893E+00
10.250	.1176E+00	-.2140E+01	.1900E+00
10.500	.1169E+00	-.2147E+01	.1906E+00
10.750	.1161E+00	-.2153E+01	.1912E+00
11.000	.1154E+00	-.2159E+01	.1918E+00
11.250	.1147E+00	-.2166E+01	.1924E+00
11.500	.1140E+00	-.2172E+01	.1930E+00
11.750	.1133E+00	-.2178E+01	.1935E+00
12.000	.1126E+00	-.2184E+01	.1940E+00
12.250	.1119E+00	-.2190E+01	.1946E+00
12.500	.1112E+00	-.2196E+01	.1951E+00
12.750	.1105E+00	-.2202E+01	.1956E+00
13.000	.1099E+00	-.2208E+01	.1960E+00
13.250	.1092E+00	-.2215E+01	.1965E+00
13.500	.1086E+00	-.2221E+01	.1970E+00
13.750	.1079E+00	-.2226E+01	.1974E+00
14.000	.1073E+00	-.2232E+01	.1978E+00
14.250	.1066E+00	-.2238E+01	.1983E+00
14.500	.1060E+00	-.2244E+01	.1987E+00
14.750	.1054E+00	-.2250E+01	.1991E+00
15.000	.1047E+00	-.2256E+01	.1995E+00
15.250	.1041E+00	-.2262E+01	.1999E+00
15.500	.1035E+00	-.2268E+01	.2003E+00
15.750	.1029E+00	-.2274E+01	.2007E+00
16.000	.1023E+00	-.2280E+01	.2010E+00
16.250	.1017E+00	-.2286E+01	.2014E+00
16.500	.1011E+00	-.2292E+01	.2018E+00
16.750	.1005E+00	-.2298E+01	.2021E+00
17.000	.9990E-01	-.2304E+01	.2025E+00
17.250	.9931E-01	-.2310E+01	.2028E+00
17.500	.9872E-01	-.2316E+01	.2031E+00
17.750	.9813E-01	-.2321E+01	.2035E+00
18.000	.9755E-01	-.2327E+01	.2038E+00
18.250	.9697E-01	-.2333E+01	.2041E+00
18.500	.9639E-01	-.2339E+01	.2044E+00
18.750	.9581E-01	-.2345E+01	.2047E+00
19.000	.9524E-01	-.2351E+01	.2050E+00
19.250	.9467E-01	-.2357E+01	.2053E+00
19.500	.9410E-01	-.2363E+01	.2056E+00
19.750	.9353E-01	-.2369E+01	.2059E+00
20.000	.9297E-01	-.2376E+01	.2062E+00
20.250	.9240E-01	-.2382E+01	.2065E+00
20.500	.9184E-01	-.2388E+01	.2068E+00
20.750	.9128E-01	-.2394E+01	.2070E+00
21.000	.9073E-01	-.2400E+01	.2073E+00
21.250	.9017E-01	-.2406E+01	.2076E+00
21.500	.8962E-01	-.2412E+01	.2078E+00
21.750	.8907E-01	-.2418E+01	.2081E+00
22.000	.8852E-01	-.2424E+01	.2084E+00
22.250	.8798E-01	-.2431E+01	.2086E+00
22.500	.8743E-01	-.2437E+01	.2089E+00

22.750	.8689E-01	-.2443E+01	.2091E+00
23.000	.8635E-01	-.2449E+01	.2094E+00
23.250	.8581E-01	-.2456E+01	.2096E+00
23.500	.8528E-01	-.2462E+01	.2098E+00
23.750	.8475E-01	-.2468E+01	.2101E+00
24.000	.8421E-01	-.2474E+01	.2103E+00
24.250	.8369E-01	-.2481E+01	.2105E+00
24.500	.8316E-01	-.2487E+01	.2108E+00
24.750	.8263E-01	-.2493E+01	.2110E+00
25.000	.8211E-01	-.2500E+01	.2112E+00
25.250	.8159E-01	-.2506E+01	.2114E+00
25.500	.8108E-01	-.2512E+01	.2117E+00
25.750	.8056E-01	-.2519E+01	.2119E+00
26.000	.8005E-01	-.2525E+01	.2121E+00
26.250	.7954E-01	-.2532E+01	.2123E+00
26.500	.7903E-01	-.2538E+01	.2125E+00
26.750	.7853E-01	-.2544E+01	.2127E+00
27.000	.7802E-01	-.2551E+01	.2129E+00
27.250	.7752E-01	-.2557E+01	.2131E+00
27.500	.7703E-01	-.2564E+01	.2134E+00
27.750	.7653E-01	-.2570E+01	.2136E+00
28.000	.7604E-01	-.2577E+01	.2138E+00
28.250	.7555E-01	-.2583E+01	.2140E+00
28.500	.7506E-01	-.2589E+01	.2142E+00
28.750	.7458E-01	-.2596E+01	.2143E+00
29.000	.7410E-01	-.2602E+01	.2145E+00
29.250	.7362E-01	-.2609E+01	.2147E+00
29.500	.7315E-01	-.2615E+01	.2149E+00
29.750	.7267E-01	-.2622E+01	.2151E+00
30.000	.7221E-01	-.2628E+01	.2153E+00
30.250	.7174E-01	-.2635E+01	.2155E+00
30.500	.7128E-01	-.2641E+01	.2157E+00
30.750	.7082E-01	-.2648E+01	.2159E+00
31.000	.7036E-01	-.2654E+01	.2161E+00
31.250	.6991E-01	-.2661E+01	.2162E+00
31.500	.6946E-01	-.2667E+01	.2164E+00
31.750	.6901E-01	-.2674E+01	.2166E+00
32.000	.6856E-01	-.2680E+01	.2168E+00
32.250	.6812E-01	-.2686E+01	.2170E+00
32.500	.6769E-01	-.2693E+01	.2171E+00
32.750	.6725E-01	-.2699E+01	.2173E+00
33.000	.6682E-01	-.2706E+01	.2175E+00
33.250	.6640E-01	-.2712E+01	.2177E+00
33.500	.6597E-01	-.2719E+01	.2179E+00
33.750	.6555E-01	-.2725E+01	.2180E+00
34.000	.6513E-01	-.2731E+01	.2182E+00
34.250	.6472E-01	-.2738E+01	.2184E+00
34.500	.6431E-01	-.2744E+01	.2186E+00
34.750	.6390E-01	-.2750E+01	.2187E+00
35.000	.6350E-01	-.2757E+01	.2189E+00
35.250	.6310E-01	-.2763E+01	.2191E+00
35.500	.6270E-01	-.2769E+01	.2193E+00
35.750	.6231E-01	-.2776E+01	.2194E+00
36.000	.6192E-01	-.2782E+01	.2196E+00

CALCIUM CHLORIDE

lower limit of molal : .100000E+01
act coeff at lowest molality: .496800E+00
upper limit of molal : .141000E+02
number of subintervals in each dm interval: .5000E+02

uncertainty in water activity (absolute) = .100000E-01
uncertainty in bal voltages (fractional) = .100000E-01

molality	mean molal solute activity coeff, (GAMMA)	ln(GAMMA)	uncertainty in ln(GAMMA)
1.250	.5573E+00	-.5846E+00	.1658E+00
1.500	.6408E+00	-.4450E+00	.1536E+00
1.750	.7476E+00	-.2909E+00	.1502E+00
2.000	.8798E+00	-.1281E+00	.1511E+00
2.250	.1041E+01	.3976E-01	.1542E+00
2.500	.1234E+01	.2104E+00	.1583E+00
2.750	.1466E+01	.3824E+00	.1629E+00
3.000	.1741E+01	.5545E+00	.1676E+00
3.250	.2067E+01	.7261E+00	.1724E+00
3.500	.2451E+01	.8965E+00	.1771E+00
3.750	.2902E+01	.1065E+01	.1818E+00
4.000	.3428E+01	.1232E+01	.1864E+00
4.250	.4042E+01	.1397E+01	.1910E+00
4.500	.4753E+01	.1559E+01	.1955E+00
4.750	.5573E+01	.1718E+01	.2000E+00
5.000	.6516E+01	.1874E+01	.2045E+00
5.250	.7594E+01	.2027E+01	.2089E+00
5.500	.8819E+01	.2177E+01	.2134E+00
5.750	.1020E+02	.2323E+01	.2178E+00
6.000	.1176E+02	.2465E+01	.2223E+00
6.250	.1350E+02	.2603E+01	.2267E+00
6.500	.1542E+02	.2736E+01	.2311E+00
6.750	.1754E+02	.2864E+01	.2356E+00
7.000	.1985E+02	.2988E+01	.2400E+00
7.250	.2234E+02	.3106E+01	.2444E+00
7.500	.2500E+02	.3219E+01	.2488E+00
7.750	.2782E+02	.3326E+01	.2532E+00
8.000	.3078E+02	.3427E+01	.2575E+00
8.250	.3383E+02	.3521E+01	.2617E+00
8.500	.3694E+02	.3609E+01	.2659E+00
8.750	.4009E+02	.3691E+01	.2700E+00
9.000	.4321E+02	.3766E+01	.2739E+00

9.250	.4626E+02	.3834E+01	.2777E+00
9.500	.4921E+02	.3896E+01	.2814E+00
9.750	.5201E+02	.3951E+01	.2849E+00
10.000	.5462E+02	.4000E+01	.2882E+00
10.250	.5702E+02	.4043E+01	.2914E+00
10.500	.5919E+02	.4081E+01	.2944E+00
10.750	.6112E+02	.4113E+01	.2972E+00
11.000	.6280E+02	.4140E+01	.2998E+00
11.250	.6423E+02	.4162E+01	.3022E+00
11.500	.6541E+02	.4181E+01	.3045E+00
11.750	.6637E+02	.4195E+01	.3066E+00
12.000	.6710E+02	.4206E+01	.3086E+00
12.250	.6763E+02	.4214E+01	.3104E+00
12.500	.6797E+02	.4219E+01	.3121E+00
12.750	.6811E+02	.4221E+01	.3136E+00
13.000	.6807E+02	.4221E+01	.3151E+00
13.250	.6784E+02	.4217E+01	.3163E+00
13.500	.6741E+02	.4211E+01	.3175E+00
13.750	.6678E+02	.4201E+01	.3185E+00
14.000	.6592E+02	.4188E+01	.3193E+00

MANGANESE CHLORIDE

lower limit of molal : .100000E+01
act coeff at lowest molality: .475400E+00
upper limit of molal : .120000E+02
number of subintervals in each dm interval: .5000E+02

uncertainty in water activity (absolute) = .100000E-01
uncertainty in bal voltages (fractional) = .100000E-01

molality	mean molal solute activity coeff, (GAMMA)	ln(GAMMA)	uncertainty in ln(GAMMA)
1.250	.5138E+00	-.6660E+00	.1671E+00
1.500	.5581E+00	-.5832E+00	.1542E+00
1.750	.6073E+00	-.4988E+00	.1500E+00
2.000	.6606E+00	-.4147E+00	.1502E+00
2.250	.7175E+00	-.3320E+00	.1525E+00
2.500	.7777E+00	-.2514E+00	.1556E+00
2.750	.8409E+00	-.1733E+00	.1592E+00
3.000	.9068E+00	-.9789E-01	.1628E+00
3.250	.9751E+00	-.2520E-01	.1664E+00
3.500	.1046E+01	.4471E-01	.1698E+00
3.750	.1118E+01	.1119E+00	.1732E+00
4.000	.1193E+01	.1765E+00	.1763E+00
4.250	.1269E+01	.2385E+00	.1793E+00
4.500	.1347E+01	.2981E+00	.1822E+00
4.750	.1427E+01	.3555E+00	.1850E+00
5.000	.1508E+01	.4107E+00	.1876E+00
5.250	.1590E+01	.4639E+00	.1901E+00
5.500	.1674E+01	.5153E+00	.1926E+00
5.750	.1759E+01	.5649E+00	.1949E+00
6.000	.1846E+01	.6130E+00	.1972E+00
6.250	.1934E+01	.6597E+00	.1993E+00
6.500	.2024E+01	.7050E+00	.2015E+00
6.750	.2115E+01	.7491E+00	.2035E+00
7.000	.2208E+01	.7921E+00	.2055E+00
7.250	.2303E+01	.8340E+00	.2075E+00
7.500	.2399E+01	.8750E+00	.2094E+00
7.750	.2497E+01	.9149E+00	.2113E+00
8.000	.2596E+01	.9539E+00	.2132E+00
8.250	.2696E+01	.9919E+00	.2150E+00
8.500	.2798E+01	.1029E+01	.2168E+00
8.750	.2900E+01	.1065E+01	.2186E+00
9.000	.3003E+01	.1100E+01	.2203E+00

9.250	.3105E+01	.1133E+01	.2220E+00
9.500	.3205E+01	.1165E+01	.2237E+00
9.750	.3303E+01	.1195E+01	.2253E+00
10.000	.3398E+01	.1223E+01	.2269E+00
10.250	.3487E+01	.1249E+01	.2285E+00
10.500	.3569E+01	.1272E+01	.2300E+00
10.750	.3642E+01	.1293E+01	.2314E+00
11.000	.3705E+01	.1310E+01	.2328E+00
11.250	.3754E+01	.1323E+01	.2340E+00
11.500	.3788E+01	.1332E+01	.2352E+00
11.750	.3804E+01	.1336E+01	.2362E+00
12.000	.3801E+01	.1335E+01	.2371E+00

MANGANESE SULFATE

lower limit of molal : .100000E+01
act coeff at lowest molality: .449000E-01
upper limit of molal : .170000E+02
number of subintervals in each dm interval: .5000E+02

uncertainty in water activity (absolute) = .100000E-01
uncertainty in bal voltages (fractional) = .100000E-01

molality	mean molal solute activity coeff, (GAMMA)	ln(GAMMA)	uncertainty in ln(GAMMA)
1.250	.3996E-01	-.3220E+01	.2345E+00
1.500	.3791E-01	-.3272E+01	.2135E+00
1.750	.3746E-01	-.3285E+01	.2058E+00
2.000	.3802E-01	-.3270E+01	.2048E+00
2.250	.3929E-01	-.3237E+01	.2068E+00
2.500	.4112E-01	-.3191E+01	.2104E+00
2.750	.4341E-01	-.3137E+01	.2145E+00
3.000	.4609E-01	-.3077E+01	.2188E+00
3.250	.4911E-01	-.3014E+01	.2231E+00
3.500	.5243E-01	-.2948E+01	.2272E+00
3.750	.5603E-01	-.2882E+01	.2312E+00
4.000	.5986E-01	-.2816E+01	.2350E+00
4.250	.6391E-01	-.2750E+01	.2386E+00
4.500	.6814E-01	-.2686E+01	.2420E+00
4.750	.7251E-01	-.2624E+01	.2452E+00
5.000	.7699E-01	-.2564E+01	.2482E+00
5.250	.8154E-01	-.2507E+01	.2512E+00
5.500	.8612E-01	-.2452E+01	.2539E+00
5.750	.9070E-01	-.2400E+01	.2565E+00
6.000	.9522E-01	-.2352E+01	.2590E+00
6.250	.9966E-01	-.2306E+01	.2614E+00
6.500	.1040E+00	-.2264E+01	.2637E+00
6.750	.1081E+00	-.2224E+01	.2659E+00
7.000	.1121E+00	-.2189E+01	.2679E+00
7.250	.1158E+00	-.2156E+01	.2699E+00
7.500	.1193E+00	-.2126E+01	.2718E+00
7.750	.1225E+00	-.2099E+01	.2736E+00
8.000	.1255E+00	-.2076E+01	.2753E+00
8.250	.1281E+00	-.2055E+01	.2769E+00
8.500	.1305E+00	-.2037E+01	.2784E+00
8.750	.1325E+00	-.2021E+01	.2799E+00
9.000	.1343E+00	-.2008E+01	.2813E+00

9.250	.1358E+00	-.1997E+01	.2827E+00
9.500	.1371E+00	-.1987E+01	.2840E+00
9.750	.1381E+00	-.1980E+01	.2852E+00
10.000	.1389E+00	-.1974E+01	.2864E+00
10.250	.1395E+00	-.1970E+01	.2875E+00
10.500	.1399E+00	-.1967E+01	.2885E+00
10.750	.1402E+00	-.1965E+01	.2896E+00
11.000	.1404E+00	-.1964E+01	.2906E+00
11.250	.1404E+00	-.1963E+01	.2915E+00
11.500	.1405E+00	-.1963E+01	.2925E+00
11.750	.1405E+00	-.1963E+01	.2934E+00
12.000	.1404E+00	-.1963E+01	.2942E+00
12.250	.1404E+00	-.1963E+01	.2951E+00
12.500	.1404E+00	-.1963E+01	.2959E+00
12.750	.1405E+00	-.1963E+01	.2968E+00
13.000	.1406E+00	-.1962E+01	.2976E+00
13.250	.1408E+00	-.1960E+01	.2984E+00
13.500	.1411E+00	-.1958E+01	.2992E+00
13.750	.1415E+00	-.1955E+01	.3000E+00
14.000	.1420E+00	-.1952E+01	.3008E+00
14.250	.1427E+00	-.1947E+01	.3015E+00
14.500	.1434E+00	-.1942E+01	.3023E+00
14.750	.1443E+00	-.1936E+01	.3031E+00
15.000	.1454E+00	-.1928E+01	.3039E+00
15.250	.1466E+00	-.1920E+01	.3047E+00
15.500	.1479E+00	-.1911E+01	.3055E+00
15.750	.1493E+00	-.1901E+01	.3064E+00
16.000	.1509E+00	-.1891E+01	.3072E+00
16.250	.1526E+00	-.1880E+01	.3080E+00
16.500	.1543E+00	-.1869E+01	.3089E+00
16.750	.1561E+00	-.1857E+01	.3097E+00
17.000	.1579E+00	-.1846E+01	.3105E+00

FERRIC CHLORIDE

lower limit of molal : .100000E+01
act coeff at lowest molality: .270000E+00
upper limit of molal : .150000E+02
number of subintervals in each dm interval: .5000E+02

uncertainty in water activity (absolute) = .100000E-01
uncertainty in bal voltages (fractional) = .100000E-01

molality	mean molal solute activity coeff, (GAMMA)	ln(GAMMA)	uncertainty in ln(GAMMA)
1.250	.3357E+00	-.1091E+01	.1292E+00
1.500	.3995E+00	-.9175E+00	.1212E+00
1.750	.4623E+00	-.7716E+00	.1194E+00
2.000	.5248E+00	-.6448E+00	.1205E+00
2.250	.5879E+00	-.5311E+00	.1231E+00
2.500	.6525E+00	-.4269E+00	.1263E+00
2.750	.7193E+00	-.3294E+00	.1298E+00
3.000	.7890E+00	-.2370E+00	.1333E+00
3.250	.8622E+00	-.1482E+00	.1368E+00
3.500	.9395E+00	-.6238E-01	.1402E+00
3.750	.1021E+01	.2125E-01	.1436E+00
4.000	.1109E+01	.1030E+00	.1469E+00
4.250	.1201E+01	.1833E+00	.1501E+00
4.500	.1300E+01	.2621E+00	.1533E+00
4.750	.1404E+01	.3395E+00	.1564E+00
5.000	.1515E+01	.4155E+00	.1594E+00
5.250	.1632E+01	.4900E+00	.1625E+00
5.500	.1756E+01	.5630E+00	.1654E+00
5.750	.1885E+01	.6341E+00	.1684E+00
6.000	.2020E+01	.7033E+00	.1713E+00
6.250	.2160E+01	.7703E+00	.1742E+00
6.500	.2305E+01	.8349E+00	.1771E+00
6.750	.2452E+01	.8968E+00	.1799E+00
7.000	.2601E+01	.9559E+00	.1827E+00
7.250	.2751E+01	.1012E+01	.1855E+00
7.500	.2899E+01	.1065E+01	.1882E+00
7.750	.3046E+01	.1114E+01	.1908E+00
8.000	.3188E+01	.1159E+01	.1934E+00
8.250	.3324E+01	.1201E+01	.1958E+00
8.500	.3454E+01	.1239E+01	.1982E+00
8.750	.3575E+01	.1274E+01	.2006E+00
9.000	.3688E+01	.1305E+01	.2028E+00

9.250	.3792E+01	.1333E+01	.2049E+00
9.500	.3887E+01	.1358E+01	.2070E+00
9.750	.3974E+01	.1380E+01	.2090E+00
10.000	.4053E+01	.1399E+01	.2109E+00
10.250	.4126E+01	.1417E+01	.2127E+00
10.500	.4194E+01	.1434E+01	.2145E+00
10.750	.4261E+01	.1449E+01	.2163E+00
11.000	.4327E+01	.1465E+01	.2181E+00
11.250	.4395E+01	.1480E+01	.2199E+00
11.500	.4468E+01	.1497E+01	.2217E+00
11.750	.4548E+01	.1515E+01	.2236E+00
12.000	.4638E+01	.1534E+01	.2257E+00
12.250	.4741E+01	.1556E+01	.2278E+00
12.500	.4858E+01	.1581E+01	.2301E+00
12.750	.4992E+01	.1608E+01	.2325E+00
13.000	.5145E+01	.1638E+01	.2352E+00
13.250	.5317E+01	.1671E+01	.2381E+00
13.500	.5509E+01	.1706E+01	.2411E+00
13.750	.5718E+01	.1744E+01	.2444E+00
14.000	.5938E+01	.1781E+01	.2479E+00
14.250	.6159E+01	.1818E+01	.2514E+00
14.500	.6364E+01	.1851E+01	.2549E+00
14.750	.6529E+01	.1876E+01	.2579E+00
15.000	.6619E+01	.1890E+01	.2603E+00

Appendix F: Plots of calculations of mean molal solute activity coefficient as a function of molality for single-electrolyte solutions

For each of the single-salt solutions studied, this appendix contains a plot of the mean molal solute activity coefficient as a function of molality. The calculations were performed using the Gibbs-Duhem equation, with the polynomial fits to the $a_w(m)$ data, as described in Chapter 1. Also included on each plot is activity coefficient data from the literature. The sources of the literature activity coefficient data are the same as those used in constructing the $a_w(m)$ polynomial fits — the abbreviations used in the figure captions to describe the literature sources have the same meaning as given in Appendix B.

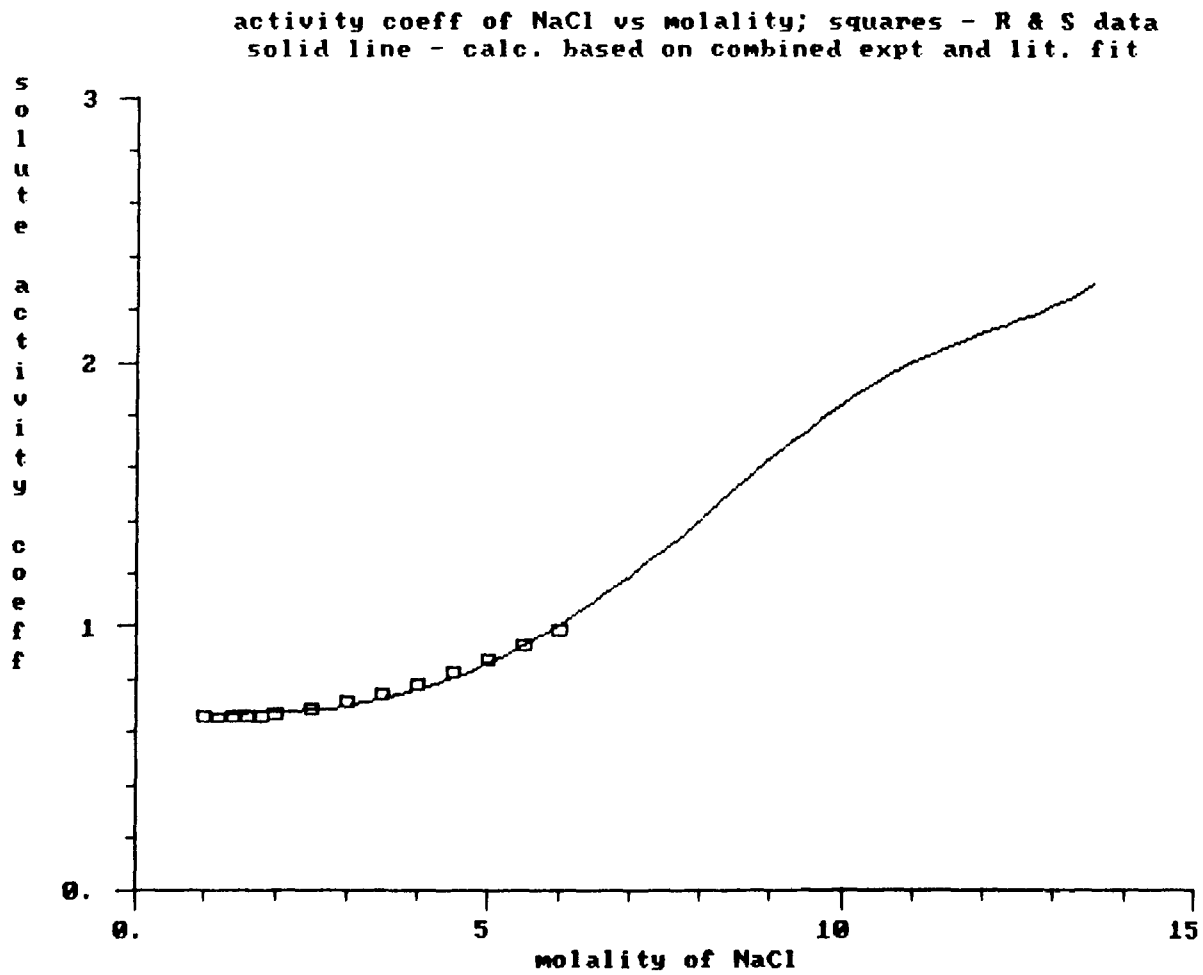
activity coeff of NaCl vs molality; squares - R & S data
solid line - calc. based on combined expt and lit. fit
solute activity coeff
3
2
1
0.
0.
5
10
15
molality of NaCl

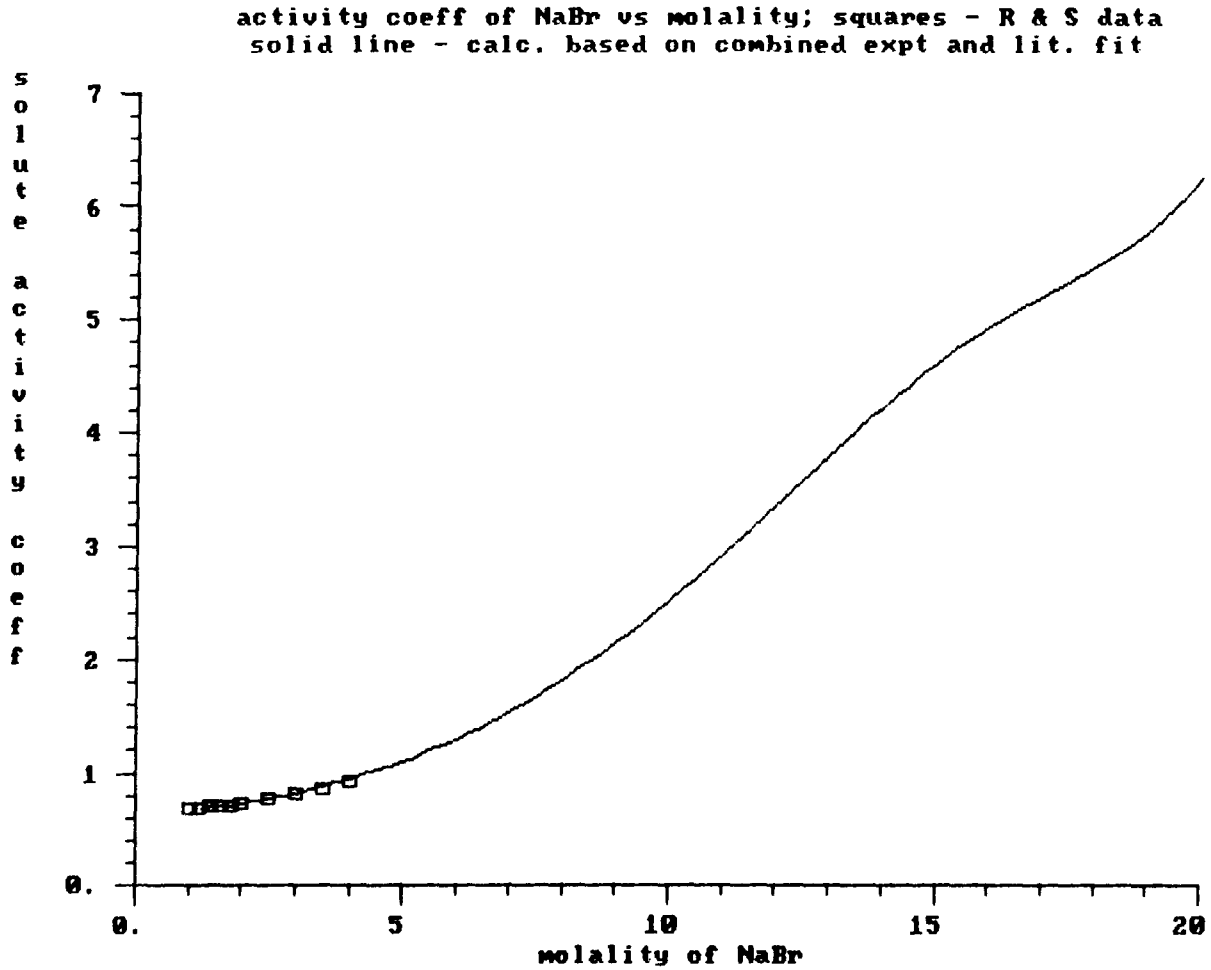
activity coeff of NaBr vs molality; squares - R & S data
solid line - calc. based on combined expt and lit. fit
solute activity coeff
7
6
5
4
3
2
1
0.
0.
5
10
15
20
molality of NaBr

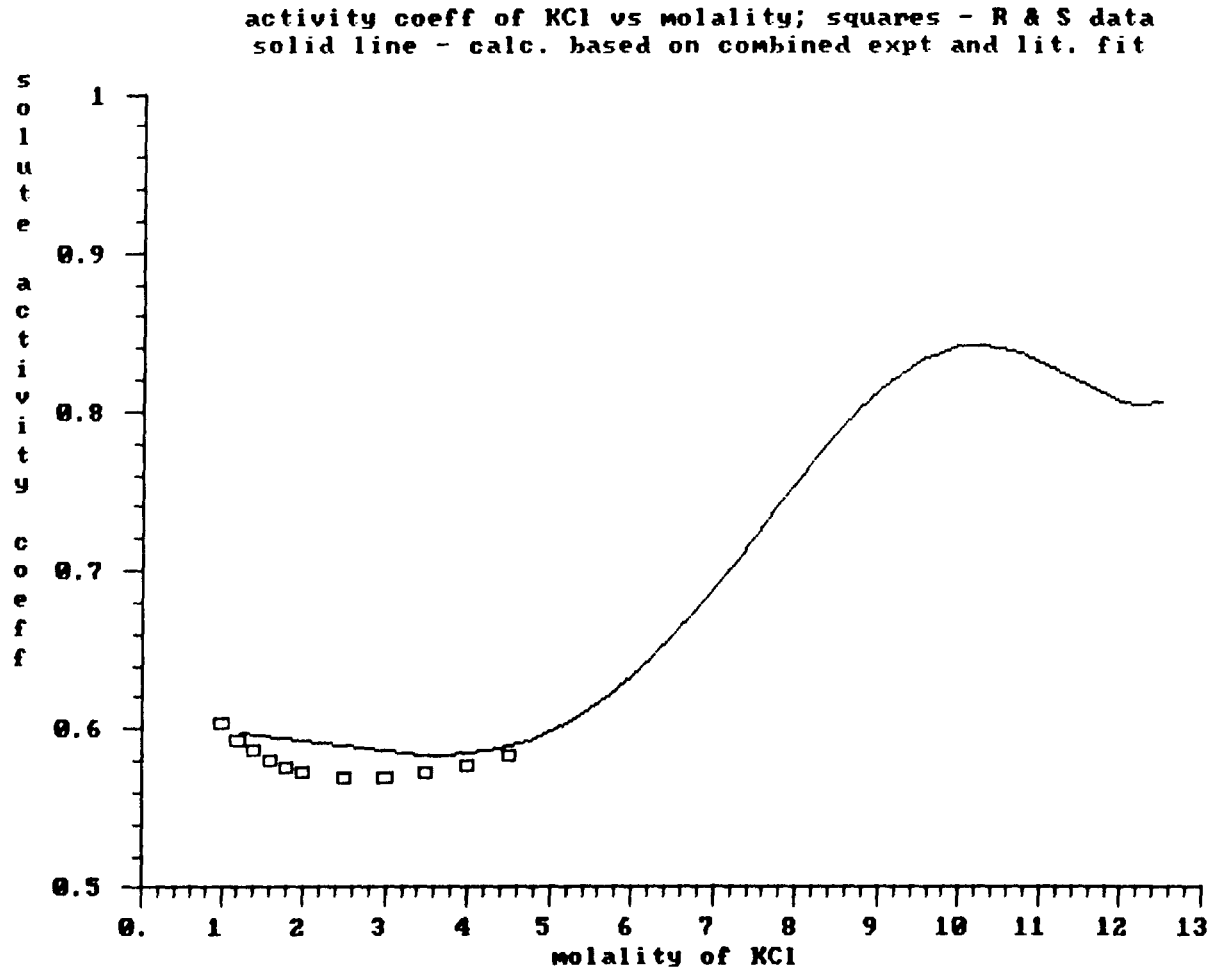
activity coeff of KCl vs molality; squares - R & S data
solid line - calc. based on combined expt and lit. fit
solute activity coeff
1
0.9
0.8
0.7
0.6
0.5
0.
1
2
3
4
5
6
7
8
9
10
11
12
13
molality of KCl

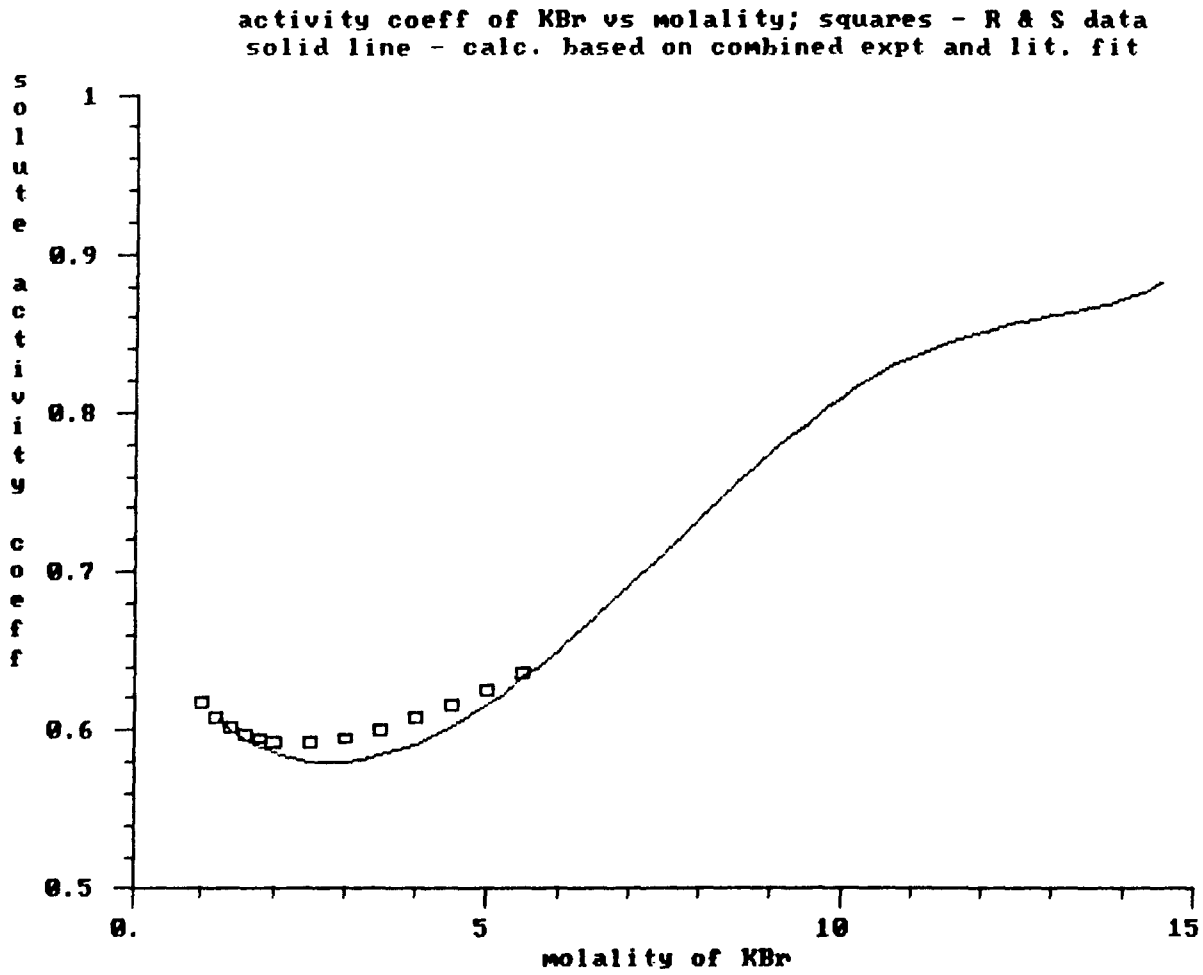
activity coeff of KBr vs molality; squares - R & S data
solid line - calc. based on combined expt and lit. fit
solute activity coeff
1
0.9
0.8
0.7
0.6
0.5
0.
5
10
15
molality of KBr

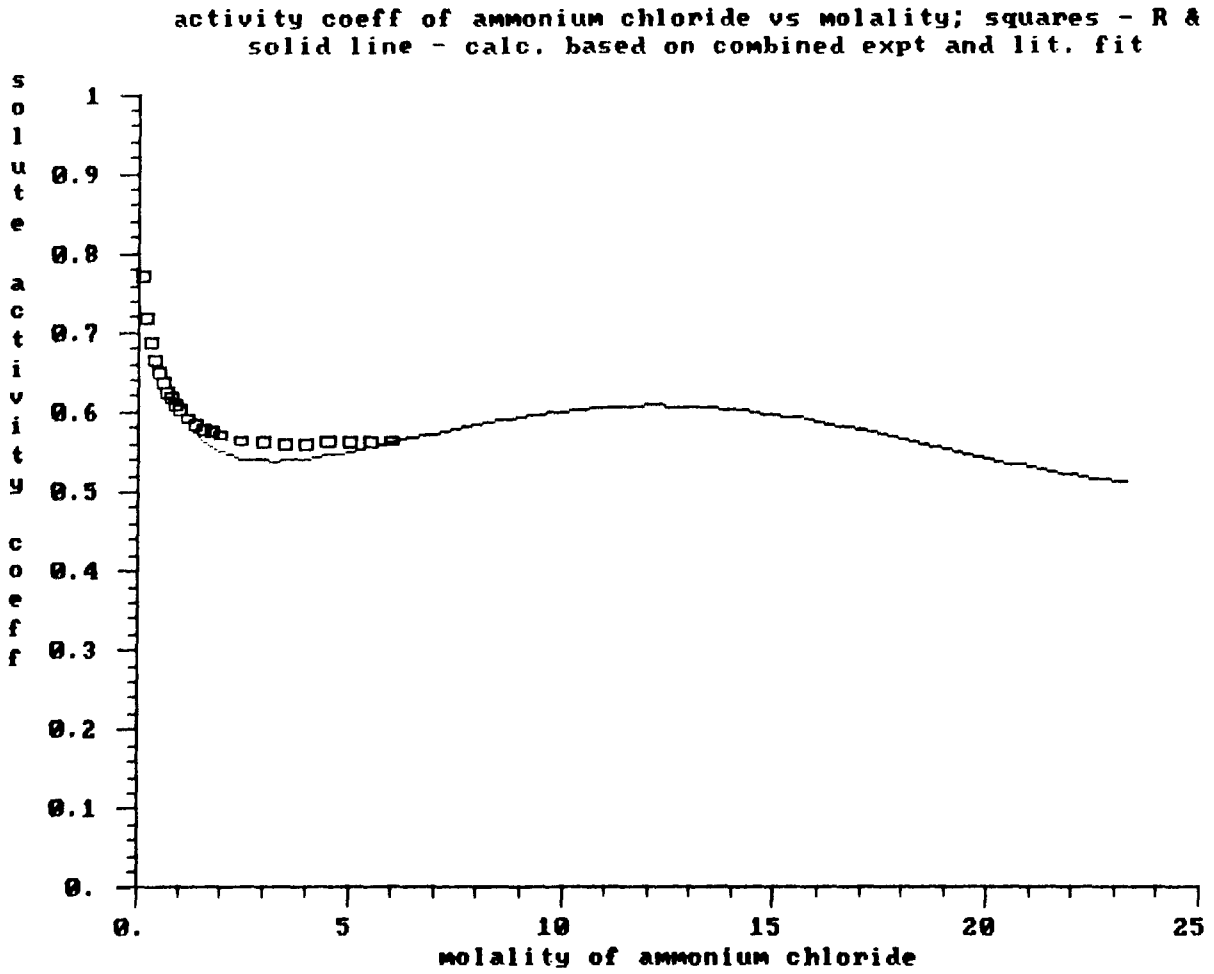
activity coeff of ammonium chloride vs molality; squares - R & S
solid line - calc. based on combined expt and lit. fit
solute activity coeff
1
0.9
0.8
0.7
0.6
0.5
0.4
0.3
0.2
0.1
0.
0.
5
10
15
20
25
molality of ammonium chloride

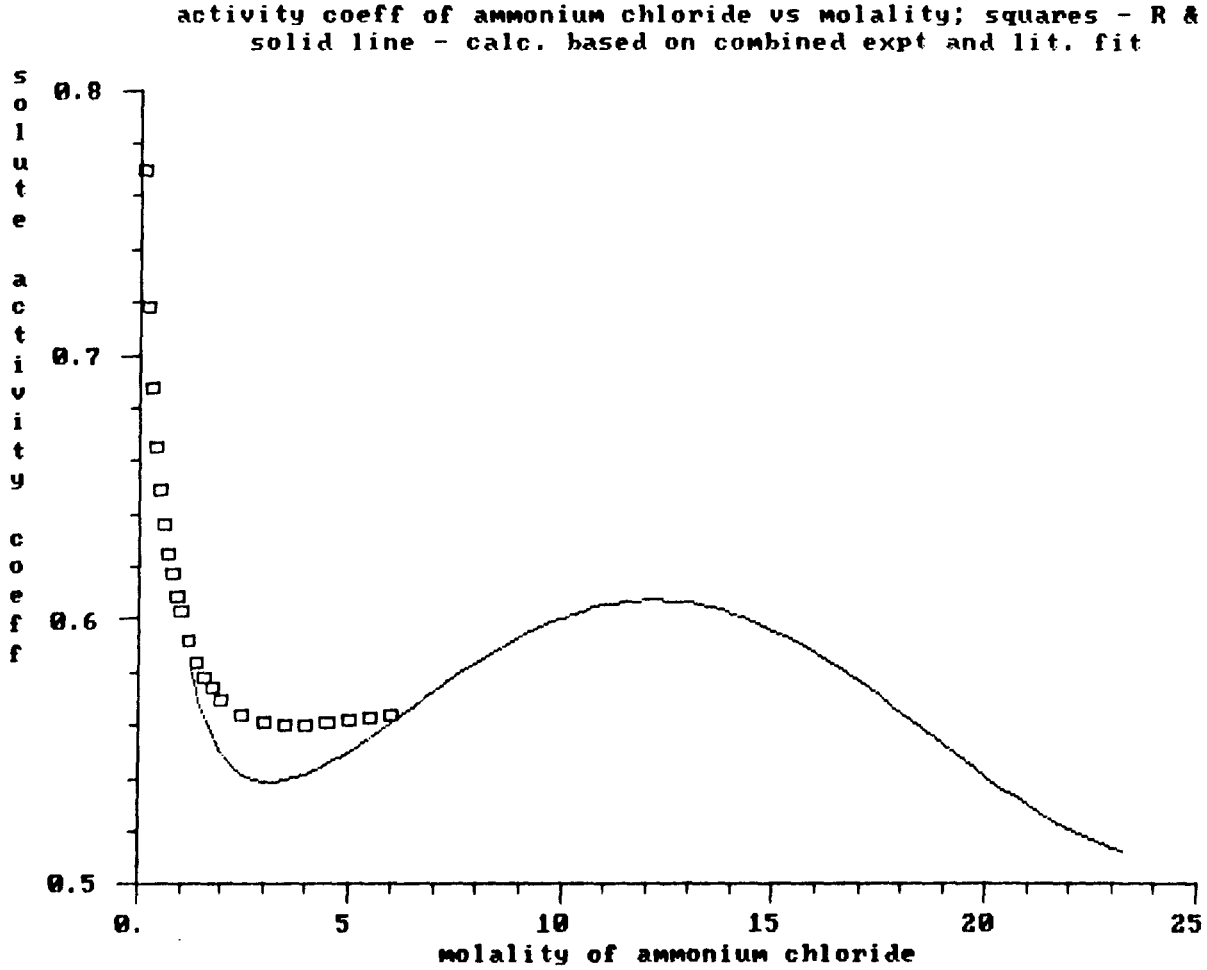
activity coeff of ammonium chloride vs molality; squares - R & S
solid line - calc. based on combined expt and lit. fit
solute activity coeff
0.8
0.7
0.6
0.5
0.
5
10
15
20
25
molality of ammonium chloride

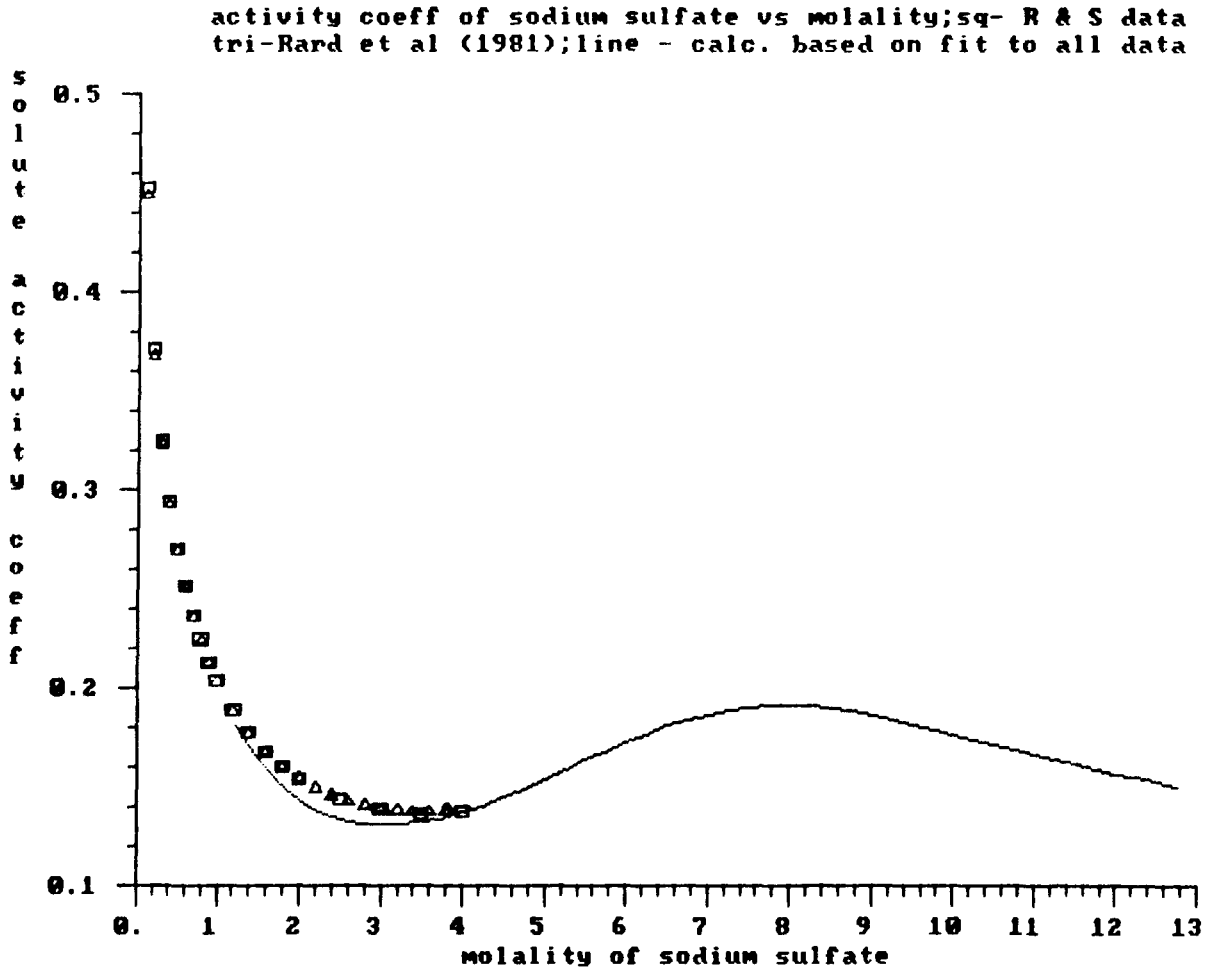
activity coeff of sodium sulfate vs molality;sq- R & S data
tri-Rard et al (1981);line - calc. based on fit to all data
solute activity coeff
0.5
0.4
0.3
0.2
0.1
0.
1
2
3
4
5
6
7
8
9
10
11
12
13
molality of sodium sulfate

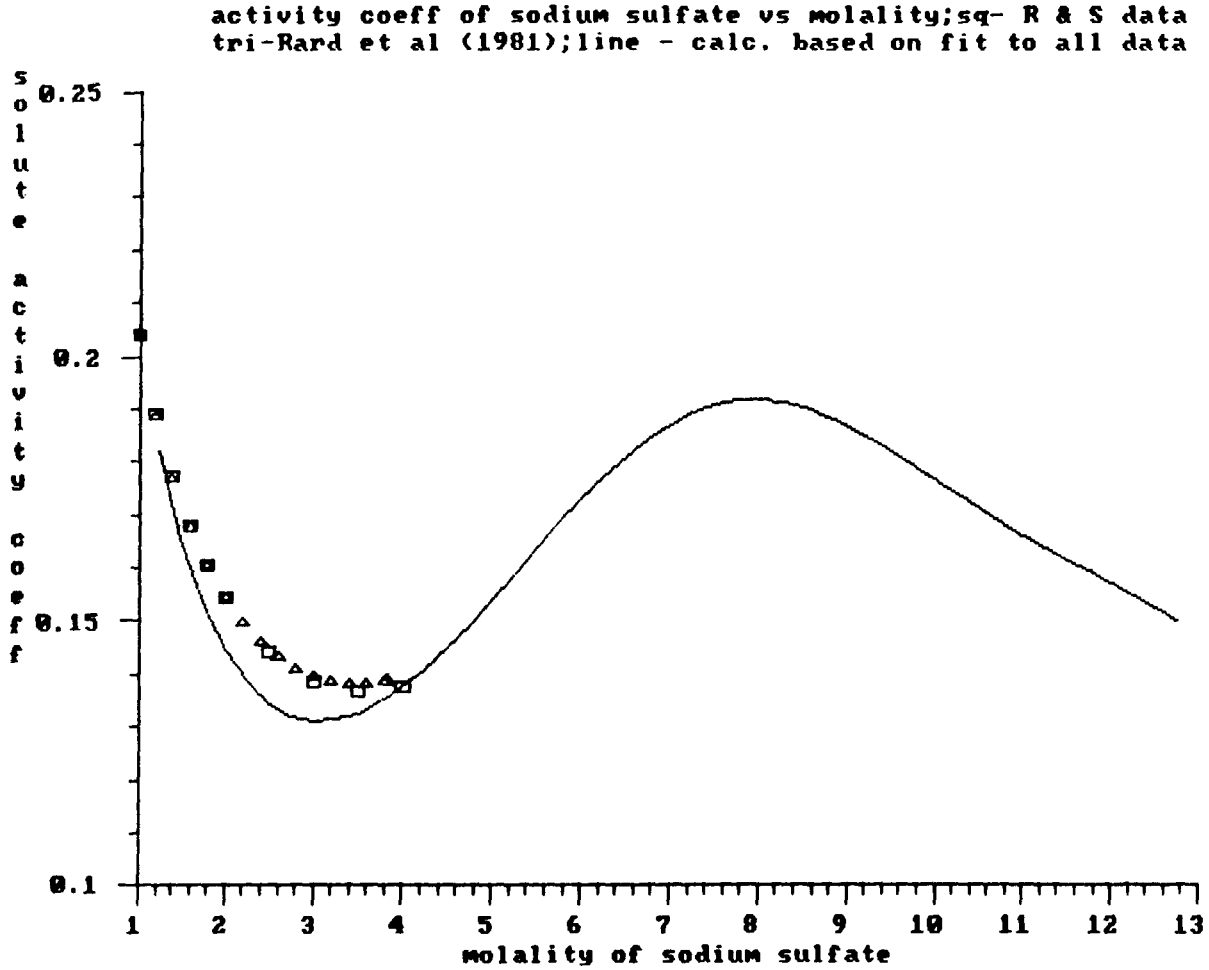
activity coeff of sodium sulfate vs molality;sq- R & S data
tri-Rard et al (1981);line - calc. based on fit to all data
solute activity coeff
0.25
0.2
0.15
0.1
1
2
3
4
5
6
7
8
9
10
11
12
13
molality of sodium sulfate

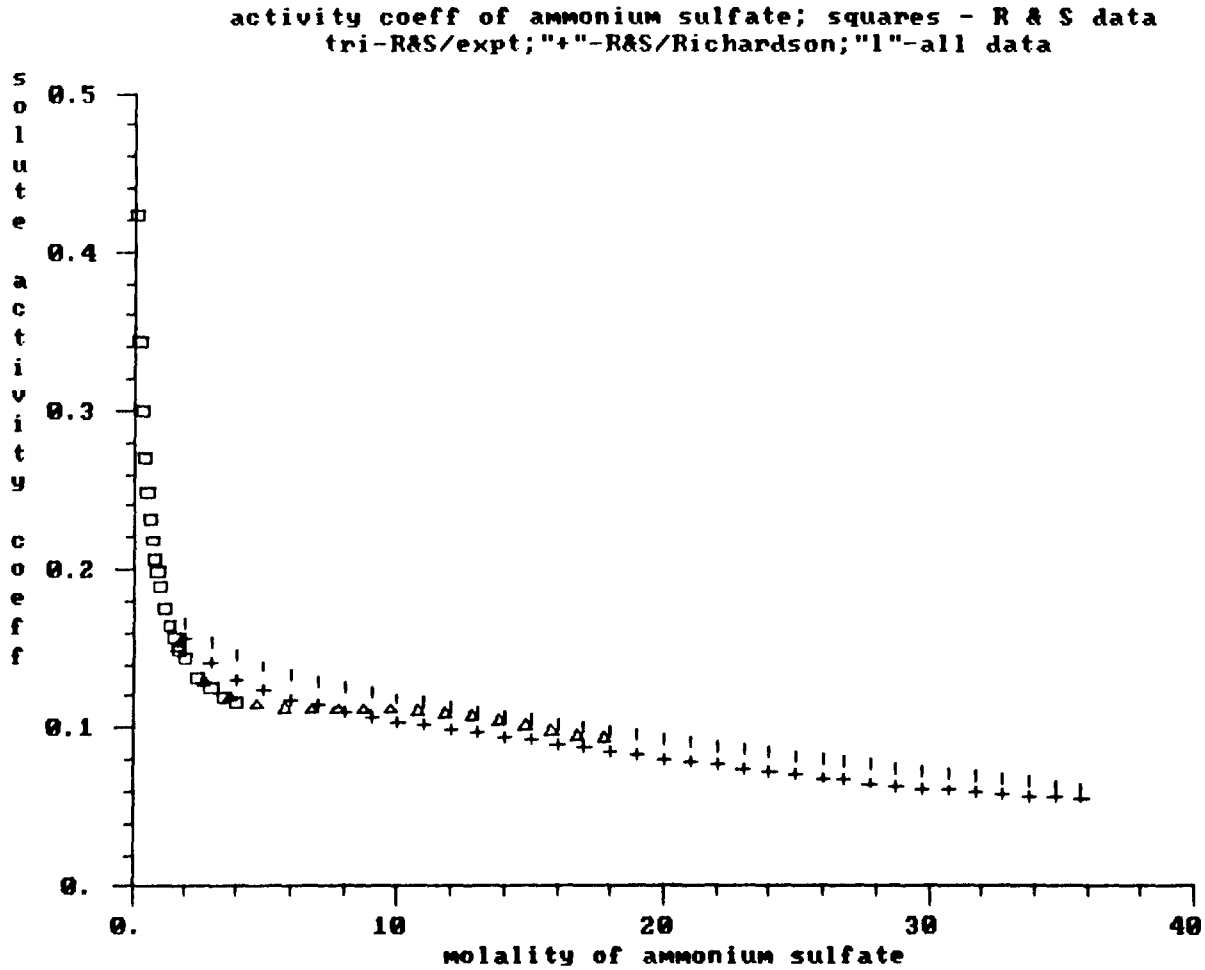
activity coeff of ammonium sulfate; squares - R & S data
tri-R&S/expt;"+"-R&S/Richardson;"l"-all data
solute activity coeff
0.5
0.4
0.3
0.2
0.1
0.
0.
10
20
30
40
molality of ammonium sulfate

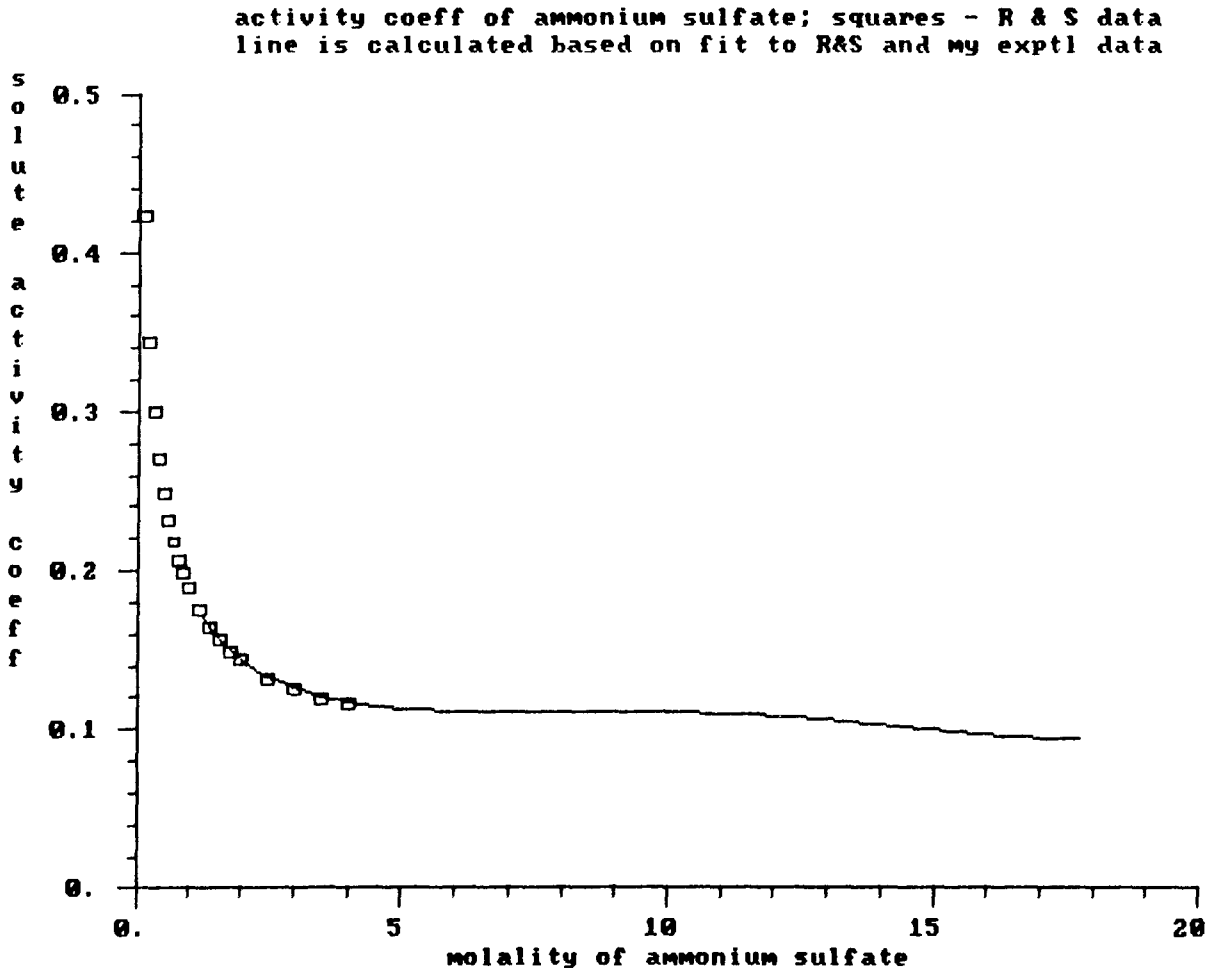
activity coeff of ammonium sulfate; squares - R & S data
line is calculated based on fit to R&S and my exptl data
solute activity coeff
0.5
0.4
0.3
0.2
0.1
0.
0.
5
10
15
20
molality of ammonium sulfate

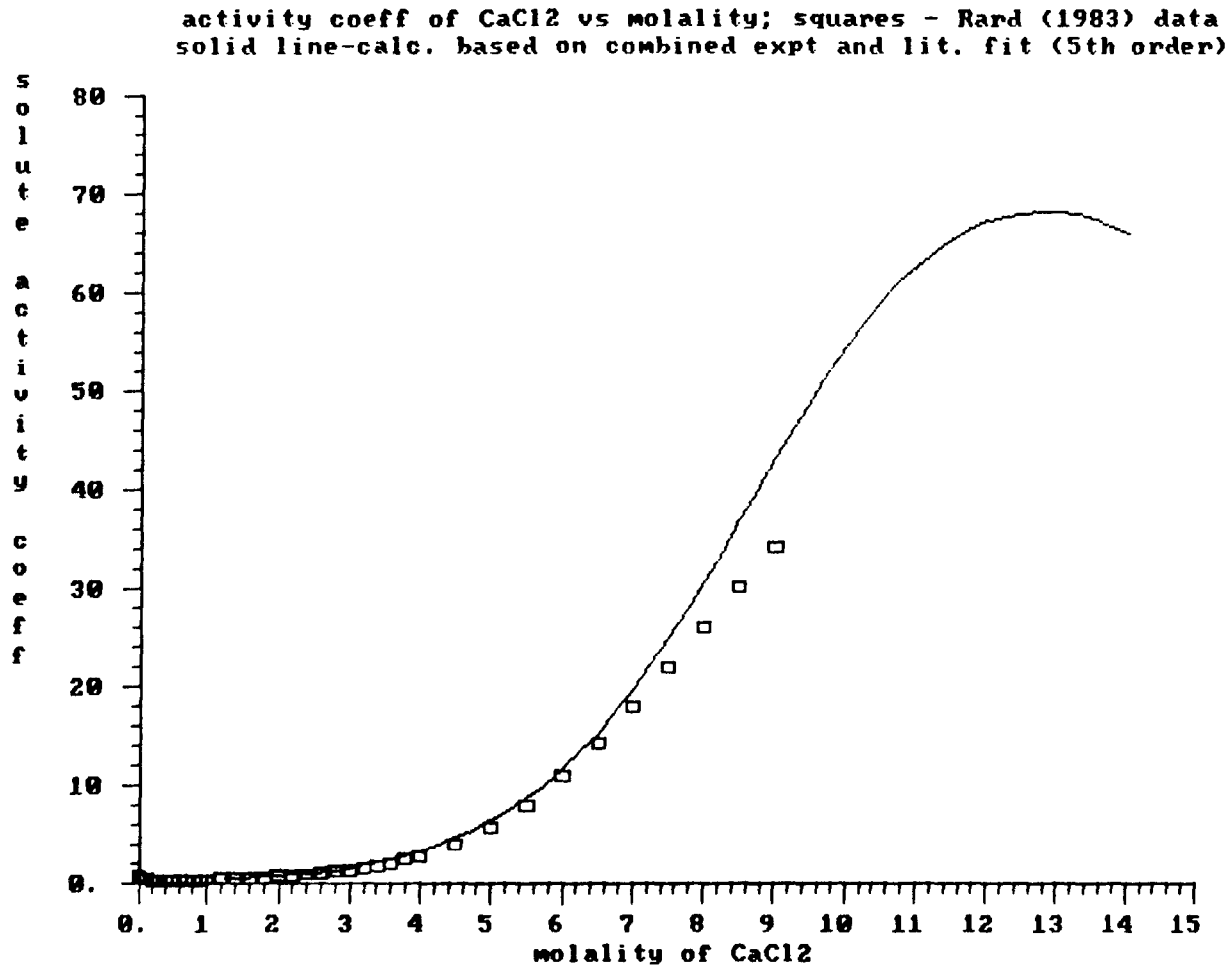
activity coeff of CaCl2 vs molality; squares - Rard (1983) data
solid line-calc. based on combined expt and lit. fit (5th order)
solute activity coeff
80
70
60
50
40
30
20
10
0.
0. 1 2 3 4 5 6 7 8 9 10 11 12 13 14 15
molality of CaCl2

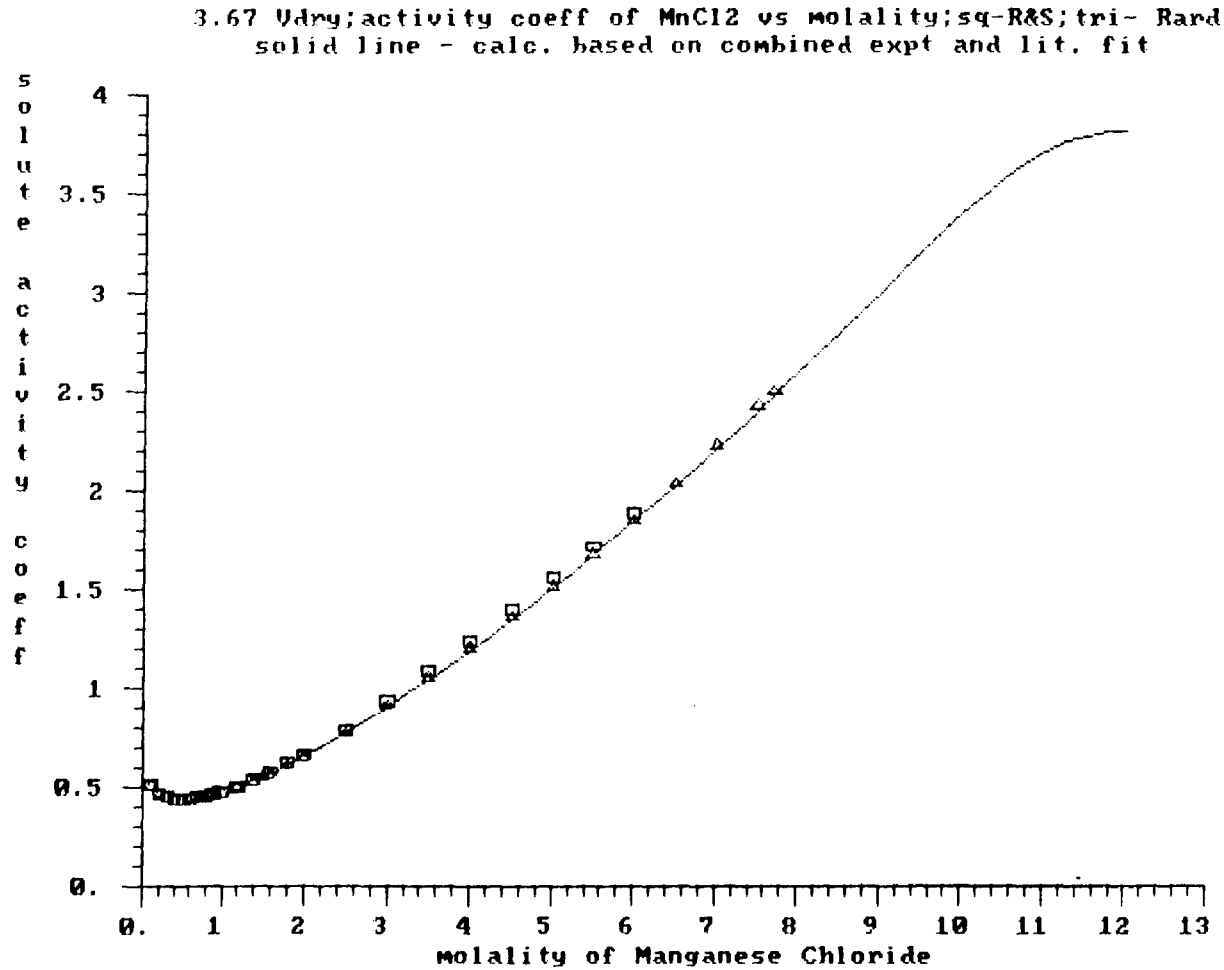
3.67 Vdry;activity coeff of MnCl2 vs molality;sq-R&S;tri- Rard
solid line - calc. based on combined expt and lit. fit
solute activity coeff
4
3.5
3
2.5
2
1.5
1
0.5
0.
0.
1
2
3
4
5
6
7
8
9
10
11
12
13
molality of Manganese Chloride

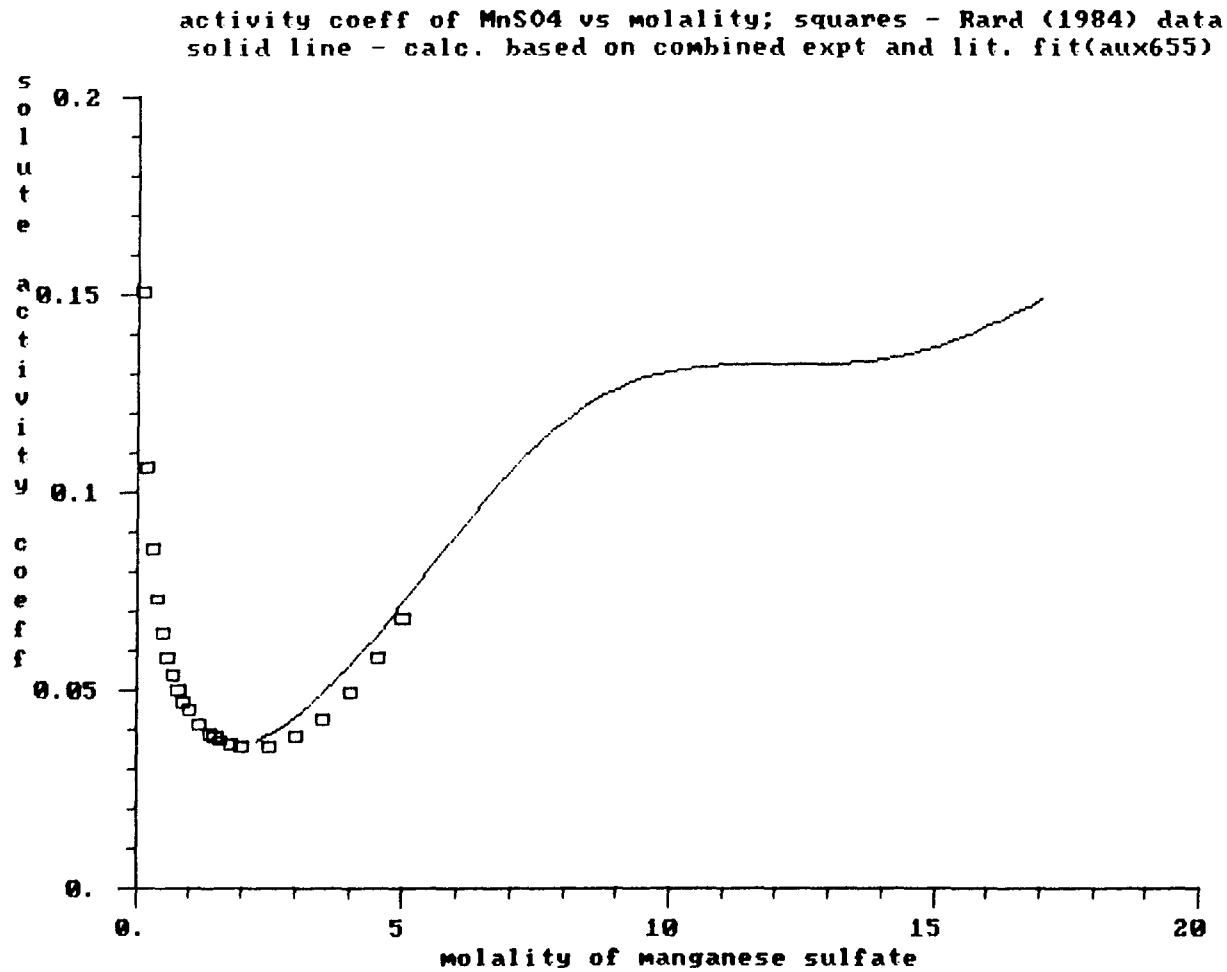
activity coeff of MnSO4 vs molality; squares - Rard (1984) data
solid line - calc. based on combined expt and lit. fit(aux655)
solute activity coeff
0.2
0.15
0.1
0.05
0.
0.
5
10
15
20
molality of manganese sulfate

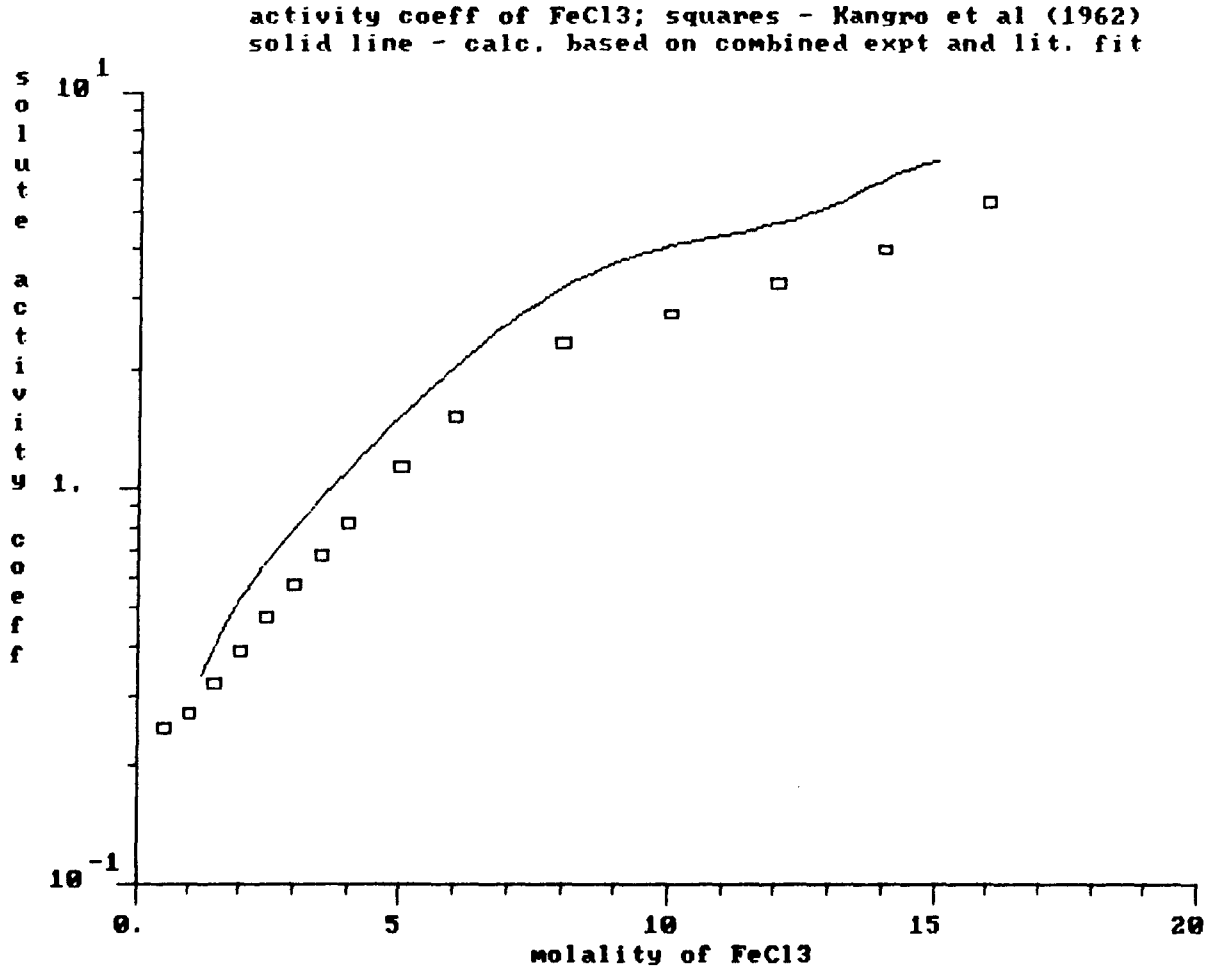
activity coeff of FeCl3; squares - Kangro et al (1962)
solid line - calc. based on combined expt and lit. fit
solute activity coeff
10^1
1.
10^-1
0.
5
10
15
20
molality of FeCl3

Appendix G: Plots of the solute activity coefficient as a function of molality in which experimental data is compared to the predictions of the local composition model of Chen et al.

This appendix contains plots corresponding to Figure 21 of Chapter 1. For further explanation and discussion of the local composition model of Chen et al., please refer to Chapter 1.

Each plot contains the following data for a particular salt:

- $\gamma_{\pm}(m)$ calculated from $a_w(m)$ polynomials (the same data as given in Appendices E and F); this data is plotted as circles
- the range of uncertainty in the calculated $\gamma_{\pm}$ (the same data as given in table form in Appendix E); this data is plotted as a short-dashed line
- $\gamma_{\pm}(m)$ calculated from the local composition model of Chen et al. using "given" parameters, *i.e.*, parameters estimated by Chen et al. from low concentration data; the parameters are given in the original paper and in Table 6 of Chapter 1; this data is plotted as a long-dashed line
- $\gamma_{\pm}(m)$ calculated from the local composition model of Chen et al. using parameters estimated in the present work from the full range of the experimental data; the parameters are given in Table 7 of Chapter 1; this data is plotted as a solid line
- $\gamma_{\pm}(m)$ data taken from the same literature sources as used in the plots of

Appendix F; this data is plotted as squares.

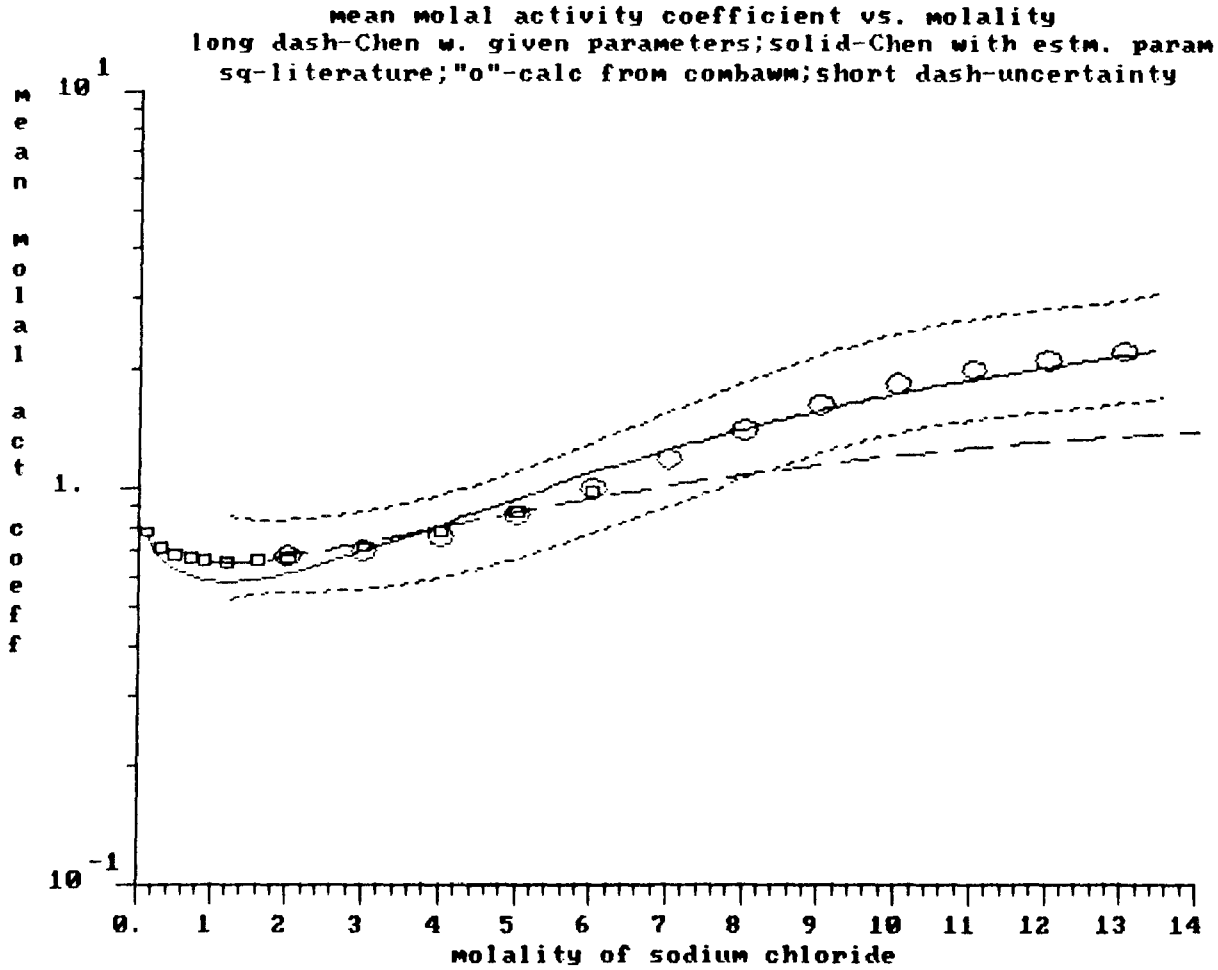
mean molal activity coefficient vs. molality
long dash-Chen w. given parameters;solid-Chen with estm. param
sq-literature;"o"-calc from combawm;short dash-uncertainty
mean molal act coeff
10 1
1.
10 -1
0. 1 2 3 4 5 6 7 8 9 10 11 12 13 14
molality of sodium chloride

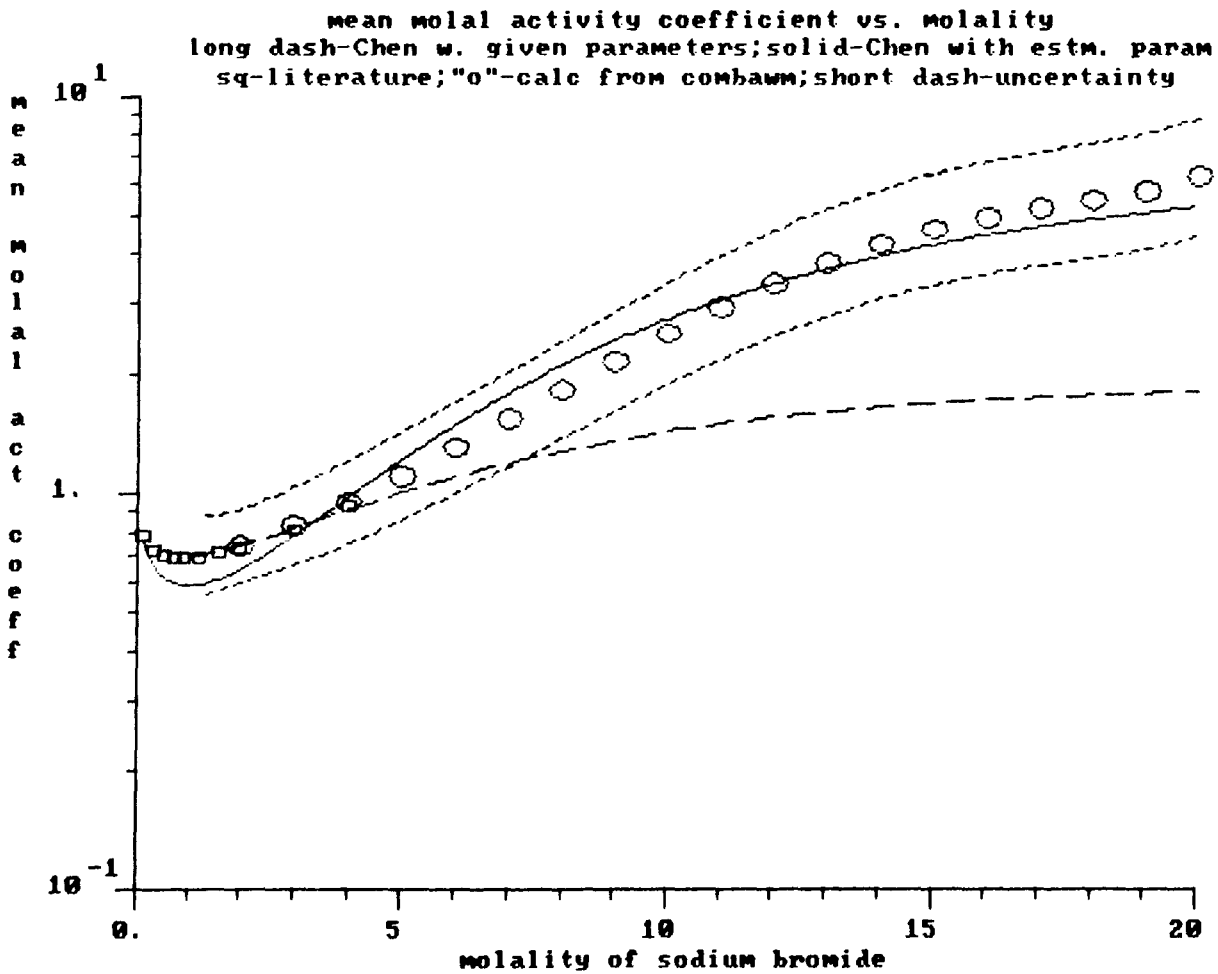
mean molal activity coefficient vs. molality
long dash-Chen w. given parameters;solid-Chen with estm. param
sq-literature;"o"-calc from combawm;short dash-uncertainty
mean molal act coeff
10 1
1.
10 -1
0.
5
10
15
20
molality of sodium bromide

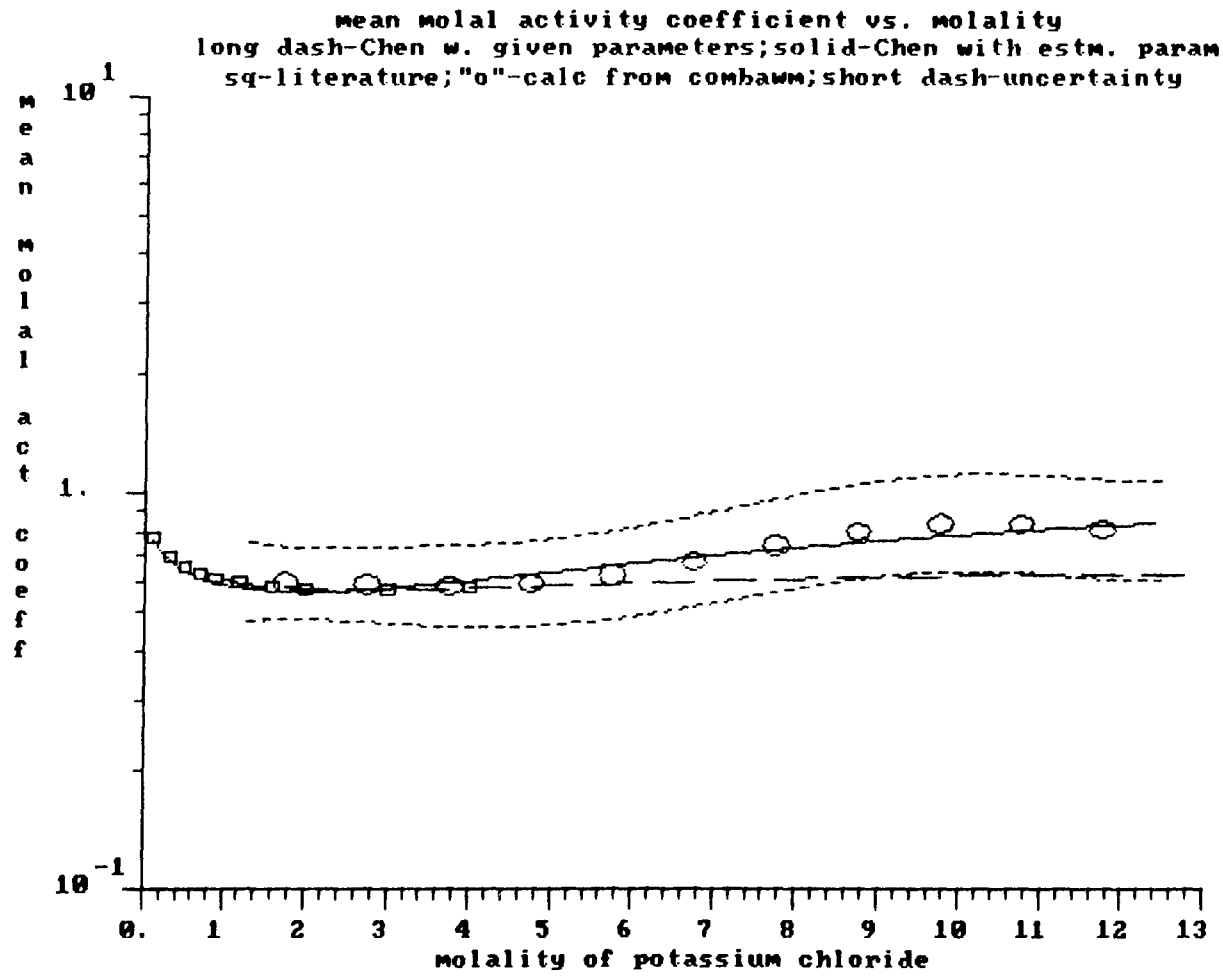
mean molal activity coefficient vs. molality
long dash-Chen w. given parameters;solid-Chen with estm. param
sq-literature;"o"-calc from combawm;short dash-uncertainty
mean molal act coeff
10 1
1.
10 -1
0. 1 2 3 4 5 6 7 8 9 10 11 12 13
molality of potassium chloride

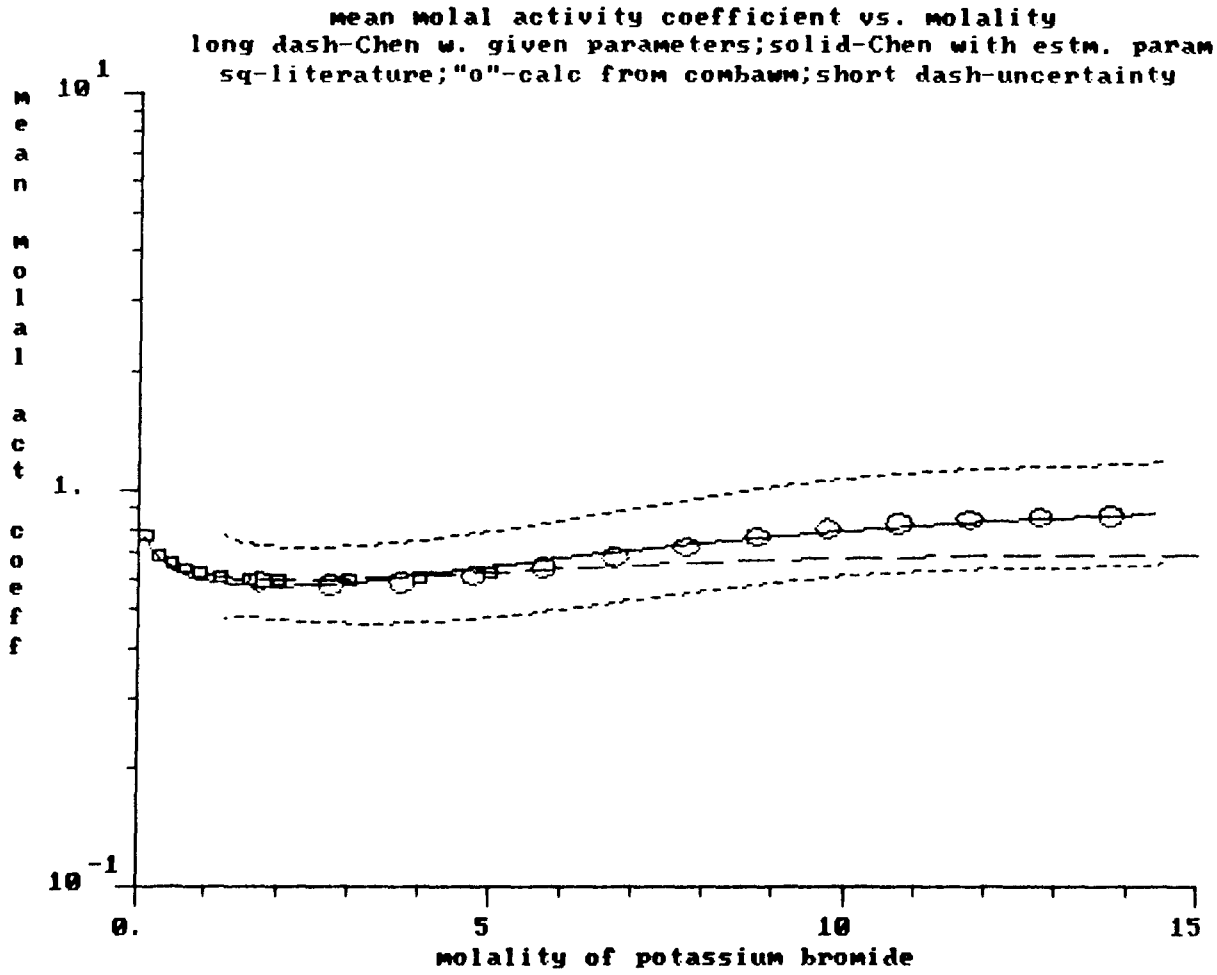
mean molal activity coefficient vs. molality
long dash-Chen w. given parameters;solid-Chen with estm. param
sq-literature;"o"-calc from combawm;short dash-uncertainty
mean molal act coeff
10 1
1.
10 -1
0.
5
10
15
molality of potassium bromide

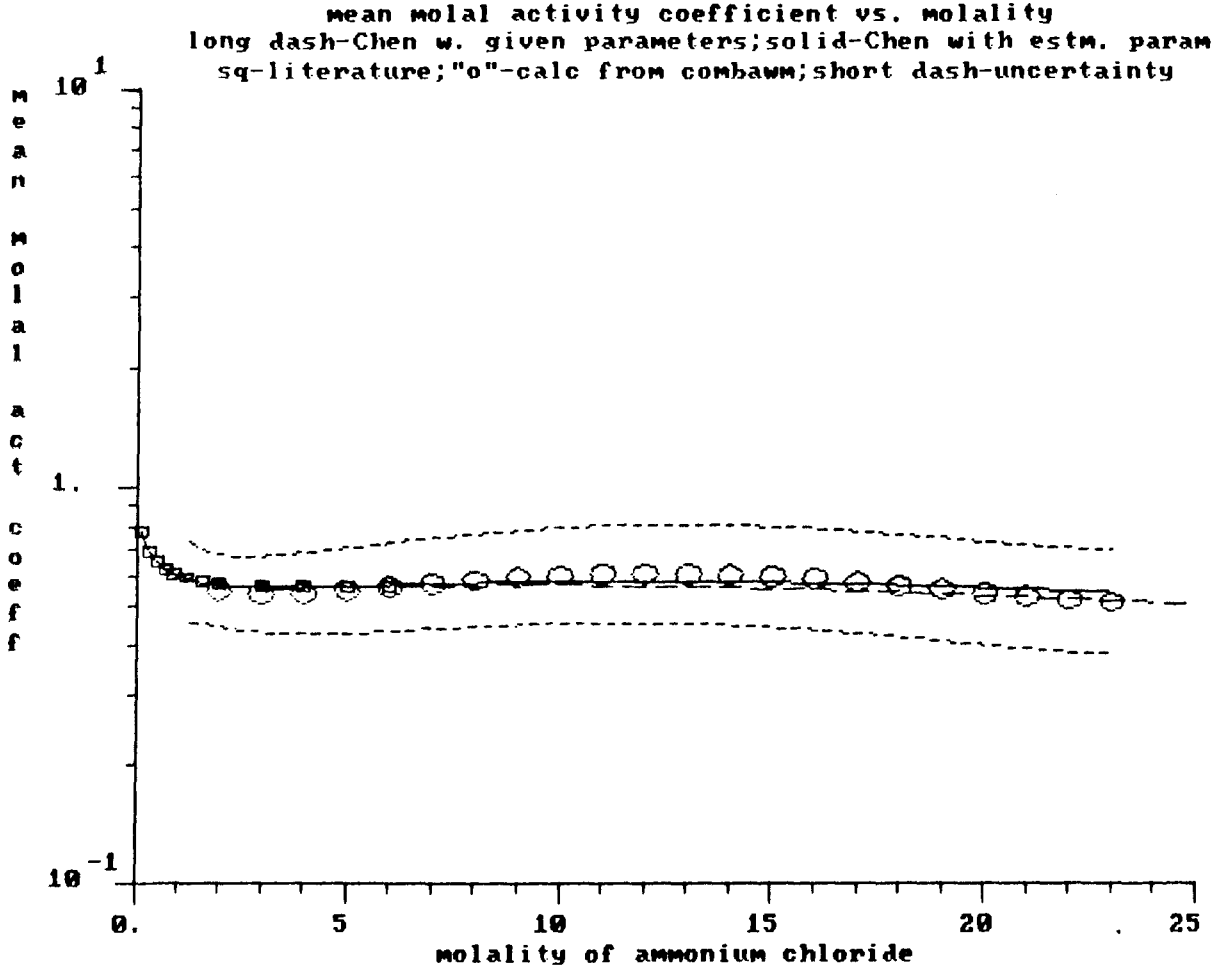
mean molal activity coefficient vs. molality
long dash-Chen w. given parameters;solid-Chen with estm. param
sq-literature;"o"-calc from combawm;short dash-uncertainty
mean molal act coeff
10 1
1.
10 -1
0.
5
10
15
20
25
molality of ammonium chloride

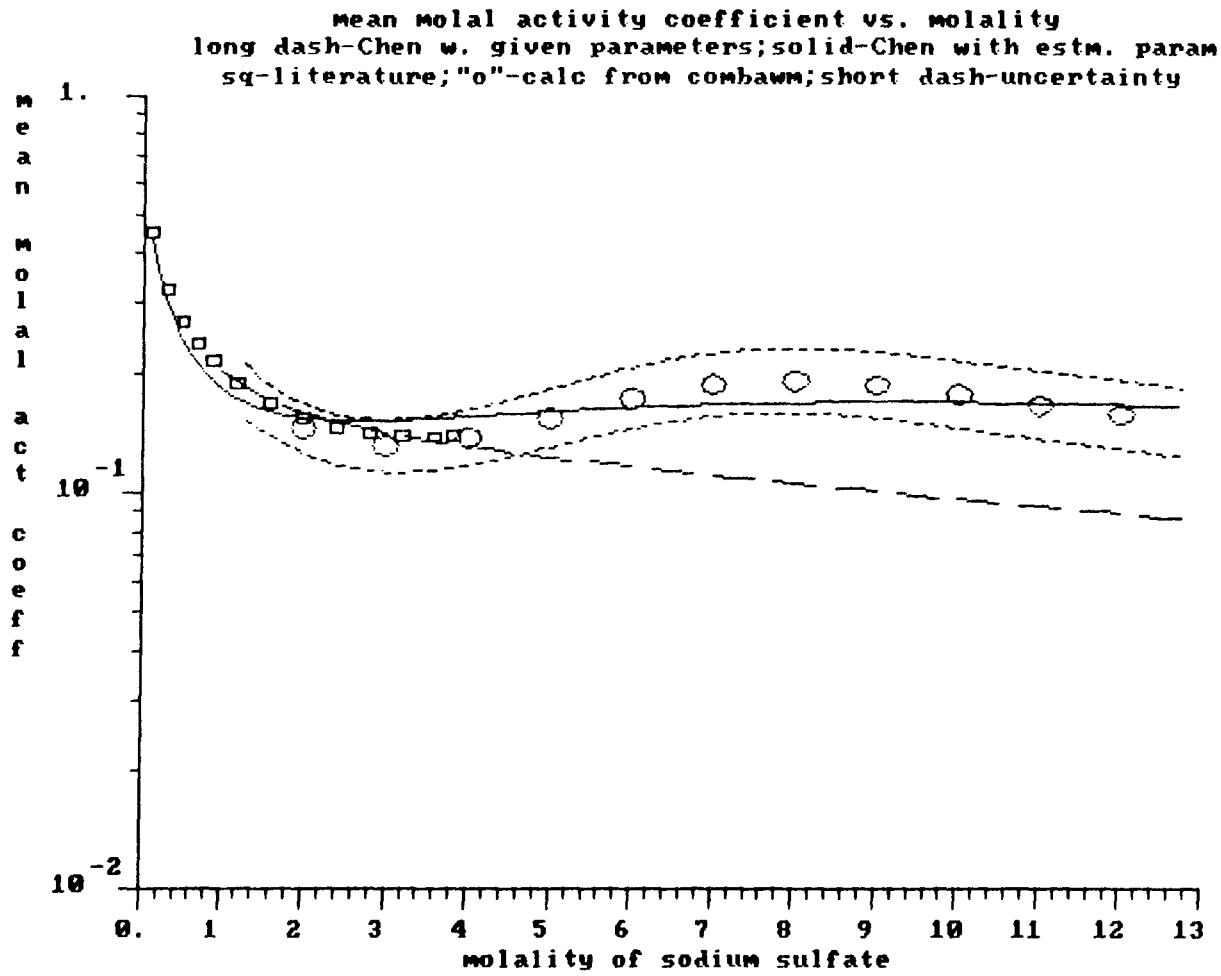
mean molal activity coefficient vs. molality
long dash-Chen w. given parameters;solid-Chen with estm. param
sq-literature;"o"-calc from combawm;short dash-uncertainty
mean molal act coeff
1.
10^-1
10^-2
0.
1
2
3
4
5
6
7
8
9
10
11
12
13
molality of sodium sulfate

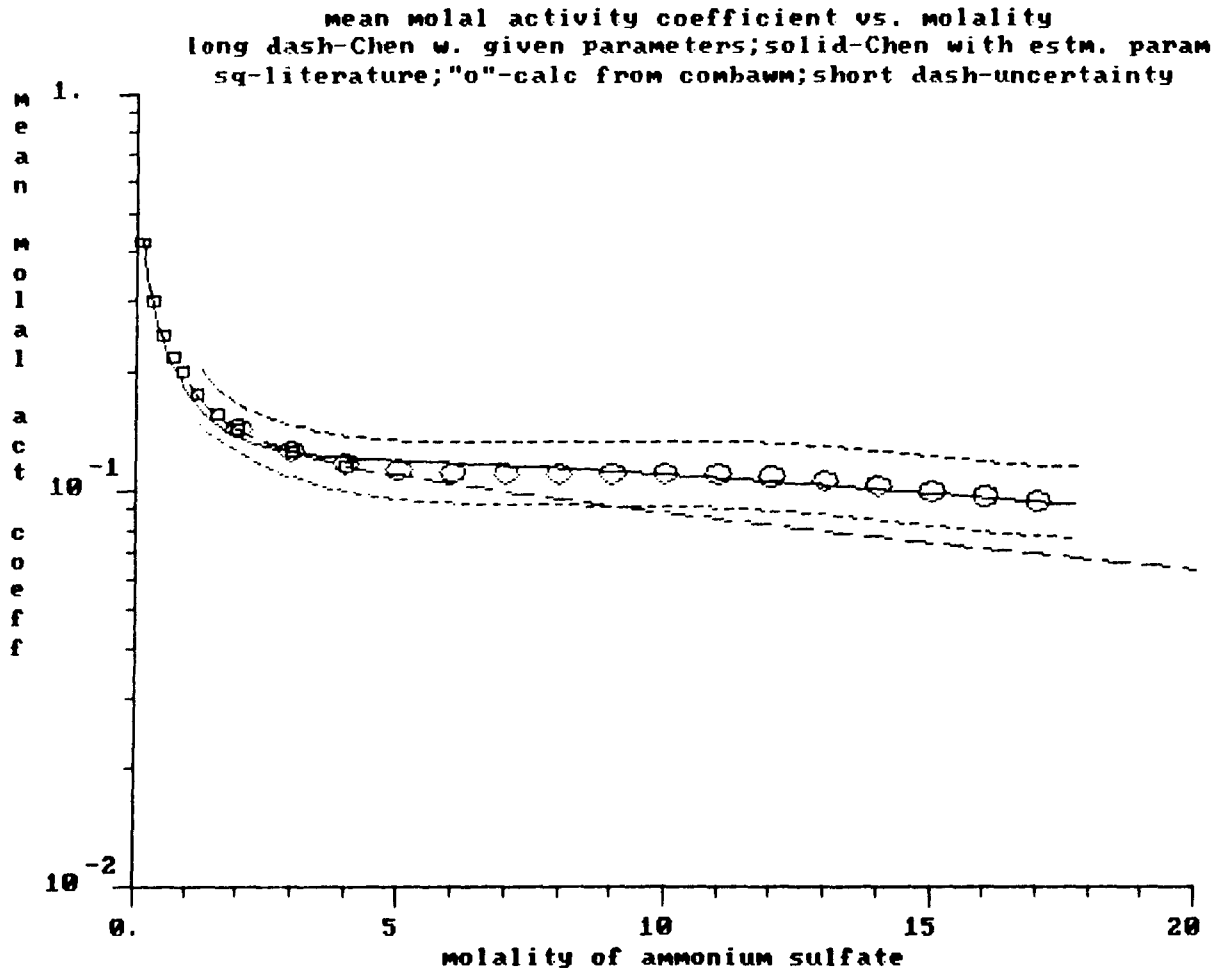
mean molal activity coefficient vs. molality
long dash-Chen w. given parameters;solid-Chen with estm. param
sq-literature;"o"-calc from combawm;short dash-uncertainty
mean molal act coeff
1.
10 -1
10 -2
0.
5
10
15
20
molality of ammonium sulfate

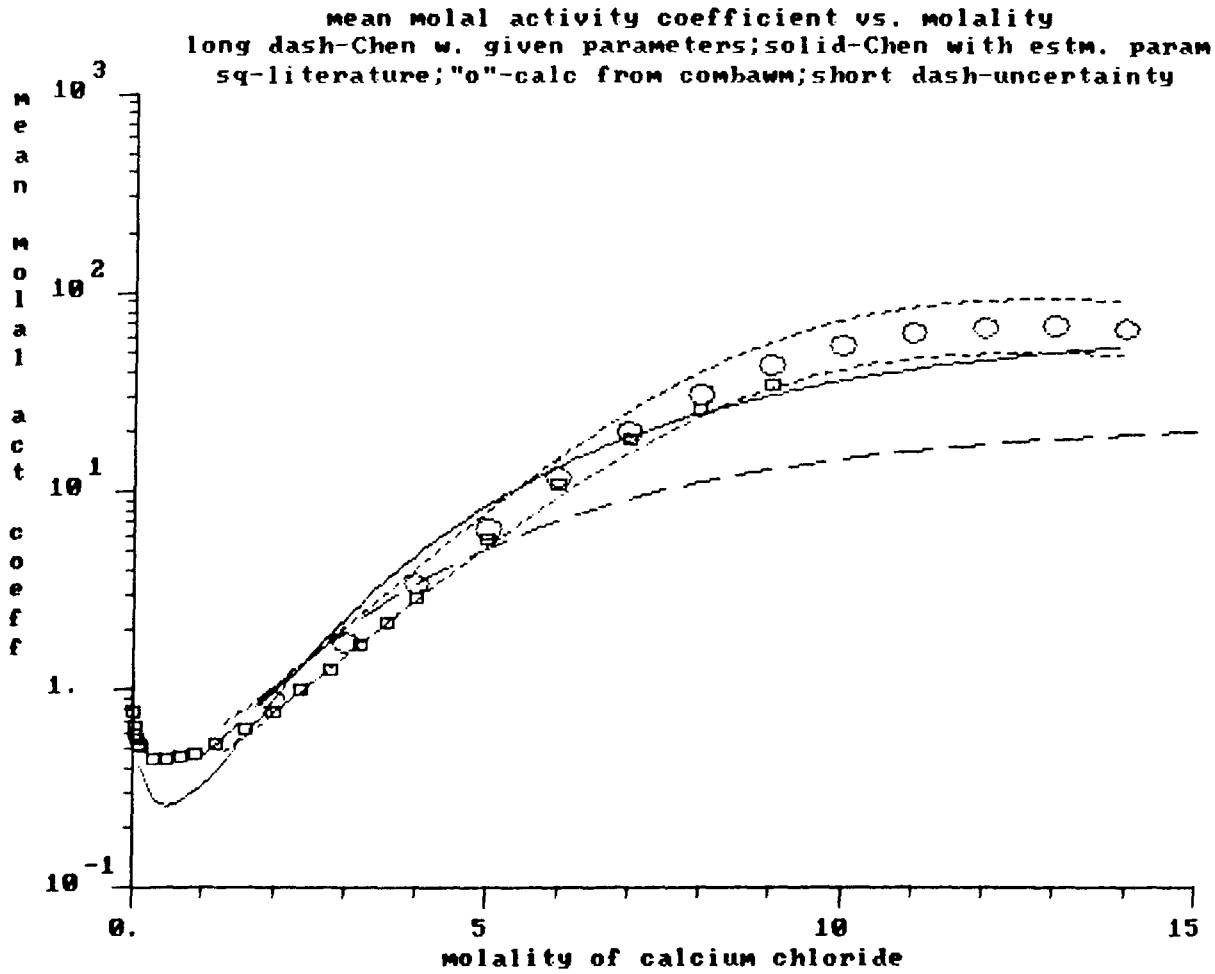
mean molal activity coefficient vs. molality
long dash-Chen w. given parameters;solid-Chen with estm. param
sq-literature;"o"-calc from combawm;short dash-uncertainty
mean molal act coeff
10^3
10^2
10^1
1.
10^-1
0.
5
10
15
molality of calcium chloride

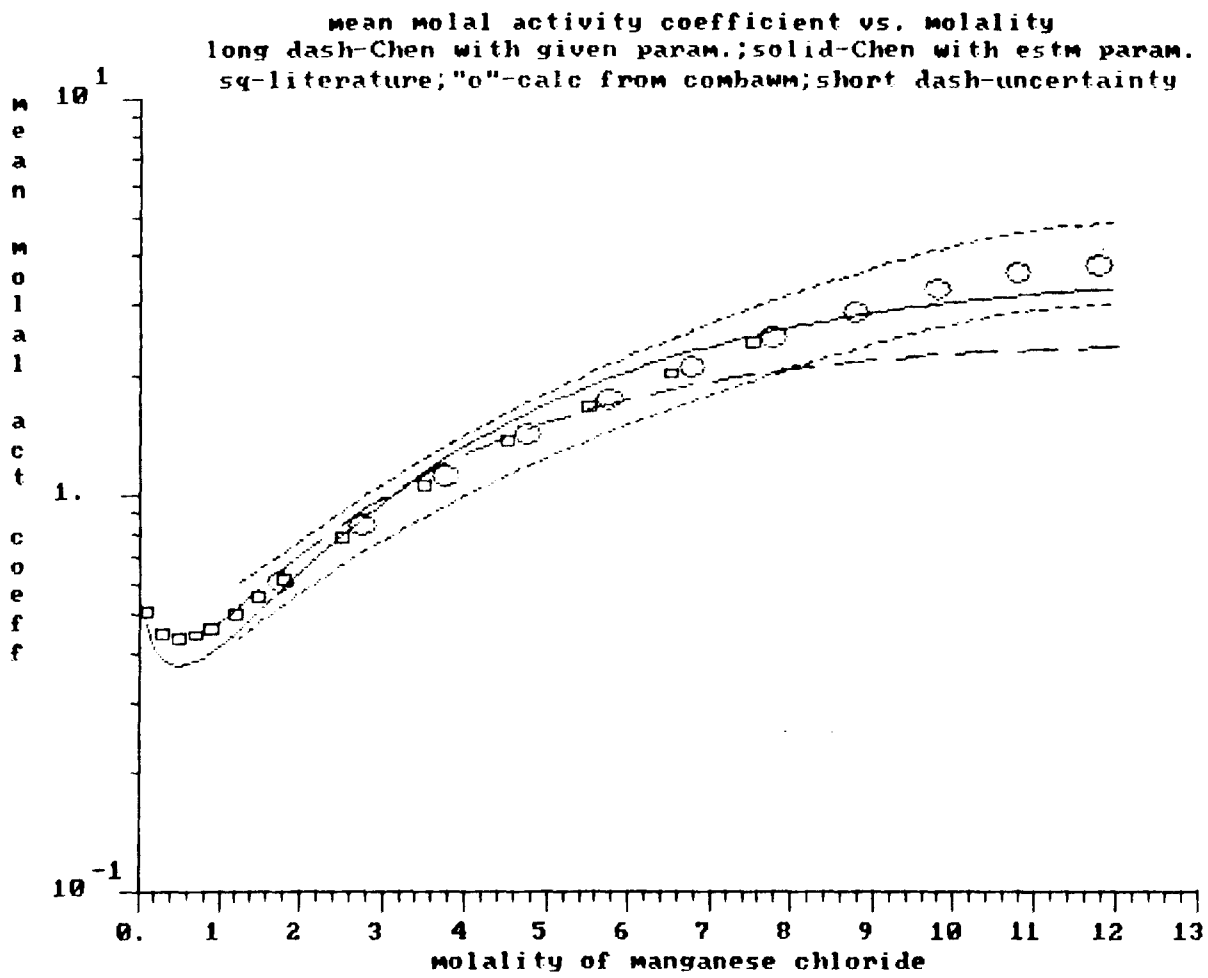
mean molal activity coefficient vs. molality
long dash-Chen with given param.;solid-Chen with estm param.
sq-literature;"o"-calc from combawm;short dash-uncertainty
mean molal act coeff
10 1
1.
10 -1
0. 1 2 3 4 5 6 7 8 9 10 11 12 13
molality of manganese chloride

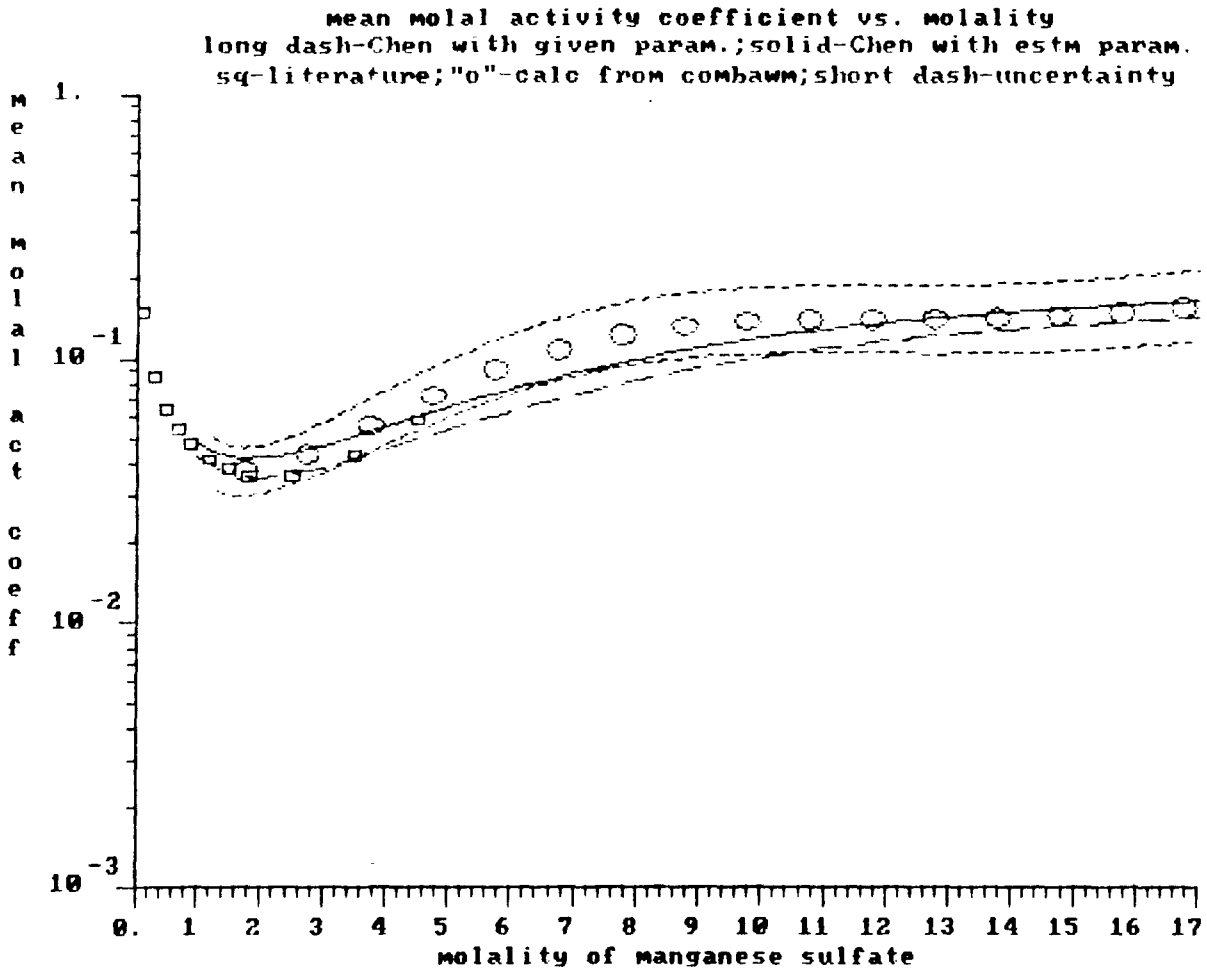
mean molal activity coefficient vs. molality
long dash-Chen with given param.;solid-Chen with estm param.
sq-literature;"o"-calc from combawm;short dash-uncertainty
mean molal act coeff
1.
10 -1
10 -2
10 -3
0. 1 2 3 4 5 6 7 8 9 10 11 12 13 14 15 16 17
molality of manganese sulfate

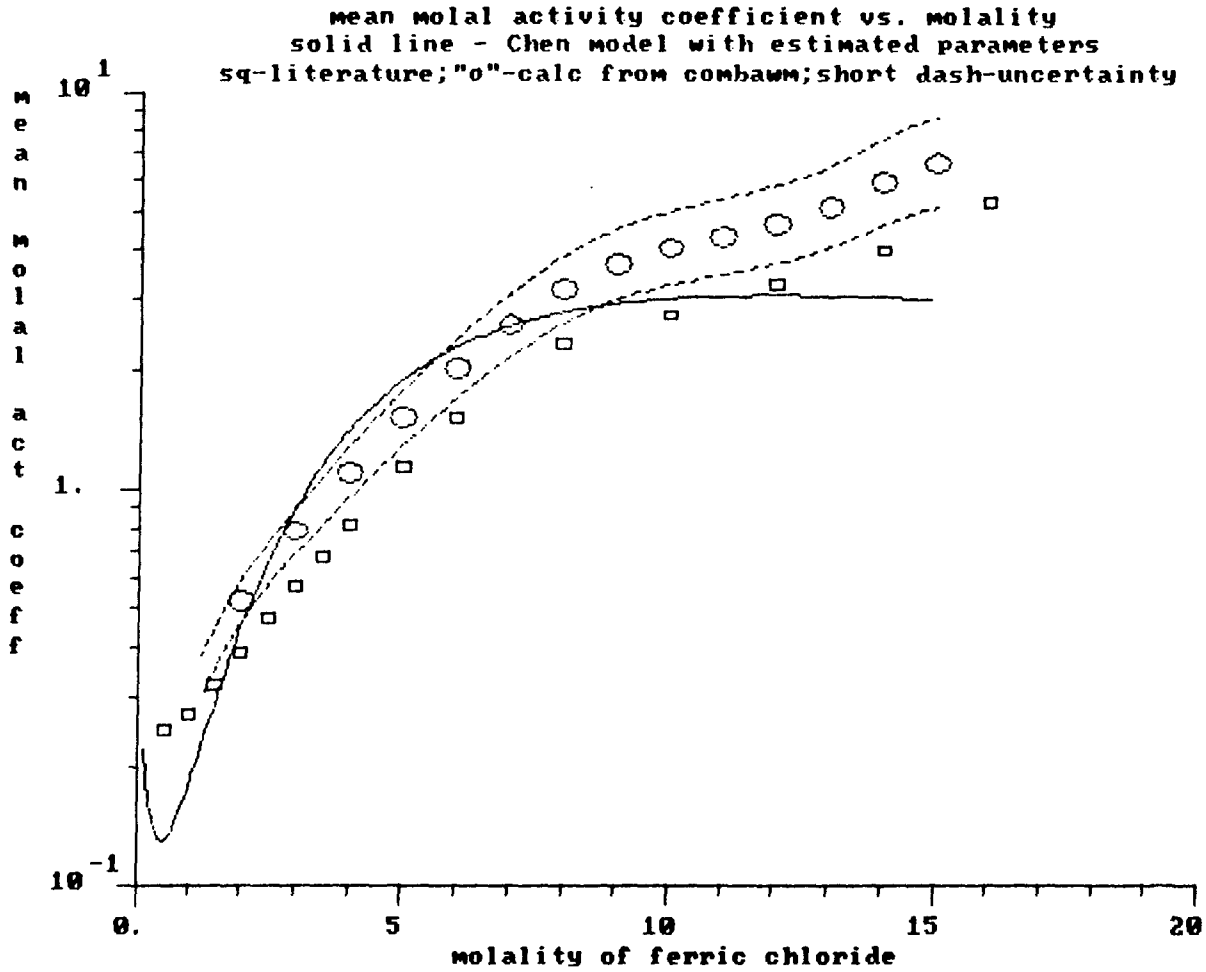
mean molal activity coefficient vs. molality
solid line - Chen model with estimated parameters
sq-literature;"o"-calc from combawm;short dash-uncertainty
mean molal act coeff
10 1
1.
10 -1
0.
5
10
15
20
molality of ferric chloride

Appendix H: Plots of water activity as a function of molality in which experimental data is compared to the predictions of the local composition model of Chen et al.

The figures in this appendix are analogous to those in Appendix G, the only difference being that the water activity instead of the solute activity coefficient is plotted as a function of molality. For further information about this model, please see Chapter 1.

Each figure contains the following data for a particular salt:

- $a_w(m)$ data from the present experiments
- $a_w(m)$ data from the literature; the same abbreviations used to describe the literature data sources in Appendix B are used in this appendix
- $a_w(m)$ data calculated from the local composition model of Chen et al. using parameters estimated from low concentration data; the parameters are given in the original paper and in Table 6 of Chapter 1; this data is described as "old" data in the figure captions
- $a_w(m)$ data calculated from the local composition model of Chen et al. using parameters estimated in this work from the full range of experimental data; the parameters are given in Table 7 of Chapter 1; this data is listed as "new" data in the figure captions
- in some of the plots, data calculated from the $a_w(m)$ polynomial fits are

given; the polynomial fits used are described in Appendices C and D and in Chapter 1

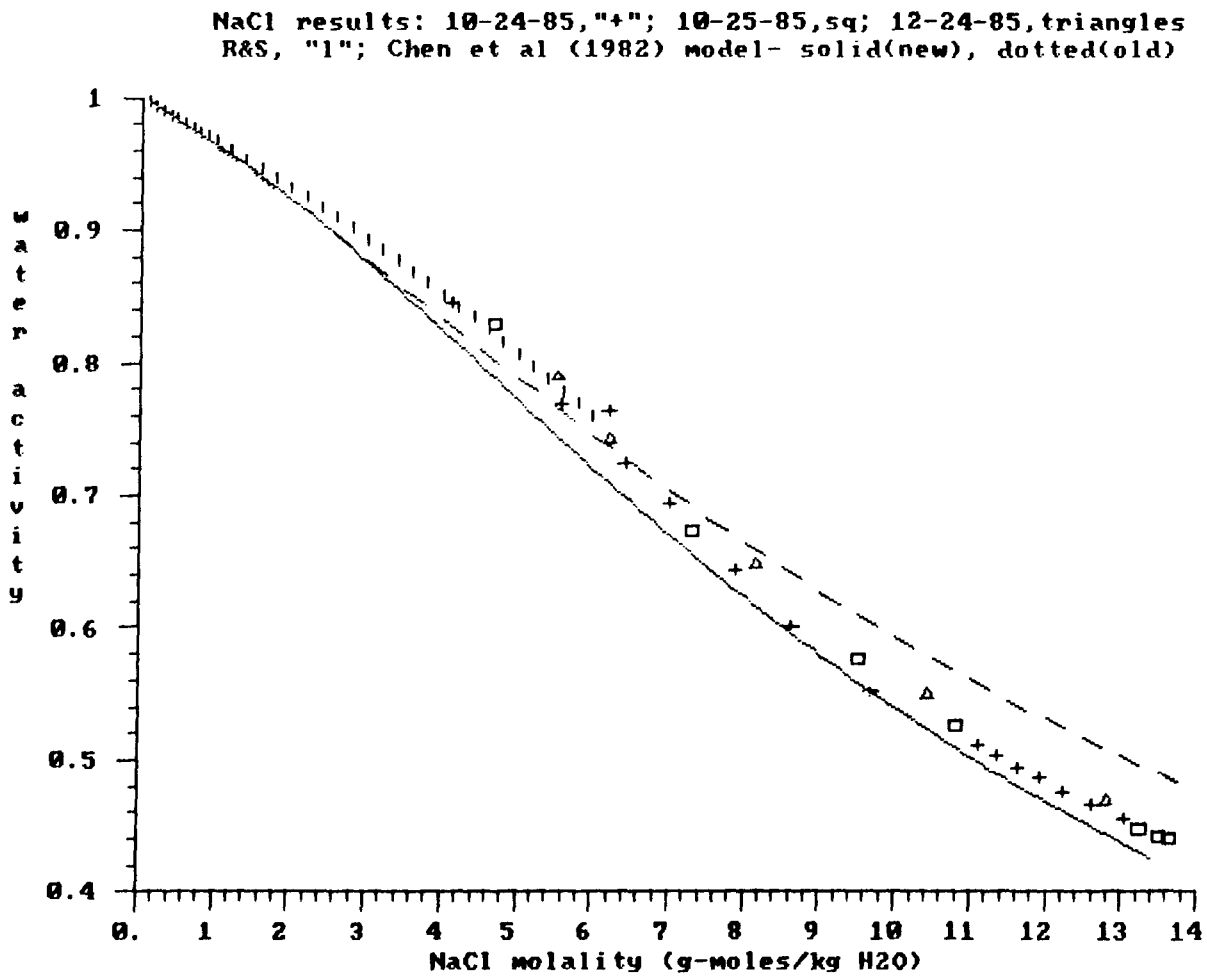
NaCl results: 10-24-85,"+"; 10-25-85,sq; 12-24-85,triangles
R&S, "l"; Chen et al (1982) model- solid(new), dotted(old)
water activity
1
0.9
0.8
0.7
0.6
0.5
0.4
0.
1
2
3
4
5
6
7
8
9
10
11
12
13
14
NaCl molality (g-moles/kg H2O)

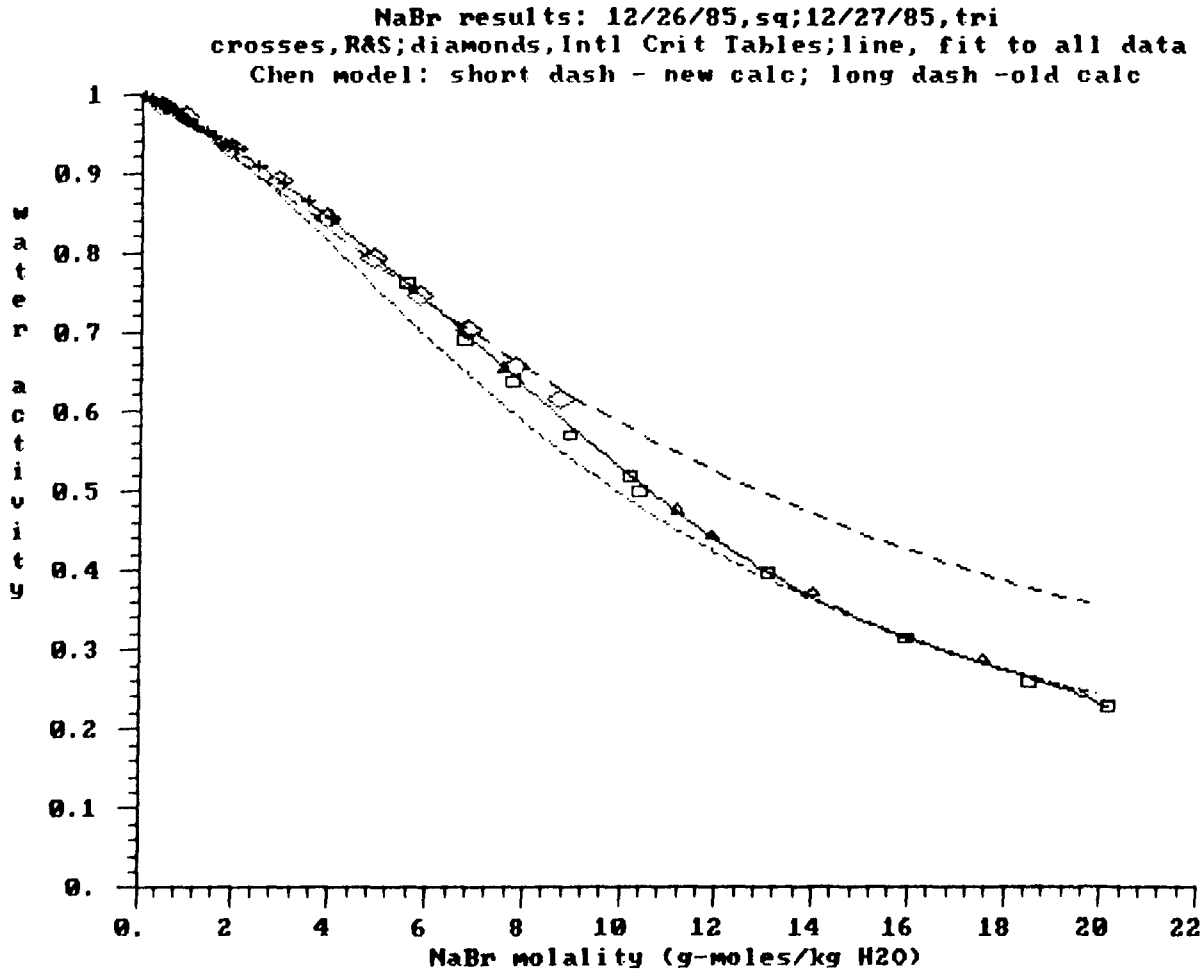
NaBr results: 12/26/85,sq;12/27/85,tri
crosses,R&S;diamonds,Intl Crit Tables;line, fit to all data
Chen model: short dash - new calc; long dash -old calc
water activity
1
0.9
0.8
0.7
0.6
0.5
0.4
0.3
0.2
0.1
0.
0.
2
4
6
8
10
12
14
16
18
20
22
NaBr molality (g-moles/kg H2O)

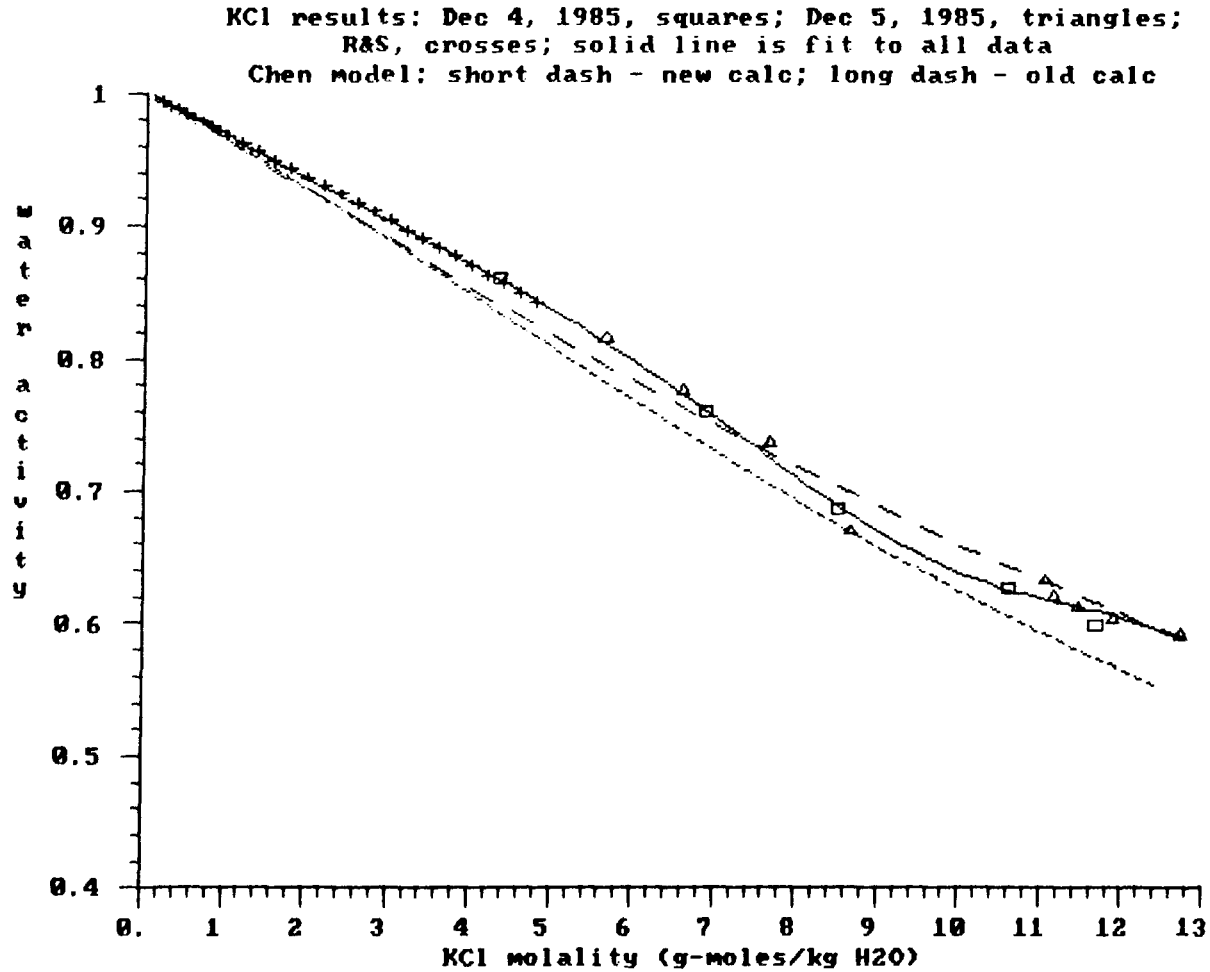
KCl results: Dec 4, 1985, squares; Dec 5, 1985, triangles;
R&S, crosses; solid line is fit to all data
Chen model: short dash - new calc; long dash - old calc
water activity
1
0.9
0.8
0.7
0.6
0.5
0.4
0.
1
2
3
4
5
6
7
8
9
10
11
12
13
KCl molality (g-moles/kg H2O)

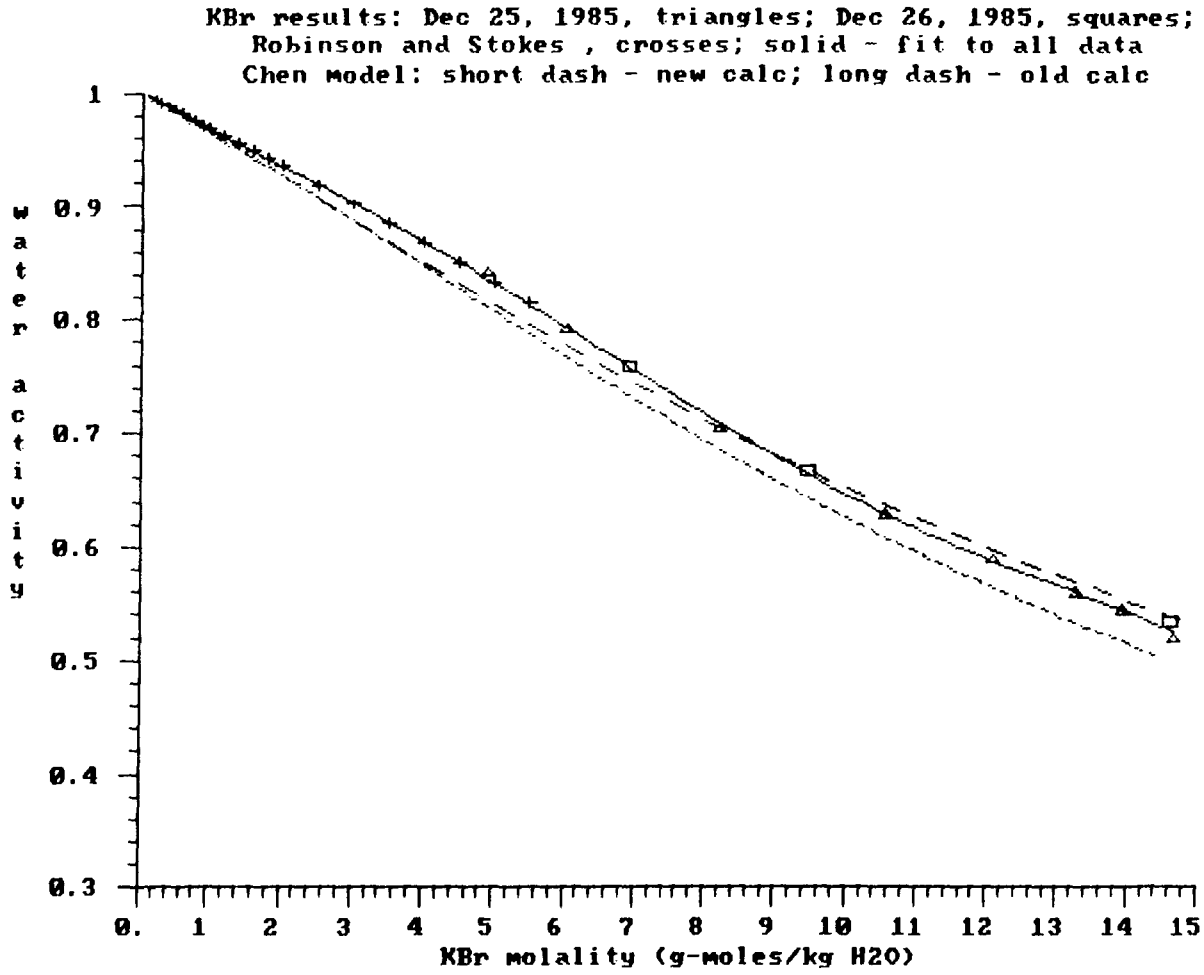
KBr results: Dec 25, 1985, triangles; Dec 26, 1985, squares;
Robinson and Stokes , crosses; solid - fit to all data
Chen model: short dash - new calc; long dash - old calc
water activity
1
0.9
0.8
0.7
0.6
0.5
0.4
0.3
0.
1
2
3
4
5
6
7
8
9
10
11
12
13
14
15
KBr molality (g-moles/kg H2O)

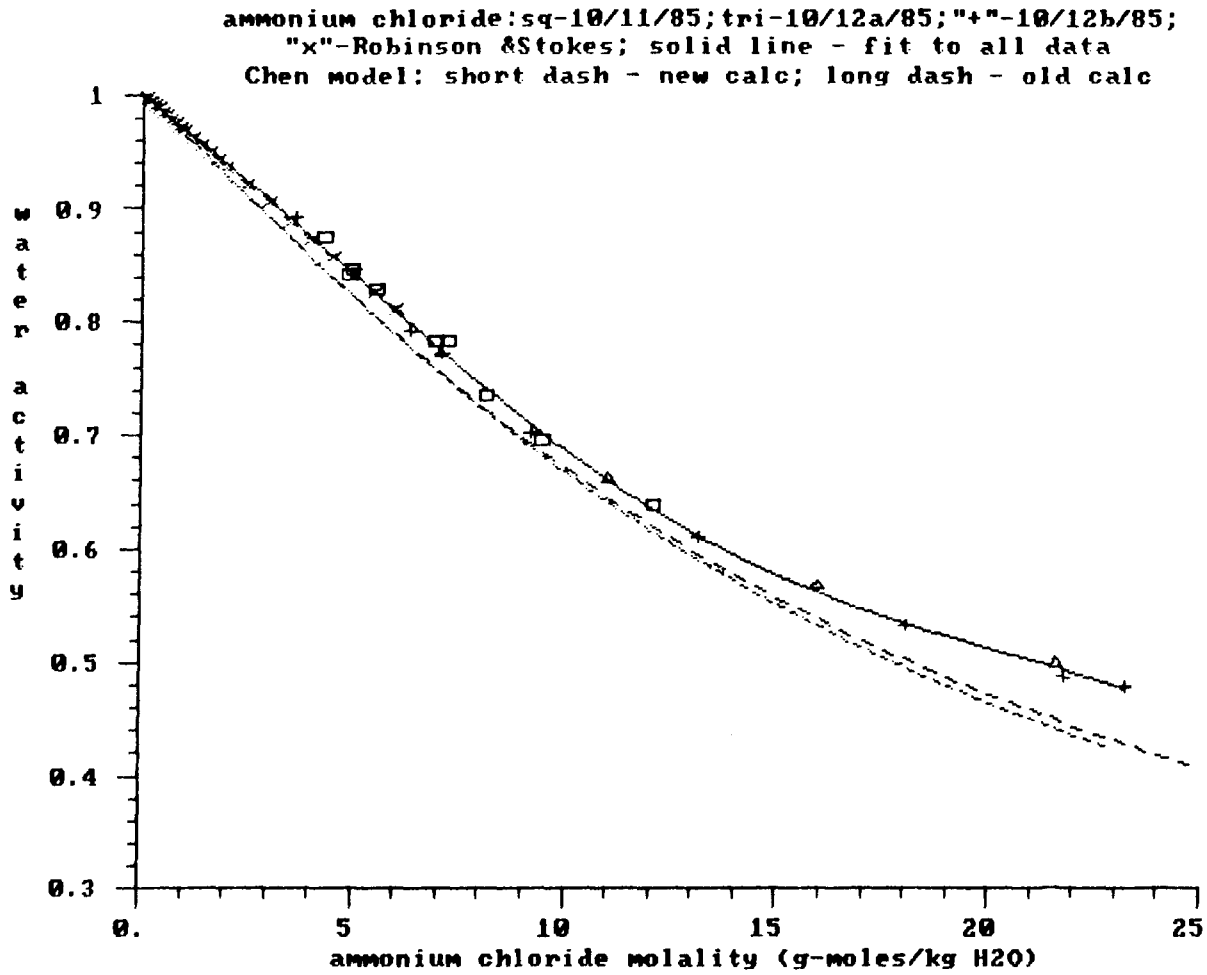
ammonium chloride:sq-10/11/85;tri-10/12a/85;"+"-10/12b/85;
"x"-Robinson &Stokes; solid line - fit to all data
Chen model: short dash - new calc; long dash - old calc
water activity
1
0.9
0.8
0.7
0.6
0.5
0.4
0.3
0.
5
10
15
20
25
ammonium chloride molality (g-moles/kg H2O)

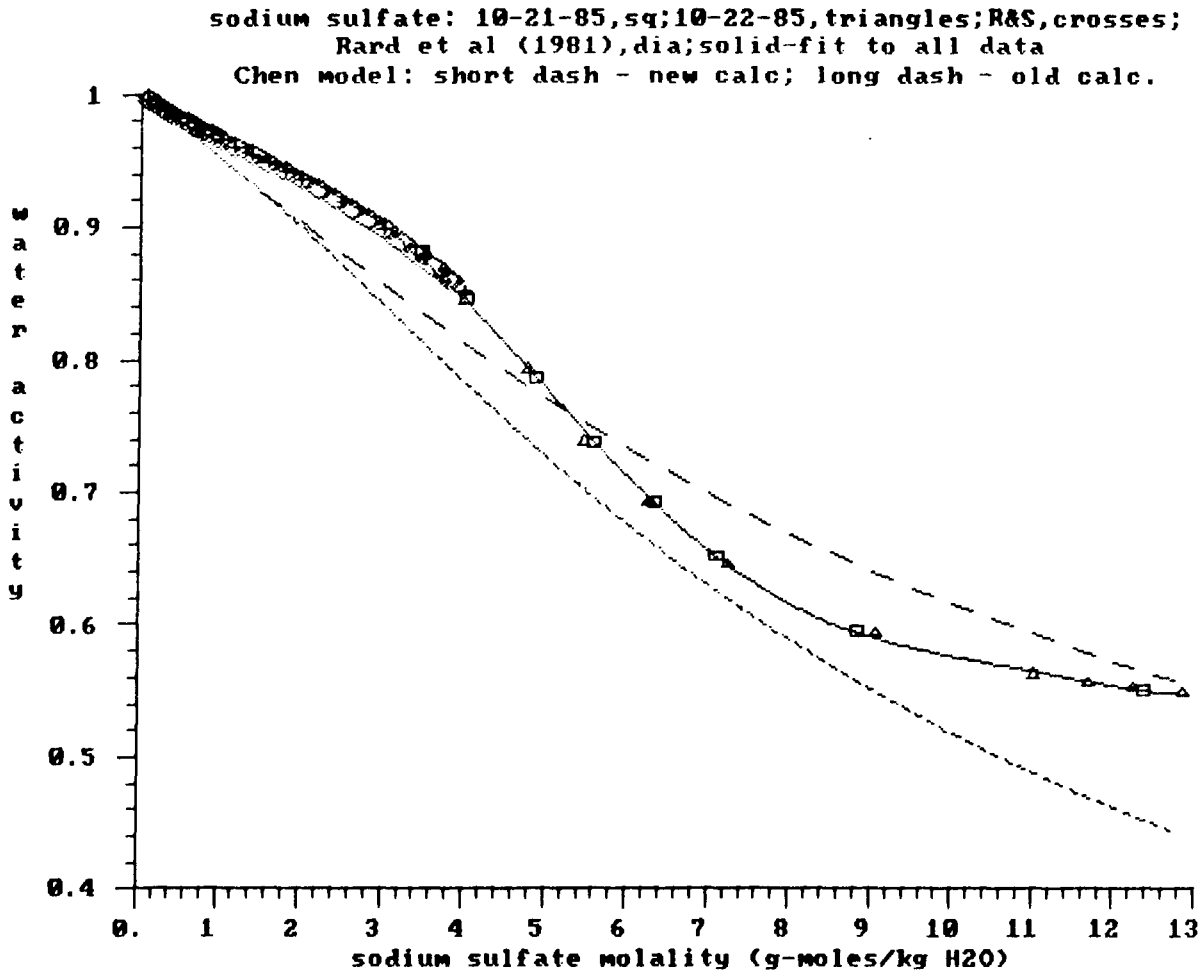
sodium sulfate: 10-21-85,sq;10-22-85,triangles;R&S,crosses;
Rard et al (1981),dia;solid-fit to all data
Chen model: short dash - new calc; long dash - old calc.
water activity
1
0.9
0.8
0.7
0.6
0.5
0.4
0.
1
2
3
4
5
6
7
8
9
10
11
12
13
sodium sulfate molality (g-moles/kg H2O)

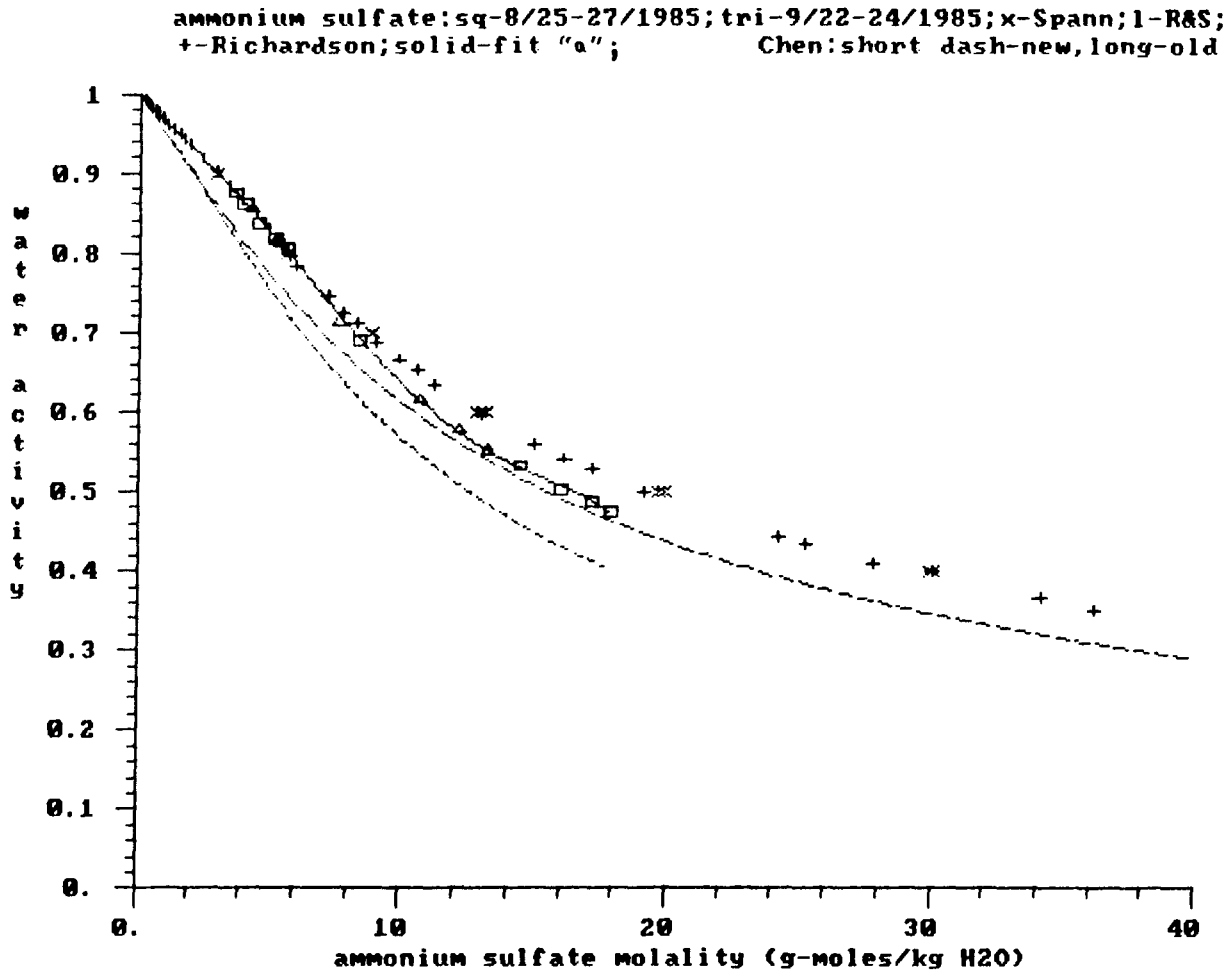
ammonium sulfate:sq-8/25-27/1985;tri-9/22-24/1985;x-Spann;1-R&S;
+-Richardson;solid-fit "a";
Chen:short dash-new,long-old
water activity
1
0.9
0.8
0.7
0.6
0.5
0.4
0.3
0.2
0.1
0.
0.
10
20
30
40
ammonium sulfate molality (g-moles/kg H2O)

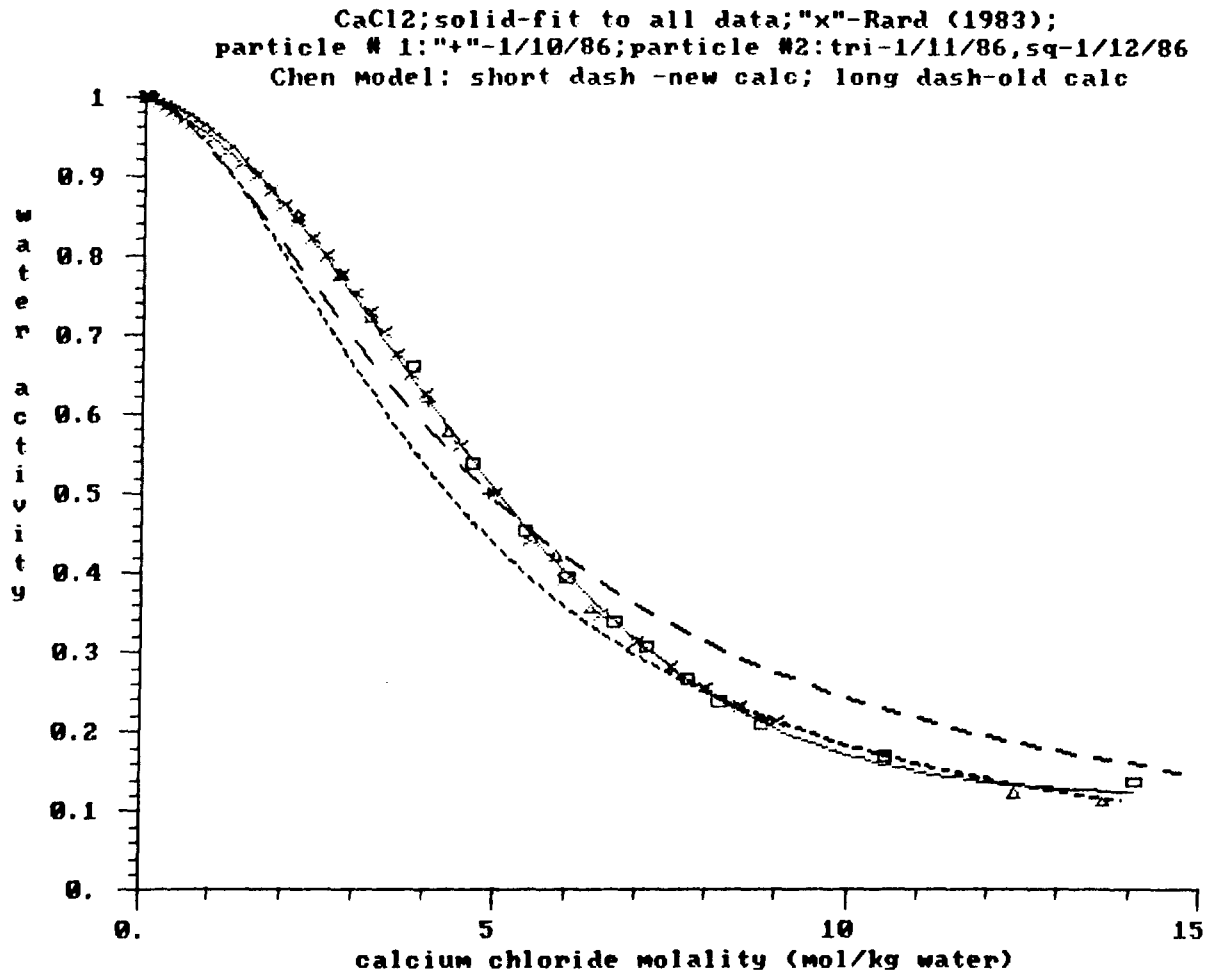
CaCl2;solid-fit to all data;"x"-Rard (1983);
particle # 1:"+"-1/10/86;particle #2:tri-1/11/86,sq-1/12/86
Chen model: short dash -new calc; long dash-old calc
water activity
1
0.9
0.8
0.7
0.6
0.5
0.4
0.3
0.2
0.1
0.
0.
5
10
15
calcium chloride molality (mol/kg water)

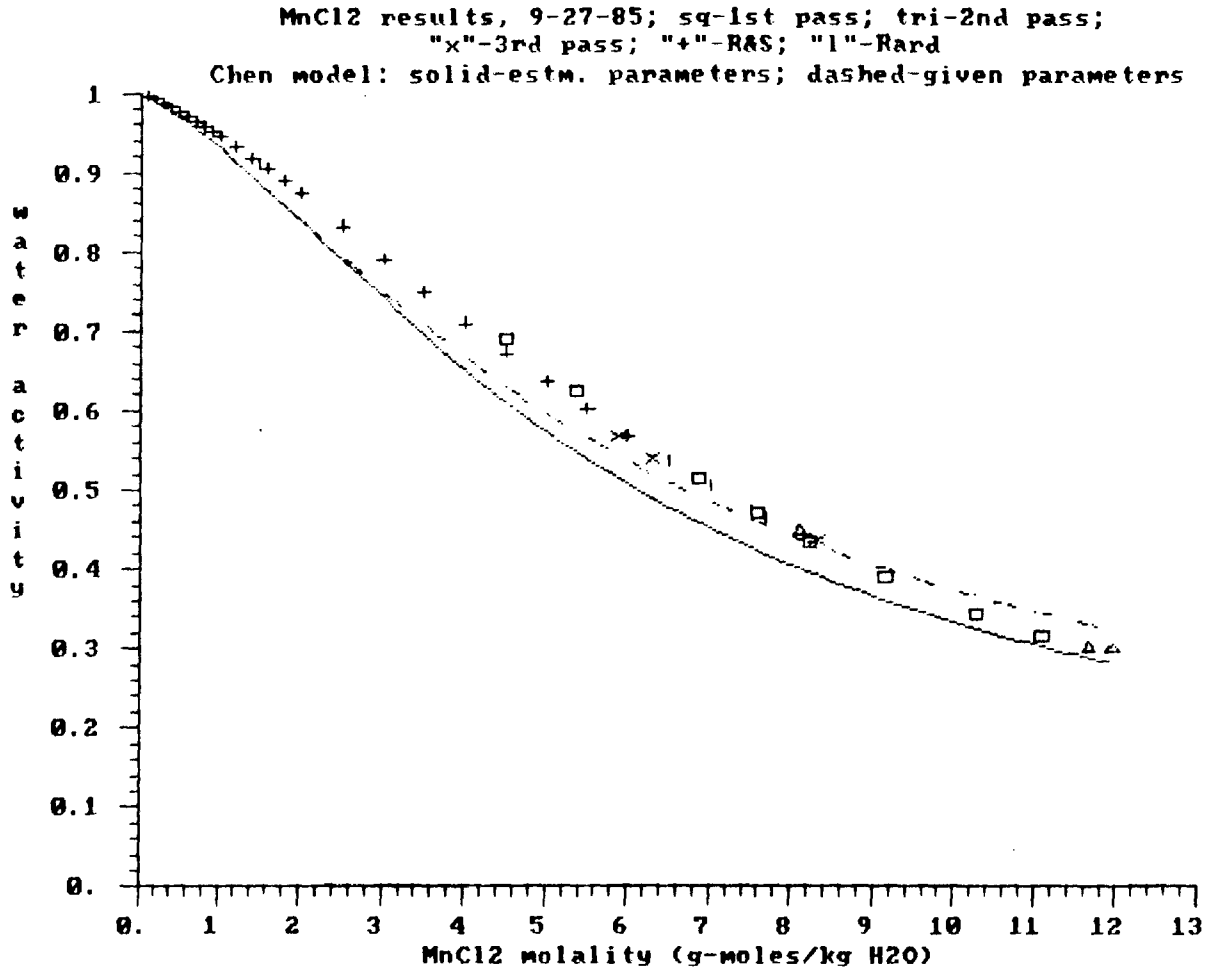
MnCl2 results, 9-27-85; sq-1st pass; tri-2nd pass;
"x"-3rd pass; "+"-R&S; "l"-Rard
Chen model: solid-estm. parameters; dashed-given parameters
water activity
1
0.9
0.8
0.7
0.6
0.5
0.4
0.3
0.2
0.1
0.
0. 1 2 3 4 5 6 7 8 9 10 11 12 13
MnCl2 molality (g-moles/kg H2O)

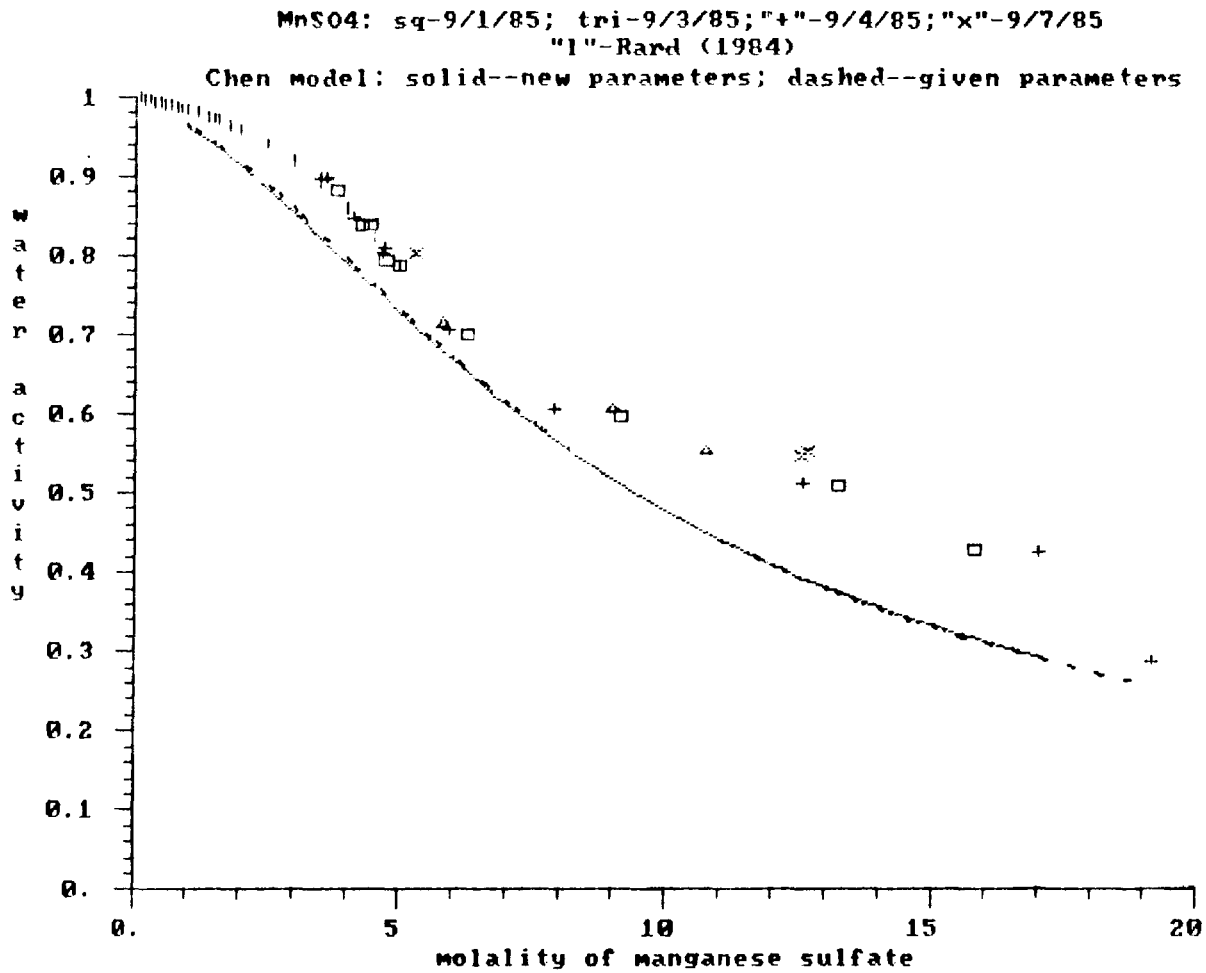
MnSO4: sq-9/1/85; tri-9/3/85;"+"-9/4/85;"x"-9/7/85
"l"-Rard (1984)
Chen model: solid--new parameters; dashed--given parameters
water activity
1
0.9
0.8
0.7
0.6
0.5
0.4
0.3
0.2
0.1
0.
0.
5
10
15
20
molality of manganese sulfate

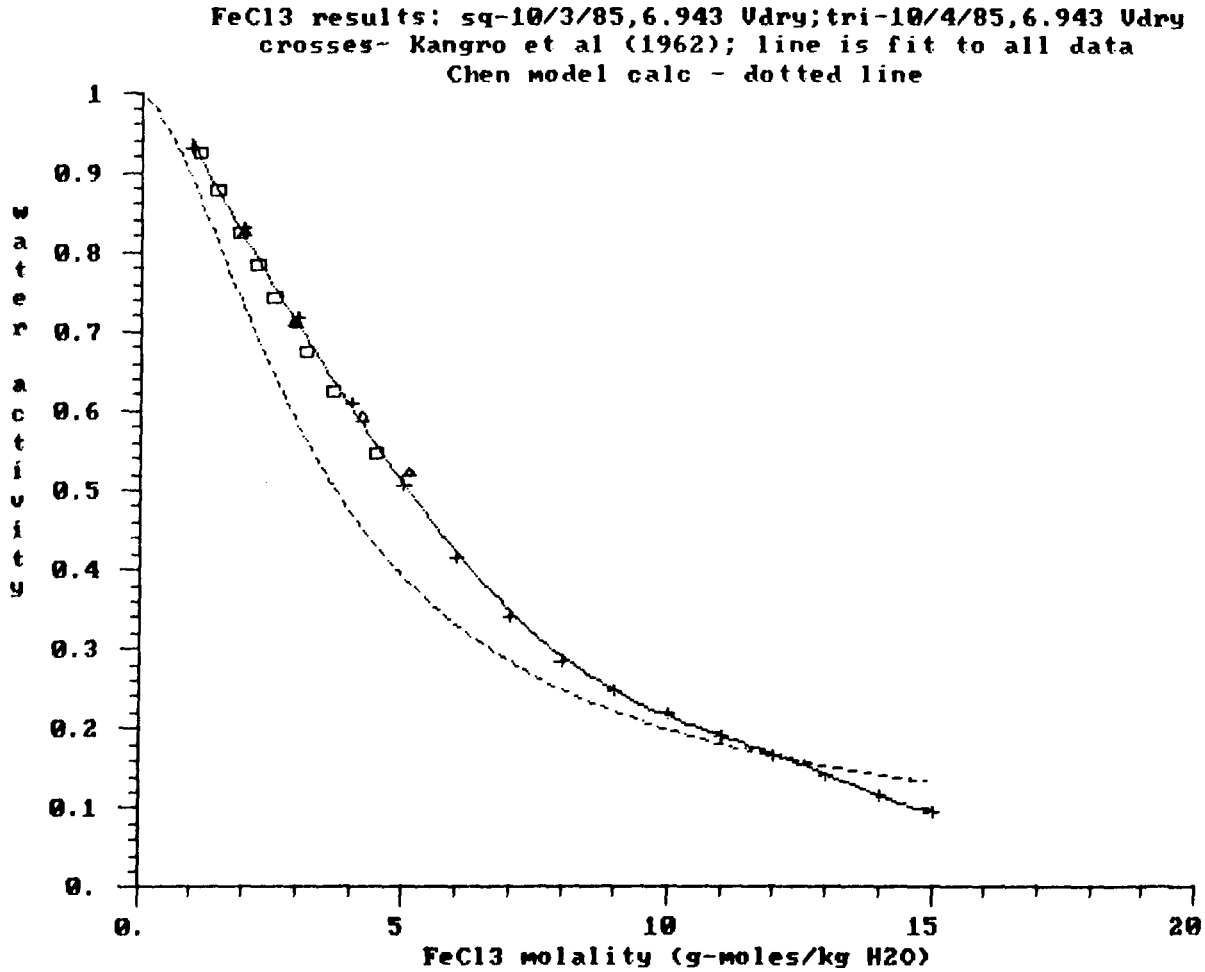
FeCl3 results: sq-10/3/85,6.943 Vdry;tri-10/4/85,6.943 Vdry
crosses- Kangro et al (1962); line is fit to all data
Chen model calc - dotted line
water activity
1
0.9
0.8
0.7
0.6
0.5
0.4
0.3
0.2
0.1
0.
0.
5
10
15
20
FeCl3 molality (g-moles/kg H2O)

Appendix I: Plots of the solute activity coefficient as a function of molality in which experimental data is compared to the predictions of Pitzer's model

This appendix contains plots corresponding to Figures 19 and 20 of Chapter 1. For further explanation and discussion of these plots and the Pitzer model, please refer to Chapter 1.

The data corresponding to the "given" parameters refers to those calculated from the parameters estimated from low concentration data; these parameters are given in Table 4 of Chapter 1. The data corresponding to the "estimated" parameters refers to those calculated from the parameters estimated from the full range of experimental data; these parameters are given in Table 5 of Chapter 1.

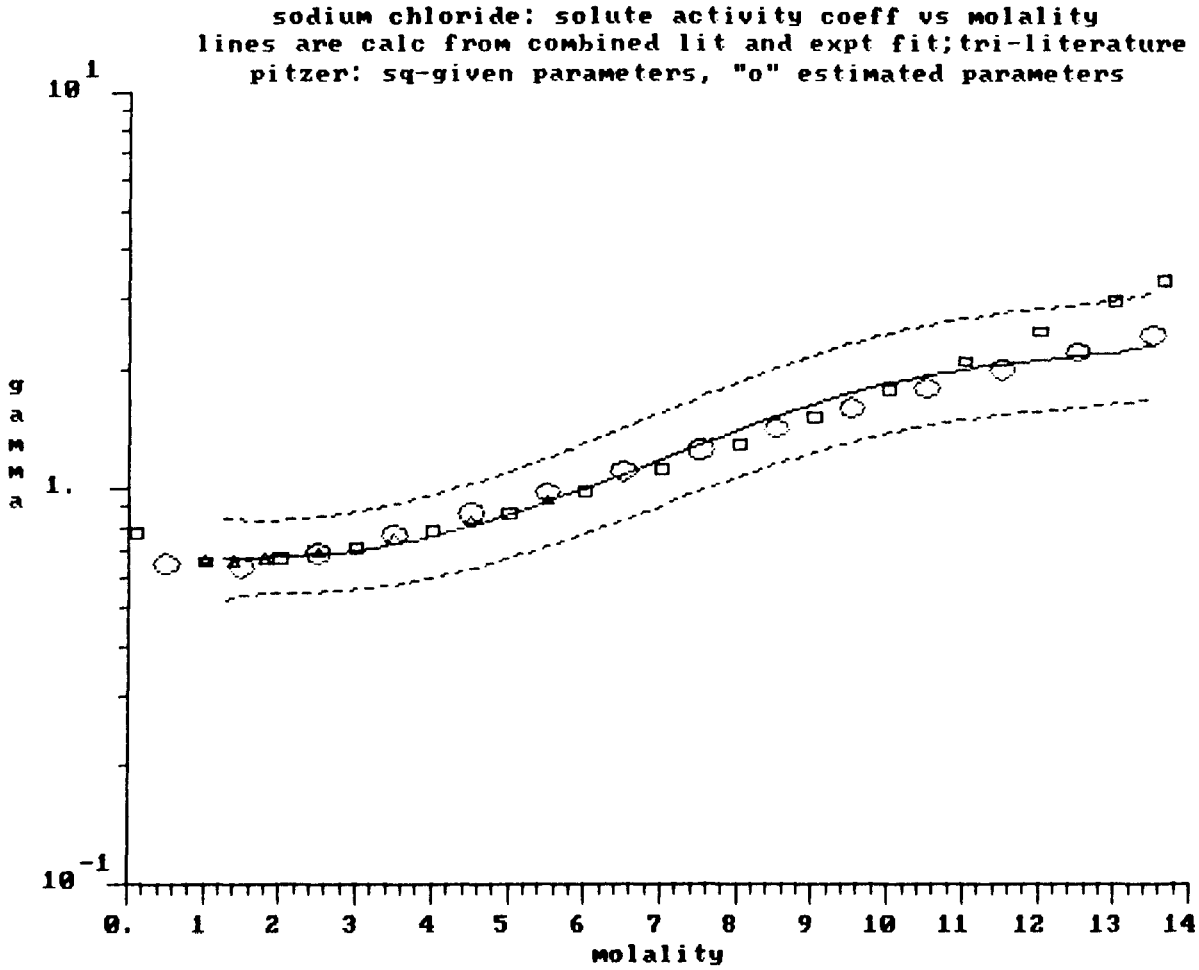
sodium chloride: solute activity coeff vs molality
lines are calc from combined lit and expt fit;tri-literature
pitzer: sq-given parameters, "o" estimated parameters
10 1
1.
10 -1
gamma
0. 1 2 3 4 5 6 7 8 9 10 11 12 13 14
molality

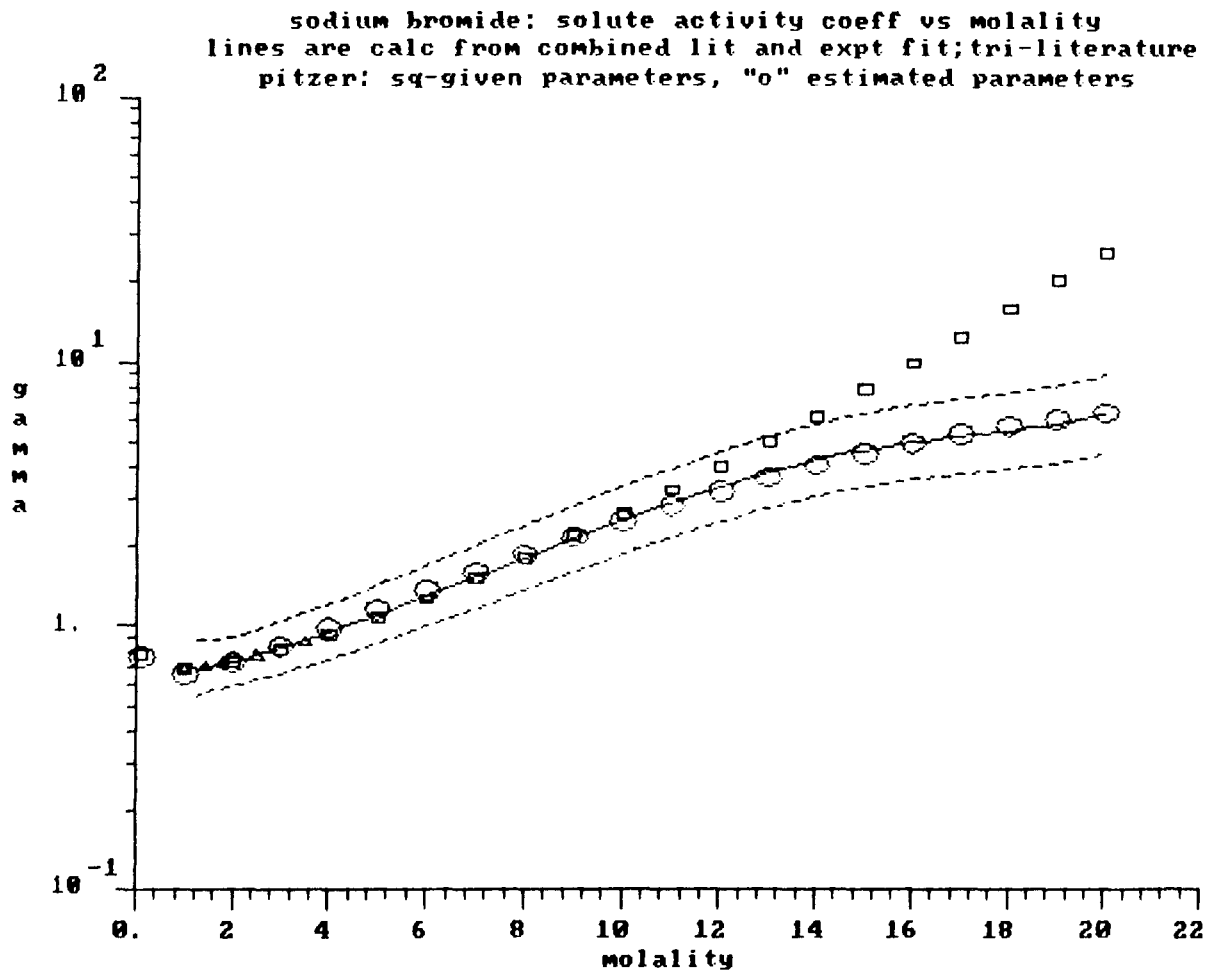
sodium bromide: solute activity coeff vs molality
lines are calc from combined lit and expt fit;tri-literature
pitzer: sq-given parameters, "o" estimated parameters
10 2
10 1
1.
10 -1
gamma
0.
2
4
6
8
10
12
14
16
18
20
22
molality

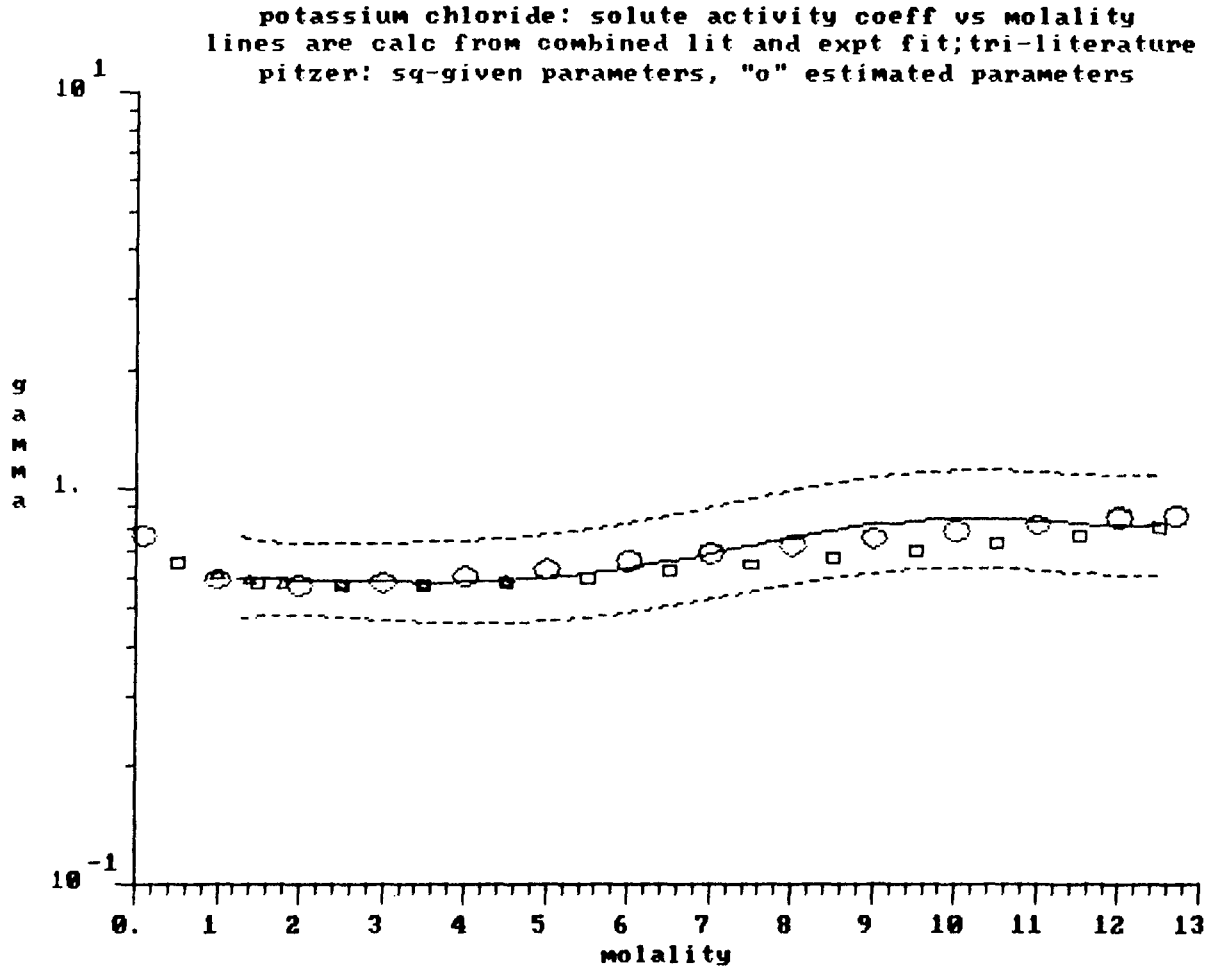
potassium chloride: solute activity coeff vs molality
lines are calc from combined lit and expt fit;tri-literature
pitzer: sq-given parameters, "o" estimated parameters
10 1
gamma
1.
10 -1
0.
1
2
3
4
5
6
7
8
9
10
11
12
13
molality

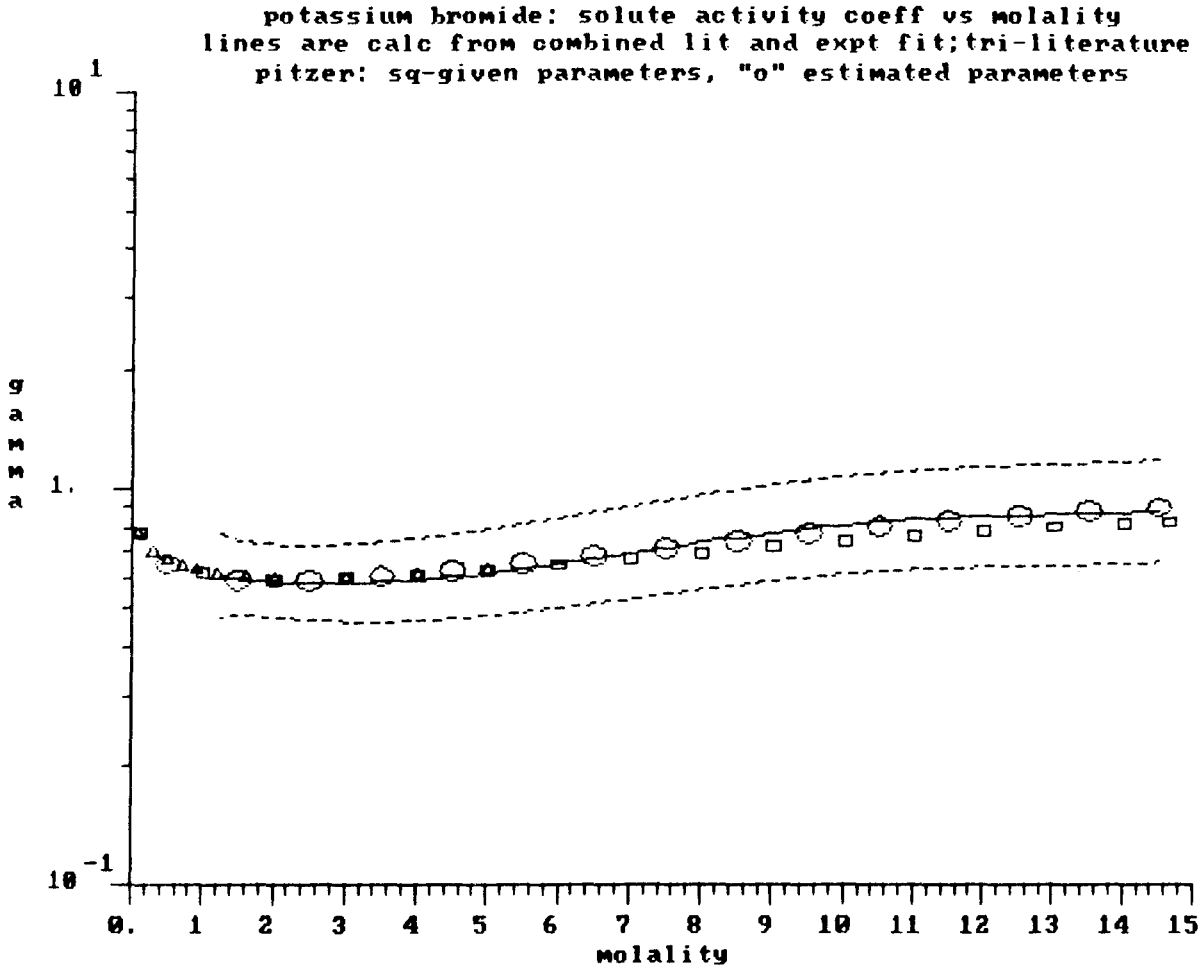
potassium bromide: solute activity coeff vs molality
lines are calc from combined lit and expt fit;tri-literature
pitzer: sq-given parameters, "o" estimated parameters
10 1
gamma
1.
10 -1
0. 1 2 3 4 5 6 7 8 9 10 11 12 13 14 15
molality

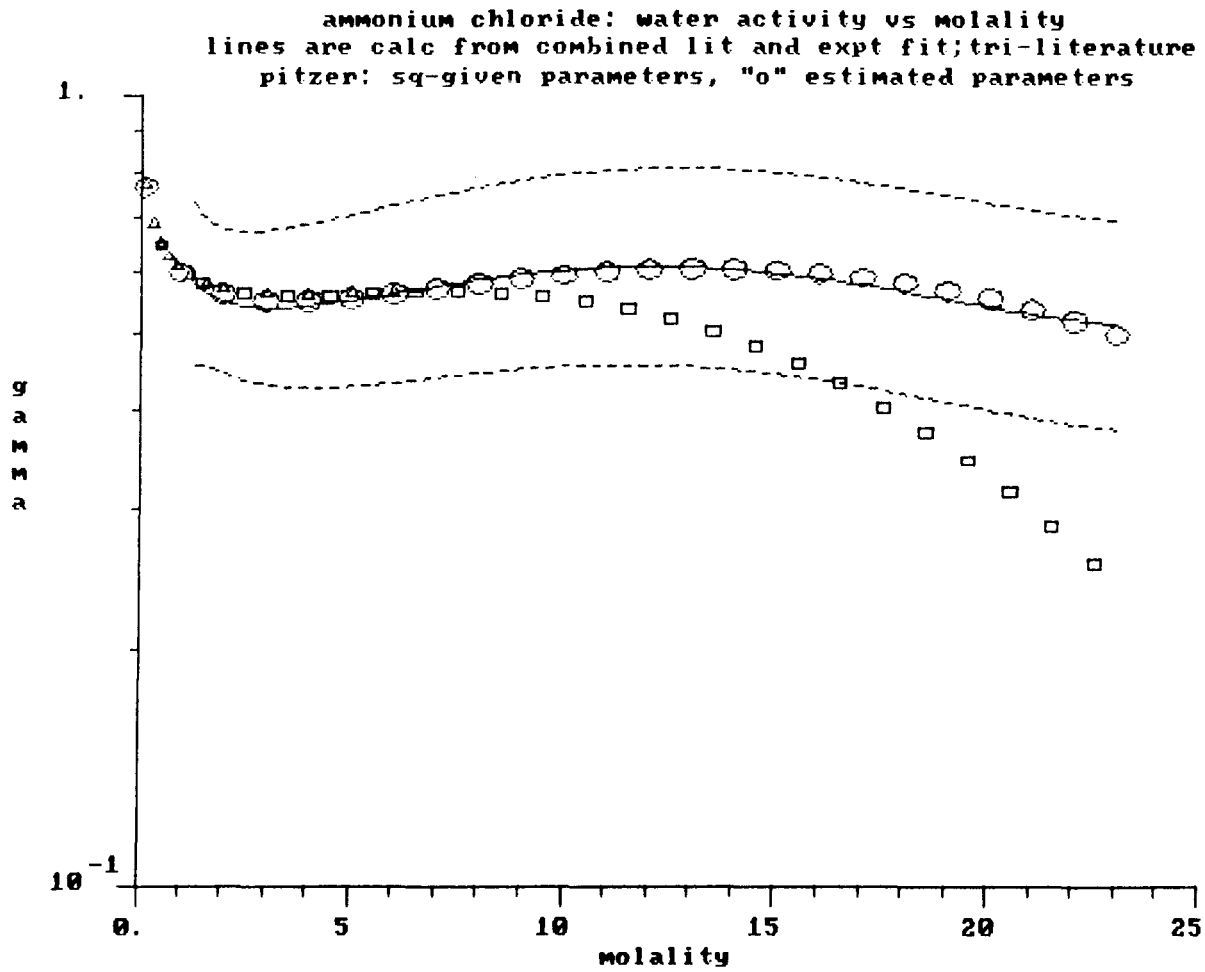
ammonium chloride: water activity vs molality
lines are calc from combined lit and expt fit;tri-literature
pitzer: sq-given parameters, "o" estimated parameters
1.
gamma
10 -1
0.
5
10
15
20
25
molality

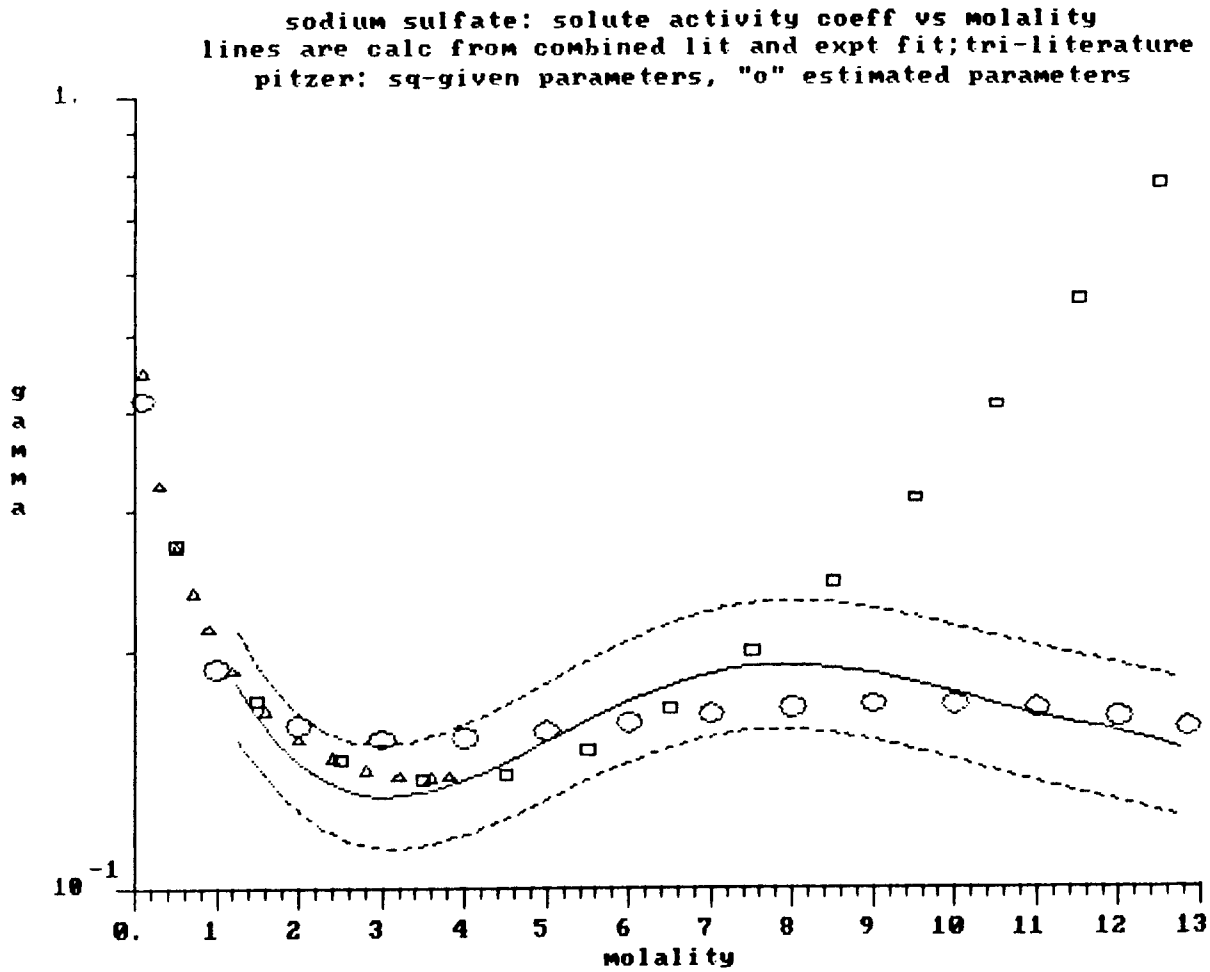
sodium sulfate: solute activity coeff vs molality
lines are calc from combined lit and expt fit;tri-literature
pitzer: sq-given parameters, "o" estimated parameters
1.
gamma
10^-1
0.
1
2
3
4
5
6
7
8
9
10
11
12
13
molality

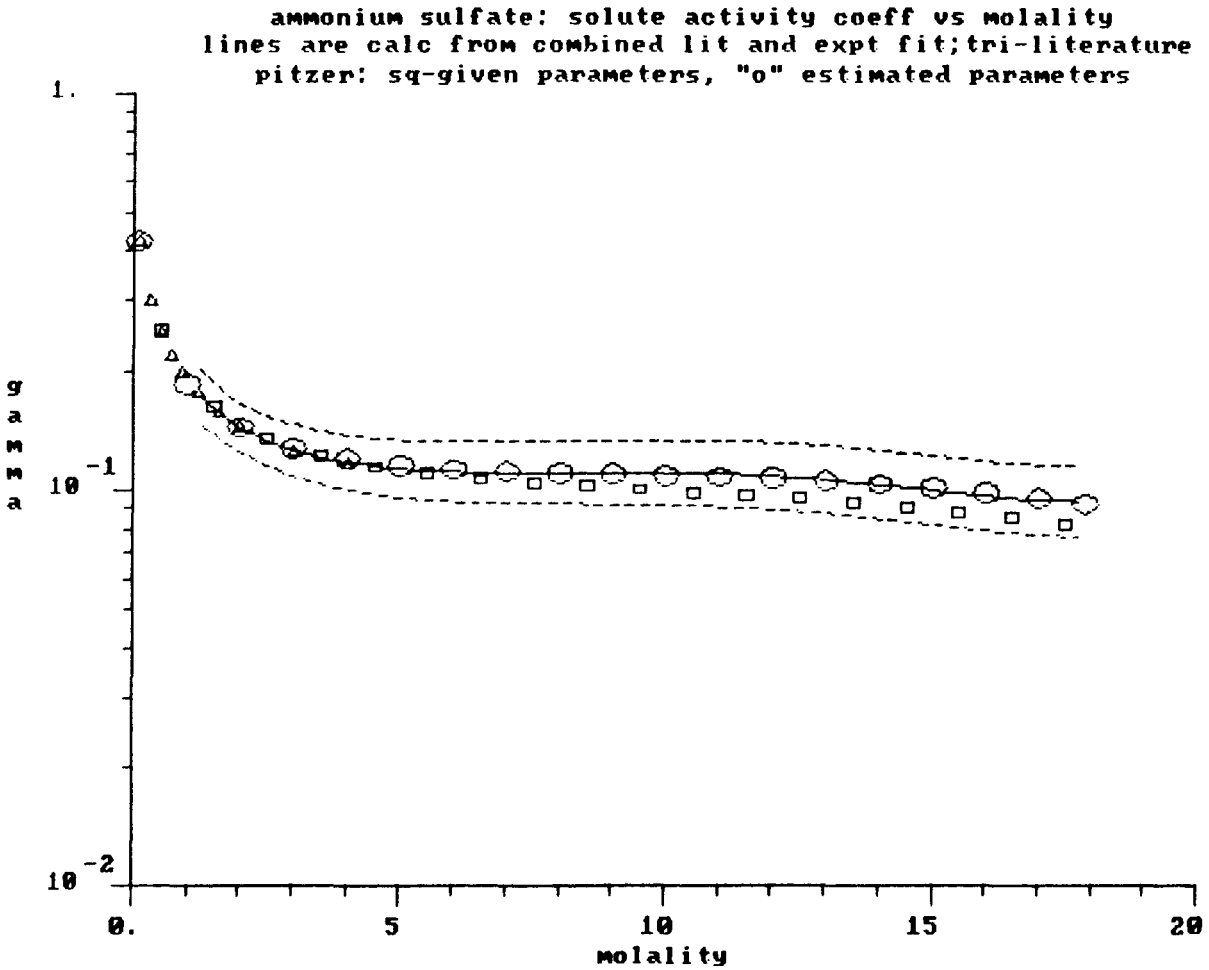
ammonium sulfate: solute activity coeff vs molality
lines are calc from combined lit and expt fit;tri-literature
pitzer: sq-given parameters, "o" estimated parameters
1.
gamma
10 -1
10 -2
0.
5
10
15
20
molality

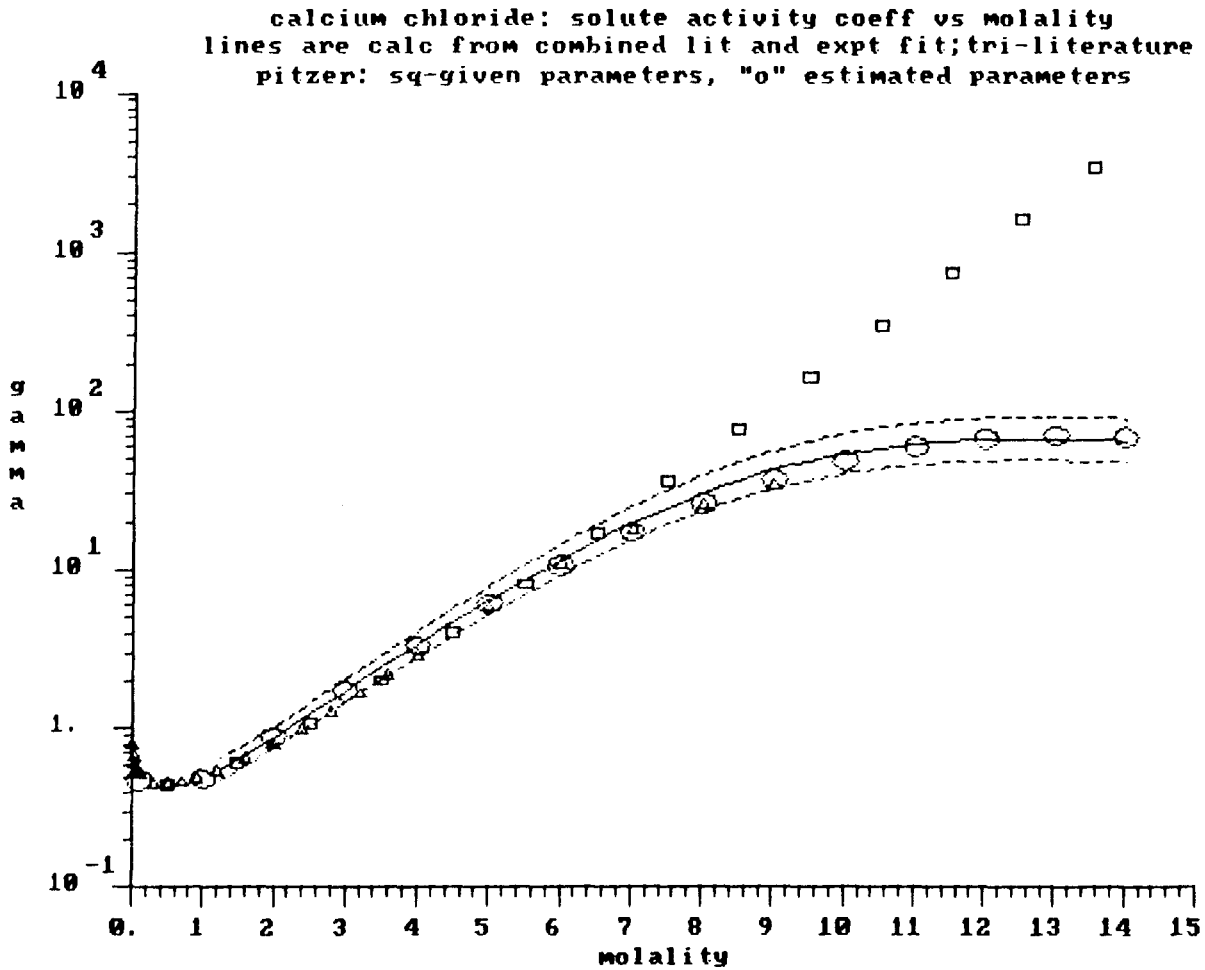
calcium chloride: solute activity coeff vs molality
lines are calc from combined lit and expt fit;tri-literature
pitzer: sq-given parameters, "o" estimated parameters
gamma
10^4
10^3
10^2
10^1
1.
10^-1
0.
1
2
3
4
5
6
7
8
9
10
11
12
13
14
15
molality

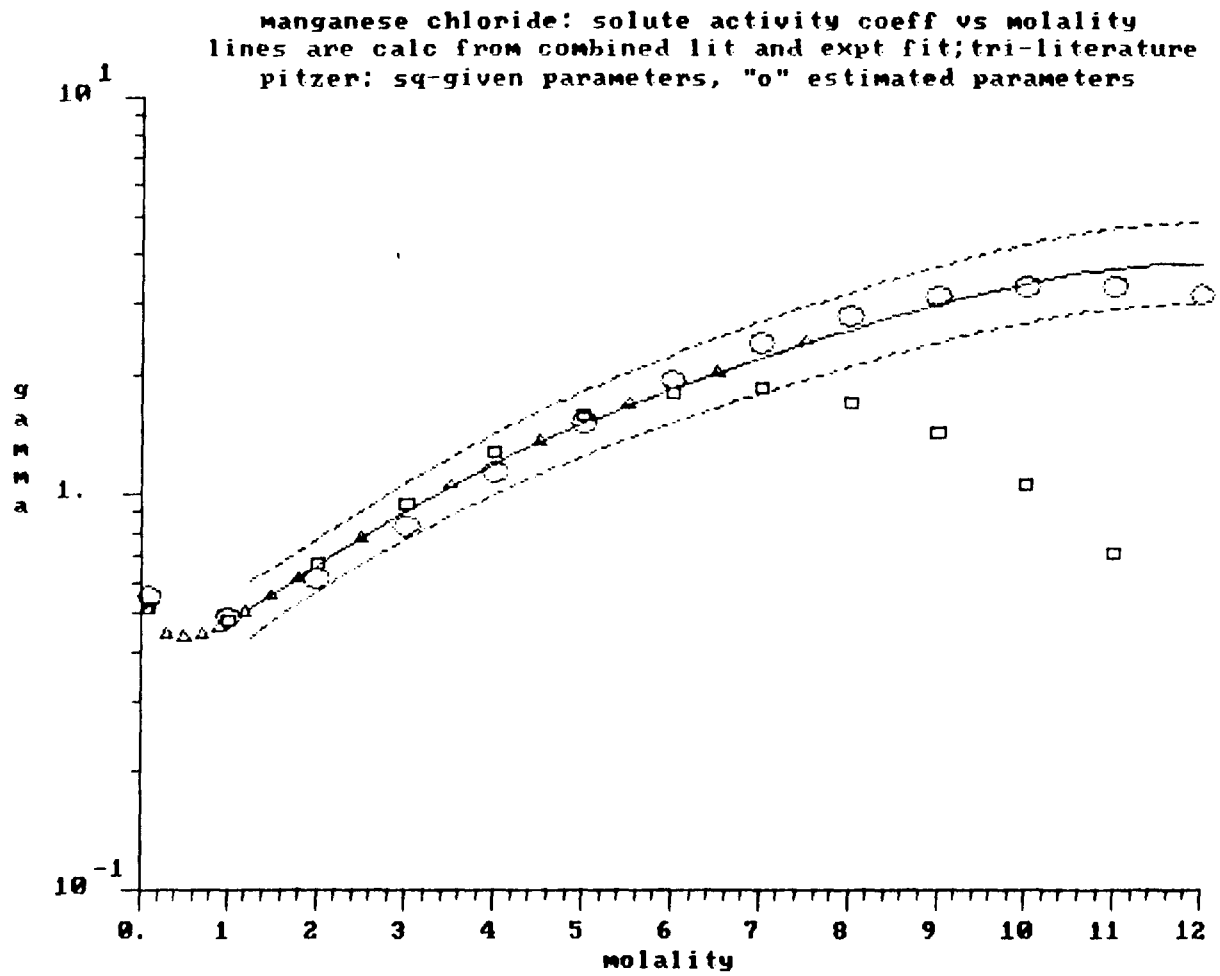
manganese chloride: solute activity coeff vs molality
lines are calc from combined lit and expt fit;tri-literature
pitzer: sq-given parameters, "o" estimated parameters
10 1
gamma
1.
10 -1
0. 1 2 3 4 5 6 7 8 9 10 11 12
molality

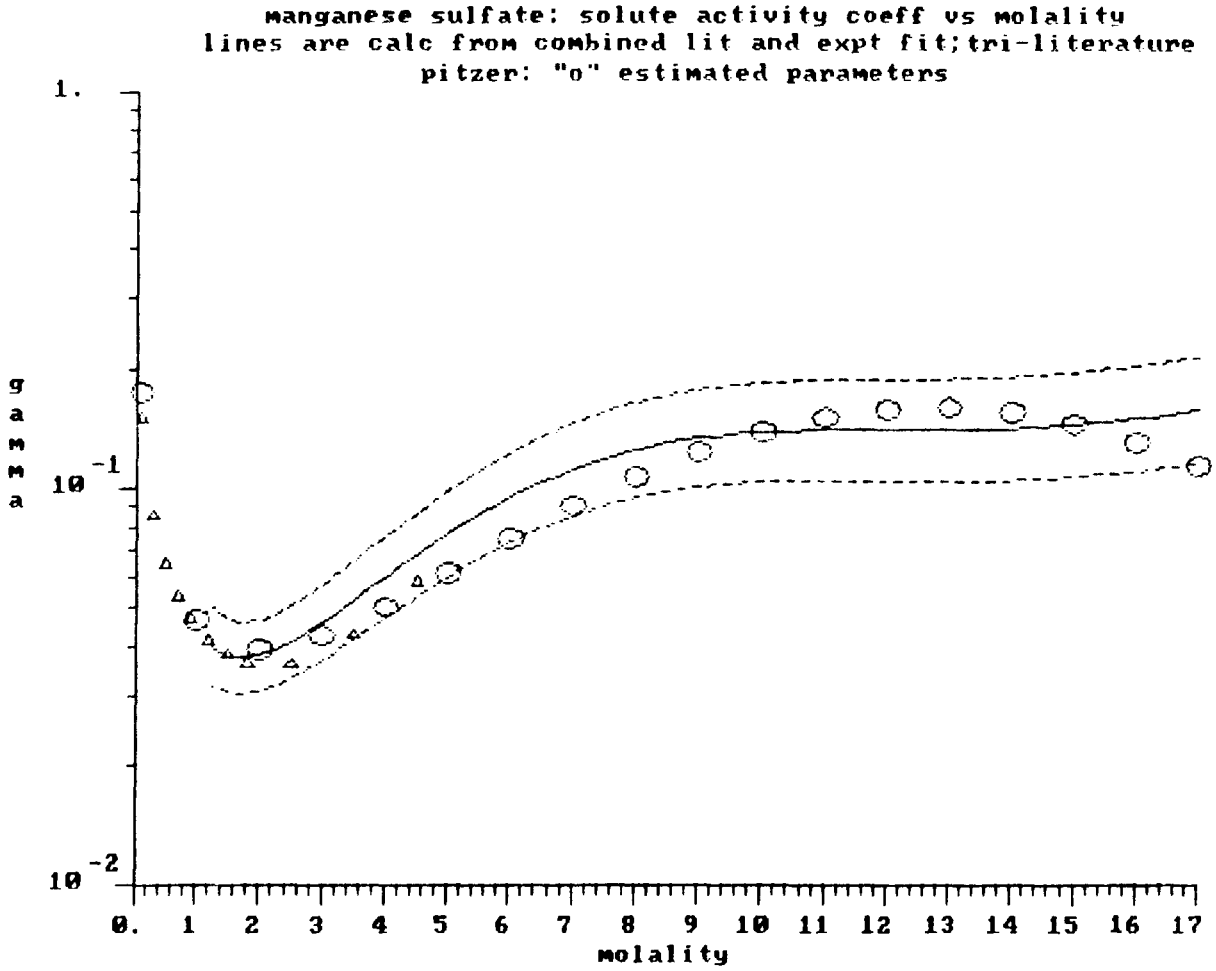
manganese sulfate: solute activity coeff vs molality
lines are calc from combined lit and expt fit;tri-literature
pitzer: "o" estimated parameters
1.
gamma
10 -1
10 -2
0. 1 2 3 4 5 6 7 8 9 10 11 12 13 14 15 16 17
molality

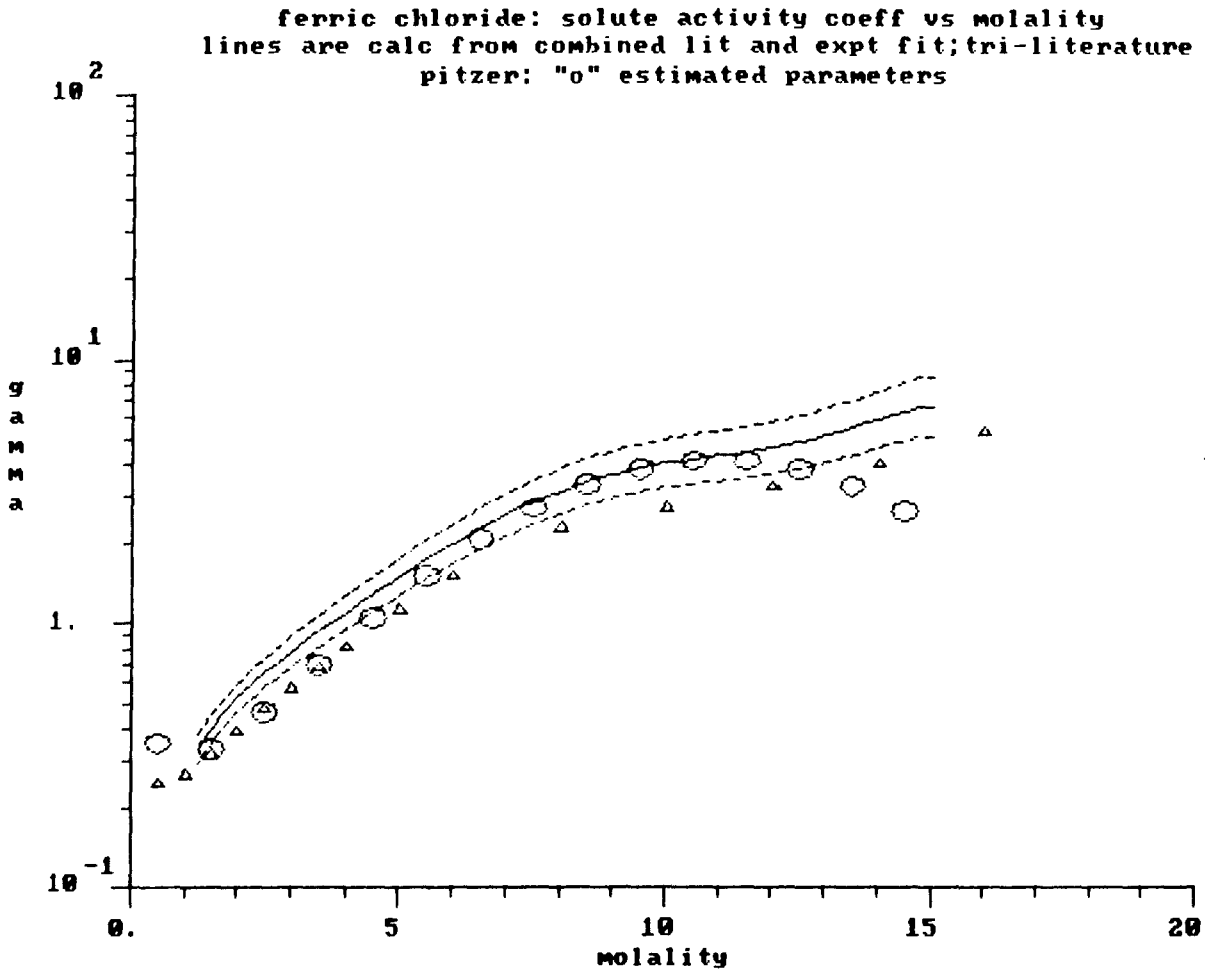
ferric chloride: solute activity coeff vs molality
lines are calc from combined lit and expt fit;tri-literature
pitzer: "o" estimated parameters
10 2
10 1
1.
10 -1
gamma
0.
5
10
15
20
molality

Appendix J: Plots of water activity as a function of molality in which experimental data is compared to the predictions of Pitzer's model

The figures in this appendix are analogous to those in Appendix I, the only difference being that the water activity instead of the solute activity coefficient is plotted as a function of molality.

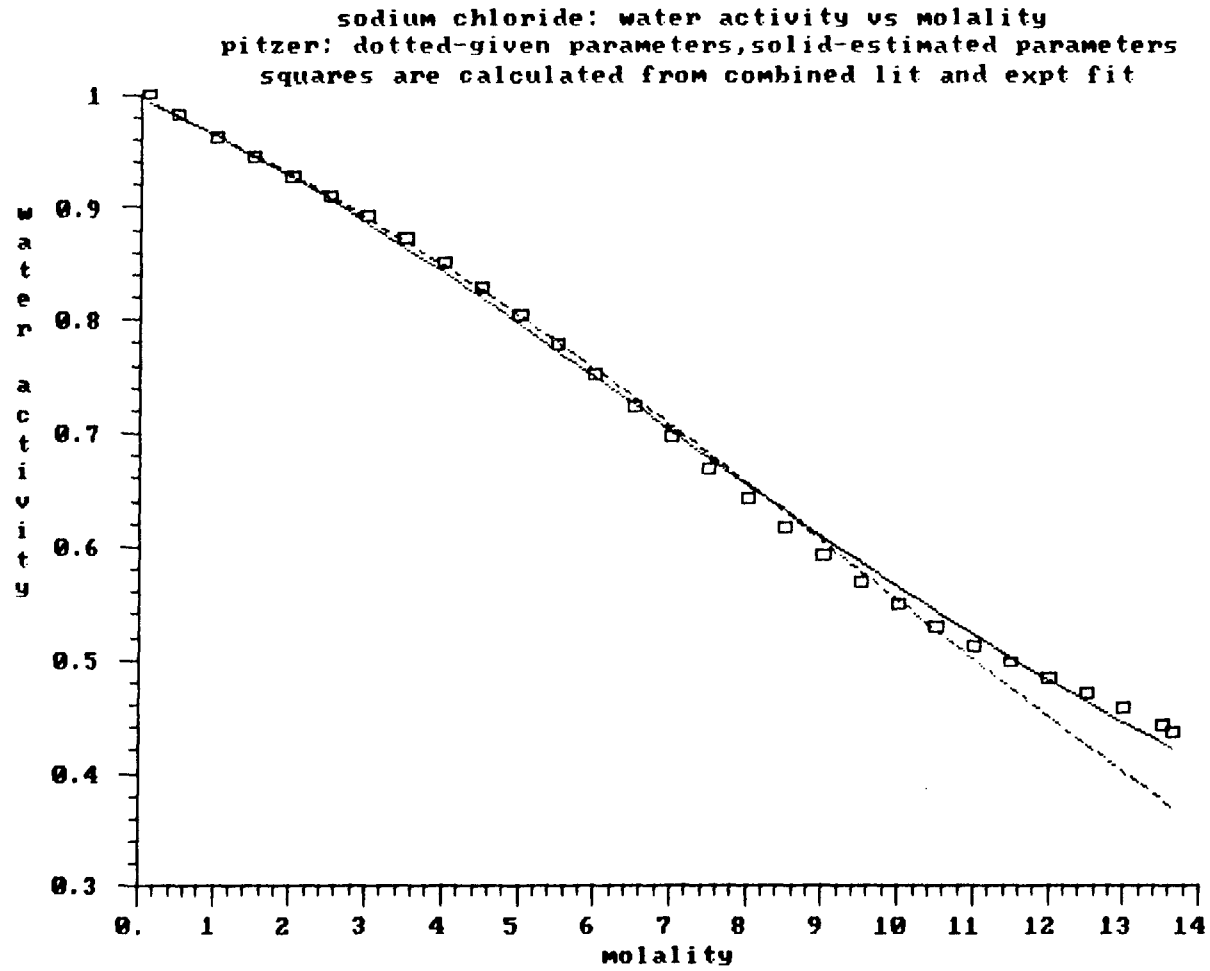
sodium chloride: water activity vs molality
pitzer: dotted-given parameters,solid-estimated parameters
squares are calculated from combined lit and expt fit
water activity
1
0.9
0.8
0.7
0.6
0.5
0.4
0.3
0.
1
2
3
4
5
6
7
8
9
10
11
12
13
14
molality

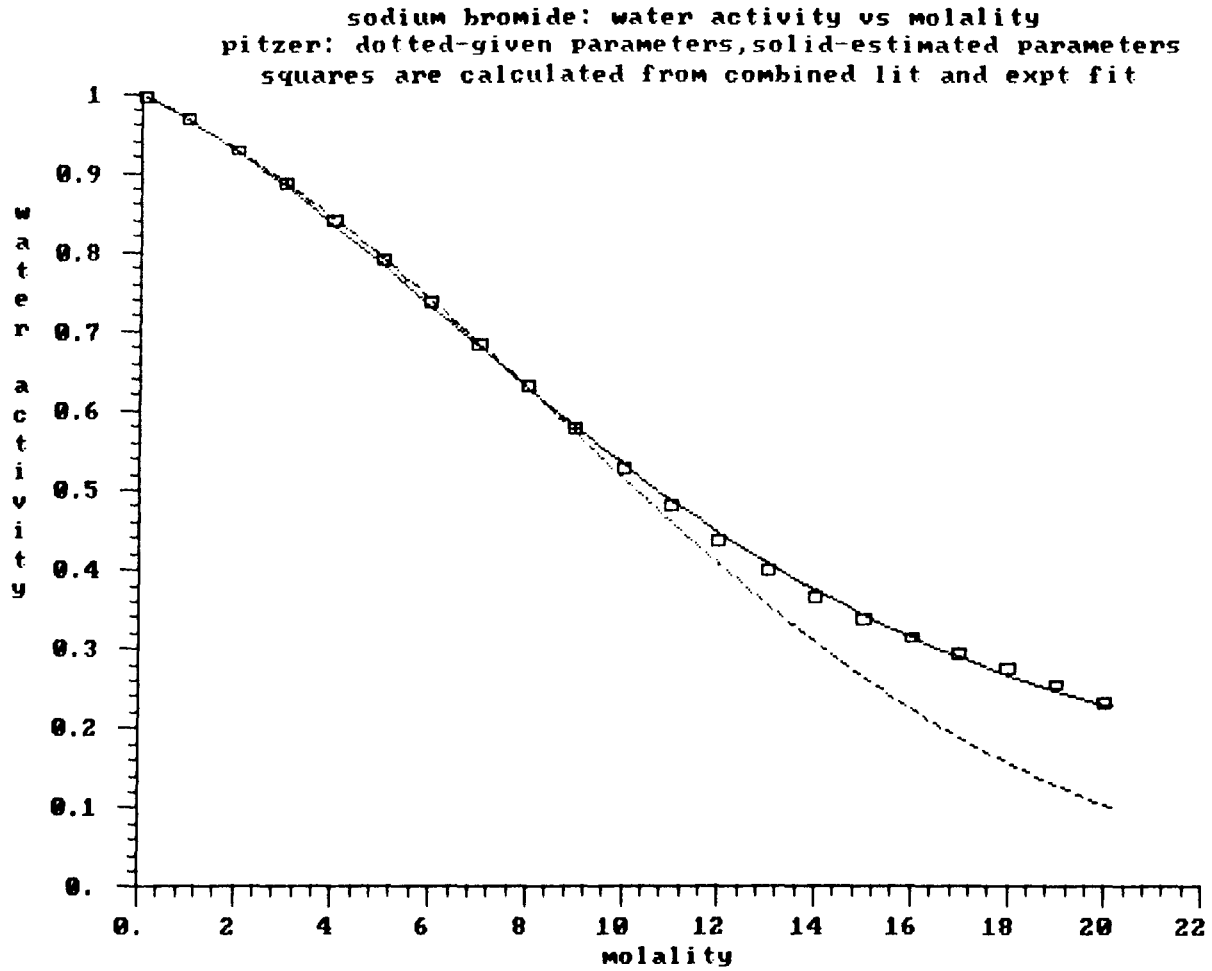
sodium bromide: water activity vs molality
pitzer: dotted-given parameters,solid-estimated parameters
squares are calculated from combined lit and expt fit
water activity
1
0.9
0.8
0.7
0.6
0.5
0.4
0.3
0.2
0.1
0.
0.
2
4
6
8
10
12
14
16
18
20
22
molality

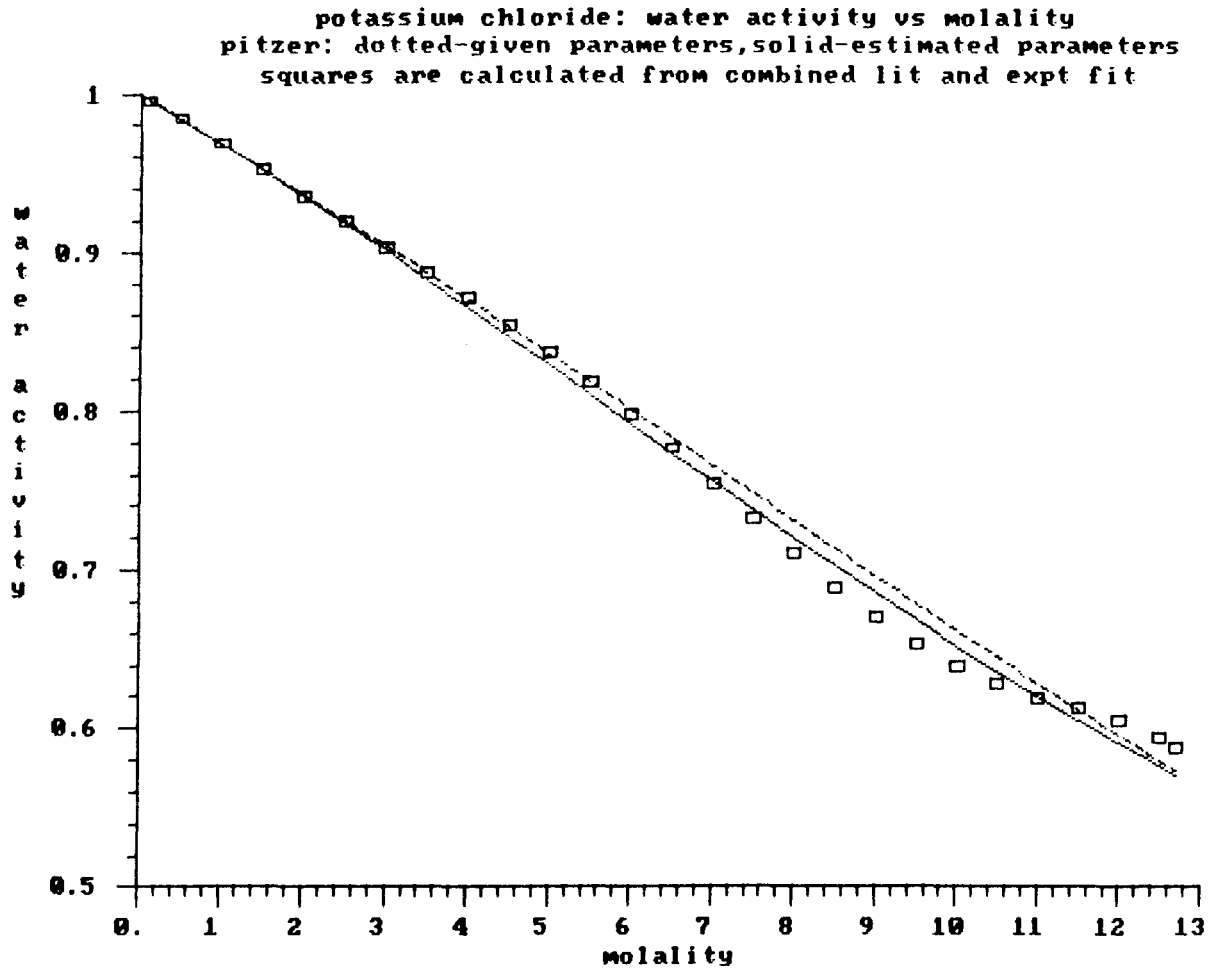
potassium chloride: water activity vs molality
pitzer: dotted-given parameters,solid-estimated parameters
squares are calculated from combined lit and expt fit
water activity
1
0.9
0.8
0.7
0.6
0.5
0.
1
2
3
4
5
6
7
8
9
10
11
12
13
molality

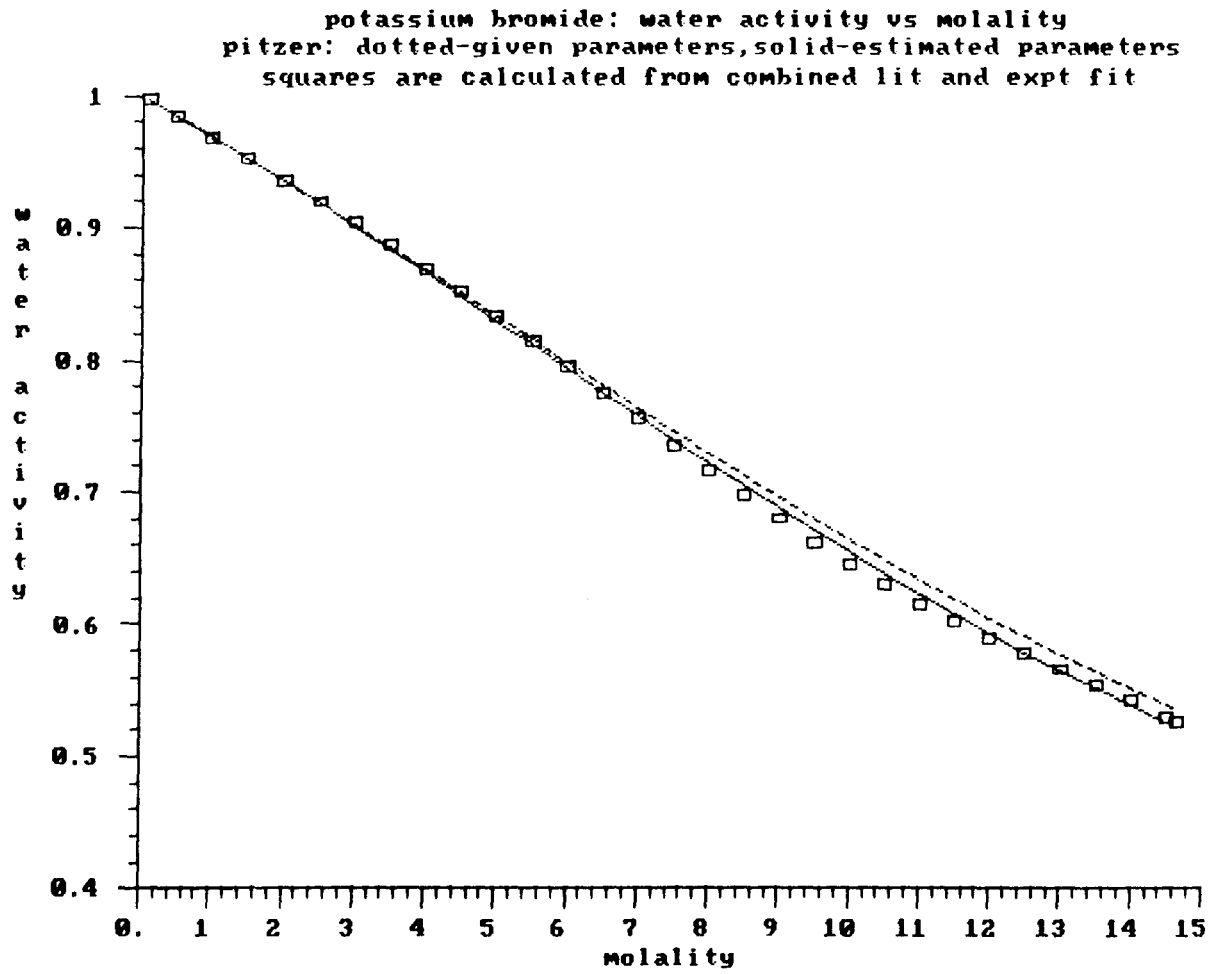
potassium bromide: water activity vs molality
pitzer: dotted-given parameters,solid-estimated parameters
squares are calculated from combined lit and expt fit
water activity
1
0.9
0.8
0.7
0.6
0.5
0.4
0.
1
2
3
4
5
6
7
8
9
10
11
12
13
14
15
molality

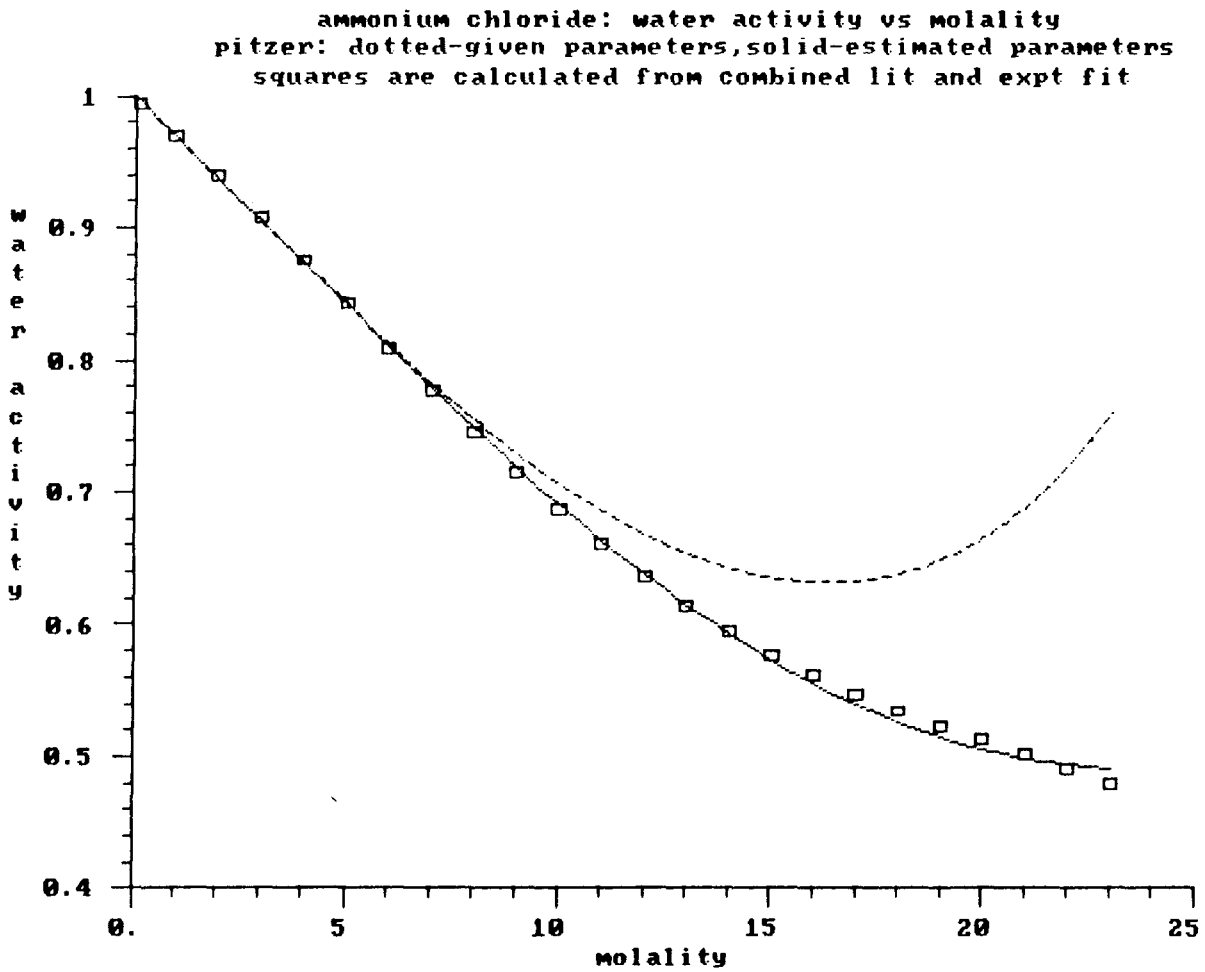
ammonium chloride: water activity vs molality
pitzer: dotted-given parameters,solid-estimated parameters
squares are calculated from combined lit and expt fit
water activity
1
0.9
0.8
0.7
0.6
0.5
0.4
0.
5
10
15
20
25
molality

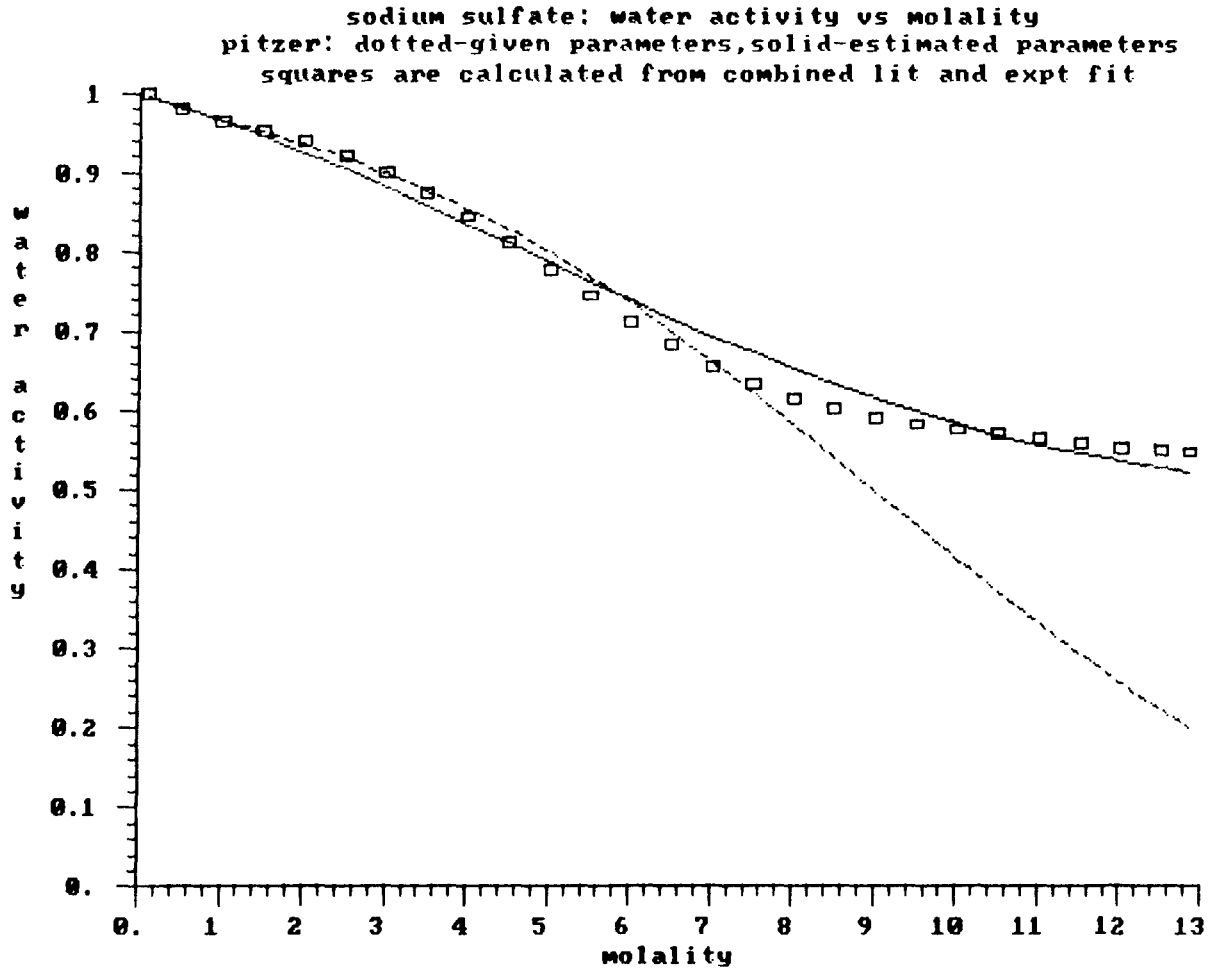
sodium sulfate: water activity vs molality
pitzer: dotted-given parameters,solid-estimated parameters
squares are calculated from combined lit and expt fit
water activity
1
0.9
0.8
0.7
0.6
0.5
0.4
0.3
0.2
0.1
0.
0.
1
2
3
4
5
6
7
8
9
10
11
12
13
molality

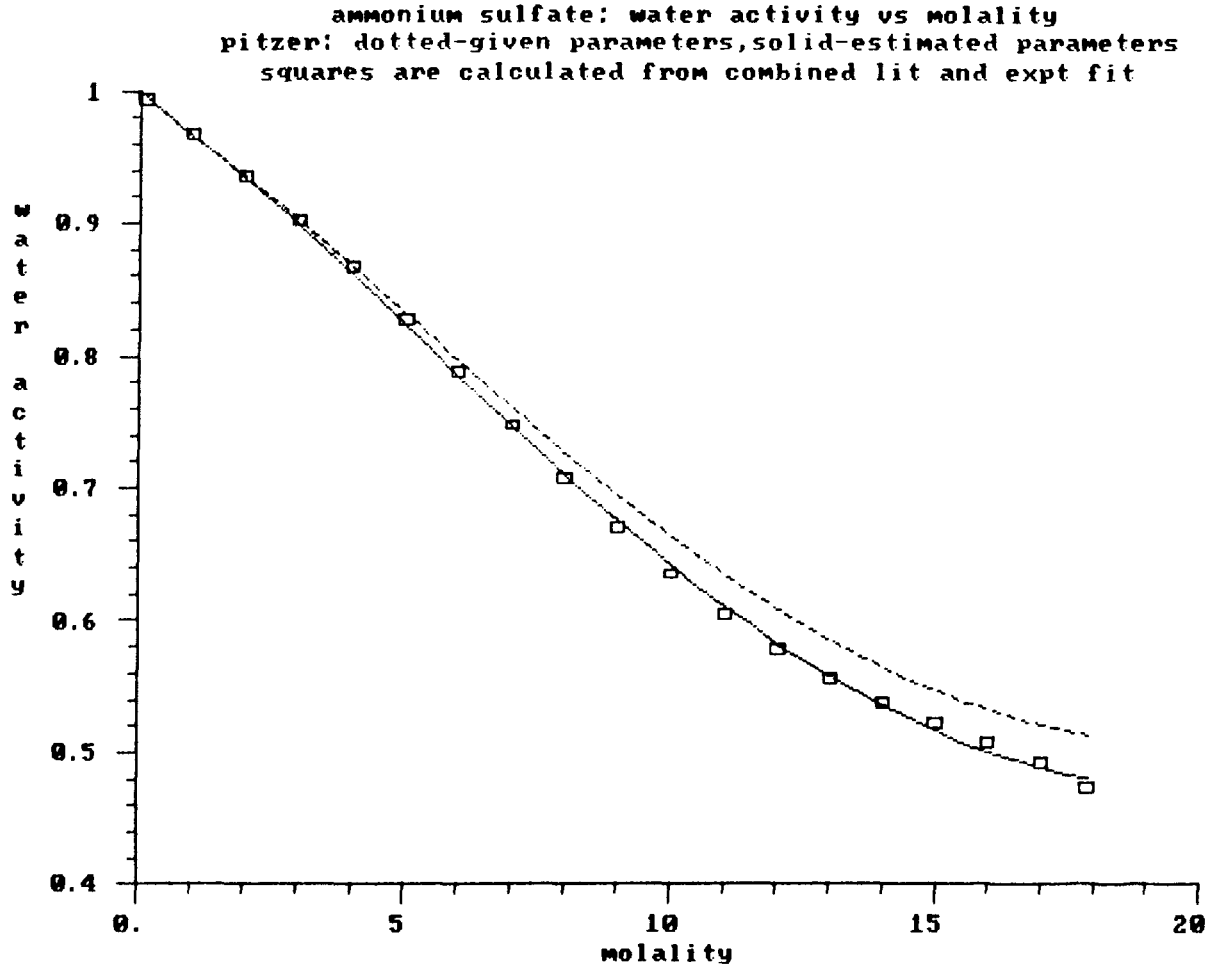
ammonium sulfate: water activity vs molality
pitzer: dotted-given parameters,solid-estimated parameters
squares are calculated from combined lit and expt fit
water activity
1
0.9
0.8
0.7
0.6
0.5
0.4
0.
5
10
15
20
molality

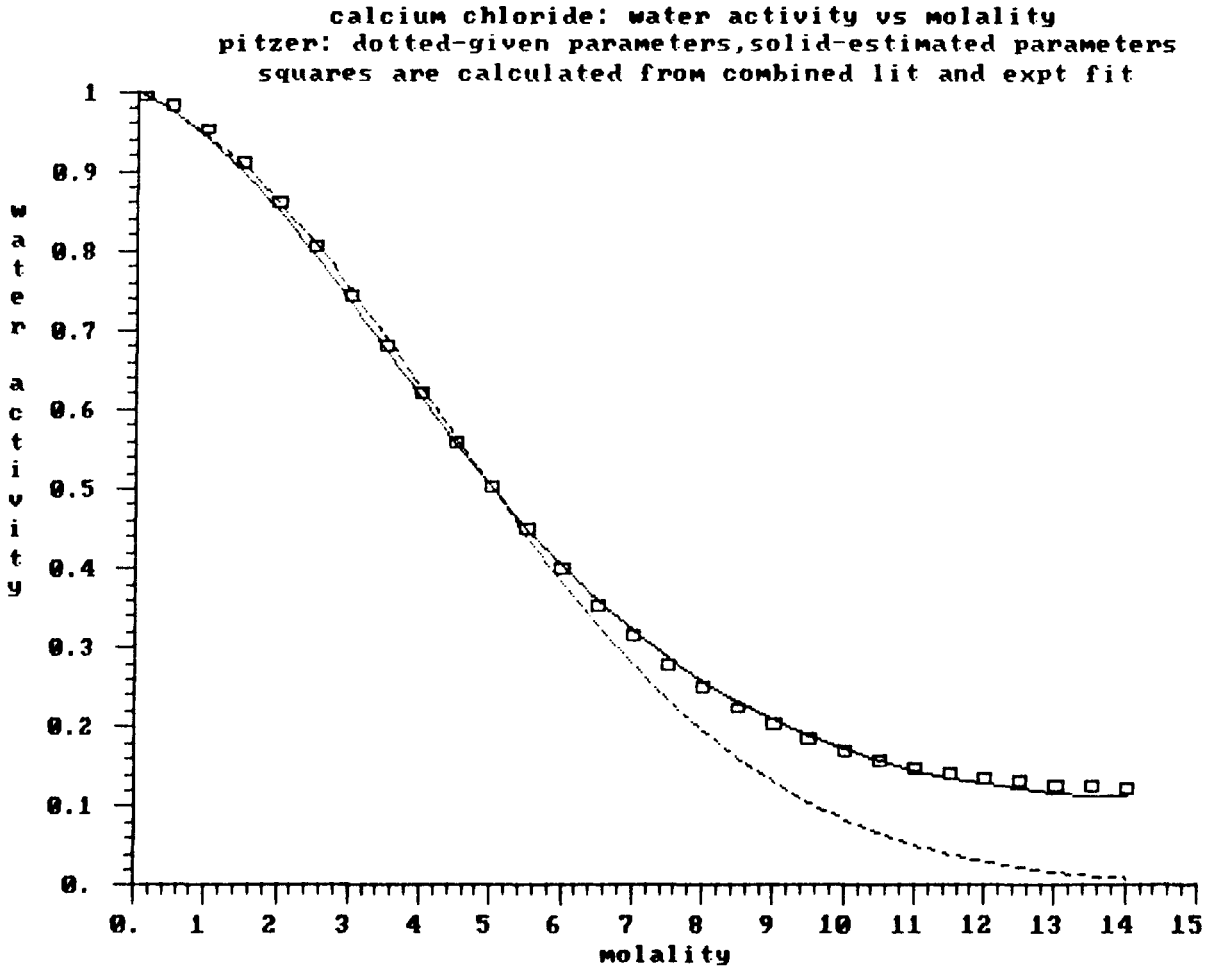
calcium chloride: water activity vs molality
pitzer: dotted-given parameters,solid-estimated parameters
squares are calculated from combined lit and expt fit
water activity
1
0.9
0.8
0.7
0.6
0.5
0.4
0.3
0.2
0.1
0.
0. 1 2 3 4 5 6 7 8 9 10 11 12 13 14 15
molality

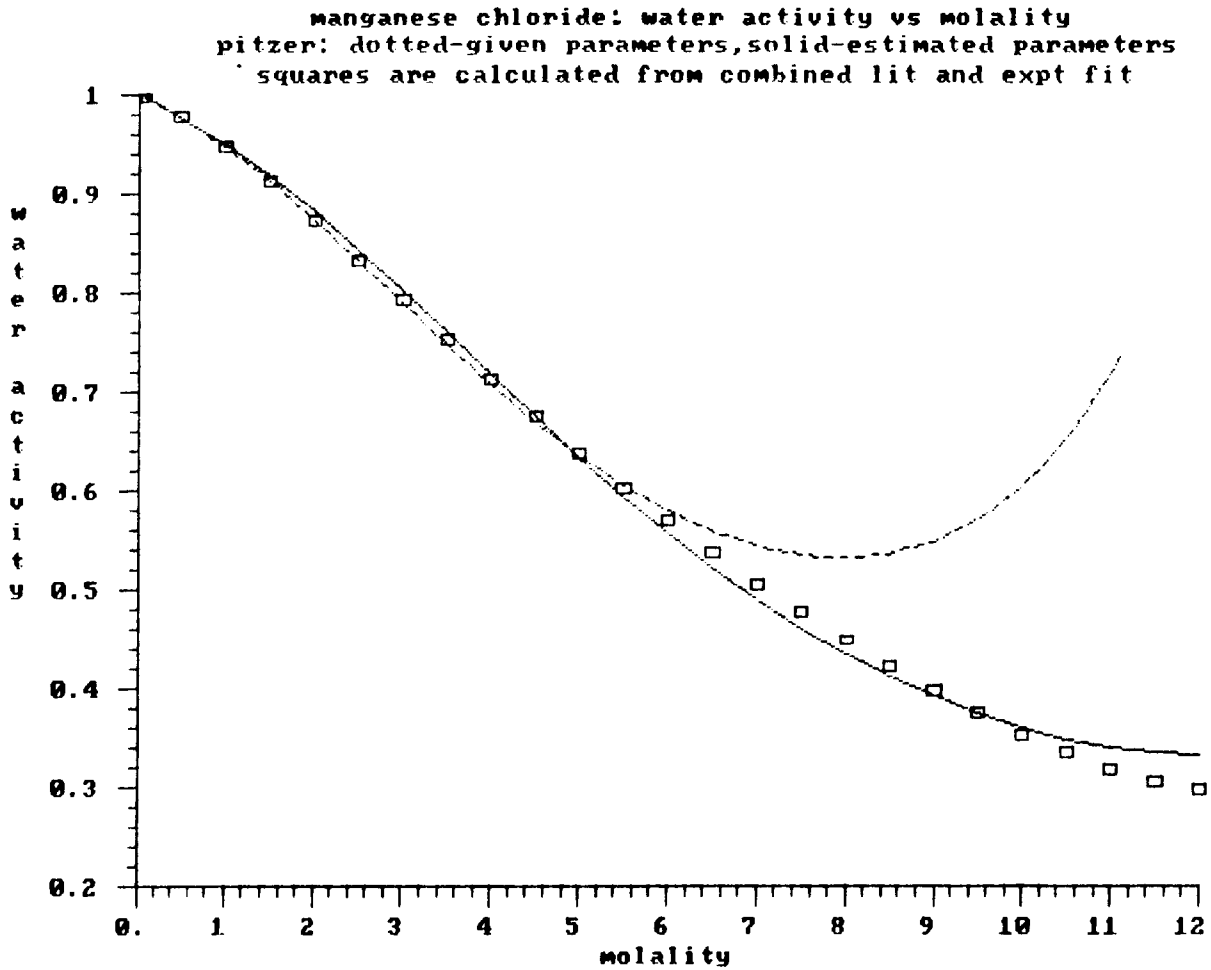
manganese chloride: water activity vs molality
pitzer: dotted-given parameters,solid-estimated parameters
squares are calculated from combined lit and expt fit
water activity
1
0.9
0.8
0.7
0.6
0.5
0.4
0.3
0.2
0.
1
2
3
4
5
6
7
8
9
10
11
12
molality

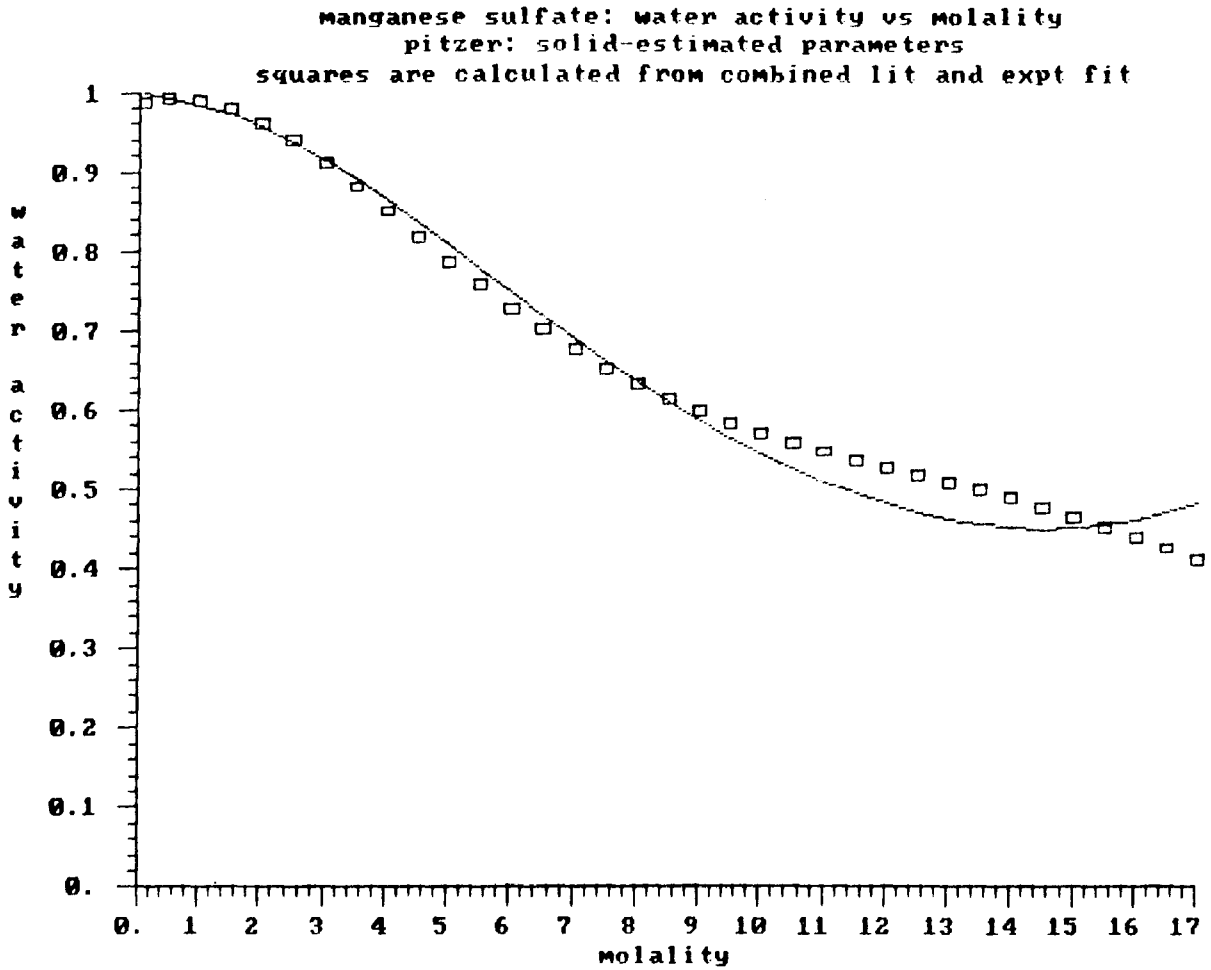
manganese sulfate: water activity vs molality
pitzer: solid-estimated parameters
squares are calculated from combined lit and expt fit
water activity
1
0.9
0.8
0.7
0.6
0.5
0.4
0.3
0.2
0.1
0.
0. 1 2 3 4 5 6 7 8 9 10 11 12 13 14 15 16 17
molality

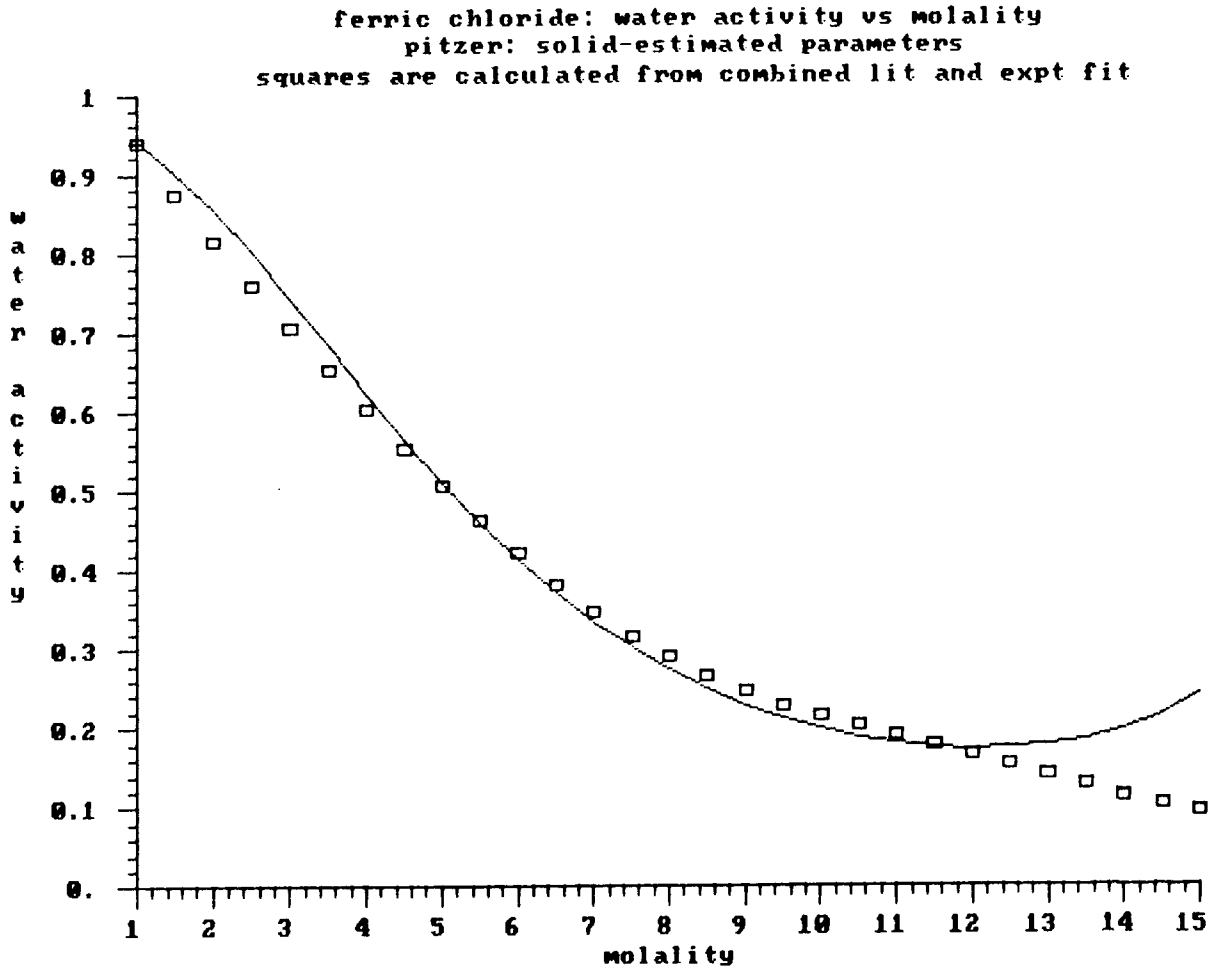
ferric chloride: water activity vs molality
pitzer: solid-estimated parameters
squares are calculated from combined lit and expt fit
water activity
1
0.9
0.8
0.7
0.6
0.5
0.4
0.3
0.2
0.1
0.
1
2
3
4
5
6
7
8
9
10
11
12
13
14
15
molality

Appendix K: Evaluation of the BET-based model of Robinson and Stokes for each of the single-electrolyte solutions studied

This appendix contains plots corresponding to Figure 22 of Chapter 1. For further explanation and discussion of these plots and the BET model, please refer to Chapter 1. In this appendix, "equation 11" refers equation 17 of Chapter 1.

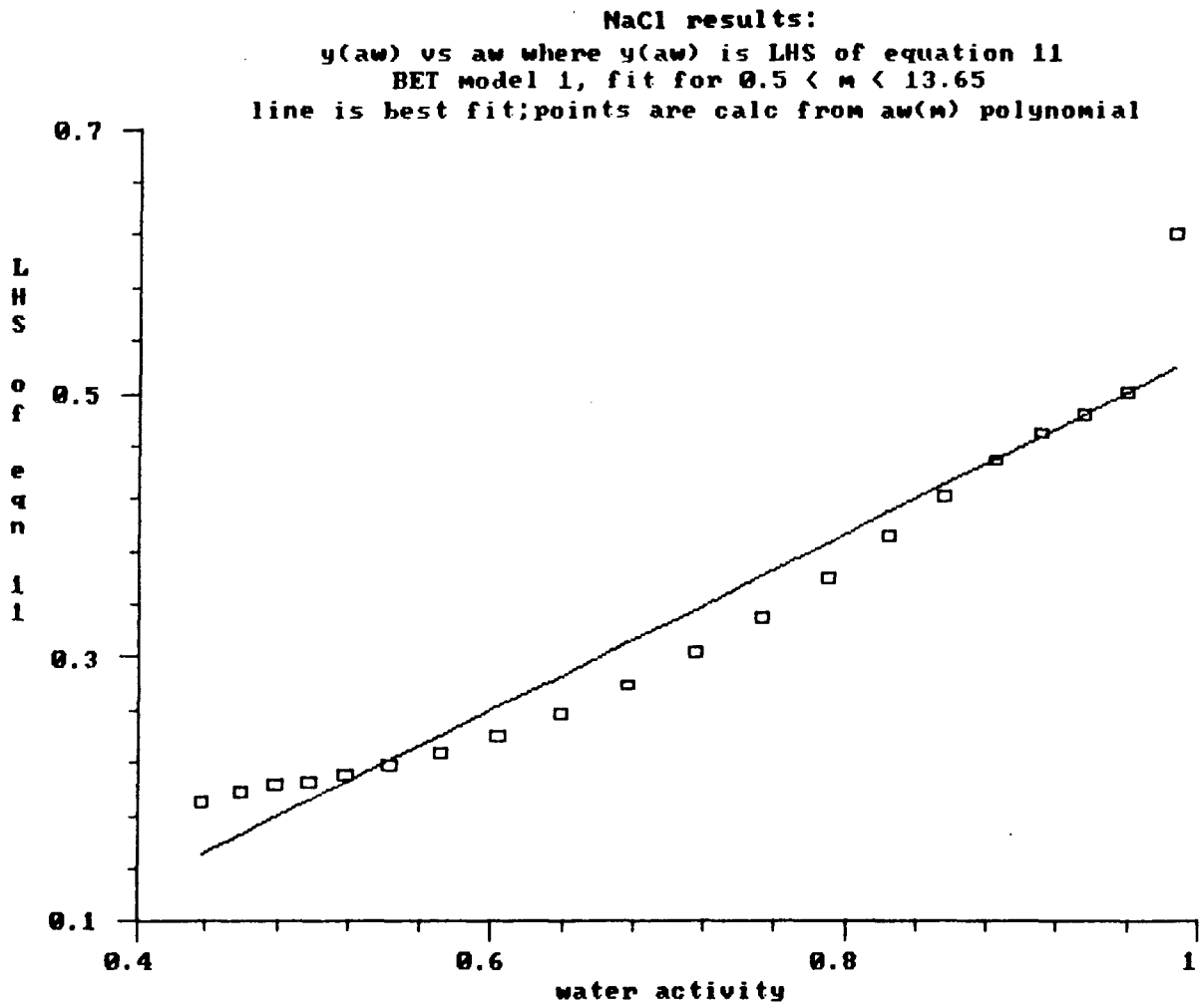
NaCl results:
y(aw) vs aw where y(aw) is LHS of equation 11
BET model 1, fit for 0.5 < m < 13.65
line is best fit;points are calc from aw(m) polynomial
0.7
0.5
0.3
0.1
LHS of eqn 11
0.4
0.6
0.8
1
water activity

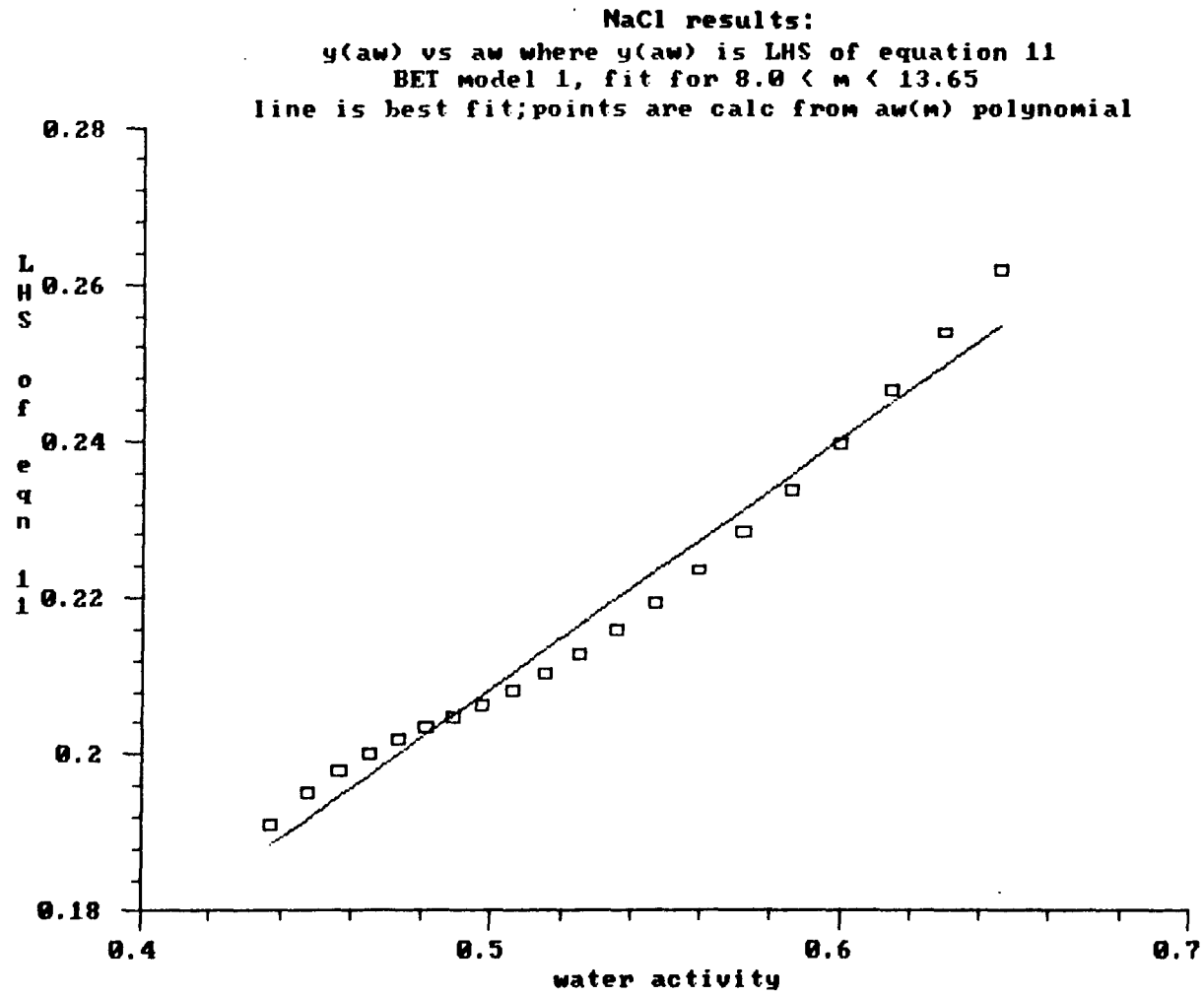
NaCl results:
y(aw) vs aw where y(aw) is LHS of equation 11
BET model 1, fit for 8.0 < m < 13.65
line is best fit;points are calc from aw(m) polynomial
LHS of eqn 11
0.28
0.26
0.24
0.22
0.2
0.18
0.4
0.5
0.6
0.7
water activity

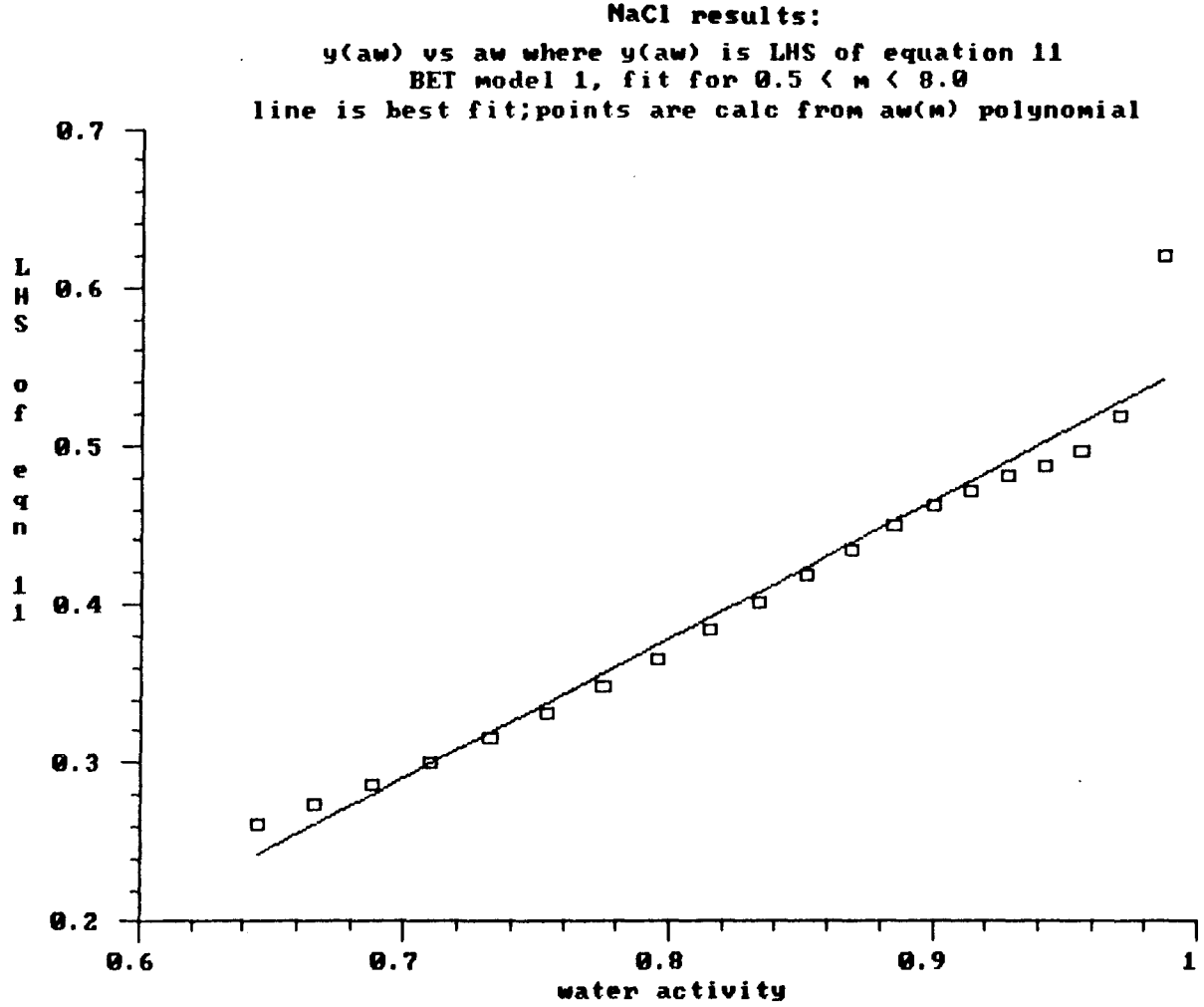
NaCl results:
y(aw) vs aw where y(aw) is LHS of equation 11
BET model 1, fit for 0.5 < m < 8.0
line is best fit;points are calc from aw(m) polynomial
LHS of eqn 11
0.7
0.6
0.5
0.4
0.3
0.2
0.6
0.7
0.8
0.9
1
water activity

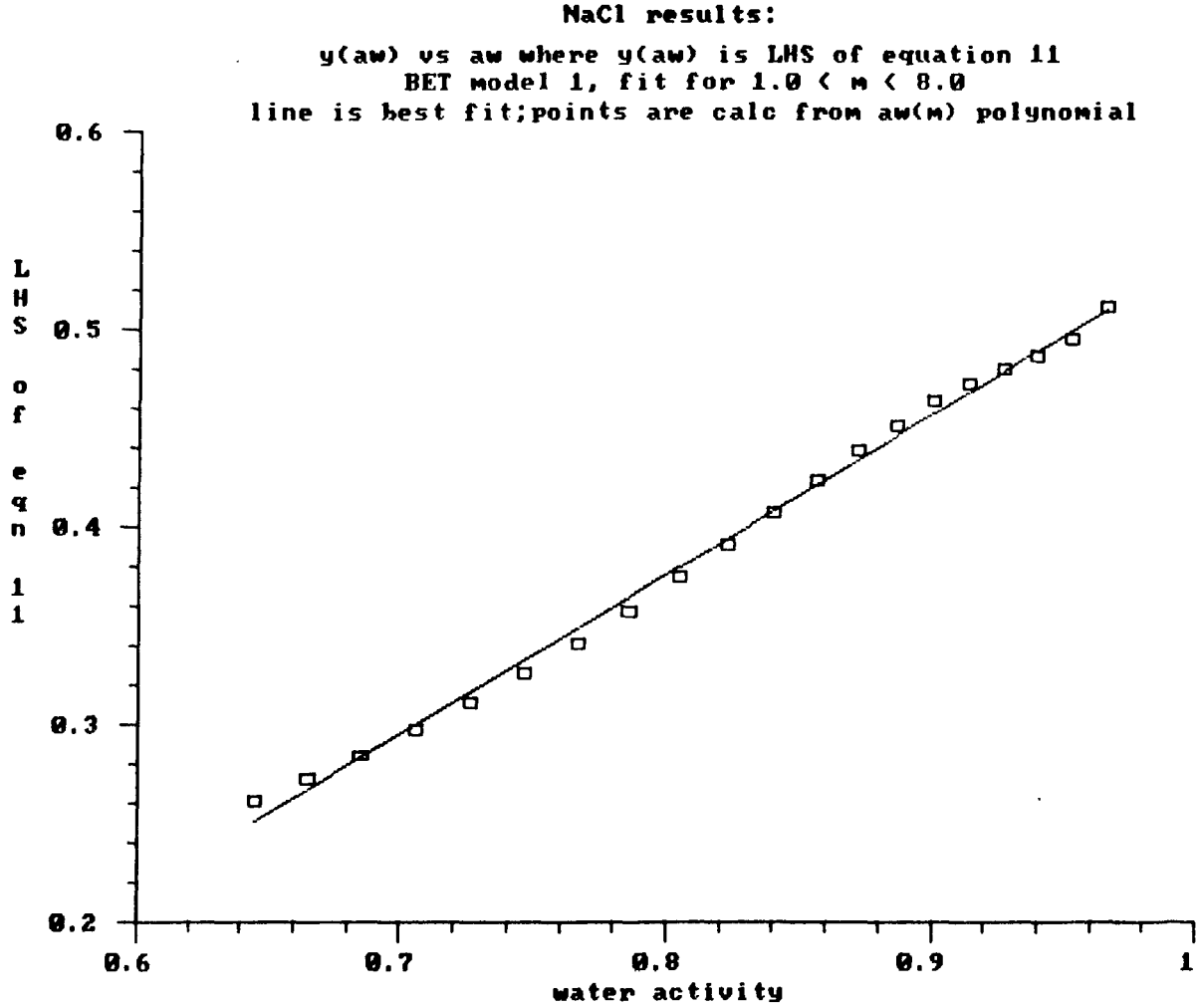
NaCl results:
y(aw) vs aw where y(aw) is LHS of equation 11
BET model 1, fit for 1.0 < m < 8.0
line is best fit;points are calc from aw(m) polynomial
LHS of eqn 11
0.6
0.5
0.4
0.3
0.2
0.6
0.7
0.8
0.9
1
water activity

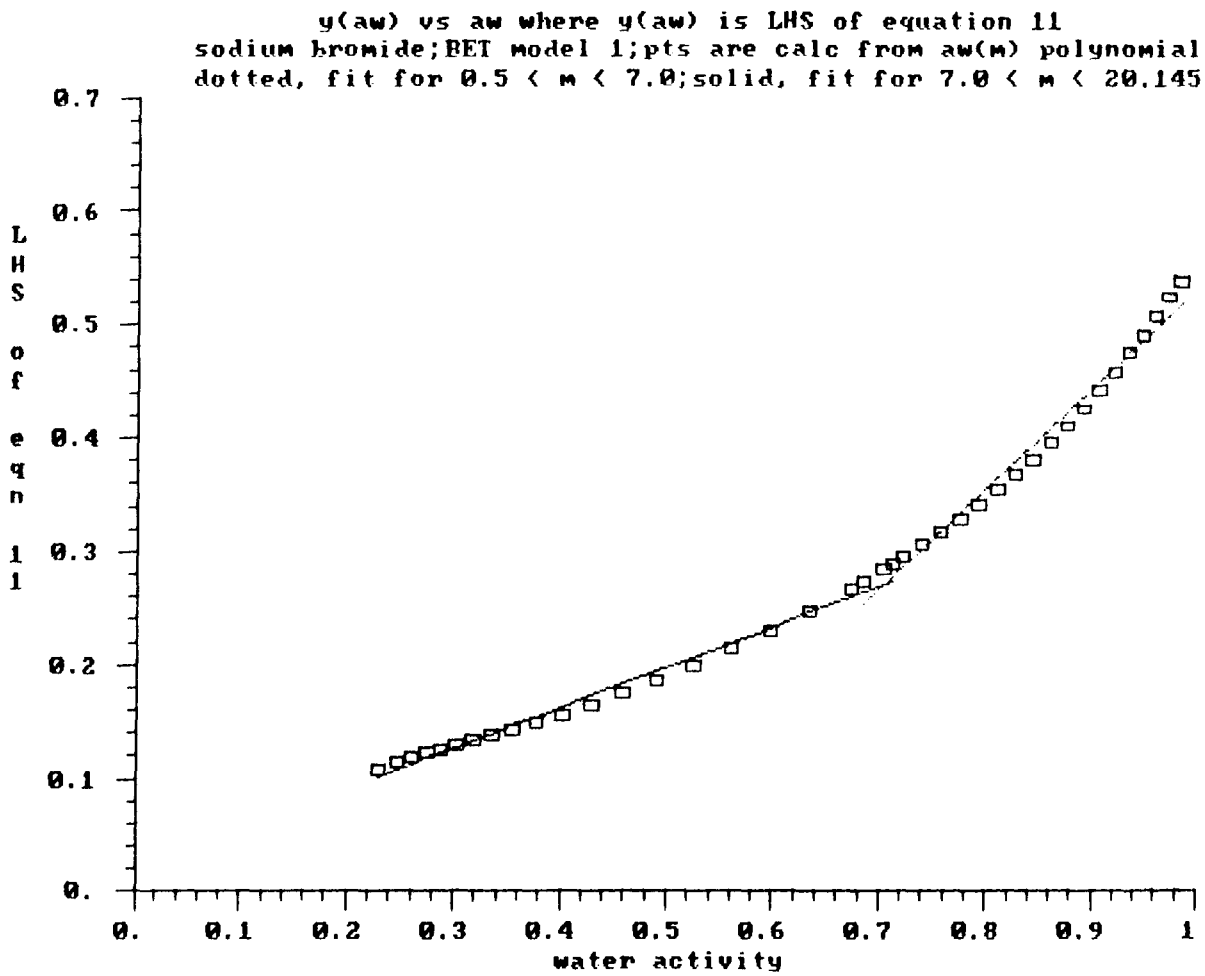
y(aw) vs aw where y(aw) is LHS of equation 11
sodium bromide;BET model 1;pts are calc from aw(m) polynomial
dotted, fit for 0.5 < m < 7.0;solid, fit for 7.0 < m < 20.145
LHS of eqn 11
0.7
0.6
0.5
0.4
0.3
0.2
0.1
0.
0.
0.1
0.2
0.3
0.4
0.5
0.6
0.7
0.8
0.9
1
water activity

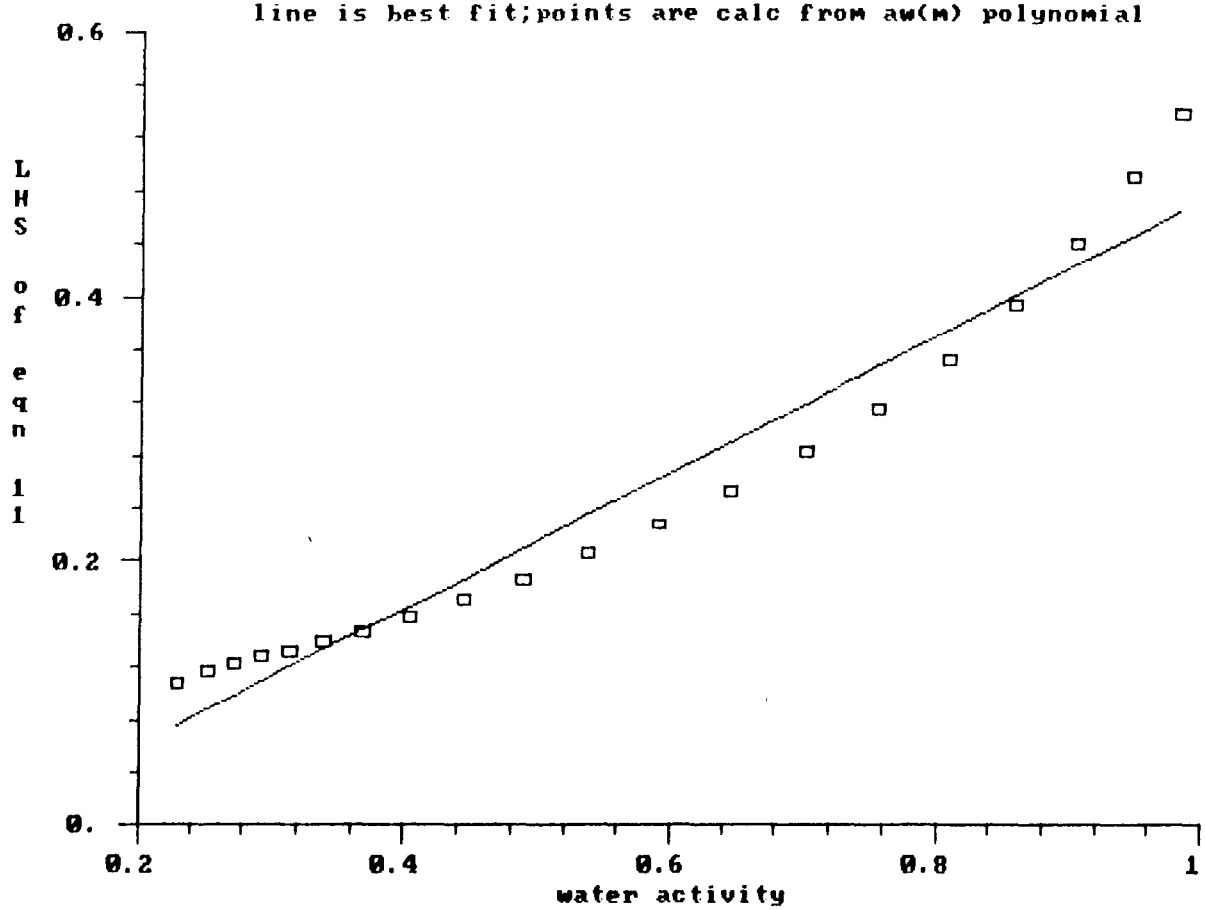
y(aw) vs aw where y(aw) is LHS of equation 11
sodium bromide; BET model 1, fit for 0.5 < m < 20.145
line is best fit;points are calc from aw(m) polynomial
LHS of eqn 11
0.6
0.4
0.2
0.
0.2
0.4
0.6
0.8
1
water activity

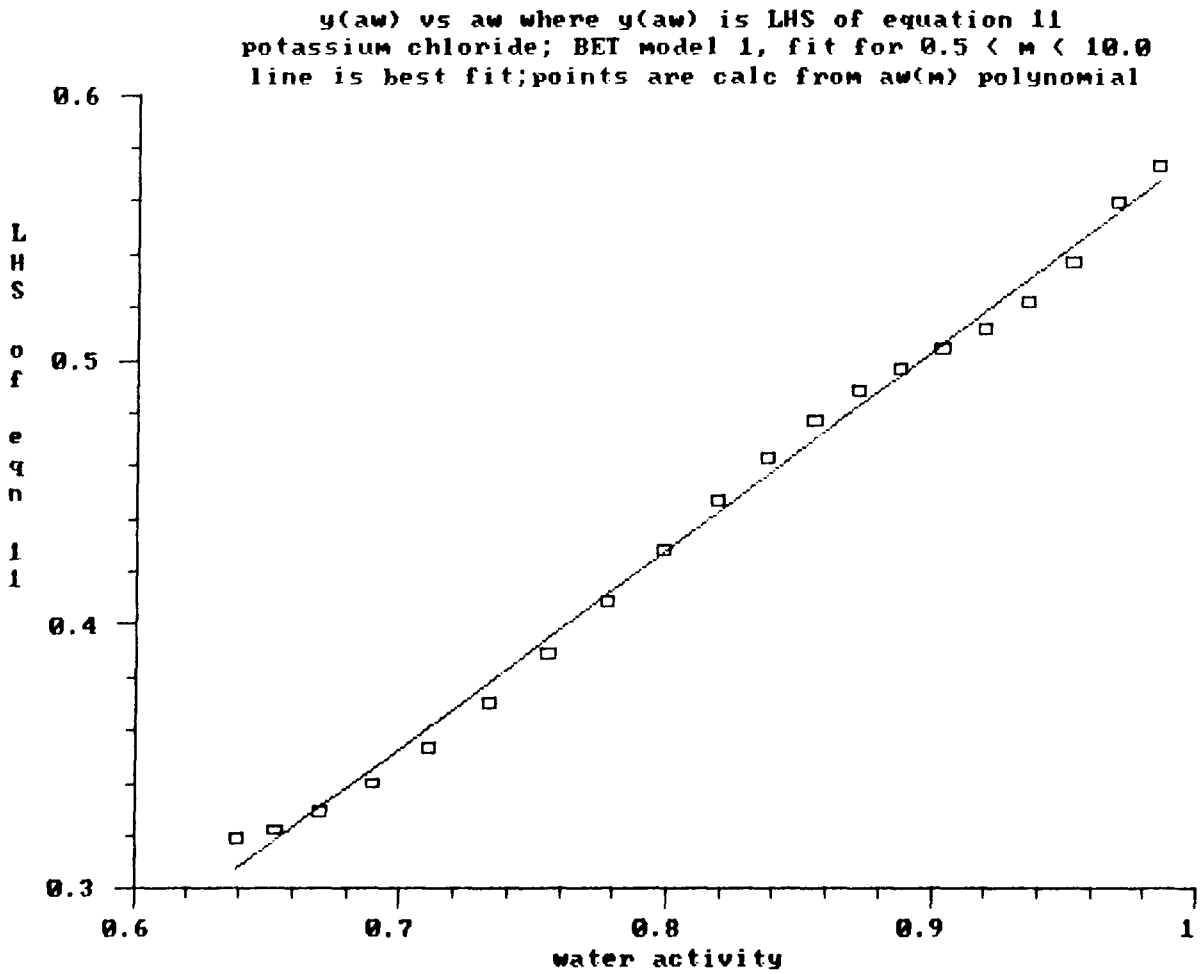
y(aw) vs aw where y(aw) is LHS of equation 11
potassium chloride; BET model 1, fit for 0.5 < m < 10.0
line is best fit;points are calc from aw(m) polynomial
LHS of eqn 11
0.6
0.5
0.4
0.3
0.6
0.7
0.8
0.9
1
water activity

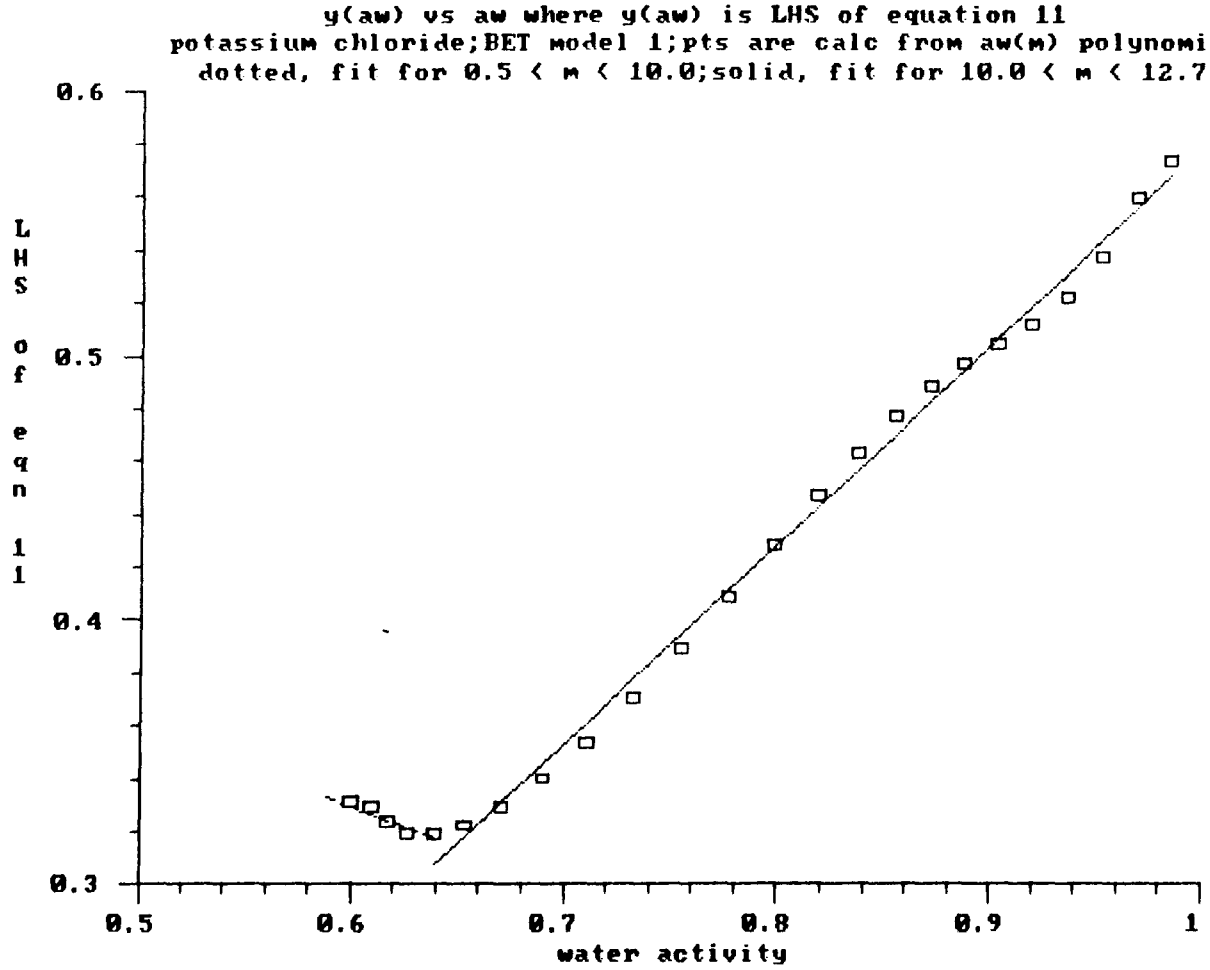
y(aw) vs aw where y(aw) is LHS of equation 11
potassium chloride;BET model 1;pts are calc from aw(m) polynomial
dotted, fit for 0.5 < m < 10.0;solid, fit for 10.0 < m < 12.7
LHS of eqn 11
0.6
0.5
0.4
0.3
0.5
0.6
0.7
0.8
0.9
1
water activity

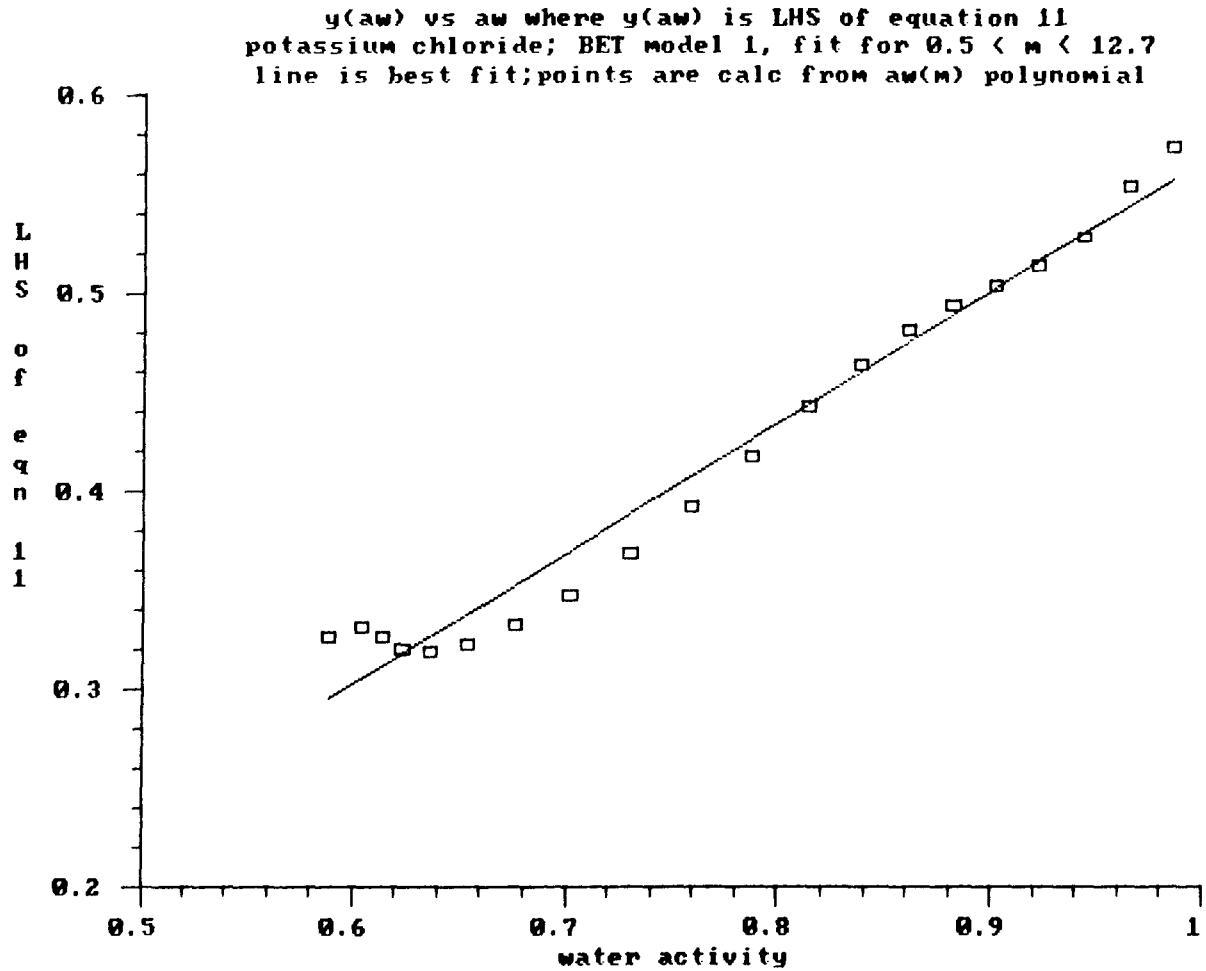
y(aw) vs aw where y(aw) is LHS of equation 11
potassium chloride; BET model 1, fit for 0.5 < m < 12.7
line is best fit;points are calc from aw(m) polynomial
LHS of eqn 11
0.6
0.5
0.4
0.3
0.2
0.5
0.6
0.7
0.8
0.9
1
water activity

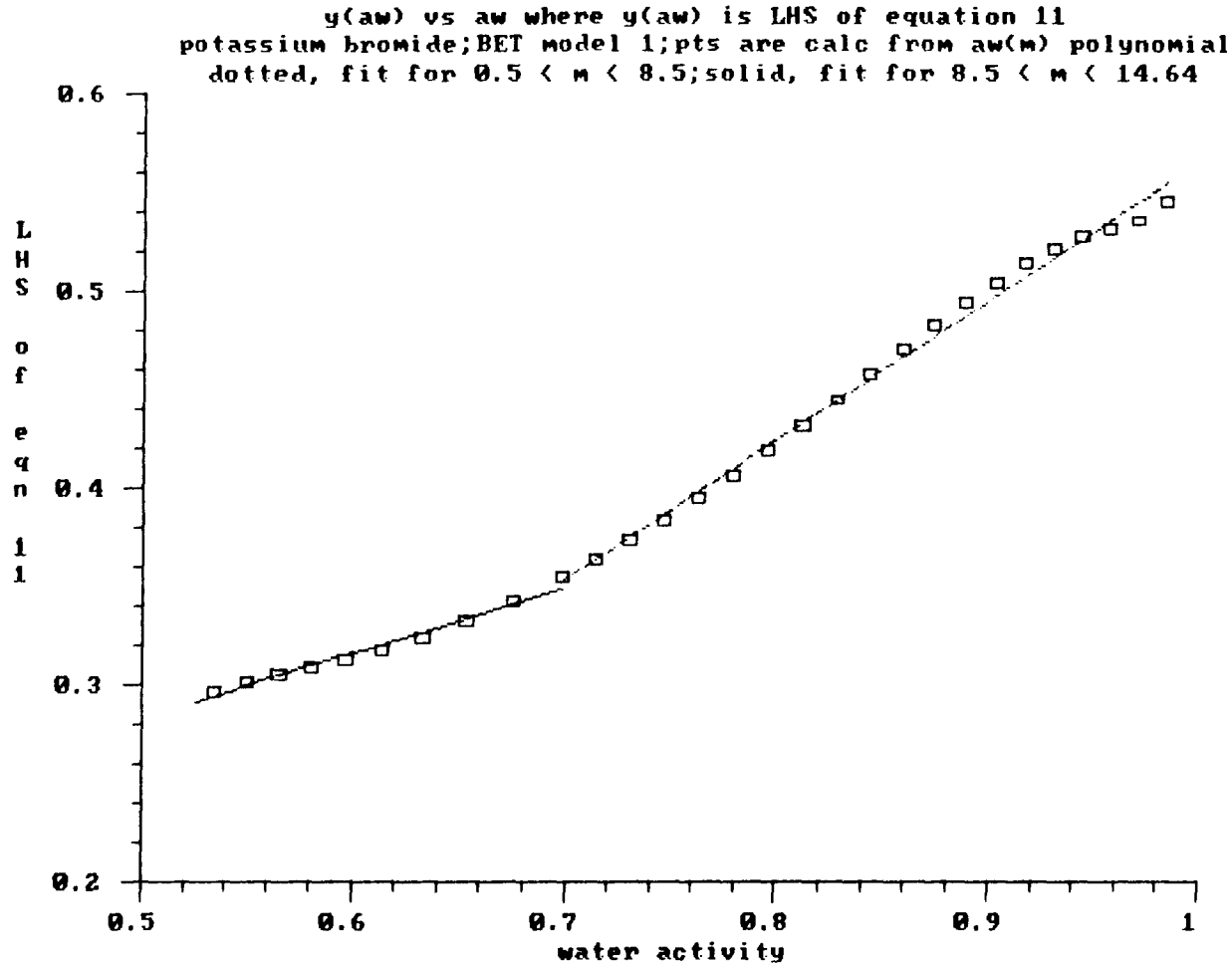
y(aw) vs aw where y(aw) is LHS of equation 11
potassium bromide;BET model 1;pts are calc from aw(m) polynomial
dotted, fit for 0.5 < m < 8.5;solid, fit for 8.5 < m < 14.64
LHS of eqn 11
0.6
0.5
0.4
0.3
0.2
0.5
0.6
0.7
0.8
0.9
1
water activity

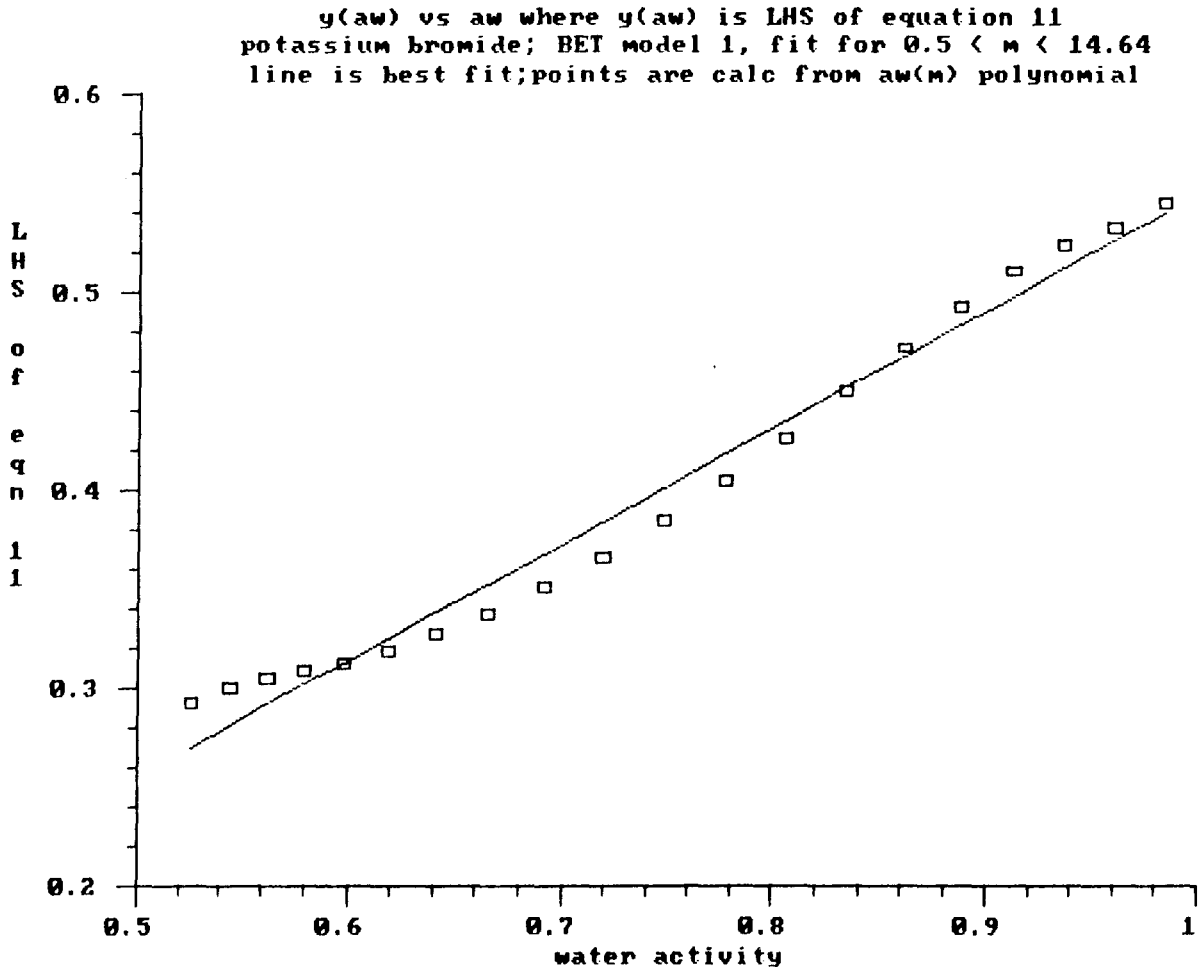
y(aw) vs aw where y(aw) is LHS of equation 11
potassium bromide; BET model 1, fit for 0.5 < m < 14.64
line is best fit;points are calc from aw(m) polynomial
LHS of eqn 11
0.6
0.5
0.4
0.3
0.2
0.5
0.6
0.7
0.8
0.9
1
water activity

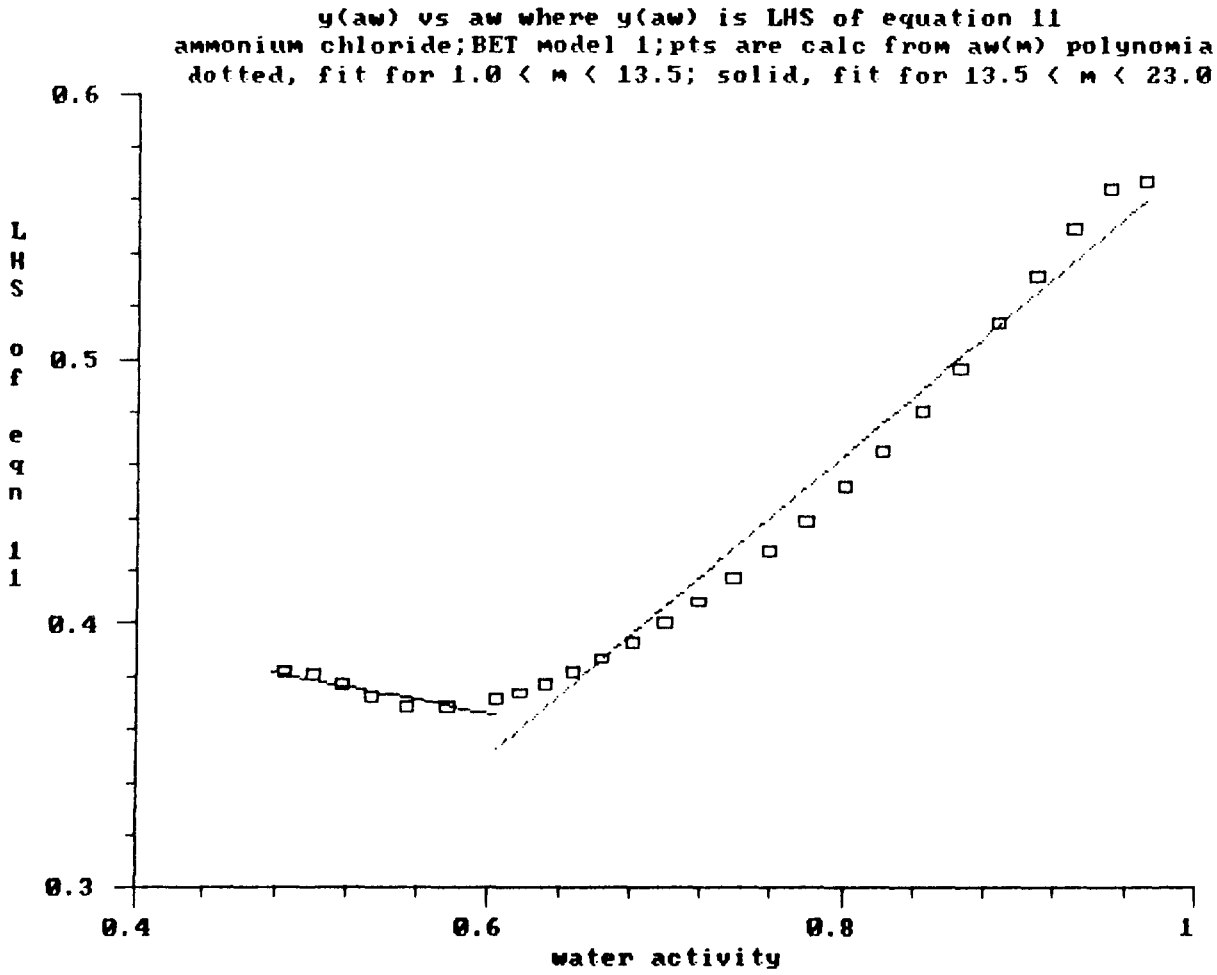
y(aw) vs aw where y(aw) is LHS of equation 11
ammonium chloride;BET model 1;pts are calc from aw(m) polynomial
dotted, fit for 1.0 < m < 13.5; solid, fit for 13.5 < m < 23.0
LHS of eqn 11
0.6
0.5
0.4
0.3
0.4
0.6
0.8
1
water activity

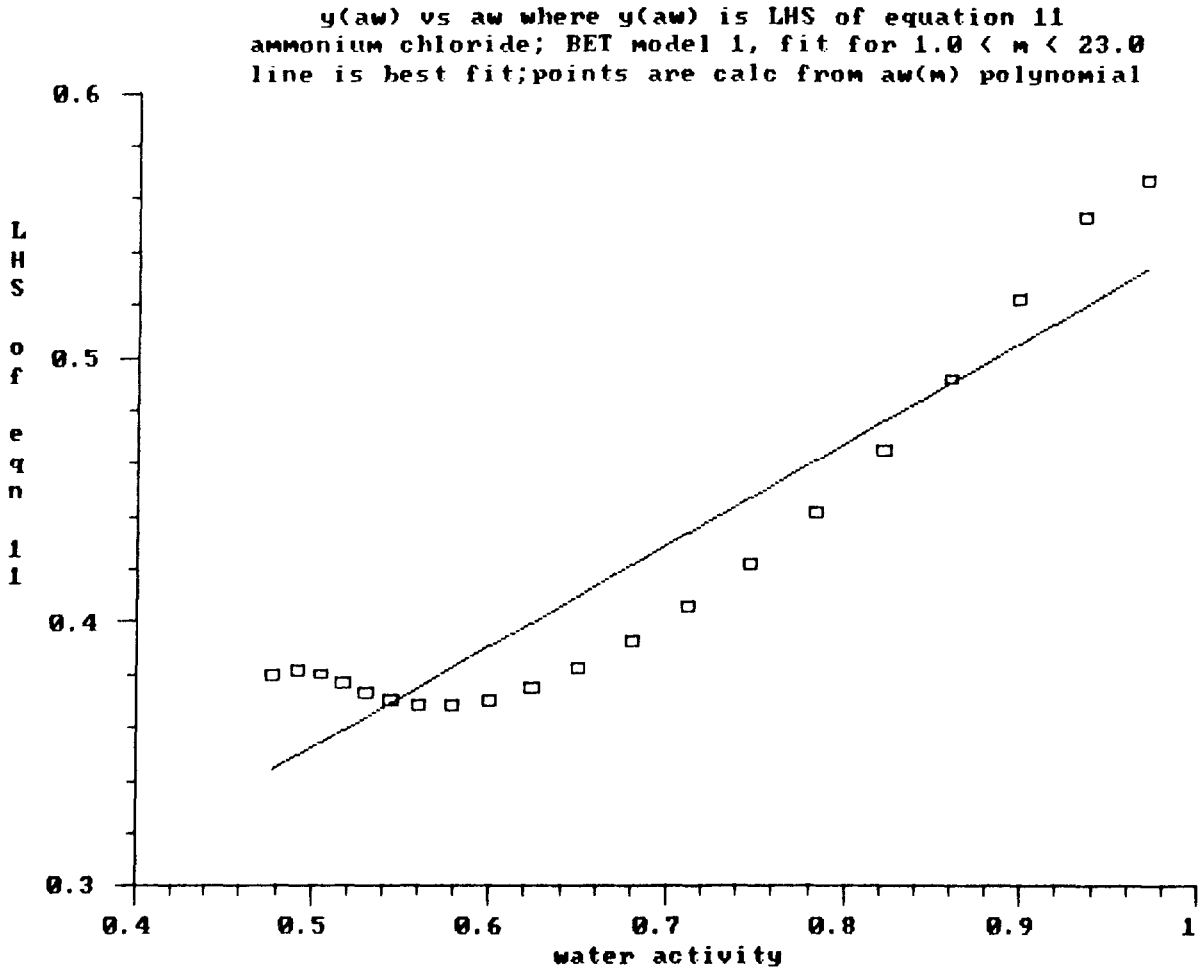
y(aw) vs aw where y(aw) is LHS of equation 11
ammonium chloride; BET model 1, fit for 1.0 < m < 23.0
line is best fit;points are calc from aw(m) polynomial
LHS of eqn 11
0.6
0.5
0.4
0.3
0.4
0.5
0.6
0.7
0.8
0.9
1
water activity

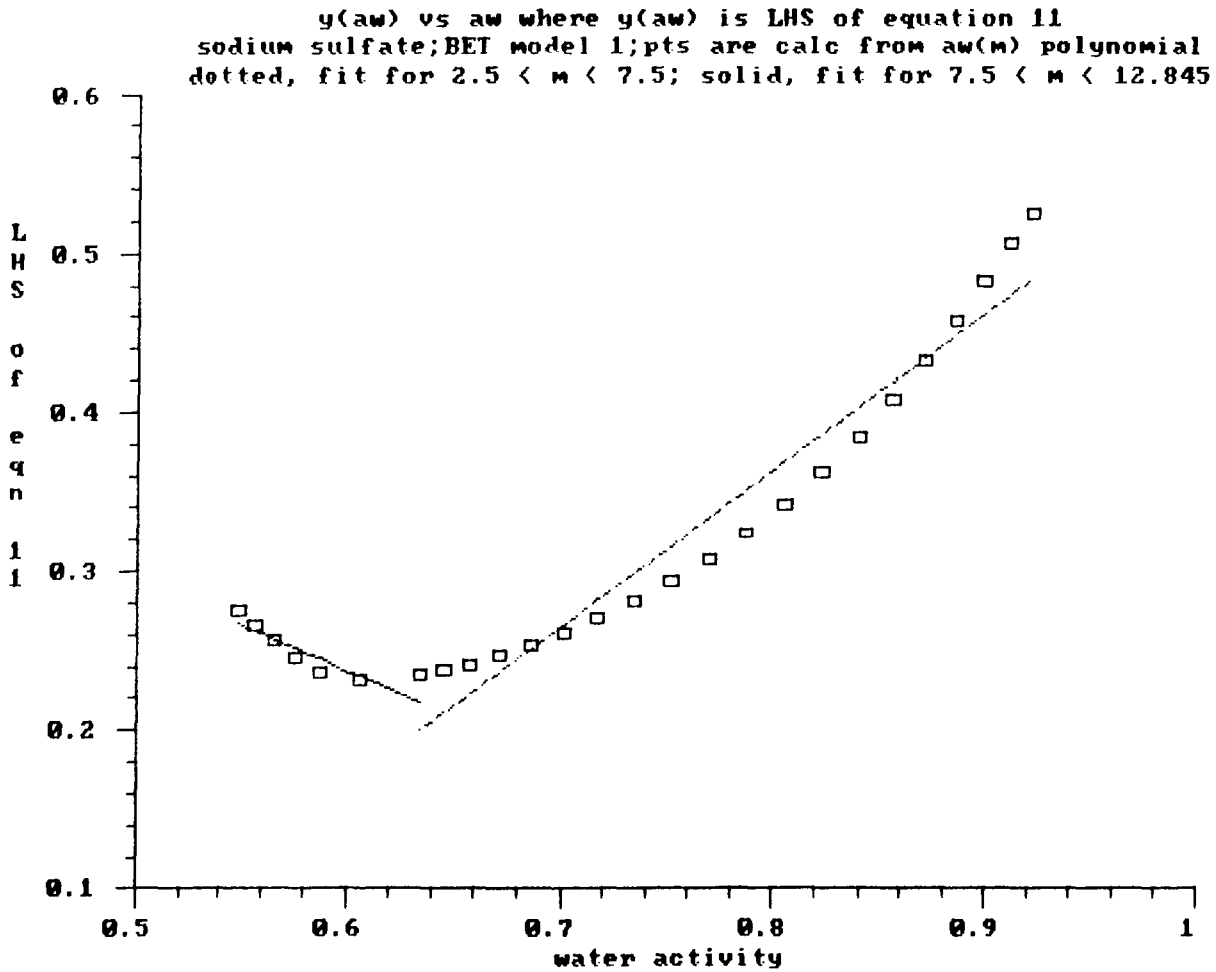
y(aw) vs aw where y(aw) is LHS of equation 11
sodium sulfate;BET model 1;pts are calc from aw(m) polynomial
dotted, fit for 2.5 < m < 7.5; solid, fit for 7.5 < m < 12.845
LHS of eqn 11
0.6
0.5
0.4
0.3
0.2
0.1
0.5
0.6
0.7
0.8
0.9
1
water activity

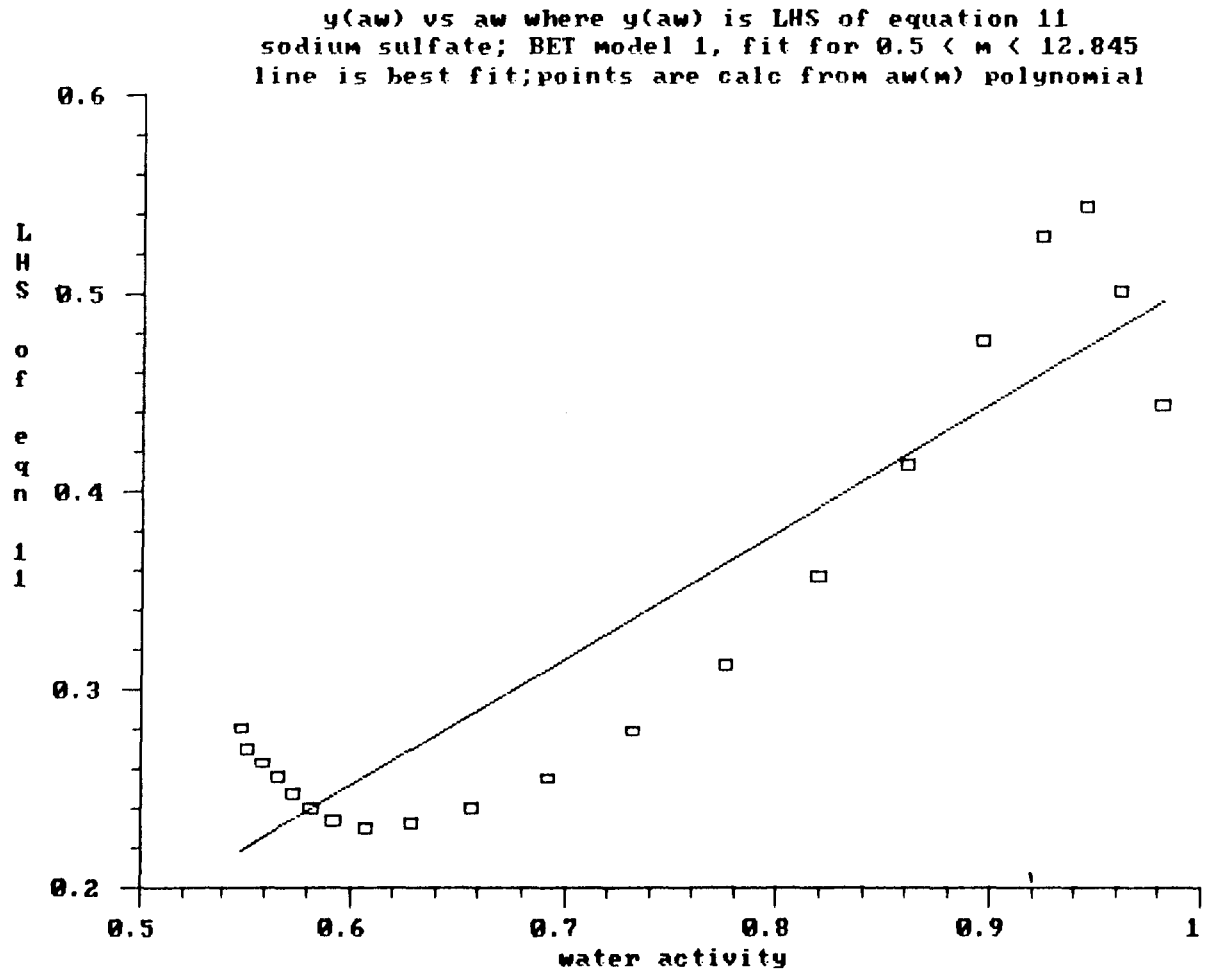
y(aw) vs aw where y(aw) is LHS of equation 11
sodium sulfate; BET model 1, fit for 0.5 < m < 12.845
line is best fit;points are calc from aw(m) polynomial
LHS of eqn 11
0.6
0.5
0.4
0.3
0.2
0.5
0.6
0.7
0.8
0.9
1
water activity

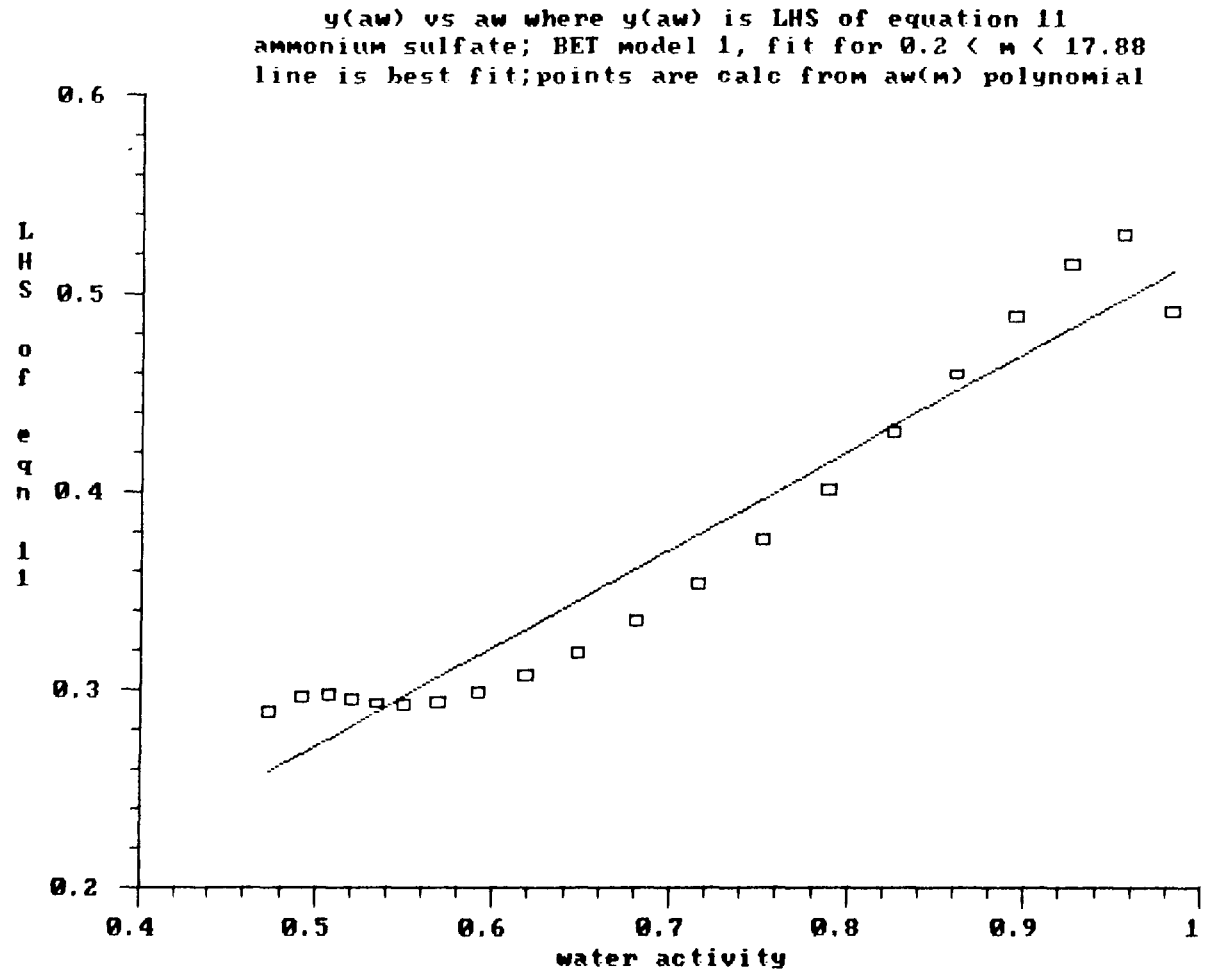
y(aw) vs aw where y(aw) is LHS of equation 11
ammonium sulfate; BET model 1, fit for 0.2 < m < 17.88
line is best fit;points are calc from aw(m) polynomial
LHS of eqn 11
0.6
0.5
0.4
0.3
0.2
0.4
0.5
0.6
0.7
0.8
0.9
1
water activity

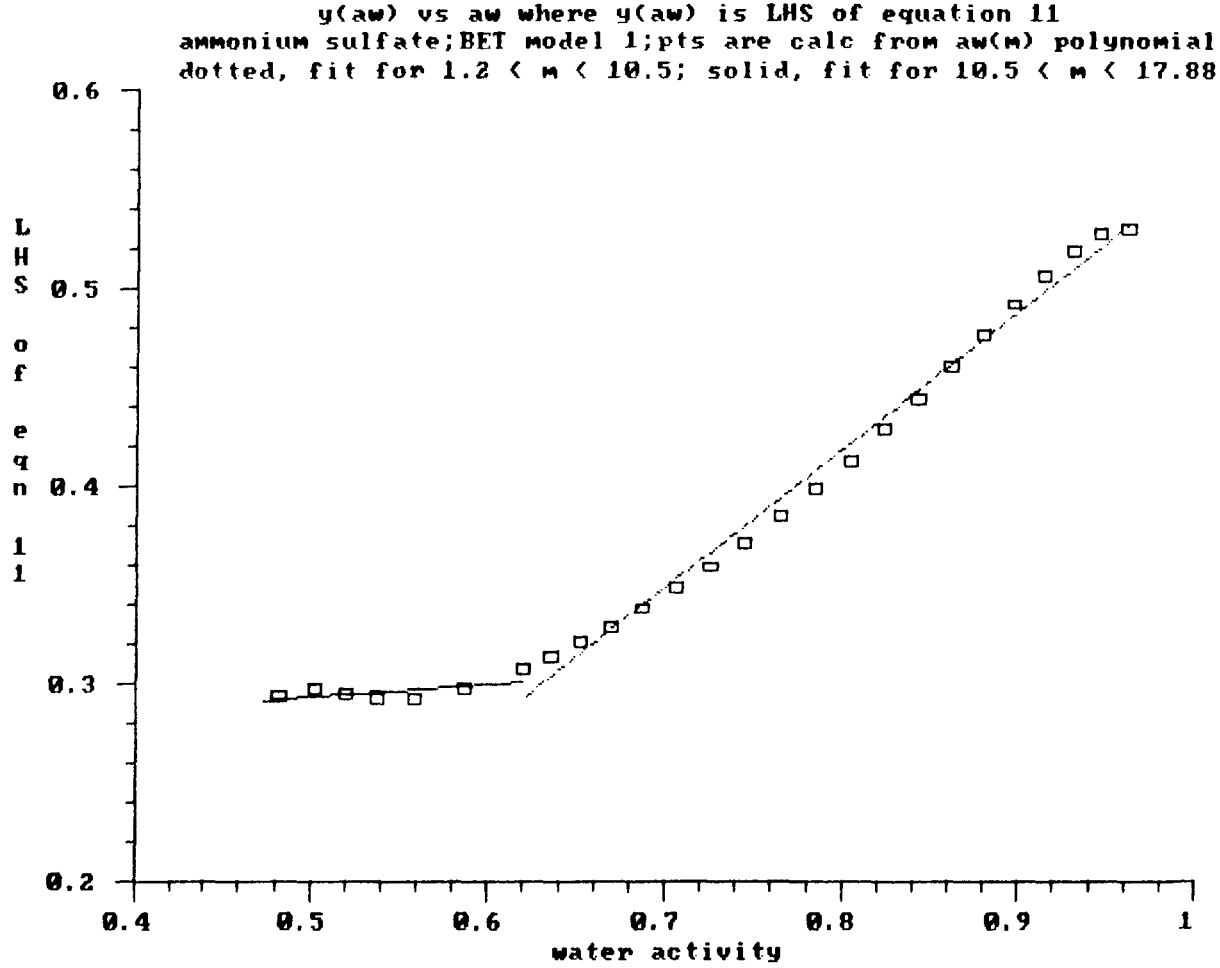
y(aw) vs aw where y(aw) is LHS of equation 11
ammonium sulfate;BET model 1;pts are calc from aw(m) polynomial
dotted, fit for 1.2 < m < 10.5; solid, fit for 10.5 < m < 17.88
LHS of eqn 11
0.6
0.5
0.4
0.3
0.2
0.4
0.5
0.6
0.7
0.8
0.9
1
water activity

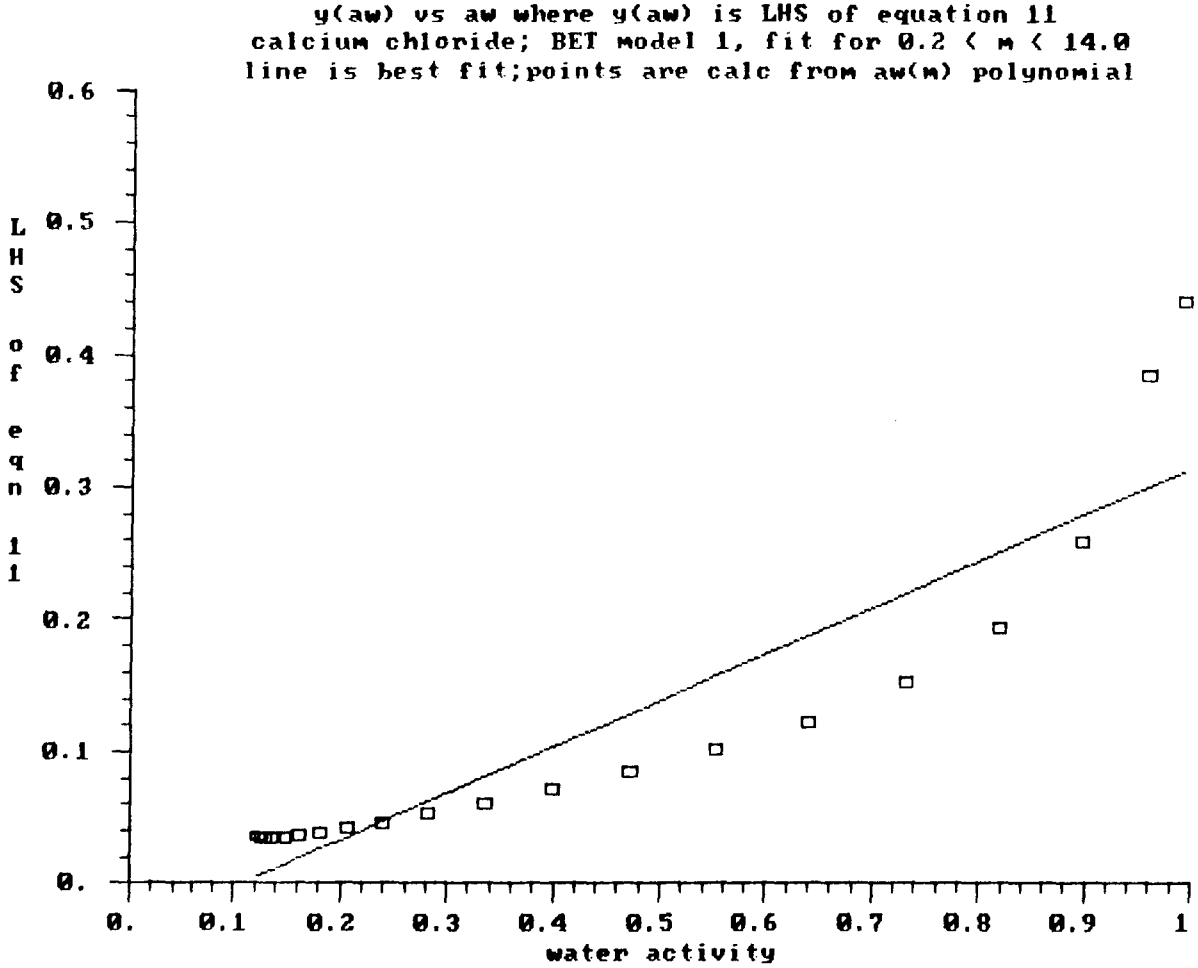
y(aw) vs aw where y(aw) is LHS of equation 11
calcium chloride; BET model 1, fit for 0.2 < m < 14.0
line is best fit;points are calc from aw(m) polynomial
LHS of eqn 11
0.6
0.5
0.4
0.3
0.2
0.1
0.
0.
0.1
0.2
0.3
0.4
0.5
0.6
0.7
0.8
0.9
1
water activity

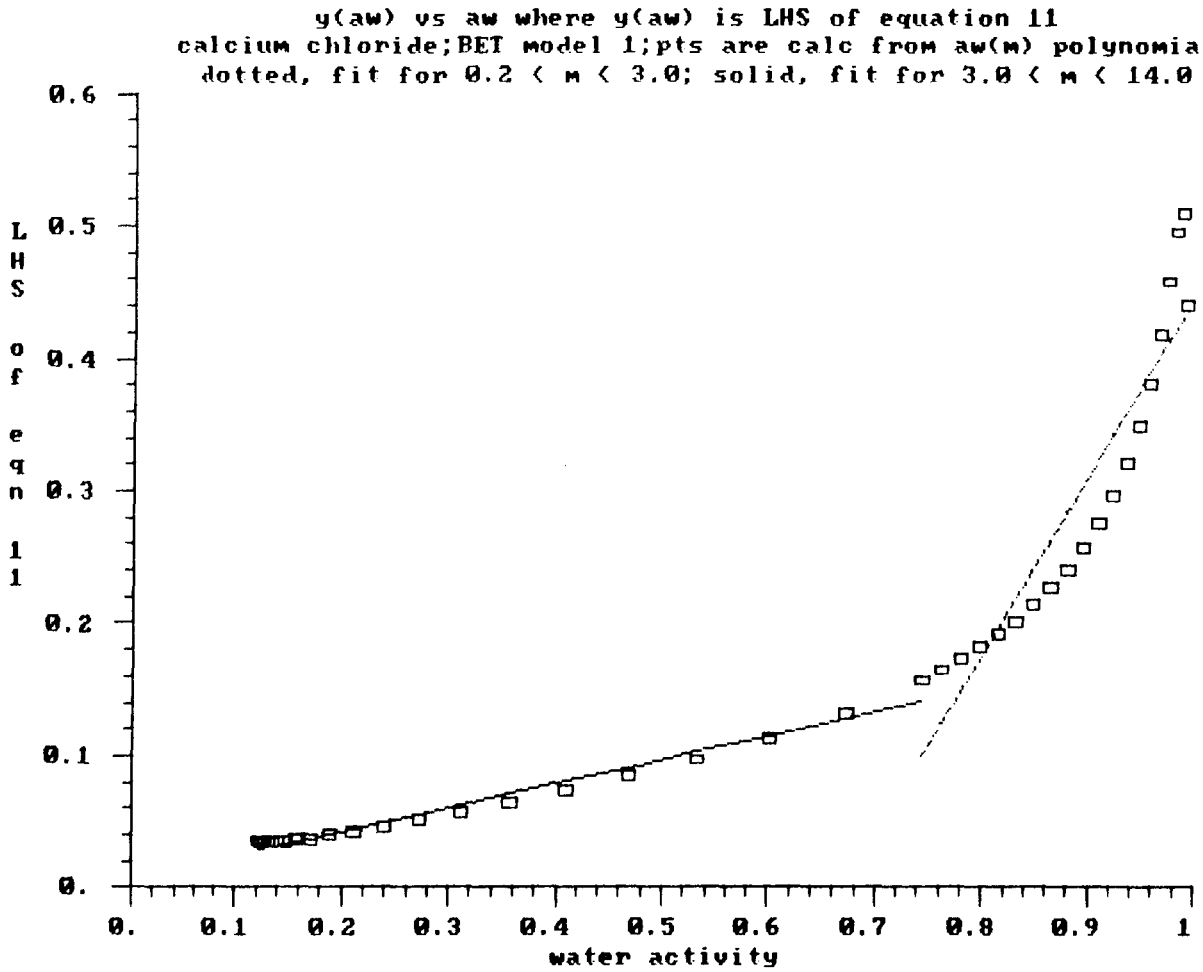
y(aw) vs aw where y(aw) is LHS of equation 11
calcium chloride;BET model 1;pts are calc from aw(m) polynomial
dotted, fit for 0.2 < m < 3.0; solid, fit for 3.0 < m < 14.0
LHS of eqn 11
0.6
0.5
0.4
0.3
0.2
0.1
0.
0.
0.1
0.2
0.3
0.4
0.5
0.6
0.7
0.8
0.9
1
water activity

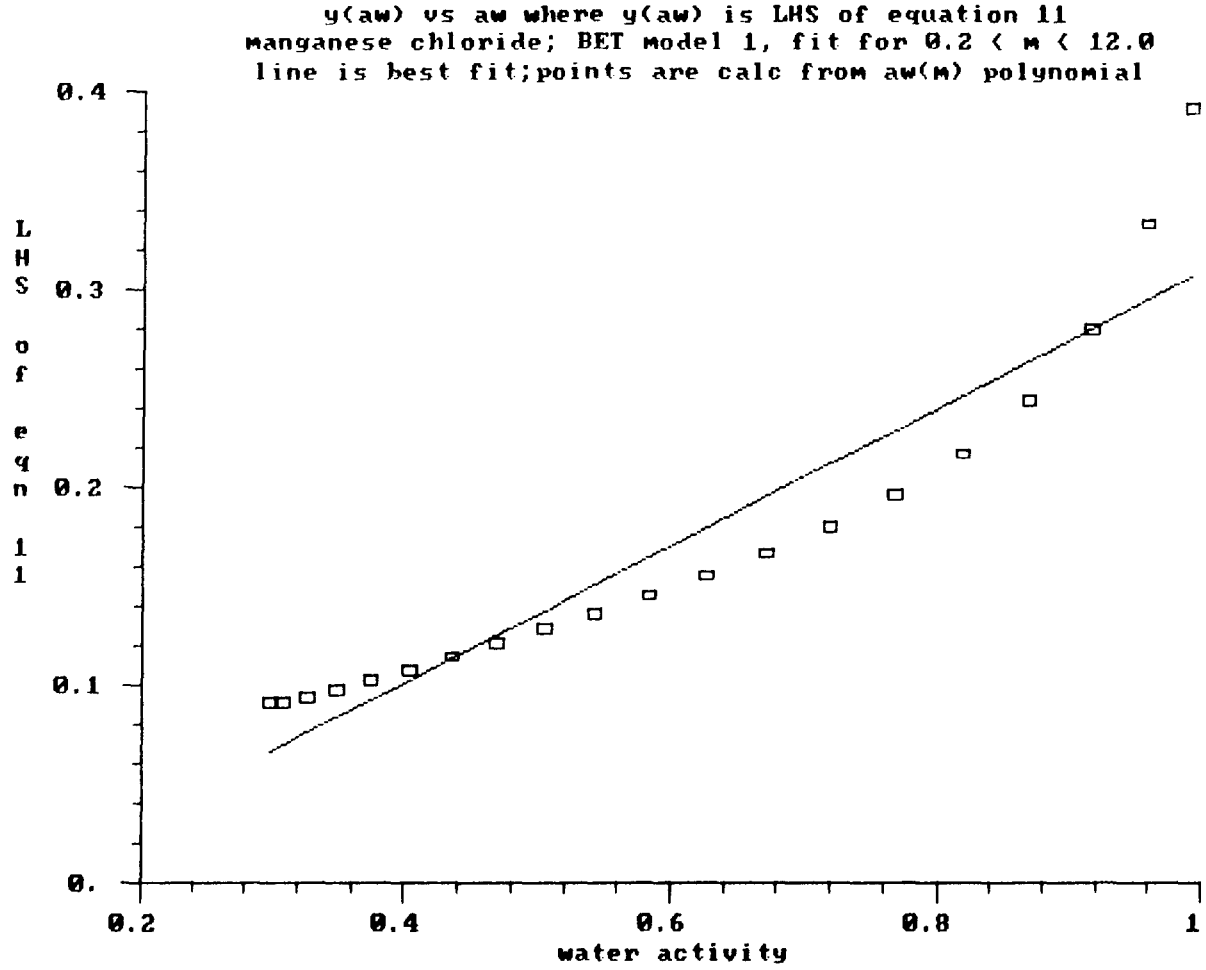
y(aw) vs aw where y(aw) is LHS of equation 11
manganese chloride; BET model 1, fit for 0.2 < m < 12.0
line is best fit;points are calc from aw(m) polynomial
LHS of eqn 11
0.4
0.3
0.2
0.1
0.
0.2
0.4
0.6
0.8
1
water activity

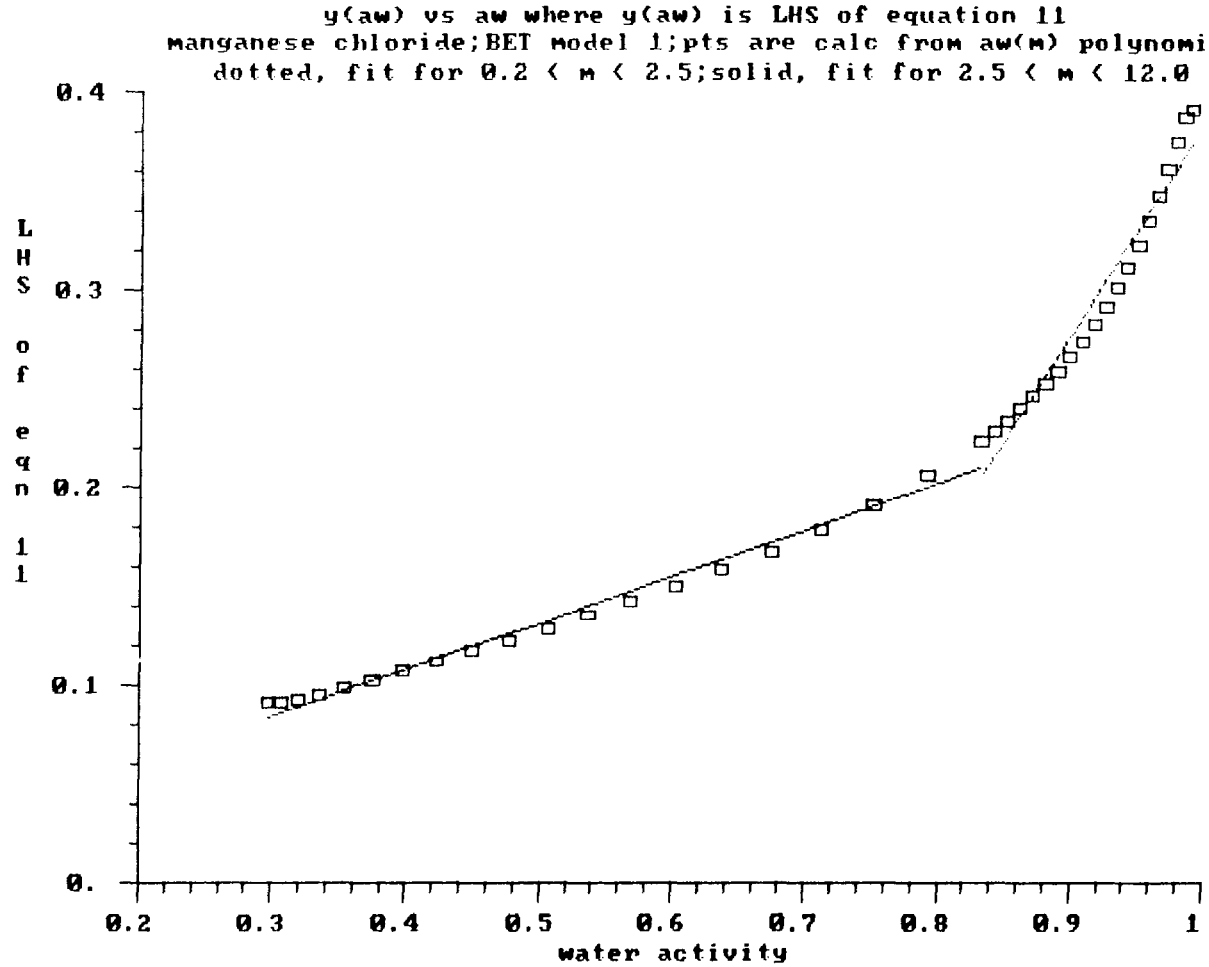
y(aw) vs aw where y(aw) is LHS of equation 11
manganese chloride;BET model 1;pts are calc from aw(m) polynomial
dotted, fit for 0.2 < m < 2.5;solid, fit for 2.5 < m < 12.0
LHS of eqn 11
0.4
0.3
0.2
0.1
0.
0.2
0.3
0.4
0.5
0.6
0.7
0.8
0.9
1
water activity

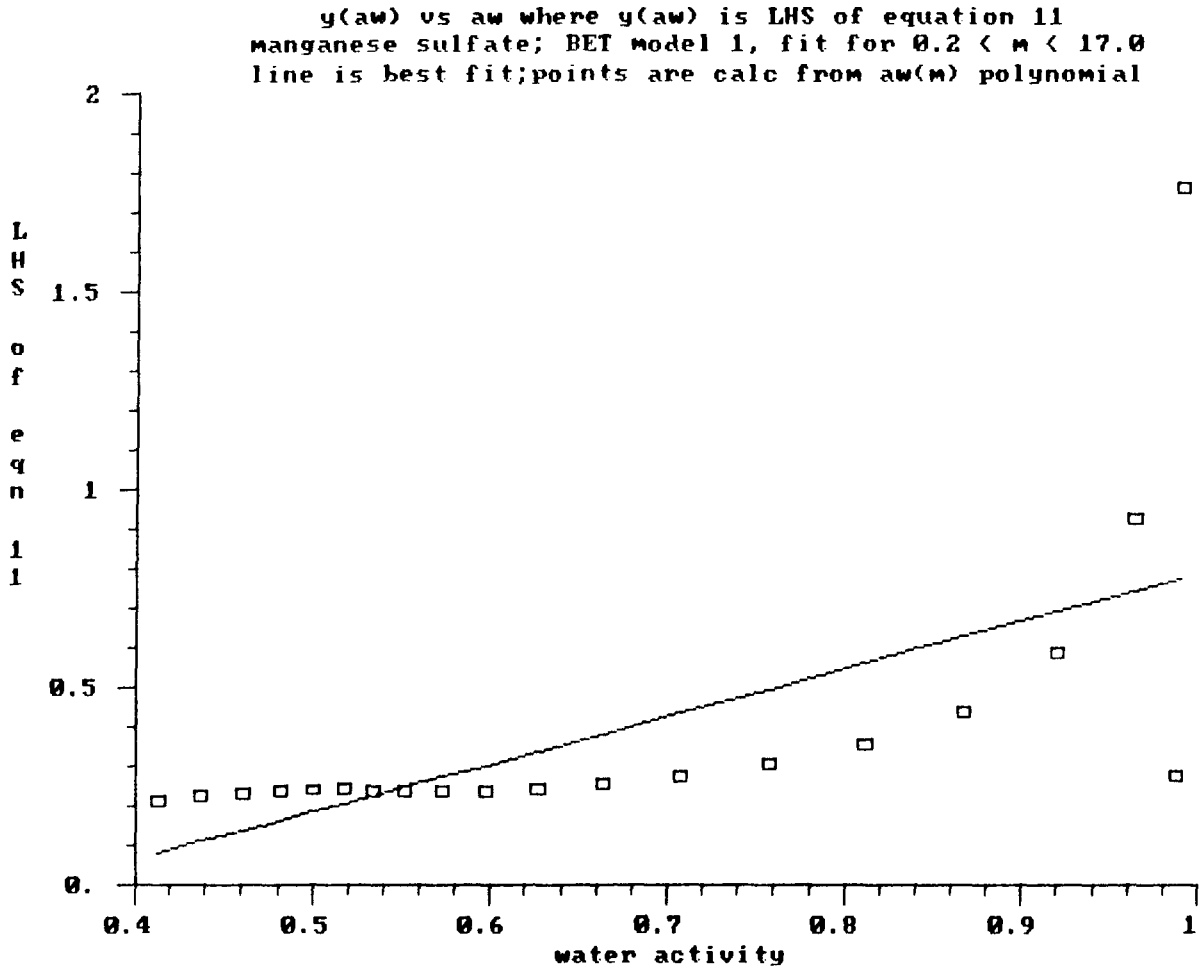
y(aw) vs aw where y(aw) is LHS of equation 11
manganese sulfate; BET model 1, fit for 0.2 < m < 17.0
line is best fit;points are calc from aw(m) polynomial
LHS of eqn 11
2
1.5
1
0.5
0.
0.4
0.5
0.6
0.7
0.8
0.9
1
water activity

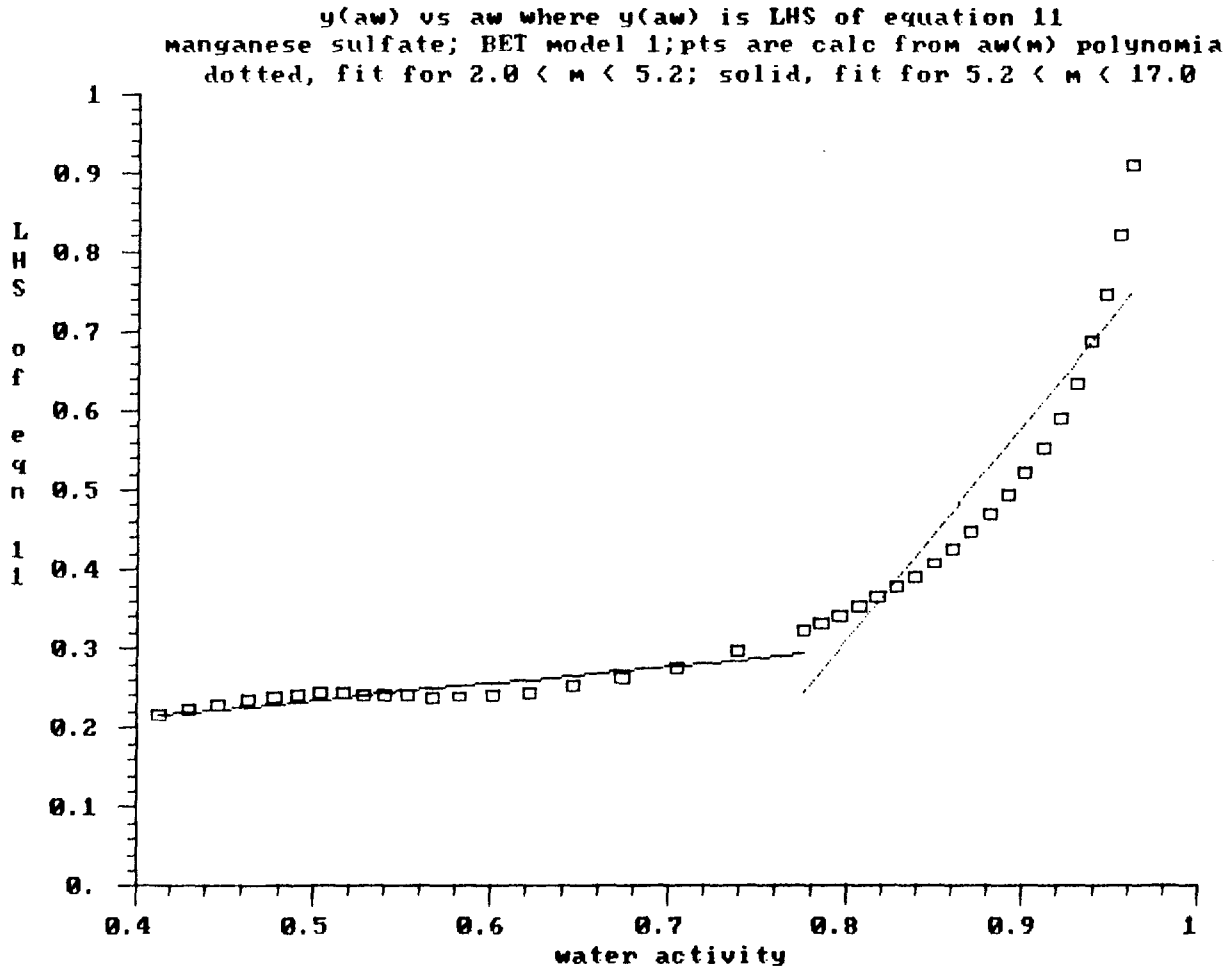
y(aw) vs aw where y(aw) is LHS of equation 11
manganese sulfate; BET model 1;pts are calc from aw(m) polynomial
dotted, fit for 2.0 < m < 5.2; solid, fit for 5.2 < m < 17.0
LHS of eqn 11
1
0.9
0.8
0.7
0.6
0.5
0.4
0.3
0.2
0.1
0.
0.4
0.5
0.6
0.7
0.8
0.9
1
water activity

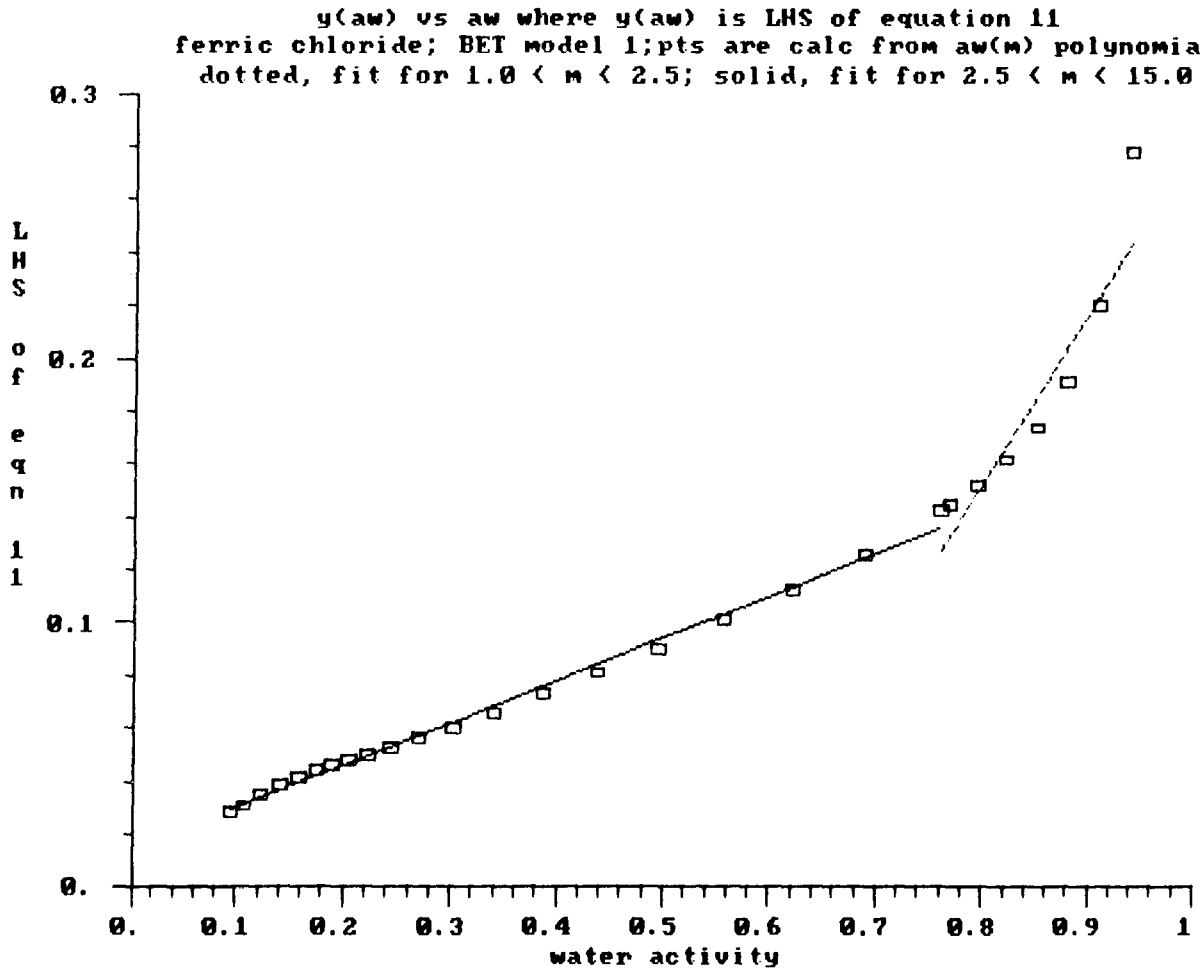
y(aw) vs aw where y(aw) is LHS of equation 11
ferric chloride; BET model 1;pts are calc from aw(m) polynomial
dotted, fit for 1.0 < m < 2.5; solid, fit for 2.5 < m < 15.0
LHS of eqn 11
0.3
0.2
0.1
0.
0.
0.1
0.2
0.3
0.4
0.5
0.6
0.7
0.8
0.9
1
water activity

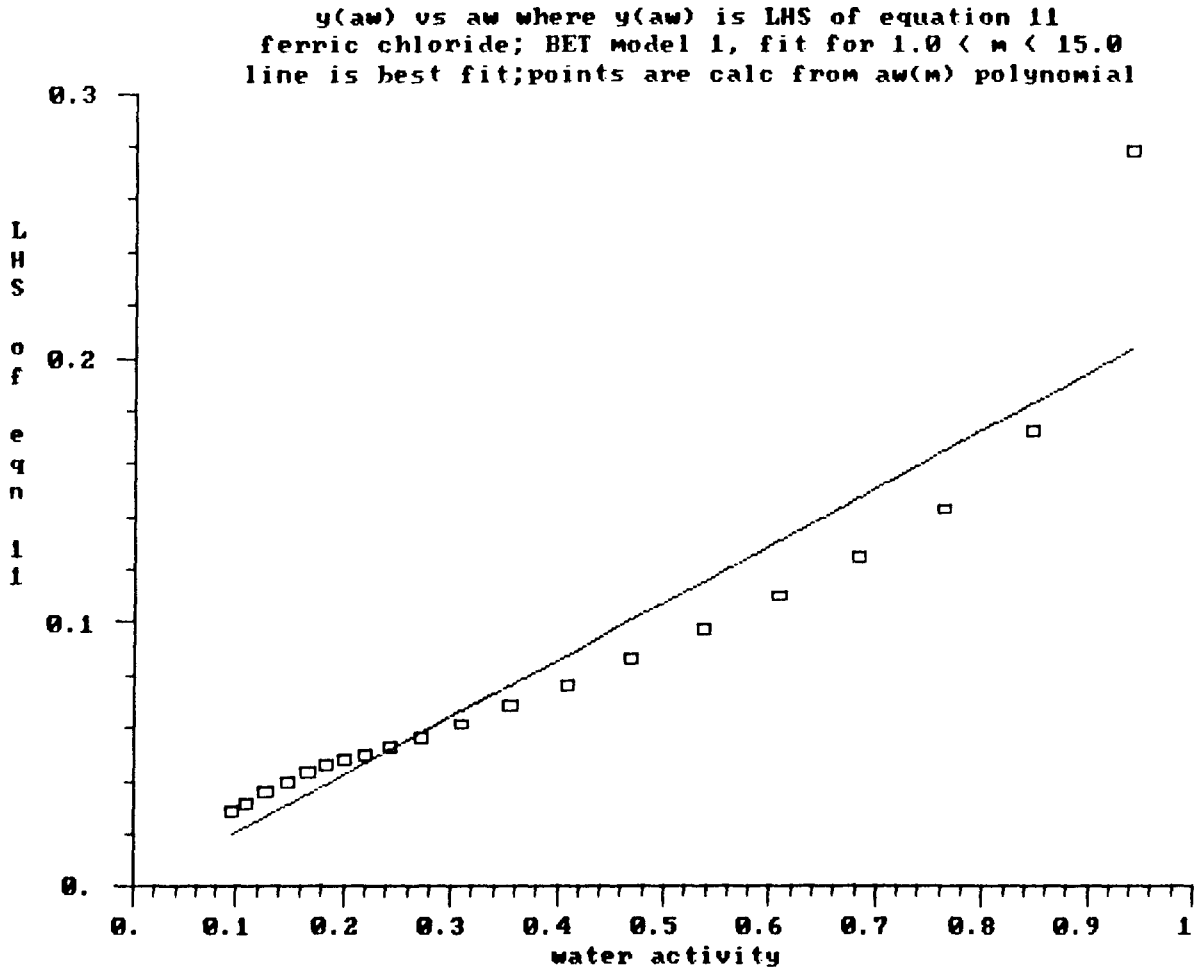
y(aw) vs aw where y(aw) is LHS of equation 11
ferric chloride; BET model 1, fit for 1.0 < m < 15.0
line is best fit;points are calc from aw(m) polynomial
LHS of eqn 11
0.3
0.2
0.1
0.
0.
0.1
0.2
0.3
0.4
0.5
0.6
0.7
0.8
0.9
1
water activity

Appendix L: Plots showing the $a_w(m)$ predictions of the BET-based model of Robinson and Stokes compared with the experimental data for each of the single-electrolyte solutions studied

In the plots in this appendix, the BET model, with parameters estimated from the plots in the previous appendix, is used to predict the $a_w(m)$ properties of single electrolyte solutions.

At some molalities for certain salts, the model became completely invalid, and the points are plotted as if the water activity was zero.

For further explanation of the BET model, please refer to Chapter 1. In this appendix, "equation 11" refers to equation 17 of Chapter 1.

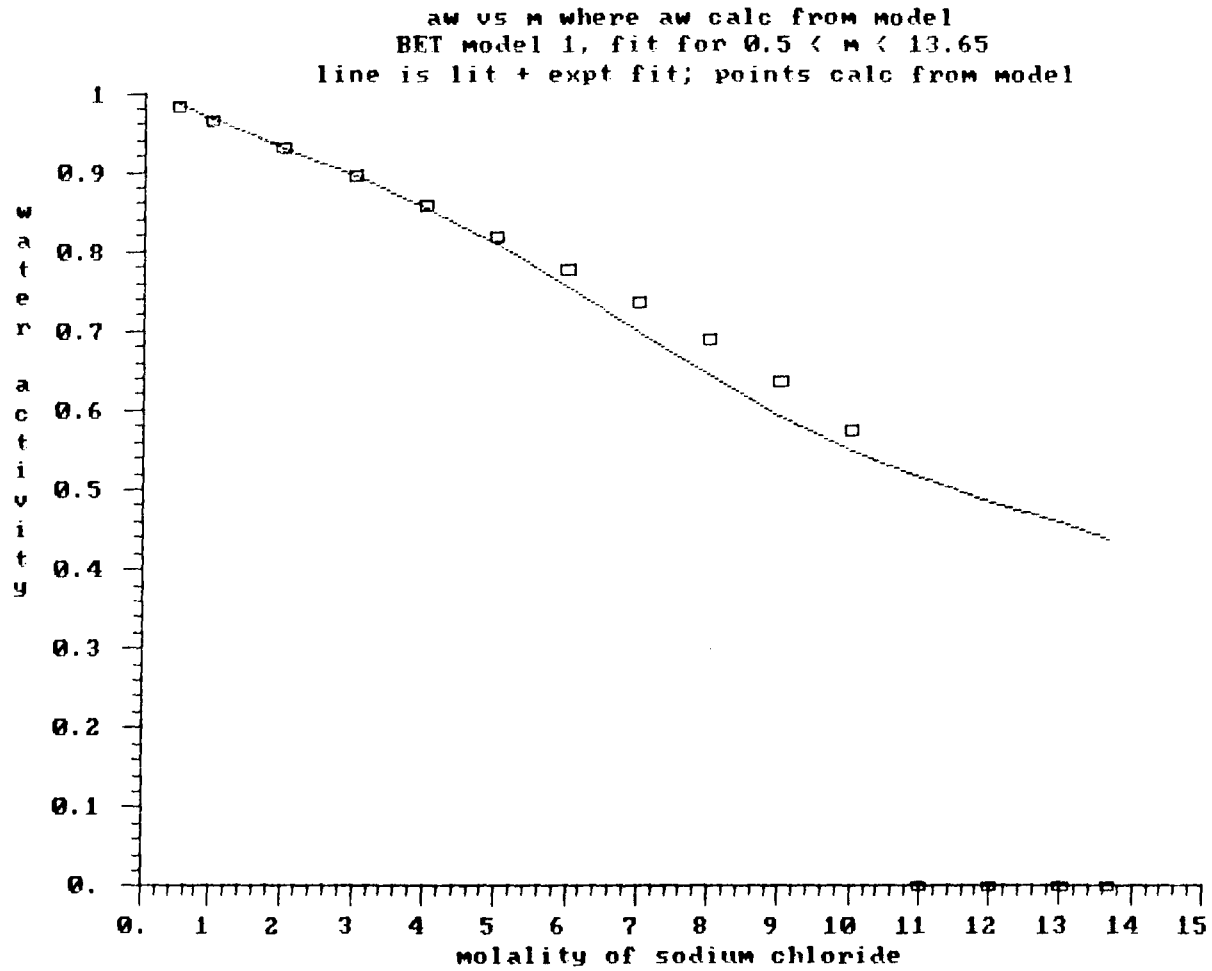
aw vs m where aw calc from model
BET model 1, fit for 0.5 < m < 13.65
line is lit + expt fit; points calc from model
water activity
1
0.9
0.8
0.7
0.6
0.5
0.4
0.3
0.2
0.1
0.
0. 1 2 3 4 5 6 7 8 9 10 11 12 13 14 15
molality of sodium chloride

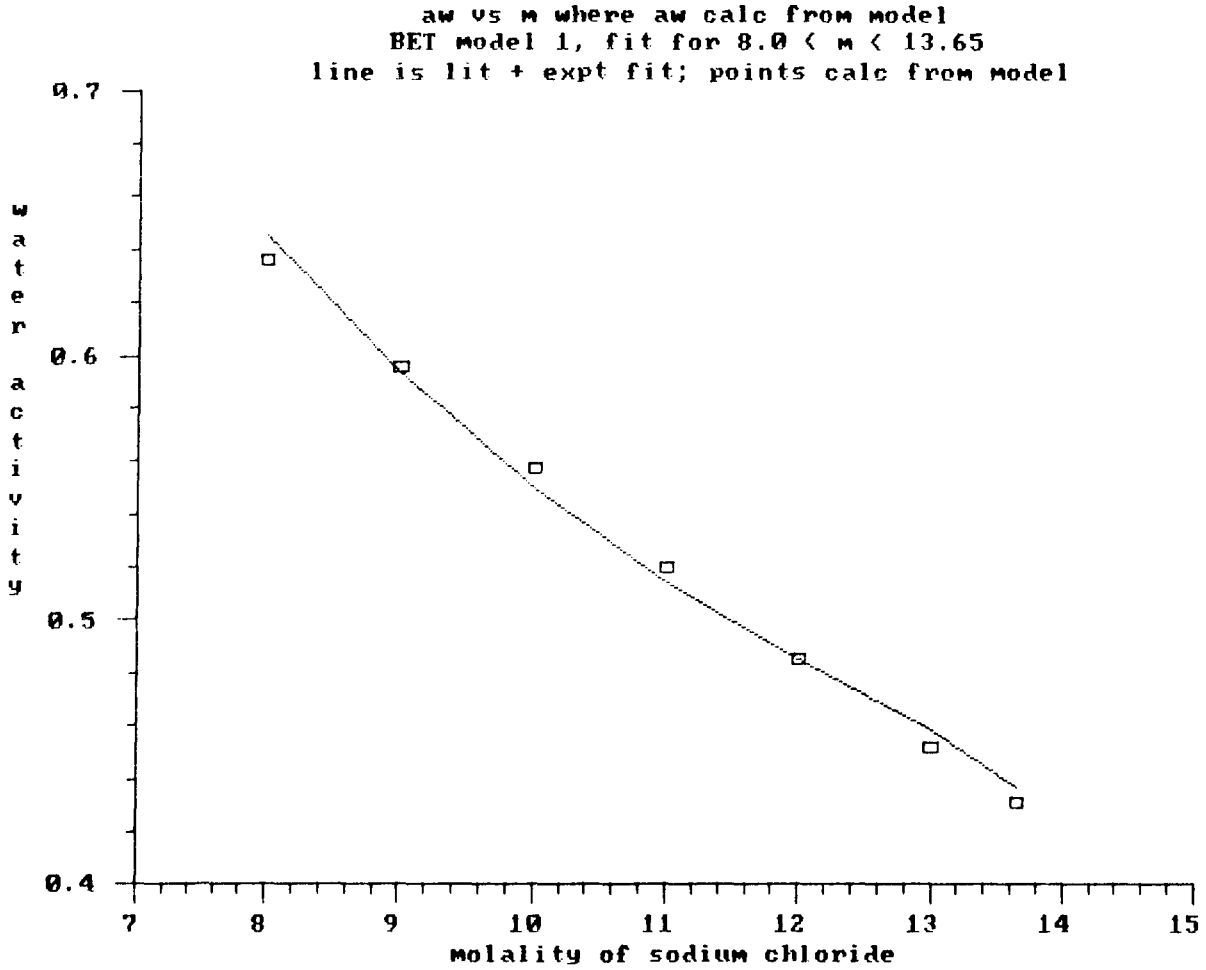
aw vs m where aw calc from model
BET model 1, fit for 8.0 < m < 13.65
line is lit + expt fit; points calc from model
water activity
0.7
0.6
0.5
0.4
7
8
9
10
11
12
13
14
15
molality of sodium chloride

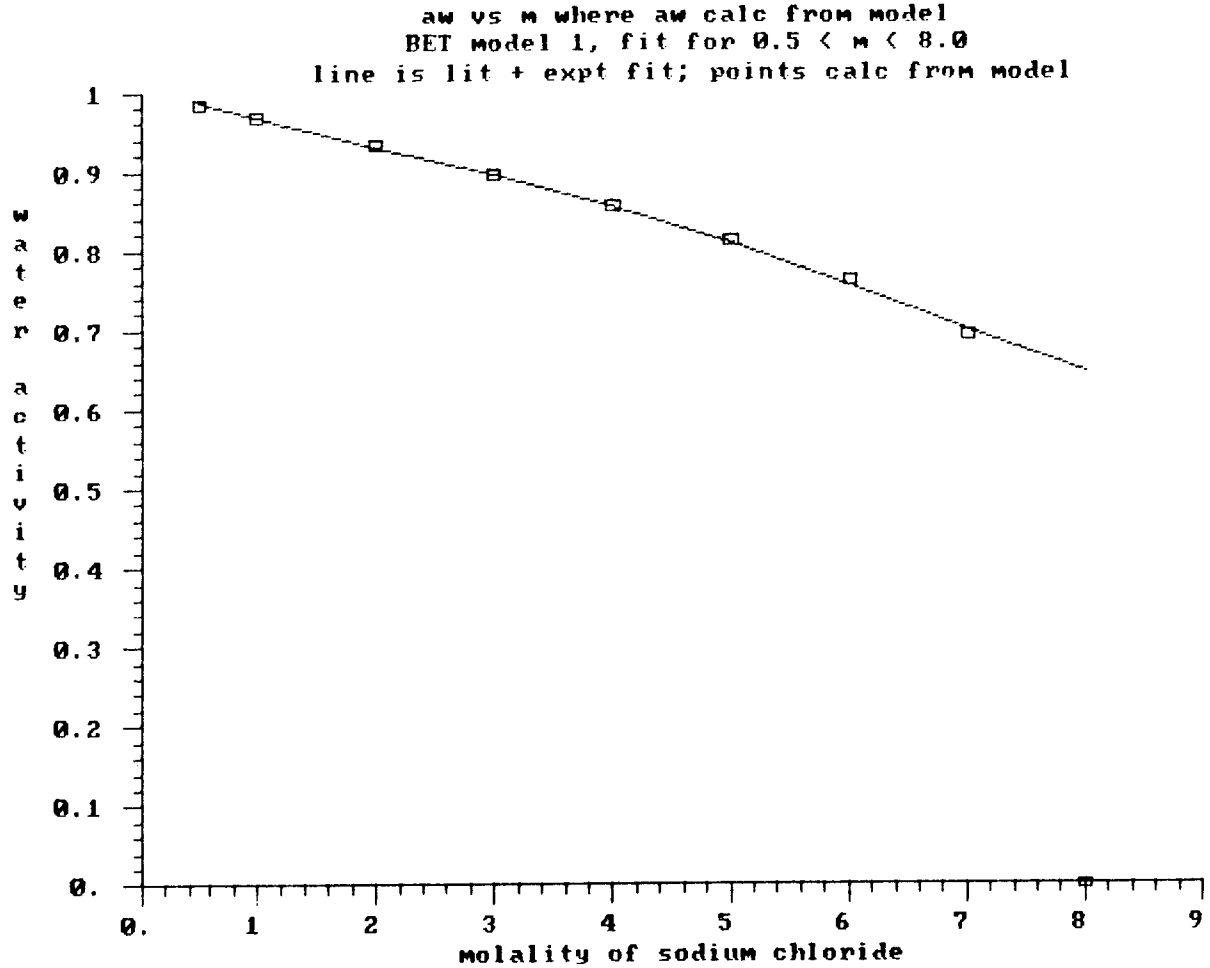
aw vs m where aw calc from model
BET model 1, fit for 0.5 < m < 8.0
line is lit + expt fit; points calc from model
water activity
1
0.9
0.8
0.7
0.6
0.5
0.4
0.3
0.2
0.1
0.
0.
1
2
3
4
5
6
7
8
9
molality of sodium chloride

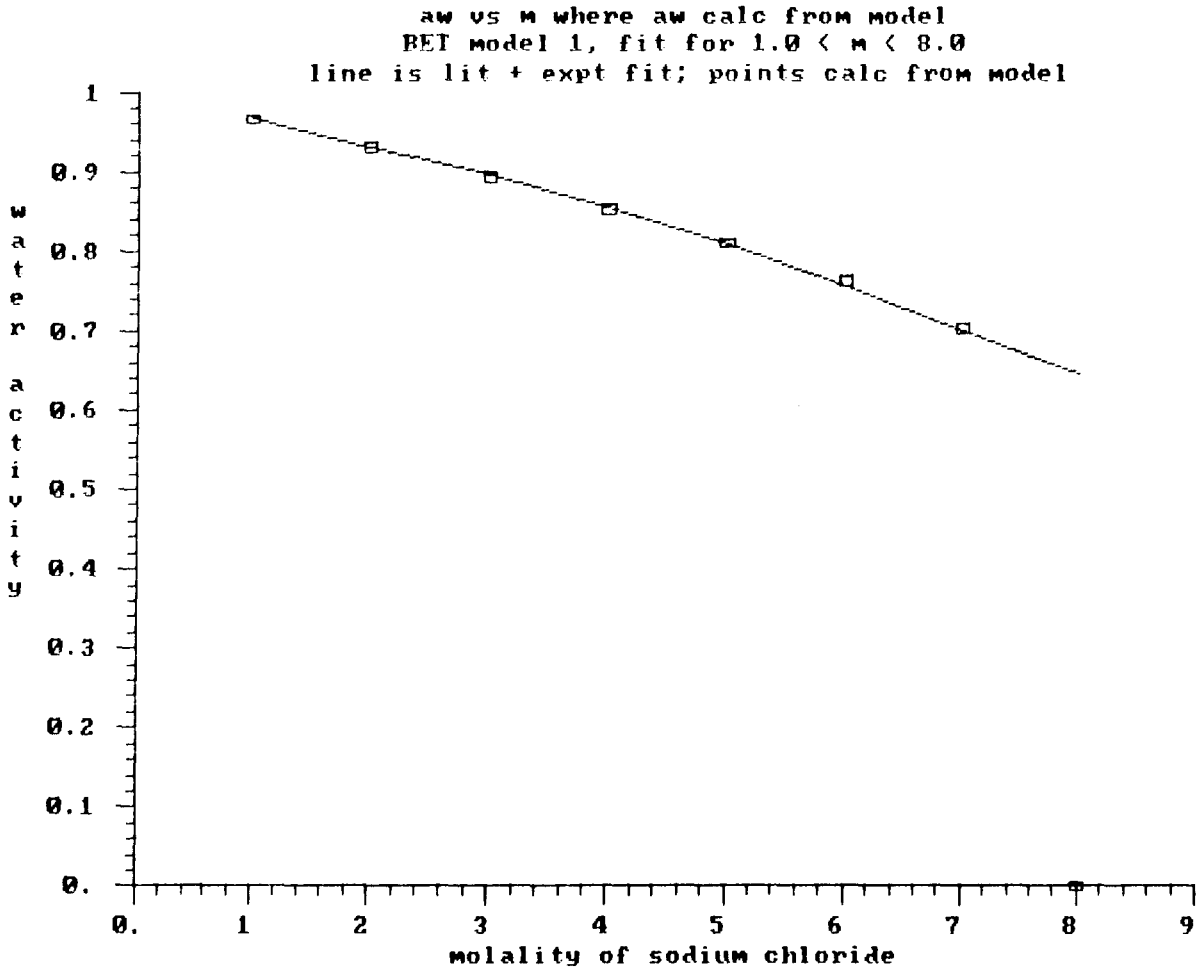
aw vs m where aw calc from model
BET model 1, fit for 1.0 < m < 8.0
line is lit + expt fit; points calc from model
water activity
1
0.9
0.8
0.7
0.6
0.5
0.4
0.3
0.2
0.1
0.
0.
1
2
3
4
5
6
7
8
9
molality of sodium chloride

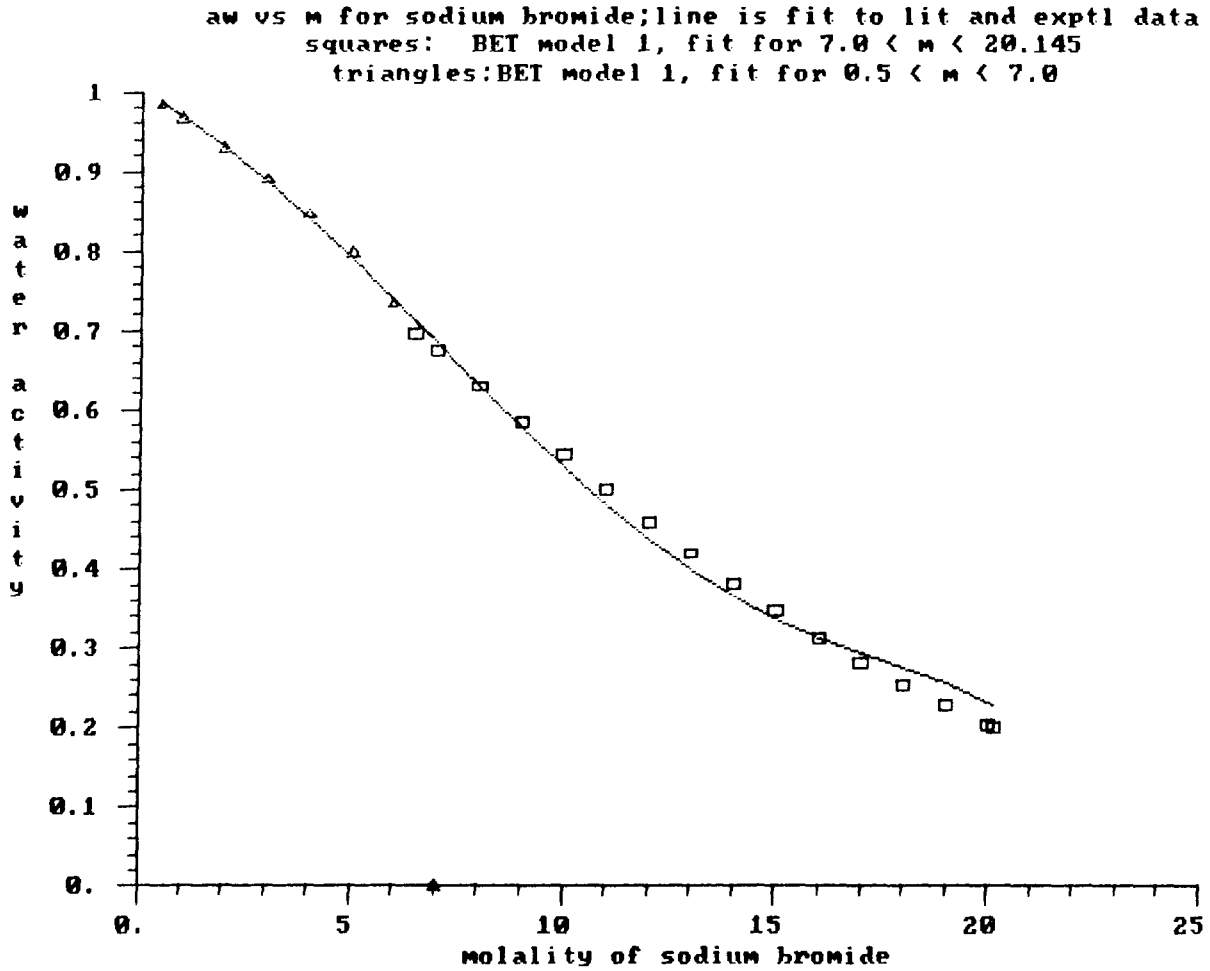
aw vs m for sodium bromide;line is fit to lit and exptl data
squares: BET model 1, fit for 7.0 < m < 20.145
triangles:BET model 1, fit for 0.5 < m < 7.0
water activity
1
0.9
0.8
0.7
0.6
0.5
0.4
0.3
0.2
0.1
0.
0.
5
10
15
20
25
molality of sodium bromide

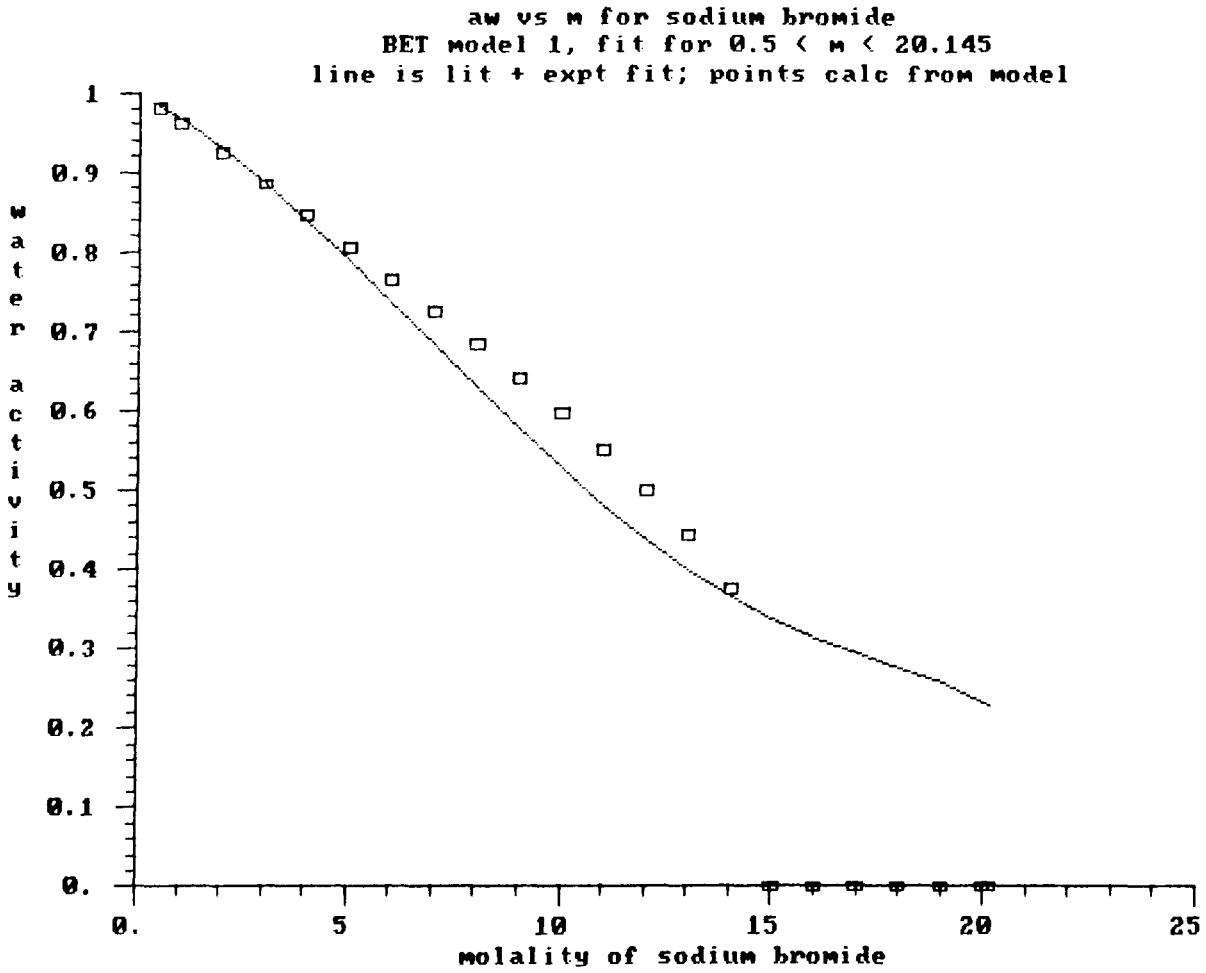
aw vs m for sodium bromide
BET model 1, fit for 0.5 < m < 20.145
line is lit + expt fit; points calc from model
water activity
1
0.9
0.8
0.7
0.6
0.5
0.4
0.3
0.2
0.1
0.
0.
5
10
15
20
25
molality of sodium bromide

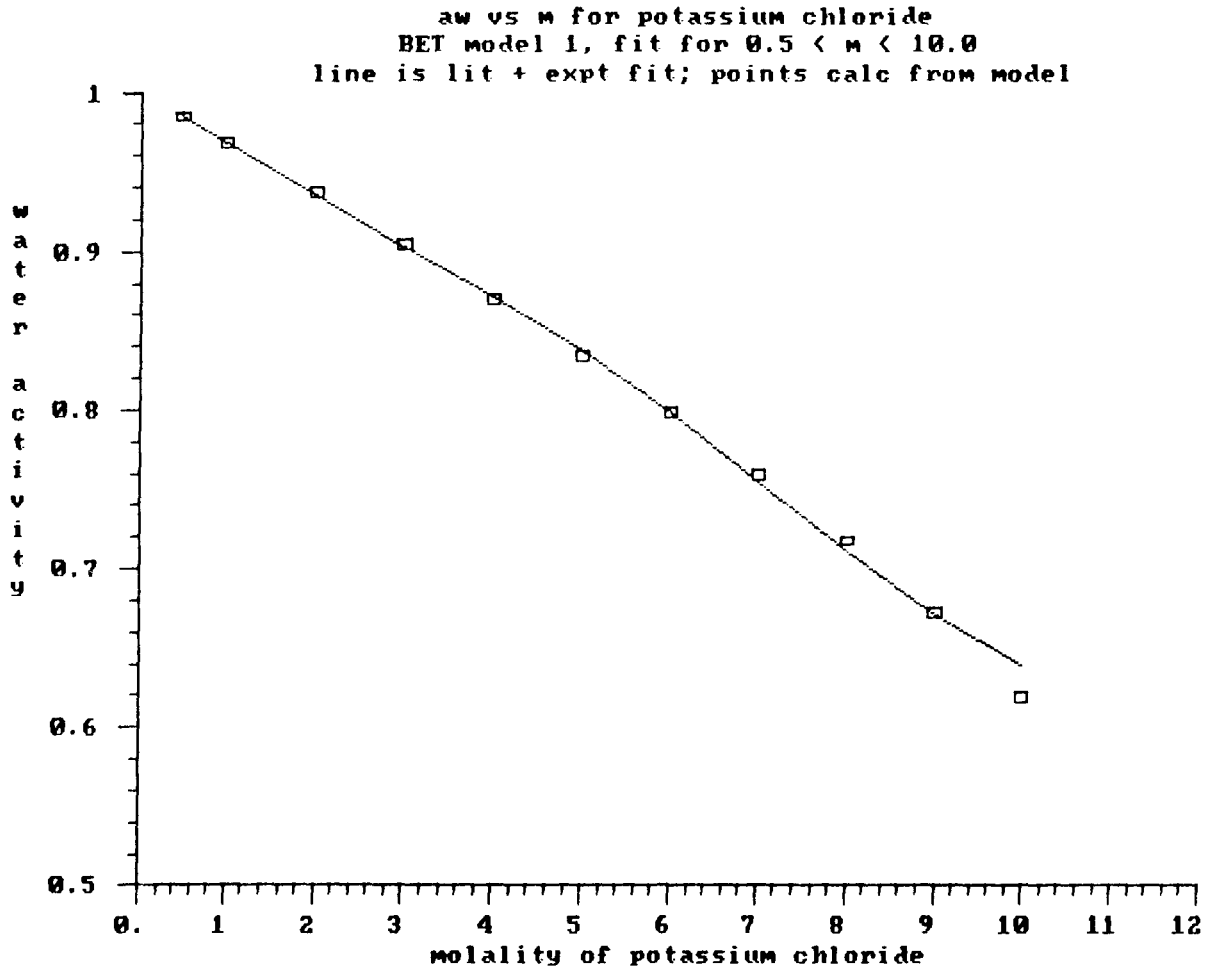
aw vs m for potassium chloride
BET model 1, fit for 0.5 < m < 10.0
line is lit + expt fit; points calc from model
water activity
1
0.9
0.8
0.7
0.6
0.5
0.
1
2
3
4
5
6
7
8
9
10
11
12
molality of potassium chloride

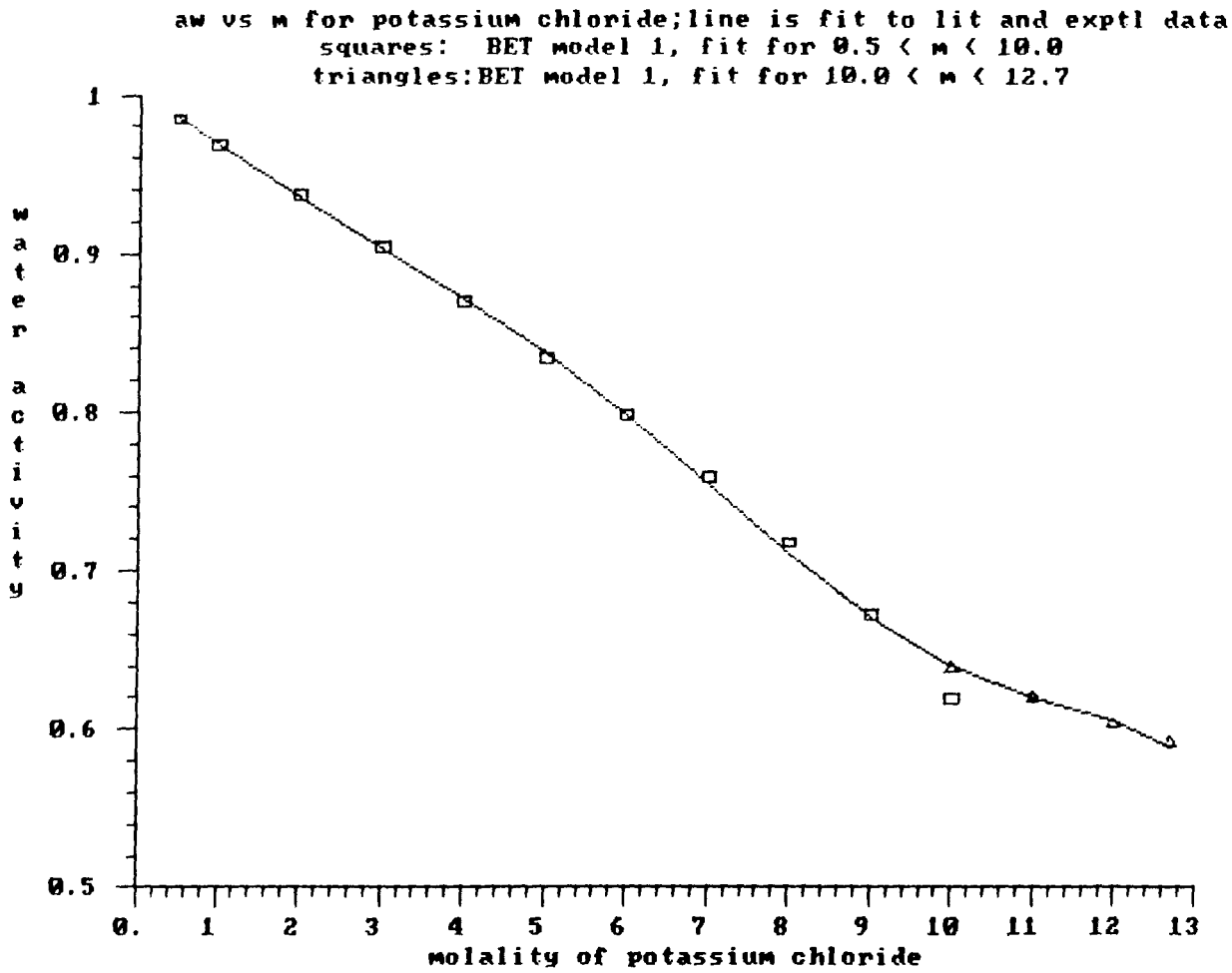
aw vs m for potassium chloride;line is fit to lit and exptl data
squares: BET model 1, fit for 0.5 < m < 10.0
triangles:BET model 1, fit for 10.0 < m < 12.7
water activity
1
0.9
0.8
0.7
0.6
0.5
0.
1
2
3
4
5
6
7
8
9
10
11
12
13
molality of potassium chloride

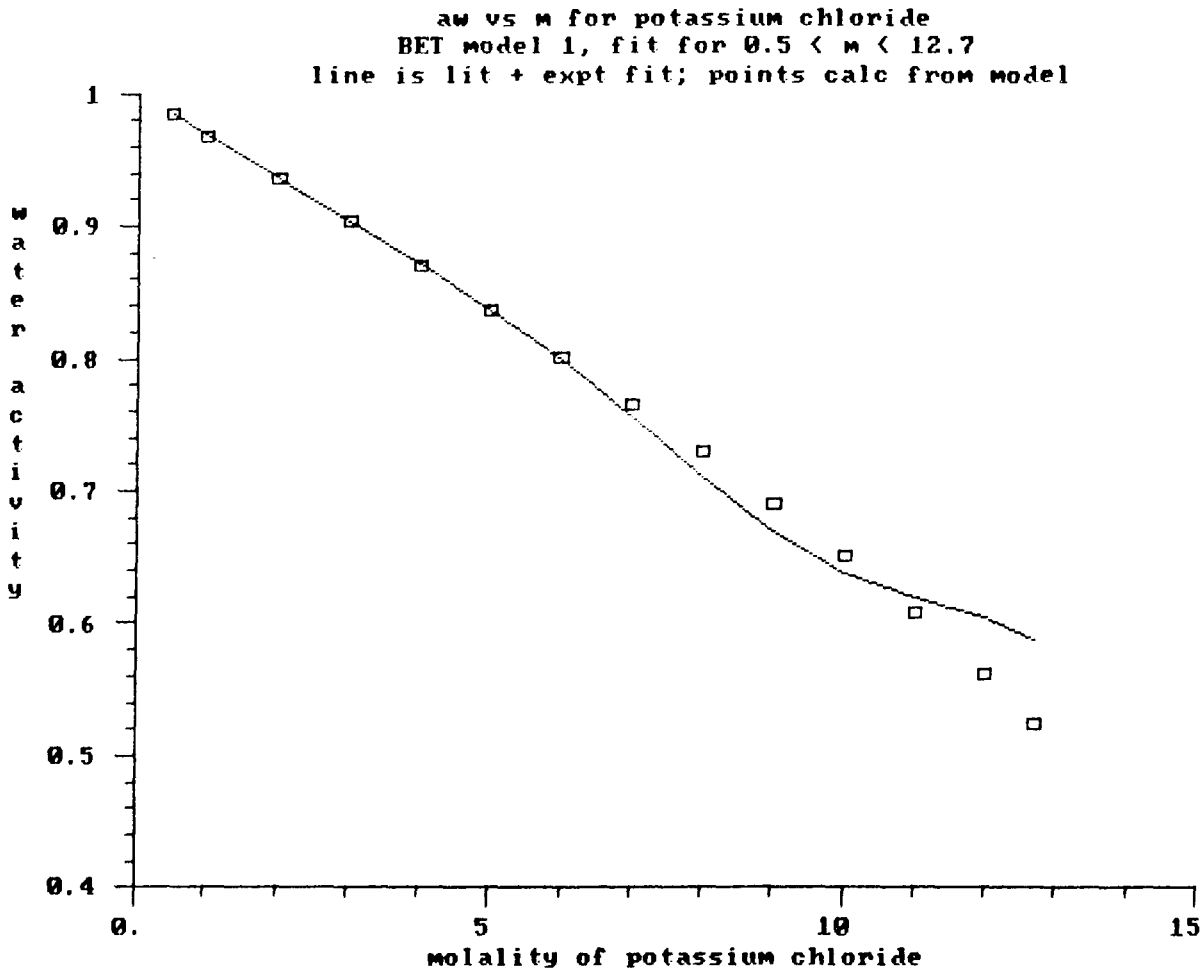
aw vs m for potassium chloride
BET model 1, fit for 0.5 < m < 12.7
line is lit + expt fit; points calc from model
water activity
1
0.9
0.8
0.7
0.6
0.5
0.4
0.
5
10
15
molality of potassium chloride

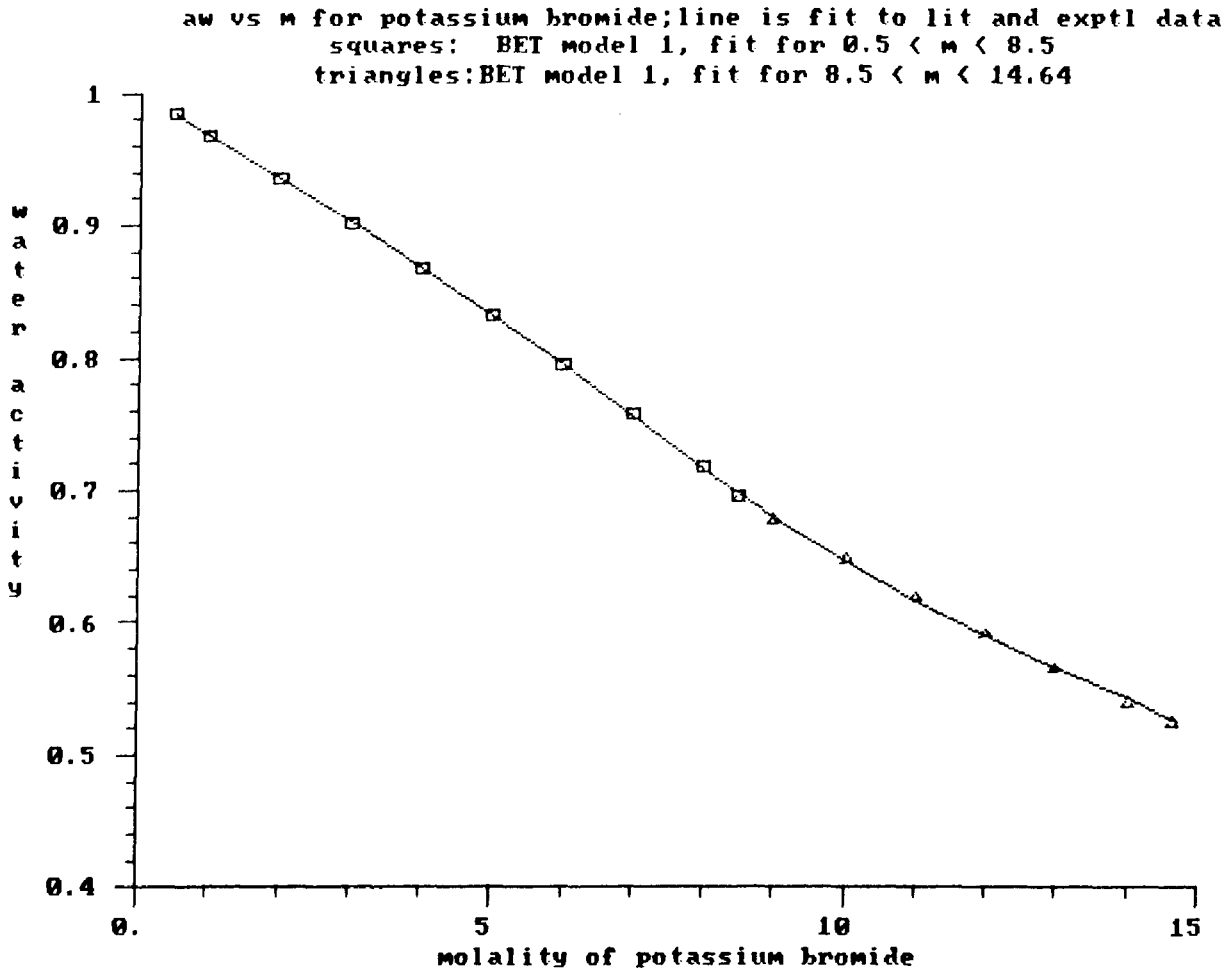
aw vs m for potassium bromide;line is fit to lit and exptl data
squares: BET model 1, fit for 0.5 < m < 8.5
triangles:BET model 1, fit for 8.5 < m < 14.64
water activity
1
0.9
0.8
0.7
0.6
0.5
0.4
0.
5
10
15
molality of potassium bromide

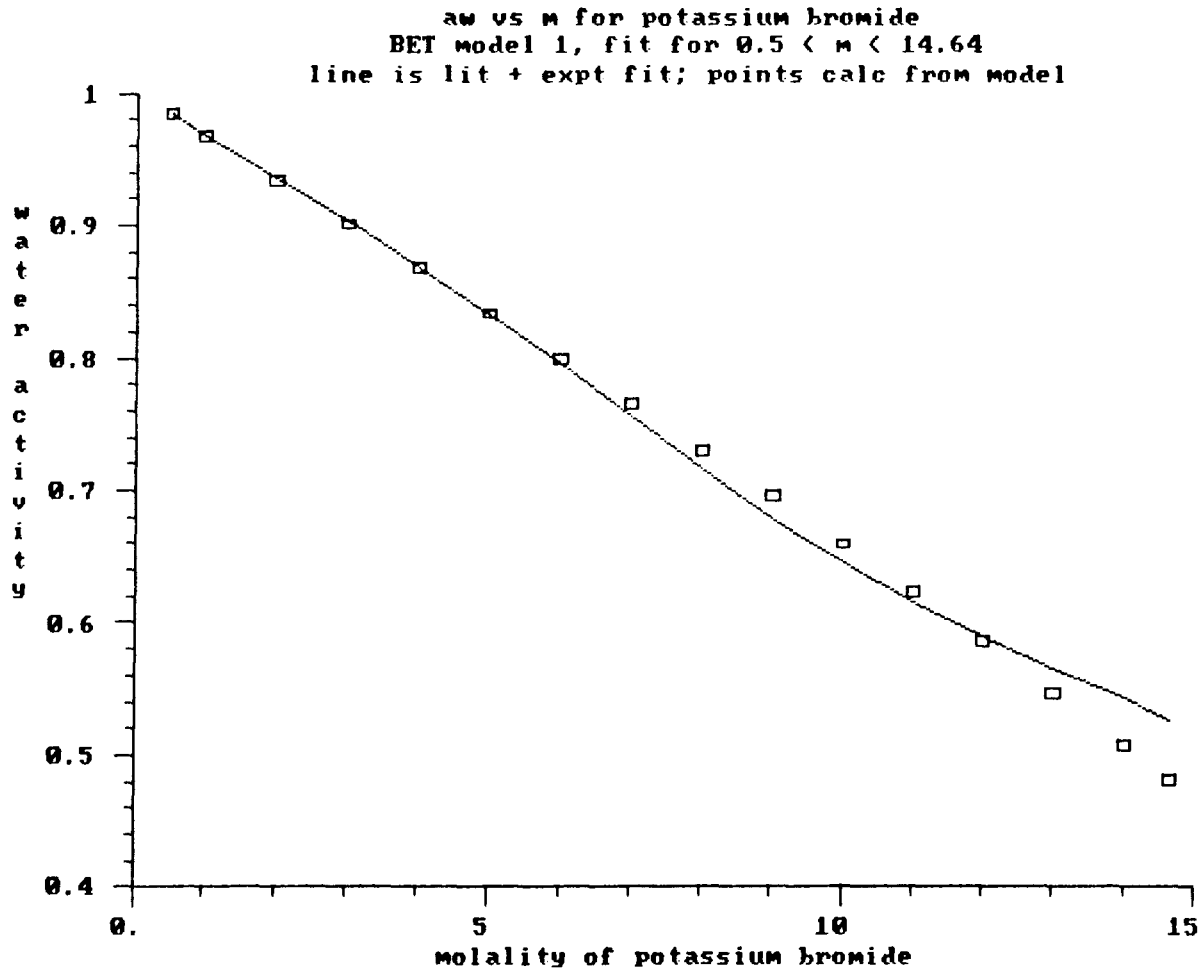
aw vs m for potassium bromide
BET model 1, fit for 0.5 < m < 14.64
line is lit + expt fit; points calc from model
water activity
1
0.9
0.8
0.7
0.6
0.5
0.4
0.
5
10
15
molality of potassium bromide

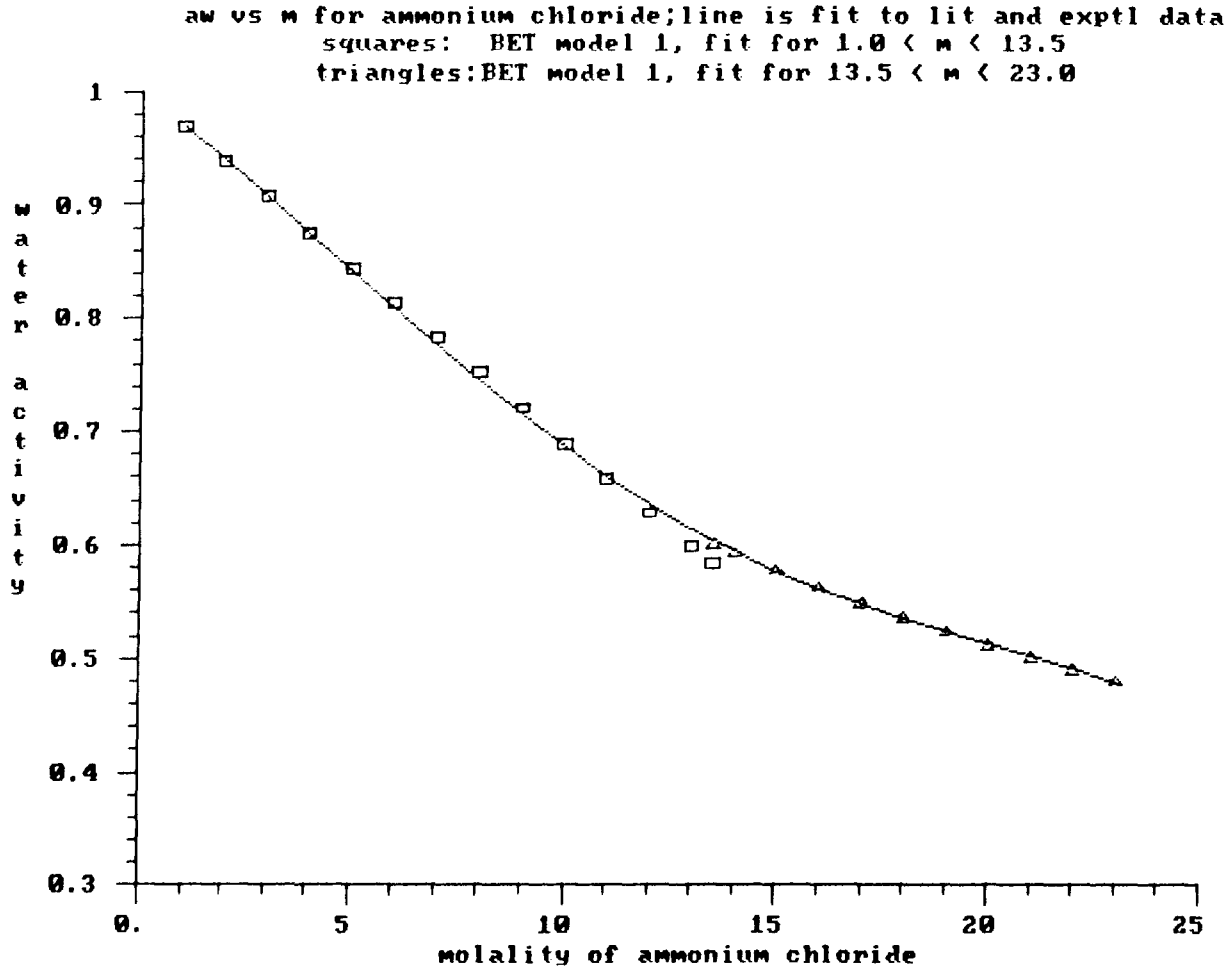
aw vs m for ammonium chloride;line is fit to lit and exptl data
squares: BET model 1, fit for 1.0 < m < 13.5
triangles:BET model 1, fit for 13.5 < m < 23.0
water activity
1
0.9
0.8
0.7
0.6
0.5
0.4
0.3
0.
5
10
15
20
25
molality of ammonium chloride

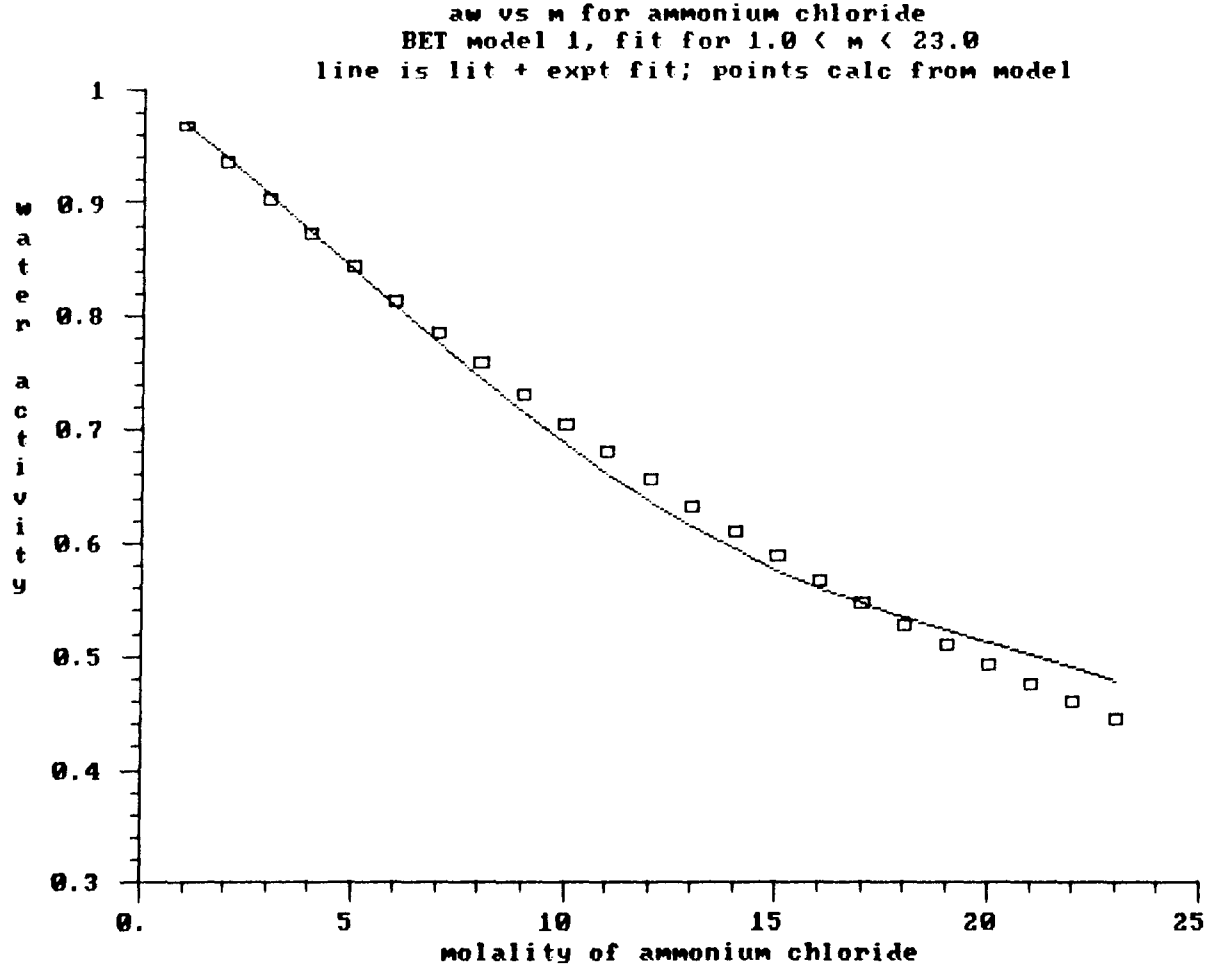
aw vs m for ammonium chloride
BET model 1, fit for 1.0 < m < 23.0
line is lit + expt fit; points calc from model
water activity
1
0.9
0.8
0.7
0.6
0.5
0.4
0.3
0.
5
10
15
20
25
molality of ammonium chloride

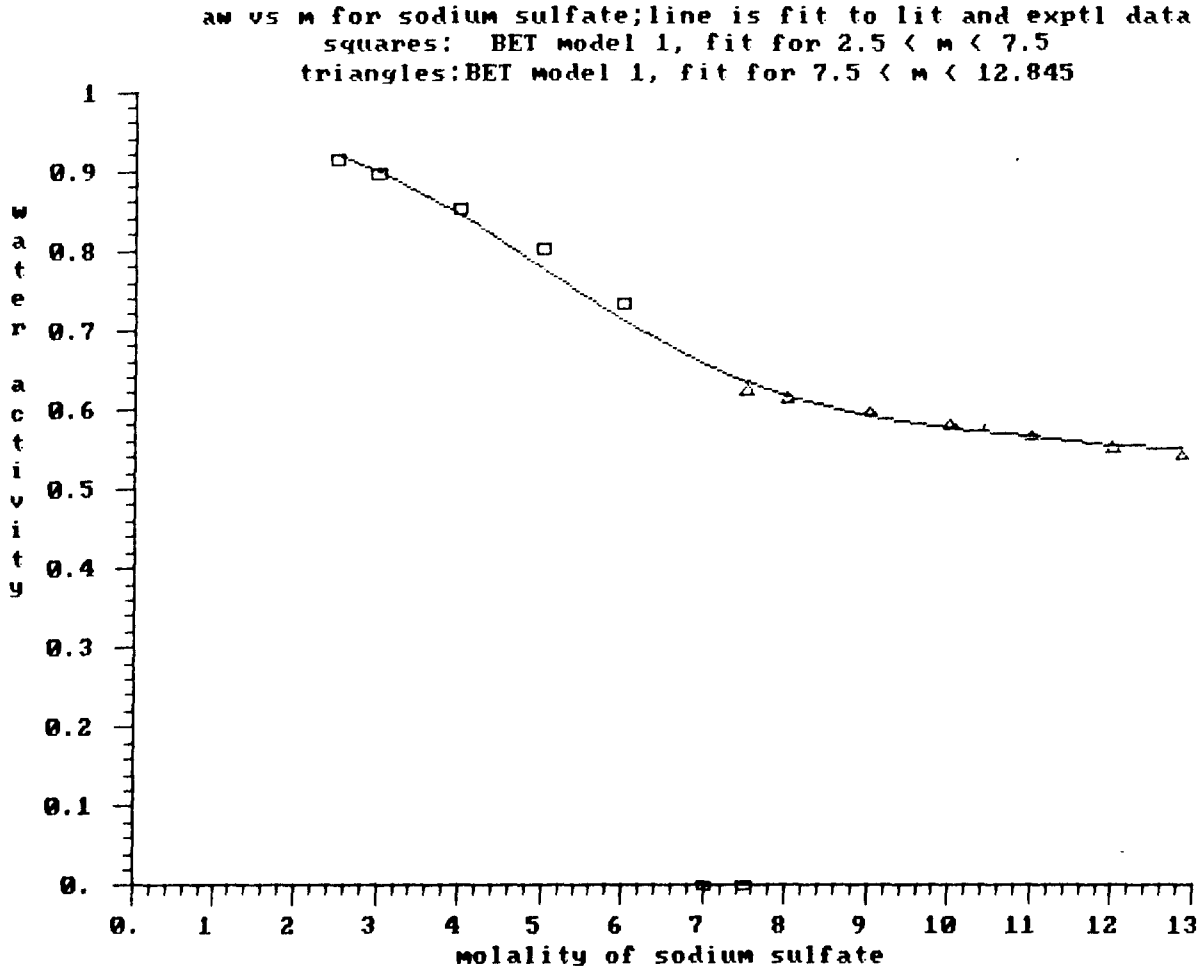
aw vs m for sodium sulfate;line is fit to lit and exptl data
squares: BET model 1, fit for 2.5 < m < 7.5
triangles:BET model 1, fit for 7.5 < m < 12.845
water activity
1
0.9
0.8
0.7
0.6
0.5
0.4
0.3
0.2
0.1
0.
0. 1 2 3 4 5 6 7 8 9 10 11 12 13
molality of sodium sulfate

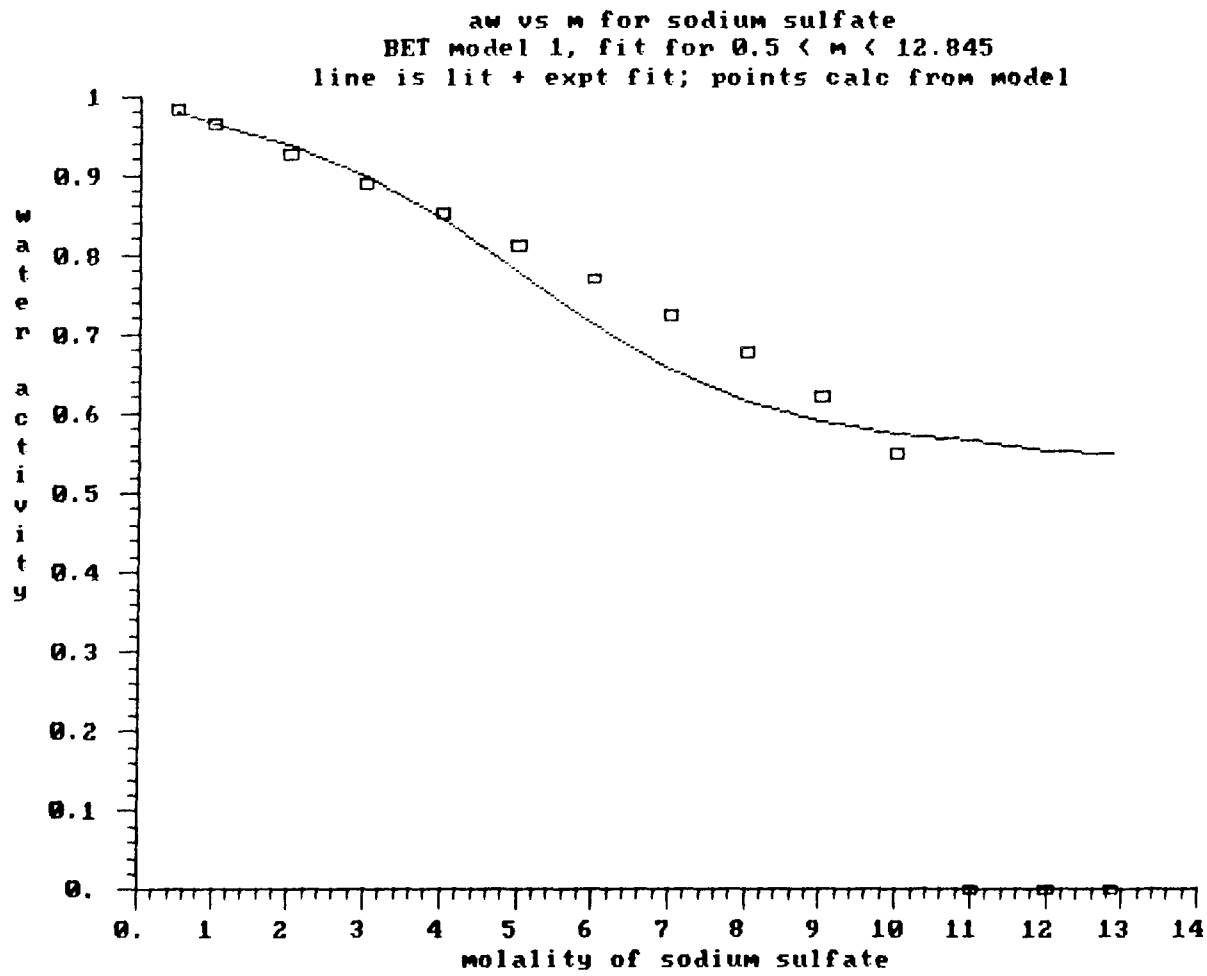
aw vs m for sodium sulfate
BET model 1, fit for 0.5 < m < 12.845
line is lit + expt fit; points calc from model
water activity
1
0.9
0.8
0.7
0.6
0.5
0.4
0.3
0.2
0.1
0.
0. 1 2 3 4 5 6 7 8 9 10 11 12 13 14
molality of sodium sulfate

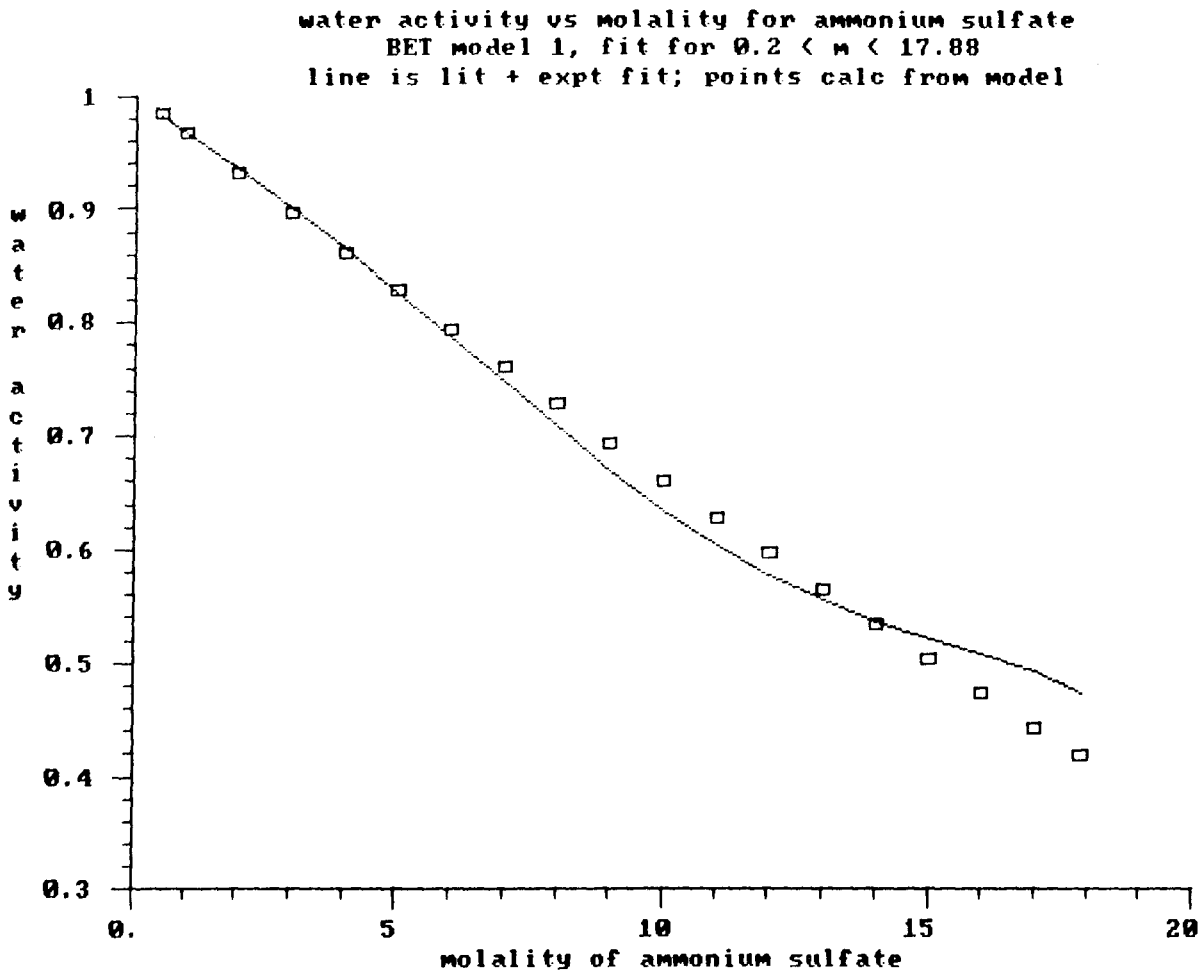
water activity vs molality for ammonium sulfate
BET model 1, fit for 0.2 < m < 17.88
line is lit + expt fit; points calc from model
water activity
1
0.9
0.8
0.7
0.6
0.5
0.4
0.3
0.
5
10
15
20
molality of ammonium sulfate

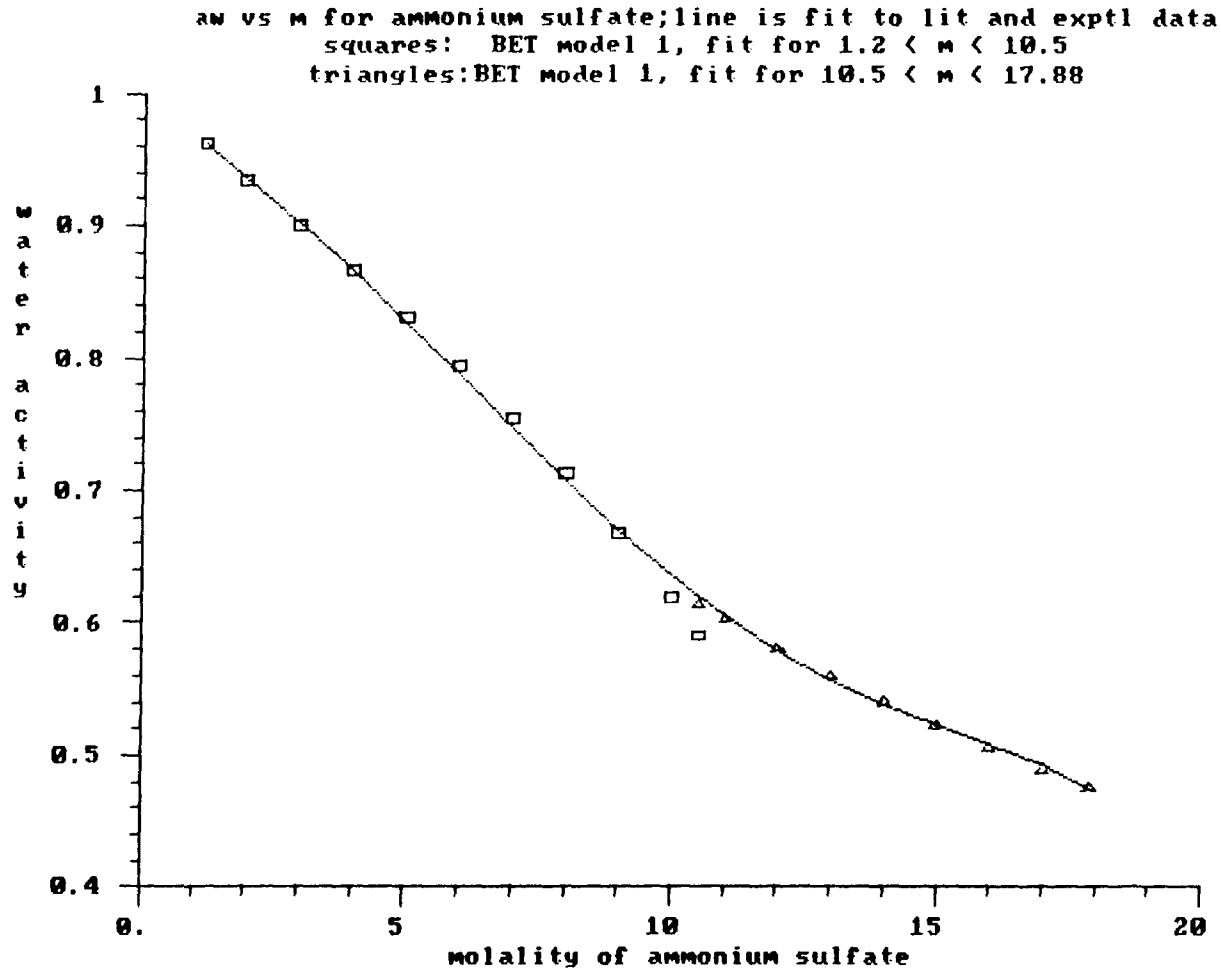
aw vs m for ammonium sulfate;line is fit to lit and exptl data
squares: BET model 1, fit for 1.2 < m < 10.5
triangles:BET model 1, fit for 10.5 < m < 17.88
water activity
1
0.9
0.8
0.7
0.6
0.5
0.4
0.
5
10
15
20
molality of ammonium sulfate

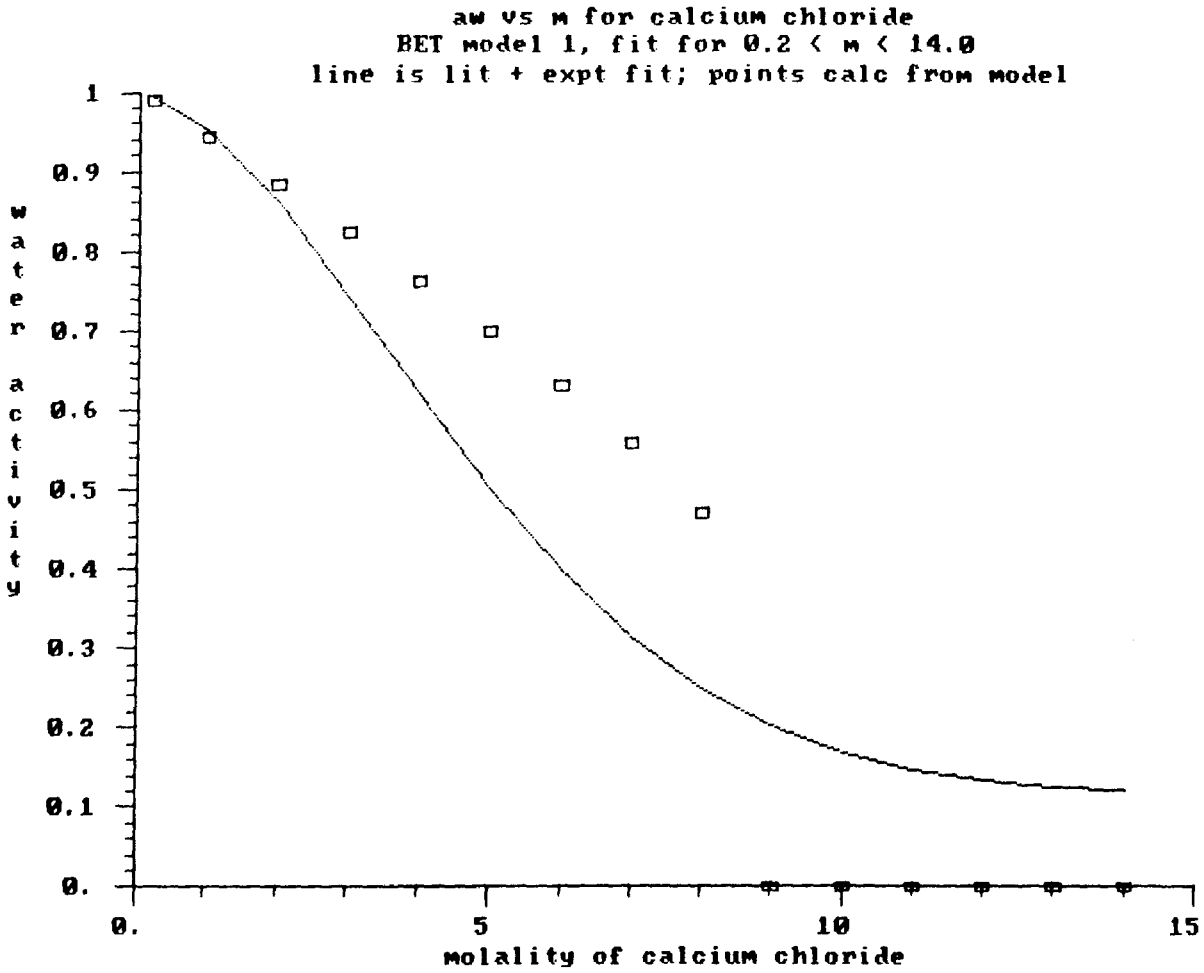
aw vs m for calcium chloride
BET model 1, fit for 0.2 < m < 14.0
line is lit + expt fit; points calc from model
water activity
1
0.9
0.8
0.7
0.6
0.5
0.4
0.3
0.2
0.1
0.
0.
5
10
15
molality of calcium chloride

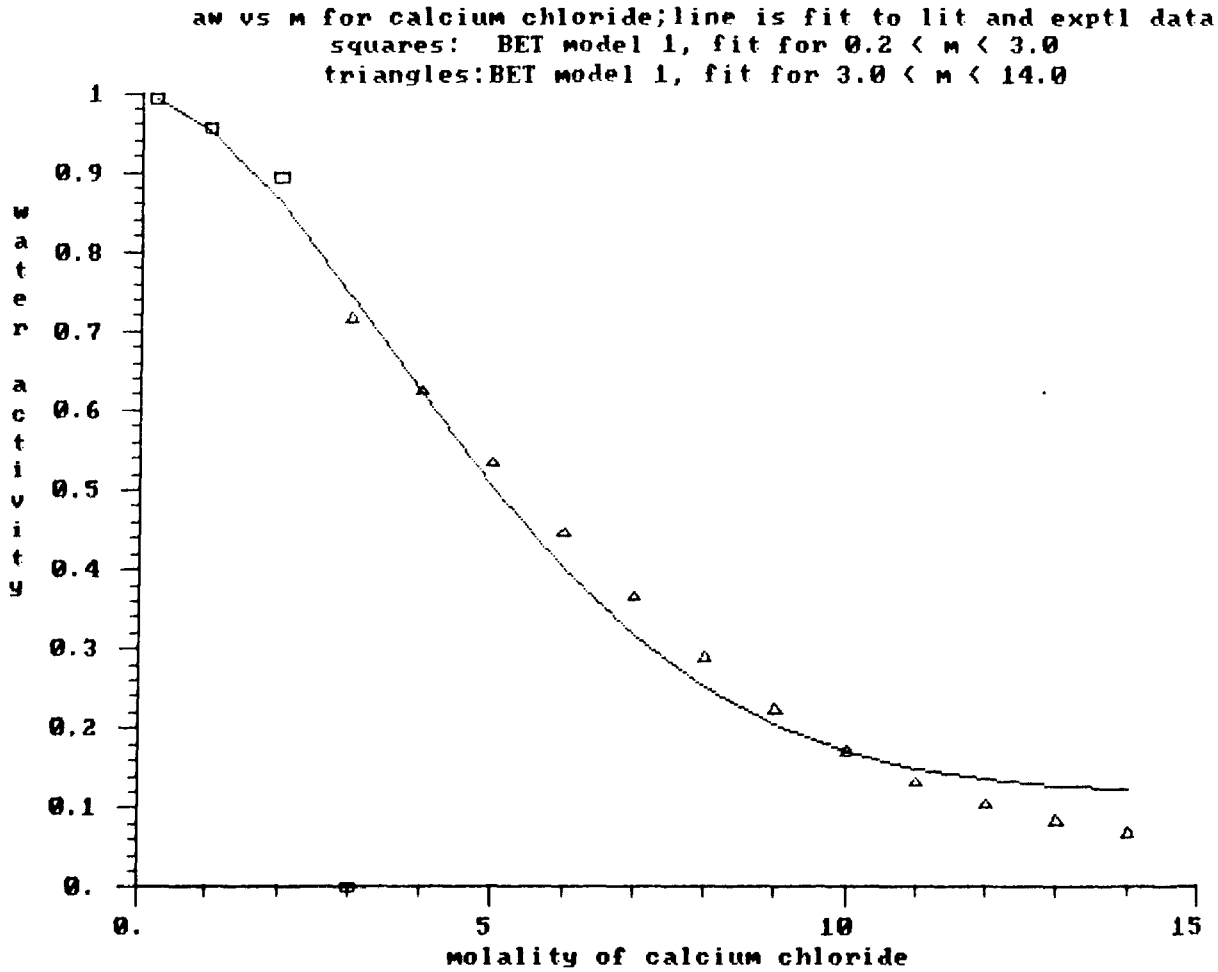
aw vs m for calcium chloride;line is fit to lit and exptl data
squares: BET model 1, fit for 0.2 < m < 3.0
triangles:BET model 1, fit for 3.0 < m < 14.0
water activity
1
0.9
0.8
0.7
0.6
0.5
0.4
0.3
0.2
0.1
0.
0.
5
10
15
molality of calcium chloride

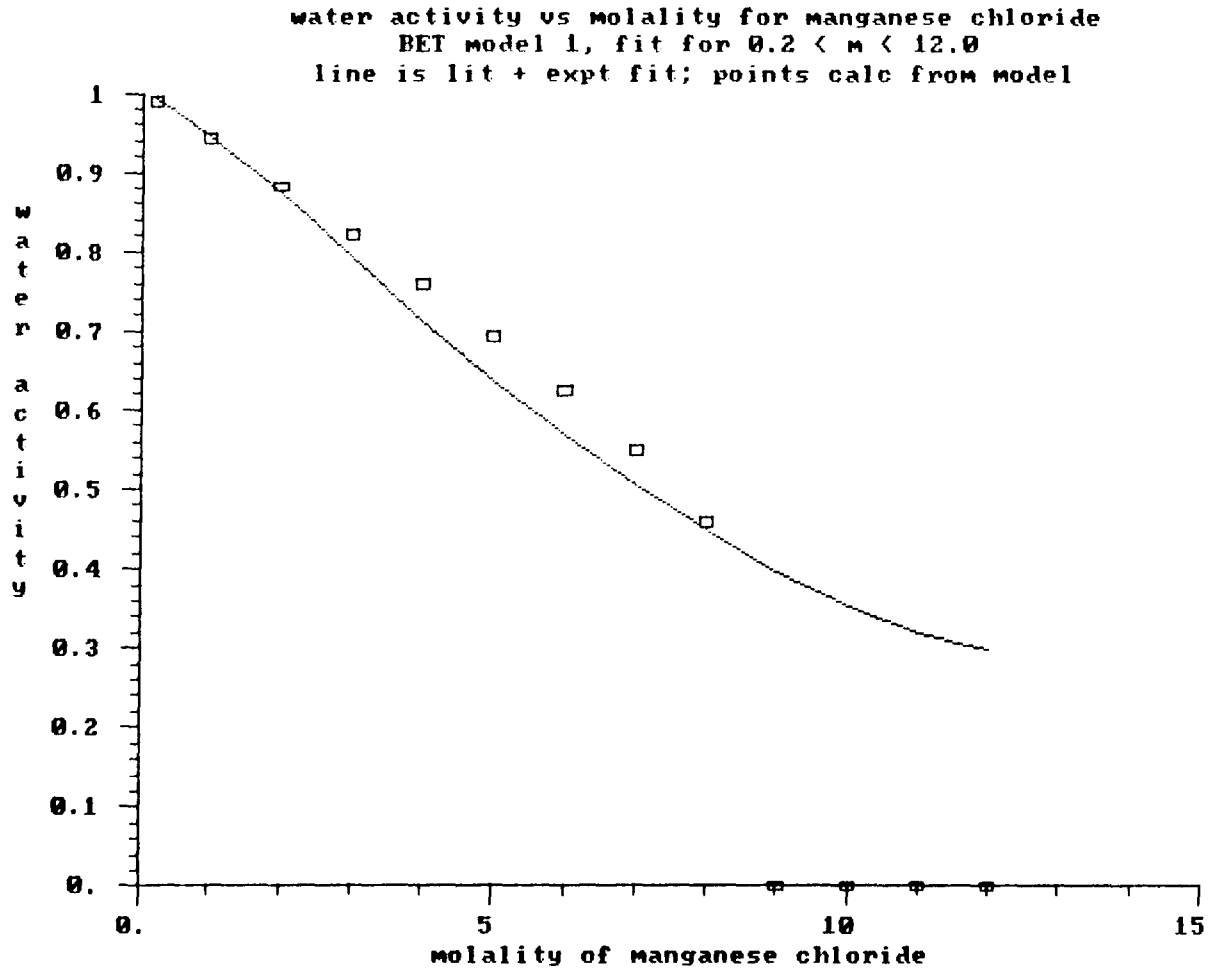
water activity vs molality for manganese chloride
BET model 1, fit for 0.2 < m < 12.0
line is lit + expt fit; points calc from model
water activity
1
0.9
0.8
0.7
0.6
0.5
0.4
0.3
0.2
0.1
0.
0.
5
10
15
molality of manganese chloride

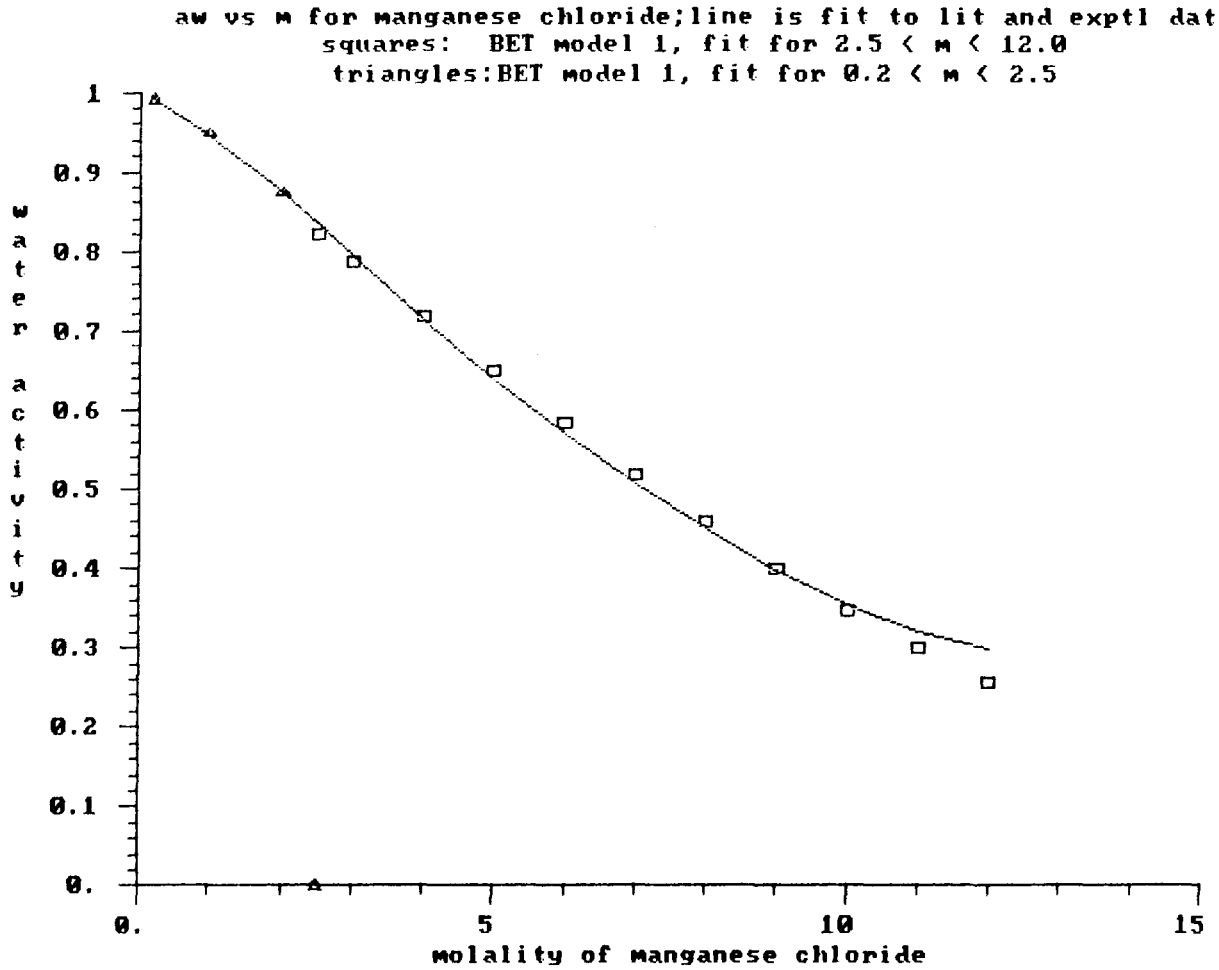
aw vs m for manganese chloride;line is fit to lit and exptl data
squares: BET model 1, fit for 2.5 < m < 12.0
triangles:BET model 1, fit for 0.2 < m < 2.5
water activity
1
0.9
0.8
0.7
0.6
0.5
0.4
0.3
0.2
0.1
0.
0.
5
10
15
molality of manganese chloride

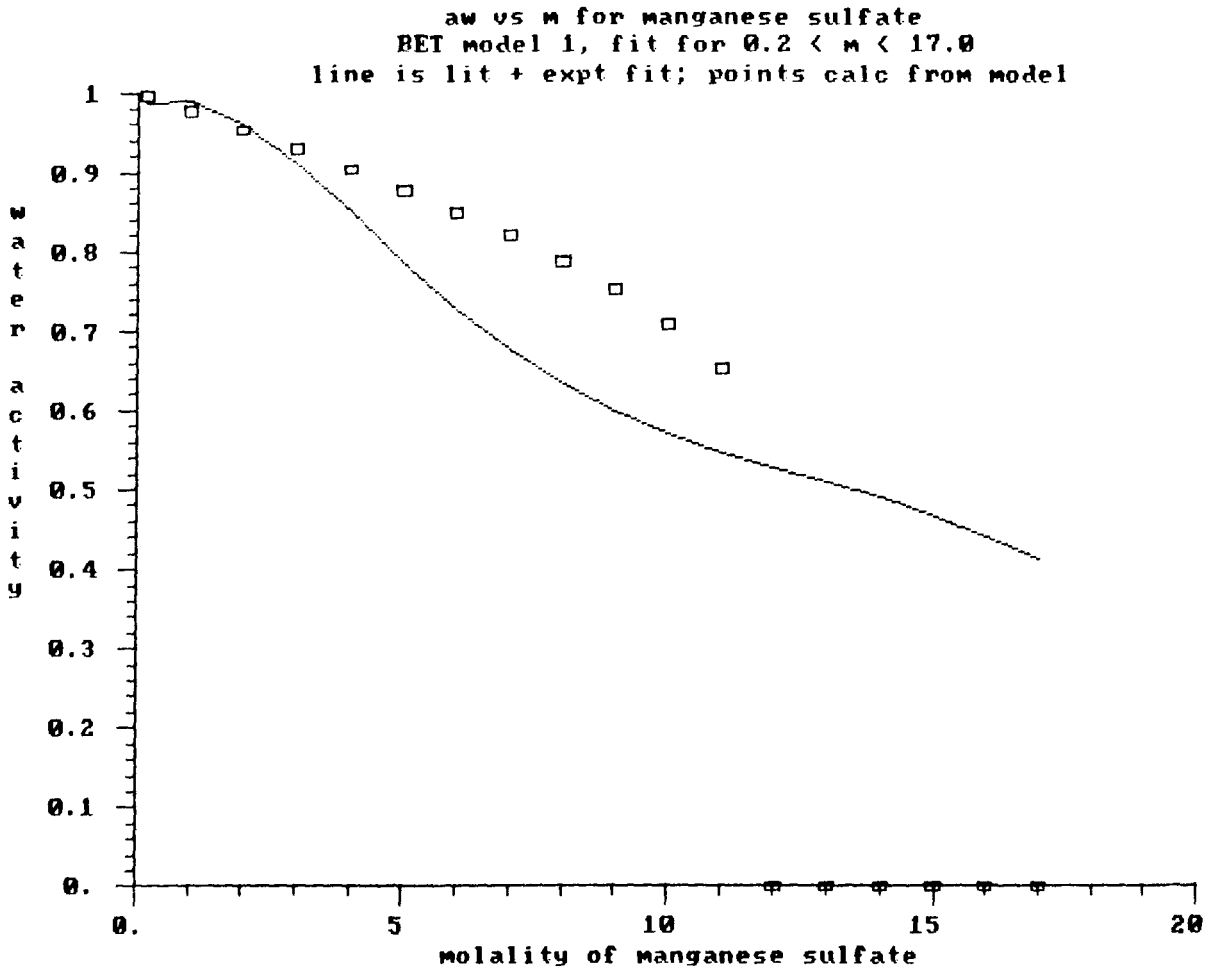
aw vs m for manganese sulfate
BET model 1, fit for 0.2 < m < 17.0
line is lit + expt fit; points calc from model
water activity
1
0.9
0.8
0.7
0.6
0.5
0.4
0.3
0.2
0.1
0.
0.
5
10
15
20
molality of manganese sulfate

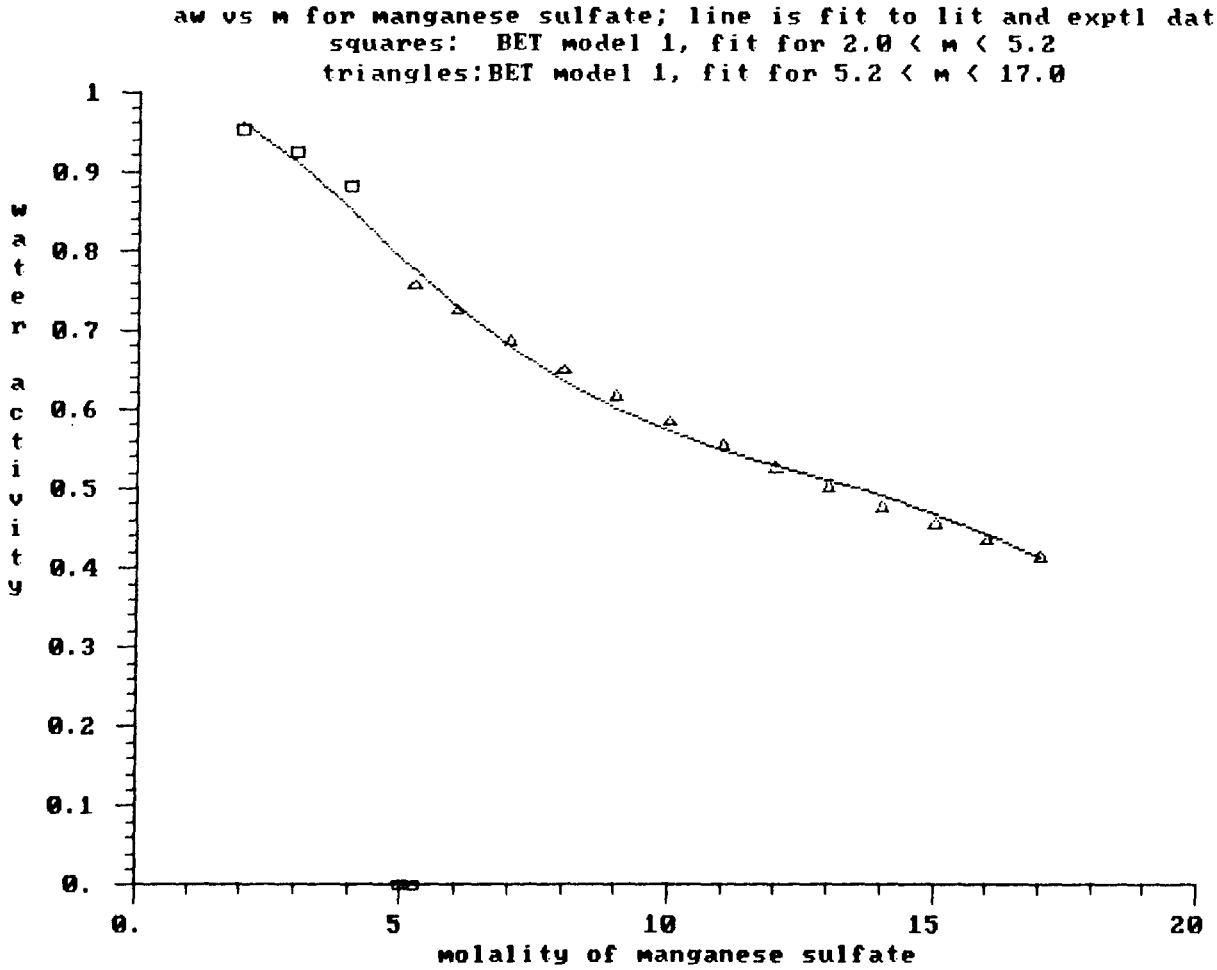
aw vs m for manganese sulfate; line is fit to lit and exptl data
squares: BET model 1, fit for 2.0 < m < 5.2
triangles:BET model 1, fit for 5.2 < m < 17.0
water activity
1
0.9
0.8
0.7
0.6
0.5
0.4
0.3
0.2
0.1
0.
0.
5
10
15
20
molality of manganese sulfate

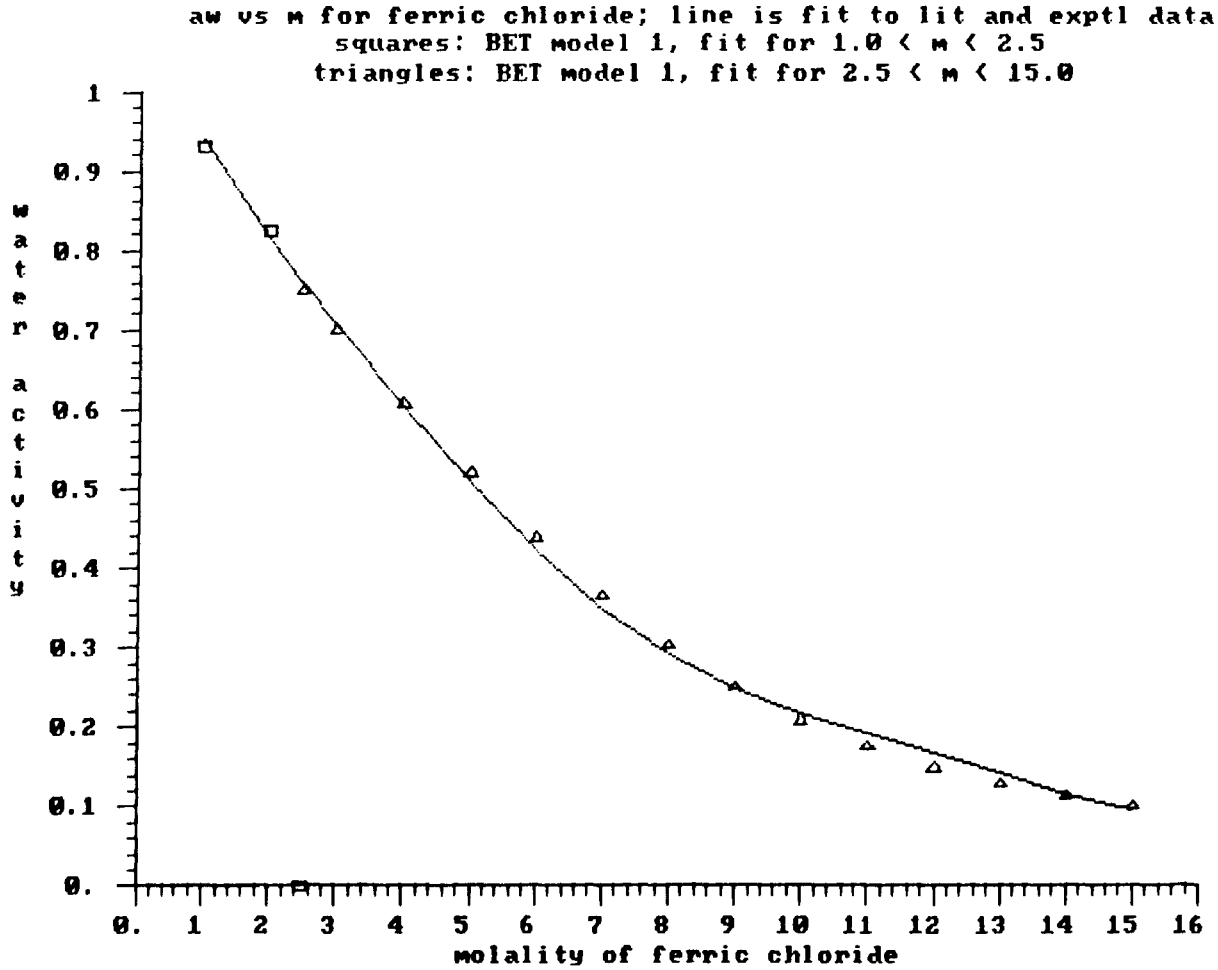
aw vs m for ferric chloride; line is fit to lit and exptl data
squares: BET model 1, fit for 1.0 < m < 2.5
triangles: BET model 1, fit for 2.5 < m < 15.0
water activity
1
0.9
0.8
0.7
0.6
0.5
0.4
0.3
0.2
0.1
0.
0. 1 2 3 4 5 6 7 8 9 10 11 12 13 14 15 16
molality of ferric chloride

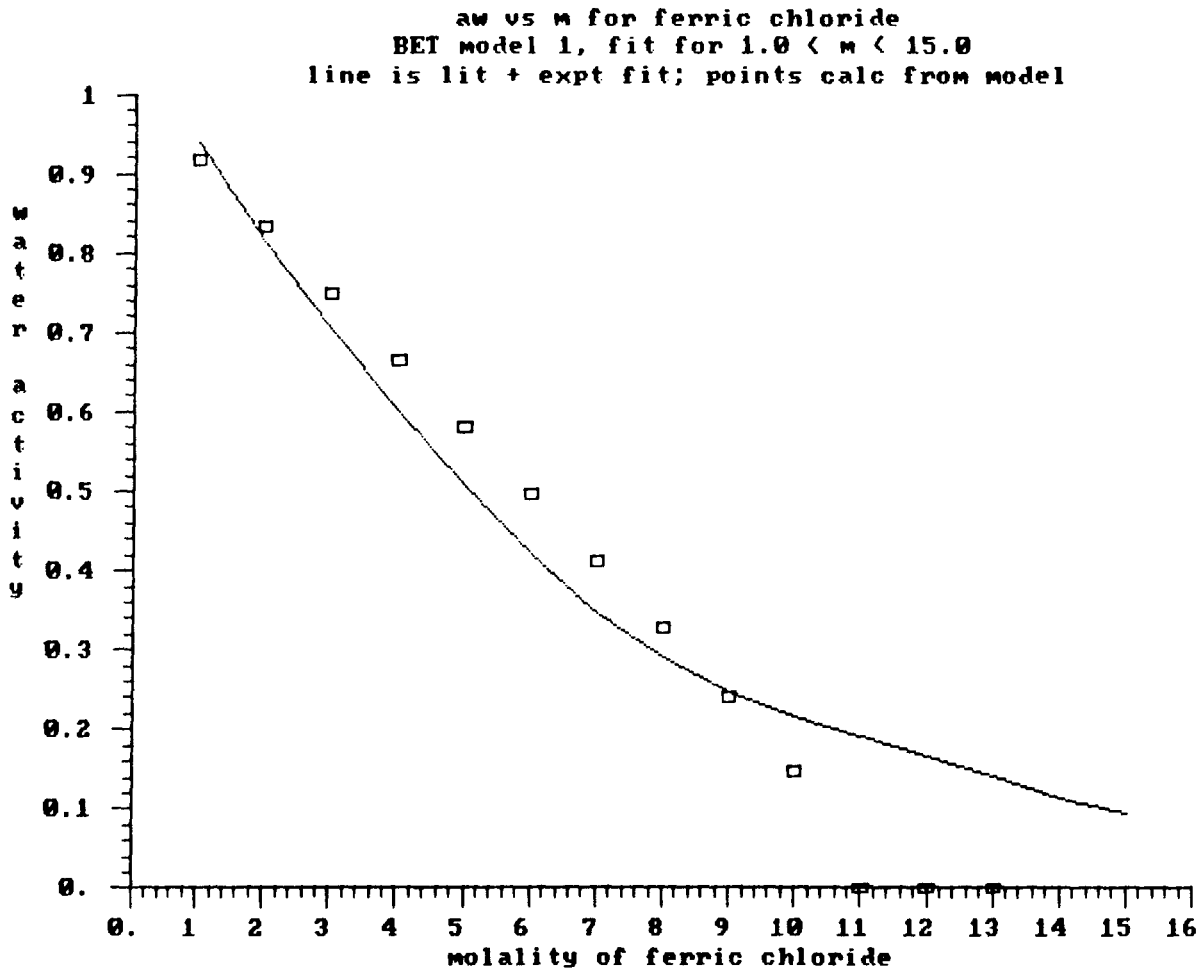
aw vs m for ferric chloride
BET model 1, fit for 1.0 < m < 15.0
line is lit + expt fit; points calc from model
water activity
1
0.9
0.8
0.7
0.6
0.5
0.4
0.3
0.2
0.1
0.
0. 1 2 3 4 5 6 7 8 9 10 11 12 13 14 15 16
molality of ferric chloride

Appendix M: Tables of experimental data for particle relative mass as a function of chamber relative humidity for mixed-electrolyte particles

This appendix documents the experimental data taken for mixed-electrolyte solutions. As in Appendix A, there are two kinds of tables included in this appendix. The tables in this appendix are very similar to those in Appendix A for single-electrolyte particles. Thus, the tables in this section will be described only briefly, with emphasis on those features which are different from those of the tables in Appendix A.

The first type of table contains essentially the "raw" experimental data. The columns of data in this first type of table have the same meanings as described in Appendix A.

In the second type of table, there are eight columns of data. Again, each line represents a datum point in which the particle mass and relative humidity had reached a steady state. This type of table contains useful quantities which have been calculated from the "raw" data of the previous type of table. For each table of the first type there is corresponding table of this second type.

In some of the tables presenting results for the NaCl – $(NH_4)_2SO_4$ mixtures studied, the dry balancing voltage is multiplied by a factor to account for the possibility of water in the dry-particle-state. In fact, for each of the three NaCl – $(NH_4)_2SO_4$ mixtures studied, there are two different tables of this sec-

ond type: one has results calculated assuming the dry particles were anhydrous; the other has results calculated assuming a particular amount of water in the crytal. This matter is discussed in detail in Chapter 2 of the text. For reasons presented in Chapter 2, the non-anhydrous dry-state assumption may be the most correct.

The columns of data in this second type of table have the following meanings.

- Column 1 contains the point label for the steady state corresponding to the earlier table for the particular experiment.
- Column 2 lists the relative humidity calculated from the dewpoint hygrometer output, the thermistor output, and the temperature difference between the particle and the thermistor. The uncertainty in this calculated relative humidity is approximately 0.01–0.02.
- Column 3 contains the weight fraction solute, calculated from the ratio of the dry to the wet balancing voltage. In some of the tables for the NaCl – $(NH_4)_2SO_4$ mixture, the dry balancing voltage is multiplied by a factor before the weight fraction solute is calculated in order to account for water in the dry-particle state.
- Columns 4 and 5 give the molalities of the various solutes.
- Column 6 lists the ionic strength of the solution, calculated on molal basis.
- Column 7 contains the water activity estimated for a this droplet con-

centration as predicted by the ZSR method. If this method could not be applied because binary data did not extend to a low-enough water activity, Column 7 is left blank.

- Column 8 contains the water activity estimated for a this droplet concentration as predicted by the RWR method. If this method could not be applied because binary data did not extend to a high-enough ionic strength, Column 8 is left blank.

MIXTURE OF SODIUM CHLORIDE AND POTASSIUM CHLORIDE
DATE OF EXPT: 11-30-85
MOLES KCL PER MOLE NACL : 1.0026

pt #	#1	880mv	Vdc(w)	Vdc(d)		comments
1	3.	13.	10.46	10.48	d	
2	3.016	30.83	10.48	10.48	d	
3	3.013	32.415	10.50	10.48	d	
4	3.011	33.13	26.90	10.48	w	partial deliq.
7	3.007	34.20	43.	10.48	w	
8	3.007	33.75	38.53	10.48	w	
9	3.008	33.16	34.53	10.48	w	
10	3.	13.	10.50	10.48	d	

DATE OF EXPT: 12-1-85
MOLES KCL PER MOLE NACL : 1.0026

pt #	#1	880mv	Vdc(w)	Vdc(d)		comments
11	3.	13.	10.69	10.67	d	
13	3.020	33.34	36.5	10.67	w	
14	3.018	32.21	31.02	10.67	w	
15	3.016	30.66	26.23	10.67	w	
16	3.014	28.74	22.56	10.67	w	
17	3.012	27.37	20.68	10.67	w	
18	3.011	26.01	10.67	10.67	d	
19	3.	13.	10.64	10.67	d	

MIXTURE OF SODIUM CHLORIDE AND POTASSIUM BROMIDE
DATES OF EXPT: 12-13-85 THROUGH 12-18-85
MOLES KBR PER MOLE NACL : 1.6142

pt #	#1	880mv	Vdc(w)	Vdc(d)		comments
1	3.	13.	11.84	11.847	d	
4	3.005	25.65	12.02	11.933	d	
5	3.	13.	11.95	11.934	d	
8	3.012	25.70	21.13	11.988	w	
9	3.012	24.84	12.04	11.990	d	
10	3.	13.	11.98	11.991	d	
11	3.	13.	12.16	12.095	d	
12	3.013	34.20	43.69	12.140	w	possibly not steady state
13	3.012	33.98	41.66	12.152	w	
14	3.012	33.34	37.06	12.156	w	
15	3.012	32.21	31.8	12.165	w	
16	3.012	30.43	26.98	12.172	w	
17	3.012	28.61	24.01	12.178	w	
18	3.012	26.03	12.21	12.181	d	
19	3.	13.	12.13	12.182	d	
21	1.5	13.	12.15	12.3	d	after 50 C cryst'n
22	3.	13.	12.56	12.56	d	
23	3.015	34.535	53.16	12.59	w	after 10 hrs waiting
24	3.014	34.16	47.80	12.59	w	
25	3.013	24.90	21.85	12.59	w	
26	3.012	24.44	21.71	12.59	w	
27	3.0115	23.74	12.60	12.59	d	
28	3.	13.	12.59	12.59	d	
30	3.011	34.00	44.0	12.60	w	
31	3.011	32.69	35.66	12.61	w	
32	3.011	31.20	30.67	12.62	w	
33	3.0115	29.39	26.51	12.63	w	
34	3.011	27.04	23.38	12.63	w	
35	3.0105	25.69	21.83	12.64	w	
36	3.010	24.67	12.70	12.64	d	
37	3.	13.	12.65	12.65	d	

DATES OF EXPT: 12-28-85 AND 12-29-85
MOLES KBR PER MOLE NACL : 1.6142

pt #	#1	880mv	Vdc(w)	Vdc(d)		comments
1	3.	13.	8.85	8.85	d	
2	3.011	34.50	41.33	8.85	w	
3	3.010	34.11	35.97	8.85	w	
4	3.009	30.40	20.50	8.85	w	
5	3.009	26.01	9.19	8.85	d	
6	3.	13.	8.865	8.85	d	
8	3.	13.	8.85	8.85	d	
9	3.	13.	8.88	8.88	d	next day
10	3.010	35.14	64.38	8.88	w	
11	3.010	34.73	49.0	8.88	w	
12	3.011	33.69	33.42	8.88	w	
13	3.010	32.49	26.28	8.88	w	
14	3.0105	30.39	20.75	8.88	w	
15	3.010	28.54	18.37	8.88	w	
16	3.010	26.98	9.25	8.88	d	
17	3.	13.	8.88	8.88	d	

MIXTURE OF SODIUM CHLORIDE AND AMMONIUM SULFATE
DATE OF EXPT: 11-24-85 (A)
MOLES AMM SULF PER MOLE NACL : 0.5002

pt #	#1	880mv	Vdc(w)	Vdc(d)		comments
1	3.008	13.	6.596	6.55	d	assume linear Vdry
2	3.010	30.68	6.47	6.54	d	decrease with pt number
3	3.009	32.36	15.23	6.53	w	
6	3.005	33.79	19.13	6.50	w	
7	3.005	33.00	17.10	6.49	w	
8	3.005	31.51	14.40	6.47	w	
9	3.004	29.84	12.75	6.46	w	
10	3.004	27.82	10.68	6.44	w	
11	3.003	26.55	9.86	6.43	w	
12	3.003	26.05	9.53	6.41	w	
13	3.002	25.73	9.44	6.39	w	
14	3.002	25.09	9.2	6.38	w	just before cryst'n
15	3.002	25.09	6.39	6.36	d	
16	3.	13.	6.36	6.36	d	

MIXTURE OF SODIUM CHLORIDE AND AMMONIUM SULFATE
DATE OF EXPT: 10-29-85
MOLES AMM SULF PER MOLE NACL : 1.0002

pt #	#1	880mv	Vdc(w)	Vdc(d)		comments
1	3.	13.	21.77	21.77	d	assuming linear decrease
2	3.015	34.16	63.31	21.68	w	in Vdry with pt number
3	3.013	33.50	55.80	21.59	w	
4	3.013	32.245	46.19	21.50	w	
5	3.013	30.52	39.56	21.41	w	
6	3.013	28.53	33.31	21.32	w	
7	3.013	25.98	28.53	21.23	w	
8	3.013	23.98	25.82	21.14	w	
9a	3.013	22.94	24.7	21.06	w	just before cryst'n
9b	3.013	22.95	21.06	21.06	d	

DATE OF EXPT: 10-31-85
MOLES AMM SULF PER MOLE NACL : 1.0002

pt #	#1	880mv	Vdc(w)	Vdc(d)		comments
1	3.	13.	13.11	13.11	d	assuming linear decrease
2	3.022	29.05	13.13	13.10	d	in Vdry with pt number
3	3.014	31.33	13.15	13.09	d	(#4 started to deliq at
5	3.014	31.59	13.17	13.08	d	just slightly higher rh)
6	3.013	31.73	13.33	13.07	d	
7	3.011	31.97	25.5	13.06	w	
9	3.010	32.93	29.95	13.04	w	
10	3.011	33.715	33.57	13.02	w	
11	3.0115	31.44	25.65	13.01	w	
12	3.0125	29.70	21.77	13.00	w	
13	3.012	32.19	26.98	12.98	w	
14	3.012	27.75	19.09	12.97	w	
15	3.013	25.16	16.79	12.95	w	
16	3.013	23.59	15.78	12.94	w	
17	3.013	22.84	15.35	12.92	w	
18	3.012	21.69	14.88	12.90	w	just before cryst'n
19	3.012	21.69	12.88	12.88	d	
20	3.	13.	12.86	12.86	d	

DATE OF EXPT: 11-23-85
MOLES AMM SULF PER MOLE NACL : 1.0029

pt #	#1	880mv	Vdc(w)	Vdc(d)		comments
1	3.019	13.	10.54	10.54	d	
2	3.015	24.19	12.99	10.56	w	
3	3.015	13.	10.58	10.58	d	

MIXTURE OF SODIUM CHLORIDE AND AMMONIUM SULFATE
DATE OF EXPT: 11-24-85 (B)
MOLES AMM SULF PER MOLE NACL : 1.9980

pt #	#1	880mv	Vdc(w)	Vdc(d)		comments
1	3.	13.	23.14	23.39	d	
2	3.011	31.46	23.39	23.39	d	
3	3.009	32.32	41.5	23.39	w	not complete deliq.
6	3.005	33.73	56.38	23.39	w	
7	3.004	33.01	50.7	23.39	w	
8	3.004	32.02	45.56	23.39	w	
9	3.004	31.04	42.09	23.39	w	
10	3.004	29.40	37.6	23.39	w	
11	3.004	27.65	33.04	23.39	w	
12	3.004	25.34	30.13	23.39	w	
13	3.003	23.84	28.77	23.39	w	
14	3.003	21.89	27.51	23.39	w	
15	3.003	20.99	27.00	23.39	w	
16	3.002	18.52	23.39	23.39	d	
17	3.	13.	23.36	23.39	d	

MIXTURE OF SODIUM CHLORIDE AND POTASSIUM CHLORIDE
DATE OF EXPT: 11-30-85
MOLES KCL/MOLE NACL : 1.00269

pt #	rh	wt. frac. sol.	NaCl molal.	KCl molal.	ionic strgth	water act. ZSR	water act. RWR
1	.1093	1.0019					
2	.6169	1.0000					
3	.7110	.9981					
4	.7596	.3896					
7	.8401	.2437	2.419	2.426	4.845	.8293	.8287
8	.8043	.2720	2.805	2.812	5.617	.7959	.7945
9	.7607	.3035	3.271	3.280	6.552	.7514	.7495
10	.1093	.9981					

DATE OF EXPT: 12-1-85
MOLES KCL/MOLE NACL : 1.00269

pt #	rh	wt. frac. sol.	NaCl molal.	KCl molal.	ionic strgth	water act. ZSR	water act. RWR
11	.1093	.9981					
13	.7781	.2923	3.101	3.109	6.211	.7681	.7662
14	.6993	.3440	3.936	3.947	7.883	.6860	.6829
15	.6077	.4068	5.148	5.162	10.310	.5967	.5834
16	.5153	.4730	6.737	6.755	13.492		
17	.4604	.5160	8.002	8.024	16.026		
18	.4132	1.0000					
19	.1093	1.0028					

MIXTURE OF SODIUM CHLORIDE AND POTASSIUM BROMIDE
DATE OF EXPT: 12-13-85 THROUGH 12-18-85
MOLES KBR/MOLE NACL : .61953

pt #	rh	wt. frac. sol.	NaCl molal.	KBr molal.	ionic strgth	water act. ZSR	water act. RWR
1	.1093	1.0006					
4	.4006	.9928					
5	.1093	.9987					
8	.4035	.5673	9.922	6.147	16.069		
9	.3773	.9958					
10	.1093	1.0009					
11	.1093	.9947					
12	.8424	.2779	2.911	1.804	4.715	.8307	.8265
13	.8243	.2917	3.116	1.930	5.046	.8166	.8117
14	.7752	.3280	3.693	2.288	5.981	.7742	.7676
15	.6974	.3825	4.688	2.904	7.592	.6937	.6871
16	.5945	.4511	6.220	3.853	10.073	.5882	.5755
17	.5094	.5072	7.788	4.825	12.612		.4959
18	.4140	.9976					
19	.1093	1.0043					
21	.0418	1.0123					
22	.1093	1.0000					
23	.8712	.2368	2.348	1.455	3.803		.8648
24	.8395	.2634	2.706	1.676	4.382	.8443	.8409
25	.3792	.5762	10.287	6.373	16.661		
26	.3657	.5799	10.445	6.471	16.916		
27	.3462	.9992					
28	.1093	1.0000					
30	.8255	.2864	3.036	1.881	4.917	.8222	.8175
31	.7288	.3536	4.139	2.564	6.704	.7386	.7318
32	.6360	.4115	5.290	3.277	8.568	.6478	.6396
33	.5436	.4764	6.885	4.265	11.150	.5514	.5388
34	.4482	.5402	8.890	5.507	14.397		
35	.4029	.5790	10.407	6.447	16.854		
36	.3720	.9953					
37	.1093	1.0000					

DATE OF EXPT: 12-28-85 AND 12-29-85
MOLES KBR/MOLE NACL : .61953

pt #	rh	wt. frac. sol.	NaCl molal.	KBr molal.	ionic strgth	water act. ZSR	water act. RWR
1	.1093	1.0000					
2	.8667	.2141	2.062	1.277	3.339	.8844	.8830
3	.8339	.2460	2.469	1.530	3.999	.8594	.8569
4	.5921	.4317	5.748	3.561	9.309	.6169	.6063
5	.4128	.9630					
6	.1093	.9983					
8	.1093	1.0000					
9	.1093	1.0000					
10	.9227	.1379	1.211	.750	1.961		.9333
11	.8860	.1812	1.675	1.038	2.712	.9072	.9064
12	.8012	.2657	2.738	1.696	4.434	.8422	.8387
13	.7150	.3379	3.861	2.392	6.254	.7610	.7542
14	.5920	.4280	5.660	3.507	9.167	.6226	.6124
15	.5059	.4834	7.080	4.386	11.466	.5411	.5293
16	.4459	.9600					
17	.1093	1.0000					

MIXTURE OF SODIUM CHLORIDE AND AMMONIUM SULFATE
DATE OF EXPT: 11-24-85 (A)
MOLES AMMSULF/MOLE NACL : .50026

pt #	rh	wt. frac. sol.	NaCl molal.	ammsulf molal.	ionic strgth	water act. ZSR	water act. RWR
1	.1097	.9930					
2	.6071	1.0108					
3	.7061	.4288	6.026	3.015	15.071	.6186	
6	.8067	.3398	4.132	2.067	10.334	.7576	.7577
7	.7482	.3795	4.911	2.457	12.282	.6972	.7138
8	.6522	.4493	6.551	3.277	16.382	.5879	
9	.5628	.5067	8.246	4.125	20.622	.5100	
10	.4757	.6030	12.195	6.101	30.497		
11	.4295	.6521	15.052	7.530	37.641		
12	.4129	.6726	16.496	8.252	41.252		
13	.4025	.6769	16.822	8.415	42.067		
14	.3829	.6935	18.165	9.087	45.427		
15	.3829	.9953					
16	.1093	1.0000					

MIXTURE OF SODIUM CHLORIDE AND AMMONIUM SULFATE
DATE OF EXPT: 11-24-85 (A)
MOLES AMMSULF/MOLE NACL : .50026
FACTOR VDRY WAS MULTIPLIED BY = .900

pt #	rh	wt. frac. sol.	NaCl molal.	ammsulf molal.	ionic strgth	water act. ZSR	water act. RWR
1	.1097	.8937					
2	.6071	.9097					
3	.7061	.3859	5.045	2.524	12.617	.6869	.7065
6	.8067	.3058	3.537	1.769	8.845	.8012	.7956
7	.7482	.3416	4.165	2.084	10.417	.7551	.7557
8	.6522	.4044	5.451	2.727	13.632	.6569	.6834
9	.5628	.4560	6.730	3.367	16.831	.5783	
10	.4757	.5427	9.528	4.767	23.828		
11	.4295	.5869	11.408	5.707	28.529		
12	.4129	.6054	12.316	6.161	30.799		
13	.4025	.6092	12.517	6.262	31.302		
14	.3829	.6241	13.332	6.670	33.341		
15	.3829	.8958					
16	.1093	.9000					

MIXTURE OF SODIUM CHLORIDE AND AMMONIUM SULFATE
DATE OF EXPT: 10-29-85
MOLES AMMSULF/MOLE NACL : 1.00017

pt #	rh	wt. frac. sol.	NaCl molal.	ammsulf molal.	ionic strgth	water act. ZSR	water act. RWR
1	.1093	1.0000					
2	.8399	.3424	2.732	2.733	10.930	.7979	.7991
3	.7875	.3869	3.311	3.312	13.246	.7426	.7554
4	.7000	.4655	4.569	4.569	18.277	.6275	
5	.5995	.5412	6.189	6.190	24.758	.5265	
6	.5062	.6400	9.329	9.331	37.321		
7	.4126	.7441	15.258	15.260	61.039		
8	.3530	.8187	23.699	23.703	94.807		
9a	.3253	.8526	30.354	30.360	121.433		
9b	.3255	1.0000					

DATE OF EXPT: 10-31-85
MOLES AMMSULF/MOLE NACL : 1.00017

pt #	rh	wt. frac. sol.	NaCl molal.	ammsulf molal.	ionic strgth	water act. ZSR	water act. RWR
1	.1093	.9992					
2	.5308	.9977					
3	.6444	.9886					
5	.6596	.9871					
6	.6677	.9752					
7	.6819	.5098	5.456	5.457	21.828	.5667	
9	.7450	.4341	4.024	4.025	16.097	.6737	
10	.8031	.3873	3.316	3.316	13.264	.7421	.7551
11	.6500	.5068	5.392	5.393	21.569	.5706	
12	.5583	.5972	7.777	7.778	31.112		
13	.6961	.4781	4.807	4.808	19.229	.6095	
14	.4747	.6757	10.934	10.935	43.740		
15	.3870	.7683	17.398	17.401	69.602		
16	.3424	.8175	23.500	23.504	94.011		
17	.3227	.8404	27.624	27.629	110.511		
18	.2939	.8669	34.181	34.187	136.743		
19	.2939	.9938					
20	.1093	.9953					

DATE OF EXPT: 11-23-85
MOLES AMMSULF/MOLE NACL : .99708

pt #	rh	wt. frac. sol.	NaCl molal.	ammsulf molal.	ionic strgth	water act. ZSR	water act. RWR
1	.1102	1.0000					
2	.3591	.8129	22.848	22.782	91.193		
3	.1100	1.0000					

MIXTURE OF SODIUM CHLORIDE AND AMMONIUM SULFATE
FACTOR Vdry WAS MULTIPLIED BY = .900
DATE OF EXPT: 10-29-85
MOLES AMMSULF/MOLE NACL : 1.00017

pt #	rh	wt. frac. sol.	NaCl molal.	ammsulf molal.	ionic strgth	water act. ZSR	water act. RWR
1	.1093	.9000					
2	.8399	.3082	2.337	2.338	9.350	.8326	.8304
3	.7875	.3482	2.803	2.804	11.214	.7914	.7937
4	.7000	.4189	3.782	3.783	15.131	.6964	
5	.5995	.4871	4.982	4.983	19.931	.5971	
6	.5062	.5760	7.128	7.130	28.518	.4831	
7	.4126	.6697	10.638	10.640	42.558		
8	.3530	.7369	14.692	14.695	58.776		
9a	.3253	.7674	17.306	17.309	69.233		
9b	.3255	.9000					

DATE OF EXPT: 10-31-85
MOLES AMMSULF/MOLE NACL : 1.00017

pt #	rh	wt. frac. sol.	NaCl molal.	ammsulf molal.	ionic strgth	water act. ZSR	water act. RWR
1	.1093	.8993					
2	.5308	.8979					
3	.6444	.8897					
5	.6596	.8884					
6	.6677	.8777					
7	.6819	.4588	4.448	4.449	17.795	.6371	
9	.7450	.3907	3.363	3.364	13.456	.7374	.7513
10	.8031	.3485	2.807	2.807	11.228	.7910	.7934
11	.6500	.4561	4.400	4.401	17.603	.6410	
12	.5583	.5374	6.096	6.097	24.386	.5313	
13	.6961	.4303	3.963	3.964	15.854	.6793	
14	.4747	.6082	8.143	8.145	32.577		
15	.3870	.6915	11.759	11.761	47.042		
16	.3424	.7357	14.607	14.609	58.435		
17	.3227	.7564	16.286	16.289	65.154		
18	.2939	.7802	18.627	18.630	74.519		
19	.2939	.8944					
20	.1093	.8958					

DATE OF EXPT: 11-23-85
MOLES AMMSULF/MOLE NACL : .99708

pt #	rh	wt. frac. sol.	NaCl molal.	ammsulf molal.	ionic strgth	water act. ZSR	water act. RWR
1	.1102	.9000					
2	.3591	.7316	14.334	14.292	57.211		
3	.1100	.9000					

MIXTURE OF SODIUM CHLORIDE AND AMMONIUM SULFATE
DATE OF EXPT: 11-24-85 (B)
MOLES AMMSULF/MOLE NACL : 1.99814

pt #	rh	wt. frac. sol.	NaCl molal.	ammsulf molal.	ionic strgth	water act. ZSR	water act. RWR
1	.1093	1.0108					
2	.6510	1.0000					
3	.7035	.5636	4.005	8.003	28.013	.5517	
6	.8020	.4149	2.199	4.393	15.378	.7503	
7	.7486	.4613	2.656	5.307	18.576	.6872	
8	.6828	.5134	3.272	6.537	22.883	.6156	
9	.6250	.5557	3.879	7.750	27.129	.5614	
10	.5421	.6221	5.104	10.199	35.702	.4805	
11	.4692	.7079	7.516	15.019	52.572		
12	.3908	.7763	10.761	21.503	75.270		
13	.3475	.8130	13.482	26.939	94.298		
14	.2975	.8502	17.605	35.177	123.136		
15	.2761	.8663	20.092	40.147	140.532		
16	.2207	1.0000					
17	.1093	1.0013					

MIXTURE OF SODIUM CHLORIDE AND AMMONIUM SULFATE
FACTOR Vdry WAS MULTIPLIED BY = .900
DATE OF EXPT: 11-24-85 (B)
MOLES AMMSULF/MOLE NACL : 1.99814

pt #	rh	wt. frac. sol.	NaCl molal.	ammsulf molal.	ionic strgth	water act. ZSR	water act. RWR
1	.1093	.9097					
2	.6510	.9000					
3	.7035	.5073	3.192	6.379	22.328	.6238	
6	.8020	.3734	1.848	3.692	12.924	.7986	.8035
7	.7486	.4152	2.202	4.399	15.400	.7499	
8	.6828	.4620	2.663	5.322	18.629	.6863	
9	.6250	.5001	3.103	6.200	21.702	.6334	
10	.5421	.5599	3.945	7.882	27.590	.5563	
11	.4692	.6371	5.445	10.880	38.084		
12	.3908	.6987	7.190	14.367	50.291		
13	.3475	.7317	8.457	16.898	59.151		
14	.2975	.7652	10.107	20.195	70.690		
15	.2761	.7797	10.973	21.926	76.751		
16	.2207	.9000					
17	.1093	.9012					

Appendix N: Plots of the weight fraction solute as a function of chamber relative humidity for mixed-electrolyte solutions; comparison of experimental data with predictions of Pitzer's model

The figures in this appendix are analogous to Figures 11–15 of Chapter 2; instead of the water activity being plotted as function of ionic strength, the weight fraction solute is plotted as function of water activity. Please see Chapter 2 for a discussion of the application of Pitzer's method to the prediction of the properties of mixed-electrolyte solutions.

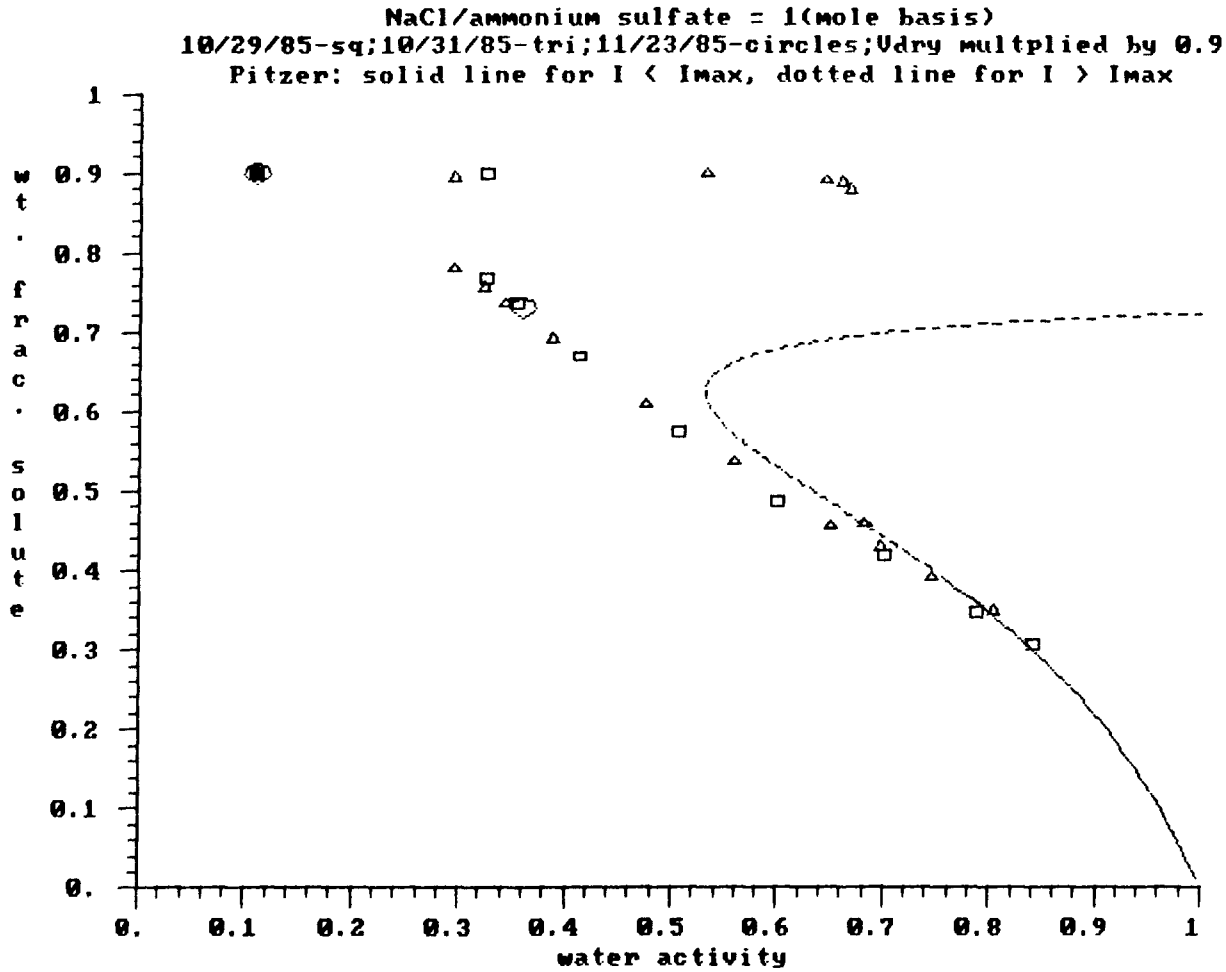
NaCl/ammonium sulfate = 1(mole basis)
10/29/85-sq;10/31/85-tri;11/23/85-circles;Vdry multplied by 0.9
Pitzer: solid line for I < Imax, dotted line for I > Imax
wt. frac. solute
1
0.9
0.8
0.7
0.6
0.5
0.4
0.3
0.2
0.1
0.
0.
0.1
0.2
0.3
0.4
0.5
0.6
0.7
0.8
0.9
1
water activity

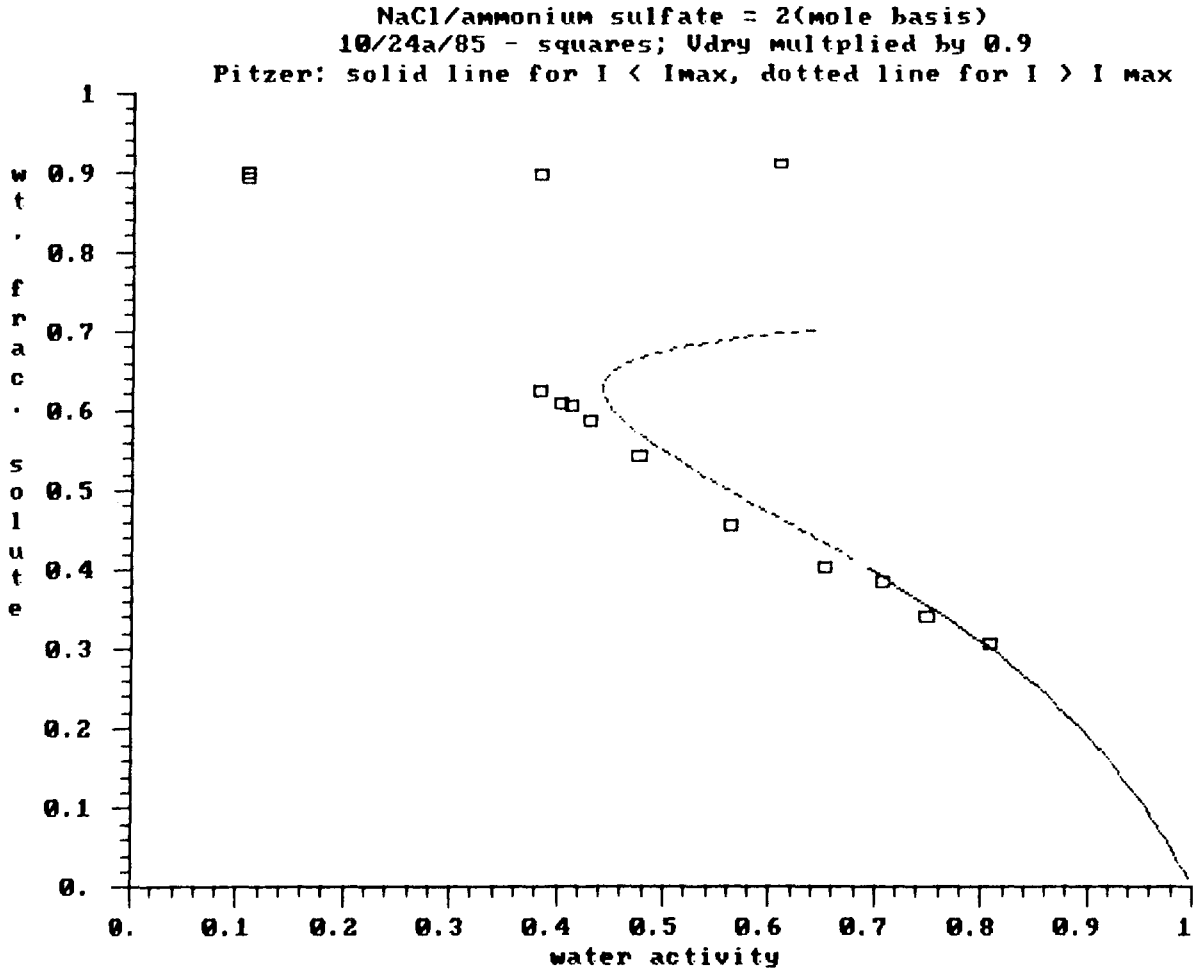
NaCl/ammonium sulfate = 2(mole basis)
10/24a/85 - squares; Vdry multplied by 0.9
Pitzer: solid line for I < Imax, dotted line for I > I max
wt. frac. solute
1
0.9
0.8
0.7
0.6
0.5
0.4
0.3
0.2
0.1
0.
0.
0.1
0.2
0.3
0.4
0.5
0.6
0.7
0.8
0.9
1
water activity

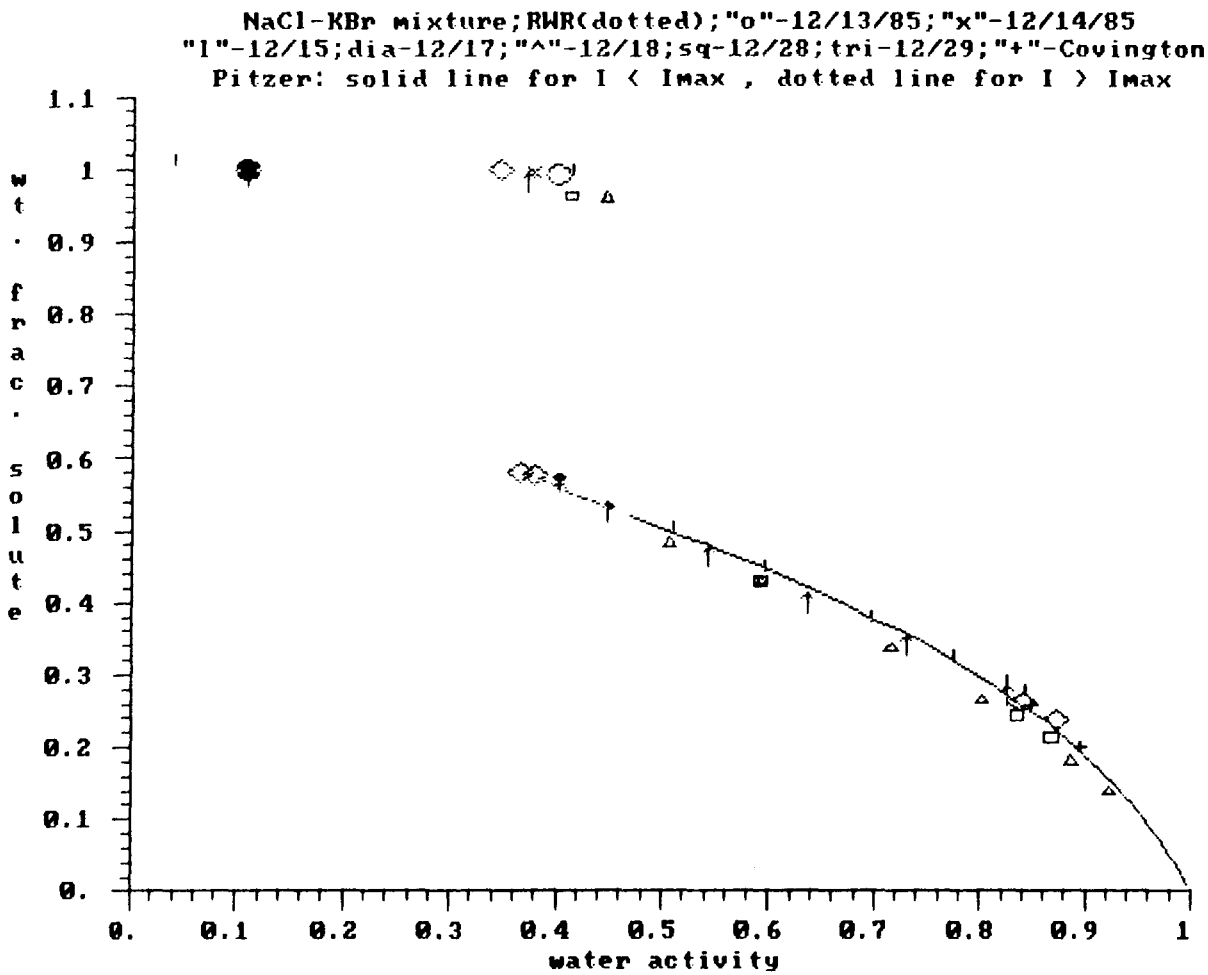
NaCl-KBr mixture;RWR(dotted);"o"-12/13/85;"x"-12/14/85
"l"-12/15;dia-12/17;"^"-12/18;sq-12/28;tri-12/29;"+"-Covington
Pitzer: solid line for I < Imax , dotted line for I > Imax
wt. frac. solute
1.1
1
0.9
0.8
0.7
0.6
0.5
0.4
0.3
0.2
0.1
0.
0.
0.1
0.2
0.3
0.4
0.5
0.6
0.7
0.8
0.9
1
water activity

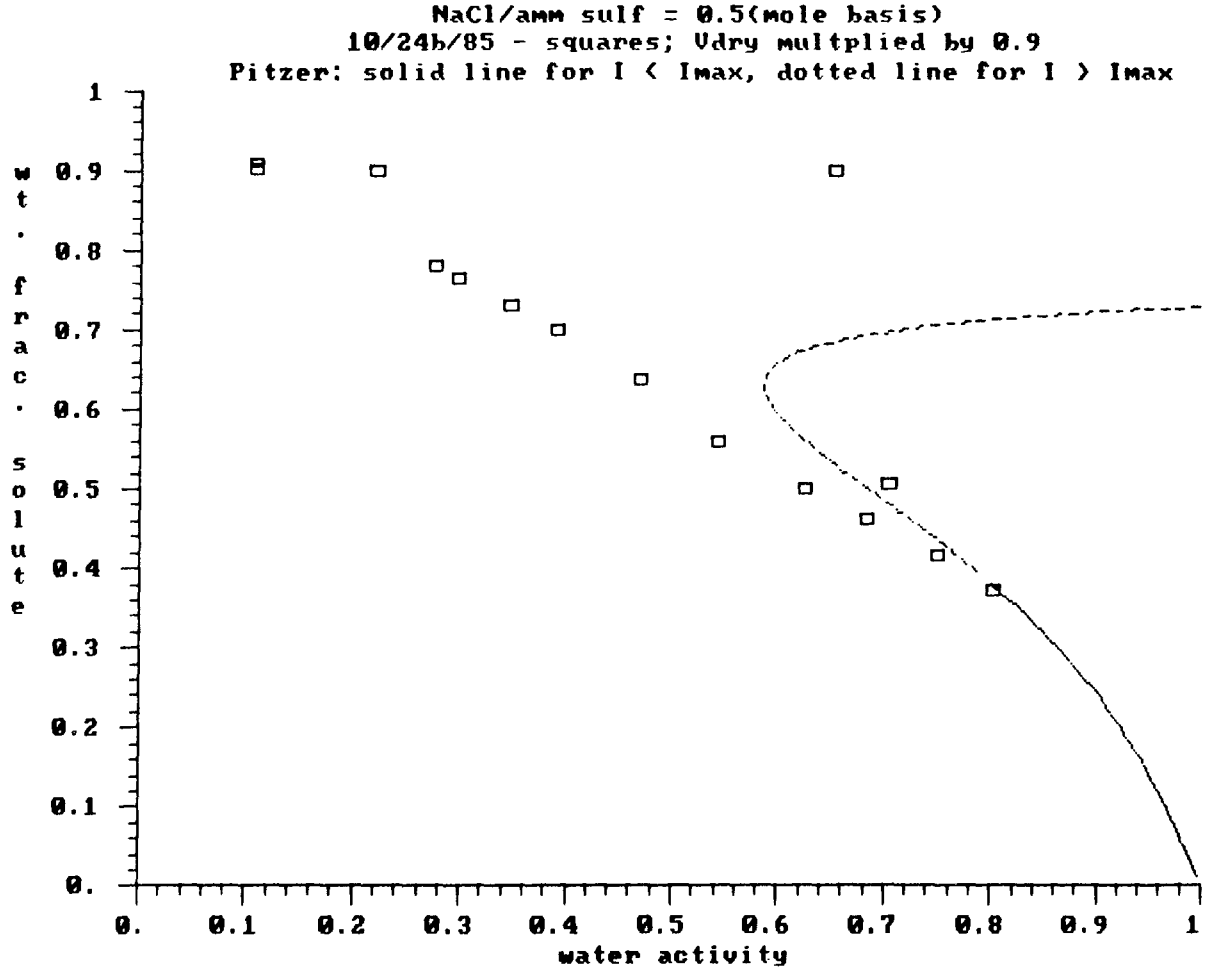
NaCl/amm sulf = 0.5(mole basis)
10/24b/85 - squares; Vdry multplied by 0.9
Pitzer: solid line for I < Imax, dotted line for I > Imax
wt. frac. solute
1
0.9
0.8
0.7
0.6
0.5
0.4
0.3
0.2
0.1
0.
0.
0.1
0.2
0.3
0.4
0.5
0.6
0.7
0.8
0.9
1
water activity

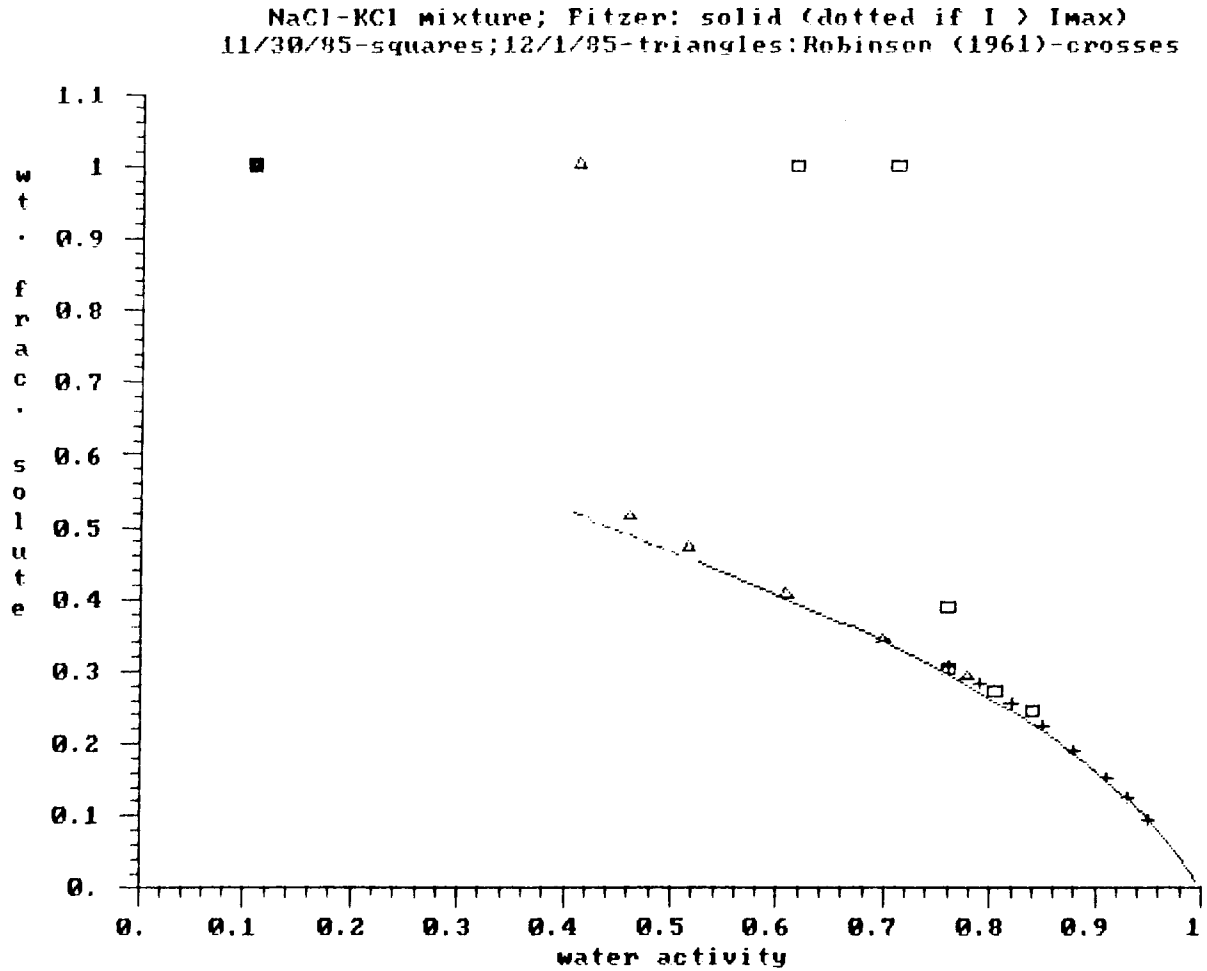
NaCl-KCl mixture; Pitzer: solid (dotted if I > Imax)
11/30/85-squares;12/1/85-triangles:Robinson (1961)-crosses
wt. frac. solute
1.1
1
0.9
0.8
0.7
0.6
0.5
0.4
0.3
0.2
0.1
0.
0.
0.1
0.2
0.3
0.4
0.5
0.6
0.7
0.8
0.9
1
water activity